UC Irvine

UC Irvine Electronic Theses and Dissertations

Title

Radical/Polar Crossover: New Methodologies and Applications in Total Synthesis & Studies Towards a Synthesis of Asperterpenoid A

Permalink

https://escholarship.org/uc/item/4pv3w78n

Author

Johnson, Lucas Kent

Publication Date

2024

Peer reviewed|Thesis/dissertation

eScholarship.org Powered by the California Digital Library
University of California

UNIVERSITY OF CALIFORNIA,
IRVINE

Radical/Polar Crossover: New Methodologies and Applications in Total Synthesis

&

Studies Towards a Synthesis of Asperterpenoid A

DISSERTATION

submitted in partial satisfaction of the requirements
for the degree of

DOCTOR OF PHILOSOPHY

in Chemistry

by

Lucas Kent Johnson

Dissertation Committee:
Professor Christopher D. Vanderwal, Chair
Professor Larry E. Overman
Professor Sergey V. Pronin

2024

Portions of Chapter 1 © 2021 American Chemical Society

Portions of Chapter 2 © 2023 Wiley-VCH Verlag GmbH & Co. KGaA

All other materials © 2024 Lucas Kent Johnson

DEDICATION

To my mother for her boundless enthusiasm and curiosity.

To my father for his endless support and patience.

To my friends for always being there.

To Chanel for everything.

"To every man, in his acquaintance with a new art, there comes a moment when that which before was meaningless first lifts, as it were, one corner of the curtain that hides its mystery, and reveals, in a burst of delight which later and fuller understanding can hardly ever equal, one glimpse of the indefinite possibilities within."

C .S. Lewis

TABLE OF CONTENTS

LIST OF FIGURES vi

LIST OF SCHEMES vii

LIST OF TABLES ix

ACKNOWLEDGEMENTS x

VITA xiii

ABSTRACT OF THE DISSERTATION xv

CHAPTER 1. THE STRUCTURAL REVISION OF PLEBEIANIOL A 1

1.1 Introduction 1
1.2 Biosynthesis of Abietane Natural Products 2
1.2.1 Diterpene Biosynthesis 2
1.2.2 Abietane Biosynthesis 4
1.3 Isolation of Plebeianiol A 4
1.3.1 The Configuration of C5 and C10 5
1.3.2 Presence of Oxidation at C11/C13 5
1.3.3 B-ring Isopropyl Transposition 6
1.4 Motivations For Synthesis 6
1.5 Retrosynthesis of Plebeianiol A 9
1.5.1 Prior Work in the Vanderwal Lab 9
1.5.2 Retrosynthesis of Plebeianiol A 10
1.6 Synthesis of Plebeianiol A 11
1.6.1 Attempted Synthesis of the Cyanophosphonate Fragment 11
1.6.2 Revised Synthesis of 1.11 12
1.6.3 Fragment Union and Completion of the Synthesis of 1.2 14
1.6.7 Completion of the Synthesis of 1.3 16
1.7 Conclusion 17
1.8 References 18
1.9 Experimental Information 20
1.9.1 Materials and Methods 20
1.9.2 Experimental Procedures 22
1.9.3 Method for Predicting ^{13}C Chemical Shifts 39
1.9.4 Supplemental References 39

CHAPTER 2. DISCOVERY OF A RADICAL-BASED ANNULATION METHOD 41

2.1 Introduction 41
2.2 Discovery of an MHAT-initiated Radical Annulation 44
2.3 Discovery of a Radical-Based Annulation Method 47

2.3.1 Reaction Optimization 47
2.3.2 Substrate Scope 49
2.4 Conclusion and Future Directions 51
2.5 Distribution of Credit 54
2.6 References 54
2.6 Experimental Information 57
2.6.1 Materials and Methods 57
2.6.2 Starting Material Synthesis 59
2.6.3 Annulation General Procedure 71
2.6.4 Experimental Procedures 71
2.6.5 Supplemental References 90
CHAPTER 3. STUDIES TOWARDS A SYNTHESIS OF ASPERTERPENOID A 91
3.1 Introduction 91
3.2 Isolation of Asperterpenoid A 92
3.3 Biosynthesis of Asperterpenoid A 92
3.3.1 Sesterterpenoid Biosynthesis 92
3.3.2 Asperterpenoid A Biosynthesis 93
3.4 Bioactivity of Asperterpenoid A 94
3.4.2 Tuberculosis 94
3.4.3 The Role of mPTPB 95
3.5 Retrosynthesis of Asperterpenoid A 96
3.5.1 Radical Disconnection 97
3.5.2 Polar Disconnection 98
3.6 Attempted Synthesis of 3.9 From Sitolactone 98
3.7 Synthesis of 3.9 From Hydrindenone 3.32 107
3.8 Synthesis of Bromide 3.12 113
3.9 Conclusions and Future Directions 114
3.10 References 116
3.11 Experimental Information 120
3.11.1 Materials and Methods 120
3.11.2 Experimental Procedures 122
3.11.3 Supplemental References 149
APPENDIX A 150
Appendix A1: NMR Data 150
Appendix A2: Predicted ^{13}C Shifts and Comparison of Spectral Data 182
APPENDIX B 194
Appendix B1: NMR Data 194
Appendix B2: X-Ray Crystallographic Data 258

APPENDIX C 274

Appendix C1: NMR Data 274

Appendix C2: X-Ray Crystallographic Data 326

LIST OF FIGURES

Figure 1.1 Abietane scaffold and representative bioactive aromatic abietanes 1

Figure 1.2 Chain-elongation of DMAPP with IPP leads to C_{5n} terpenoid natural products 2

Figure 1.3 Bifurcation of diterpenoid biosynthesis 3

Figure 1.4 Reported structure of plebeianiol A 5

Figure 1.5 Reported and proposed structures of plebeianiol A resemble known abietane 1.3 7

Figure 1.6 Linear correlation plot for 1.1 against plebeianiol A 8

Figure 1.7 Linear correlation plot for 1.2 against plebeianiol A 8

Figure 1.8 ^{13}C shift differences between 1.1 or 1.2 with plebeianiol A 9

Figure 3.1 Two modes of ring fusion in trans-hydrindane sesterterpenoids 91

Figure 3.2 Structure of asperterpenoid A (3.1) 92

Figure 3.3 Two modes of cyclization initiate canonical sesterterpenoid biosynthesis 93

Figure 3.4 Representative TB chemotherapeutics and associated modes of inhibition 95

LIST OF SCHEMES

Scheme 1.1 Biosynthesis of aromatic abietanes intercepts miltiradiene 4

Scheme 1.2 Proposed rearrangement of ferruginol leads to totaranes and semperviranes 6

Scheme 1.3 Synthesis of a related abietane natural product 10

Scheme 1.4 Retrosynthetic analysis of 1.2 11

Scheme 1.5 Synthesis of acetonide-protected cyanophosphonate precursor 1.19 12

Scheme 1.6 Nucleophilic displacement with iodide 1.19 proves unsuccessful 12

Scheme 1.7 A change in protecting group permits homologation to nitrile 1.30 14

Scheme 1.8 Synthesis of polycyclization precursor 1.32 14

Scheme 1.9 Completion of the synthesis of 1.2 15

Scheme 1.10 Work by González studies the autoxidation processes of abietane carbinols 16

Scheme 1.11 Observed solvent effects facilitate autoxidation of 1.2 to 1.3 17

Scheme 2.1 Robinson annulation by Baran and coworkers in their synthesis of pallambins 41

Scheme 2.2 Danheiser annulation by Shenvi and coworkers in their synthesis of (±)-GB18 42

Scheme 2.3 Hauser–Kraus annulation by Pronin and coworkers in a synthesis of acremoxanthone A 42

Scheme 2.4 Biginelli condensation by Overman and coworkers aids the synthesis of batzelladine A 43

Scheme 2.5 Radical annulation by Curran and coworkers in the synthesis of camptothecin 43

Scheme 2.6 MHAT-initiated annulation by Pronin and coworkers in the synthesis of forskolin . 44

Scheme 2.7 Proposed mechanism for HAT-initiated radical bicyclization 45

Scheme 2.8 Functional group reorganization leads to annulation reaction concept 45

Scheme 2.9 Simple mechanism for MHAT-initiated annulation 46

Scheme 2.10 Retrosynthesis of hamigeran F (2.53) 52

Scheme 2.11 Synthesis of model arene 2.59 52

Scheme 2.12 Synthesis of model arene 2.61 52

Scheme 2.13 Annulation attempts with 2.59 or 2.61 53

Scheme 2.14 Photoredox-mediated annulation cascade by Yoshimitu and coworkers 54

Scheme 3.1 Proposed biosynthesis of asperterpenoid A 94
Scheme 3.2 Disconnection of asperterpenoid A prioritizes two fragment coupling approaches . 97
Scheme 3.3 Disconnection of the common intermediate by radical fragment coupling..... 97
Scheme 3.4 Retrosynthetic analysis of β,γ-unsaturated ketone 3.9 98
Scheme 3.5 Disconnection of the common intermediate by polar fragment coupling 98
Scheme 3.6 Desaturation and cuprate conjugate addition to sitolactone 99
Scheme 3.7 Work by Trauner reveals an unexpected epimerization 100
Scheme 3.8 Epimerization/isomerization of 3.15..... 102
Scheme 3.9 Alternate approaches to epimerization..... 103
Scheme 3.10 Synthesis of enone 3.21 104
Scheme 3.11 Proposed mechanistic pathway converting 3.25a to 3.25b..... 105
Scheme 3.12 Stereoselective hydrogenolysis of 3.21..... 105
Scheme 3.13 Synthesis of keto-acid 3.28 106
Scheme 3.14 Photocatalytic oxidative dehomologation leads to 3.29 106
Scheme 3.15 Mozingo reduction of sitolactone leads to lactone 3.31 107
Scheme 3.16 Ding's synthesis of hydrindenone 3.32 inspires a new strategy to 3.9..... 107
Scheme 3.17 Regulated chemical access complicates synthesis of hydrindenone 3.9..... 108
Scheme 3.18 The discovery of a tandem HWE/Nef reaction enables synthesis of 3.35 109
Scheme 3.19 Reported conditions leading to ketoaldehye 3.40 prove irreproducible 109
Scheme 3.20 Synthesis of hydrindenone 3.32 by Fallis and coworkers 110
Scheme 3.21 Efforts to intercept epoxide 3.41 are unsuccessful 110
Scheme 3.22 Adaptation of chemistry by Fallis and coworkers enables synthesis of enone 3.9 111
Scheme 3.23 Early derivatizations of 3.32 and proposed synthesis of 3.13..... 113
Scheme 3.24 Synthesis of allylic alcohol 3.56 114
Scheme 3.25 Bromination of 3.12 proves challenging..... 114
Scheme 3.26 Proposed endgame sequence permitting synthesis of asperterpenoid A (3.1) 115

LIST OF TABLES

Table 2.1 Reaction optimization with acrylonitrile 48

Table 2.2 Arene substrate scope 50

Table 2.3 Electron-deficient alkene scope 51

Table 3.1 Optimization of cuprate conjugate addition to 3.14 101

ACKNOWLEDGEMENTS

The body of work described over the next few hundred pages or so wouldn't have been possible without the tremendous and immediate support of many, many people in my life – in this way, this thesis is as much yours as it is mine. A million times, thank you.

Chris, thank you for taking me under your wing as a fledgling graduate student. Under your mentorship, I've had the opportunity to mature as a scientist in ways that I couldn't possibly have predicted. Your pure passion for the field of synthesis and your knack for dreaming up beautiful chemistry is deeply inspiring, and your attentiveness to everyone in the group has always been without limits – thank you for so carefully cultivating such a wonderful place to do science. Thank you for challenging me and thank you for stoking my fire.

To Professor Larry Overman and Professor Sergey Pronin, thank you for reading this far! But seriously, thank you for your continued mentorship and the many helpful discussions you've entertained on my behalf over the past five years. Larry, I'm so grateful to have had the opportunity to discuss and share my chemistry with you on several occasions – I always left with so much more than I entered with. I am *still* working my way through your publication list, and I will plan a dive trip to the Coral Sea. Sergey, thanks for always responding to my last-minute e-mails and agreeing to meet at a moment's notice. You surprised me several times when you'd drop by FRH 4003A to chat, lab coat and all.

To Professor William Alston and Professor Scott Fier, thank you for laying the foundation on which I stand today. Only through your thoughtful support was I able to continue along this journey, and I feel extremely lucky to have learned the fundamentals from each of you. I still routinely refer to your notes when I get hung up on something.

The experiences I had at Takeda were critical to my development as a professional chemist and solidified my career aspirations. To Lily Kwok, thanks for teaching me how to work efficiently in lab and how to triage reactions. I will always remember our fun lunch trips to Convoy! To Derek Cole, Gloria Hernández, Phong Vu, Joanne Miura, Dan Scheibe, Andy Jennings, Mark Sabat, Andy Flick, Steve Woodhead, Dan Carney, Jason Green, Antoine Henninot, thanks for the many encouraging conversations we had about chemistry, graduate school, life in industry, and life itself. I look forward to catching up with you soon!

I have to thank Darius Vrubliauskas for being such a positive influence and outstanding role model as a scientist during my first year in the group. Thanks for going out on a limb for me,

but despite your best efforts I'm still a fairly lousy chess player. Night Shift was a truly memorable experience under your reign. To that end, I thank the Night Shift crew for weathering the highly unusual circumstances of a global pandemic and making the experience, dare I say, enjoyable. You know who you are, and without you the Night Shift wouldn't have been the very special experience it was. It still feels like some sort of crazy dream.

Gratitude is due to our most talented postdoctoral scholars, especially Jonathan Chung, Fabian Hörmann, Nick Magann, and Ibrahim Çelik. Jono, I look forward to planning many more ski trips with you and Griffin. Thanks for helping me through many hard times early on, and for always lifting our spirits. Fabi, it's Friday again. I hope you always remember that you *can* eat the skin of a banana, too. Nick, just how are you always so cool-headed about everything? Thanks for setting the bar high on the back end of this whole thing and showing us how to really get it done. Ibo, thanks for knowing more named reactions than the rest of the lab combined. But seriously, thanks for your positivity, willingness to problem-solve, and love of kebabs. Thank you all for being not only incredible scientists, but great friends as well.

I spent a lot of time in the trenches with Griffin Barnes, Jane Supantanapong, and Bonnie Park. Griffin, it's been an absolute blast working with you. Thanks for putting up with the clean room banter and so selflessly helping us all solve problems that weren't ever your own. You will make an outstanding PI and I very much look forward to hearing about the illustrious academic career that your future certainly holds. I'm so grateful for our friendship and I know we'll stay in touch, no doubt. Jane, thanks always for being such a ray of sunshine in lab – Chanel and I are so excited to visit you and Darius in Thailand! Also, thanks for always sharing treats before seminar. Bonnie, your creativity in chemistry is admirable – you always have a way of seeing things that no one else does. Your ability to bring a fresh perspective to the table is always appreciated, and I know the very near future holds exciting opportunities for you. It has been an absolute privilege to work with the three of you over the past five years, and I look forward to staying in touch as our paths play out ahead of us.

When I started in lab, Ryan Kozlowski and Riley Mills were already two peas in a pod. I am grateful for their sustained light-heartedness and routine satire. Thanks to Bonnie Pak for making many quiet mornings less quiet and more fun – you are a real one. I'm grateful to Joe Capani not only for putting me up during visitation weekend, but for the many laughs we shared over the years. To Natalie Dwulet and Scott Niman, thanks for showing us how to grind. Scott, It still makes me laugh that we were trying to make the same thing for so long and just never talked about it.

Thanks to Phil and Hanh, who held in there during the pandemic and stuck it out - it's been a pleasure to overlap with you both. Matt, Mira, Jon, and Brandon, it's been surreal to watch the four of you develop into talented, capable, and successful scientists over the past year – please stay in touch! Seamus and Theo, the two of you are the new guard for the Vanderwal Lab and I couldn't be more impressed. You both have bright futures ahead and I look forward to seeing what you accomplish in the coming years.

Thanks to Evan Horn, Sharon Michalak, Mary Beth Daub, Allen Hong, Jon Lam, Theo Michels, Dave Martin, and Grant Shibuya. Thanks to Chuck Dooley, Leah Salituro, Bryant Lim, Paul Carlson, Matt Duong, and Jess Pazienza. Thanks to Tyler Allred. Thanks to Nick Foy, Will Thomas, Sarah Bredenkamp, Daniel Essayan, Brandon Cooper, and Amy Cheung. Thanks to Taylor Thane, Claire Herbert, Nadia Hirbawi, and Patricia Lin. Thanks to Gretchen Guaglianone. Thanks to Martin Stang. Thanks to Chris Dicksion. I can't imagine completing this task without the exchanges I had with you all, routine or otherwise.

To the friends outside UCI who got me through this: Andre Ramoska, Joe Maltese, Tyler Suss, Bryson Nugent, Brice Murtaugh, and Collin Rodarte – thanks for always being there for me. Thanks for getting me out of lab and onto the beach when I needed it most – I am so grateful for our friendship, and I look forward to many more years of it to come.

To Dad, thanks for always being so supportive. You shared with me your deep curiosity in the world around us and taught me how to see the bigger picture from the details. You challenged me to never stop learning. Thanks for pushing me to grow and encouraging me to blaze my own trail.

To Chanel, thank you for everything. I can't believe we met at such a tumultuous moment in time and I can't tell you how grateful I am for the opportunity that was our meeting. You quickly became my rock through all of the hardships that this process has entailed; you patiently listened to all of my frustrations along the way and were always able to provide a positive perspective. I couldn't possibly imagine making it this far without you. I love you so much and I am so excited to begin this next chapter with you.

I thank the American Chemical Society for permission to include portions of Chapter 1, which were originally published in *Organic Letters*. I thank Wiley-VCH Verlag GmbH & Co. KGaA for permission to include portions of Chapter 2, which were originally published in *Angewandte Chemie International Edition*.

VITA

Lucas Kent Johnson

EDUCATION

University of California, Irvine
Ph.D., Chemistry 2024

Arizona State University
B.S., Biochemistry (conc. Medicinal Chemistry) 2017

University of California, Santa Cruz 2012
B.A., Anthropology (conc. Medical Anthropology)

EXPERIENCE

Graduate Student Researcher 2020 – 2024
Department of Chemistry, University of California, Irvine
Advisor: Professor Christopher D. Vanderwal
-Total synthesis and structural revision of plebeianiol A.
-Development of a new radical/polar crossover method for annulation of allyl arenes with electron-deficient alkenes.
-Synthetic studies towards a total synthesis of asperterpenoid A.

Graduate Student Teaching Assistant 2019 – 2024
Department of Chemistry, University of California, Irvine
-Teaching assistant for lecture and lab series in general and organic chemistry.

Intern, Medicinal Chemistry 2018 – 2019
Takeda Pharmaceuticals
-Design, synthesis, purification, and characterization of novel chemical compounds for three discrete therapeutic targets.

Undergraduate Student Researcher 2017 – 2017
School of Molecular Sciences, Arizona State University
Advisor: Professor George R. Pettit II
-Synthesis of dolaisoleuine and efforts towards (+)-pancratistatin benzoate.

PUBLICATIONS

Johnson, L. K.; Barnes, G. L.; Fernandez, S. A.; Vanderwal, C. D. Hydrogen-Atom-Transfer-Initiated Radical/Polar Crossover Annulation Cascade for Expedient Access to Complex Tetralins. *Angew. Chem. Int. Ed.* **2023,** e202303228.

Johnson, L. K.; Niman, S. W.; Vrubliauskas, D.; Vanderwal, C. D. Stereocontrolled Synthesis and Structural Revision of Plebeianiol A. *Org. Lett.* **2021,** 23, 9569–9573.

PRESENTATIONS

"Cobalt-Catalyzed Radical/Polar Crossover: New Methodologies and Applications in Total Synthesis" — May 2023
Saddleback College, Mission Viejo, CA

"Cobalt-Catalyzed Annulation via Hydrogen Atom Transfer: Expedient Access to Arene-Fused Cycloalkanes" — Sept 2022
28th Congress of the International Society of Heterocyclic Chemistry
UC Santa Barbara, Santa Barbara, CA

AWARDS

Chemistry Graduate Dissertation Fellowship	Sept 2023
Harold Friedemann Chemistry Scholarship	May 2016
ACS Chemistry Student of the Year	May 2016
Dr. Steve Sworder Memorial Mathematics Scholarship	May 2015
NSF S-STEM Scholarship	May 2015
Summer Science Research Scholarship	May 2015

ABSTRACT OF THE DISSERTATION

Radical/Polar Crossover: New Methodologies and Applications in Total Synthesis

&

Studies Towards a Synthesis of Asperterpenoid A

by

Lucas Kent Johnson

Doctor of Philosophy in Chemistry

University of California, Irvine, 2024

Professor Christopher D. Vanderwal, Chair

This dissertation describes work completed in several areas of ongoing research in the Vanderwal Lab. Chapter 1 describes the family of natural products known as the abietane diterpenoids, the structural anomaly plebeianiol A, and our synthetic endeavor to elucidate the authentic structure of this natural product. Chapter 2 describes the development of a new radical/polar crossover annulation method using metal-hydride hydrogen atom transfer (MHAT) catalysis. Finally, Chapter 3 details our investigation into a synthetic route towards the sesterterpenoid natural product, asperterpenoid A.

CHAPTER 1. THE STRUCTURAL REVISION OF PLEBEIANIOL A

1.1 Introduction

Species of plants within the *Salvia* genus of the Lamiaceae family are found on nearly every continent.[1] Renowned for their applications in traditional medicine, these plants possess a variety of chemical constituents that can be divided into several groups, the largest of which are the abietane diterpenoids.[2] Within this group, congeners displaying an aromatic C ring comprise the subgroup of aromatic abietanes (**Figure 1.1**). This class of natural products exhibit an array of therapeutically-relevant properties including antiviral, antibacterial, antimalarial, antifungal, antitumor, anti-inflammatory, and immunosuppressive activities.[2]

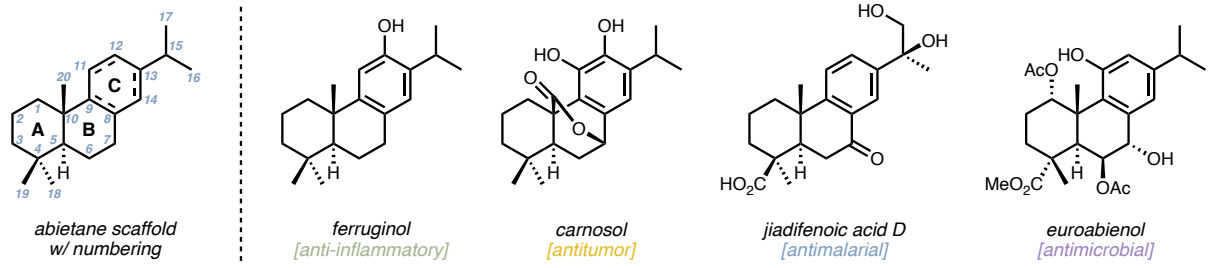


Figure 1.1 *Abietane scaffold and representative bioactive aromatic abietanes*

The aromatic abietane diterpenoids possess an octahydrophenanthrene ring system and are differentiated by the degree and pattern of oxygenation that decorates this core. Evidently, these subtle changes in the oxygenation have a dramatic effect on the biological properties observed in each abietane natural product.

1.2 Biosynthesis of Abietane Natural Products

1.2.1 Diterpene Biosynthesis

Fundamentally, all terpene natural products are derived from just two C_5 monomers: isopentenyl diphosphate (IPP) and its structural isomer dimethylallyl diphosphate (DMAPP). Two families of enzymes are essential to this process; through the action of a prenyltransferase (PT), one or more subunits of IPP are added to DMAPP through a chain elongation process which permits the biosynthesis of C_{5n} terpene precursors (**Figure 1.2**).[3]

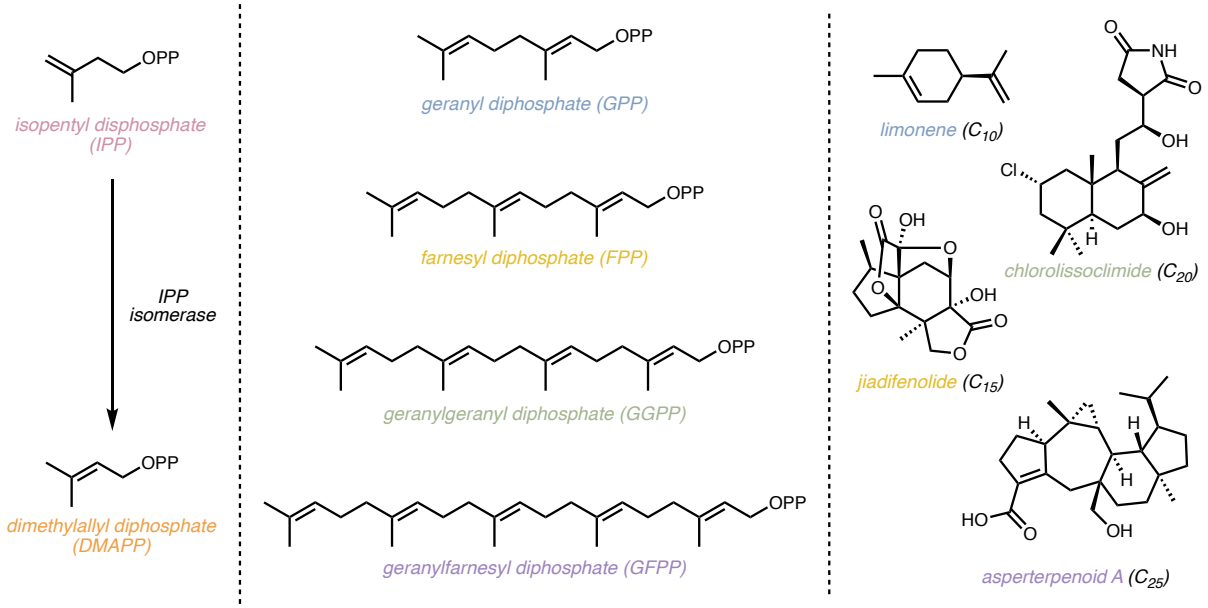


Figure 1.2 *Chain-elongation of DMAPP with IPP leads to C_{5n} terpenoid natural products*

These precursors typically become the subject of complex reaction cascades that are entirely mediated by terpene synthases (TS).[4] Produced by bacteria, fungi, and plants alike, terpene synthases are classified by the mode in which the cyclization cascade is initiated: class I terpene synthases initiate cyclization through metal-mediated loss of diphosphate ("tail-to-head"), whereas class II terpene synthases initiate cyclization through an alkene (or epoxide) protonation

event ("head-to-tail").[4,5] Not surprisingly, these two modes of action have different consequences regarding the details of cyclization cascade.

In the biosynthesis of diterpenoid natural products, GGPP may be the substrate for either class I or class II diterpene synthases (**Figure 1.3**). The action of a particular class I diterpene synthase on GGPP typically facilitates a distinct cyclization cascade in its entirety. By controlling which alkenes participate in the cascade, class I diterpene synthases produce a dazzling series of molecular scaffolds. Conversely, class II diterpene synthases first direct the formation of copalyl diphosphate (CPP). Still possessing the reactive diphosphate group, the subsequent action of a class I diterpene synthase on CPP couples the metal-mediated loss of diphosphate coupled with elimination, rearrangement, or further cyclization events to complete scaffold formation. In this way, many diterpene natural products share CPP as a discrete biosynthetic intermediate and it is this detail that leads to their grouping as the so-called "labdane-related" diterpenoids.

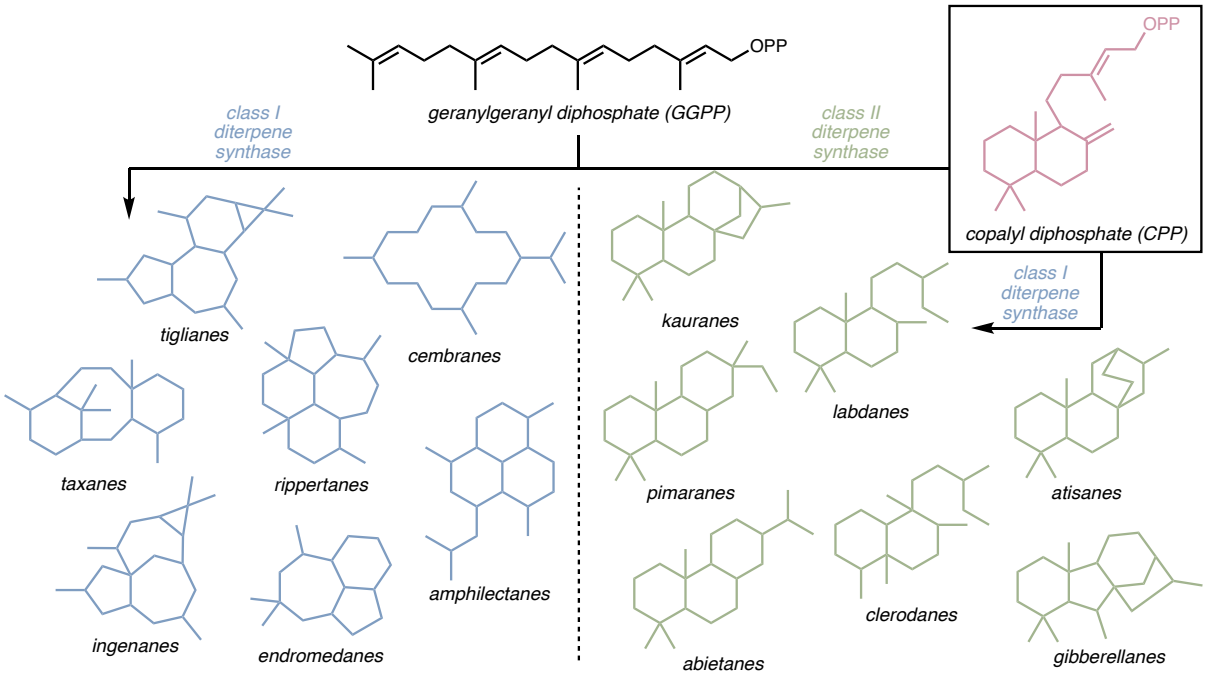
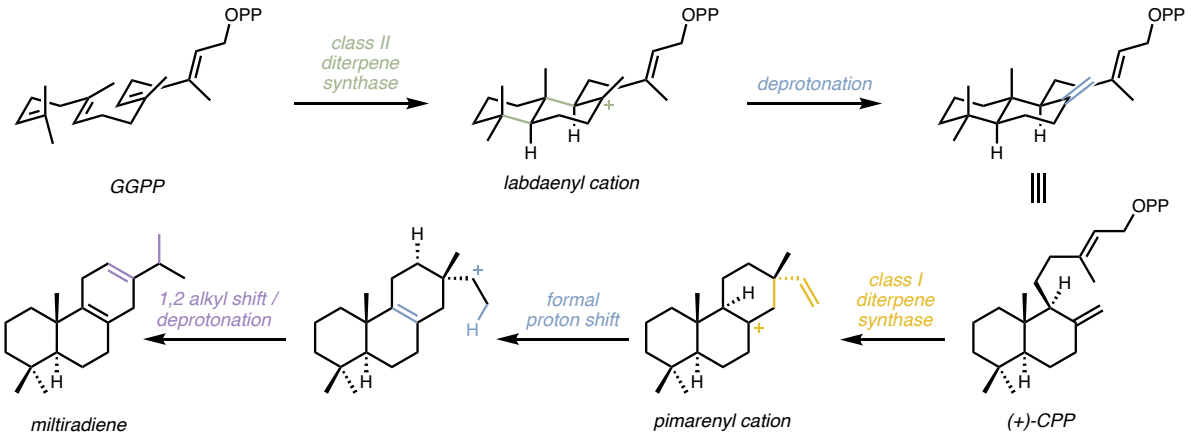


Figure 1.3 *Bifurcation of diterpenoid biosynthesis*

1.2.2 Abietane Biosynthesis

As labdane-related diterpenoids, abietanes are biosynthesized by a cyclization cascade that intercepts CPP (**Scheme 1.1**).[6] The first stage of abietane biosynthesis is characterized by the specific action of a class II diterpene synthase on geranylgeranyl diphosphate (GGPP). Enzyme-mediated protonation of the terminal alkene in GGPP facilitates a bicyclization event that closes the A/B decalin ring system and simultaneously generates the labdaenyl cation. Subsequent deprotonation by a basic residue in the terpene synthase active site completes the synthesis of copalyl diphosphate (CPP).[6] In the second stage of abietane biosynthesis, a class I diterpene synthase couples the loss of the diphosphate group with closure of the C ring. It is proposed that the nascent pimarenyl cation is converted to miltiradiene through a series of elementary steps.[7] Though miltiradiene can spontaneously aromatize under aerobic conditions, this process is mediated enzymatically.[8]

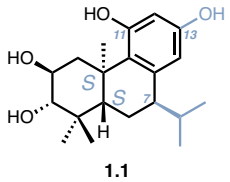
Scheme 1.1 *Biosynthesis of aromatic abietanes intercepts miltiradiene*



1.3 Isolation of Plebeianiol A

In 2015, Liang and Wu reported the isolation of a novel aromatic abietane from *Salvia plebeia* R. Br., which they named plebeianiol A (**Figure 1.4**).[9] Working exclusively from 2D NMR data, the group assigned the structure of plebeianiol A as **1.1**. Assuming that plebeianiol A is an

aromatic abietane natural product, several aspects of the proposed structure and isolation report led us to believe the structure may have been misassigned. There are three structural details in **1.1** that contradict the biosynthetic origins of these compound: (1) C5 and C10 are assigned an absolute configuration of *S*; (2) the C ring bears oxidation at C11 *and* C13; and (3) the isopropyl unit is located on the B ring at C7.



1.1

Figure 1.4 *Reported structure of plebeianiol A*

1.3.1 The Configuration of C5 and C10

The assigned absolute configurations of C5 and C10 as *S* implicates that (–)-CPP is produced from GGPP as a biosynthetic intermediate.[6] While (–)-CPP-producing class II diterpene synthases are ubiquitous in nature, studies investigating the biogeneses of abietane or abietane-type natural products to date have only ever observed and characterized class II diterpene synthases that produce (+)-CPP.[7,10–14] Though not entirely inconceivable, it seems highly unlikely that *Salvia plebeia* R. Br. would be an evolutionary outlier in this case. This notion is further corroborated by the authors' co-isolation of several other previously described abietane natural products derived from (+)-CPP.

1.3.2 Presence of Oxidation at C11/C13

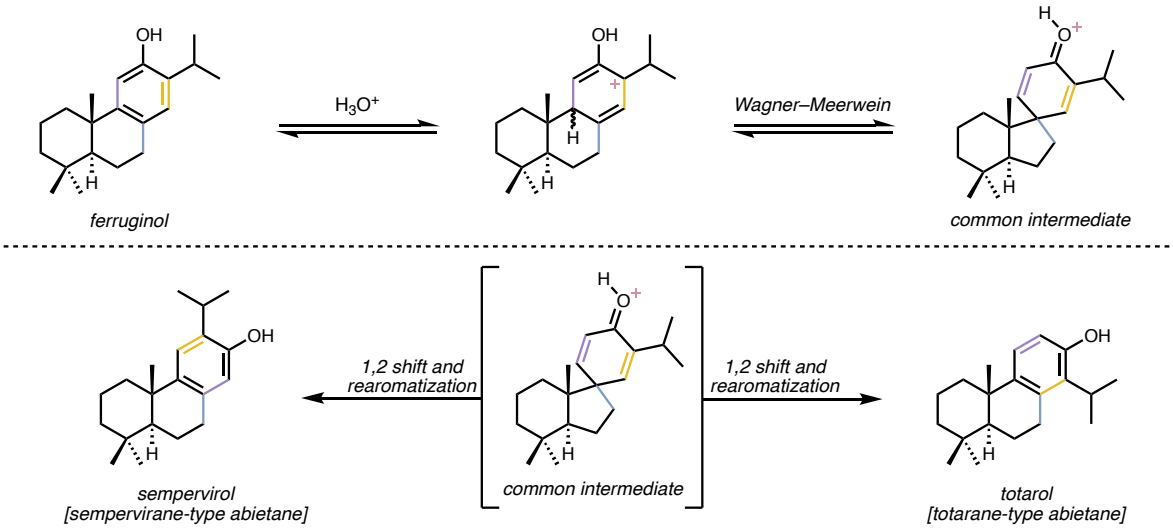
Oxidation events in nature are transforms mediated almost entirely by cytochrome P450 (CYP) enzymes.[15] Site-selective oxidation of ferruginol at C11 or C12 is shown to be directed by CYP76AH4 or CYP76AH24, respectively.[8,16] C13 oxidation, however, is significantly less common among the aromatic abietanes. Indeed, this position almost always bears the vestigial isopropyl

group, which itself is the product of C ring closure. Because these processes are so highly conserved evolutionarily in abietane biosynthesis, the presence of oxidation at C13 in plebeianiol A necessitates outright deletion or otherwise transposition of the C13 isopropyl group.

1.3.3 B-ring Isopropyl Transposition

The assignment of the isopropyl group to C7 is the most problematic detail of the three. In all known abietane natural products, the isopropyl group is located on the aromatic C ring. Almost always located at C13, the isopropyl group may also be displayed at C12 or C14. This 1,2-transposition is proposed to occur via an acid-mediated dearomative ring contraction of ferruginol, followed by a Wagner–Meerwein-type ring expansion event, and provides entry to sempervirane and totarane natural products (**Scheme 1.2**).[17]

Scheme 1.2 *Proposed rearrangement of ferruginol leads to totaranes and semperviranes*



1.4 Motivations For Synthesis

Ultimately, our group initiated synthetic studies not towards **1.1** but instead its structural isomer **1.2**, which we supposed might be the authentic structure of plebeianiol A (**Figure 1.5**).

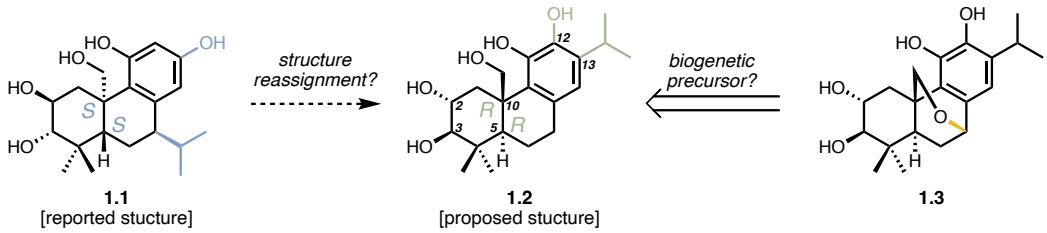


Figure 1.5 *Reported and proposed structures of plebeianiol A resemble known abietane* ***1.3***

In **1.2**, the absolute configurations of C5 and C10 are restored to *R*. On the basis that all known abietanes appear to be derived from (+)-CPP, here this choice implicates (+)-CPP as a precursor to plebeianiol A. **1.2** bears C12 oxidation, a decision that renders possible repositioning of the C7 isopropyl group in **1.1** to C13 in **1.2**. Lastly, the absolute configurations of C2 and C3 have been changed from *S* to *R*; what seems an arbitrary decision was in fact predicated on the reported isolation and characterization of another abietane natural product, **1.3**.[18] If identified as plebeianiol A, it could be the case that **1.2** is the biogenetic precursor to **1.3**.

Confident in our analysis thus far, we nevertheless sought another means by which to interrogate the legitimacy of **1.1** as the assigned structure of plebeianiol A. Inspired by relatively the recent work of Rychnovsky, we felt our hypothesis might be further informed by computational methods. Here, prediction of ^{13}C chemical shifts for both structures could facilitate a head-to-head comparison against the spectral data for plebeianiol A as reported by Liang and coworkers. It is generally understood that the absolute error – measured by the difference between the chemical shifts of authentic spectral data against chemical shifts determined computationally – should always be comparatively smaller in cases where structure and spectra are matched correctly. [19–22]

Subjecting **1.1** and **1.2** to the predictive method described by Rychnovsky provided unique ^{13}C chemical shifts for both structures.[23] While the distinction between the two data sets was interesting enough by itself, comparing each set with the real spectral data yielded a startling result

(**Figures 1.6** to **1.8**). When the resonances are tabulated in order of decreasing shift, the predicted chemical shifts for **1.1** deviate on average by approximately 5.9 ppm, with four signals deviating by more than 10.0 ppm. Conversely, for **1.2** the predicted chemical shifts deviate on average by only 1.7 ppm, with no single deviation greater than 5.7 ppm. Further motivated by these results, we began our investigation into the synthesis of **1.2**.

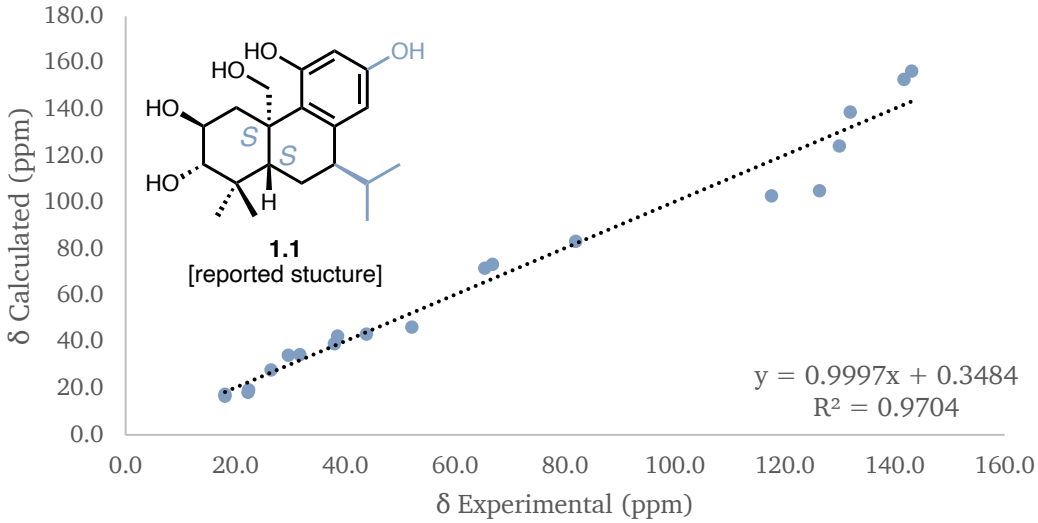


Figure 1.6 *Linear correlation plot for* ***1.1*** *against plebeianiol A*

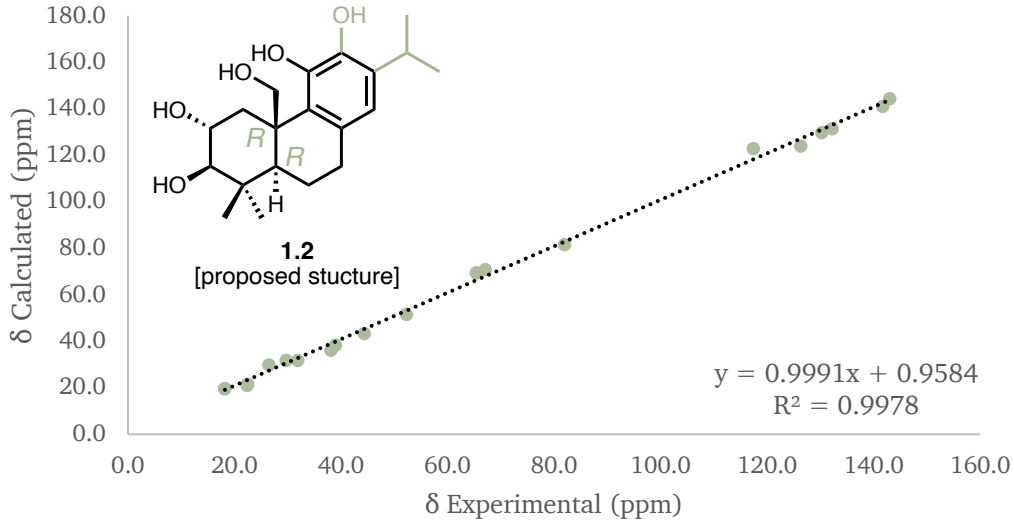


Figure 1.7 *Linear correlation plot for* ***1.2*** *against plebeianiol A*

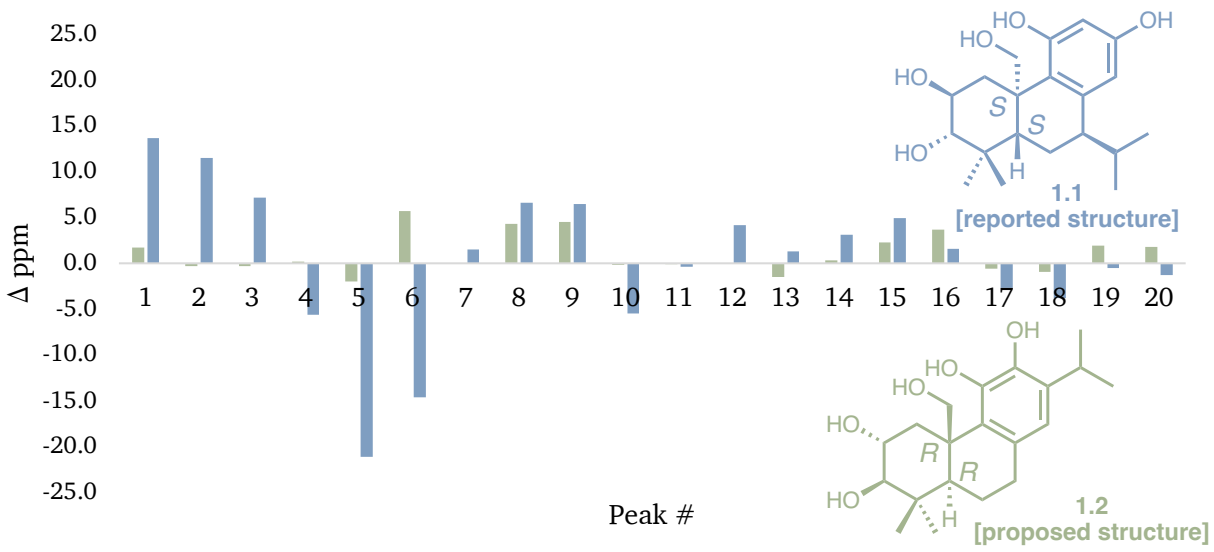


Figure 1.8 *^{13}C shift differences between **1.1** or **1.2** (predicted) with plebeianiol A (experimental)*

1.5 Retrosynthesis of Plebeianiol A

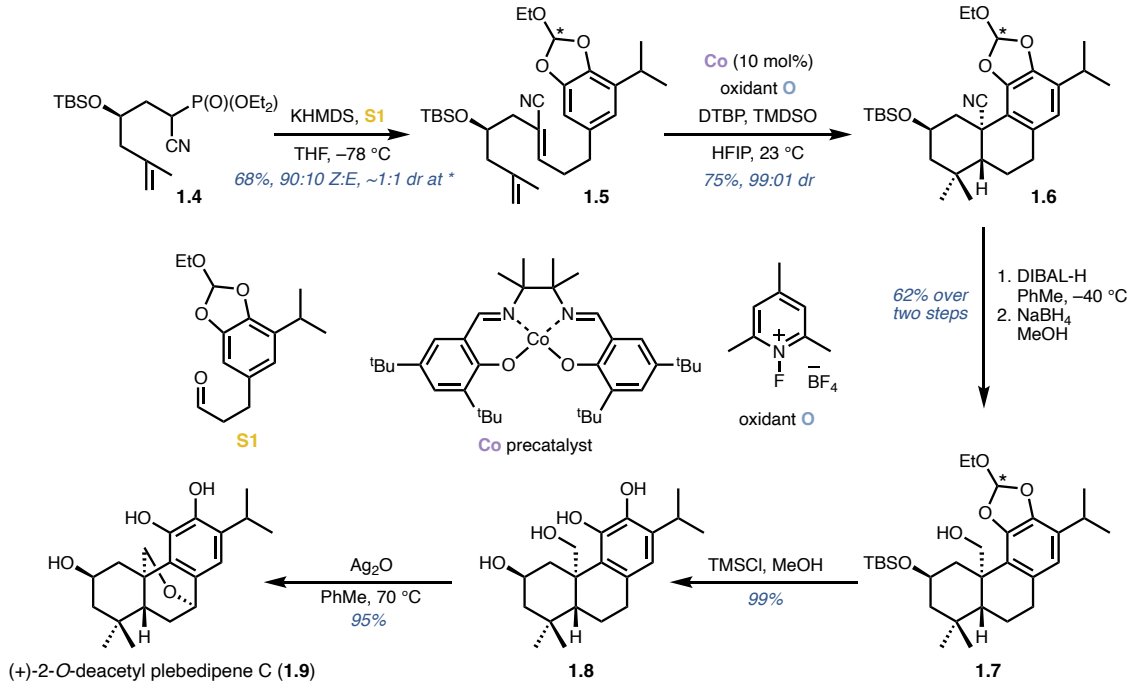
1.5.1 Prior Work in the Vanderwal Lab

Our strategy towards **1.2** was motivated by the recent completion of a closely-related project initiated by former group member, Dr. Darius Vrubliauskas. Initially disclosing the discovery of a cobalt-catalyzed MHAT-initiated radical bicyclization, Darius's subsequent work examined the influence of pendant functionality with respect to the stereoselectivity of this transformation.[24,25] Ultimately, Darius applied this chemistry to efficiently access four aromatic abietane natural products.

One representative synthesis is shown in **Scheme 1.3**, wherein the abietane core is generated in 75% yield as a single diastereomer (**1.6**). The requisite polyene substrates were in each case generated by a convergent Horner–Wadsworth–Emmons (HWE) alkenylation. In this way, the linear precursors could be split into two fragments of similar complexity: alkenyl cyanophosphonate **1.4** and aryl aldehyde **S1**. Subsequent adjustment of the C20 oxidation state (abietane numbering) and global deprotection leads to a tetraol intermediate (**1.8**) that can be

subjected to tandem oxidation/cycloetherification mediated by silver(I) oxide. Slight modifications of the synthetic route used to access (+)-2-*O*-deacetyl plebedipene C (**1.9**) would allow us to disconnect **1.2** in a similar fashion.

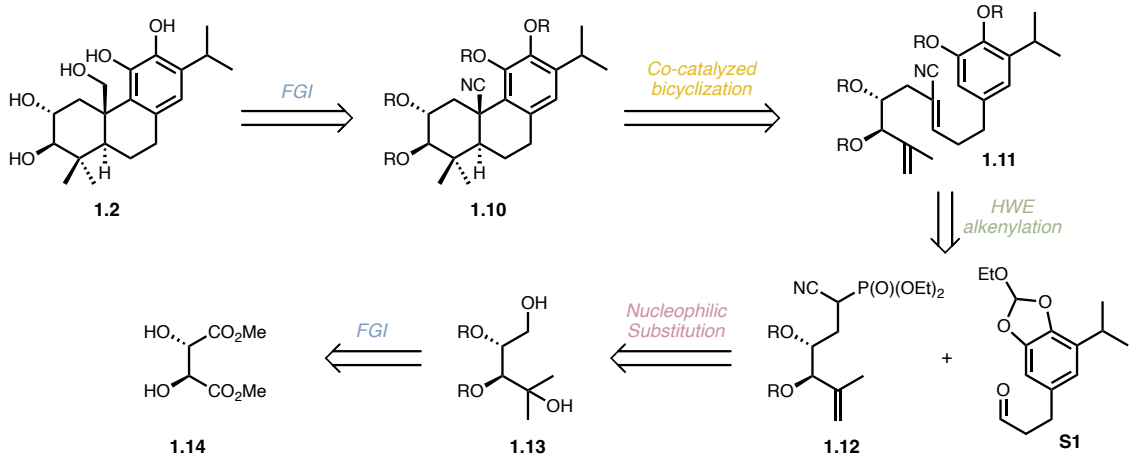
Scheme 1.3 *Synthesis of a related abietane natural product*



1.5.2 Retrosynthesis of Plebeianiol A

Guided by similar logic, a retrosynthesis of **1.2** was readily fashioned (**Scheme 1.4**). Functional group interconversion reduces pentaol target **1.2** to nitrile intermediate (**1.10**), which itself is the immediate product of the cobalt-catalyzed radical bicyclization. The unsaturated nitrile **1.11** may be disconnected by HWE to two fragments. With sufficient amounts of aldehyde **S1** still on hand, the challenge could at this point be reduced to an efficient synthesis of cyanophosphonate **1.12**. In the earliest stages of this work, analysis of the stereodiad present in **1.12** led Darius to propose (–)-dimethyl tartrate (**1.14**) as a starting point.

Scheme 1.4 *Retrosynthetic analysis of* ***1.2***

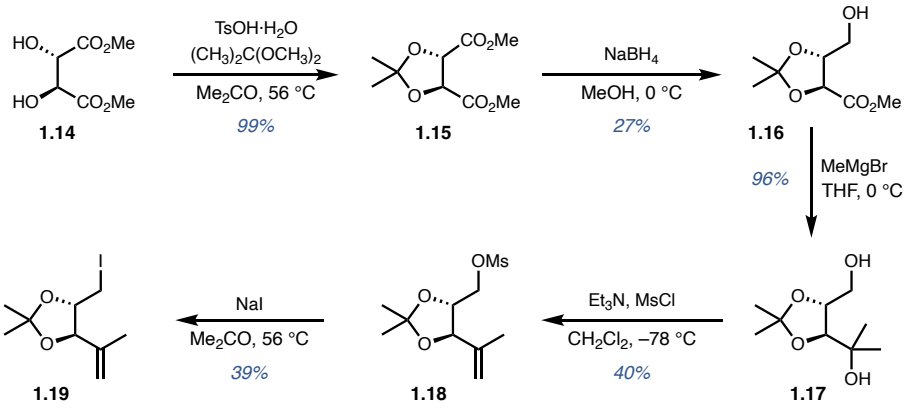


1.6 Synthesis of Plebeianiol A

1.6.1 Attempted Synthesis of the Cyanophosphonate Fragment

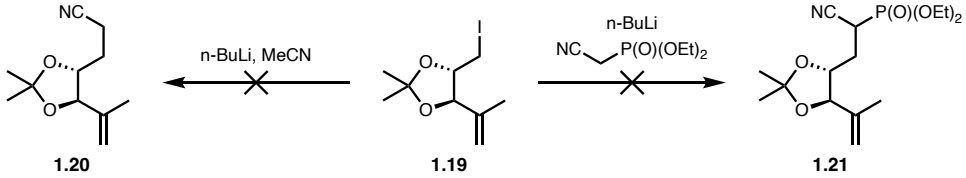
Synthesis of a suitable cyanophosphonate fragment commenced from commercially-available (–)-dimethyl tartrate (**1.14**, **Scheme 1.5**). (–)-Dimethyl tartrate was masked as the acetonide (**1.15**) and subsequently reduced by sodium borohydride to generate primary alcohol **1.16**. Though a relatively low-yielding process, this transformation could be performed on gram scale and, as the starting material and diol byproduct were readily separable, enabled sufficient throughput of the desired carbinol to test downstream chemistry. Sequential 1,2-addition by methylmagnesium bromide formed diol **1.17**. Exposing this material to methanesulfonyl chloride in the presence of triethylamine facilitated a tandem mesylation/elimination process that generated both the 1,1-disubstituted alkene as well as a primary mesylate (**1.18**); a Finkelstein reaction of the mesylate granted access to iodide **1.19**.

Scheme 1.5 *Synthesis of acetonide-protected cyanophosphonate precursor* ***1.19***



Much to our surprise, attempts to displace the iodide of **1.19** with carbon nucleophiles were ultimately futile (**Scheme 1.6**). Because nitrile-stabilized carbanions are strong nucleophiles that eagerly engage electrophiles in alkylation reactions, the failure of these transformations is attributed to an insurmountable kinetic barrier under the reaction conditions required.

Scheme 1.6 *Nucleophilic displacement with iodide* ***1.19*** *proves unsuccessful*



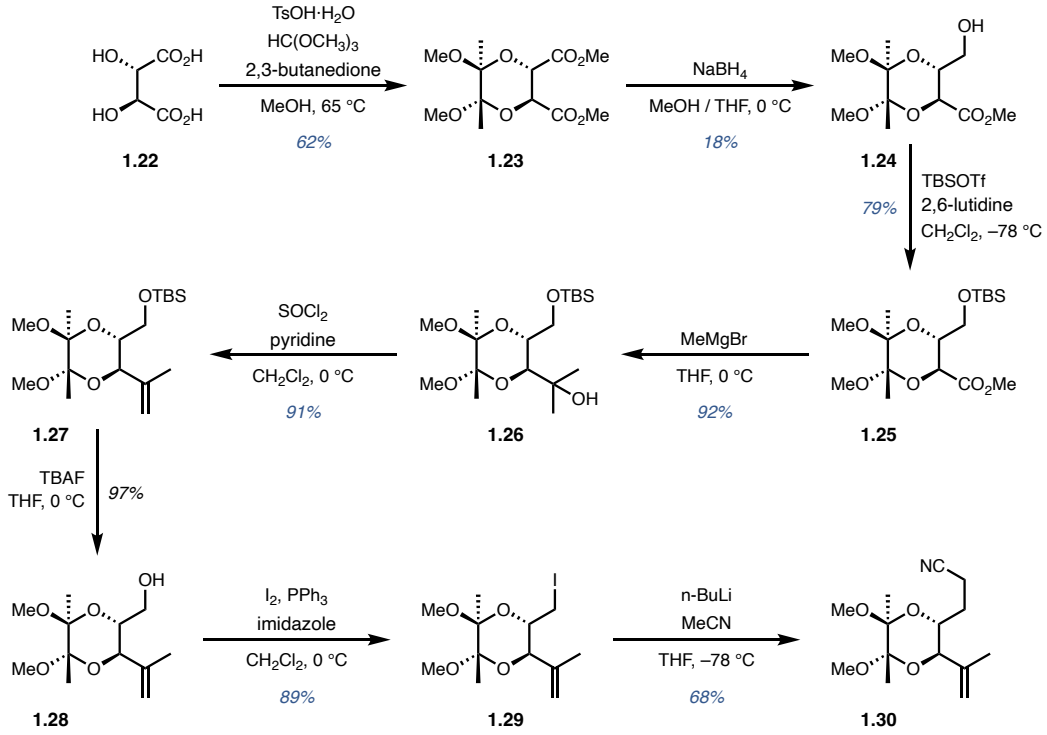
1.6.2 Revised Synthesis of ***1.11***

Forced to regroup, a second strategy was soon devised wherein we opted to exchange the acetonide protecting group for a butanedione diacetal (BDA) protecting group. Driven thermodynamically by favorable anomeric interactions, the dioxane ring generated by this protecting group predictably adopts a chair-like conformation, a detail that we reasoned might have several valuable consequences.[26,27] First, the conformational rigidity of the BDA protecting group might confer an additional layer of stereocontrol during the radical bicyclization key to our proposed synthesis of **1.2**. Second, installation and removal of the BDA protecting group could be

accomplished under roughly the same conditions as the acetonide group, which meant that the rest of synthesis could be left intact. Lastly, we wondered if the greater ring size of the dioxane system might enable a suitable trajectory for nucleophile approach in the hindered alkylation step.

Conversion of (–)-tartaric acid (**1.22**) to *bis*-ester **1.23** was followed by partial reduction to generate carbinol **1.24** (**Scheme 1.7**). Despite the scant yield, separation of **1.24** from the statistical reaction mixture was objectively trivial and granted us sufficient material to move forward. Because of the relatively low yields obtained during the tandem mesylation/elimination sequence used in the synthesis of **1.18**, we were encouraged at this point to perform these steps separately. In this way, we first protected carbinol **1.24** as the corresponding TBS ether **1.25**, which was then treated with two equivalents of methylmagnesium bromide to yield tertiary alcohol **1.26**. Thionyl chloride facilitated elimination of the tertiary alcohol to provide alkene **1.27**. Following deprotection of the TBS group, one-step conversion of **1.28** to alkyl iodide **1.29** was accomplished with a Garegg–Samuelsson reaction. Overall, the sequence converting **1.24** to **1.29** provided a four-fold increase in material throughput when compared with the analogous sequence used to transform **1.16** to **1.19**. Although several attempts to react **1.28** with the appropriate cyanophosphonate nucleophile always returned our starting material unchanged, we soon made a crucial discovery: the iodide could be successfully displaced with lithiated acetonitrile! Through this pivotal transformation we were able to obtain homologated nitrile **1.30** and thus the penultimate intermediate in our synthesis of the cyanophosphonate coupling partner.

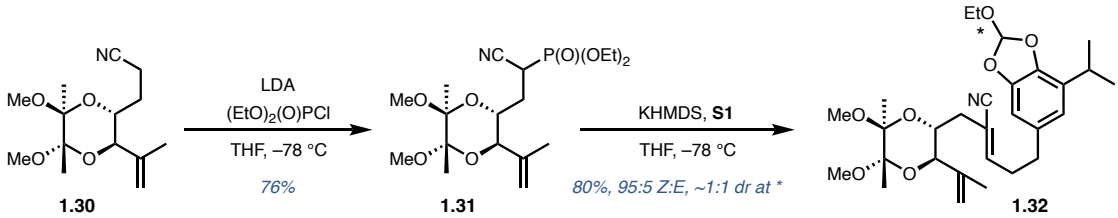
Scheme 1.7 *A change in protecting group permits homologation to nitrile* ***1.30***



1.6.3 Fragment Union and Completion of the Synthesis of ***1.2***

Deprotonation of **1.29** with LDA followed by the addition of diethyl chlorophosphate generated cyanophosphonate **1.31** as an inconsequential mixture of diastereomers (**Scheme 1.8**). At this stage, the convergent coupling between fragments **1.31** and **S1** was achieved via Horner–Wadsworth–Emmons alkenylation.

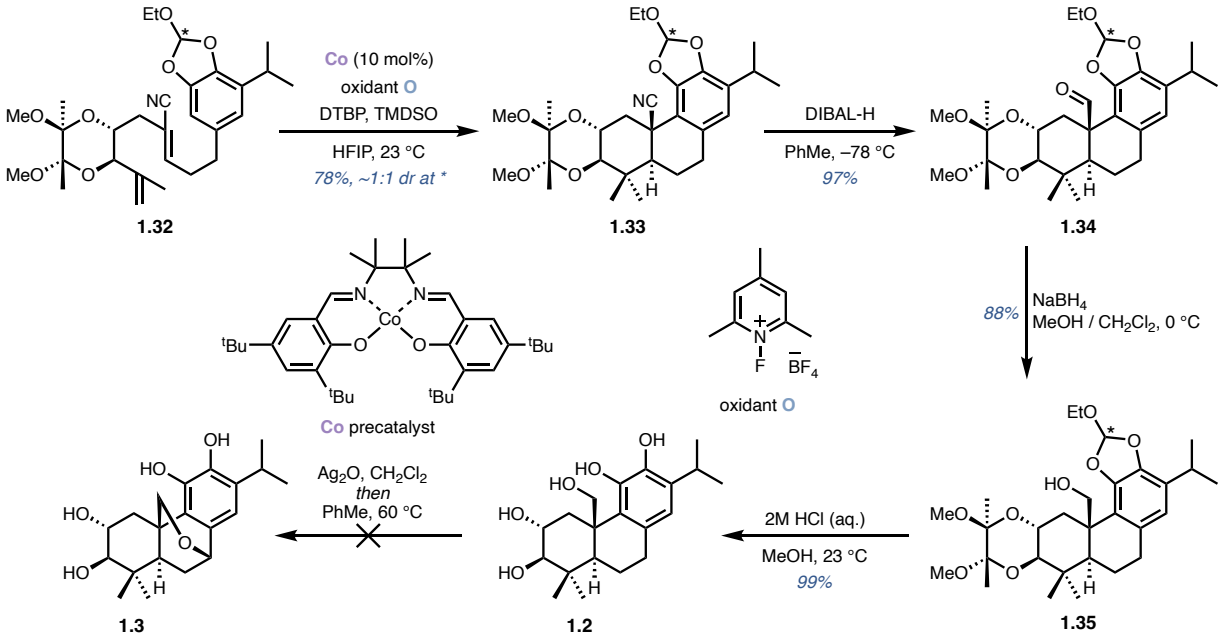
Scheme 1.8 *Synthesis of polycyclization precursor* ***1.32***



Subjecting **1.32** to modified conditions for cobalt-catalyzed radical bicyclization smoothly generated pentacycle **1.33** as a mixture of orthoformate diastereomers (**Scheme 1.9**). The

observed instability of the orthoformate group under the standard reaction conditions necessitated inclusion of 2,6-di-*tert*-butylpyridine (DTBP) as a buffering agent and granted us meaningful levels of material throughput. To obtain the carbinol in **1.2**, a two-step sequence was utilized in which the nitrile was first reduced under the action of DIBAL-H. Hydrolysis of the resulting imine provided neopentylic aldehyde **1.34**, which could be further reduced with sodium borohydride to generate alcohol **1.35**. Exposure of **1.35** to methanolic HCl facilitated global deprotection of the orthoester and BDA protecting groups to generate pentaol **1.2** in near-quantitative yield.

Scheme 1.9 *Completion of the synthesis of* ***1.2***



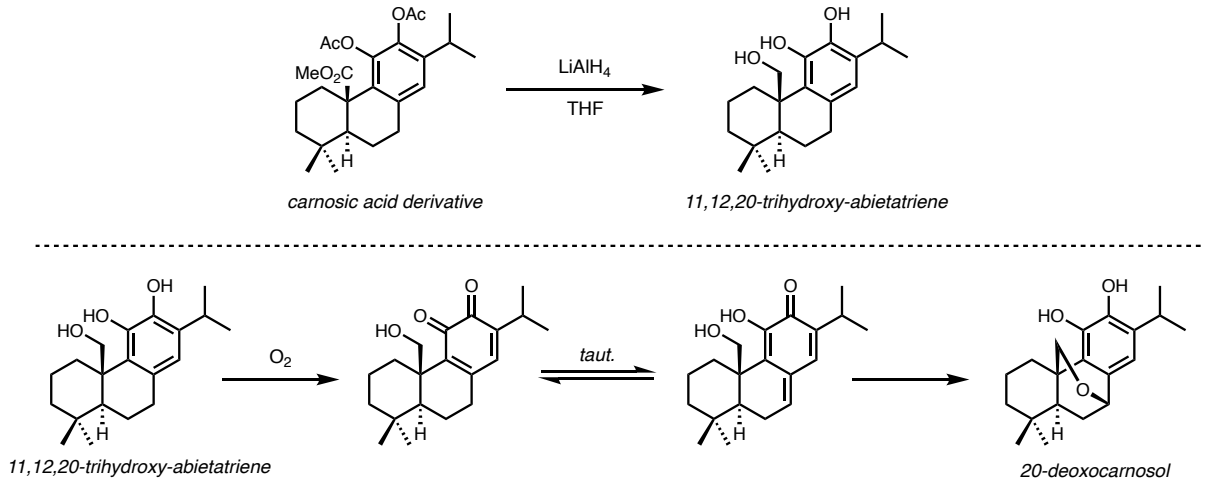
A comparison of the ^{13}C data for **1.2** with those reported in the isolation of plebeianiol A revealed near-congruence between the two data sets, strongly suggesting the correct structure for plebeianiol A is, in fact, **1.2**. This argument was further strengthened by direct comparison of 2D NMR spectra (COSY, HMQC, HMBC) and specific rotation data obtained for **1.2**. With our primary objective secured, we next tasked ourselves with the challenge of converting **1.2** to **1.3**. Given that a similar tandem oxidation/cycloetherification sequence had been performed in the synthesis of

(+)-2-*O*-deacetyl plebedipene C (**Scheme 1.3**), we were surprised when our attempts to apply this chemistry to **1.2** were less successful; only trace amounts of **1.3** were ever detected and so we set about investigating this sequence in greater detail.

*1.6.7 Completion of the Synthesis of **1.3***

Performing this transformation stepwise would reveal valuable information about the intended reaction: though **1.2** could be smoothly converted to the *ortho*-quinone, it appeared that the elevated temperatures required for its tautomerization (and thus the desired ring-closure event) instead led to various modes of decomposition of this intermediate. A search of the literature proved insightful: in their attempts to reduce the C20 acid function of carnosic acid derivatives, González and coworkers frequently observed small amounts of 20-deoxocarnosol.[28,29] The authors ultimately concluded that autoxidation of the desired triol during workup was responsible for formation of this byproduct (**Scheme 1.10**); a similar observation was made nearly twenty years earlier.[30]

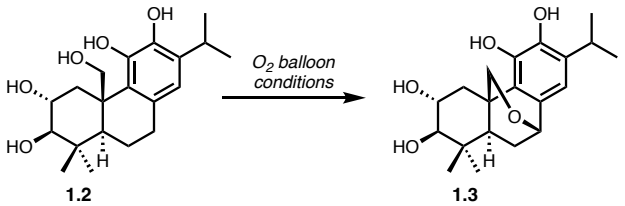
Scheme 1.10 *Work by González studies the autoxidation processes of abietane carbinols*



Subjecting **1.2** to the conditions described by González revealed trace conversion of the starting material to a new compound whose spectral data nicely matched those reported for **1.3**.

With relatively few parameters to study, we opted to examine the reaction solvent mixture and what role (if any) it might play regarding the efficiency of this transformation (**Scheme 1.11**). The results of the screen indicated that the oxidation/cycloetherification sequence is indeed subject to interesting solvent effects: in an aprotic environment (entries 1–3) the conversion of **1.2** to **1.3** is very slow – likely on the order of weeks – but in a protic environment **1.2** is much more rapidly converted to **1.3** (entries 4–6). Heating the reaction mixture proved to have a synergistic effect and permitted a decrease in reaction time from two days to several hours. Isolation of the major product from the reaction mixture allowed its conclusive identification as known abietane **1.3**.

Scheme 1.11 *Observed solvent effects facilitate autoxidation of* ***1.2*** *to* ***1.3***



1.2 **1.3**

entry	solvent	T (°C)	t (h)	conversion (%)
1	EtOAc / hexanes	23	60	tr.
2	CH_2Cl_2 / pentane	23	48	tr.
3	Et_2O / pentane	23	48	tr.
4	EtOH / pentane	23	48	40
5	EtOH	30	2	66
6	EtOH	40	2	99

1.7 Conclusion

The synthesis of **1.2** and **1.3** represent yet another successful application of the cobalt-catalyzed radical bicyclization technology previously developed in the group, here used to fashion the A/B/C ring system of the aromatic abietane scaffold *en route* to **1.2**. Leveraging recent accomplishments in the group's synthesis of other abietane natural products, our strategy prioritized a highly convergent HWE alkenylation and allowed us to disconnect the acyclic precursor to two key fragments. During our earliest efforts to generate cyanophosphonate **1.21**, we observed that the choice of an acetonide protecting group precluded engagement of carbon

nucleophiles with the alkyl iodide substrate. A revised route using the BDA protecting group revealed itself to be more suitable and allowed access to **1.31**.

While the synthetic route to this fragment was less than ideal, it facilitated an expedient synthesis of **1.2** and **1.3**, and confirmed our suspicions about the assigned structure of plebeianiol A. Careful and clever work by a former group member, Dr. Scott Niman, would significantly improve the sequence used to generate **1.31**; the details of this route may be found in our publication.[31]

1.8 References

(1) Wu, Y.-B.; Ni, Z.-Y.; Shi, Q.-W.; Dong, M.; Kiyota, H.; Gu, Y.-C.; Cong, B. *Chem. Rev.* **2012**, *112*, 5967–6026.

(2) González, M. A. *Nat. Prod. Rep.* **2015**, *32*, 684–704.

(3) Dewick, P. M. *Nat. Prod. Rep.* **2002**, *19*, 181–222.

(4) Christianson, D. W. *Chem. Rev.* **2017**, *117*, 11570–11648.

(5) Pronin, S. V.; Shenvi, R. A. *Nature Chem* **2012**, *4*, 915–920.

(6) Peters, R. J. *Nat. Prod. Rep.* **2010**, *27*, 1521.

(7) Gao, W.; Hillwig, M. L.; Huang, L.; Cui, G.; Wang, X.; Kong, J.; Yang, B.; Peters, R. J. *Org. Lett.* **2009**, *11*, 5170–5173.

(8) Zi, J.; Peters, R. J. *Org. Biomol. Chem.* **2013**, *11*, 7650–7652.

(9) Zhang, B.-B.; He, B.-Q.; Sun, J.-B.; Zeng, B.; Shi, X.-J.; Zhou, Y.; Niu, Y.; Nie, S.-Q.; Feng, F.; Liang, Y.; Wu, F.-H. *Molecules* **2015**, *20*, 14879–14888.

(10) Peters, R. J.; Ravn, M. M.; Coates, R. M.; Croteau, R. B. *J. Am. Chem. Soc.* **2001**, *123*, 8974–8978.

(11) Stofer Vogel, B.; Wildung, M. R.; Vogel, G.; Croteau, R. *J. Biol. Chem.* **1996**, *271*, 23262–23268.

(12) Kuźma, Ł. In *Plant Cell and Tissue Differentiation and Secondary Metabolites*; Ramawat, K. G., Ekiert, H. M., Goyal, S., Eds.; Reference Series in Phytochemistry; Springer International Publishing: Cham, 2021; pp 561–584.

(13) Božić, D.; Papaefthimiou, D.; Brückner, K.; Vos, R. C. H. de; Tsoleridis, C. A.; Katsarou, D.; Papanikolaou, A.; Pateraki, I.; Chatzopoulou, F. M.; Dimitriadou, E.; Kostas, S.; Manzano, D.; Scheler, U.; Ferrer, A.; Tissier, A.; Makris, A. M.; Kampranis, S. C.; Kanellis, A. K. *PLOS ONE* **2015**, *10*, e0124106.

(14) Scheler, U.; Brandt, W.; Porzel, A.; Rothe, K.; Manzano, D.; Božić, D.; Papaefthimiou, D.; Balcke, G. U.; Henning, A.; Lohse, S.; Marillonnet, S.; Kanellis, A. K.; Ferrer, A.; Tissier, A. *Nat. Commun.* **2016**, *7*, 12942.

(15) Ortiz de Montellano, P. R. *Chem. Rev.* **2010**, *110*, 932–948.

(16) Ignea, C.; Athanasakoglou, A.; Ioannou, E.; Georgantea, P.; Trikka, F. A.; Loupassaki, S.; Roussis, V.; Makris, A. M.; Kampranis, S. C. *PNAS*, **2016**, *113*, 3681–8686.

(17) Bendall, J.; Cambie, R. *Aust. J. Chem.* **1995**, *48*, 883.

(18) Xiong, Y.; Qu, W.; Sun, J.; Wang, M.; Liang, J. *Phytochem. Lett.* **2013**, *6*, 457–460.

(19) Forsyth, D. A.; Sebag, A. B. *J. Am. Chem. Soc.* **1997**, *119*, 9483–9494.

(20) Duan, Z.-K.; Lv, T.-M.; Song, G.-S.; Wang, Y.-X.; Lin, B.; Huang, X.-X. *Nat. Prod. Res.* **2020**, 1–8.

(21) Meiler, J.; Sanli, E.; Junker, J.; Meusinger, R.; Lindel, T.; Will, M.; Maier, W.; Köck, M. *J. Chem. Inf. Comput. Sci.* **2002**, *42*, 241–248.

(22) Bagno, A. *Chem. Eur. J.* **2001**, *7*, 1652–1661.

(23) Rychnovsky, S. D. *Org. Lett.* **2006**, *8*, 2895–2898.

(24) Vrubliauskas, D.; Vanderwal, C. D. *Angew. Chem. Int. Ed.* **2020**, *59*, 6115–6121.

(25) Vrubliauskas, D.; Gross, B. M.; Vanderwal, C. D. *J. Am. Chem. Soc.* **2021**, *143*, 2944–2952.

(26) Lence, E.; Castedo, L.; González-Bello, C. *Chem. Soc. Rev.* **2008**, *37*, 1689.

(27) Ley, S. V.; Polara, A. *J. Org. Chem.* **2007**, *72*, 5943–5959.

(28) González, A. G.; Andrés, L. S.; Luis, J. G.; Brito, I.; Rodríguez, M. L. *Phytochemistry* **1991**, *30*, 4067–4070.

(29) Antonio G. Gonzalez; Carmen M. Rodriguez; Javier G. Luis. *J. Chem. Res. (S)* **1988**, 114–115.

(30) Wenkert, E.; Fuchs, A.; McChesney, J. D. *J. Org. Chem.* **1965**, *30*, 2931–2934.

(31) Johnson, L. K.; Niman, S. W.; Vrubliauskas, D.; Vanderwal, C. D. *Org. Lett.* **2021**, *23*, 9569–9573.

1.9 Experimental Information

1.9.1 Materials and Methods

All reactions were performed in oven-dried (120 °C) or flame-dried glassware under an atmosphere of dry argon unless otherwise noted. Reaction solvents including dichloromethane (CH_2Cl_2, Fisher, HPLC Grade), hexanes (Fisher, HPLC Grade), diethyl ether (Et_2O, Fisher, BHT stabilized, HPLC Grade), benzene (PhH, Fisher, HPLC Grade), tetrahydrofuran (THF, Fisher, HPLC Grade), and toluene (PhMe, Fisher, HPLC Grade) were dried by percolation through a column packed with neutral alumina and a column packed with Q5 reactant, a supported copper catalyst for scavenging oxygen, under a positive pressure of argon. Hexafluoroisopropanol ($(CF_3)_2CHOH$, Oakwood) was degassed prior to use by sparging with argon for 15 minutes. Solvents for workup and chromatography were hexanes (Fisher or EMD, ACS Grade), ethyl acetate (EtOAc, Fisher, ACS Grade), dichloromethane (CH_2Cl_2, Fisher, ACS Grade), and diethyl ether (Et_2O, Fisher, ACS Grade).

Column chromatography was performed using EMD Millipore 60 Å (0.040-0.063 mm) mesh silica gel (SiO_2). Analytical and preparative thin-layer chromatography was performed on Merck silica gel 60 F254 TLC plates. Visualization was accomplished with UV (254 or 210 nm), and *p*-anisaldehyde, vanillin, potassium permanganate ($KMnO_4$), 2,4-dinitrophenylhydrazine (2,4-DNP), or ceric ammonium molybdate (CAM) and heat as developing agents. Chloroform-*d* ($CDCl_3$, 99.8% D, DLM-7) and C_6D_6 (99.5% D, DLM-1-100, dried over activated alumina [5 wt%]) were purchased from Cambridge Isotope Laboratories. K_2CO_3 (anhydrous, 99%, Alfa Aesar), $NaHCO_3$ (ACS grade, Fisher), NaOH (ACS grade, Macron or Fisher), 1-fluoro-2,4,6-trimethylpyridinium tetrafluoroborate (TCI or Sigma Aldrich, 95-99%), and 1,1,3,3-tetramethyldisiloxane (TMDSO, 97%, Acros Organics) were purchased commercially and used without further purification.

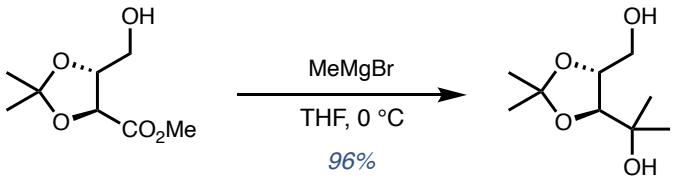
Triethylamine (EMD, CaH_2) and pyridine (Alfa Aesar, CaH_2) were distilled from the indicated drying agents prior to use.

Proton and carbon magnetic resonance spectra (^{1}H NMR and ^{13}C NMR) were recorded at 298 K on a Bruker CRYO500 (500 MHz, ^{1}H; 125 MHz, ^{13}C) or a Bruker AVANCE600 (600 MHz, ^{1}H; 151 MHz, ^{13}C) spectrometer with solvent residual as the internal standard for ^{1}H NMR: $CHCl_3$ at 7.26 ppm, and C_6HD_5 at 7.16 ppm and solvent as internal standard for ^{13}C NMR: $CDCl_3$ at 77.16 ppm and C_6D_6 at 128.06 ppm. ^{1}H NMR data are reported as follows: chemical shift, multiplicity (s = singlet, d = doublet, t = triplet, q = quartet, h = heptet, dd = doublet of doublets, ddd = doublet of doublet of doublets, td = triplet of doublets, tdd = triplet of doublet of doublets, qd = quartet of doublets, m = multiplet, br = broad signal), coupling constants (Hz), and integration. The raw fid files were processed into the included NMR spectra using MestReNova 14.3 (Mestrelab Research S.L.).

High resolution mass spectra (HRMS) were recorded either on a Waters LCT Premier S2 spectrometer using ESI-TOF (electrospray ionization-time of flight) or a Waters GCT Premier spectrometer using CI-TOF (chemical ionization-time of flight) and data are reported in the form of (m/z).

*Please note that the syntheses of **1.19** and **1.31** presented below were ultimately not used in the final route to **1.2** and **1.3**; in some cases characterization is limited.*

1.9.2 Experimental Procedures

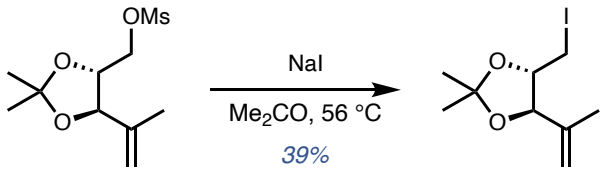


1.16 **1.17**

Methyl ester **1.16**[1] (100 mg, 0.53 mmol, 1 equiv.) was dissolved in dry THF (6.6 mL) and cooled to 0 °C. Methylmagnesium bromide (3.0 M, 701 µL, 2.10 mmol, 4 equiv.) was added by syringe and the reaction mixture was stirred while warming to 23 °C over 30 minutes. The reaction was quenched with saturated aqueous NH_4Cl (3 mL) to form a biphasic mixture. The layers were separated, and the aqueous layer was further extracted with EtOAc (3 x 3 mL). The combined organic extracts were dried over Na_2SO_4 and concentrated under reduced pressure. The crude residue was purified by flash column chromatography (SiO_2, 0–60% EtOAc in hexanes) to afford **1.17** (96 mg, 96%).

^{1}H NMR (500 MHz, $CDCl_3$) δ 4.09 (dt, J = 8.2, 4.1 Hz, 1H), 3.82 (dd, J = 11.9, 4.1 Hz, 1H), 3.75 (d, J = 8.2 Hz, 1H), 3.68 (dd, J = 11.8, 4.1 Hz, 1H), 1.44 (s, 3H), 1.42 (s, 3H), 1.28 (s, 3H), 1.21 (s, 3H).

TLC: R_f = 0.30 (100% Et_2O, visualized by $KMnO_4$)



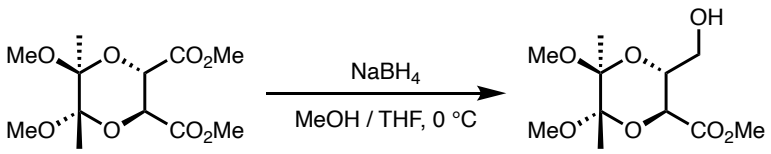
1.18 **1.19**

Mesylate **1.18**[2] (430 mg, 1.72 mmol, 1 equiv.) and NaI (515 mg, 3.44 mmol, 2 equiv.) were dissolved in acetone (4.3 mL). The reaction mixture was placed to stir in a pre-heated oil bath at 65 °C for 48 hours. After cooling to 23 °C, the stir bar was removed and reaction mixture was concentrated under reduced pressure. The crude residue was resuspended in Et_2O (5 mL) and diluted with H_2O (5 mL) to form a biphasic mixture. The layers were separated, and the organic phase was washed with saturated aqueous $Na_2S_2O_3$ (3 mL), H_2O (3 mL), brine (3 mL), dried over Na_2SO_4, and concentrated under reduced pressure. Purification by flash column chromatography (SiO_2, 0–10% Et_2O in hexanes) afforded **1.19** (190 mg, 39%) as a clear oil.

^{1}H NMR (500 MHz, $CDCl_3$) δ 5.11 – 5.08 (m, 1H), 5.02 – 4.98 (m, 1H), 4.17 (d, J = 8.0 Hz, 1H), 3.65 (ddd, J = 8.0, 5.4, 3.9 Hz, 1H), 3.36 (dd, J = 10.9, 3.9 Hz, 1H), 3.21 (dd, J = 10.9, 5.4 Hz, 1H), 1.77 (d, J = 1.3 Hz, 3H), 1.50 – 1.47 (m, 3H), 1.44 (s, 3H).

^{13}C NMR (151 MHz, $CDCl_3$) δ 141.1, 115.2, 109.5, 85.1, 77.5, 27.5, 27.3, 17.5, 5.7.

TLC: R_f = 0.44 (10% Et_2O in hexanes, visualized by CAM)



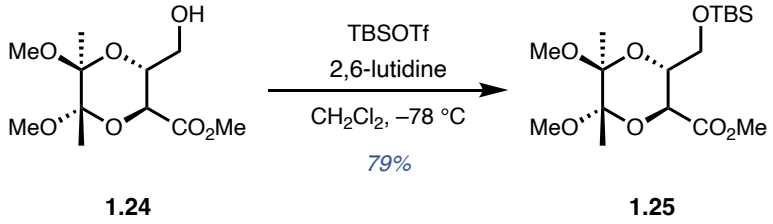
1.23 **1.24**

Based on a previously reported procedure.[1] Butanedione diacetal **1.23**[3] (20.0 g, 68.5 mmol, 1 equiv.) was dissolved in MeOH : THF (1:1, 137 mL) and cooled to 0 °C. $NaBH_4$ (1.30 g, 34.2 mmol, 0.4 equiv.) was added in four portions over 1 hour, then the resulting mixture was stirred for 1 hour. The reaction was quenched with the addition of H_2O (40 mL) and concentrated under

reduced pressure. The opaque residue was redissolved in EtOAc (175 mL) then transferred to a separatory funnel and washed with brine (2 x 40 mL). The combined aqueous washes were back-extracted with EtOAc (3 x 60 mL). The combined organic layers were washed with brine (2 x 30 mL), dried over Na_2SO_4, and concentrated under reduced pressure. The crude residue was purified by flash column chromatography (SiO_2, 50% CH_2Cl_2 in hexanes *then* 50% EtOAc in hexanes to afford **1.24** (3.2 g, 18%).

^{1}H NMR (500 MHz, $CDCl_3$) δ 4.40 (d, J = 10.1 Hz, 1H), 3.95 (ddd, J = 10.0, 4.9, 3.6 Hz, 1H), 3.80 – 3.70 (m, 5H), 3.30 (s, 3H), 3.28 (s, 3H), 2.12 (t, J = 6.7 Hz, 1H), 1.37 (s, 3H), 1.31 (s, 3H).

TLC: R_f = 0.20 (9:1 hexanes:EtOAc, visualized by CAM)

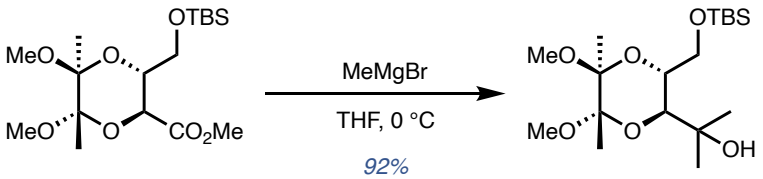


1.24 **1.25**

Carbinol **1.24** (816 mg, 3.09 mmol, 1 equiv.) and 2,6-lutidine (565 µL, 7.72 mmol, 2.5 equiv.) were dissolved in dry CH_2Cl_2 (3 mL) and cooled to –78 °C. TBSOTf (852 µL, 3.71 mmol, 1.2 equiv.) was added dropwise and the reaction mixture was stirred for 2 hours. The reaction was quenched with MeOH (50 µL) and diluted with additional CH_2Cl_2 (15 mL). The opaque solution was transferred to a separatory funnel and washed with aqueous HCl (2 M, 2 x 10 mL), brine, (10 mL), dried over Na_2SO_4, and concentrated under reduced pressure to afford **1.25** (930 mg, ~79%).

^{1}H NMR (500 MHz, $CDCl_3$) δ 4.25 (d, J = 10.0 Hz, 1H), 3.96 (dt, J = 10.1, 5.1 Hz, 1H), 3.75 (s, 3H), 3.71 (dd, J = 6.6, 5.1 Hz, 2H), 3.28 (app s, 6H), 1.34 (s, 3H), 1.28 (s, 3H), 0.88 (s, 9H).

TLC: R_f = 0.72 (50% EtOAc in hexanes, visualized by CAM)

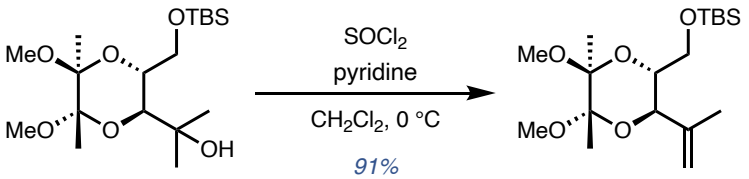


1.25 **1.26**

Methyl ester **1.25** (805 mg, 2.13 mmol, 1 equiv.) was dissolved in dry THF (27 mL) and cooled to 0 °C. Methylmagnesium bromide (2.7 M, 2.13 mL, 5.75 mmol, 2.7 equiv.) was added by syringe and the reaction mixture was stirred while warming to 23 °C for 1 hour. The reaction was quenched with saturated aqueous NH_4Cl (5 mL). Most of the solvent was removed under reduced pressure and the remaining volume was then diluted with Et_2O (10 mL) and H_2O (10 mL). The layers were separated, and then the aqueous phase was further extracted with Et_2O (4 x 10 mL). The combined organic extracts were washed with brine (40 mL) and concentrated under reduced pressure to afford **1.26** (743 mg, ~92%).

^{1}H NMR (500 MHz, $CDCl_3$) δ 4.63 (s, 1H), 3.85 (dd, J = 10.7, 8.5 Hz, 1H), 3.79 – 3.72 (m, 1H), 3.68 (dd, J = 10.7, 2.7 Hz, 1H), 3.45 (d, J = 9.5 Hz, 1H), 3.24 (app s, 6H), 1.28 (s, 3H), 1.26 – 1.24 (m, 9H), 0.91 (s, 9H), 0.12 (s, 6H).

TLC: R_f = 0.51 (50% Et_2O in hexanes, visualized by CAM)

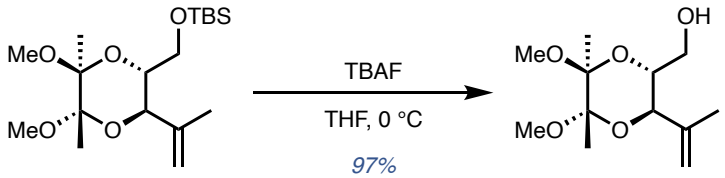


1.26 **1.27**

$SOCl_2$ (1.6 mL, 22 mmol, 2 equiv.) was added dropwise by syringe to a solution of carbinol **1.26** (4.2 g, 11 mmol, 1 equiv.) and pyridine (3.6 mL, 44 mmol, 4 equiv.) in dry CH_2Cl_2 (222 mL) at 0 °C. The resulting mixture was stirred for 2 hours at 0 °C. The reaction was quenched slowly with saturated aqueous $NaHCO_3$ (10 mL) and the biphasic solution that formed was then transferred to a separatory funnel. The phases were separated, and the organic extract was carefully washed with saturated aqueous $NaHCO_3$ (80 mL), aqueous HCl (2 M, 3 x 80 mL), brine (80 mL), dried over Na_2SO_4, and concentrated under reduced pressure to afford **1.27** (3.65 g, ~91%).

^{1}H NMR (500 MHz, $CDCl_3$) δ 5.01 (s, 1H), 4.95 (s, 1H), 4.01 (d, J = 10.0 Hz, 1H), 3.76 (dt, J = 9.6, 4.5 Hz, 1H), 3.58 (d, J = 4.7 Hz, 2H), 3.27 (s, 3H), 3.23 (s, 3H), 1.81 (s, 3H), 1.28 (overlapping s, 3H), 1.27 (overlapping s, 3H), 0.88 (s, 9H), 0.05 (overlapping s, 3H), 0.04 (overlapping s, 3H).

TLC: R_f = 0.56 (15% EtOAc in hexanes, visualized by $KMnO_4$)



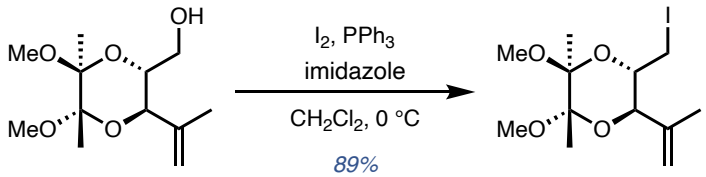
1.27 **1.28**

Silyl ether **1.27** (3.65 g, 10.1 mmol, 1 equiv.) was dissolved in dry THF (20.3 mL) and cooled to 0 °C. TBAF (1.0 M in THF, 12.2 mL, 12.2 mmol, 1.2 equiv.) was added dropwise by syringe and the resulting reaction mixture was stirred for 12 hours. The stir bar was removed and the reaction mixture was concentrated under reduced pressure. The crude residue obtained was purified by flash column chromatography (SiO_2, 30% EtOAc in hexanes) to afford **1.28** (2.41 g, 97%).

^{1}H NMR (500 MHz, $CDCl_3$) δ 5.03 (s, 1H), 5.01 – 4.97 (m, 1H), 4.08 (d, J = 10.0 Hz, 1H), 3.83 (ddd, J = 10.0, 6.4, 3.6 Hz, 1H), 3.60 – 3.52 (m, 2H), 3.28 (s, 3H), 3.25 (s, 3H), 1.80 (s, 3H), 1.32 (s, 3H), 1.29 (s, 3H).

^{13}C NMR (151 MHz, $CDCl_3$) δ 141.9, 116.2, 99.0, 98.9, 73.5, 69.8, 62.3, 48.1 (2C), 18.3, 17.8, 17.8.

TLC: R_f = 0.24 (30% EtOAc in hexanes, visualized by $KMnO_4$)



1.28 **1.29**

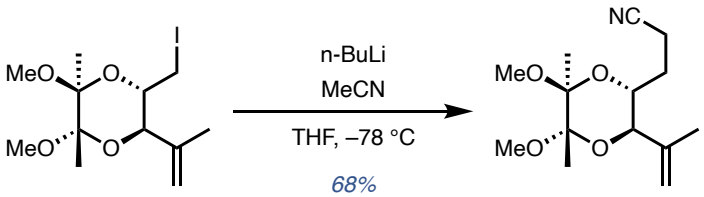
PPh_3 (2.19 g, 8.36 mmol, 1.1 equiv.) and imidazole (1.14 g, 16.7 mmol, 2.2 equiv.) were suspended in dry CH_2Cl_2 (19 mL) and stirred at 23 °C until a homogenous solution had formed. The solution was cooled to 0 °C and iodine (1.93 g, 8.36 mmol, 1.1 equiv.) was quickly added. The mixture was stirred for 20 minutes, then **1.28** (1.87 g, 7.60 mmol, 1 equiv.) was added

dropwise as a solution in dry CH_2Cl_2 (4 mL). After stirring overnight, the reaction was quenched with H_2O (15 ml) and diluted with CH_2Cl_2 (10 mL). The layers were separated and aqueous layer was further extracted with CH_2Cl_2 (3 x 15 mL). The combined organic extracts were washed with brine (2 x 15 mL), dried over Na_2SO_4, and concentrated under reduced pressure. The crude residue was purified by flash column chromatography (SiO_2, 4% EtOAc in hexanes) to afford **1.29** (2.40 g, ~89%).

^{1}H NMR (500 MHz, $CDCl_3$) δ 5.06 – 5.04 (m, 1H), 5.03 – 4.99 (m, 1H), 3.94 (d, J = 9.6 Hz, 1H), 3.78 (td, J = 9.7, 2.3 Hz, 1H), 3.35 (s, 3H), 3.25 (s, 3H), 3.18 (dd, J = 10.7, 2.4 Hz, 1H), 3.02 (dd, J = 10.7, 9.7 Hz, 1H), 1.79 (s, 3H), 1.34 (s, 3H), 1.29 (s, 3H).

HRMS (ES+) *m/z* calc'd for $C_{12}H_{21}IO_4$ $[M–I]^+$: 229.1440, found 229.1448.

TLC: R_f = 0.65 (30% EtOAc, in hexanes, visualized by $KMnO_4$)



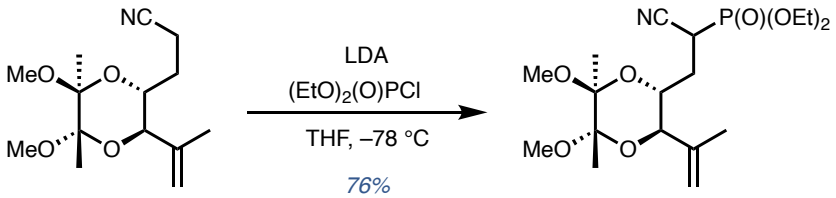
1.29 **1.30**

A solution of dry MeCN (196 µL, 3.77 mmol, 2.5 equiv.) and dry THF (7.5 mL) was cooled to –78 °C. *n*-butyllithium (2.8M in hexanes, 1.35 mL, 3.77 mmol, 2.5 equiv.) was added by syringe to form a bright pink solution. **1.29** (537 mg, 1.51 mmol, 1 equiv.) was added as a solution in dry THF (1.5 mL). The reaction mixture was stirred while warming to 0 °C and monitored for completion by TLC. When TLC analysis indicated full consumption of **1.29**, the reaction was

quenched with saturated aqueous NH_4Cl (20 mL) and diluted with Et_2O (20 mL) to form a biphasic solution. The layers were separated and the aqueous layer was further extracted with Et_2O (2 x 20 mL). The combined organic extracts were washed with brine (40 mL), dried over Na_2SO_4, and concentrated under reduced pressure. The crude residue was purified by flash column chromatography (SiO_2, 20% EtOAc in hexanes) to afford **1.30** (276 mg, ~68%).

^{1}H NMR (500 MHz, $CDCl_3$) δ 5.03 – 4.98 (m, 2H), 3.92 (d, J = 9.5 Hz, 1H), 3.86 (td, J = 10.0, 2.8 Hz, 1H), 3.30 (s, 3H), 3.26 (s, 3H), 2.60 – 2.45 (m, 2H), 1.80 (s, 3H), 1.77 – 1.71 (m, 1H), 1.70 – 1.62 (m, 1H), 1.31 (s, 3H), 1.29 (s, 3H).

TLC: R_f = 0.44 (30% EtOAc in hexanes, visualized by CAM)



1.30 **1.31**

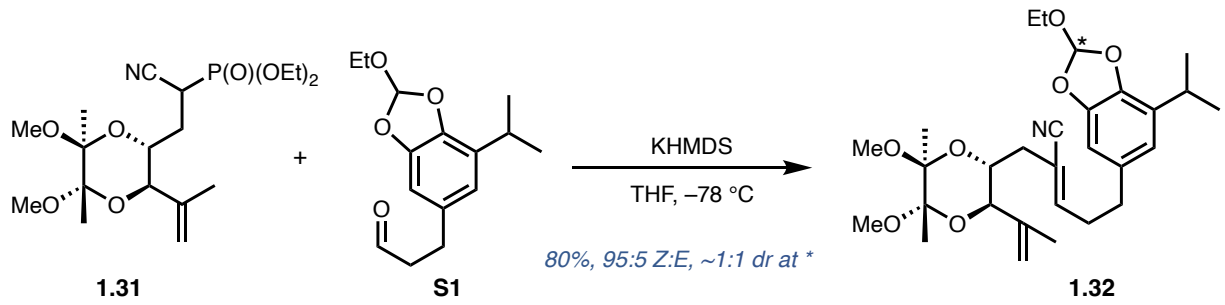
n-Butyllithium (2.8 M in hexanes, 2.37 mL, 6.65 mmol, 2.1 equiv.) was added to a solution of diisopropylamine (979 µL, 6.96 mmol, 2.2 equiv.) in dry THF (14 mL) at –78 °C. The resulting solution was warmed to 0 °C and stirred for 30 minutes, then once more cooled down to –78 °C. **1.30** (852 mg, 3.17 mmol, 1 equiv.) was added dropwise as solution in THF (3 mL). After stirring for 30 minutes, diethylchlorophosphonate (505 µL, 3.48 mmol, 1.1 equiv.) was added dropwise and the reaction mixture was stirred for 2 hours. The reaction was quenched with NH_4Cl : H_2O (20

mL) to form a biphasic mixture. The layers were separated, and the aqueous layer was further extracted with EtOAc (3 x 20 mL). The combined organic extracts were washed with brine (20 mL), dried over Na_2SO_4, and concentrated under reduced pressure. The crude residue was purified by flash column chromatography (SiO_2, 40–50% EtOAc in hexanes) to afford **1.31** (971 mg, 76%) as a 90:10 mixture of diastereomers.

Note: ^{1}H signals are reported for the major diastereomer

^{1}H NMR (500 MHz, $CDCl_3$) δ 5.02 (s, 1H), 5.01 (s, 1H), 4.29 – 4.19 (m, 4H), 4.05 – 3.99 (m, 1H), 3.92 (d, J = 9.7 Hz, 1H), 3.44 – 3.35 (m, 1H), 3.33 (s, 3H), 3.25 (s, 3H), 1.87 (m, 2H), 1.81 (s, 3H), 1.38 (t, J = 7.0 Hz, 6H), 1.30 (overlapping s, 3H), 1.29 (overlapping s, 3H).

TLC: R_f = 0.25 (60% EtOAc in hexanes, visualized by CAM)



A solution of cyanophosphonate **1.31** (509 mg, 1.26 mmol, 1.0 equiv.) in dry PhMe (14.0 mL) was cooled to –78 °C. KHMDS (0.5 M in PhMe, 2.5 mL, 1.26 mmol, 1.0 equiv.), was added dropwise by syringe over 5 minutes. The resulting orange solution was placed in an ice bath to stir at 0 °C for 5 minutes and then cooled once more to –78 °C. A solution of **S1**[4] in dry PhMe (3.0 mL) was added dropwise by syringe and the reaction mixture stirred for 3 hours. The reaction was quenched with the addition of saturated aqueous ammonium chloride (15.0 mL) and then diluted with

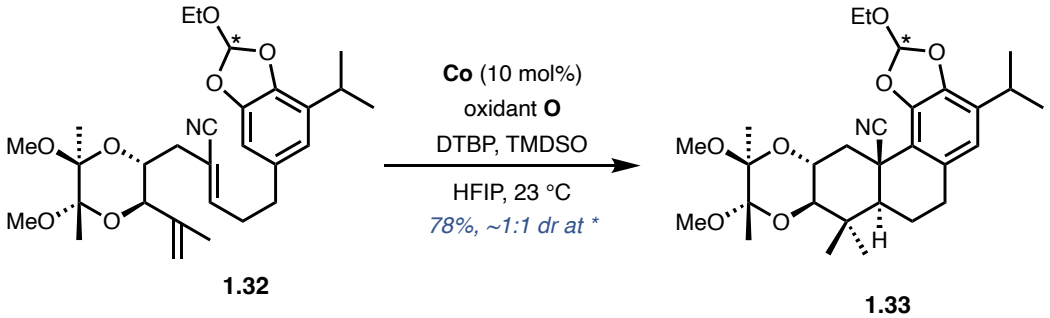
deionized water (5.0 mL). The biphasic solution was transferred to a separatory funnel and the layers were separated. The aqueous layer was extracted with Et_2O (3 x 15.0 mL). The combined organic extracts were washed with brine (15.0 mL), dried over sodium sulfate, filtered, and concentrated under reduced pressure. The crude residue was purified by flash column chromatography (SiO_2, 6% EtOAc in hexanes), providing diene **1.32** (518 mg, 1.01 mmol, 80%, >91:09 *Z*:*E*, ~95% purity) as a faint yellow oil.

^{1}H NMR (500 MHz, $CDCl_3$) δ 6.81 (s, 1H), 6.53 (app d, J = 9.1 Hz, 2H), 6.27 – 6.20 (m, 1H), 4.97 (app d, J = 6.5, 2H), 3.96 – 3.86 (m, 2H), 3.67 (q, J = 7.1 Hz, 2H), 3.29 – 3.14 (m, 6H), 2.99 (h, J = 7.0 Hz, 1H), 2.72 – 2.54 (m, 4H), 2.23 (d, J = 14.3 Hz, 1H), 2.16 (dd, J = 14.4, 8.7 Hz, 1H), 1.78 (bs, 3H), 1.32 – 1.15 (m, 15H).

^{13}C NMR (151 MHz, $CDCl_3$) δ 149.3, 149.3, 145.8, 145.8, 141.8, 141.6, 133.7, 133.7, 129.4, 119.3, 118.6, 117.3, 116.6, 111.3, 105.9, 105.8, 98.9, 98.9, 77.4, 76.3, 67.0, 58.9, 48.0, 48.0, 47.9, 35.8, 34.7, 34.7, 33.4, 33.3, 29.2, 22.2, 22.1, 17.9, 17.6, 17.6, 14.9.

HRMS (ESI) *m/z* calc'd for $C_{29}H_{41}NO_7$ $[M+Na]^+$: 538.2781, found 538.2773.

TLC: R_f = 0.20 (9:1 hexanes:EtOAc, visualized by CAM)



1.32 **1.33**

Diene **1.32** (208 mg, 0.40 mmol, 1.0 equiv.), cobalt(II) precatalyst (24.5 mg, 0.04 mmol, 0.1 equiv.), 1-fluoro-2,4,6-trimethylpyridinium tetrafluoroborate (275 mg, 1.21 mmol, 3.0 equiv.), and 2,6-di-*tert*-butylpyridine (0.2 mL, 0.81 mmol, 2.0 equiv.) were placed in a vial open to air and dissolved in HFIP (9.0 mL). The vial was capped with a rubber septum and sealed with parafilm. The septum was vented with a syringe needle and the solution was sparged under positive pressure with an Ar balloon for 15 minutes. The vent was removed from the septum to leave the solution under Ar and TMDSO (0.2 mL, 1.21 mmol, 3.0 equiv.) was added dropwise by syringe over 5 minutes. The reaction mixture was allowed to stir for 4 hours. The mixture was concentrated under reduced pressure. The crude residue was purified by flash column chromatography (SiO_2, 4% EtOAc in hexanes), providing nitrile **1.33** (163 mg, 0.32 mmol, 78%) as a white foam. It was isolated as a mixture of diastereomers at the orthoester stereogenic center. These isomers could be separated (SiO_2, 2–4% EtOAc in hexanes) but assignment of absolute configuration could not be made.

More polar diastereomer **1.33a** (relative configuration unassigned):

^{1}H NMR (600 MHz, $CDCl_3$) δ 6.91 (s, 1H), 6.51 (s, 1H), 4.15 (ddd, J = 12.2, 10.1, 4.1 Hz, 1H), 3.68 (dq, J = 9.4, 7.2 Hz, 1H), 3.58 (dq, J = 9.4, 7.1 Hz, 1H), 3.41 (dd, J = 13.0, 4.1 Hz, 1H), 3.35 (s, 3H), 3.26 – 3.22 (m, 4H), 3.00 (h, J = 7.0 Hz, 1H), 2.93 (dd, J = 16.6, 4.3 Hz, 1H), 2.80 (ddd, J = 17.0, 12.6, 5.9 Hz, 1H), 2.07 – 2.00 (m, 1H), 1.81 (qd, J = 12.7, 5.2 Hz, 1H), 1.63 (t, J = 12.6 Hz, 1H), 1.41 (dd, J = 12.0, 1.6 Hz, 1H), 1.31 (s, 6H), 1.26 – 1.22 (m, 9H), 1.18 (s, 3H), 1.12 (s, 3H).

^{13}C NMR (151 MHz, $CDCl_3$) δ 143.4, 142.2, 129.9, 129.5, 121.7, 120.3, 118.5, 116.3, 99.8, 99.4, 77.4, 64.8, 57.9, 51.0, 48.3, 47.8, 38.6, 38.2, 37.4, 30.8, 28.9, 27.1, 22.2, 22.0, 21.3, 17.9, 15.3, 15.0.

HRMS (ESI) *m/z* calc'd for $C_{29}H_{41}NO_7$ $[M+Na]^+$: 538.2781, found 538.2799.

TLC: R_f = 0.23 (9:1 hexanes:EtOAc, visualized by CAM)

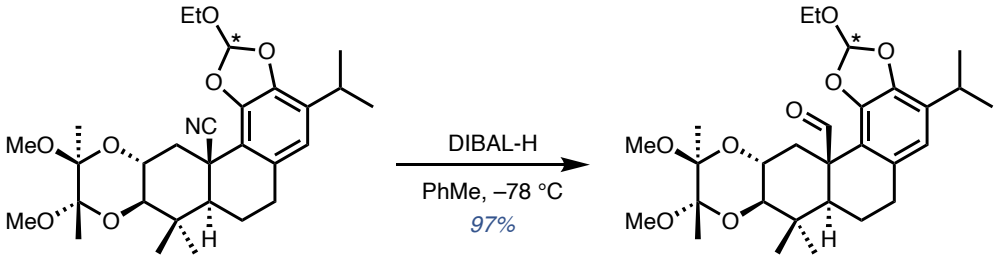
Less polar diastereomer **1.33b** (relative configuration unassigned):

^{1}H NMR (600 MHz, $CDCl_3$) δ 6.92 (s, 1H), 6.51 (s, 1H), 4.15 (ddd, *J* = 12.2, 10.1, 4.1 Hz, 1H), 3.62 (qd, *J* = 7.0, 5.1 Hz, 2H), 3.41 (dd, *J* = 13.0, 4.1 Hz, 1H), 3.34 (s, 3H), 3.26 – 3.23 (m, 4H), 3.00 (h, *J* = 7.0 Hz, 1H), 2.95 (dd, *J* = 16.6, 3.9 Hz, 1H), 2.84 – 2.75 (m, 1H), 2.06 – 1.99 (m, 1H), 1.82 (qd, *J* = 12.9, 5.2 Hz, 1H), 1.63 (t, *J* = 12.6 Hz, 1H), 1.41 (dd, *J* = 12.0, 1.6 Hz, 1H), 1.32 (s, 3H), 1.31 (s, 3H), 1.26 – 1.23 (m, 9H), 1.18 (s, 3H), 1.11 (s, 3H).

^{13}C NMR (151 MHz, $CDCl_3$) δ 143.5, 142.3, 129.9, 129.4, 121.9, 120.4, 118.7, 116.1, 99.8, 99.4, 77.4, 64.7, 58.5, 51.0, 48.2, 47.9, 38.7, 38.3, 37.2, 30.8, 28.9, 27.1, 22.1, 22.1, 21.4, 17.9, 17.9, 15.3, 15.0.

HRMS (ESI) *m/z* calc'd for $C_{29}H_{41}NO_7$ $[M+Na]^+$: 538.2781, found 538.2790.

TLC: R_f = 0.25 (9:1 hexanes:EtOAc, visualized by CAM)



1.33 **1.34**

Nitrile **1.33** (29 mg, 0.058 mmol, 1.0 equiv.) was dissolved in dry PhMe (3.0 mL) under Ar and cooled to –78 °C. DIBAL-H (0.5 M in PhMe, 0.93 mL, 0.47 mmol, 8.0 equiv.) was added dropwise by syringe. The resulting suspension was stirred at –78 °C for 3 hours. The reaction mixture was warmed to 0 °C and diluted with PhMe (3 mL). The reaction was quenched with the addition of saturated aqueous Rochelle salt (4 mL). The biphasic solution was allowed to stir vigorously for 12 hours at room temperature. The organic layer was separated, acidified with HCO_2H (1.0 mL), and diluted with deionized water (1 mL). The resulting biphasic solution was allowed to stir vigorously for 30 minutes. The organic layer was collected and washed with brine (10 mL), dried over sodium sulfate, and concentrated under reduced pressure to afford aldehyde **1.34** (28 mg, 0.054 mmol, 97%) as a white foam, which was used without further purification.

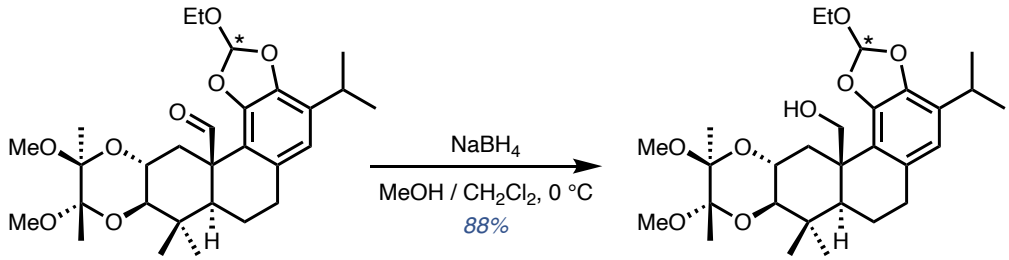
*NMR data for this compound are reported for the compound derived from the less polar diastereomer **1.33b** (at the orthoester).*

^{1}H NMR (500 MHz, $CDCl_3$) δ 9.80 (s, 1H), 6.81 (s, 1H), 6.57 (s, 1H), 3.93 (td, J = 11.5, 4.3 Hz, 1H), 3.59 (q, J = 7.1 Hz, 2H), 3.51 (dd, J = 12.7, 4.4 Hz, 1H), 3.35 (s, 3H), 3.27 – 3.21 (m, 4H), 3.06 – 2.95 (m, 2H), 2.95 – 2.85 (m, 1H), 2.12 (qd, J = 12.9, 5.3 Hz, 1H), 1.97 (dd, J = 13.7, 6.2 Hz, 1H), 1.68 (d, J = 12.5 Hz, 1H), 1.39 (d, J = 10.3 Hz, 2H), 1.31 (s, 3H), 1.29 (s, 3H), 1.27 – 1.19 (m, 10H), 1.10 (s, 3H), 0.86 (s, 3H).

^{13}C NMR (151 MHz, $CDCl_3$) δ 196.7, 144.8, 142.3, 131.3, 129.5, 120.4, 118.3, 113.5, 99.8, 99.3, 77.8, 64.3, 58.3, 52.5, 52.2, 48.1, 47.8, 38.2, 33.0, 31.1, 28.8, 26.4, 22.2, 22.1, 18.1 (2 C), 17.9, 16.3, 15.0.

HRMS (ESI) *m/z* calc'd for $C_{29}H_{42}O_8$ $[M+Na]^+$: 541.2777, found 541.2792.

TLC: R_f = 0.23 (9:1 hexanes:EtOAc, visualized by CAM)



1.34 **1.35**

Aldehyde **1.34** (90 mg, 0.17 mmol, 1.0 equiv.) was dissolved in MeOH/CH_2Cl_2 (1:3, 4.3 mL) and cooled to 0 °C in an ice bath. Sodium borohydride (33 mg, 0.87 mmol, 5.0 equiv.) was added in one portion and the resulting mixture allowed to stir for 3 hours. The reaction was quenched with the addition of EtOAc (3 mL) and saturated aqueous ammonium chloride (5 mL). The biphasic solution was stirred vigorously for 12 hours and then diluted with EtOAc (12.0 mL) and deionized water (15 mL). The organic layer was separated and washed with brine (20 mL), dried over sodium sulfate, and concentrated under reduced pressure. The crude residue was purified by flash column chromatography (SiO_2, 20% EtOAc in hexanes), providing carbinol **1.35** (79 mg, 0.15 mmol, 88%) as a translucent foam.

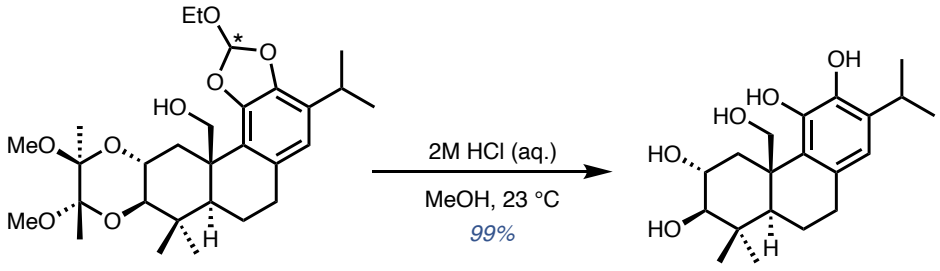
NMR data for this compound are reported for the compound derived from the less polar diastereomer ***1.33b*** *(at the orthoester).*

^{1}H NMR (600 MHz, $CDCl_3$) δ 6.83 (s, 1H), 6.53 (s, 1H), 6.57 (s, 1H), 4.00 (d, *J* = 11.4 Hz, 1H), 3.93 (d, *J* = 11.4 Hz, 1H), 3.93 – 3.87 (m, 1H), 3.61 (tdd, *J* = 19.6, 9.0, 6.6 Hz, 2H), 3.30 (s, 3H), 3.27 – 3.21 (m, 4H), 3.11 (dd, *J* = 13.1, 4.1 Hz, 1H), 3.00 (h, *J* = 7.0 Hz, 1H), 2.94 (dd, *J* = 16.9, 6.2 Hz, 1H), 2.87 – 2.79 (m, 1H), 1.94 (qd, *J* = 12.6, 6.6 Hz, 1H), 1.8 (dd, *J* = 13.3, 7.7 Hz, 1H), 1.57 – 1.50 (m, 2H), 1.31 (s, 3H), 1.30 (s, 3H), 1.27 – 1.20 (m, 9H), 1.09 (s, 3H), 1.01 (s, 3H).

^{13}C NMR (151 MHz, $CDCl_3$) δ 143.3, 141.4, 130.5, 128.2, 122.4, 120.4, 117.7, 99.7, 99.3, 78.6, 66.9, 64.4, 58.2, 51.2, 48.1, 47.8, 44.4, 38.1, 35.9, 30.5, 28.8, 28.5, 22.3, 22.1, 18.4, 18.1, 18.0, 17.6, 15.1.

HRMS (ES+) *m/z* calc'd for $C_{29}H_{44}O_8$ $[M+Na]^+$: 543.2934, found 543.2932.

TLC: R_f = 0.21 (96:4 CH_2Cl_2:EtOAc, visualized by CAM)



1.35 **1.2**

Carbinol **1.35** (9.2 mg, 18 µmol, 1.0 equiv.) was dissolved in dry MeOH (1.5 mL). HCl (2.0 M aqueous, 1.5 mL) was added. The reaction mixture was stirred at room temperature for 3 hours,

producing a clear solution that was slowly concentrated under reduced pressure to afford plebeianiol A (**1.2**) (6.2 mg, 18 µmol, >99%) as a white film.

^{1}H NMR (500 MHz, DMSO-d_6) δ 9.63 (br s, 1H), 7.54 (br s, 1H), 6.57 (br s, 1H), 6.36 (s, 1H), 4.11 (d, J = 10.0 Hz, 1H), 3.71 (d, J = 10.0 Hz, 1H), 3.58 (ddd, J = 11.7, 9.4, 3.9 Hz, 1H), 3.34 (dd, J = 13.4, 4.0 Hz, 1H), 3.11 (h, J = 7.0 Hz, 1H), 2.85 (d, J = 9.4 Hz, 1H), 2.78 – 2.68 (m, 2H), 1.71 – 1.59 (m, 1H), 1.51 (qd, J = 12.1, 7.7 Hz, 1H), 1.28 (d, J = 12.0 Hz, 1H), 1.12 (d, J = 6.8 Hz, 3H), 1.11 (d, J = 6.8 Hz, 3H), 1.01 (s, 3H), 0.99 – 0.93 (m, 1 H), 0.78 (s, 3H).

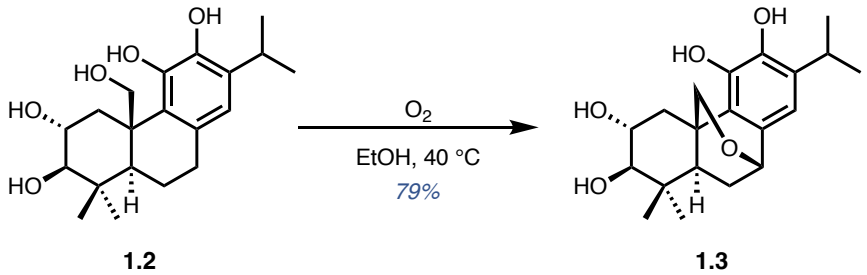
^{13}C NMR (151 MHz, DMSO-d_6) δ 143.0, 141.7, 132.1, 130.2, 126.3, 117.4, 81.9, 67.0, 65.4, 52.3, 44.3, 38.9, 38.1, 31.8, 29.7, 26.4, 22.5, 22.4, 18.2 (2 C).

HRMS (ES+) *m/z* calc'd for $C_{20}H_{30}O_5$ $[M+Na]^+$: 373.1991, found 373.1991

TLC: R_f = 0.20 (92:8 CH_2Cl_2:MeOH, visualized by CAM)

$[\alpha]^{22.8}_D$ +26.2 (c = 1.0, MeOH) [observed]

$[\alpha]^{27}_D$ +25.8 (c = 0.1, MeOH) [literature[5]]



1.2 **1.3**

Plebeianiol A (**1.2**) (1.6 mg, 0.0046 mmol, 1.0 equiv.) was dissolved in EtOH (1.0 mL) and the vial capped with a rubber septum. The septum was vented with a syringe needle and the solution was sparged under positive pressure with an O_2 balloon for 5 minutes. The cap was replaced and the vial was sealed with electrical tape. The solution was placed in a pre-heated oil bath and stirred at 40 °C for 4 hours. The reaction mixture was concentrated under reduced pressure and purified by flash column chromatography (SiO_2, 1:9 EtOH:PhH with 2% AcOH) to give ether **1.3** (1.1 mg, 0.003 mmol, 79%) as an orange oil.

*The spectral data for **1.3** were in good accord with those previously published.*[6]

^{1}H NMR (600 MHz, $CDCl_3$) δ 6.52 (s, 1H), 4.61 (d, *J* = 3.5 Hz, 1H), 4.06 (d, *J* = 8.5 Hz, 1H), 3.49 (ddd, *J* = 11.9, 9.3, 4.2 Hz, 1H), 3.23 (h, *J* = 6.8 Hz, 1H), 2.88 (dd, *J* = 9.1, 3.4 Hz, 2H), 2.68 (dd, *J* = 14.3, 11.9 Hz, 1H), 2.11 (dd, *J* = 14.2, 4.3 Hz, 1H), 1.92 (dd, *J* = 7.6, 3.8 Hz, 1H), 1.43 – 1.36 (m, 2H), 1.13 (d, *J* = 6.8 Hz, 3H), 1.11 (d, *J* = 6.8 Hz, 3H), 0.98 (s, 3H), 0.86 (s, 3H).

^{13}C NMR (151 MHz, $CDCl_3$) δ 142.3, 140.7, 133.2, 132.0, 128.1, 111.2, 81.6, 69.6, 68.6, 67.0, 43.0, 39.9, 39.3, 37.2, 29.4, 28.9, 26.2, 22.9, 22.8, 15.8.

HRMS (ES–) *m/z* calc'd for $C_{20}H_{28}O_5$ $[M–H]^-$: 347.1859, found 347.1866.

TLC: R_f = 0.20 (1:9 EtOH:PhH with 2% AcOH, visualized by CAM)

$[\alpha]^{22}_D$ –19.3 (c = 0.5, *i*-PrOH)

Note: There is no optical rotation data for this compound reported in the literature.

1.9.3 Method for Predicting ^{13}C Chemical Shifts

All calculations were performed using Spartan 18[7] on structures **1.1** and **1.2** in the gas phase. First, a distribution of conformers was calculated with Molecular Mechanics MMFF. All conformers exceeding 13 kcal/mol were discarded. The remaining conformers were subjected to an equilibrium geometry calculation using HF/3-21G and then assigned an alignment score. Any duplicates (conformers that shared an align score and relative energy) were discarded as well as any conformers exceeding 5 kcal/mol. All remaining conformers were refined using a single point energy calculation with ωB97X-D/6-31G* and all conformers exceeding 3 kcal/mol were discarded. [For example for **1.1**]: At this point 9 conformers remained, and they were subjected to a final energy refinement with ωB97XD/6-311+G(2df,2p)[6-311G*] with NMR prediction using ωB97X-D/6-31G*. Each of the 9 conformers were assigned a Boltzmann weight and the Boltzmann averaged ^{13}C shifts are reported for **1.1** in **Appendix A: A2**.

1.9.4 Supplemental References

(1) Batsanov, A. S.; Michael J. Begley; Fletcher, R. J.; Murphy, J. A.; Sherburn, M. S. *J. Chem. Soc., Perkin Trans. 1* **1995**, No. 10, 1281.

(2) Hayashi, Y.; Miyakoshi, N.; Kitagaki, S.; Mukai, C. *Org. Lett.* **2008**, *10*, 2385–2388.

(3) G. Banwell, M.; N. Buckler, J.; D. Schwartz, B. *Heterocycles* **2017**, *95*, 290.

(4) Vrubliauskas, D.; Gross, B. M.; Vanderwal, C. D. *J. Am. Chem. Soc.* **2021**, *143*, 2944–2952.

(5) Zhang, B.-B.; He, B.-Q.; Sun, J.-B.; Zeng, B.; Shi, X.-J.; Zhou, Y.; Niu, Y.; Nie, S.-Q.; Feng, F.; Liang, Y.; Wu, F.-H. *Molecules* **2015**, *20*, 14879–14888.

(6) Xiong, Y.; Qu, W.; Sun, J.; Wang, M.; Liang, J. *Phytochem. Lett.* **2013**, *6*, 457–460.

(7) Shao, Y.; Gan, Z.; Epifanovsky, E.; Gilbert, A. T. B.; Wormit, M.; Kussmann, J.; Lange, A. W.; Behn, A.; Deng, J.; Feng, X.; Ghosh, D.; Goldey, M.; Horn, P. R.; Jacobson, L. D.; Kaliman, I.; Khaliullin, R. Z.; Kuś, T.; Landau, A.; Liu, J.; Proynov, E. I.; Rhee, Y. M.; Richard, R. M.; Rohrdanz, M. A.; Steele, R. P.; Sundstrom, E. J.; Woodcock III, H. L.; Zimmerman, P. M.; Zuev, D.; Albrecht, B.; Alguire, E.; Austin, B.; Beran, G. J. O.; Bernard, Y. A.; Berquist, E.; Brandhorst, K.; Bravaya, K. B.; Brown, S. T.; Casanova, D.; Chang, C.-M.; Chen, Y.; Chien, S. H.; Closser, K. D.; Crittenden, D.

L.; Diedenhofen, M.; DiStasio Jr., R. A.; Do, H.; Dutoi, A. D.; Edgar, R. G.; Fatehi, S.; Fusti-Molnar, L.; Ghysels, A.; Golubeva-Zadorozhnaya, A.; Gomes, J.; Hanson-Heine, M. W. D.; Harbach, P. H. P.; Hauser, A. W.; Hohenstein, E. G.; Holden, Z. C.; Jagau, T.-C.; Ji, H.; Kaduk, B.; Khistyaev, K.; Kim, J.; Kim, J.; King, R. A.; Klunzinger, P.; Kosenkov, D.; Kowalczyk, T.; Krauter, C. M.; Lao, K. U.; Laurent, A. D.; Lawler, K. V.; Levchenko, S. V.; Lin, C. Y.; Liu, F.; Livshits, E.; Lochan, R. C.; Luenser, A.; Manohar, P.; Manzer, S. F.; Mao, S.-P.; Mardirossian, N.; Marenich, A. V.; Maurer, S. A.; Mayhall, N. J.; Neuscamman, E.; Oana, C. M.; Olivares-Amaya, R.; O'Neill, D. P.; Parkhill, J. A.; Perrine, T. M.; Peverati, R.; Prociuk, A.; Rehn, D. R.; Rosta, E.; Russ, N. J.; Sharada, S. M.; Sharma, S.; Small, D. W.; Sodt, A.; Stein, T.; Stück, D.; Su, Y.-C.; Thom, A. J. W.; Tsuchimochi, T.; Vanovschi, V.; Vogt, L.; Vydrov, O.; Wang, T.; Watson, M. A.; Wenzel, J.; White, A.; Williams, C. F.; Yang, J.; Yeganeh, S.; Yost, S. R.; You, Z.-Q.; Zhang, I. Y.; Zhang, X.; Zhao, Y.; Brooks, B. R.; Chan, G. K. L.; Chipman, D. M.; Cramer, C. J.; Goddard III, W. A.; Gordon, M. S.; Hehre, W. J.; Klamt, A.; Schaefer III, H. F.; Schmidt, M. W.; Sherrill, C. D.; Truhlar, D. G.; Warshel, A.; Xu, X.; Aspuru-Guzik, A.; Baer, R.; Bell, A. T.; Besley, N. A.; Chai, J.-D.; Dreuw, A.; Dunietz, B. D.; Furlani, T. R.; Gwaltney, S. R.; Hsu, C.-P.; Jung, Y.; Kong, J.; Lambrecht, D. S.; Liang, W.; Ochsenfeld, C.; Rassolov, V. A.; Slipchenko, L. V.; Subotnik, J. E.; Van Voorhis, T.; Herbert, J. M.; Krylov, A. I.; Gill, P. M. W.; Head-Gordon, M. *Molecular Physics* **2015**, *113*, 184–215.

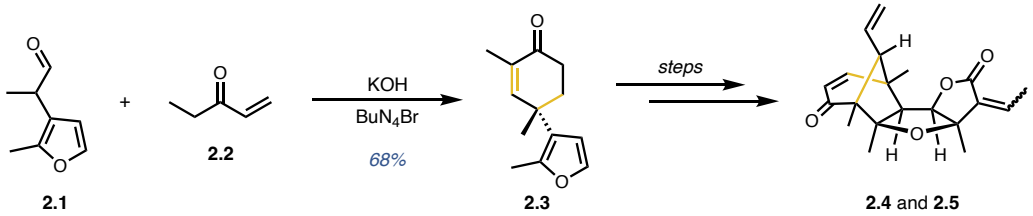
CHAPTER 2. DISCOVERY OF A RADICAL-BASED ANNULATION METHOD

2.1 Introduction

Forming two carbon–carbon bonds and one new ring, annulation reactions are powerful stepwise transformations that permit a rapid increase in molecular complexity. Indeed, these reactions are so important to organic chemists that many bear the names of the scientists who first discovered or popularized them. Typically, annulation reactions are designed around the bifunctional reactivity of each given component along the intended reaction pathway. As annulation transforms can vastly simplify target molecules in a retrosynthetic sense, these reactions find frequent applications in concise total syntheses of complex natural products.

In their synthesis of pallambins C and D, the Baran group utilized a Robinson annulation in the construction of intermediate **2.3** (**Scheme 2.1**).[1] Treatment of furfuryl alcohol derivative **2.1**. in with aqueous potassium hydroxide and ethyl vinyl ketone (**2.2**) facilitated Michael addition followed by an intramolecular aldol condensation. The derived enone **2.3** was subsequently converted to pallambins C and D (**2.4** and **2.5**) after ten additional steps.

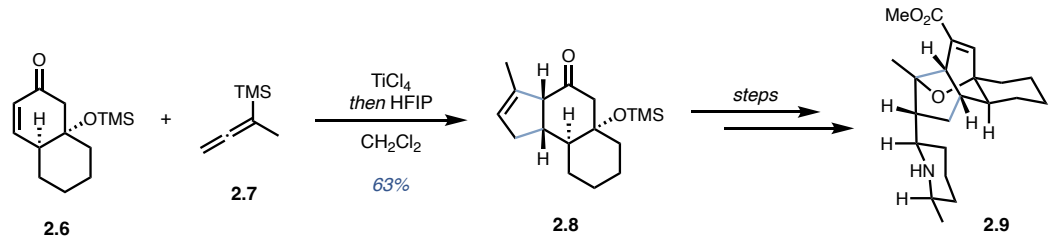
Scheme 2.1 *Robinson annulation by Baran and coworkers in their synthesis of pallambins C and D*



Shenvi and coworkers recently disclosed the first synthesis of the *Galbulimima* alkaloid, GB18.[2] The authors' use of a highly stereoselective Danheiser annulation permitted the stepwise formation of the cyclopentene ring in **2.8** (**Scheme 2.2**). The addition of HFIP facilitated *in situ*

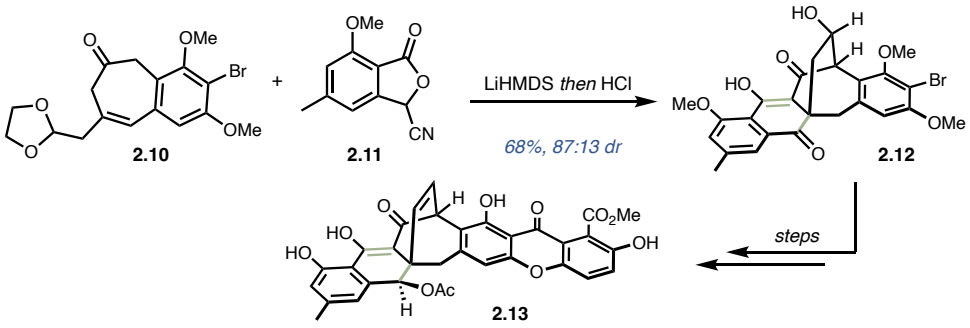
protodesilylation of the annulation product while mitigating unwanted alkene isomerization and β-elimination processes observed under more traditional conditions.

Scheme 2.2 *Danheiser annulation by Shenvi and coworkers in their synthesis of (±)-GB18*



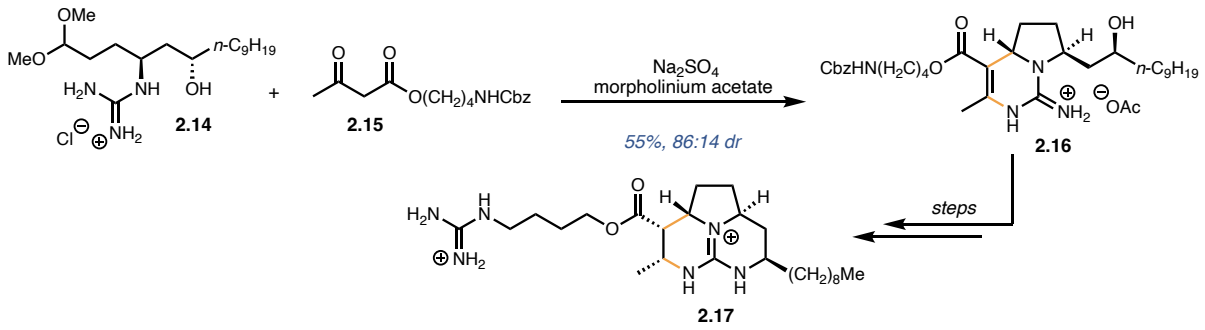
Pronin's synthesis of acremoxanthone A features a highly convergent Hauser–Kraus annulation between phthalide **2.11** and benzocycloheptanone **2.10** (**Scheme 2.3**).[3] The authors propose that the reaction conditions permit alkene isomerization of the alkene in **2.10**; the subsequently formed enone then undergoes Michael addition with the nitrile-stabilized carbanion of **2.11** followed by Dieckmann condensation with the neighboring lactone. Hydrolysis of the acetal protecting group facilitates an intramolecular aldol reaction that closes the bridging ring.

Scheme 2.3 *Hauser–Kraus annulation by Pronin and coworkers in a synthesis of acremoxanthone A*



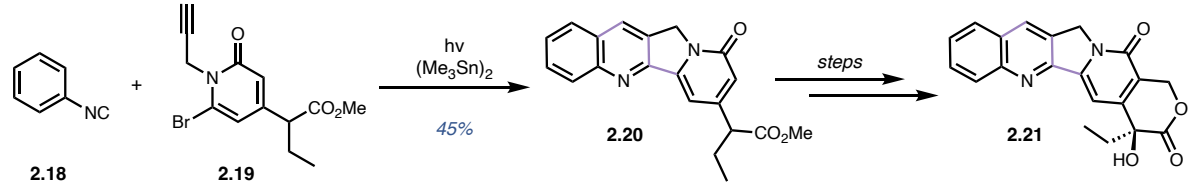
In their synthesis of batzelladine D, Overman and coworkers applied a Biginelli condensation between guanidine **2.14** and β-ketoester **2.15** (**Scheme 2.4**).[4] Normally a three component reaction, by tethering the aldehyde and guanidine functions the authors were able to effect a stereoselective bicyclization that established the *anti* relationship between the methine hydrogens of the pyrrolidine ring.

Scheme 2.4 *Biginelli condensation by Overman and coworkers aids the synthesis of batzelladine A*



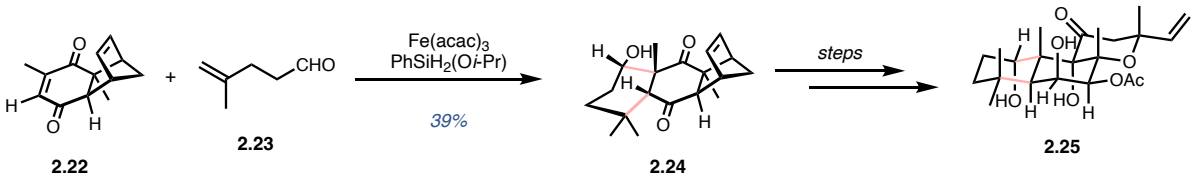
Coupled with its therapeutic potential as a topoisomerase I inhibitor, the alluring polycyclic scaffold of camptothecin has drawn the interest of total synthesis groups for decades. While many early syntheses of camptothecin disconnected the quinoline ring via Friedlander synthesis, Curran and coworkers saw the opportunity to leverage a carefully designed annulation cascade in what would become a highly convergent synthesis of the natural product (**Scheme 2.5**).[5] Irradiation of hexamethylditin facilitates the formation of a stannyl radical that can abstract bromine from **2.19**. The pyridone radical engages the isonitrile function of phenylisocyanide (**2.18**), and sequential intermolecular cyclizations followed by oxidative rearomatization leads to tetracycle **2.20**.

Scheme 2.5 *Radical annulation by Curran and coworkers in the synthesis of camptothecin*



More recently, Pronin and coworkers described a synthesis of forskolin in which a radical/polar crossover annulation enabled the coupling of enedione **2.22** with aldehyde **2.23** (**Scheme 2.6**).[6] In the key step, Giese addition is followed by single-electron reduction to generate a reactive enolate. The intramolecular aldol that follows completes the formation of forskolin's decalin core in a highly diastereoselective manner.

Scheme 2.6 *MHAT-initiated annulation by Pronin and coworkers in the synthesis of forskolin*



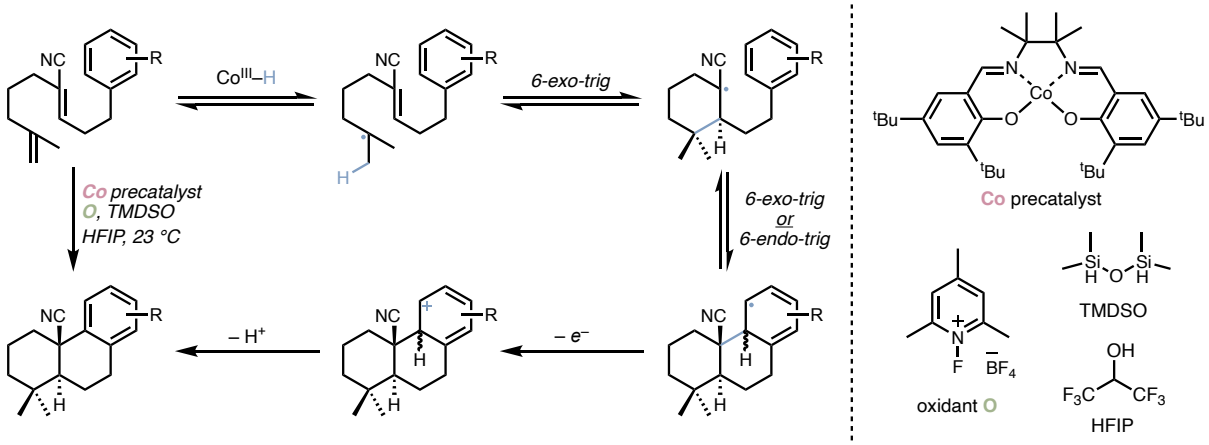
2.2 Discovery of an MHAT-initiated Radical Annulation

Over the last twenty years, hydrofunctionalization of alkenes by metal-hydride hydrogen atom transfer (MHAT) has emerged as an exceptionally useful tool in synthetic organic chemistry. Metal hydrides react with alkenes to generate radical intermediates with Markovnikov selectivity, which parallels the regioselectivity observed in Brønsted-acid based methods of alkene activation that involves carbocation formation. Unlike reactions involving the generation of carbocationic intermediates, MHAT-initiated transformations typically occur under comparatively milder conditions. This detail permits unique or otherwise highly useful chemoselectivity and makes chemistry within this manifold particularly attractive.[7–9] Currently, MHAT-initiated hydrofunctionalization enables the construction of a variety of bonds to carbon, including C–H, C–C, C–N, C–O, and C–X (X = Cl or Br). Thus, easily accessible alkene intermediates are readily converted into a multitude of useful and important functionalities present in natural products and terminal synthetic compounds alike.

Our group recently disclosed a method for stereoselective radical bicyclizations initiated by cobalt-catalyzed hydrogen atom transfer (HAT).[10] Empirical evidence supports several key details about this transformation: (1) the two bond-forming events of the cyclization proceed in a stepwise fashion with radical intermediates; (2) the cascade is almost certainly terminated via single-electron oxidation; (3) this process leads to an irreversible radical/polar crossover event (**Scheme**

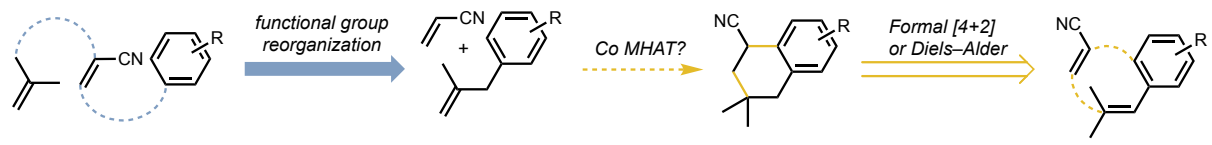
2.7). Altogether, these findings led us to speculate whether other reaction types might be realized with this chemistry.

Scheme 2.7 *Proposed mechanism for HAT-initiated radical bicyclization*



We reasoned that reorganization of the reactive functional groups might enable an annulation cascade initiated by HAT (**Scheme 2.8**). Conceptually, this transformation represents a formal [4+2] cycloaddition between styrene (4π component) and an electron deficient alkene (2π component) followed by rearomatization. The pericyclic variant of this transformation is a challenging reaction that is largely limited to systems involving tethered reactive groups, aryne intermediates, or radical cation intermediates generated by photoredox catalysis.[11–17] Such a method would naturally benefit from the unique chemoselectivity characteristic of transformations operating within the radical manifold.

Scheme 2.8 *Functional group reorganization leads to annulation reaction concept*

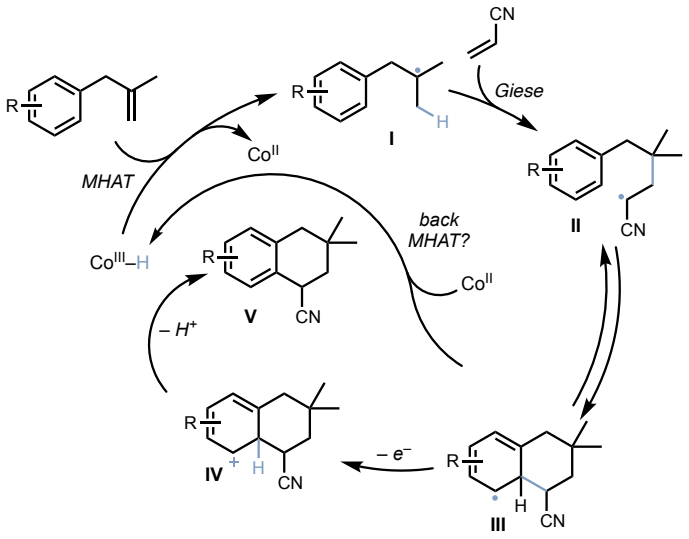


In this way, this chemistry might enable expedient access to a broad range of tetralin products. Tetralins are ubiquitous among structures of secondary metabolites and pharmaceutical

compounds alike, and so the importance of reactions that quickly provide access to these scaffolds cannot but overstated. Critically important tetralin-containing compounds include A-ring aromatic steroids, morphinans, aryltetralin lignins (e.g. podophyllotoxin), 2-aminotetralins (e.g. sertraline/Zoloft), doxorubicin, and ergot alkaloids.

Mechanistically, this annulation could be achieved in a mode analogous to bicyclization (**Scheme 2.9**). Generated *in situ*, $Co^{III}-H$ transfers a hydrogen atom to the substrate to generate tertiary alkyl radical **I**; Giese addition of **I** to an electron-deficient alkene (in this case, acrylonitrile) forms radical adduct **II**. **II** engages the electron-rich arene in a second bond-forming event, which leads (transiently) to loss of aromaticity and generates cyclohexadienyl radical **III**. The depicted chemoselectivity of this sequence ultimately relies on the relative polarity of each radical species and its philicity for one coupling partner over another.[18–22] Aromaticity is most likely restored through a single-electron oxidation/deprotonation process, but back-HAT to a cobalt complex (as proposed by Shenvi) might also be operative; both paths ultimately converge to **V.**[23]

Scheme 2.9 *Simple mechanism for MHAT-initiated annulation*



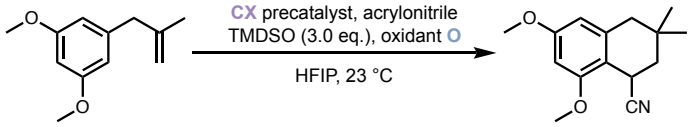
2.3 Discovery of a Radical-Based Annulation Method

2.3.1 Reaction Optimization

Our preliminary efforts targeted annulation between acrylonitrile and methallyl arene **S2.26**, whose pattern of π-electron-donating methoxy substituents proved optimal in our group's bicyclization studies.[10] The initial reaction conditions we settled on approximated those that worked best for the intramolecular bicyclization chemistry: 10 mol% of a bulky cobalt(II) precatalyst and three equivalents each of the siloxane reductant TMDSO and the oxidant *N*-fluorocollidinium tetrafluoroborate, all in HFIP at 23 °C. Following an initial hit, we identified several reaction parameters that we would investigate in our optimization studies; our findings are summarized in **Table 2.1**.

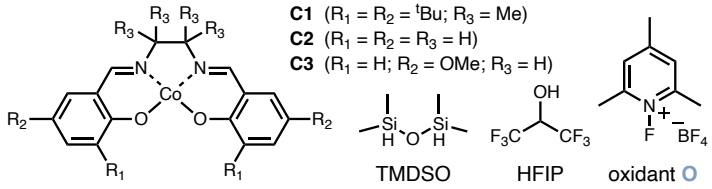
Focusing on the stoichiometry of the two reaction partners, we observed a five-fold excess of acrylonitrile to be optimal. As the first carbon–carbon bond-formation event is intermolecular, using less than two equivalents of the radical acceptor (entry 1) led to a dramatic increase in problematic side reactions of **S2.26** including hydrogenation, hydrofluorination, hydroalkoxylation, and alkene isomerization – all of which are known processes that this chemistry has otherwise been optimized for.[23–27] With higher concentrations of acrylonitrile we could reliably obtain good yields of **2.26** (entries 2–3) but using more than five equivalents (entry 4) proved deleterious to reaction outcome.

Table 2.1 *Reaction optimization with acrylonitrile*



S2.26 **2.26**

Entry	*precatalyst (mol%)*	*Conc. (M)*	*Acceptor (equiv.)*	*Ox. (equiv.)*	*Temp (°C)*	*Yield (%)*
1	C1 (10)	0.10	1	3	23	52
2	C1 (10)	0.10	2	3	23	72
3	C1 (10)	0.10	5	3	23	75
4	C1 (10)	0.10	10	3	23	69
5	C1 (10)	0.10	5	3	23	77
6	C2 (10)	0.10	5	3	23	74
7	C3 (10)	0.10	5	3	23	59
8	C1 (10)	0.10	5	3	35	92
9	C1 (10)	0.10	5	3	50	92
10	C1 (10)	0.10	5	2	35	77
11	C1 (2)	0.10	5	2	35	72
12	C2 (2)	0.10	5	2	35	45
13	C3 (2)	0.10	5	2	35	45
14	C1 (2)	0.20	5	2	35	57
15	C1 (2)	0.05	5	2	35	77
16	C1 (2)	0.03	5	2	35	84



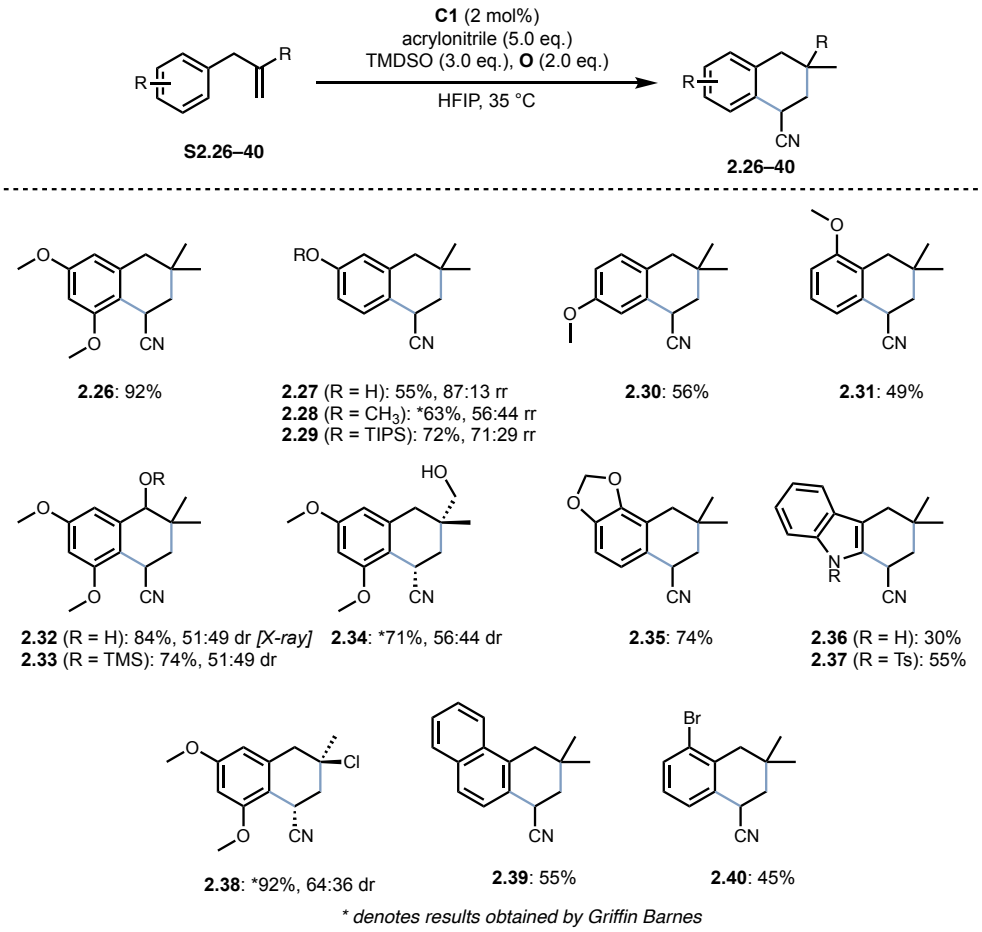
As ligand structure can generally confer selectivity regarding product distribution, we decided to briefly sample this parameter here (entries 5–7).[28–33] Ultimately, we found bulky precatalyst **C1** to perform with the highest efficiency; use of less-hindered **C2** or more electron-rich **C3** led to decreased formation of **2.26**. The most meaningful increase in yield was realized by increasing reaction temperature (entries 8–9), revealing for these reaction partners a relationship that appears to plateau around 35 °C. Reducing the amount of precatalyst (entries 11–13) proved deleterious to the overall reaction outcome. While this observed drop in yield could be somewhat recovered by running the reaction at lower concentrations (entry 15–16), the opposite effect was observed at higher concentration (entry 14), altogether elucidating the system's sensitivity to several parameters regarding overall reaction efficiency.

An analogous optimization study was performed in parallel for cyclohexenone but will not be discussed here; this work was conducted by my colleague, Griffin Barnes, with whom I gratefully share this work with.

2.3.2 Substrate Scope

Exploration of the scope of the allyl arene revealed several important trends (**Table 2.2**). Applying the standard conditions, we found greatest success with 3- or 5-substituted electron-rich arenes (**2.26**, **2.27–2.29**); this pattern was also observed in our group's development of the bicyclization methodology. Attempts to transform analogous 2- or 4-functionalized arenes (**2.30** and **2.31**) resulted in poorer reaction outcomes, suggesting a sensitivity of the radical trapping event that facilitates ring closure and concomitant generation of a cyclohexadienyl radical intermediate. Notably, several important and useful functional groups are tolerated under the reaction conditions (**2.32–2.40**). Electron-deficient arenes are purposely not included in the substrate scope as our earlier work demonstrated these systems to be incompatible with the oxidative termination mode operative in this transformation.

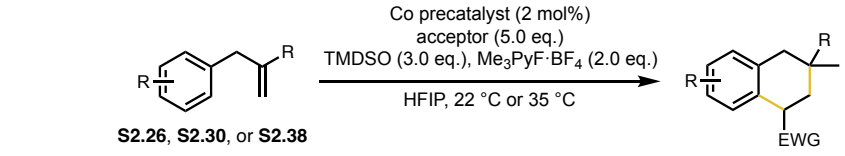
Table 2.2 *Arene substrate scope*

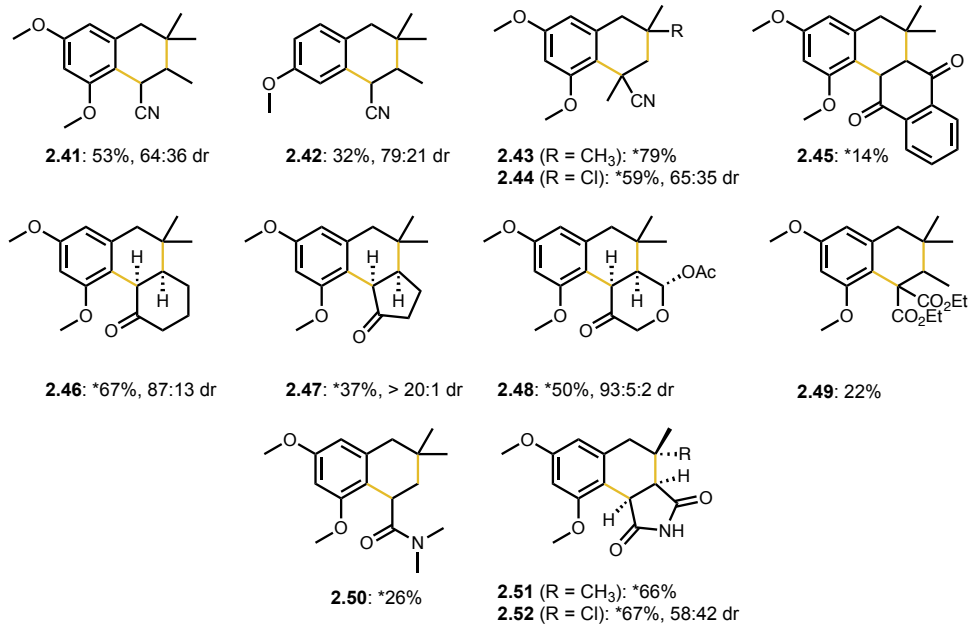


** denotes results obtained by Griffin Barnes*

Next, we investigated the scope of electron-deficient alkenes that might participate in the desired annulation. While substitution at the α position (**2.43** and **2.44**) appears to be well-tolerated for acyclic acceptors, the reaction appears to be more sensitive to β substitution (compare **2.26** versus **2.41**). Once again, 3- or 5- substitution patterns appear to improve the reaction outcome (compare **2.41** versus **2.42**). We note that moderate to good yields were obtained with cyclic enones and maleimides alike, and in some cases the reaction displays interesting diastereoselectivity (**2.42**, **2.46**, **2.47**, and **2.48**). Attempts to perform the annulation with naphthoquinone or alkylidene malonate were much less efficient as these substrates were readily reduced under the reaction conditions (**2.45** and **2.49**).

Table 2.3 *Electron-deficient alkene scope*





** denotes results obtained by Griffin Barnes*

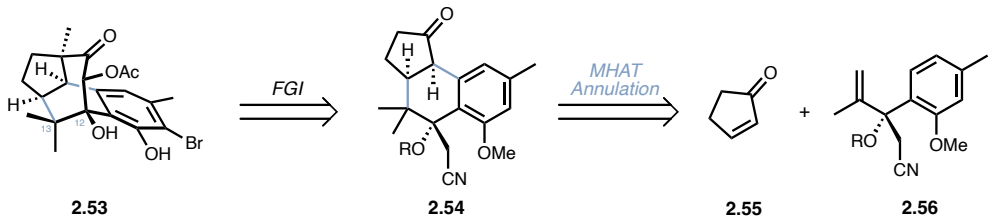
2.4 Conclusion and Future Directions

The discovery of a novel method permitting the annulation of allylarenes with electron-deficient alkenes was developed through functional group reorganization of our bicyclization chemistry. The method is operationally simple, proceeds under relatively mild conditions, and tolerates several important and sensitive functionalities. Based on our prior work, the reaction mechanism likely proceeds via radical/polar crossover facilitated by oxidative rearomatization of the arene function.

Briefly, we considered the application of this method towards a synthesis of hamigeran F (**2.53**, **Scheme 2.10**).[34] Several transformations conglomerate to disconnect the seven-membered

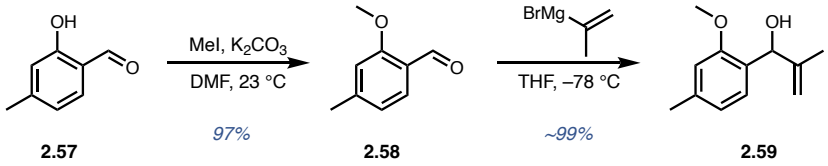
ring in **2.53** and in this way lead back to a tetralin intermediate (**2.54**), which is the annulation product of **2.56** with cyclopentenone **2.55**.

Scheme 2.10 *Retrosynthesis of hamigeran F (**2.53**)*



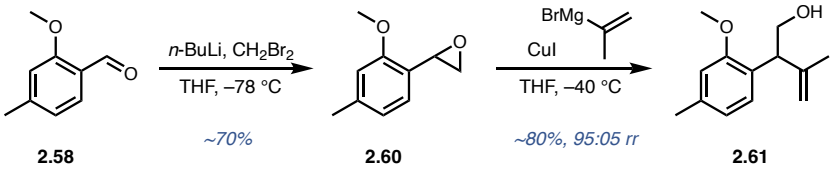
Because the annulation of **2.26** with cyclopentenone had revealed itself to be a rather inefficient process (**2.47**, **Table 2.3**), we were interested in the construction of a model system of **2.56** that we felt would allow us to test the feasibility of the intended annulation (**Scheme 2.11**). Methylation of phenol **2.57** followed by 1,2-addition of the appropriate Grignard reagent provided us with allylarene **2.59**.

Scheme 2.11 *Synthesis of model arene **2.59***



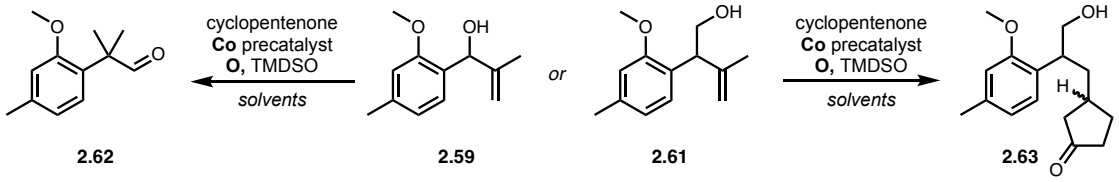
Similarly, we derivatized **2.58** in parallel to a homologated variant of **2.59** (**2.61**, **Scheme 2.12**). Treatment of benzaldehyde **2.58** with lithiated dibromomethane allowed smooth formation of styrene oxide **2.60**. Exposure of **2.60** to the cuprate derived from isopropenylmagnesium bromide permitted highly regioselective opening of the epoxide to form carbinol **2.61**.

Scheme 2.12 *Synthesis of model arene **2.61***



Unfortunately, neither substrate would prove competent for the intended transformation (**Scheme 2.13**). Our attempts to effect annulation of **2.59** with cyclopentenone exclusively formed the semipinacol rearrangement product **2.62**; this transformation has been previously reported by Pronin and coworkers under very similar conditions, and so the outcome here is not entirely surprising.[35] Separately, a variety of conditions applied to **2.61** only led to the formation of what we presently suspect to be Giese product **2.63**. Following Giese addition, a putative α-ketone radical could be conceivably transformed to **2.63** by several pathways, including 1,5 hydrogen atom transfer.

Scheme 2.13 *Annulation attempts with* ***2.59*** *or* ***2.61***



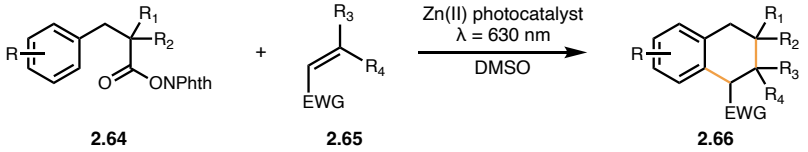
2.62 **2.59** **2.61** **2.63**

In this way, it appears that reduction of the putative α-ketone radical is faster than the dearomative C–C bond formation event, a detail that is likely informed by the unfavorable pattern of arene substitution (*vide supra*). Analogous experiments attempting annulation between **2.59** or **2.61** and acrylonitrile also formed exclusively the Giese adduct – an outcome that we had never previously observed with this alkene partner. Together, these results specifically indicate that **2.59** and **2.61** are unsuitable for the annulation method described. Successful application of this chemistry towards a synthesis of hamigeran F will necessitate judicious arene substitution such that efficient annulation with the challenging acceptor cyclopentenone is possible.

More recently, Yoshimitsu and coworkers described a new method for the synthesis of tetralins using photoredox catalysis (**Scheme 2.14**).[36] In this work, excitation of a zinc(II) porphyrin photocatalyst with red light facilitates conversion of a redox-active *N*-

acyloxyphthalimide (**2.64**) to the corresponding tertiary alkyl radical which is capable of intercepting electron deficient alkenes (**2.65**). In that the termination mode is oxidative and involves dearomative cyclohexadienyl radical formation, we were unsurprised to find many similarities in both the method's substrate scope and its limitations alike.

Scheme 2.14 *Photoredox-mediated annulation cascade described by Yoshimitu and coworkers*



2.5 Distribution of Credit

Griffin Barnes and Sebastian Fernandez are acknowledged for their significant contributions to the work described in section **2.3**. Griffin optimized the annulation of **S2.26** with cyclohexenone and with Sebastian Fernandez investigated the scope of electron-deficient alkenes; the full details of this work may be found in our publication.[37]

2.6 References

(1) Martinez, L. P.; Umemiya, S.; Wengryniuk, S. E.; Baran, P. S. *J. Am. Chem. Soc.* **2016**, *138*, 7536–7539.

(2) Woo, S.; Shenvi, R. A. *Nature* **2022**, *606*, 917–921.

(3) Holmbo, S. D.; Pronin, S. V. *J. Am. Chem. Soc.* **2018**, *140*, 5065–5068.

(4) Cohen, F.; Overman, L. E.; Ly Sakata, S. K. *Org. Lett.* **1999**, *1*, 2169–2172.

(5) Curran, D. P.; Liu, H. *J. Am. Chem. Soc.* **1992**, *114*, 5863–5864.

(6) Thomas, W. P.; Schatz, D. J.; George, D. T.; Pronin, S. V. *J. Am. Chem. Soc.* **2019**, *141*, 12246–12250.

(7) Crossley, S. W. M.; Obradors, C.; Martinez, R. M.; Shenvi, R. A. *Chem. Rev.* **2016**, *116*, 8912–9000.

(8) Green, S. A.; Crossley, S. W. M.; Matos, J. L. M.; Vásquez-Céspedes, S.; Shevick, S. L.; Shenvi, R. A. *Acc. Chem. Res.* **2018**, *51*, 2628–2640.

(9) Shevick, S. L.; Wilson, C. V.; Kotesova, S.; Kim, D.; Holland, P. L.; Shenvi, R. A. *Chem. Sci.* **2020**, *11*, 12401–12422.

(10) Vrubliauskas, D.; Vanderwal, C. D. *Angew. Chem. Int. Ed.* **2020**, *59*, 6112–6121.

(11) Pan, L.-N.; Wang, Q.; Sun, J.; Yan, C.-G. *Asian J. Org. Chem.* **2021**, *10*, 2591–2595.

(12) Kubo, T.; Fujita, T.; Ichikawa, J. *Chem. Lett.* **2020**, *49*, 264–266.

(13) Zhang, G.; Lin, Y.; Luo, X.; Hu, X.; Chen, C.; Lei, A. *Nat. Commun.* **2018**, *9*, 1225.

(14) Wang, L.; Wu, F.; Chen, J.; Nicewicz, D. A.; Huang, Y. *Angew. Chem. Int. Ed.* **2017**, *56*, 6896–6900.

(15) Zheng, M.; Wu, F.; Chen, K.; Zhu, S. *Org. Lett.* **2016**, *18*, 3554–3557.

(16) Li, W.; Zhou, L.; Zhang, J. *Chem. Eur. J.* **2016**, *22*, 1558–1571.

(17) Wagner-Jauregg, T. *Justus Liebigs Ann. Chem.* **1931**, *491*, 1–13.

(18) Parsaee, F.; Senarathna, M. C.; Kannangara, P. B.; Alexander, S. N.; Arche, P. D. E.; Welin, E. R. *Nat. Rev. Chem.* **2021**, *5*, 486–499.

(19) Ruffoni, A.; Mykura, R. C.; Bietti, M.; Leonori, D. *Nat. Synth.* **2022**, *1*, 682–695.

(20) De Vleeschouwer, F.; Van Speybroeck, V.; Waroquier, M.; Geerlings, P.; De Proft, F. *Org. Lett.* **2007**, *9*, 2721–2724.

(21) Shinohara, H.; Imamura, A. *Bull. Chem. Soc. Jpn.* **1979**, *52*, 3265–3270.

(22) Roberts, B. P. *Chem. Soc. Rev.* **1999**, *28*, 25–35.

(23) Crossley, S. W. M.; Barabé, F.; Shenvi, R. A. *J. Am. Chem. Soc.* **2014**, *136*, 16788–16791.

(24) Shigehisa, H.; Aoki, T.; Yamaguchi, S.; Shimizu, N.; Hiroya, K. *J. Am. Chem. Soc.* **2013**, *135*, 10306–10309.

(25) Shigehisa, H.; Nishi, E.; Fujisawa, M.; Hiroya, K. *Org. Lett.* **2013**, *15*, 5158–5161.

(26) Iwasaki, K.; Wan, K. K.; Oppedisano, A.; Crossley, S. W. M.; Shenvi, R. A. *J. Am. Chem. Soc.* **2014**, *136*, 1300–1303.

(27) Discolo, C. A.; Touney, E. E.; Pronin, S. V. *J. Am. Chem. Soc.* **2019**, *141*, 17527–17532.

(28) Palucki, M.; Finney, N. S.; Pospisil, P. J.; Güler, M. L.; Ishida, T.; Jacobsen, E. N. *J. Am. Chem. Soc.* **1998**, *120*, 948–954.

(29) Kochem, A.; Kanso, H.; Baptiste, B.; Arora, H.; Philouze, C.; Jarjayes, O.; Vezin, H.; Luneau, D.; Orio, M.; Thomas, F. *Inorg. Chem.* **2012**, *51*, 10557–10571.

(30) Ford, D. D.; Nielsen, L. P. C.; Zuend, S. J.; Musgrave, C. B.; Jacobsen, E. N. *J. Am. Chem. Soc.* **2013**, *135*, 15595–15608.

(31) Chiang, L.; Allan, L. E. N.; Alcantara, J.; Wang, M. C. P.; Storr, T.; Shaver, M. P. *Dalton Trans.* **2014**, *43*, 4295–4304.

(32) Chiang, L.; Herasymchuk, K.; Thomas, F.; Storr, T. *Inorg. Chem.* **2015**, *54*, 5970–5980.

(33) Yuan, Y.-C.; Mellah, M.; Schulz, E.; David, O. R. P. *Chem. Rev.* **2022**, *122*, 8841–8883.

(34) Singh, A. J.; Dattelbaum, J. D.; Field, J. J.; Smart, Z.; Woolly, E. F.; Barber, J. M.; Heathcott, R.; Miller, J. H.; Northcote, P. T. *Org. Biomol. Chem.* **2013**, *11*, 8041.

(35) Touney, E. E.; Foy, N. J.; Pronin, S. V. *J. Am. Chem. Soc.* **2018**, *140*, 16982–16987.

(36) Okanishi, Y.; Takemoto, O.; Kawahara, S.; Hayashi, S.; Takanami, T.; Yoshimitsu, T. *Org. Lett.* **2024**, *26*, 3929–3934.

(37) Johnson, L. K.; Barnes, G. L.; Fernandez, S. A. Vanderwal, C. D. *Angew. Chem. Int. Ed.* **2023**, *62*, e202303228.

2.6 Experimental Information

2.6.1 Materials and Methods

All reactions were performed in oven-dried (120 °C) or flame-dried glassware under an atmosphere of dry argon unless otherwise noted. Reaction solvents including dichloromethane (CH_2Cl_2, Fisher, HPLC Grade), hexanes (Fisher, HPLC Grade), diethyl ether (Et_2O, Fisher, BHT stabilized, HPLC Grade), benzene (PhH, Fisher, HPLC Grade), tetrahydrofuran (THF, Fisher, HPLC Grade), and toluene (PhMe, Fisher, HPLC Grade) were dried by percolation through a column packed with neutral alumina and a column packed with Q5 reactant, a supported copper catalyst for scavenging oxygen, under a positive pressure of argon. Hexafluoroisopropanol ($(CF_3)_2CHOH$, Oakwood) was degassed prior to use by sparging with argon for 15 minutes. Solvents for workup and chromatography were hexanes (Fisher or EMD, ACS Grade), ethyl acetate (EtOAc, Fisher, ACS Grade), dichloromethane (CH_2Cl_2, Fisher, ACS Grade), and diethyl ether (Et_2O, Fisher, ACS Grade).

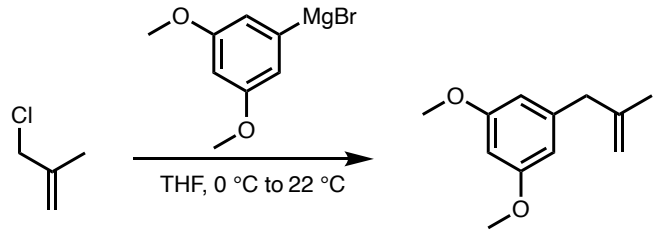
Column chromatography was performed using EMD Millipore 60 Å (0.040-0.063 mm) mesh silica gel (SiO_2). Analytical and preparative thin-layer chromatography was performed on Merck silica gel 60 F254 TLC plates. Visualization was accomplished with UV (254 or 210 nm), and *p*-anisaldehyde, vanillin, potassium permanganate ($KMnO_4$), 2,4-dinitrophenylhydrazine (2,4-DNP), or ceric ammonium molybdate (CAM) and heat as developing agents. Chloroform-*d* ($CDCl_3$, 99.8% D, DLM-7) and C_6D_6 (99.5% D, DLM-1-100, dried over activated alumina [5 wt%]) were purchased from Cambridge Isotope Laboratories. K_2CO_3 (anhydrous, 99%, Alfa Aesar), $NaHCO_3$ (ACS grade, Fisher), NaOH (ACS grade, Macron or Fisher), 1-fluoro-2,4,6-trimethylpyridinium tetrafluoroborate (TCI or Sigma Aldrich, 95-99%), and 1,1,3,3-tetramethyldisiloxane (TMDSO, 97%, Acros Organics) were purchased commercially and used without further purification.

Triethylamine (EMD, CaH_2) and pyridine (Alfa Aesar, CaH_2) were distilled from the indicated drying agents prior to use.

Proton and carbon magnetic resonance spectra (^1H NMR and ^{13}C NMR) were recorded at 298 K on a Bruker CRYO500 (500 MHz, ^1H; 125 MHz, ^{13}C) or a Bruker AVANCE600 (600 MHz, ^1H; 151 MHz, ^{13}C) spectrometer with solvent residual as the internal standard for ^1H NMR: $CHCl_3$ at 7.26 ppm, and C_6HD_5 at 7.16 ppm and solvent as internal standard for ^{13}C NMR: $CDCl_3$ at 77.16 ppm and C_6D_6 at 128.06 ppm. ^1H NMR data are reported as follows: chemical shift, multiplicity (s = singlet, d = doublet, t = triplet, q = quartet, h = heptet, dd = doublet of doublets, ddd = doublet of doublet of doublets, td = triplet of doublets, tdd = triplet of doublet of doublets, qd = quartet of doublets, m = multiplet, br = broad signal), coupling constants (Hz), and integration. The raw fid files were processed into the included NMR spectra using MestReNova 14.3 (Mestrelab Research S.L.).

High resolution mass spectra (HRMS) were recorded either on a Waters LCT Premier S2 spectrometer using ESI-TOF (electrospray ionization-time of flight) or a Waters GCT Premier spectrometer using CI-TOF (chemical ionization-time of flight) and data are reported in the form of (m/z).

2.6.2 Starting Material Synthesis



S2.26

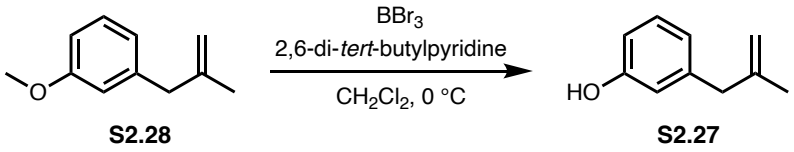
3-Chloro-2-methylprop-1-ene (3.3 mL, 33 mmol) was dissolved in THF (52 mL) and cooled to 0 °C under an argon atmosphere. (3,5-Dimethoxyphenyl)magnesium bromide[1] (38 mL of THF solution, 0.73 M, 28 mmol) was added dropwise by syringe. The reaction was allowed to stir while warming to 22 °C. After 16 hours the reaction was diluted with Et_2O (100 mL), quenched with saturated aqueous NH_4Cl (100 mL) and extracted with Et_2O (50 mL). The combined organic extracts were washed with 1.0 M NaOH (100 mL), brine (100 mL), and dried over Na_2SO_4. The crude residue was concentrated under reduced pressure and purified by vacuum distillation (155 °C at 4 mm Hg) using a Kugelröhr distillation apparatus to provide alkene **S2.26** (3.5 g, 66%).

^{1}H NMR (500 MHz, $CDCl_3$): δ 6.36 (d, *J* = 2.3 Hz, 2H), 6.32 (t, *J* = 2.3 Hz, 1H), 4.82 (s, 1H), 4.77 (s, 1H), 3.78 (s, 6H), 3.26 (s, 2H), 1.68 (s, 3H).

^{13}C NMR (126 MHz, $CDCl_3$): δ 160.8, 144.9, 142.3, 112.3, 107.1, 98.2, 55.4, 45.1, 22.2.

HRMS (ESI+): *m/z* calc'd for $C_{12}H_{16}O_2$ $[M+H]^+$: 193.1228, found 193.1225.

TLC: R_f = 0.56 (EtOAc:hexanes = 30:70, visualized by CAM).



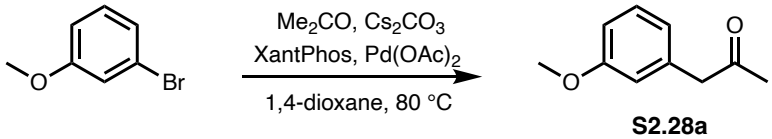
S2.28 **S2.27**

A solution of alkene **S2.28** (50 mg, 0.31 mmol) and 2,6-di-*tert*-butylpyridine (139 µL, 0.62 mmol) in CH_2Cl_2 (3.1 mL) under an argon atmosphere was cooled to 0 °C with an ice bath. Boron tribromide (617 µL of 1.0 M in heptane, 0.62 mmol) was added dropwise by syringe. The reaction mixture was allowed to stir for 5 hours, then quenched with saturated aqueous sodium bicarbonate (3 mL). The layers were separated and the aqueous layer was then extracted with $CHCl_3$ (2 x 3 mL). The combined organic extracts were washed with brine (3 mL), dried over Na_2SO_4, and concentrated under reduced pressure. The crude residue was purified by flash chromatography (SiO_2, 0–5% EtOAc in hexanes) to provide phenol **S2.27** (40 mg, 87%).

^{1}H NMR (600 MHz, $CDCl_3$): δ 7.19 – 7.13 (m, 1H), 6.77 (d, J = 7.5 Hz, 1H), 6.71 – 6.66 (m, 2H), 4.82 (s, 1H), 4.76 – 4.73 (m, 2H), 3.27 (s, 2H), 1.68 (s, 3H).

^{13}C NMR (151 MHz, $CDCl_3$): δ 155.6, 145.0, 141.9, 129.6, 121.7, 115.9, 113.2, 112.2, 44.6, 22.2.

TLC: R_f = 0.31 (EtOAc:hexanes = 20:80, visualized by p-anisaldehyde)



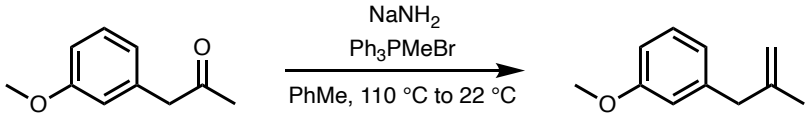
S2.28a

Based on a reported procedure.[2,3] 3-Bromoanisole (439 mg, 2.36 mmol), $Pd(OAc)_2$ (26 mg, 0.12 mmol), XantPhos (136 mg, 0.24 mmol), and Cs_2CO_3 (1.54 g, 4.72 mmol) were added to a flask equipped with a reflux condenser. 1,4-Dioxane (9.4 mL) and acetone (2.40 mL, 33.0 mmol) were

added to the reaction mixture, which was then placed to stir in a preheated 80 °C oil bath. After 17 hours the reaction vessel was removed from the oil bath and allowed to cool to 22 °C. The reaction mixture was filtered through Celite (5 g), eluting with EtOAc (3 x 10 mL). The filtrate was washed with brine (30 mL), water (30 mL), dried over Na_2SO_4, and concentrated under reduced pressure. The crude residue was purified by flash chromatography (SiO_2, 0–5% EtOAc in hexanes) to obtain ketone **S2.28a** (298 mg, 77%). The spectral data matched those reported in the literature.[2]

^{1}H NMR (500 MHz, $CDCl_3$): δ 7.27 – 7.23 (m, 1H), 6.84 – 6.78 (m, 2H), 6.76 – 6.74 (m, 1H), 3.80 (s, 3H), 3.66 (s, 2H), 2.15 (s, 3H).

TLC: R_f = 0.17 (EtOAc:hexanes = 10:90, visualized by p-anisaldehyde)



S2.28a **S2.28**

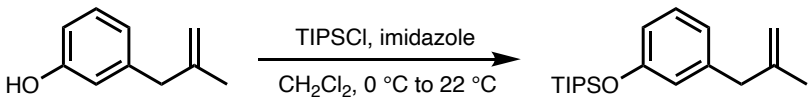
A flame-dried flask charged with Ph_3PMeBr (9.5 g, 27 mmol) was placed under vacuum and submerged in a preheated 110 °C oil bath for 2 hours. The flask was backfilled with argon and $NaNH_2$ (1.3 g, 33 mmol) was added at once. The heterogenous mixture was suspended in PhMe (89 mL) and stirred for 2 hours. The reaction vessel was removed from the oil bath and allowed to cool to 22 °C.

Methylene triphenylphosphorane (22 mL 0.30 M in PhMe, 6.7 mmol) was added to a solution of ketone **S2.28a** (273 mg, 1.66 mmol) in PhMe (20 mL) and the reaction mixture was allowed to stir. After 16 hours the reaction was quenched with saturated aqueous NH_4Cl (40 mL) and

extracted with hexanes (20 mL). The combined organic extracts were washed with water (40 mL), then brine (40 mL), dried over Na_2SO_4, and concentrated under reduced pressure. The crude residue was purified by flash chromatography (SiO_2, 0–10% CH_2Cl_2 in hexanes) to obtain alkene **S2.28** (178 mg, 66%). The spectral data matched those reported in the literature.[4]

^{1}H NMR (500 MHz, $CDCl_3$): δ 7.24 – 7.17 (m, 1H), 6.81 – 6.73 (m, 3H), 4.81 (s, 1H), 4.75 (s, 1H), 3.80 (s, 3H), 3.30 (s, 2H), 1.68 (s, 3H).

TLC: R_f = 0.38 (CH_2Cl_2:hexanes = 20:80, visualized by p-anisaldehyde)



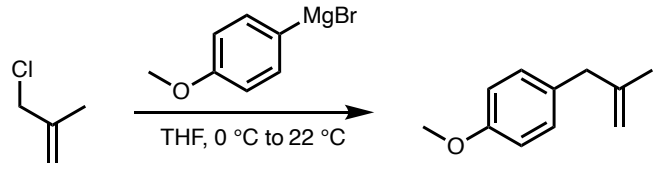
S2.27 **S2.29**

A solution of phenol **S2.27** (9 mg, 0.06 mmol) and imidazole (10 mg, 0.15 mmol) in CH_2Cl_2 (304 µL) was cooled to 0 °C with an ice bath. Triisopropylsilyl chloride (13 µL, 0.06 mmol) was added dropwise by syringe and the reaction mixture was then stirred for 5 hours. The reaction mixture was diluted with CH_2Cl_2 (500 µL) and washed with water (500 µL). Next, the organic extract was washed with 1.0 M NaOH (500 µL), brine (1 mL), dried over Na_2SO_4, and concentrated under reduced pressure. The crude residue was purified by flash chromatography (SiO_2, 100% hexanes) to provide **S2.29** (12 mg, 64%).

^{1}H NMR (600 MHz, $CDCl_3$): δ 7.15 – 7.09 (m, 1H), 6.76 (d, *J* = 7.7 Hz, 1H), 6.75 – 6.71 (m, 2H), 4.80 (s, 1H), 4.72 (s, 1H), 3.26 (s, 2H), 1.66 (s, 3H), 1.28 – 1.19 (m, 3H), 1.10 (d, *J* = 7.4 Hz, 18H).

^{13}C NMR (151 MHz, $CDCl_3$): δ 156.2, 145.3, 141.4, 129.2, 121.9, 120.7, 117.8, 112.0, 44.7, 22.1, 18.1, 12.8.

TLC: R_f = 0.37 (hexanes, visualized by p-anisaldehyde).



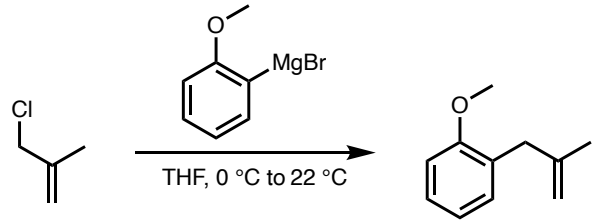
S2.30

3-Chloro-2-methylprop-1-ene (2.4 mL, 24 mmol) was dissolved in THF (7.5 mL) and cooled to 0 °C under an argon atmosphere. (4-Methoxyphenyl)magnesium bromide[5] (30 mL of 0.62 M in THF, 19 mmol) was added dropwise by syringe. The reaction was allowed to stir while warming to 22 °C. After 21 hours the reaction was diluted with Et_2O (100 mL), quenched with saturated aqueous NH_4Cl (100 mL) and extracted with Et_2O (2 x 50 mL). The combined organic extracts were washed with saturated aqueous sodium bicarbonate (100 mL), then brine (100 mL), and dried over $MgSO_4$. The crude residue was concentrated under reduced pressure and purified by vacuum distillation (90 °C at 4 mm Hg) using a kugelrohr distillation apparatus to provide alkene **S2.30** (2.3 g, 77%). The spectral data matched those reported in the literature.[6]

^{1}H NMR (499 MHz, $CDCl_3$): δ 7.10 (d, *J* = 8.6 Hz, 2H), 6.84 (d, *J* = 8.6 Hz, 2H), 4.79 (s, 1H), 4.71 (s, 1H), 3.80 (s, 3H), 3.26 (s, 2H), 1.67 (s, 3H).

HRMS (CI+): *m/z* calc'd for $C_{11}H_{14}O$ $[M]^+$: 162.1045, found 162.1044.

TLC: R_f = 0.41 (hexanes:EtOAc = 10:90, visualized by CAM).



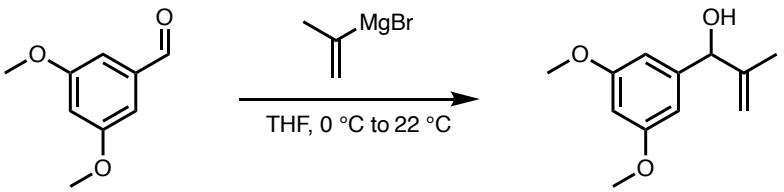
S2.31

3-Chloro-2-methylprop-1-ene (1.1 mL, 11 mmol) was dissolved in THF (8 mL) and cooled to 0 °C under an argon atmosphere. (2-Methoxyphenyl)magnesium bromide[5] (27 mL of 0.34 M in THF, 9.3 mmol) was added dropwise by syringe. The reaction was allowed to stir while warming to 22 °C. After 22 hours the reaction was quenched with saturated aqueous NH_4Cl (20 mL) and extracted with EtOAc (3 x 15 mL). The combined organic extracts were washed with 1.0 M NaOH (30 mL) then brine (30 mL), and dried over Na_2SO_4. The crude residue was concentrated under reduced pressure and purified by flash chromatography (SiO_2, 100% hexanes) to provide alkene **S2.31** (840 mg, 56%).

^{1}H NMR (500 MHz, $CDCl_3$): δ 7.20 (td, *J* = 7.8, 1.8 Hz, 1H), 7.13 (dd, *J* = 7.5, 1.8 Hz, 1H), 6.92 – 6.83 (m, 2H), 4.78 (s, 1H), 4.63 (s, 1H), 3.82 (s, 3H), 3.34 (s, 2H), 1.73 (s, 3H).

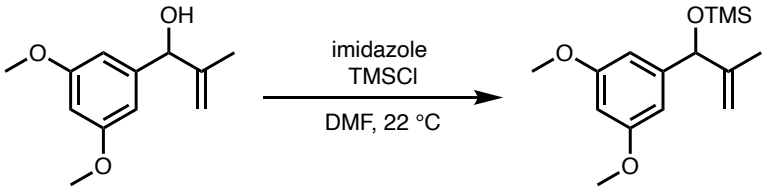
^{13}C NMR (126 MHz, $CDCl_3$): δ 157.7, 145.1, 130.5, 128.4, 127.4, 120.5, 111.4, 110.6, 55.6, 37.9, 22.7.

TLC: R_f = 0.41 (EtOAc:hexanes = 10:90, visualized by CAM).



S2.32

Carbinol **S2.32** was prepared according to a previously reported procedure.[7] The spectral data matched those reported in the literature.[7]



S2.32 **S2.33**

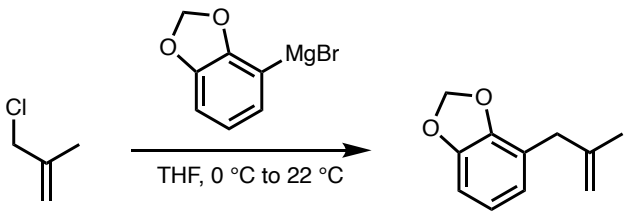
Alcohol **S2.32** (50 mg, 0.24 mmol) and imidazole (114 mg, 1.68 mmol) were dissolved in DMF (2.4 mL) under an argon atmosphere. TMSCl (152 µL, 1.20 mmol) was added dropwise by syringe and the reaction stirred at 22 °C. After 3 hours the reaction was quenched with $NaHCO_3$ (10 mL) to form a biphasic mixture, which was further diluted with $CHCl_3$ (10 mL) and water (40 mL). The layers were separated and the aqueous layer again extracted with $CHCl_3$ (3 x 10 mL). The combined organic extracts were washed with brine (40 mL), dried over Na_2SO_4, and concentrated under reduced pressure. The crude residue was purified by flash chromatography (SiO_2, CH_2Cl_2) to obtain trimethylsilyl ether **S2.33** (49 mg, 73%).

^{1}H NMR (500 MHz, $CDCl_3$): δ 6.52 (dd, *J* = 2.4, 0.7 Hz, 2H), 6.34 (t, *J* = 2.3 Hz, 1H), 5.09 – 5.07 (m, 1H), 5.04 (s, 1H), 4.87 – 4.85 (m, 1H), 3.78 (s, 6H), 1.56 (dd, *J* = 1.6, 0.9 Hz, 3H), 0.11 (s, 9H).

^{13}C NMR (126 MHz, $CDCl_3$): δ 160.7, 147.6, 145.7, 111.7, 104.4, 98.9, 78.4, 55.4, 17.5, 0.2.

HRMS (ESI+): *m/z* calc'd for $C_{15}H_{24}O_3Si$ $[M+Na]^+$: 303.1393, found 303.1406.

TLC: R_f = 0.67 (CH_2Cl_2, visualized by CAM).



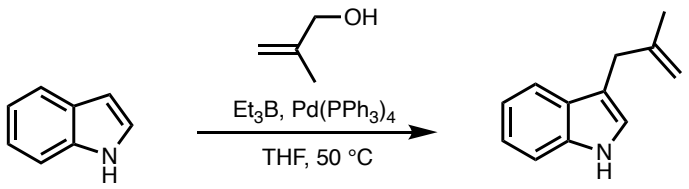
S2.35

Magnesium (41 mg, 1.7 mmol) and a small crystal of I_2 were added to a flame-dried round bottom flask equipped with a stir bar under an argon atmosphere. The heterogenous mixture was diluted in THF (1 mL) and dibromoethane (22 µL, 0.26 mmol) was added dropwise by syringe. After bubbling ceased, the reaction mixture was diluted with additional THF (4.2 mL) and cooled to 0 °C. 4-Bromobenzo[1,3]dioxole[8] (26 µL, 0.26 mmol) was then added dropwise by syringe to the cooled flask. The reaction mixture was allowed to stir for 30 minutes. The remaining 4-bromobenzo[1,3]dioxole (229 µL, 2.35 mmol) was then added to the reaction mixture and the flask was placed to stir at 50 °C in a pre-heated oil bath for 3 hours. The reaction vessel was removed from the oil bath and cooled to 0 °C. Next, 3-Chloro-2-methylprop-1-ene (0.26 mL, 2.6 mmol) was added dropwise by syringe. The reaction was then allowed to stir while warming to 22 °C for 16 hours. The reaction was quenched with saturated aqueous NH_4Cl (5 mL) and extracted with EtOAc (3 x 5 mL). The layers were separated and the combined organic extracts were washed with brine (10 mL), dried over Na_2SO_4, and concentrated under reduced pressure. The crude residue was dry-loaded onto Celite (2 g) and purified by flash chromatography (SiO_2, 0–10% CH_2Cl_2 in hexanes) to provide **S2.35** (115 mg, 50%).

^{1}H NMR (600 MHz, $CDCl_3$): δ 6.77 (t, *J* = 7.7 Hz, 1H), 6.71 (dd, *J* = 7.7, 1.3 Hz, 1H), 6.67 (dd, *J* = 7.8, 1.3 Hz, 1H), 5.93 (s, 2H), 4.81 (s, 1H), 4.72 (s, 1H), 3.29 (s, 2H), 1.74 (s, 3H).

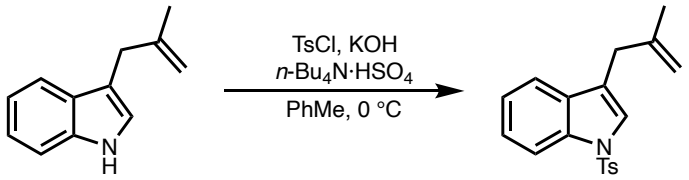
^{13}C NMR (151 MHz, $CDCl_3$): δ 147.2, 145.9, 143.9, 123.2, 121.5, 121.3, 111.9, 106.8, 100.6, 37.8, 22.4.

TLC: R_f = 0.29 (CH_2Cl_2:hexanes = 10:90, visualized by CAM)



S2.36

Indole **S2.36** was prepared according to a previously reported procedure.[9] The spectral data matched those reported in the literature.[9]



S2.36 **S2.37**

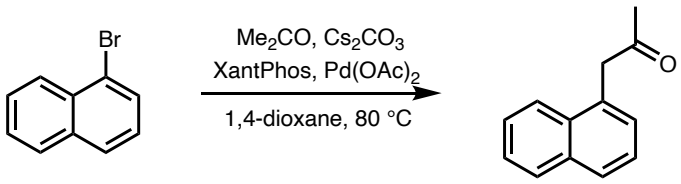
Based on a reported procedure.[10] A solution of indole **S10** (20 mg, 0.12 mmol), tetrabutylammonium hydrogensulfate (4 mg, 0.01 mmol), and 4-toluenesulfonyl chloride (27 mg, 0.14 mmol) in toluene (470 µL) under an argon atmosphere was cooled to 0 °C with an ice bath. 10.0 M KOH (160 µL, 1.60 mmol) was added dropwise by syringe to create a biphasic mixture. The mixture was stirred vigorously at 0 °C for six hours, at which time analysis by TLC indicated

full consumption of the starting material. The reaction was then diluted with H_2O (1 mL), toluene (1 mL), and the layers were separated. The aqueous layer was extracted once more with toluene (2 x 1 mL) and the combined organic extracts were then washed with brine (3 mL), dried over Na_2SO_4, and concentrated under reduced pressure. The crude residue was purified by flash chromatography (SiO_2, 0–30% CH_2Cl_2 in hexanes) to obtain indole tosylate **S2.36** (31 mg, 83%) as a colorless oil.

^{1}H NMR (600 MHz, $CDCl_3$): δ 7.98 (d, *J* = 8.3 Hz, 1H), 7.74 (d, *J* = 8.5 Hz, 2H), 7.48 (d, *J* = 7.8 Hz, 1H), 7.36 (s, 1H), 7.30 (t, *J* = 7.8 Hz, 1H), 7.21 (t, J = 7.9, 1H), 7.19 (d, J = 8.3, 2H), 4.84 (s, 1H), 4.77 (s, 1H), 3.37 (s, 2H), 2.33 (s, 3H), 1.70 (s, 3H).

^{13}C NMR (151 MHz, $CDCl_3$): δ 144.9, 143.1, 135.6, 135.4, 131.3, 129.9, 126.9, 124.7, 124.0, 123.1, 120.9, 120.0, 113.9, 112.4, 33.9, 22.3, 21.7.

TLC: R_f = 0.13 (CH_2Cl_2:hexanes = 30:70, visualized by UV).



S2.39a

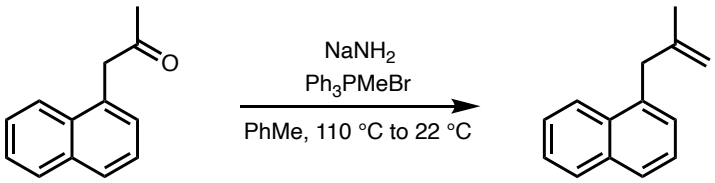
Based on a reported procedure.[2,3] 2-Bromonaphthalene[11] (300 mg, 1.46 mmol), $Pd(OAc)_2$ (16 mg, 0.07 mmol), XantPhos (84 mg, 0.15 mmol), and Cs_2CO_3 (949 mg, 2.91 mmol) were added to a flask equipped with a reflux condenser. 1,4-Dioxane (5.8 mL) and acetone (1.50 mL, 20.4 mmol) were added to the reaction mixture, which was then placed to stir in a preheated 80 °C oil bath. After 21 hours the reaction vessel was removed from the oil bath and allowed to cool to 22 °C. The

reaction mixture was diluted with EtOAc (45 mL) and brine (100 mL). The layers were separated and the organic extract was washed with water (100 mL), filtered through Celite (5 g), dried over Na_2SO_4, and concentrated under reduced pressure. The crude residue was purified by flash chromatography (SiO_2, 0–10% EtOAc in hexanes) to obtain ketone **S2.39a** (161 mg, 60%). The spectral data matched those reported in the literature.[12]

^{1}H NMR (500 MHz, $CDCl_3$): δ 7.89 (t, *J* = 8.3 Hz, 2H), 7.82 (d, *J* = 8.3 Hz, 1H), 7.56 – 7.49 (m, 2H), 7.46 (t, *J* = 7.6 Hz, 1H), 7.40 (d, *J* = 7.0 Hz, 1H), 4.12 (s, 2H), 2.12 (s, 3H).

^{13}C NMR (126 MHz, $CDCl_3$): δ 207.0, 134.0, 132.3, 131.2, 128.9, 128.3, 128.2, 126.7, 126.0, 125.7, 123.9, 49.3, 29.1.

TLC: R_f = 0.20 (EtOAc:hexanes = 10:90, visualized by $KMnO_4$)



S2.39a **S2.39**

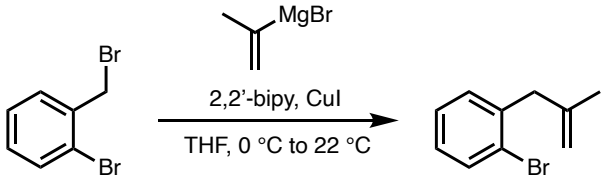
A flame-dried flask charged with Ph_3PMeBr (614 mg, 1.72 mmol) was placed under vacuum and submerged in a preheated 110 °C oil bath for 2 hours. The flask was backfilled with argon and $NaNH_2$ (84 mg, 2.15 mmol) was added at once. The heterogenous mixture was suspended in PhMe (6.4 mL) and stirred for 2 hours. The reaction vessel was then removed from the oil bath and allowed to cool to 22 °C.

Methylene triphenylphosphorane (1.6 mL 0.28 M in PhMe, 0.43 mmol) was added to a solution of ketone **S2.39a** (20 mg, 0.11 mmol) in PhMe (1.1 mL) and the reaction mixture was allowed to stir. After 17 hours the reaction was quenched with saturated aqueous NH_4Cl (4 mL) and extracted with hexanes (2 x 3 mL). The combined organic extracts were washed with water (6 mL), then brine (6 mL), dried over Na_2SO_4, and concentrated under reduced pressure. The crude residue was purified by flash chromatography (SiO_2, 100% hexanes) to obtain alkene **S2.39** (12 mg, 61%). The spectral data matched those reported in the literature.[12]

^{1}H NMR (500 MHz, $CDCl_3$): δ 8.08 – 7.99 (m, 1H), 7.90 – 7.83 (m, 1H), 7.76 (d, J = 8.2 Hz, 1H), 7.53 – 7.45 (m, 2H), 7.43 (dd, J = 8.2, 7.0 Hz, 1H), 7.35 (d, J = 6.9 Hz, 1H), 4.88 (s, 1H), 4.64 (s, 1H), 3.80 (s, 2H), 1.80 (s, 3H).

^{13}C NMR (126 MHz, $CDCl_3$): δ 144.8, 135.9, 134.0, 132.6, 128.7, 127.3, 127.1, 125.8, 125.6, 125.6, 124.5, 112.4, 41.7, 22.9.

TLC: R_f = 0.38 (hexanes, visualized by $KMnO_4$)



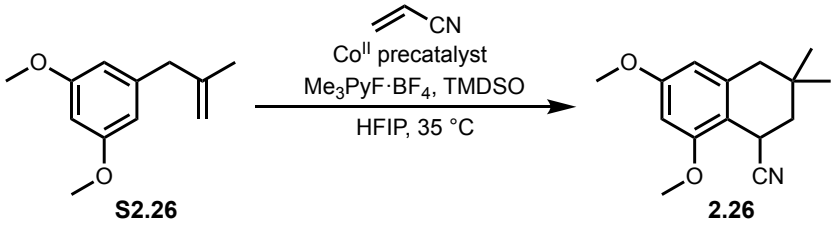
S2.40

Alkene **S2.40** was prepared according to a previously reported procedure.[13] The spectral data matched those reported in the literature.[13]

2.6.3 Annulation General Procedure

Starting material (1.0 eq.) and 1-fluoro-2,4,6-trimethylpyridinium tetrafluoroborate (2.0 eq.) were added to a vial open to air. The vial was fitted with a septum, evacuated under reduced pressure and refilled under an argon atmosphere. Separately, HFIP was degassed by sparging with argon for 15 minutes before use. Solutions of the cobalt precatalyst (2 mol%) and the electron deficient alkene (5.0 eq.) in HFIP were added sequentially by syringe. HFIP was added to adjust the final reaction concentration to 0.1 M relative to starting material. The dark green solution was stirred for five minutes at the indicated reaction temperature and then a solution of TMDSO (3.0 eq.) in HFIP was added dropwise by syringe. Gradual color changes occur over time as the reaction progresses. The mixture was stirred until consumption of starting material was observed as determined by TLC or GCMS analysis. Then the mixture was concentrated in vacuo, dissolved in CH_2Cl_2 and passed through a plug (SiO_2, EtOAc:hexanes = 50:50 to 75:25) to remove paramagnetic impurities. Unless otherwise noted, subsequent purification by flash chromatography or preparative TLC (SiO_2) permitted isolation of desired product.

2.6.4 Experimental Procedures



S2.26 **2.26**

The general procedure for annulation was used with the modifications below to transform alkene **S2.26** (10.0 mg, 52.0 µmol) and acrylonitrile (14 mg, 17 µL, 260 µmol). The crude mixture was purified using flash chromatography (SiO_2, EtOAc:hexanes = 7:93) to provide **2.26** (11.7 mg, 92%) as a colorless oil.

Co^{II} precatalyst: C1 (10 mol%).

Oxidant: $Me_3PyF{\cdot}BF_4$ (3.0 equiv).

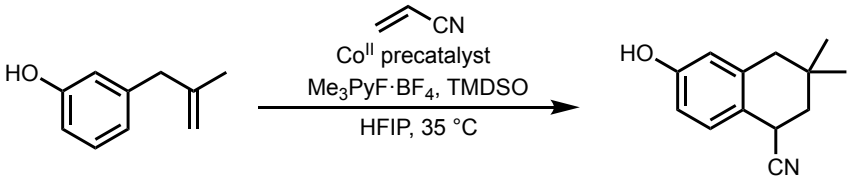
Reaction time: 40 min.

^{1}H NMR (500 MHz, $CDCl_3$): δ 6.34 (d, *J* = 2.4 Hz, 1H), 6.22 (d, *J* = 2.4 Hz, 1H), 3.91 (apparent t, *J* = 6.6 Hz, 1H), 3.88 (s, 3H), 3.79 (s, 3H), 2.58 (d, *J* = 16.3 Hz, 1H), 2.46 (d, *J* = 16.3 Hz, 1H), 1.96 (dd, *J* = 13.9, 5.7 Hz, 1H), 1.91 (dd, *J* = 13.7, 7.2 Hz, 1H), 1.14 (s, 3H), 0.97 (s, 3H).

^{13}C NMR (126 MHz, $CDCl_3$): δ 160.4, 158.6, 138.5, 122.4, 109.7, 105.5, 96.7, 55.7, 55.4, 43.5, 39.4, 29.6, 28.1, 27.7, 23.7.

HRMS (ESI+): *m/z* calc'd for $C_{15}H_{19}NO_2$ $[M+Na]^+$: 268.1313, found: 268.1317.

TLC: R_f = 0.39 (EtOAc:hexanes = 30:70, visualized by CAM).



S2.27 **2.27**

The general procedure for annulation was used with the modifications below to transform alkene **S2.27** (10.4 mg, 70 µmol) and acrylonitrile (19 mg, 23 µL, 351 µmol). The crude mixture was purified using flash chromatography (SiO_2, EtOAc:hexanes = 0:100 to 20:80 gradient) then by preparative TLC (SiO_2, acetone:Et_2O:hexanes = 26.5:12:61.5) to provide **2.27** as an inseparable mixture of regioisomers (7.8 mg, rr = 90:10, 55%) as a clear oil.

Co^{II} precatalyst: C1.

Reaction time: 16 h.

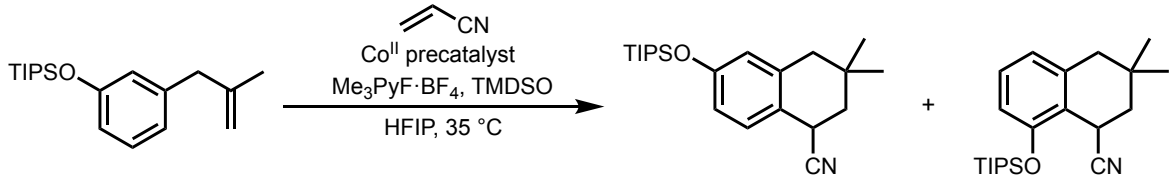
Major regioisomer **2.27**:

^{1}H NMR (600 MHz, $CDCl_3$): δ 7.32 (d, J = 8.4 Hz, 1H), 6.71 (dd, J = 8.4, 2.6 Hz, 1H), 6.56 (d, J = 2.7 Hz, 1H), 4.78 (s, 1H), 3.96 (dd, J = 10.6, 6.1 Hz, 1H), 2.61 (d, J = 16.4 Hz, 1H), 2.45 (d, J = 16.4 Hz, 1H), 1.98 (ddd, J = 13.1, 6.1, 1.9 Hz, 1H), 1.88 (dd, J = 13.2, 10.5 Hz, 1H), 1.12 (s, 3H), 0.93 (s, 3H).

^{13}C NMR (151 MHz, $CDCl_3$): δ 155.3, 137.6, 129.8, 122.5, 120.8, 116.2, 114.2, 43.0, 40.0, 30.1, 29.7, 28.4, 25.5.

HRMS (ESI+): *m/z calc'd* for $C_{13}H_{15}NO$ $[M+Na]^+$: 224.1051, found 224.1049.

TLC: R_f = 0.36 (hexanes:acetone:Et_2O = 5:2:1, visualized by PMA).



S2.29 **2.29A** **2.29B**

The general procedure for annulation was used with the modifications below to transform alkene **S2.29** (10.3 mg, 34 µmol) and acrylonitrile (9 mg, 11 µL, 169 µmol). The crude mixture was purified using flash chromatography (SiO_2, EtOAc:hexanes = 0:100 to 20:80 gradient) to provide **2.29** as a mixture of regioisomers (8.7 mg, rr = 71:29, 72%). The regioisomers **2.29A** and **2.29B**

could be separated by preparative TLC (SiO_2, 5% THF + 7.5% Et_2O + 87.5% hexanes) as a clear oil.

Co^{II} precatalyst: C1.

Reaction time: 16 h.

Major regioisomer **2.29A**:

^{1}H NMR (500 MHz, $CDCl_3$): δ 7.29 (d, *J* = 8.4 Hz, 1H), 6.75 (dd, *J* = 8.4, 2.6 Hz, 1H), 6.59 (d, *J* = 2.6 Hz, 1H), 3.96 (dd, *J* = 10.6, 6.2 Hz, 1H), 2.61 (d, *J* = 16.4 Hz, 1H), 2.43 (dd, *J* = 16.5, 1.9 Hz, 1H), 1.97 (ddd, *J* = 13.1, 6.2, 1.9 Hz, 1H), 1.88 (dd, *J* = 13.2, 10.5 Hz, 1H), 1.24 (septet, *J* = 7.3 Hz, 3H), 1.11 (s, 3H), 1.09 (d, *J* = 7.4 Hz, 18H), 0.92 (s, 3H).

^{13}C NMR (151 MHz, $CDCl_3$): δ 155.8, 137.2, 129.3, 122.6, 120.9, 120.8, 118.5, 43.1, 40.1, 30.2, 29.7, 28.4, 25.5, 18.1, 12.8.

HRMS (ESI+): *m/z* calc'd for $C_{22}H_{35}NOSi$ $[M+Na]^+$: 380.2386, found 380.2384.

TLC: R_f = 0.40 (hexanes:Et_2O:THF = 88:7:5, visualized by CAM).

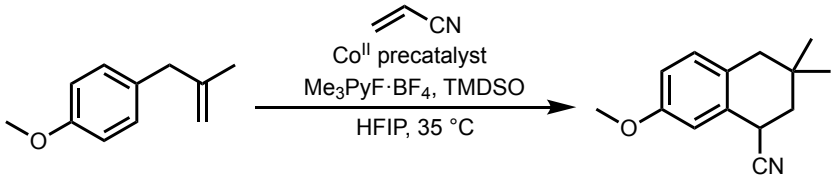
Minor regioisomer **2.29B**:

^{1}H NMR (500 MHz, $CDCl_3$): δ 7.08 (t, *J* = 7.8 Hz, 1H), 6.70 (d, *J* = 8.1 Hz, 1H), 6.67 (d, *J* = 7.7 Hz, 1H), 3.97 (dd, *J* = 7.3, 5.2 Hz, 1H), 2.62 (d, *J* = 16.3 Hz, 1H), 2.50 (d, *J* = 16.3 Hz, 1H), 2.01 (ddd, *J* = 13.7, 5.3, 1.3 Hz, 1H), 1.93 (dd, *J* = 13.7, 7.4 Hz, 1H), 1.40 (septet, *J* = 7.5 Hz, 3H), 1.18 (d, *J* = 7.5 Hz, 9H), 1.16 (s, 3H), 1.13 (d, *J* = 7.5 Hz, 9H), 0.98 (s, 3H).

^{13}C NMR (151 MHz, $CDCl_3$): δ 154.3, 138.1, 128.6, 122.1, 122.0, 115.3, 43.3, 39.7, 29.6, 28.5, 27.6, 24.5, 18.3, 18.3, 13.3.

HRMS: *m/z* calc'd for $C_{22}H_{35}NOSi$ $[M+Na]^+$: 380.2386, found 380.2393.

TLC: R_f = 0.45 (hexanes:Et_2O:THF = 88:7:5, visualized by CAM).



S2.30 **2.30**

The general procedure for annulation was used with the modifications below to transform alkene **S2.30** (10.2 mg, 62.9 µmol) and acrylonitrile (17 mg, 21 µL, 315 µmol). The crude mixture was purified using flash chromatography (SiO_2, 0–50% CH_2Cl_2 in hexanes) to provide **2.30** (7.6 mg, 56%) as a clear oil.

Co^{II} precatalyst: C1.

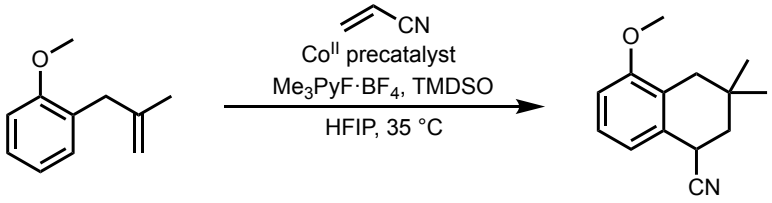
Reaction time: 23 h.

^{1}H NMR (500 MHz, $CDCl_3$): δ 7.00 (d, *J* = 8.6 Hz, 1H), 6.98 (d, *J* = 2.8 Hz, 1H), 6.81 (dd, *J* = 8.4, 2.7 Hz, 1H), 4.00 (dd, *J* = 10.6, 6.2 Hz, 1H), 3.81 (s, 3H), 2.59 (d, *J* = 16.1 Hz, 1H), 2.45 (dd, *J* = 16.1, 1.9 Hz, 1H), 1.98 (ddd, *J* = 13.2, 6.2, 1.9 Hz, 1H), 1.88 (dd, *J* = 13.3, 10.6 Hz, 1H), 1.12 (s, 3H), 0.93 (s, 3H).

^{13}C NMR (126 MHz, $CDCl_3$): δ 158.3, 131.0, 129.4, 127.8, 122.2, 114.9, 112.7, 55.5, 42.0, 39.9, 30.2, 29.9, 29.3, 25.4.

HRMS (CI+): *m/z* calc'd for $C_{14}H_{17}NO$ $[M]^+$: 215.1310, found 215.1317.

TLC: R_f = 0.18 (hexanes:CH_2Cl_2 = 50:50, visualized by CAM)



S2.31 **2.31**

The general procedure for annulation was used with the modifications below to transform alkene **S2.31** (11.0 mg, 67.9 µmol) and acrylonitrile (18 mg, 22 µL, 339 µmol). The crude mixture was purified using flash chromatography (SiO_2, CH_2Cl_2:hexanes = 0:100 to 40:60 gradient) to provide **2.31** (7.2 mg, 49%) as a clear oil.

Co^{II} precatalyst: C1.

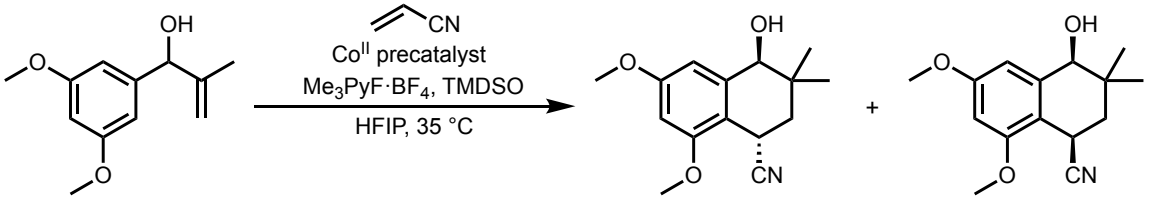
Reaction time: 18 h.

^{1}H NMR (500 MHz, $CDCl_3$): δ 7.21 (t, *J* = 8.0 Hz, 1H), 7.10 (d, *J* = 7.8 Hz, 1H), 6.78 (d, *J* = 8.1 Hz, 1H), 4.04 (dd, *J* = 10.9, 6.0 Hz, 1H), 3.82 (s, 3H), 2.60 (d, *J* = 17.5 Hz, 1H), 2.39 (d, *J* = 17.4 Hz, 1H), 1.97 (ddd, *J* = 13.1, 6.0, 1.9 Hz, 1H), 1.88 (dd, *J* = 13.1, 10.8 Hz, 1H), 1.15 (s, 3H), 0.93 (s, 3H).

^{13}C NMR (126 MHz, $CDCl_3$): δ 157.7, 129.7, 127.0, 124.9, 122.3, 120.3, 109.1, 55.5, 39.5, 36.2, 30.6, 29.1, 29.0, 25.8.

HRMS (CI+): *m/z* calc'd for $C_{14}H_{17}NO$ $[M]^+$: 215.1310, found 215.1316.

TLC: R_f = 0.25 (CH_2Cl_2:hexanes = 40:60, visualized by CAM).



S2.32 **2.32A** **2.32B**

The general procedure for annulation was used with the modifications below to transform alkene **S2.32** (13.5 mg, 65 µmol) and acrylonitrile (17 mg, 21 µL, 324 µmol). The crude mixture was purified using flash chromatography (SiO_2, CH_2Cl_2:hexanes = 0:100 to 40:60 gradient) to provide **2.32** as mixture of diastereomers (14.2 mg, dr = 50:50, 84%) as a clear oil. The diastereomers were resolved by preparative TLC (SiO_2, MeCN:CH_2Cl_2 = 4:96) and the more polar diastereomer was recrystallized by vapor diffusion using a pentane/Et_2O system.

Co^{II} precatalyst: C1.

Reaction time: 26 h.

Higher R_f diastereomer **2.32A**:

^{1}H NMR (500 MHz, $CDCl_3$): δ 6.61 (d, *J* = 2.5 Hz, 1H), 6.44 (d, *J* = 2.5 Hz, 1H), 4.26 (d, *J* = 5.0 Hz, 1H), 3.92 (t, *J* = 6.5Hz, 1H), 3.89 (s, 3H), 3.82 (s, 3H), 2.22 (dd, *J* = 14.0, 7.4 Hz, 1H), 1.88 (dd, *J* = 14.0, 5.6 Hz, 1H), 1.66 (d, *J* = 5.8 Hz, 1H), 1.14 (s, 3H), 0.98 (s, 3H).

^{13}C NMR (126 MHz, $CDCl_3$): δ 161.1, 158.3, 140.5, 122.1, 109.5, 104.6, 98.4, 75.8, 55.9, 55.6, 35.1, 34.1, 25.7, 23.3, 22.5.

HRMS (ESI+): *m/z* calc'd for $C_{15}H_{19}NO_3$ $[M+Na]^+$: 284.1263, found 284.1250.

TLC: R_f = 0.29 (MeCN:CH_2Cl_2 = 4:96, visualized by CAM).

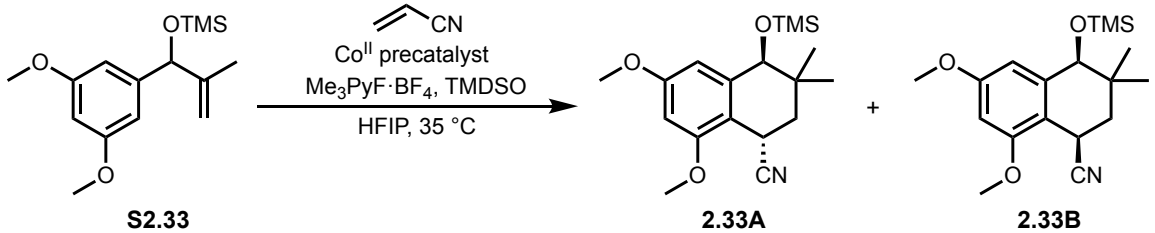
Lower R_f diastereomer **2.32B**:

^{1}H NMR (500 MHz, $CDCl_3$): δ 6.66 (d, *J* = 2.5 Hz, 1H), 6.43 (d, *J* = 2.5 Hz, 1H), 4.19 (d, *J* = 6.7 Hz, 1H), 3.89 (s, 3H), 3.85 (t, *J* = 6.7 Hz, 1H), 3.82 (s, 3H), 2.22 (dd, *J* = 14.0, 5.9 Hz, 1H), 1.91 (dd, *J* = 14.0, 7.4 Hz, 1H), 1.74 (d, *J* = 7.1 Hz, 1H), 1.13 (s, 3H), 0.98 (s, 3H).

^{13}C NMR (126 MHz, $CDCl_3$): δ 161.1, 158.4, 140.4, 122.0, 109.6, 104.1, 98.3, 76.2, 55.9, 55.6, 35.8, 34.0, 25.9, 23.2, 21.9.

HRMS (ESI+): *m/z* calc'd for $C_{15}H_{19}NO_3$ $[M+Na]^+$: 284.1263, found 284.1262.

TLC: R_f = 0.21 (MeCN:CH_2Cl_2 = 4:96, visualized by CAM).



S2.33 **2.33A** **2.33B**

The general procedure for annulation was used with the modifications below to transform alkene **S2.33** (9.5 mg, 34 µmol) and acrylonitrile (9 mg, 11 µL, 170 µmol). The crude mixture was purified using flash chromatography (SiO_2, acetone:hexanes = 0:100 to 10:90 gradient) to provide 7 as inseparable mixture of diastereomers (8.4 mg, dr = 50:50, 74%) as a clear oil. Conversion of isolated alcohols **2.32A** and **2.32B** permitted assignment of signals to stereoisomers **2.33A** and **2.33B** as indicated below.

Co^{II} precatalyst: C1.

Reaction time: 2 h.

Higher R_f diastereomer **2.33A**:

^{1}H NMR (500 MHz, $CDCl_3$): δ 6.46 (d, J = 2.4 Hz, 1H), 6.40 (d, J = 2.4 Hz, 1H), 4.29 (s, 1H), 3.91 (dd, J = 7.8, 5.9 Hz, 1H), 3.88 (s, 3H), 3.81 (s, 3H), 2.24 (dd, J = 13.9, 7.7 Hz, 1H), 1.84 (dd, J = 13.9, 5.8 Hz, 1H), 1.07 (s, 3H), 0.87 (s, 3H), 0.18 (s, 9H).

^{13}C NMR (151 MHz, $CDCl_3$): δ 160.6, 158.2, 141.3, 122.5, 109.5, 104.7, 97.9, 55.9, 55.5, 35.7, 34.7, 29.9, 26.2, 23.3, 22.8, 0.9.

HRMS (ESI+): *m/z calc'd* for $C_{18}H_{27}NO_3Si$ $[M+Na]^+$: 356.1658, found 356.1658.

TLC: R_f = 0.16 (acetone:hexanes = 4:94, visualized by CAM).

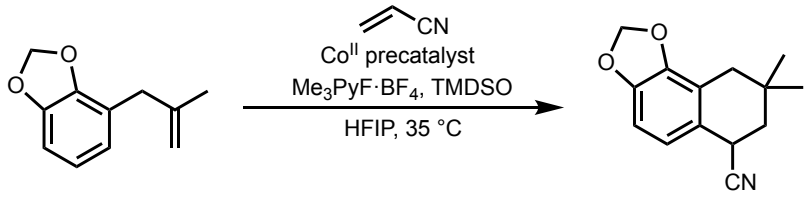
Lower R_f diastereomer **2.33B**:

^{1}H NMR (500 MHz, $CDCl_3$): δ 6.46 (d, J = 2.4 Hz, 1H), 6.41 (d, J = 2.4 Hz, 1H), 4.18 (s, 1H), 3.88 (s, 3H), 3.84 (dd, J = 7.9, 6.3 Hz, 1H), 3.81 (s, 1H), 2.27 (dd, J = 13.8, 6.2 Hz, 1H), 1.86 (dd, J = 13.9, 7.8 Hz, 1H), 1.06 (s, 3H), 0.87 (s, 3H), 0.18 (s, 9H).

^{13}C NMR (151 MHz, $CDCl_3$): δ 160.5, 158.3, 141.2, 122.2, 109.7, 104.8, 97.9, 55.9, 55.5, 35.6, 34.6, 29.9, 25.9, 23.2, 23.0, 0.9.

HRMS (ESI+): *m/z calc'd* for $C_{18}H_{27}NO_3Si$ $[M+Na]^+$: 356.1658, found 356.1647.

TLC: R_f = 0.14 (acetone:hexanes = 4:96, visualized by CAM).



S2.35 **2.35**

The general procedure for annulation was used with the modifications below to transform alkene **S2.35** (10.1 mg, 57 µmol) and acrylonitrile (15 mg, 19 µL, 287 µmol). The crude mixture was purified using flash chromatography (SiO_2, EtOAc:hexanes = 0:100 to 10:90 gradient) to provide **2.35** (9.0 mg, 74%) as a clear oil.

Co^{II} precatalyst: C1.

Reaction time: 16 h.

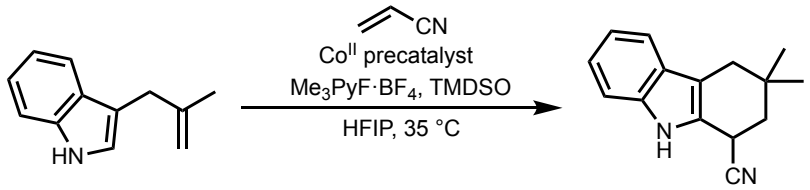
^{1}H NMR (600 MHz, $CDCl_3$): δ 6.97 (d, *J* = 8.1 Hz, 1H), 6.73 (d, *J* = 8.1 Hz, 1H), 5.97 (dd, *J* = 6.6, 1.5 Hz, 2H), 3.98 (dd, *J* = 10.8, 5.9 Hz, 1H), 2.50 (d, *J* = 16.9 Hz, 1H), 2.45 (d, *J* = 16.8

Hz, 1H), 1.97 (ddd, J = 13.2, 5.9, 1.8 Hz, 1H), 1.88 (dd, J = 13.2, 10.7 Hz, 1H), 1.16 (s, 3H), 0.95 (s, 3H).

^{13}C NMR (151 MHz, $CDCl_3$): δ 146.5, 145.8, 122.5, 122.3, 121.5, 118.2, 106.9, 101.4, 39.9, 36.0, 30.3, 29.0, 28.4, 25.6.

HRMS (ESI+): *m/z* calc'd for $C_{14}H_{15}NO_2$ $[M+Na]^+$: 252.1001, found 252.1001.

TLC: R_f = 0.23 (EtOAc:hexanes = 10:90, visualized by CAM).



S2.36 **2.36**

The general procedure for annulation was used with the modifications below to transform alkene **S2.36** (9.5 mg, 56 µmol) and acrylonitrile (15 mg, 18 µL, 278 µmol). The crude mixture was purified using flash chromatography (SiO_2, CH_2Cl_2:hexanes = 0:100 to 70:30 gradient) to provide **2.36** (3.7 mg, 30%) as a clear oil.

Co^{II} precatalyst: C1.

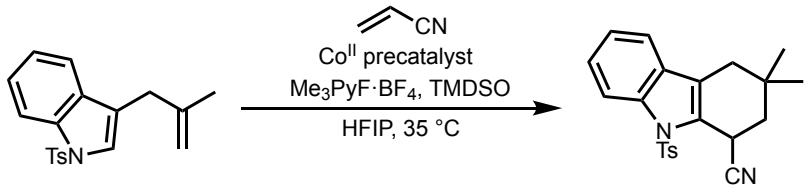
Reaction time: 17 h.

^{1}H NMR (499 MHz, $CDCl_3$): δ 8.06 (s, 1H), 7.47 (d, J = 7.8 Hz, 1H), 7.36 (d, J = 8.2 Hz, 1H), 7.22 (t, J = 7.6 Hz, 1H), 7.13 (t, J = 7.5 Hz, 1H), 4.05 (dd, J = 9.0, 6.7 Hz, 1H), 2.63 – 2.52 (m, 2H), 2.10 – 1.99 (m, 2H), 1.22 (s, 3H), 1.01 (s, 3H).

^{13}C NMR (151 MHz, $CDCl_3$): δ 136.7, 127.4, 124.2, 123.0, 120.1, 120.0, 118.7, 112.1, 111.3, 40.2, 34.4, 30.9, 30.1, 25.8, 24.4.

HRMS (CI+): *m/z* calc'd for $C_{15}H_{16}N_2$ $[M]^+$: 224.1313, found 224.1314.

TLC: R_f = 0.19 (CH_2Cl_2:hexanes = 70:30, visualized by CAM).



S2.37 **2.37**

The general procedure for annulation was used with the modifications below to transform alkene **S2.37** (9.7 mg, 30 µmol) and acrylonitrile (8 mg, 10 µL, 149 µmol). The crude mixture was purified using flash chromatography (SiO_2, EtOAc:hexanes = 0:100 to 10:90 gradient) to provide **2.37** (6.2 mg, 55%) as an opaque oil.

Co^{II} precatalyst: C1.

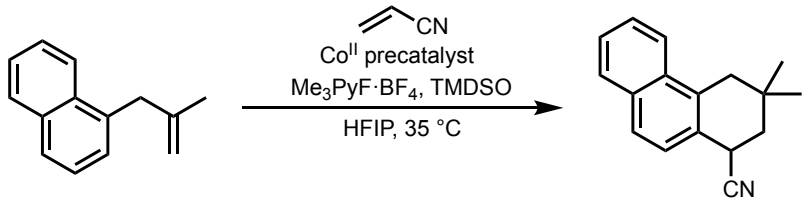
Reaction time: 23 h.

^{1}H NMR (500 MHz, $CDCl_3$): δ 8.03 (d, *J* = 8.4 Hz, 1H), 7.78 (d, *J* = 8.4 Hz, 2H), 7.38 (d, *J* = 7.7 Hz, 1H), 7.34 (td, *J* = 7.8, 1.3 Hz, 1H), 7.25 (td, *J* = 7.5, 1.0 Hz, 1H), 7.20 (d, *J* = 7.9 Hz, 2H), 4.58 – 4.52 (m, 1H), 2.57 (d, *J* = 16.5 Hz, 1H), 2.42 (dd, *J* = 16.6, 2.1 Hz, 1H), 2.33 (s, 3H), 2.12 (ddd, *J* = 13.7, 4.4, 1.2 Hz, 1H), 2.05 (dd, *J* = 13.7, 6.6 Hz, 1H), 1.25 (s, 3H), 1.10 (s, 3H).

^{13}C NMR (126 MHz, $CDCl_3$): δ 145.2, 137.0, 135.3, 130.0, 129.6, 127.1, 126.1, 125.8, 123.9, 121.8, 120.4, 119.1, 115.0, 40.5, 34.8, 29.9, 29.2, 27.4, 25.6, 21.7.

HRMS (ESI+): *m/z* calc'd for $C_{22}H_{22}N_2O_2S$ $[M+Na]^+$: 401.1300, found 401.1284.

TLC: R_f = 0.28 (EtOAc:hexanes = 20:80, visualized by CAM)



S2.39 **2.39**

The general procedure for annulation was used with the modifications below to transform alkene **S2.39** (10.5 mg, 58 µmol) and acrylonitrile (15 mg, 19 µL, 288 µmol). The crude mixture was purified using flash chromatography (SiO_2, EtOAc:hexanes = 0:100 to 5:95 gradient) to provide **2.39** (7.5 mg, 55%) as a clear oil.

Co^{II} precatalyst: C1.

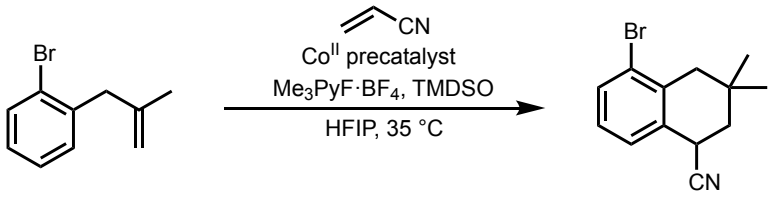
Reaction time: 18 h.

^{1}H NMR (499 MHz, $CDCl_3$): δ 8.00 (d, J = 8.2 Hz, 1H), 7.85 (dd, J = 7.8, 1.7 Hz, 1H), 7.76 (d, J = 8.5 Hz, 1H), 7.60 – 7.48 (m, 3H), 4.22 (dd, J = 10.3, 6.2 Hz, 1H), 3.01 (d, J = 16.9 Hz, 1H), 2.92 (d, J = 16.9 Hz, 1H), 2.10 (ddd, J = 13.1, 6.2, 1.7 Hz, 1H), 2.02 (dd, J = 13.1, 10.2 Hz, 1H), 1.27 (s, 3H), 1.02 (s, 3H).

^{13}C NMR (125 MHz, $CDCl_3$): δ 133.1, 132.4, 131.6, 128.8, 127.3, 126.7, 126.2, 125.9, 125.4, 123.2, 122.3, 39.4, 39.1, 30.6, 29.9, 29.6, 26.1.

HRMS (CI+): *m/z calc'd* for C17H17N $[M]^+$: 235.1361, found 235.1354.

TLC: R_f = 0.35 (EtOAc:hexanes = 10:90, visualized by CAM).



S2.40 **2.40**

The general procedure for annulation was used with the modifications below to transform alkene **S2.40** (9.8 mg, 46 µmol) and acrylonitrile (12 mg, 15 µL, 232 µmol). The crude mixture was purified using flash chromatography (SiO_2, EtOAc:hexanes = 0:100 to 4:94 gradient) to provide **2.40** (5.5 mg, 45%) as a clear oil.

Co^{II} precatalyst: C1.

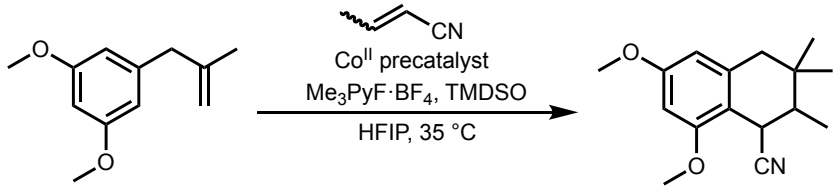
Reaction time: 6 h.

^{1}H NMR (499 MHz, $CDCl_3$): δ 7.54 (d, *J* = 7.9 Hz, 1H), 7.47 (d, *J* = 7.7 Hz, 1H), 7.12 (t, *J* = 7.8 Hz, 1H), 4.07 (dd, *J* = 10.9, 6.0 Hz, 1H), 2.67 (d, *J* = 17.4 Hz, 1H), 2.54 (d, *J* = 17.4 Hz, 1H), 2.00 (ddd, *J* = 13.2, 6.0, 1.8 Hz, 1H), 1.89 (dd, *J* = 13.2, 10.8 Hz, 1H), 1.18 (s, 3H), 0.96 (s, 3H).

^{13}C NMR (126 MHz, $CDCl_3$): δ 135.5, 132.5, 131.1, 127.8, 127.7, 126.5, 121.7, 43.4, 39.5, 30.4, 29.8, 29.5, 25.8.

HRMS (ESI+): *m/z* calc'd for $C_{13}H_{18}BrN$ $[M+Na]^+$: 286.0207, found 286.0199.

TLC: R_f = 0.35 (EtOAc:hexanes = 10:90, visualized by CAM).



S2.26 **2.41**

The general procedure for annulation was used with the modifications below to transform alkene **S2.26** (10.0 mg, 52 µmol) and acrylonitrile (14 mg, 17 µL, 260 µmol). The crude mixture was purified using preparative TLC (SiO_2, hexanes:Et_2O:EtOAc = 10:6:1) to provide **2.41** as an inseparable mixture of diastereomers (7.1 mg, dr = 66:34, 53%) as a clear oil.

Co^{II} precatalyst: C1.

Reaction time: 3 h.

(Major diastereomer)

^{1}H NMR (500 MHz, $CDCl_3$): δ 6.33 (s, 1H), 6.21 (s, 1H), 3.88 (s, 3H), 3.78 (s, 3H), 3.37 (dd, *J* = 9.8, 1.3 Hz, 1H), 2.67 (d, *J* = 16.3 Hz, 1H), 2.42 (d, *J* = 16.3 Hz, 1H), 2.01 (dq, *J* = 9.7, 6.8 Hz, 1H), 1.19 (d, *J* = 6.8 Hz, 3H), 1.09 (s, 3H), 0.72 (s, 3H).

^{13}C NMR (151 MHz, $CDCl_3$): δ 160.3, 158.4, 138.5, 122.5, 110.3, 105.3, 96.7, 55.7, 55.4, 44.9, 42.6, 32.8, 30.8, 28.8, 19.5, 14.8.

(Minor diastereomer)

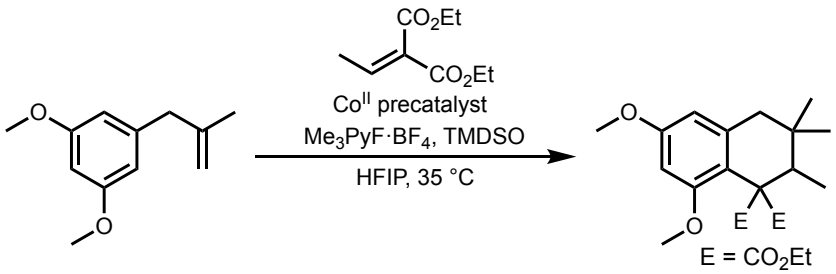
^{1}H NMR (500 MHz, $CDCl_3$): δ 6.33 (s, 1H), 6.21 (s, 1H), 3.91 (d, *J* = 6.4 Hz, 1H), 3.88 (s, 3H), 3.79 (s, 3H), 2.59 (d, *J* = 16.6 Hz, 1H), 2.53 (d, *J* = 16.6 Hz, 1H), 1.86 (p, *J* = 6.9 Hz, 1H), 1.27 (d, *J* = 7.1 Hz, 1H), 1.04 (s, 3H), 1.02 (s, 3H).

^{13}C NMR (151 MHz, $CDCl_3$): δ 160.4, 158.3, 138.4, 120.1, 111.1, 105.0, 96.5, 55.8, 55.5, 45.7, 38.6, 32.5, 30.8, 29.1, 20.3, 13.9.

(Reported for mixture of stereoisomers)

HRMS (ESI+): *m/z* calc'd for $C_{16}H_{21}NO_2$ $[M+Na]^+$: 282.1470, found 282.1479.

TLC: R_f = 0.43 (hexanes:Et_2O:EtOAc = 10:6:1, visualized by CAM).



S2.26 **2.49**

The general procedure for annulation was used with the modifications below to transform alkene **S2.26** (30.0 mg, 156 µmol) and diethyl 2-ethylidenemalonate (156 mg, 153 µL, 781 µmol). The crude mixture was purified using flash chromatography (SiO_2, CH_2Cl_2) then preparative TLC (SiO_2, acetone:hexanes = 30:70) to provide **2.49** (13 mg, 22%) as a clear oil.

Co^{II} precatalyst: C1.

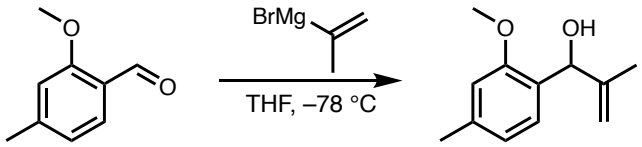
Reaction time: 16 h.

^{1}H NMR (500 MHz, $CDCl_3$): δ 6.29 (d, J = 2.5 Hz, 1H), 6.21 (d, J = 2.5 Hz, 1H), 4.24 – 4.08 (m, 3H), 4.07 – 3.98 (m, 1H), 3.79 (s, 3H), 3.69 (s, 3H), 2.67 (d, J = 16.3 Hz, 1H), 2.52 (d, J = 16.3 Hz, 1H), 2.36 (q, J = 7.2 Hz, 1H), 1.24 – 1.12 (m, 9H), 1.00 (s, 3H), 0.82 (s, 3H).

^{13}C NMR (126 MHz, $CDCl_3$): δ 172.5, 170.1, 159.6, 159.2, 138.0, 117.5, 104.9, 97.0, 61.2, 60.7, 59.3, 55.5, 55.2, 46.3, 46.2, 33.1, 30.2, 21.2, 14.2, 14.1, 12.4.

HRMS (ESI+): *m/z calc'd* for $C_{21}H_{30}O_6$ $[M+Na]^+$: 401.1940, found 401.1952.

TLC: R_f = 0.41 (acetone:hexanes = 30:70, visualized by PMA).

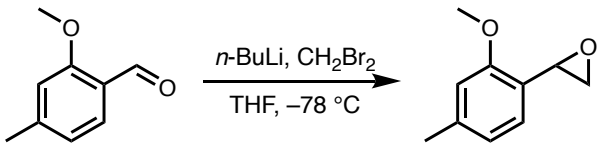


2.58 **2.59**

A solution of **2.58**[14] (250 mg, 1.66 mmol, 1 equiv.) in THF (1 mL) was added to a solution of isopropenylmagnesium bromide (0.44 M, 4.54 mL, 2.00 mmol, 1.2 equiv.) in dry THF (8.3 mL) at –78 °C. The reaction mixture was stirred overnight while warming to 23 °C. The reaction was quenched with saturated aqueous NH_4Cl (15 mL). The layers were separated and the aqueous phase was further extracted with EtOAc (2 x 5 mL). The combined organic extracts were washed with H_2O (10 mL), brine (15 mL), dried over Na_2SO_4, and concentrated under reduced pressure to afford **2.59** (320 mg, ~99%). The material was used without purification.

^{1}H NMR (500 MHz, $CDCl_3$): δ 7.15 (d, J = 7.6 Hz, 1H), 6.76 (d, J = 8.2 Hz, 1H), 6.71 (s, 1H), 5.34 (d, J = 5.6 Hz, 1H), 5.11 (d, J = 0.9 Hz, 1H), 4.95 (app q, J = 1.5 Hz, 1H), 3.84 (s, 3H), 2.61 (d, J = 5.8 Hz, 1H), 2.35 (s, 3H), 1.68 (s, 3H).

TLC: R_f = 0.35 (EtOAc:hexanes = 20:80, visualized by *p*-anisaldehyde).



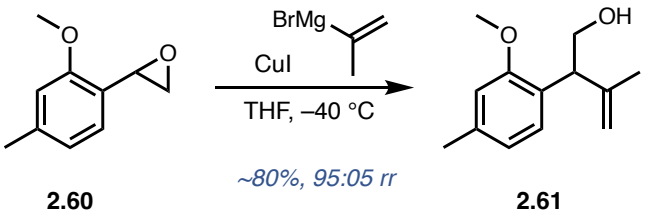
2.58 **2.60**

Dibromomethane (56 µL, 0.80 mmol, 1.2 equiv.) was added to a solution of **2.58**[14] (100 mg, 0.67 mmol, 1 equiv.) in dry THF (3.3 mL) at –78 °C. *n*-Butyllithium (2.38 M in hexanes, 310 µL, 0.73 mmol, 1.1 equiv.) was added dropwise and the reaction mixture was left to stir overnight while warming to 23 °C. The reaction was quenched with saturated aqueous NH_4Cl (3 mL) and the layers were separated. The aqueous phase was further extracted with EtOAc (2 x 5 mL), then the combined organic extracts were dried over Na_2SO_4 and concentrated under reduced pressure. The crude residue was purified by flash column chromatography (basic Al_2O_3, Grade IV, 1.7 g, 0–5% Et_2O in hexanes) to afford **2.60** (77 mg, ~70%).

^{1}H NMR (600 MHz, $CDCl_3$): δ 7.02 (d, J = 7.6 Hz, 1H), 6.77 – 6.74 (m, 1H), 6.70 (s, 1H), 4.17 (dd, J = 4.1, 2.7 Hz, 1H), 3.86 (s, 3H), 3.12 (dd, J = 5.7, 4.1 Hz, 1H), 2.71 (dd, J = 5.7, 2.7 Hz, 1H), 2.35 (s, 3H).

^{13}C NMR (151 MHz, $CDCl_3$): δ 158.2, 139.1, 125.1, 123.2, 121.4, 111.3, 55.5, 50.6, 48.4, 21.7.

HRMS (ESI+): *m/z* calc'd for $C_{10}H_{12}O_2$ $[M+H]^+$: 165.0916, found 165.0911.



Isopropenylmagnesium bromide (0.44 M, 350 µL, 0.15 mmol, 2.5 equiv.) was added dropwise to a solution of copper(I) iodide (2.3 mg, 0.012 mmol, 0.2 equiv.) in dry THF (200 µL) at –40 °C. The resulting mixture was stirred for 15 minutes, then a solution of **2.60** (10 mg, 0.061 mmol, 1 equiv.) in dry THF (200 µL) was added. The reaction mixture was stirred at –40 °C for 20 minutes and then removed from the cooling bath and stirred for 1 hour while warming to 23 °C. The reaction was quenched with saturated aqueous NH_4Cl (0.5 mL), stirred vigorously for 30 minutes, and then diluted with H_2O (1 mL) and Et_2O (1 mL). The layers were separated and the aqueous phase was further extracted with Et_2O (2 x 1 mL). The combined organic extracts were washed with saturated aqueous NH_4Cl (3 mL), brine (3 mL), dried over Na_2SO_4, and concentrated under reduced pressure to afford **2.61** (10 mg, ~80%).

^{1}H NMR (500 MHz, $CDCl_3$): δ 7.05 (d, J = 7.7 Hz, 1H), 6.76 – 6.73 (m, 1H), 6.71 (s, 1H), 5.03 (s, 1H), 4.91 (s, 1H), 3.98 – 3.94 (m, 1H), 3.93 – 3.89 (m, 1H), 3.84 – 3.80 (m, 4H), 2.34 (s, 3H), 1.68 (s, 3H).

^{13}C NMR (126 MHz, $CDCl_3$): δ 157.7, 145.3, 137.9, 127.8, 125.4, 121.4, 111.9, 111.5, 64.3, 55.6, 46.9, 22.8, 21.6.

TLC: R_f = 0.28 (EtOAc:hexanes = 20:80, visualized by *p*-anisaldehyde).

2.6.5 Supplemental References

(1) Matsuki, H.; Okubo, K.; Takaki, Y.; Niihori, Y.; Mitsui, M.; Kayahara, E.; Yamago, S.; Kobayashi, K. *Angew. Chem. Int. Ed.* **2021**, *60*, 998–1003.

(2) Hesp, K. D.; Lundgren, R. J.; Stradiotto, M. *J. Am. Chem. Soc.* **2011**, *133*, 5194–5197.

(3) Palucki, M.; Buchwald, S. L. *J. Am. Chem. Soc.* **1997**, *119*, 11108–11109.

(4) Seomoon, D.; Lee, K.; Kim, H.; Lee, P. H. *Chem. Eur. J.* **2007**, *13*, 5197–5206.

(5) Cromwell, S.; Sutio, R.; Zhang, C.; Such, G. K.; Lupton, D. W. *Angew. Chem. Int. Ed.* **2022**, *61*, e202206647.

(6) Zhao, K.; Knowles, R. R. *J. Am. Chem. Soc.* **2022**, *144*, 137–144.

(7) Sudhakar, G.; Satish, K. *Chem. Eur. J.* **2015**, *21*, 6475–6480.

(8) Kobayashi, Y.; Lalitnorasate, P.; Kaneko, Y.; Kiyotsuka, Y.; Endo, Y. *Tetrahedron Lett.* **2010**, *51*, 6018–6021.

(9) Kimura, M.; Futamata, M.; Mukai, R.; Tamaru, Y. *J. Am. Chem. Soc.* **2005**, *127*, 4592–4593.

(10) Wang, K.; Liu, Z. *Synth. Commun.* **2009**, *40*, 144–150.

(11) Tang, R.-J.; Milcent, T.; Crousse, B. *J. Org. Chem.* **2018**, *83*, 930–938.

(12) MacMillan, J. W. M.; McGuire, R. T.; Stradiotto, M. *Chem. Eur. J.* **2022**, *28*.

(13) Watson, I. D. G.; Ritter, S.; Toste, F. D. *J. Am. Chem. Soc.* **2009**, *131*, 2056–2057.

(14) Kumari, A.; Suresh, M.; Singh, R. B. *Tetrahedron* **2021**, *92*, 132282.

CHAPTER 3. STUDIES TOWARDS A SYNTHESIS OF ASPERTERPENOID A

3.1 Introduction

Owing to their striking molecular architectures and broad biological activities, sesterterpenoid natural products have long attracted the interests of organic chemists. The smallest component of the terpenome (n = ~1000), these natural products are comprised of five isoprene units and have been isolated from fungi, bacteria, lichens, plants, insects, and marine sponges alike.[1,2] Within this subclass, fewer still belong to the so-called *trans*-hydrindane sesterterpenoids; the carbocyclic skeleton of these natural products includes a *trans*-hydrindane ring system bearing an isopropyl group, whose relationship with the hydrindane angular methyl may be *anti* or *syn* respectively (**Figure 3.1**).[3] Curiously, the hydrindane ring system in these natural products is systematically fused to rest of the scaffold in one of two ways: across C4/C5 or across C5/C6. This observation has led to an additional layer of useful subtyping within the sesterterpenoids, wherein C4/C5 fusion is termed type B and C5/C6 fusion is termed type A.[4,5]

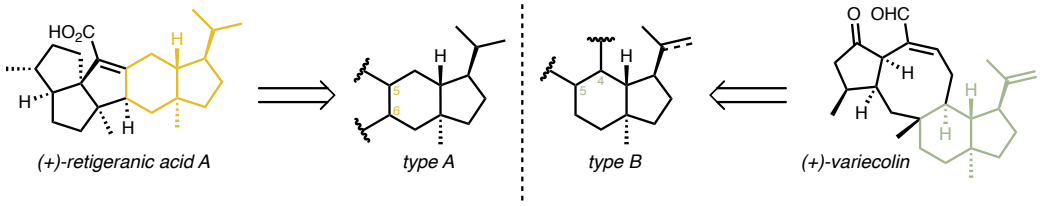


Figure 3.1 *Two modes of ring fusion in trans-hydrindane sesterterpenoids*

Thus, retigeranic acid A is a type A *trans*-hydrindane sesterterpenoid and variecolin is a type B *trans*-hydrindane sesterterpenoid. As the focus of seemingly-countless synthetic endeavors (and with the latter still evading the efforts of total synthesis), these two natural products exemplify the risks and rewards associated with the enterprise of total synthesis among the *trans*-hydrindane sesterterpenoid natural products.[6–18]

3.2 Isolation of Asperterpenoid A

The sesterterpenoid natural product known as asperterpenoid A (**3.1**) was first isolated in 2013 from endophytic marine fungus *Aspergillus* sp. 16-5c (**Figure 3.2**).[19] Extraction of fungal mycelia and the rice growth medium provided the authors with 6.8 g of an organic residue that was chromatographed to provide 0.8 mg (0.01 wt%) of **3.1**.[19] The authors were able to unambiguously determine the structure of **3.1** structure by single-crystal X-ray diffraction which confirmed the new sesterterpenoid ring system.[19]

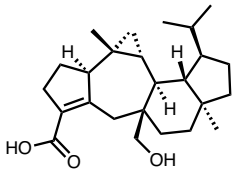


Figure 3.2 *Structure of asperterpenoid A* ***(3.1)***

3.3 Biosynthesis of Asperterpenoid A

3.3.1 Sesterterpenoid Biosynthesis

All sesterterpenoid natural products are derived from the activity of sesterterpene synthases. While the processes of chain-elongation and cyclization are traditionally performed by individual enzymes, fungi produce bifunctional enzymes that couple the two functions together over two discrete domains: the C-terminal domain acts as the prenyl transferase (PT) that facilitates the synthesis of geranylfarnesyl diphosphate (GFPP) whereas the N-terminal domain acts as the terpene synthase (TS) subunit that facilities highly controlled polycyclizations of GFPP.[1] Subsequent modifications to the sesterterpenoid skeleton are performed by downstream tailoring enzymes.

Naturally, preorganization of GFPP in the TS active site enables the selective participation of a pair of alkenes during the first step of the cyclization cascade (**Figure 3.3**). It is presently

believed that all sesterterpene synthases initiate cyclization of GFPP through one of two discrete modes based on the cationic intermediate that forms; type A cyclization (C1 with alkenes IV and V) leads to 5/15 bicyclic cation **3.2** while type B cyclization (C1 with alkenes III and IV) leads to 5/11 bicyclic cation **3.3**.[20–22] Notably, the specific configuration of the cyclopentane stereotriad is not uniformly determined by the mode of cyclization but rather by the specific identity of the sesterterpene synthase.

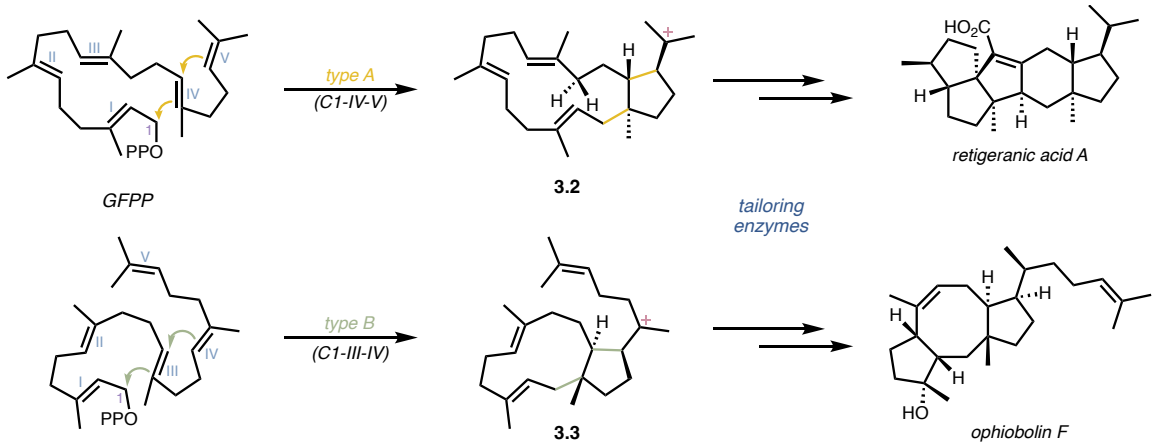


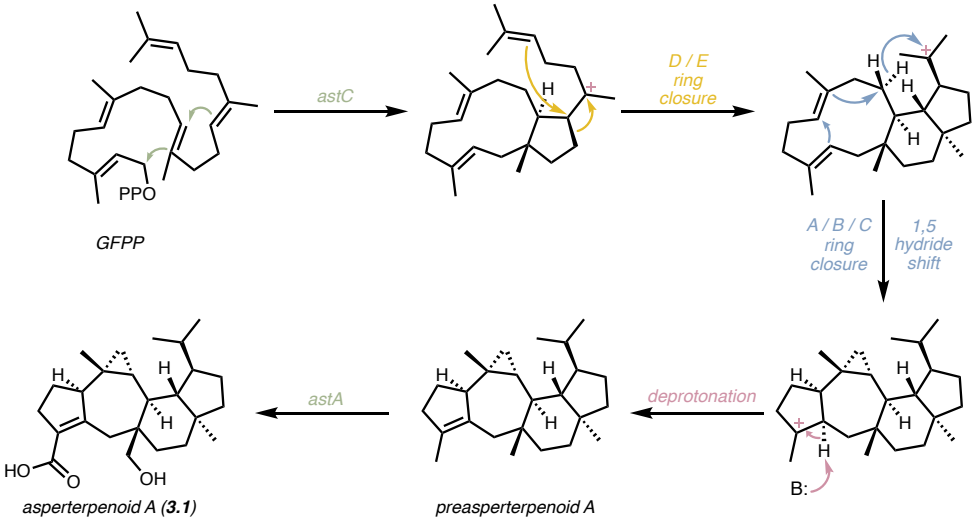
Figure 3.3 *Two modes of cyclization initiate canonical sesterterpenoid biosynthesis*

3.3.2 Asperterpenoid A Biosynthesis

In 2017, analysis of the *Talaromyces verruculosus* (previously *Penicillium verruculosum* TPU1311) genome enabled the discovery and characterization of a gene cluster that appeared to be related to sesterterpene biosynthesis.[23] Heterologous expression in *Aspergillus oryzae* NSAR1 revealed that the gene product is a type B sesterterpene synthase, which they named PvPs, and that one role of PvPS is to convert GFPP to preasperterpenoid A.[23] Separately, a three gene cluster (*astA–C*) discovered in *Talaromyces wortmannii* ATCC 26942 was also shown to produce preasperterpenoid A; the authors would later determine that the amino acid sequences of AstC and PvPS are highly similar (71% identity).[24] Direct conversion of preasperterpenoid A to asperterpenoid A is guided by a CYP450 oxidase that itself is the gene product of *astB*.[24]

A proposed mechanism for the cyclization of GFPP to form preasperterpenoid A is provided below (**Scheme 3.1**) and is strongly corroborated by a series of labeling experiments. In these studies, all 25 isotopomers of ($^{13}C_1$)GFPP were prepared and converted by PvPS to preasperterpenoid A; analysis of the spectral data in each case revealed ^{13}C incorporation in appropriate accord with the mechanism depicted.[23]

Scheme 3.1 *Proposed biosynthesis of asperterpenoid A*



3.4 Bioactivity of Asperterpenoid A

In the isolation report, the authors note that asperterpenoid A inhibits *Mycobacterium tuberculosis* protein tyrosine phosphatase B (*m*PTPB; IC_{50} = 2.2 μM); this protein is essential to the survival of bacterial cells that cause the infectious disease known as tuberculosis (TB).

3.4.2 Tuberculosis

Prehistoric in origin, the root cause of tuberculosis was not established until 1882 when Robert Koch identified the bacterial species now known as *Mycobacterium tuberculosis*.[25–27] Approximately one third of the global population has active TB or is otherwise infected with *M. tuberculosis*. Conventional measures for the prevention, diagnosis, and treatment of TB have waned

in efficacy over the past century and as a result TB remains the second leading cause of death due to infectious disease.[26] The emergence of multi-drug resistant TB (MDR-TB) and extensive-drug resistant TB (XDR-TB) has only exacerbated this public health crisis.[27–29]

Infections causing tuberculosis are treated with a combination of several antibiotics that render *M. tuberculosis* unviable through one of three usual modes: (1) inhibition of transcription; (2) inhibition of translation; or (3) inhibition of cell wall synthesis (**Figure 3.4**).[30,31] Phenotypic variation in *M. tuberculosis* promotes drug tolerance or outright resistance.[31] Such outcomes are also common in cases where a variety of geographical or sociological conditions lead to inadequate diagnosis or treatment of TB.

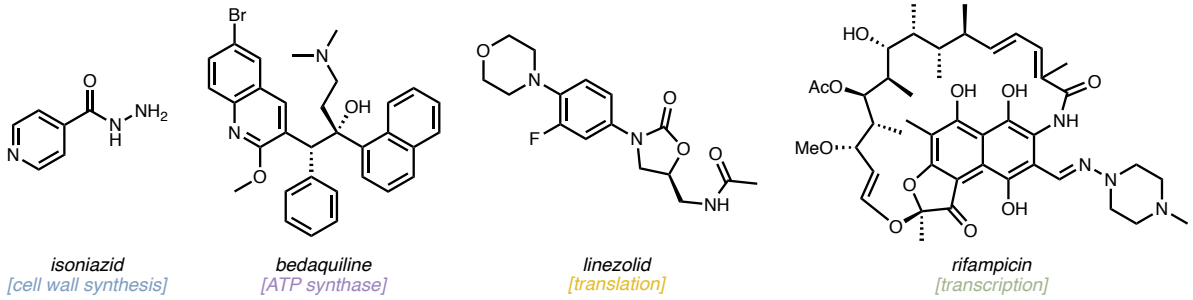


Figure 3.4 *Representative TB chemotherapeutics and associated modes of inhibition*

Remediation of treatment in MDR- and XDR-TB cases will likely benefit from drugs that operate orthogonally to existing chemotherapeutics, and so the discovery and validation of new therapeutic targets for TB treatment remains a valuable endeavor.

3.4.3 The Role of mPTPB

As an intracellular pathogen, *M. tuberculosis* is known to especially proliferate in host macrophage cells.[32] This unusual choice of refuge is facilitated by proteins secreted by *M. tuberculosis*; these so-called virulence factors are essential in that they enable *M. tuberculosis* to evade detection by the host immune system.[33] *M. tuberculosis* protein tyrosine phosphatase B

(*m*PTPB) is a virulence factor that is suspected to remove phosphoryl groups from host proteins, and in this way is implicated in the disruption of cytokine signaling pathways that would otherwise lead to host immune response.[34,35] Disruption of *m*PTPB via gene deletion or small molecule inhibition has been demonstrated to restore immune function and attenuate the pathogenicity of *M. tuberculosis*.[33,35–37] While the human proteome encodes for a number of tyrosine phosphatases, none of these are orthologs to *m*PTPB, and so treatments promoting *m*PTPB inhibition are expected to display high selectivity profiles with minimal side effects.[37] Altogether, *m*PTPB holds demonstrable potential as a therapeutic target for the treatment of TB and is complementary to the antibiotic regimen that is typically prescribed (*vide supra*).

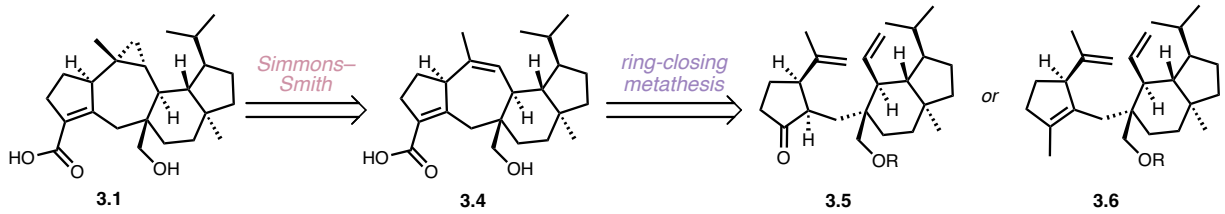
Because the tertiary structure of *m*PTPB possesses several discrete binding pockets, a variety of molecular scaffolds have been utilized in the design of *m*PTPB inhibitors.[38] Despite their great potential, *m*PTPB inhibitors remain absent in the pipeline and marketplace alike; invariably, efforts to develop small molecule candidates targeting *m*PTPB have struggled to achieve the necessary balance of potency, selectivity, and efficacy.[36,39] The binding mode of asperterpenoid A to *m*PTPB is presently unknown and could inform the rational design of novel *m*PTPB inhibitors that circumvent the issues otherwise precluding their successful development. The low relative natural abundance of asperterpenoid A therefore warrants the efforts of total synthesis to permit an investigation into this matter.

3.5 Retrosynthesis of Asperterpenoid A

Our analysis of the pentacyclic framework of asperterpenoid A suggested that efficient synthesis of the natural product might be best realized through strategies that target a convergent fragment coupling (**Scheme 3.2**). To this end, we first disconnected the cyclopropane ring in asperterpenoid A back to cycloheptene **3.4**. The cycloheptene ring in **3.4** could likely be generated

through ring-closing metathesis, and in this way we were led to consider of various permutations of suitable tricyclic intermediates that might each be the products of fragment coupling. We ultimately settled on tricyclic intermediates **3.5** and **3.6**, which we reasoned could be put together by a radical or polar coupling strategies respectively.

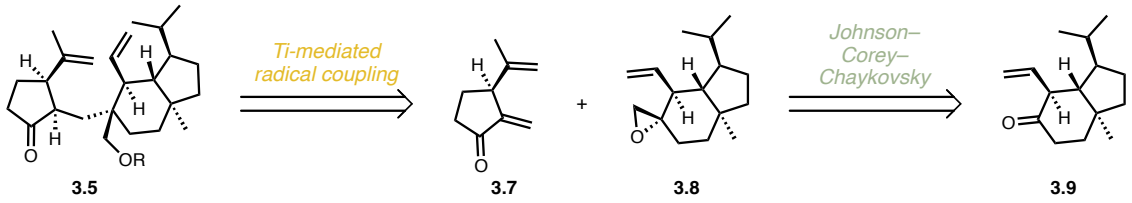
Scheme 3.2 *Disconnection of asperterpenoid A prioritizes two fragment coupling approaches*



3.5.1 Radical Disconnection

Based on work by Nugent and RajanBabu, we proposed that the synthesis of **3.5** might be achieved via a titanocene-mediated radical fragment coupling between **3.7** and **3.8** (**Scheme 3.3**).[40] Considering these two fragments, it seemed that a practical synthesis of **3.7** could be quickly realized from cyclopentenone. Retrosynthetic analysis of **3.8** suggests disconnection of the epoxide to β-γ unsaturated ketone **3.9**, a fragment whose synthesis would ultimately prove most capricious.

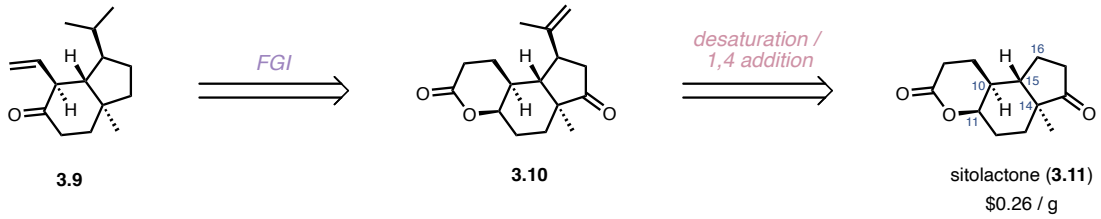
Scheme 3.3 *Disconnection of the common intermediate by radical fragment coupling*



At first glance, the *trans*-hydrindane ring and carbonyl function in **3.9** suggests Hajos–Parrish ketone as a quintessential starting point for the synthesis. While a very reasonable choice as a precursor to **3.9**, a more thoughtful analysis led us to designate sterol-derived sitolactone (**3.11**) as our point of entry (**Scheme 3.4**).[41] We valued this choice for several reasons: (1) the presence of oxidation at C11 (asperterpenoid A numbering) could provide the requisite ketone

function in **3.9**; (2) oxidative dehomologation of the lactone could be used to form the vinyl group in **3.9**; (3) the absolute configurations of C10 / C14 / C15 (asperterpenoid A numbering) in the *trans*-hydrindane system are the same as those found in asperterpenoid A; (4) the carbonyl function at C18 (asperterpenoid A numbering) could be used to introduce the isopropyl group located at C16; and (5) the cost of **3.11** is quite low ($0.26 per gram).

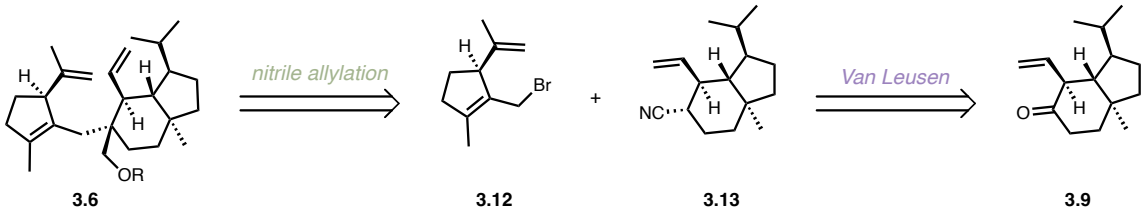
Scheme 3.4 *Retrosynthetic analysis of β,γ-unsaturated ketone* ***3.9***



3.5.2 Polar Disconnection

In a similar manner, synthesis of **3.6** might be realized through an ionic coupling between the known bromide **3.12** and the nitrile-stabilized carbanion of **3.13** (**Scheme 3.5**). The nitrile function of **3.13** could be introduced via Van Leusen homologation of the same β,γ-unsaturated ketone (**3.9**). We found the coincidence of intermediate **3.9** meaningful in that it would permit both strategies to be explored at once.

Scheme 3.5 *Disconnection of the common intermediate by polar fragment coupling*

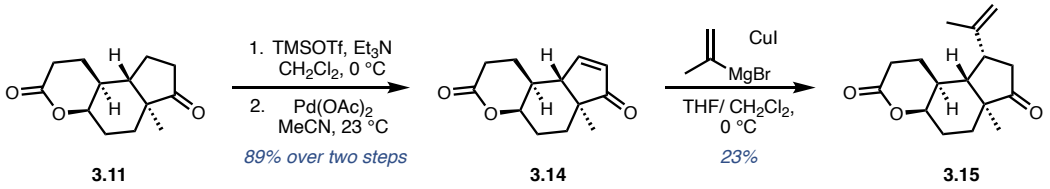


3.6 Attempted Synthesis of 3.9 From Sitolactone

Our efforts to generate **3.9** commenced with the introduction of unsaturation to the cyclopentanone ring of sitolactone via Saegusa–Ito oxidation (**Scheme 3.6**). Exactly following a

procedure by Gui and coworkers, formation of the requisite enoxysilane proved to be a complicated matter.[42] In all cases, the written procedure generated a statistical mixture of enoxysilane and silyl ketene acetal products. A solution was eventually determined in which syringe pump-addition of TMSOTf over two hours to a cold solution of sitolactone and triethylamine led to exclusive formation of the desired enoxysilane. Though this material could be purified, we found it convenient to directly subject the crude enoxysilane to Saegusa–Ito oxidation using modified conditions reported by Danishefsky which allowed us to obtain enone **3.14** in 89% over two steps.[43] In their synthesis of ritterazine B, the Reisman group was able to introduce unsaturation to a similar hydrindanone ring system through an α-bromination/elimination sequence; unfortunately this chemistry was unsuccessful in its application here.[44] Such a result suggests that neither of the vicinal protons in the substrate adopt a suitable *anti*-periplanar arrangement that would otherwise facilitate E2 elimination of bromide. Nevertheless, enone **3.14** represents a suitable substrate for 1,4 addition chemistry utilizing cuprate nucleophiles; in this case the cuprate generated from isopropenylmagnesium bromide and copper(I) iodide led to incorporation of the isopropenyl group exclusively from the *re* face of **3.14** to form **3.15** in low yield; here, the configuration of the newly-formed stereogenic center is opposite that found in asperterpenoid A.

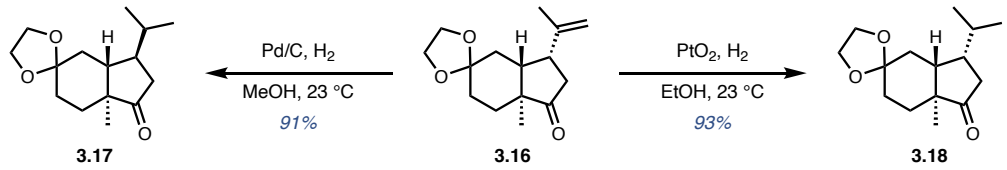
Scheme 3.6 *Desaturation and cuprate conjugate addition to sitolactone*



This was not entirely unsurprising, as a similar result had been obtained by Trauner and coworkers in the synthesis of (–)-nitidasin. Importantly, the authors discovered that the allylic methine in **3.16** was epimerized under hydrogenating conditions, and ultimately found this event

to be highly dependent on the identity of the transition metal catalyst used (**Scheme 3.7**).[3,45,46] While systems employing platinum(IV) oxide provided ketone **3.18** as the major product, reducing systems with palladium unexpectedly formed its epimer **3.17**.

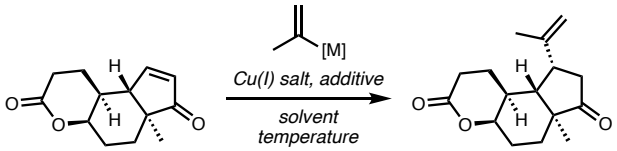
Scheme 3.7 *Work by Trauner reveals an unexpected epimerization*



Because our group's relatively recent synthesis of wickerols A and B featured a conjugate addition whose stereochemical outcome was highly sensitive to the reaction conditions employed, we presumed that the stereochemical outcome of cuprate addition to **3.14** might similarly be perturbed. If unsuccessful, we reasoned that we could epimerize this stereocenter (à la Trauner) during palladium-mediated hydrogenation of the alkene in **3.15**.

With the two-fold goal of improving yield and reversing the stereochemical outcome, our initial experiments (**Table 3.1**, entries 1–3) revealed that temperature plays a significant role regarding product distribution and overall yield of the 1,4 adduct. In a mixture THF and CH_2Cl_2 we found that higher reaction temperatures (entries 1–2) led to formation of numerous byproducts (not characterized). Lowering the reaction temperature to –78 °C (entry 3) resulted in high selectivity for the desired 1,4 adduct. Switching the ethereal solvent from THF to diethyl ether (entry 4) results in an erosion of this product selectivity and indicates that both solvent and temperature are important parameters for this transformation. Several typical copper(I) sources were also considered (entries 5-7); here CuBr·Me_2S was found to be superior to CuCl, CuCN, or CuI. Use of the lithiocuprate (entry 8) also failed to reverse the stereochemical outcome.

Table 3.1 *Optimization of cuprate conjugate addition to* ***3.14***



3.14 **3.15**

Entry	*Solvent*	*[M]*	*CuX*	*T (°C)*	*dr*	*Additive*	*Yield*[a]
1	THF:CH_2Cl_2 (5:3)	MgBr	CuI	0	99:01	–	23%
2	THF:CH_2Cl_2 (5:3)	MgBr	CuI	–42	99:01	–	27%
3	THF:CH_2Cl_2 (5:3)	MgBr	CuI	–78	99:01	–	48%
4	Et_2O:CH_2Cl_2 (5:3)	MgBr	CuI	–78	99:01	–	30%
5	THF:CH_2Cl_2 (5:3)	MgBr	CuBr·Me_2S	–78	99:01	–	53%
6	THF:CH_2Cl_2 (5:3)	MgBr	CuCl	–78	99:01	–	52%
7	THF:CH_2Cl_2 (5:3)	MgBr	CuCN	–78	99:01	–	35%
8	THF:CH_2Cl_2 (5:3)	Li	CuBr·Me_2S	–78	99:01	–	40%
9	THF:CH_2Cl_2 (5:3)	MgBr	CuBr·Me_2S	–78	99:01	TMSCl (5 eq.)	51%
10	THF:CH_2Cl_2 (5:3)	MgBr	CuBr·Me_2S	–78	99:01	HMPA (5 eq.)	35% (+20% rsm)
11	THF:CH_2Cl_2 (5:3)	MgBr	CuBr·Me_2S	–78	99:01	BF_3·OEt_2 (5 eq.)	52%
12	THF:CH_2Cl_2 (5:3)	MgBr	CuBr·Me_2S	–78	99:01	DMPU (5 eq.)	26%
13	THF:CH_2Cl_2 (5:3)	MgBr	CuBr·Me_2S	–78	99:01	HMPA (5 eq.) + TMSCl (5 eq.)	66%
14	THF:CH_2Cl_2 (5:3)	MgBr[b]	CuBr·Me_2S[b]	–78	99:01	–	59%
15	THF:CH_2Cl_2 (5:3)	MgBr[b]	CuBr·Me_2S[b]	–78	99:01	HMPA (5 eq.) + TMSCl (5 eq.)	74%

[a]yields by ^{1}H NMR w/ 5,6-dibromobenzo[1,3]dioxole standard; [b]1.6 eq. of magnesiocuprate formed; full consumption of SM observed in all cases unless noted

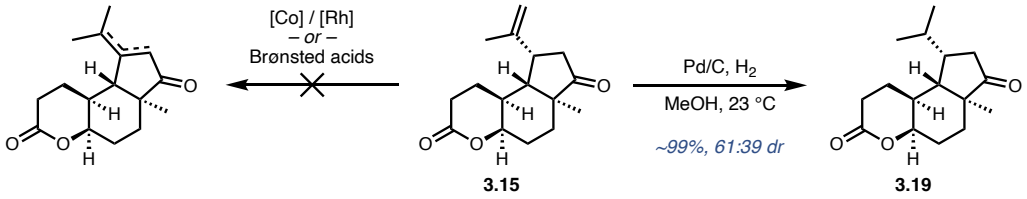
TMSCl, BF_3·OEt_2, and HMPA are frequently incorporated as additives in cuprate conjugate addition reactions. Their discrete roles in various copper-based transformations have been the subject of numerous works and are still hotly debated to this day.[47–56] Testing their effects in this system (entries 9–13), we found the inclusion of either TMSCl or BF_3·OEt_2 (entry 9 and entry 11) had no effect on reaction outcome. Use of highly polar, aprotic cosolvents such as HMPA or DMPU (entry 10 and entry 12) resulted in dramatically lower yields. Though poorly understood, TMSCl and HMPA are believed to display unusual synergistic effects when used together. Such a result was also observed in this system, where inclusion of both additives (entry 13) increased the yield of **3.15** to 66%. Separately, we found that increasing the amount of magnesiocuprate in the

reaction (entry 14) also served to increase the yield of **3.15**. Combining entries 13 and 14, we were able to obtain 74% of ketone **3.15** as a single diastereomer.

While we had succeeded in our efforts to improve the overall efficiency of this transformation, we only ever observed formation of the undesired stereoisomer. We conclude that the steric encumbrance of the lactone ring precludes nucleophilic addition to the *si* face of the π system. Fighting an uphill battle on this front, we decided it would be more meaningful to investigate chemistry that might permit epimerization of this stereocenter.

We discovered that palladium-mediated hydrogenation of the alkene in the **3.15** also facilitated epimerization, in this case leading to a 61:39 mixture of diastereomers in which the undesired stereoisomer (**3.19**) was the major component (**Scheme 3.8**). Efforts to isomerize the disubstituted alkene of **3.15** using a variety of transition-metal- or Brønsted-acid-mediated transformations all proved unsuccessful and either returned only starting material or otherwise facilitated its decomposition.[57,58]

Scheme 3.8 *Epimerization/isomerization of* ***3.15***

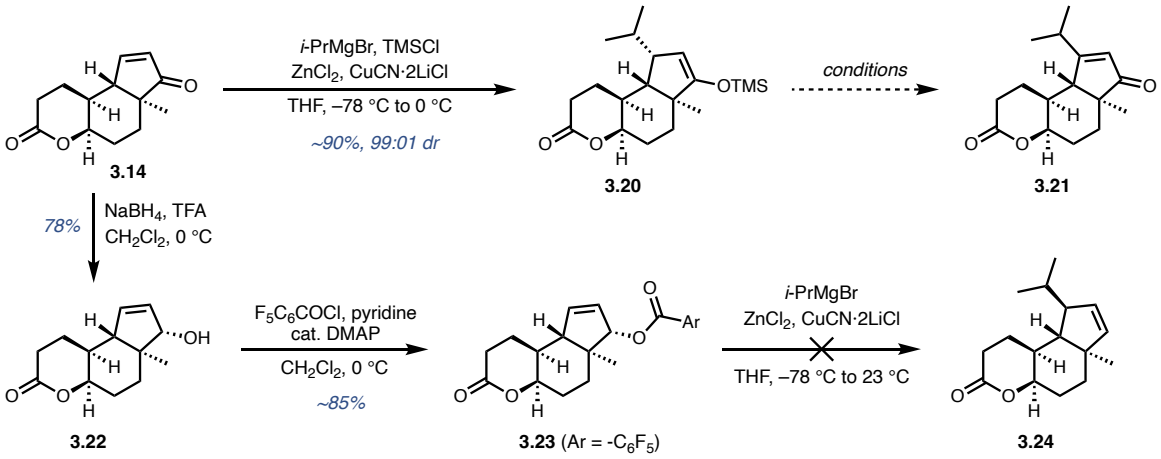


Stymied by these results but undeterred, we explored two new approaches. Our earlier experiments had revealed that trapping of the enolate produced in the conjugate addition was a highly efficient process. We reasoned that enoxysilane **3.20** might be leveraged in various ways to access to enone **3.21**, in which the stereochemical outcome of the cuprate conjugate addition is rendered inconsequential (**Scheme 3.9**). The propensity of cuprate-based nucleophiles to add from

the convex face of enone **3.14** led us to reason that hydride delivery to **3.21** might display similar selectivity.

At the same time, we were drawn to work by Knochel and coworkers in which cuprates derived from dialkylzinc reagents were utilized in highly selective *anti*-S_N2'-type allylic substitutions.[59,60] While we could easily derivatize enone **3.14** to pentafluorobenzoyl ester **3.22**, we were surprised to find that exposure of this material to the reaction conditions required for this transformation returned only starting material (**Scheme 3.9**). It appears that each component is so strongly biased towards opposing modes of addition that the result is no reaction. The outcome here prompted us at this time to consider other ways in which the nascent enolate or enoxysilane might be repurposed to access **3.21** via difunctionalized intermediates.

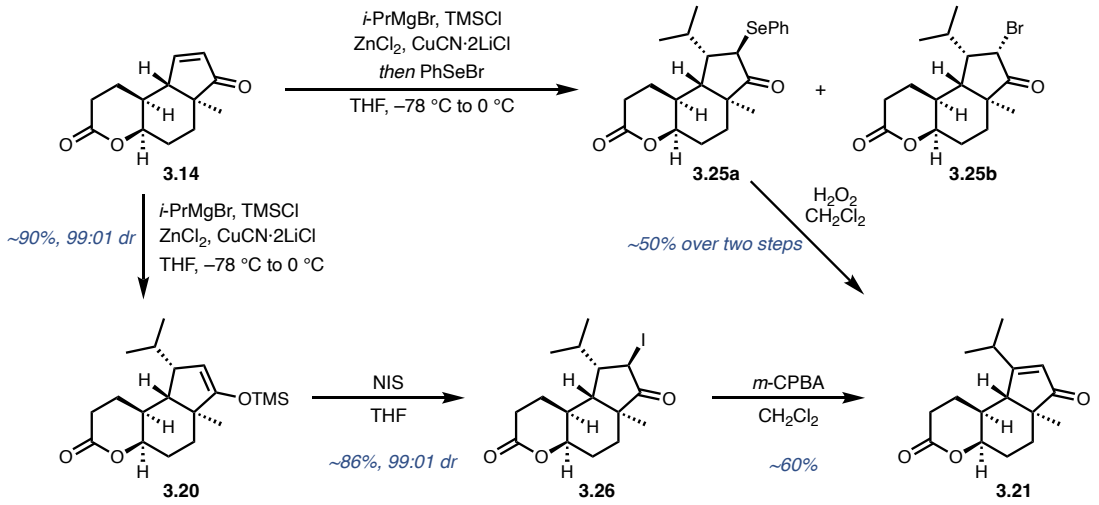
Scheme 3.9 *Alternate approaches to epimerization*



To this end, we were interested in synthesis of selenoether **3.25a** and iodide **3.26**, as oxidation of these functional groups is known to facilitate syn eliminations (**Scheme 3.10**). While PhSeCl proved unsuitable for electrophilic selenylation of **3.14**, the use of PhSeBr smoothly converted the enoxysilane formed *in situ* to an inseparable mixture of desired selenoether **3.25a**

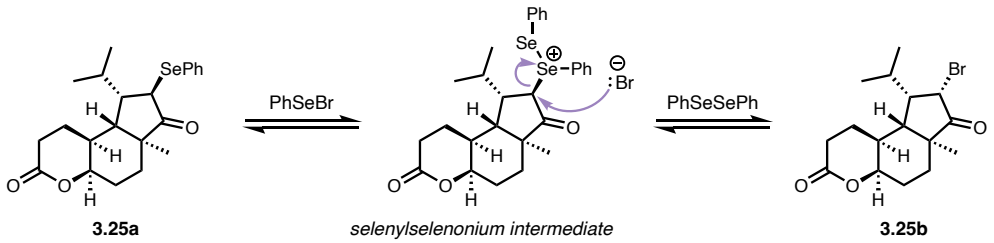
and bromide **3.25b**. We determined that the crude mixture could be carried through the oxidation step which trivialized the separation of the bromide impurity.

Scheme 3.10 *Synthesis of enone* ***3.21***



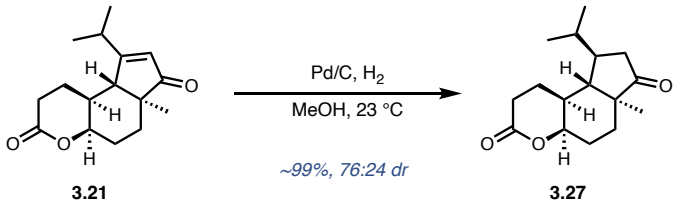
The highly stereoselective processes leading to the formation of **3.25a** and **3.25b** initially appear to be at odds with one another and warrant further discussion. Attempting to mitigate formation of **3.25b**, we found that using fewer equivalents of PhSeBr led to increased recovery of protodesilylated **3.20** following workup**.** Conversely, using more equivalents of PhSeBr led to pronounced formation of bromide **3.25b**. Unable to escape formation of this byproduct, we were forced to make several conclusions about this transformation: (1) selenoether **3.25a** is an intermediate *en route* to bromide **3.25b**; (2) this process likely involves a selenylselenonium species; (3) formation and subsequent displacement of this leaving group is at least as fast as selenylation of the enoxysilane (**Scheme 3.11**). That selenide **3.25a** and bromide **3.25b** were only ever detected as single stereoisomers strongly supports the notion that this process probably occurs via an S_N2-type mechanism.

Scheme 3.11 *Proposed mechanistic pathway converting* ***3.25a*** *to* ***3.25b***



Separately, we found that exposure of enoxysilane **3.20** to NIS smoothly formed iodide **3.26** in approximately 86% yield as a single stereoisomer. In the presence of a peroxyacid, **3.26** can be converted to an iodoso intermediate (not isolated) that presumably participates in *syn*-type elimination to form enone **3.21**.[61,62] Subsequent palladium-mediated hydrogenation of enone **3.21** (obtained by either method) generated an 76:24 mixture of ketone diastereomers in favor of the desired stereoisomer (**3.27**), and confirmed our hypothesis that hydride delivery might proceed from the convex face of **3.21** (**Scheme 3.12**).

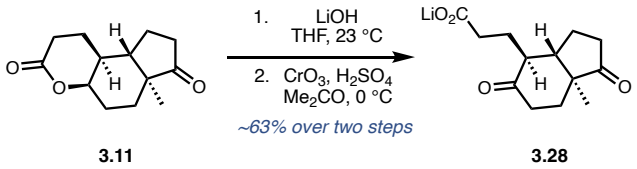
Scheme 3.12 *Stereoselective hydrogenolysis of* ***3.21***.



It seems reasonable that other reducing systems (e.g. $[(Ph_3P)CuH]_6$, $RhCl(PPh_3)_3$, PtO_2) might more selectively inform the stereochemical outcome of this transformation, but these were not explored at this time. Through the pair of stepwise sequences described above we had effectively reversed the outcome of the cuprate conjugate addition at the cost of increased step count and reduced material throughput.

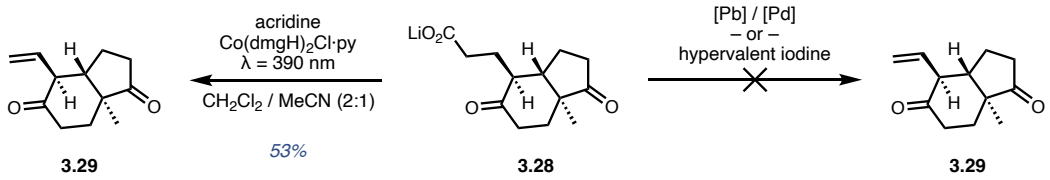
Tangentially, we had explored chemistry on the lactone ring of sitolactone. Conversion of sitolactone to keto-acid **3.28** was accomplished according to the procedure of Gui (**Scheme 3.13**).

Scheme 3.13 *Synthesis of keto-acid* ***3.28***



Oxidative dehomologation of carboxylic acids is traditionally accomplished with lead tetraacetate or hypervalent iodine reagents in the presence of a copper(II) acetate, but these conditions were found unfit for application in this system (**Scheme 3.14**).[63–66] Palladium-mediated methods for oxidative dehomologation of carboxylic acids also failed to produce the desired outcome.[67,68] Based on a similar result observed by Stoltz and coworkers, we believe that the high temperatures required in these experiments might also facilitate ketone enolization and relactonization; such a process likely renders the substrate inert to the desired transformation.[69] Around this time we had discovered a photocatalytic method for oxidative dehomologation of carboxylic acids reported by Larionov and coworkers; application of this chemistry resulted in smooth formation of the desired β,γ-unsaturated ketone **3.29**.[70]

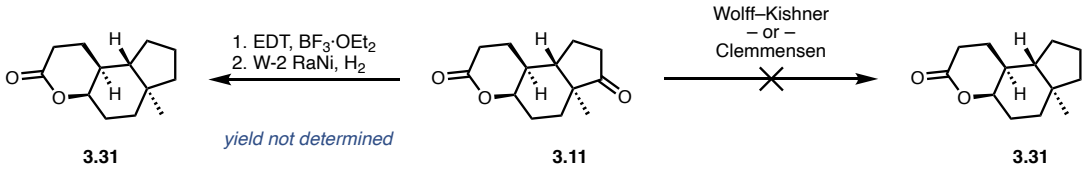
Scheme 3.14 *Photocatalytic oxidative dehomologation leads to* ***3.29***



Around the same time, a parallel series of experiments led us to believe that the ketone function in sitolactone was all but impervious to its removal. After screening a variety of methods for carbonyl deletion, we found conditions reported by Mozingo to be most promising (**Scheme**

3.15).[71–74] While the dithiane of sitolactone could be formed in 78% yield, attempts to desulfurize this material with W-2 Raney nickel proved sluggish unless the reaction was conducted under a hydrogen atmosphere. Though spectroscopic analysis (GCMS and ^{1}H NMR) of the crude reaction mixture strongly corroborated the intended result, attempts to isolate lactone **3.31** were complicated by its coelution with several related impurities that precluded full characterization. In different scenarios we might have endeavored further along this route, but we ultimately deprioritized the synthesis of **3.9** from sitolactone.

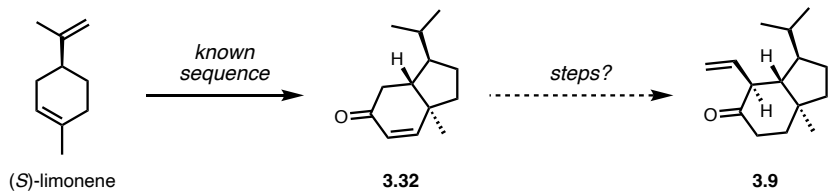
Scheme 3.15 *Mozingo reduction of sitolactone leads to lactone* ***3.31***



3.7 Synthesis of 3.9 From Hydrindenone 3.32

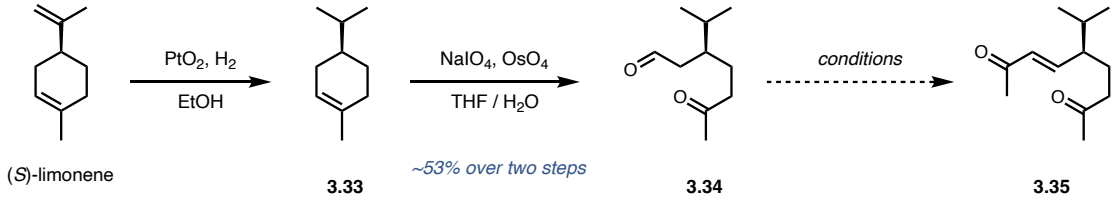
Though sitolactone appeared to be an excellent starting point for the synthesis of asperterpenoid A, our work in this area led us consider other alternatives. Specifically, we were drawn to a recent synthesis of retigeranic acid A by Ding and coworkers; beginning from (*S*)-limonene, the Ding group was able to intercept the hydrindenone intermediate **3.32** over six steps.[10] Objectively, we reasoned that chemical manipulation of **3.32** might allow its conversion to β,γ-unsaturated ketone **3.9** (**Scheme 3.16**).

Scheme 3.16 *Ding's synthesis of hydrindenone* ***3.32*** *inspires a new strategy to* ***3.9***



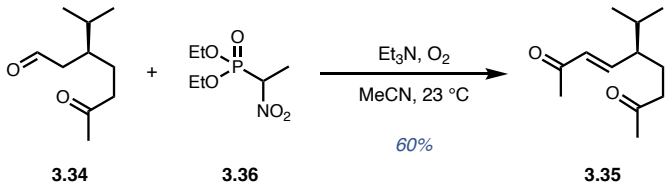
Following the two-step sequence described by Ding and coworkers, chemoselective reduction with Adam's catalyst under a hydrogen atmosphere provided cyclic alkene **3.33** (**Scheme 3.17**). Lemieux–Johnson oxidative cleavage of **3.33** enabled synthesis of ketoaldehyde **3.34** in 53% over two steps. The two carbon homologation that the Ding group utilized to access enone **3.34** required the use of the DEA regulated chemical nitroethane.[75] While we were able to contact an approved supplier, the lead time for delivery of this chemical coupled with EH&S policies in place regarding rendered this option unsuitable.

Scheme 3.17 *Regulated chemical access complicates the direct synthesis of hydrindenone* ***3.9***



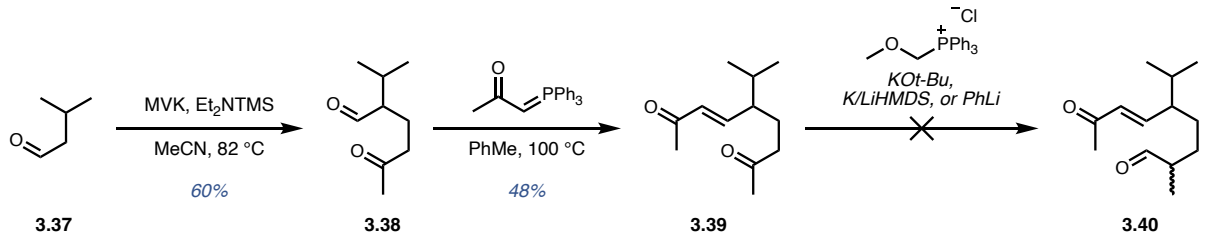
Understanding that the mechanism of this transformation is thought to proceed through a discrete nitroalkene intermediate, we wondered if we might access this same intermediate through Horner–Wadsworth–Emmons alkenylation of the aldehyde in **3.34**. It seemed plausible that subjection of the putative nitroalkene product to otherwise identical reaction conditions might facilitate Nef oxidation to **3.35**. Synthesis of a known nitrophosphonate reagent (**3.36**) allowed us to test this hypothesis. Exposure of the ketoaldehyde **3.34** to **3.36** in the presence of triethylamine and oxygen promoted conversion to the desired enone in good yield (**Scheme 3.18**). While synthesis of nitroalkenes in this manner has been previously described, to the best of our knowledge there are no examples of these reagents being used to intentionally facilitate tandem HWE/Nef reactions.[76,77]

Scheme 3.18 *The discovery of a tandem HWE/Nef reaction enables synthesis of* ***3.35***



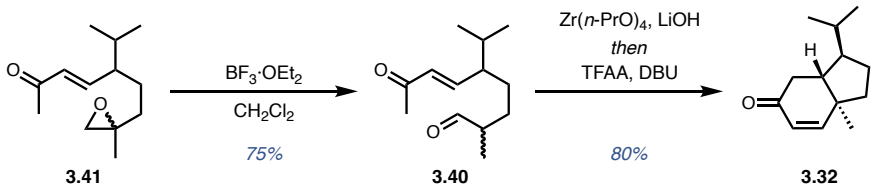
Another strategy towards enone **3.35** was explored in parallel (**Scheme 3.19**). Following literature precedent, enamine-mediated Michael addition between isovalderaldehyde and methyl vinyl ketone granted access to racemic ketoaldehyde **3.38**. While not ideal for the total synthesis of asperterpenoid A, we reasoned that this material could be used to test the efficacy of downstream chemistry. Wittig homologation of **3.38** allowed the synthesis of enone **3.39** at which point our attempts to reproduce the chemistry reported by Ding and coworkers to generate **3.40** were entirely unsuccessful. Despite our screening of several reaction parameters (base, temperature, reagent stoichiometry), we never observed the chemoselectivity reported.[10]

Scheme 3.19 *Reported conditions leading to ketoaldehye* ***3.40*** *prove irreproducible*



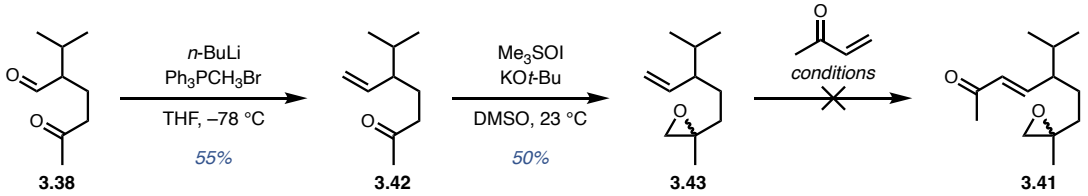
Around this time we discovered that an earlier synthesis of hydrindenone **3.32** had been reported by Fallis and coworkers (**Scheme 3.20**).[78] While both groups intercepted enone **3.40** in their routes, Fallis produced this intermediate via Meinwald rearrangement of epoxide **3.41**. It seemed that if we could access this epoxide, we might be able to circumvent the problems we had run into in our efforts to replicate the Wittig chemistry described by Ding.

Scheme 3.20 *Synthesis of hydrindenone* ***3.32*** *by Fallis and coworkers*



We hoped to divert the Michael product (**3.38)** obtained previously to epoxide **3.41** through a short sequence (**Scheme 3.21**). Wittig methylenation of the aldehyde in **3.38** provided alkenyl ketone **3.42** in 55% yield. Next, Johnson–Corey–Chaykovsky conditions allowed for the synthesis of epoxide **3.43** as an inseparable mixture of diastereomers. At this point in time, we envisioned that ruthenium-mediated cross metathesis between the alkene of **3.43** and methyl vinyl ketone would allow us to intercept **3.41**. While Lewis-basic functions can be problematic in metathesis reactions, epoxides generally appear to be the exception. Unfortunately, we only ever observed traces of the desired enone **3.41**, leading us to conclude that the epoxide in **3.43** is problematic for catalyst turnover.

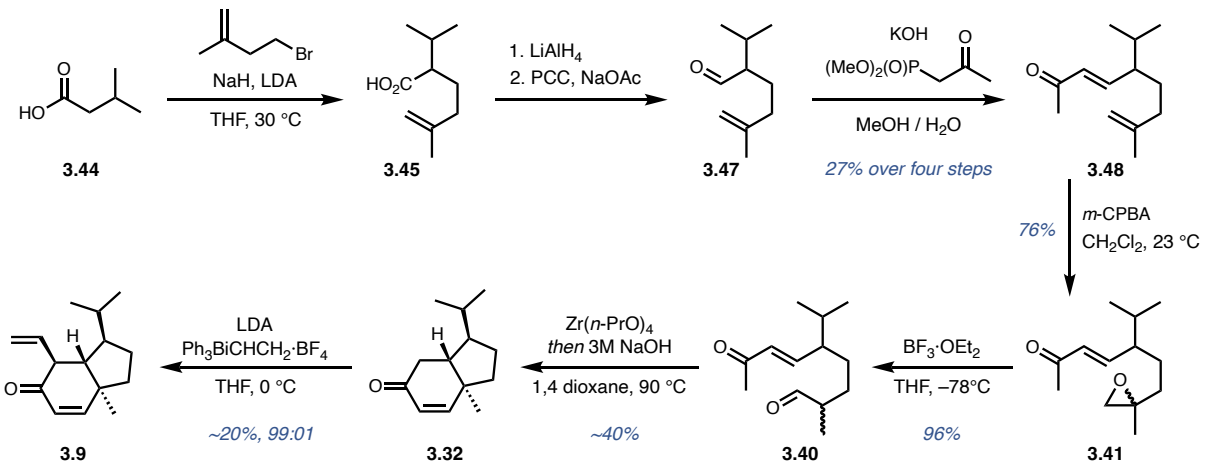
Scheme 3.21 *Efforts to intercept epoxide* ***3.41*** *are unsuccessful*



At this point we opted to utilize the route to **3.32** explicitly described by Fallis (**Scheme 3.22**).[78] Alkylation of isovaleric acid followed by reduction with lithium aluminum hydride provided an alkenyl alcohol (**3.46**, not depicted) that under the action of pyridinium chlorochromate could be converted to aldehyde **3.47**. Horner–Wadsworth–Emmons homologation of this aldehyde was accomplished with dimethyl acetonylphosphonate and in this way the four step sequence was used to access alkenyl enone **3.48** in 27% over four steps. Subsequent

epoxidation of the disubstituted alkene in **3.48** provided **3.41** in 76% yield as an approximately equal mixture of diastereomers. Our attempts to effect Meinwald rearrangement as described by Fallis and coworkers initially proved unsuccessful; using the reaction conditions as reported, we always observed the significant formation of an isomeric byproduct (not characterized). While other conditions reported to promote Meinwald rearrangement of epoxides were explored ($HClO_4$, $Bi(OTf)_3$, $InCl_3$), a brief solvent screen revealed that switching the reaction solvent from CH_2Cl_2 to THF arrested the formation of this unwanted byproduct and allowed synthesis of ketoaldehyde **3.40** in 96%.[79–81] We suspect that the Lewis-basic solvent THF plays an important role in attenuating both the availability of $BF_3{\cdot}OEt_2$ to substrate and its relative Lewis acidity.

Scheme 3.22 *Adaptation of chemistry by Fallis and coworkers enables synthesis of enone* ***3.9***



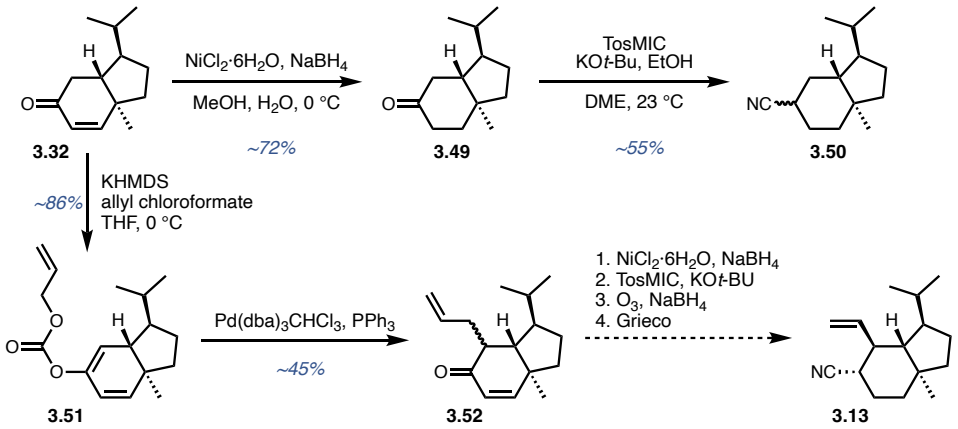
Modifications to the reaction conditions reported by Ding at last enabled the stereoselective conversion of enone **3.40** to the desired hydrindenone **3.32**. It must be mentioned that using the exact conditions described by either group only ever led to the formation of ketol intermediates, which proved resistant to elimination under the explicit reaction conditions reported. With hydrindenone in hand, we could finally consider chemistry that might facilitate vinylation of **3.32**. While several multi-step methods permit vinylation of carbonyl compounds, we were drawn to a

new method described by Rawal that could potentially accomplish this transformation in a single step. Application of this chemistry enabled a stereoselective vinylation that formed the desired β,γ-unsaturated ketone **3.9**. Unfortunately, the yield of this transformation was very low and we were unsure how to best proceed regarding its optimization.

As we were running low on material, we opted to investigate workarounds to this transformation while also using **3.32** as a model system to explore other downstream manipulations we knew we would need to perform on the target substrate (**Scheme 3.23**). We discovered that reduction of the unsaturated enone in **3.32** could be accomplished via the action of nickel boride generated *in situ*; this reaction permitted access to hydrindanone **3.49** in ~72% yield and we anticipate these conditions could enable chemoselective reduction of the enone in the presence of an alkene.[82] Though lacking a vinyl group, we were curious to see if **3.50** might be receptive to van Leusen homologation. Indeed, application of the original conditions described by van Leusen and coworkers facilitated homologation to the nitrile as a presumably inconsequential mixture of stereoisomers.[83]

While we had trouble directly allylating the enolate derived from **3.32**, the allyl enol carbonate **3.51** could be easily prepared. Excitingly, exposure of this material to a palladium(0) catalyst in the presence of a phosphine ligand appears to permit highly stereoselective allylation of **3.52**, but significant overlap in the ^{1}H NMR spectrum precluded the assignment of this new stereogenic center.[84] Lacking material, we were forced to halt our investigation at this time.

Scheme 3.23 *Early derivatizations of* ***3.32*** *and proposed synthesis of* ***3.13***

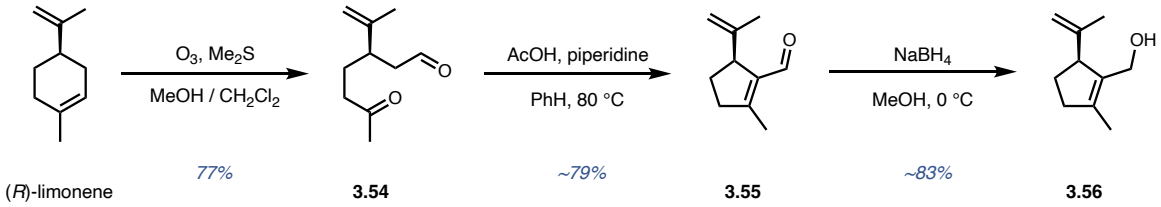


We believe that derivatization of **3.52** will eventually permit a synthesis of the desired nitrile coupling partner **3.13**. Though several viable permutations are possible, one plausible sequence is presented in **Scheme 3.22**: nickel boride-mediated conjugate reduction followed by van Leusen homologation might produce an alkenyl nitrile intermediate. Reductive ozonolysis and subsequent Grieco elimination of the primary carbinol could be used to procure requisite coupling partner **3.13**.

3.8 Synthesis of Bromide 3.12

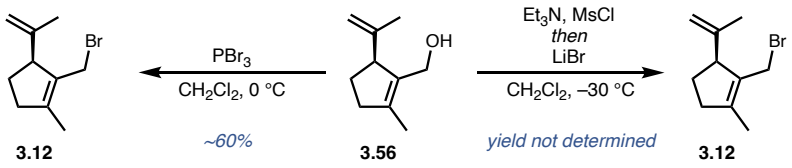
In conjunction with our synthetic efforts towards nitrile **3.13**, we initiated studies regarding the synthesis of bromide **3.12** from allylic alcohol **3.56** (**Scheme 3.24**). Based on a three-step protocol reported by Babu and coworkers, ozonolysis of (*R*)-limonene could be used to access ketoaldehyde **3.54**.[85] Heating **3.54** in the presence of acetic acid and piperidine generated the unsaturated aldehyde **3.55** which could be reduced with sodium borohydride to access to carbinol **3.56** in acceptable yields.

Scheme 3.24 *Synthesis of allylic alcohol* ***3.56***



Although straightforward, we found efficient conversion of this material to bromide **3.12** a somewhat capricious task. While unable to tolerate the conditions of the Appel reaction, we found the substrate could be converted to the bromide under the action of phosphorus tribromide or by *in situ* formation of the allylic mesylate and nucleophilic displacement with bromide (**Scheme 3.25**). In all cases, the desired bromide was formed with various byproducts that complicated our isolation efforts. It seems entirely reasonable that a dedicated optimization effort will substantially improve the observed outcome of this transformation.

Scheme 3.25 *Bromination of* ***3.12*** *proves challenging*



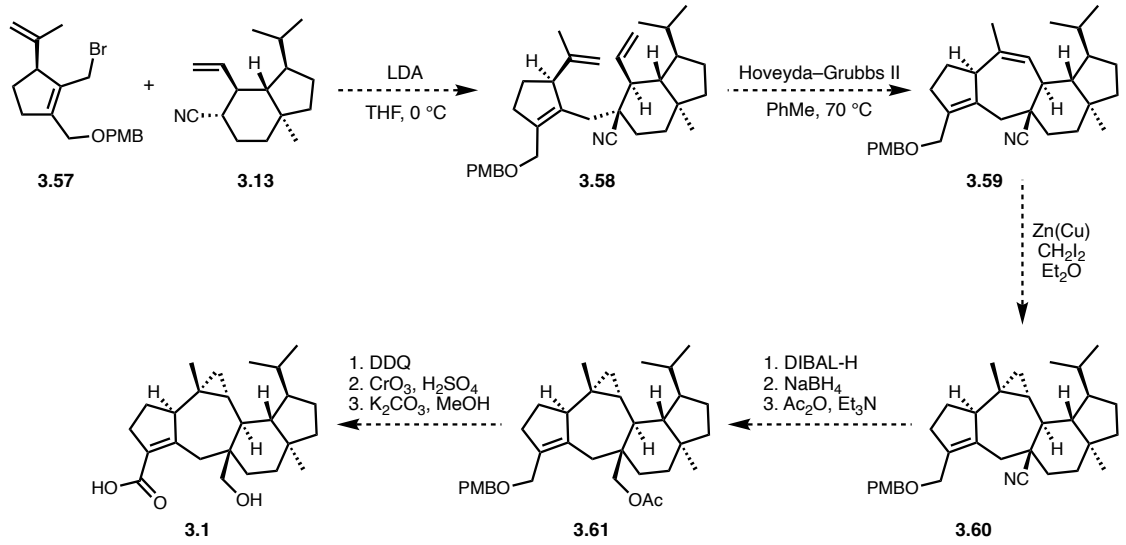
3.9 Conclusions and Future Directions

In conclusion, two iterations of our convergent fragment coupling strategy for the synthesis of asperterpenoid A were explored. In the first route, we prioritized the synthesis of an epoxide fragment required for the radical coupling approach. The undesirable outcome of a highly stereoselective cuprate addition led us to consider workarounds by which we might persist in our efforts towards the synthesis of this fragment. After careful consideration, we deprioritized this route and redesigned our synthesis of this fragment so as to incorporate results obtained by Ding

and coworkers. Unfortunately, we were unable to reproduce a key transformation reported in this work which forced us to abandon this shorter route in favor of a slightly longer synthesis described by Fallis and coworkers. In doing so, we were finally able to validate our proposed fragment synthesis and simultaneously explore derivatization of a related intermediate. At the same time, we secured a route to the bromide coupling partner required for the nitrile alkylation approach.

The project remains active in the group and it seems reasonable that a synthesis of both fragments will be achieved shortly, at which point the two key steps of the synthesis can be investigated (**Scheme 3.26**). If ionic fragment coupling successfully leads to the formation of **3.58**, it seems plausible that ring-closing metathesis should form only diene **3.59**. Introduction of the final carbon could be accomplished through a stereoselective Simmons–Smith cyclopropanation, which we anticipate occurring on the convex face of the **3.59**. In **3.60**, the oxidation state of C21 is too high while the oxidation state of C19 is too low; a series of functional group manipulations and could conceivably lead to asperterpenoid A.

Scheme 3.26 *Proposed endgame sequence permitting synthesis of asperterpenoid A (**3.1**)*



3.10 References

(1) Li, K.; Gustafson, K. R. *Nat. Prod. Rep.* **2021**, *38*, 1251–1281.

(2) Liu, Y.; Wang, L.; Jung, J. H.; Zhang, S. *Nat. Prod. Rep.* **2007**, *24*, 1401.

(3) Hog, D. T.; Mayer, P.; Trauner, D. *J. Org. Chem.* **2012**, *77*, 5838–5843.

(4) Hog, D. T. A Unified Approach toward Astellatol, Nitiol, and YW 3548. Ph.D. Thesis, Ludwig-Maximilians-Universität München, Munich, Germany, **2013**.

(5) Huber, F. M. E. The Total Synthesis of (–)-Nitidasin, Synthetic Studies Toward Astellatol and Retigeranic Acid B, and Development of Novel Photochromic Ligands for L-type Voltage-gated Calcium Channels. Ph.D. Thesis, Ludwig-Maximilians-Universität München, Munich, Germany, **2014**.

(6) Piers, E.; Boulet, S. L. *Tetrahedron Letters* **1997**, *38*, 8815–8818.

(7) Molander, G. A.; Quirmbach, M. S.; Silva, L. F.; Spencer, K. C.; Balsells, J. *Org. Lett.* **2001**, *3*, 2257–2260.

(8) Krout, M. R.; Henry, C. E.; Jensen, T.; Wu, K.-L.; Virgil, S. C.; Stoltz, B. M. *J. Org. Chem.* **2018**, *83*, 6995–7009.

(9) Chen, X.; Yao, W.; Zheng, H.; Wang, H.; Zhou, P.-P.; Zhu, D.-Y.; Wang, S.-H. *J. Am. Chem. Soc.* **2023**.

(10) Sun, D.; Chen, R.; Tang, D.; Xia, Q.; Zhao, Y.; Liu, C.-H.; Ding, H. *J. Am. Chem. Soc.* **2023**.

(11) Corey, E. J.; Desai, M. C.; Engler, T. A. *J. Am. Chem. Soc.* **1985**, *107*, 4339–4341.

(12) Engler, T. A. In *Strategies and Tactics in Organic Synthesis*; Elsevier, 1989; Vol. 2, pp 91–121.

(13) Hudlicky, T.; Fleming, A.; Radesca, L. *J. Am. Chem. Soc.* **1989**, *111*, 6691–6707.

(14) Wright, Jonathan.; Drtina, G. J.; Roberts, R. A.; Paquette, L. A. *J. Am. Chem. Soc.* **1988**, *110*, 5806–5817.

(15) Wender, P. A.; Singh, S. K. *Tetrahedron Letters* **1990**, *31*, 2517–2520.

(16) Paquette, L. A.; Wright, J.; Drtina, G. J.; Roberts, R. A. *J. Org. Chem.* **1987**, *52*, 2960–2962.

(17) Wang, X.; Li, D.; Zhang, J.; Gong, J.; Fu, J.; Yang, Z. *Org. Lett.* **2021**, *23*, 5092–5097.

(18) Zhang, J.; Wang, X.; Li, S.; Li, D.; Liu, S.; Lan, Y.; Gong, J.; Yang, Z. *Chem. Eur. J.* **2015**, *21*, 12596–12600.

(19) Huang, X.; Huang, H.; Li, H.; Sun, X.; Huang, H.; Lu, Y.; Lin, Y.; Long, Y.; She, Z. *Org. Lett.* **2013**, *15*, 721–723.

(20) Minami, A.; Ozaki, T.; Liu, C.; Oikawa, H. *Nat. Prod. Rep.* **2018**, *35*, 1330–1346.

(21) Luo, P.; Huang, J.-H.; Lv, J.-M.; Wang, G.-Q.; Hu, D.; Gao, H. *Nat. Prod. Rep.* **2024**.
(22) Mitsuhashi, T.; Abe, I. In *Progress in the Chemistry of Organic Natural Products 111*; Kinghorn, A. D., Falk, H., Gibbons, S., Kobayashi, J., Asakawa, Y., Liu, J.-K., Eds.; Progress in the Chemistry of Organic Natural Products; Springer International Publishing: Cham, 2020; pp 1–79.
(23) Mitsuhashi, T.; Rinkel, J.; Okada, M.; Abe, I.; Dickschat, J. S. *Chem. Eur. J.* **2017**, *23*, 10053–10057.
(24) Huang, J.-H.; Lv, J.-M.; Wang, Q.-Z.; Zou, J.; Lu, Y.-J.; Wang, Q.-L.; Chen, D.-N.; Yao, X.-S.; Gao, H.; Hu, D. *Org. Biomol. Chem.* **2019**, *17*, 248–251.
(25) Hershkovitz, I.; Donoghue, H. D.; Minnikin, D. E.; Besra, G. S.; Lee, O. Y.-C.; Gernaey, A. M.; Galili, E.; Eshed, V.; Greenblatt, C. L.; Lemma, E.; Bar-Gal, G. K.; Spigelman, M. *PLOS ONE* **2008**, *3*, e3426.
(26) Gagneux, S. *Nat. Rev. Microbiol.* **2018**, *16*, 202–213.
(27) Lawn, S. D.; Zumla, A. I. *The Lancet* **2011**, *378*, 57–72.
(28) Shenoi, S.; Friedland, G. *Annual Review of Medicine* **2009**, *60*, 307–320.
(29) Tuberculosis (TB) https://www.who.int/news-room/fact-sheets/detail/tuberculosis.
(30) Brammachary, U.; Ramachandra, V.; Palavesam, S.; Kapalamurthy, V. R. C.; Muralidhar, A.; Muthaiah, M.; Brammachary, U.; Ramachandra, V.; Palavesam, S.; Kapalamurthy, V. R. C.; Muralidhar, A.; Muthaiah, M. IntechOpen, 2022.
(31) Dartois, V. A.; Rubin, E. J. *Nat. Rev. Microbiol.* **2022**, *20*, 685–701.
(32) Ahmad, F.; Rani, A.; Alam, A.; Zarin, S.; Pandey, S.; Singh, H.; Hasnain, S. E.; Ehtesham, N. Z. *Front. Immunol.* **2022**, *13*.
(33) Zhou, B.; He, Y.; Zhang, X.; Xu, J.; Luo, Y.; Wang, Y.; Franzblau, S. G.; Yang, Z.; Chan, R. J.; Liu, Y.; Zheng, J.; Zhang, Z.-Y. *PNAS* **2010**, *107*, 4573–4578.
(34) Koul, A.; Herget, T.; Klebl, B.; Ullrich, A. *Nat. Rev. Microbiol.* **2004**, *2*, 189–202.
(35) Singh, R.; Rao, V.; Shakila, H.; Gupta, R.; Khera, A.; Dhar, N.; Singh, A.; Koul, A.; Singh, Y.; Naseema, M.; Narayanan, P. R.; Paramasivan, C. N.; Ramanathan, V. D.; Tyagi, A. K. *Mol. Microbiol.* **2003**, *50*, 751–762.
(36) Vickers, C. F.; Silva, A. P. G.; Chakraborty, A.; Fernandez, P.; Kurepina, N.; Saville, C.; Naranjo, Y.; Pons, M.; Schnettger, L. S.; Gutierrez, M. G.; Park, S.; Kreiswith, B. N.; Perlin, D. S.; Thomas, E. J.; Cavet, J. S.; Tabernero, L. *J. Med. Chem.* **2018**, *61*, 8337–8352.
(37) Ruddraraju, K. V.; Aggarwal, D.; Zhang, Z.-Y. *Microorganisms* **2021**, *9*, 14.
(38) Grundner, C.; Ng, H.-L.; Alber, T. *Structure* **2005**, *13*, 1625–1634.

(39) Cheng, S.; Wang, Q.; Chen, X.; Chen, J.; Wang, B.; Chen, D.; Shen, D.; Tian, J.; Ye, F.; Lu, Y.; Huang, H.; Lu, Y.; Zhang, D. *Bioorg. Med. Chem.* **2022**, *73*, 117006.

(40) RajanBabu, T. V.; Nugent, W. A. *J. Am. Chem. Soc.* **1994**, *116*, 986–997.

(41) Nakamatsu, T.; Beppu, T.; Arima, K. *Agric. Biol. Chem.* **1983**, *47*, 1449–1454.

(42) Deng, J.; Ning, Y.; Tian, H.; Gui, J. *J. Am. Chem. Soc.* **2020**, *142*, 4690–4695.

(43) Zhang, Y.; Danishefsky, S. J. *J. Am. Chem. Soc.* **2010**, *132*, 9567–9569.

(44) Nakayama, Y.; Maser, M. R.; Okita, T.; Dubrovskiy, A. V.; Campbell, T. L.; Reisman, S. E. *J. Am. Chem. Soc.* **2021**, *143*, 4187–4192.

(45) Yoshikai, N.; Nakamura, E. *Chem. Rev.* **2012**, *112*, 2339–2372.

(46) Yamamoto, Y. *Angew. Chem. Int. Ed.* **1986**, 25, 947–959.

(47) Nakamura, E.; Mori, S. *Angew. Chem. Int. Ed.* **2000**, *39*, 3750–3771.

(48) Bertz, S. H.; Miao, G.; Rossiter, B. E.; Snyder, J. P. *J. Am. Chem. Soc.* **1995**, *117*, 11023–11024.

(49) Cabezas, J. A.; Oehlschlager, A. C. *J. Am. Chem. Soc.* **1997**, *119*, 3878–3886.

(50) Yamamoto, Y.; Nemoto, H.; Ibuka, T. *Journal of Japan Oil Chemists' Society* **1990**, *39*, 881–887.

(51) Lipshutz, B. H.; Sengupta, S. In *Organic Reactions*; John Wiley & Sons, Ltd, 2004; pp 135–631.

(52) Horiguchi, Y.; Komatsu, M.; Kuwajima, I. *Tetrahedron Letters* **1989**, *30*, 7087–7090.

(53) Horiguchi, Y.; Matsuzawa, S.; Nakamura, E.; Kuwajima, I. *Tetrahedron Letters* **1986**, *27*, 4025–4028.

(54) Woodward, S. *Chem. Soc. Rev.* **2000**, *29*, 393–401.

(55) Crossley, S. W. M.; Barabé, F.; Shenvi, R. A. *J. Am. Chem. Soc.* **2014**, *136*, 16788–16791.

(56) Grieco, P. A.; Nishizawa, M.; Marinovic, N.; Ehmann, W. J. *J. Am. Chem. Soc.* **1976**, *98*, 7102–7104.

(57) Calaza, M. I.; Hupe, E.; Knochel, P. *Org. Lett.* **2003**, *5*, 1059–1061.

(58) Nakata, K.; Kiyotsuka, Y.; Kitazume, T.; Kobayashi, Y. *Org. Lett.* **2008**, *10*, 1345–1348.

(59) Reich, H. J.; Peake, S. L. *J. Am. Chem. Soc.* **1978**, *100*, 4888–4889.

(60) Kim, S.; Fuchs, P. L. *Tetrahedron Letters* **1994**, *35*, 7163–7166.

(61) Bacha, J. D.; Kochi, J. K. *Tetrahedron* **1968**, *24*, 2215–2226.

(62) Carlson, G. L.; Belobaba, D. T. E.; Hofmann, A. F.; Wedmid, Y. *Steroids* **1977**, *30*, 787–793.

(63) Giner, J. L.; Djerassi, C. *J. Am. Chem. Soc.* **1991**, *113*, 1386–1393.

(64) Concepcion, J. I.; Francisco, C. G.; Freire, R.; Hernandez, R.; Salazar, J. A.; Suarez, E. *J. Org. Chem.* **1986**, *51*, 402–404.

(65) Le Nôtre, J.; Scott, E. L.; Franssen, M. C. R.; Sanders, J. P. M. *Tetrahedron Letters* **2010**, *51*, 3712–3715.

(66) Liu, Y.; Kim, K. E.; Herbert, M. B.; Fedorov, A.; Grubbs, R. H.; Stoltz, B. M. *Adv. Synth. Catal.* **2014**, *356*, 130–136.

(67) Liu, Y.; Virgil, S. C.; Grubbs, R. H.; Stoltz, B. M. *Angew. Chem. Int. Ed.* **2015**, *54*, 11800–11803.

(68) Nguyen, V. T.; Nguyen, V. D.; Haug, G. C.; Dang, H. T.; Jin, S.; Li, Z.; Flores-Hansen, C.; Benavides, B. S.; Arman, H. D.; Larionov, O. V. *ACS Catal.* **2019**, *9*, 9485–9498.

(69) Mozingo, R.; Wolf, D. E.; Harris, S. A.; Folkers, K. *J. Am. Chem. Soc.* **1943**, *65*, 1013–1016.

(70) Wolfrom, M. L.; Karabinos, J. V. *J. Am. Chem. Soc.* **1944**, *66*, 909–911.

(71) Rentner, J.; Kljajic, M.; Offner, L.; Breinbauer, R. *Tetrahedron* **2014**, *70*, 8983–9027.

(72) Bender, M.; Schmidtmann, M.; Summons, R. E.; Rullkötter, J.; Christoffers, J. *Chem. Eur. J.* **2015**, *21*, 12501–12508.

(73) Umemiya, S.; Nishino, K.; Sato, I.; Hayashi, Y. *Chem. Eur. J.* **2014**, *20*, 15753–15759.

(74) Frnaklin, A. S. *Synlett* **2000**, *2000*, 1154–1156.

(75) Fujii, M. *Chem. Lett.* **1992**, *21*, 933–934.

(76) Attah-Poku, S. K.; Chau, F.; Yadav, V. K.; Fallis, A. G. *J. Org. Chem.* **1985**, *50*, 3418–3419.

(77) Orru, R. V. A.; Mayer, S. F.; Kroutil, W.; Faber, K. *Tetrahedron* **1998**, *54*, 859–874.

(78) Löser, P. S.; Rauthe, P.; Meier, M. a. R.; Llevot, A. *Phil. Trans. R. Soc. A* **2020**, 378, 20190267.

(79) Nicolaou, K. C.; Shi, L.; Lu, M.; Pattanayak, M. R.; Shah, A. A.; Ioannidou, H. A.; Lamani, M. *Angew. Chem. Int. Ed.* **2014**, *53*, 10970–10974.

(80) Khurana, J. M.; Sharma, P. *Bull. Chem. Soc. Jpn.* **2004**, *77*, 549–552.

(81) Oldenziel, O. H.; Van Leusen, D.; Van Leusen, A. M. *J. Org. Chem.* **1977**, *42*, 3114–3118.

(82) Tsuji, J.; Minami, I.; Shimizu, I. *Tetrahedron Letters* **1983**, *24*, 1793–1796.

(83) Srikrishna, A.; Babu, N. C. *Tetrahedron Letters* **2001**, *42*, 4913–4914.

3.11 Experimental Information

3.11.1 Materials and Methods

All reactions were performed in oven-dried (120 °C) or flame-dried glassware under an atmosphere of dry argon unless otherwise noted. Reaction solvents including dichloromethane (CH_2Cl_2, Fisher, HPLC Grade), hexanes (Fisher, HPLC Grade), diethyl ether (Et_2O, Fisher, BHT stabilized, HPLC Grade), benzene (PhH, Fisher, HPLC Grade), tetrahydrofuran (THF, Fisher, HPLC Grade), and toluene (PhMe, Fisher, HPLC Grade) were dried by percolation through a column packed with neutral alumina and a column packed with Q5 reactant, a supported copper catalyst for scavenging oxygen, under a positive pressure of argon. Hexafluoroisopropanol ($(CF_3)_2CHOH$, Oakwood) was degassed prior to use by sparging with argon for 15 minutes. Solvents for workup and chromatography were hexanes (Fisher or EMD, ACS Grade), ethyl acetate (EtOAc, Fisher, ACS Grade), dichloromethane (CH_2Cl_2, Fisher, ACS Grade), and diethyl ether (Et_2O, Fisher, ACS Grade).

Column chromatography was performed using EMD Millipore 60 Å (0.040-0.063 mm) mesh silica gel (SiO_2). Analytical and preparative thin-layer chromatography was performed on Merck silica gel 60 F254 TLC plates. Visualization was accomplished with UV (254 or 210 nm), and *p*-anisaldehyde, vanillin, potassium permanganate ($KMnO_4$), 2,4-dinitrophenylhydrazine (2,4-DNP), or ceric ammonium molybdate (CAM) and heat as developing agents. Chloroform-*d* ($CDCl_3$, 99.8% D, DLM-7) and C_6D_6 (99.5% D, DLM-1-100, dried over activated alumina [5 wt%]) were purchased from Cambridge Isotope Laboratories. K_2CO_3 (anhydrous, 99%, Alfa Aesar), $NaHCO_3$ (ACS grade, Fisher), NaOH (ACS grade, Macron or Fisher), 1-fluoro-2,4,6-trimethylpyridinium tetrafluoroborate (TCI or Sigma Aldrich, 95-99%), and 1,1,3,3-tetramethyldisiloxane (TMDSO, 97%, Acros Organics) were purchased commercially and used without further purification.

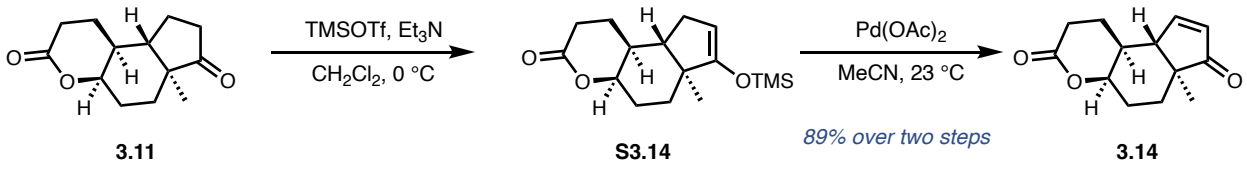
Triethylamine (EMD, CaH_2) and pyridine (Alfa Aesar, CaH_2) were distilled from the indicated drying agents prior to use.

Proton and carbon magnetic resonance spectra (^{1}H NMR and ^{13}C NMR) were recorded at 298 K on a Bruker CRYO500 (500 MHz, ^{1}H; 125 MHz, ^{13}C) or a Bruker AVANCE600 (600 MHz, ^{1}H; 151 MHz, ^{13}C) spectrometer with solvent residual as the internal standard for ^{1}H NMR: $CHCl_3$ at 7.26 ppm, and C_6HD_5 at 7.16 ppm and solvent as internal standard for ^{13}C NMR: $CDCl_3$ at 77.16 ppm and C_6D_6 at 128.06 ppm. ^{1}H NMR data are reported as follows: chemical shift, multiplicity (s = singlet, d = doublet, t = triplet, q = quartet, h = heptet, dd = doublet of doublets, ddd = doublet of doublet of doublets, td = triplet of doublets, tdd = triplet of doublet of doublets, qd = quartet of doublets, m = multiplet, br = broad signal), coupling constants (Hz), and integration. The raw fid files were processed into the included NMR spectra using MestReNova 14.3 (Mestrelab Research S.L.).

High resolution mass spectra (HRMS) were recorded either on a Waters LCT Premier S2 spectrometer using ESI-TOF (electrospray ionization-time of flight) or a Waters GCT Premier spectrometer using CI-TOF (chemical ionization-time of flight) and data are reported in the form of (*m/z*).

*Please note that characterization for compounds **3.50–3.52** is limited; the best available data is presented in its existing state and, where appropriate, these limitations are noted.*

3.11.2 Experimental Procedures



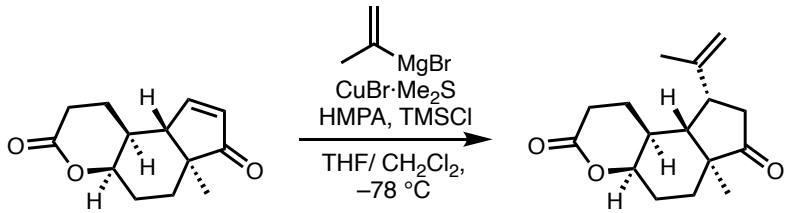
Based on a previously reported procedure.[1] Ketone **3.11** (500 mg, 2.25 mmol, 1.0 equiv.) was dissolved in dry CH_2Cl_2 (22.5 mL) and cooled to 0 °C. Triethylamine (941 µL, 6.75 mmol, 3.0 equiv.) was added by syringe in one portion. TMSOTf (829 µL, 4.50 mmol, 2.0 equiv.) was added via syringe pump at a rate of 1 equivalent per hour over two hours. The reaction mixture was stirred for one additional hour, then quenched with saturated aqueous $NaHCO_3$ (20 mL). The layers were separated and the aqueous phase was extracted with CH_2Cl_2 (3 x 20 mL). The combined organic extracts were washed with brine (50 mL), dried with Na_2SO_4, and concentrated under reduced pressure. The crude enoxysilane **S3.14** (611 mg) was used without purification in the next step.

^{1}H NMR (600 MHz, $CDCl_3$) δ 4.53 – 4.50 (m, 1H), 4.48 (dd, J = 3.2, 1.2 Hz, 1H), 2.56 – 2.39 (m, 2H), 2.11 – 1.95 (m, 4H), 1.90 – 1.80 (m, 3H), 1.76 (dddd, J = 13.6, 7.0, 5.8, 3.2 Hz, 1H), 1.54 – 1.48 (m, 2H), 0.89 (s, 3H), 0.19 (s, 9H).

^{13}C NMR (151 MHz, $CDCl_3$) δ 172.7, 164.5, 98.6, 79.2, 44.6, 44.2, 31.4, 28.5, 27.9, 27.5, 26.6, 21.6, 14.3, 0.2.

Crude enoxysilane **S3.14** (611 mg, 2.02 mmol, 1.0 equiv.) was dissolved in dry MeCN (40.5 mL). Palladium(II) acetate (545 mg, 2.43 mmol, 1.2 equiv.) was added in one portion. The reaction mixture was stirred for two hours, then loaded neat onto SiO_2 (30 g), eluted with EtOAc (3 x 60

mL), and concentrated under reduced pressure to an orange oil. The crude oil was dry loaded onto Celite (10 g) and purified by flash column chromatography (SiO_2, 50 g, 0–20% acetone in hexanes) to provide **3.14** (402 mg; 89% over two steps) as a tan solid. The spectral data matched those reported in the literature.[1]



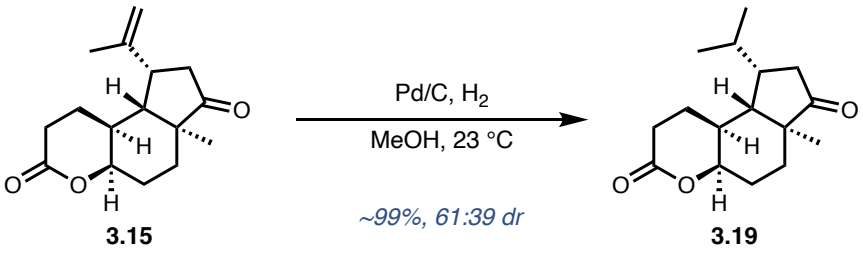
$CuBr{\cdot}Me_2S$ (14.9 mg, 72.6 µmol, 1.6 equiv.) was suspended in dry THF (462 µL) and cooled to –78 °C with a dry ice/acetone cooling bath. Isopropenylmagnesium bromide (0.44 M, 330 µL, 145 µmol, 3.2 equiv.) was added dropwise by syringe to form an orange solution, which was stirred at –78 °C for 45 minutes. TMSCl (28.7 µL, 227 µmol, 5 equiv.) and HMPA (39.5 µL, 227 µmol, 5 equiv.) were added sequentially by syringe. Enone **3.14** (10.0 mg, 45.4 µmol, 1.0 equiv.) was added as a solution in CH_2Cl_2 (295 µL). The reaction mixture was stirred at –78 °C for one hour, removed from the cooling bath, and quenched with saturated aqueous NH_4Cl : 30% NH_4OH (9:1, 2 mL). The biphasic mixture was diluted with Et_2O and stirred vigorously for one hour. The layers were separated, and the aqueous phase was further extracted with Et_2O (5 x 2 mL). The combined organic extracts were washed with brine (5 mL), dried over anhydrous $MgSO_4$, and concentrated under reduced pressure. The crude residue was purified by flash column chromatography (SiO_2, 2 g, 0–15% acetone in hexanes) to afford **3.15** (8.8 mg, 74%) as a crystalline solid. The solid was recrystallized by vapor diffusion using a hexanes/EtOAc system to obtain a single crystal suitable for X-ray diffraction.

^{1}H NMR (500 MHz, $CDCl_3$) δ 4.95 (s, 1H), 4.86 (s, 1H), 4.56 (q, J = 3.1 Hz, 1H), 2.93 (t, J = 8.2 Hz, 1H), 2.66 (dd, J = 19.3, 2.1 Hz, 1H), 2.62 – 2.54 (m, 2H), 2.53 – 2.45 (m, 2H), 2.28 – 2.20 (m, 1H), 2.12 (dd, J = 13.4, 7.2 Hz, 1H), 2.08 (dq, J = 15.1, 3.1 Hz, 1H), 1.94 – 1.85 (m, 2H), 1.83 (s, 3H), 1.63 – 1.59 (m, 2H), 1.08 (s, 3H).

^{13}C NMR (151 MHz, $CDCl_3$) δ 219.7, 172.8, 145.9, 113.3, 77.6, 47.1, 46.4, 42.6, 40.0, 31.6, 29.0, 27.3, 26.5, 25.2, 21.8, 16.8.

HRMS (CI+) *m/z calc'd* for $C_{16}H_{22}O_3$ $[M]^+$: 262.1569, found 262.1564.

TLC: R_f = 0.26 (30% acetone in hexanes, visualized by CAM)



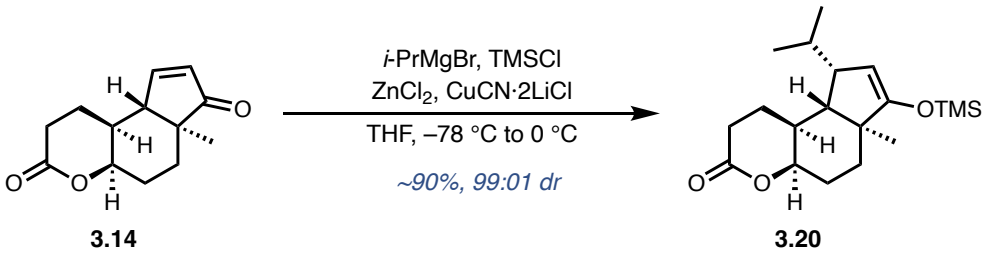
10% Pd/C (4 mg, 0.004 mmol, 0.1 eq.) was added in one portion to a solution of alkenyl ketone **3.15** (10 mg, 0.038 mmol, 1 equiv.) in MeOH (380 µL). The reaction mixture was stirred for 16 hours under a balloon atmosphere of hydrogen, then filtered through Celite (500 mg) and concentrated under reduced pressure to afford crude **3.19** (10 mg, ~99%) as a 61:39 mixture of diastereomers. An analytical sample of **3.19** was separately obtained through the protodesilylation of **3.20**.

^{1}H NMR (600 MHz, $CDCl_3$) δ 4.53 (app q, J = 3.1 Hz, 1H), 2.60 – 2.46 (m, 3H), 2.41 – 2.38 (m, 2H), 2.25 (dtd, J = 13.6, 8.3, 5.1 Hz, 1H), 2.07 (dq, J = 15.1, 2.9 Hz, 1H), 2.01 – 1.95 (m, 2H), 1.90 – 1.77 (m, 3H), 1.63 – 1.59 (m, 2H), 1.09 (s, 3H), 1.05 (d, J = 6.7 Hz, 3H), 0.94 (d, J = 6.4 Hz, 3H).

^{13}C NMR (151 MHz, $CDCl_3$) δ 221.0, 173.0, 77.3, 47.3, 46.3, 43.9, 42.2, 32.0, 31.4, 29.4, 27.3, 26.3, 24.2, 22.4, 22.0, 16.5.

HRMS (ES+) *m/z* calc'd for $C_{22}H_{28}SeO_3$ $[M+Na]^+$: 443.1103, found 443.1086.

TLC: R_f = 0.30 (10% EtOAc in CH_2Cl_2, visualized by CAM)



Preparation of CuCN·2LiCl solution:

Anhydrous LiCl (9.6 mg, 0.23 mmol, 5.0 equiv.) and CuCN (10 mg, 0.11 mmol, 2.5 equiv.) were suspended in THF (300 µL) and stirred vigorously until homogenous - approximately 15 minutes.

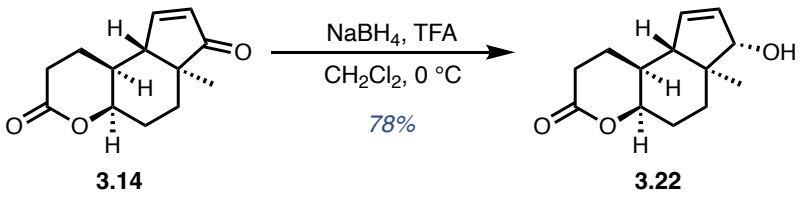
Preparation of i-Pr_2Zn:

Anhydrous $ZnCl_2$ (15 mg, 0.11 mmol, 2.5 equiv.) was suspended in dry THF (300 µL) and cooled to 0 °C with an ice/water bath. Isopropylmagnesium bromide (0.40 M, 570 µL, 0.23 mmol, 5 equiv.) was added dropwise, then the reaction mixture was removed from the cooling bath and stirred for 15 minutes while warming to 23 °C.

A solution of CuCN·2LiCl (see above) was added dropwise to a freshly prepared solution of *i*-Pr_2Zn (see above) at –78 °C. The organometallic mixture was stirred at this temperature for 30 minutes. Enone **3.14** (10 mg, 0.045 mmol, 1 equiv.) and TMSCl (29 µL, 0.23 mmol, 5 equiv.) were added dropwise as a solution in dry THF (600 µL). The reaction mixture was stirred at 0 °C for 30 minutes and quenched with the addition of saturated aqueous $NaHCO_3$ (2 mL). The biphasic mixture was diluted with saturated aqueous NH_4Cl : 30% NH_4OH (9:1, 2 mL) at which point the layers were separated. The aqueous phase was further extracted with EtOAc (4 x 2 mL) and the combined organic extracts were washed with saturated aqueous NH_4Cl : 30% NH_4OH (9:1, 4 mL), brine : saturated aqueous $NaHCO_3$ (1:1, 6 mL), and concentrated under reduced pressure to afford **3.20** (14 mg, ~90%) as a clear oil that could be used without further purification.

^{1}H NMR (600 MHz, $CDCl_3$) δ 4.71 (d, J = 3.1 Hz, 1H), 4.51 (app q, J = 3.2 Hz, 1H), 2.54 – 2.41 (m, 2H), 2.35 – 2.29 (m, 1H), 2.20 – 2.13 (m, 1H), 2.11 – 2.07 (m, 1H), 2.06 – 2.02 (m, 1H), 2.02 – 1.98 (m, 1H), 1.88 – 1.72 (m, 3H), 1.50 (dd, J = 13.2, 4.3 Hz, 1H), 1.45 (ddd, J = 12.8, 5.1, 2.2 Hz, 1H), 1.08 (s, 3H), 0.95 (d, J = 6.7 Hz, 3H), 0.86 (d, J = 6.6 Hz, 3H), 0.20 (s, 9H).

TLC: R_f = 0.65 (10% EtOAc in CH_2Cl_2, visualized by CAM)



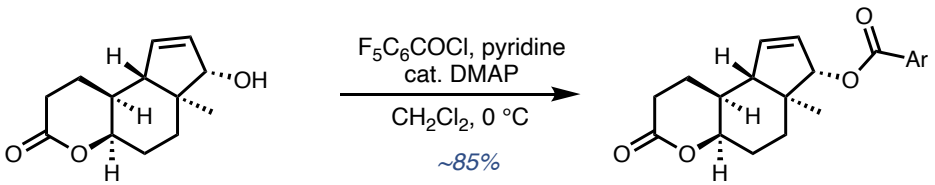
3.14 **3.22**

Based on a previously reported procedure.[1] Trifluoroacetic acid (100 µL, 1.4 mmol, 30 equiv.) was added dropwise to a suspension of $NaBH_4$ (6.9 mg, 0.18 mmol, 4 equiv.) in dry CH_2Cl_2 (610 µL). The heterogeneous mixture was gently stirred for 10 minutes at 23 °C, then **3.14** (10 mg, 0.045 mmol, 1 equiv.) was added as a solution in dry CH_2Cl_2 (300 µL). The heterogeneous reaction mixture was stirred for 1 hour and then the reaction was quenched with saturated aqueous Na_2CO_3 (3 mL). The layers were separated and the aqueous phase was further extracted with CH_2Cl_2. The combined organic extracts were washed with brine, dried over Na_2SO_4, and concentrated under reduced pressure. The crude residue was purified by flash column chromatography (SiO_2, 2 g, 0–10% EtOAc in CH_2Cl_2) to provide **3.22** (7.8 mg, 78%) a clear oil. The spectral data matched those reported previously.[1]

^{1}H NMR (500 MHz, $CDCl_3$) δ 5.84 (dt, J = 4.2, 1.9 Hz, 1H), 5.77 (ddd, J = 5.9, 3.3, 1.3 Hz, 1H), 4.52 (q, J = 2.9 Hz, 1H), 4.40 (s, 1H), 2.56 – 2.40 (m, 2H), 2.33 (ddd, J = 12.3, 4.8, 2.7 Hz, 1H), 2.19 – 2.12 (m, 2H), 2.09 – 2.02 (m, 1H), 1.94 – 1.86 (m, 1H), 1.85 – 1.79 (m, 1H), 1.76 (dd, J = 12.8, 4.5 Hz, 1H), 1.70 (ddd, J = 12.4, 5.3, 1.9 Hz, 1H), 1.65 (d, J = 7.3 Hz, 1H), 0.88 (s, 3H).

HRMS (ES+) *m/z* calc'd for $C_{13}H_{18}O_3$ $[M+Na]^+$: 245.1154, found 245.1165.

TLC: R_f = 0.11 (10% EtOAc in CH_2Cl_2, visualized by CAM)



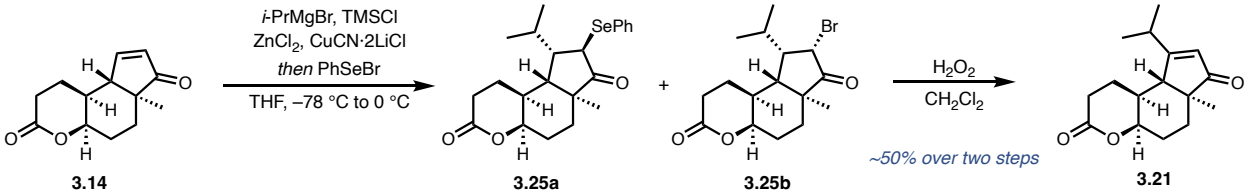
3.22 **3.23**

Allyl alcohol **3.22** (10 mg, 0.045 mmol, 1 equiv.), pyridine (8.7 µL, 0.11 mmol, 2.4 equiv.), and DMAP (0.5 mg, 0.005 mmol, 0.1 equiv.) were dissolved in dry CH_2Cl_2 (450 µL). 2,3,4,5,6-pentafluorobenzoyl chloride (7.8 µL, 0.054 mmol, 1.2 equiv.) was added dropwise and then the reaction mixture was stirred for 1 hour. The reaction was quenched with saturated aqueous NH_4Cl (2 mL) and diluted with EtOAc (2 mL). The layers were separated, and the aqueous phase was further extracted with EtOAc (4 x 2 mL). The combined organic extracts were washed with saturated aqueous $NaHCO_3$ (4 mL), brine (4 mL), dried over Na_2SO_4, and concentrated under reduced pressure to afford crude **3.23** (16 mg, ~85%)

^{1}H NMR (500 MHz, $CDCl_3$) δ 6.01 (d, J = 5.6 Hz, ll1H), 5.89 – 5.83 (m, 1H), 5.60 (s, 1H), 4.55 – 4.50 (m, 1H), 2.59 – 2.42 (m, 3H), 2.26 – 2.18 (m, 2H), 2.10 – 2.03 (m, 1H), 1.98 – 1.89 (m, 2H), 1.83 (dt, J = 10.6, 6.9 Hz, 1H), 1.77 – 1.73 (m, 1H), 1.71 – 1.54 (m, 1H), 0.97 (s, 3H).

HRMS (ES+) *m/z* calc'd for $C_{20}H_{17}F_5O_4$ $[M]^+$: 416.1047, found 416.1039.

TLC: R_f = 0.56 (10% EtOAc in CH_2Cl_2, visualized by CAM)



Preparation of CuCN·2LiCl solution:

Anhydrous LiCl (9.6 mg, 0.23 mmol, 5.0 equiv.) and CuCN (10 mg, 0.11 mmol, 2.5 equiv.) were suspended in THF (300 µL) and stirred vigorously until homogenous - approximately 15 minutes.

Preparation of i-Pr_2Zn:

Anhydrous $ZnCl_2$ (15 mg, 0.11 mmol, 2.5 equiv.) was suspended in dry THF (300 µL) and cooled to 0 °C with an ice/water bath. Isopropylmagnesium bromide (0.40 M, 570 µL, 0.23 mmol, 5 equiv.) was added dropwise, then the reaction mixture was removed from the cooling bath and stirred for 15 minutes while warming to 23 °C.

A solution of CuCN·2LiCl (see above) was added dropwise to a freshly prepared solution of *i*-Pr_2Zn (see above) at –78 °C. The organometallic mixture was stirred at this temperature for 30 minutes. Enone **3.14** (10 mg, 0.045 mmol, 1 equiv.) and TMSCl (29 µL, 0.23 mmol, 5 equiv.) were added dropwise as a solution in dry THF (600 µL). The bright yellow reaction mixture was stirred at 0 °C for 30 minutes. Phenylselenyl bromide (96 mg, 0.41 mmol, 9 equiv.) was added as a solution in dry THF (500 µL) and the emerald mixture that formed was stirred at 0 °C for 2 hours. The reaction was quenched with the addition of saturated aqueous NH_4Cl (2 mL) and diluted with NH_4Cl : 30% NH_4OH (9:1, 1 mL). The layers were separated, and the aqueous phase was further extracted with Et_2O (7 x 2 mL). The combined organic extracts were washed with brine (4 mL), dried over Na_2SO_4, and concentrated under reduced pressure to form a mixture of desired **3.25a** and bromide **3.25b** (24 mg, ~40% purity). The crude selenide **3.25a** could be used in the following step without purification. An analytical sample was obtained in a separate experiment by purification with flash column chromatography (SiO_2, 2 g, 0–2% EtOAc in CH_2Cl_2).

^{1}H NMR (600 MHz, $CDCl_3$) δ 7.62 – 7.59 (m, 2H), 7.40 – 7.36 (m, 1H), 7.33 – 7.29 (m, 2H), 4.46 (app q, J = 3.1 Hz, 1H), 3.85 (d, J = 1.1 Hz, 1H), 2.51 – 2.41 (m, 2H), 2.33 (dt, J = 16.7, 6.3 Hz, 1H), 2.14 – 2.08 (m, 2H), 2.04 – 1.99 (m, 1H), 1.87 – 1.83 (m, 1H), 1.82 – 1.75 (m, 2H), 1.67 –

1.61 (m, 2H), 1.53 (td, J = 13.5, 4.1 Hz, 1H), 1.08 (s, 3H), 0.98 (d, J = 6.6 Hz, 3H), 0.86 (d, J = 6.3 Hz, 3H).

^{13}C NMR (151 MHz, $CDCl_3$) δ 216.9, 172.4, 136.9, 129.51, 129.46, 127.7, 77.4, 60.5, 50.84, 50.80, 46.4, 44.3, 31.9, 31.6, 30.2, 27.1, 26.4, 23.8, 22.10, 22.07, 16.8, 14.3.

HRMS (ES+) *m/z* calc'd for $C_{22}H_{28}SeO_3$ $[M+Na]^+$: 443.1103, found 443.1086.

TLC: R_f = 0.24 (2% EtOAc in CH_2Cl_2, visualized by CAM)

3.21: Aqueous H_2O_2 (30 wt%, 23 µL, 0.23 mmol, 10 equiv.) was added via Hamilton syringe to a stirring solution of crude **3.25a** (24 mg, ~40% purity, 0.023 mmol, 1 equiv.) in CH_2Cl_2 (500 µL) at 23 °C. After 1 hour, the reaction was quenched with the addition of saturated aqueous $NaHCO_3$ (1 mL). The layers were separated, and the aqueous phase was extracted with EtOAc (3 x 2 mL). The combined organic extracts were washed with brine (3 mL), dried with anhydrous Na_2SO_4, and concentrated under reduced pressure. The crude residue was then purified by flash column chromatography (SiO_2, 2 g, 0–10% EtOAc in CH_2Cl_2), allowing separation of both the desired enone **3.21** (5 mg, ~90%) and the bromide impurity **3.25b**.

Enone **3.21**:

^{1}H NMR (500 MHz, $CDCl_3$) δ 5.82 (dd, J = 2.8, 1.2 Hz, 1H), 4.57 (q, J = 3.2 Hz, 1H), 2.84 (dd, J = 12.6, 2.8 Hz, 1H), 2.66 – 2.56 (m, 2H), 2.56 – 2.47 (m, 2H), 2.35 – 2.28 (m, 1H), 2.15 – 2.08 (m, 2H), 2.03 – 1.95 (m, 1H), 1.81 (td, J = 13.2, 4.7 Hz, 1H), 1.72 (ddd, J = 13.4, 5.6, 2.1 Hz, 1H), 1.21 (d, J = 6.6 Hz, 3H), 1.13 (d, J = 6.9 Hz, 3H), 1.12 (s, 3H).

^{13}C NMR (151 MHz, $CDCl_3$) δ 211.1, 183.8, 172.2, 124.4, 78.7, 52.6, 48.9, 31.6, 30.4, 27.3, 26.5, 24.4, 23.1, 21.6, 21.4, 20.6.

HRMS (ES+) *m/z* calc'd for $C_{16}H_{22}O_3$ $[M+Na]^+$: 285.1467, found 285.1460.

TLC: R_f = 0.19 (10% EtOAc in CH_2Cl_2, visualized by CAM)

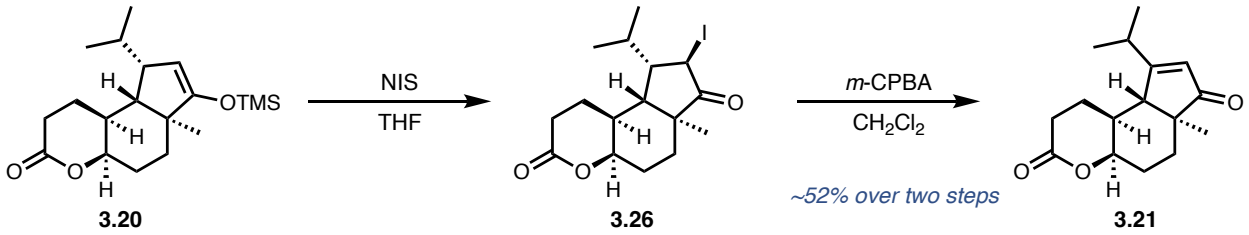
Bromide **3.25b**

^{1}H NMR (600 MHz, $CDCl_3$) δ 4.55 (q, *J* = 3.0 Hz, 1H), 4.27 (d, *J* = 1.0 Hz, 1H), 2.64 – 2.59 (m, 1H), 2.58 – 2.48 (m, 3H), 2.23 (dtd, *J* = 13.8, 7.8, 5.9 Hz, 1H), 2.13 (dd, *J* = 11.1, 6.3 Hz, 1H), 2.11 – 2.07 (m, 1H), 1.92 – 1.72 (m, 5H), 1.13 (s, 3H), 1.09 (overlapping d, *J* = 6.8 Hz), 1.08 (overlapping d, *J* = 6.3 Hz)

^{13}C NMR (151 MHz, $CDCl_3$) δ 213.9, 172.4, 77.17 (overlapping $CDCl_3$; please see DEPTQ), 54.0, 50.2, 46.3, 43.4, 31.7, 31.5, 30.9, 27.1, 26.4, 23.9, 22.1, 21.9, 16.7.

HRMS (CI+) *m/z* calc'd for $C_{16}H_{23}BrO_3$ $[M]^+$: 342.0831, found 342.0840.

TLC: R_f = 0.50 (10% EtOAc in CH_2Cl_2, visualized by CAM)



NIS (10 mg, 0.046 mmol, 1.2 equiv.) was added at once to a stirring solution of enoxysilane **3.20** (13 mg, 0.039 mmol, 1 equiv.) in dry THF (190 µL). The reaction mixture was stirred at 23 °C for 1 hour, then the reaction was quenched with the addition of saturated aqueous $Na_2S_2O_3$ (2 mL).

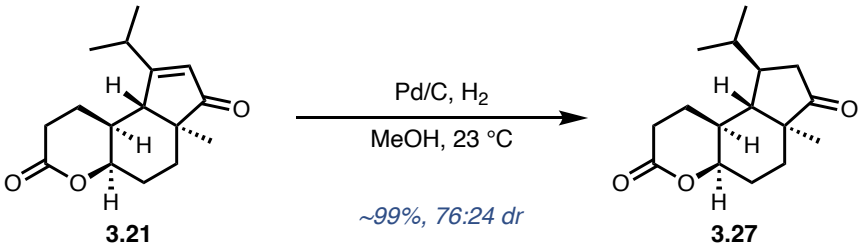
The layers of the newly-formed biphasic mixture were separated, and the aqueous phase was further extracted with EtOAc (3 x 2 mL). The combined organic extracts were washed with brine (6 mL), dried over anhydrous Na_2SO_4, and concentrated under reduced pressure to afford crude **3.26** (13 mg, approx. 86%), which was used without purification in the following step.

^{1}H NMR (500 MHz, $CDCl_3$) δ 4.65 (s, 1H), 4.56 (app q, J = 3.1 Hz, 1H), 2.73 (dd, J = 13.3, 5.9 Hz, 1H), 2.62 – 2.49 (m, 3H), 2.27 – 2.17 (m, 1H), 2.10 – 2.05 (m, 2H), 1.93 – 1.82 (m, 2H), 1.81 – 1.73 (m, 3H), 1.12 (s, 3H), 1.08 (d, J = 6.5 Hz, 3H), 1.06 (d, J = 6.8 Hz, 3H).

HRMS (CI+) *m/z* calc'd for $C_{16}H_{23}IO_3$ $[M]^+$: 390.0692, found 390.0707.

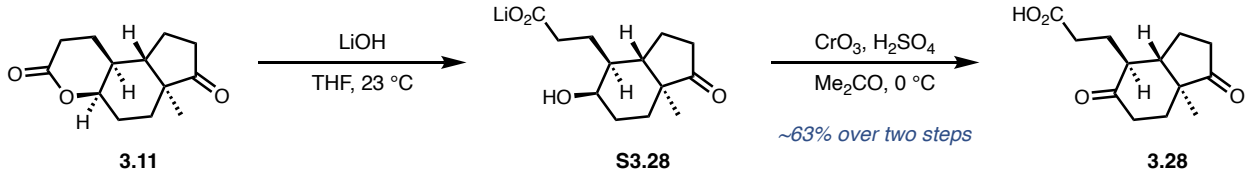
TLC: R_f = 0.65 (10% EtOAc in CH_2Cl_2, visualized by CAM)

Iodide **3.26** was suspended in dry CH_2Cl_2 (560 µL) and cooled to 0 °C with an ice/water bath. A solution of *m*-CPBA (11 mg, 0.067 mmol, 2 equiv.) in dry CH_2Cl_2 (1.1 mL) was added dropwise. After 10 hours, the reaction was quenched with the addition of saturated aqueous $NaHCO_3$ (2 mL). The biphasic mixture was extracted with EtOAc (2 x 2 mL) and then the combined organic extracts were washed with saturated aqueous $Na_2S_2O_3$ (4 mL), saturated aqueous $NaHCO_3$ (4 mL), brine (4 mL), dried over anhydrous sodium sulfate, and concentrated under reduced pressure to afford crude enone **3.21** (5.2 mg, approx. 60%) as an opaque oil. The spectra matched those obtained previously via oxidation/elimination of selenide **3.25a**.



10% Pd/C (6 mg, 0.006 mmol, 0.3 eq.) was added in one portion to a solution of enone **3.21** (5.4 mg, 0.21 mmol, 1 equiv.) in MeOH (500 µL). The reaction mixture was stirred for 2 hours under a balloon atmosphere of hydrogen, then filtered through Celite (200 mg) and concentrated under reduced pressure to afford crude ketone **3.27** (5.4 mg, ~99%) as a 76:24 mixture of diastereomers.

TLC: R_f = 0.30 (10% EtOAc in CH_2Cl_2, visualized by CAM)



Sitolactone (**3.11)** (50 mg, 0.22 mmol, 1 equiv.) and LiOH·H_2O (14 mg, 0.34 mmol, 1.5 equiv.) were suspended in THF : H_2O (3:1, 750 µL). The reaction mixture was stirred for 48 hours at 23 °C, then the stir bar was removed and the mixture was concentrated under reduced pressure to form lithium carboxylate **S3.28** (50 mg, ~90%) as an opaque wax. The crude material was used immediately in the following step.

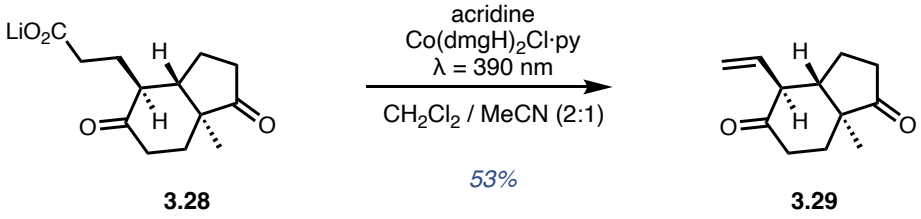
^{1}H NMR (500 MHz, D_2O) δ 4.03 (q, J = 2.7 Hz, 1H), 3.76 – 3.64 (m, 1H), 2.54 (dd, J = 20.0, 8.6 Hz, 1H), 2.37 – 2.28 (m, 1H), 2.26 – 2.16 (m, 2H), 2.05 – 1.98 (m, 1H), 1.83 – 1.78 (m, 3H), 1.77 – 1.64 (m, 3H), 1.61 – 1.45 (m, 3H), 0.92 (s, 3H).

TLC: R_f = 0.17 (70% EtOAc in hexanes + 1% AcOH, visualized by CAM)

HRMS (ES–) *m/z* calc'd for $C_{13}H_{20}O_4$ $[M–H]^-$: 239.1283, found 239.1278.

Based on a previously reported procedure.[2] Lithium carboxylate **S3.28** (50 mg, 0.20 mmol, 1 equiv.) was dissolved in H_2O (510 µL) and cooled to 0 °C. A solution of Jones' reagent (2.5 M in H_2O, 650 µL, 1.6 mmol, 8 equiv.) was added dropwise. After stirring for 5 hours, the reaction was quenched with *i*-PrOH (1 mL) and the mixture dilute with brine (1 mL). The biphasic solution was transferred to a separatory funnel and extracted with EtOAc (3 x 20 mL). The combined organic extracts were washed with water (5 x 5 mL), brine (10 mL), dried over Na_2SO_4 and concentrated under reduced pressure to afford ketoacid **3.28** (35 mg, ~70%). The spectral data matched those previously reported.[2]

TLC: R_f = 0.20 (70% EtOAc in hexanes + 1% AcOH, visualized by CAM)



3.28 **3.29**

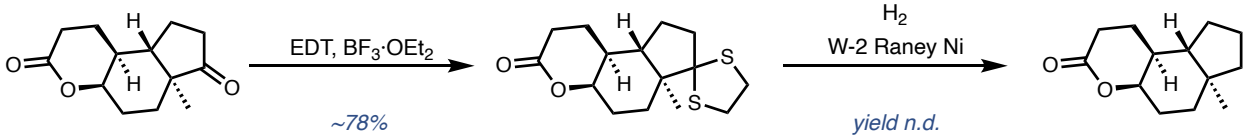
3.29: Lithium carboxylate **3.28**[2] (10 mg, 0.042 mmol, 1 equiv.), $Co(dmgH)_2Cl{\cdot}py$ (0.85 mg, 0.002 mmol, 0.05 equiv.), and acridine (1.5 mg, 0.008 mmol, 0.2 equiv) were suspended in a mixture of degassed CH_2Cl_2 and degassed MeCN (2:1, 300 µL). The reaction mixture was irradiated with blue LED light (Kessil, λ = 390 nm) and stirred for 2 hours. The stir bar was removed and the reaction mixture was concentrated under reduced pressure to form a dark residue that was subsequently purified by flash column chromatography (SiO_2, 1.5 g, 10% acetone in hexanes) to afford alkenyl ketone **3.29** (4.3 mg, 53%) as a clear oil.

^{1}H NMR (500 MHz, $CDCl_3$) δ 5.76 (ddd, *J* = 17.2, 10.3, 8.6 Hz, 1H), 5.28 (dd, *J* = 10.3, 1.6 Hz, 1H), 5.12 (dd, *J* = 17.2, 1.4 Hz, 1H), 3.06 (dd, *J* = 12.9, 8.7 Hz, 1H), 2.59 – 2.47 (m, 3H), 2.26 – 2.17 (m, 1H), 2.05 – 2.00 (m, 1H), 1.99 – 1.90 (m, 2H), 1.74 – 1.63 (m, 2H), 1.19 (s, 3H).

Please note that the carbonyl resonances could not be conclusively assigned from the spectra obtained. (n = 10/12 carbon signals reported)

^{13}C NMR (125 MHz, $CDCl_3$) δ 133.0, 119.2, 56.0, 49.3, 47.2, 37.1, 36.1, 30.3, 22.9, 13.6.

TLC: R_f = 0.17 (10% acetone in hexanes, visualized by CAM)



3.11 **3.30** **3.31**

$BF_3{\cdot}Et_2O$ (63 µL, 0.50 mmol, 1.1 equiv.) was added to a solution of sitolactone (**3.11**) (100 mg, 0.45 mmol, 1 equiv.) and 1,2-ethanedithiol (57 µL, 0.68 mmol, 1.5 equiv.) in dry CH_2Cl_2 (900 µL). After stirring for 8 hours, the reaction mixture was diluted with H_2O (2 mL) and the layers were

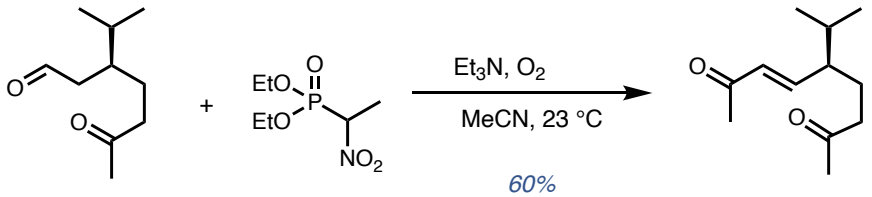
separated. The aqueous layer was further extracted with EtOAc (2 x 2 mL), then the combined organic extracts were washed with saturated aqueous $NaHCO_3$ (4 mL), brine (4 mL), dried over Na_2SO_4, and concentrated under reduced pressure. The crude residue was purified by flash column chromatography (SiO_2, 10 g, 20% acetone in hexanes) to afford dithiane **3.30** (105 mg, 78%) as a clear oil.

^{1}H NMR (500 MHz, $CDCl_3$) δ 4.48 (app q, J = 2.7 Hz, 1H), 3.31 – 3.17 (m, 3H), 3.14 – 3.06 (m, 1H), 2.59 – 2.43 (m, 3H), 2.38 (ddd, J = 14.8, 9.5, 5.1 Hz, 1H), 2.11 – 1.98 (m, 3H), 1.96 – 1.85 (m, 2H), 1.83 – 1.70 (m, 3H), 1.42 – 1.36 (m, 1H), 1.26 (qd, J = 12.0, 5.1 Hz, 1H), 0.96 (s, 3H).

HRMS (ES+) *m/z* calc'd for $C_{15}H_{22}O_2S_2$ $[M+Na]^+$: 321.0959, found 321.0963.

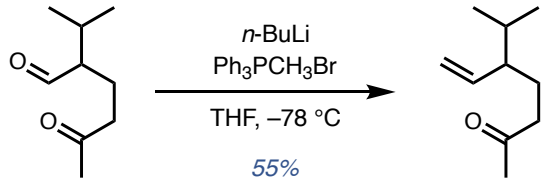
TLC: R_f = 0.37 (50% EtOAc in hexanes, visualized by PMA)

A solution of Raney Nickel (590 mg, 10 mmol, 300 equiv.) in EtOH (1.3 mL) was added to a vial containing **3.11** (10 mg, 0.034 mmol, 1 equiv.) and a stir bar. The heterogeneous mixture was placed to stir in a preheated oil bath at 60 °C under a balloon atmosphere of hydrogen. After 48 hours the reaction mixture was filtered through SiO_2 (1 g, elute w/ EtOAc) and concentrated under reduced pressure.



3.34 **3.36** **3.35**

Ketoaldehyde **3.34**[3] (10 mg, 0.059 mmol, 1 equiv.) and alkylphosphonate **3.36**[4] (25 mg, 0.12 mmol, 2 equiv.) were dissolved in MeCN (290 µL). Triethylamine (25 µL, 0.18 mmol, 3 equiv.) was added by syringe and the reaction mixture was stirred at 23 °C with no effort made to exclude air or water. After 36 hours the reaction mixture was diluted with EtOAc (2 mL) and quenched with 1 M HCl : brine (1:1, 4 mL). The layers were separated and the aqueous layer was further extracted with EtOAc (2 x 2 mL). The combined organic extracts were washed with $NaHCO_3$: brine (1:1, 4 mL), dried over anhydrous Na_2SO_4, and concentrated under reduced pressure. The crude reside was purified by flash column chromatography (SiO_2, 1.8 g, 0–20% EtOAc in hexanes) to afford **3.35** (7 mg, 60%) as a clear oil. The spectral data matched those previously reported.[3]



3.38 **3.42**

Methyltriphenylphosphonium bromide (8.2 g, 23 mmol, 1.9 equiv.) was suspended in dry THF (110 mL) and cooled to –78 °C. A solution of *n*-butyllithium (2.65 M in hexanes, 8.2 mL, 1.8 equiv.) was added dropwise and the mixture was stirred at –78 °C for 20 minutes. The reaction mixture was warmed to 0 °C for 15 minutes. The solution of ylide was cooled to –78 °C and then ketoaldehyde **3.38**[5] (1.9 g, 12 mmol, 1 equiv.) was added quickly as solution in dry THF (10 mL). The reaction mixture was stirred for 30 minutes, then removed from the cooling bath and stirred for 1 hour while warming to 23 °C. The reaction was quenched with saturated aqueous NH_4Cl (80 mL) and the biphasic solution that formed was diluted with H_2O (20 mL). The layers were separated and the aqueous phase was further extracted with Et_2O (3 x 20 mL). The combined

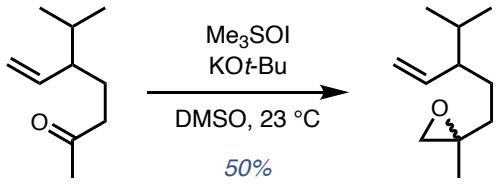
organic extracts were washed with brine (2 x 30 mL), dried over anhydrous $MgSO_4$, and concentrated under reduced pressure (*Note:* ***3.42*** *is volatile; solvent removed at P = 90 mmHg*). The crude residue was purified by flash column chromatography (SiO_2, 35 g, 10% Et_2O in hexanes) then distilled under reduced pressure (b.p. = 66–74 °C at 40 mmHg) to afford alkenyl ketone **3.42** (1.0 g, 55%).

^{1}H NMR (500 MHz, $CDCl_3$) δ 5.50 (dt, J = 17.1, 9.7 Hz, 1H), 5.04 (dd, J = 10.3, 2.2 Hz, 1H), 4.93 (dd, J = 17.1, 2.2 Hz, 1H), 2.47 – 2.39 (m, 1H), 2.37 – 2.29 (m, 1H), 2.12 (s, 3H), 1.79 – 1.67 (m, 2H), 1.63 – 1.53 (m, 1H), 1.50 – 1.41 (m, 1H), 0.89 (d, J = 6.7 Hz, 3H), 0.84 (d, J = 6.8 Hz, 3H).

^{13}C NMR (125 MHz, $CDCl_3$) δ 209.5, 140.4, 116.3, 50.5, 42.1, 32.0, 30.2, 25.8, 20.7, 19.2.

HRMS (CI+) *m/z* calc'd for $C_{10}H_{18}O$ $[M]^+$: 154.1358, found 154.1362.

TLC: R_f = 0.31 (10% Et_2O in hexanes, visualized by PMA)



3.42 **3.43**

Anhydrous potassium *tert*-butoxide (3.42 g, 30.5 mmol, 5 equiv.) was dissolved in DMSO (15.2 mL) and stirred for 15 minutes at 23 °C. The solution of DMSO and KO*t*-Bu was transferred by syringe to a vial containing a stir bar and trimethylsulfoxonium iodide (6.71 g, 30.5 mmol, 5 equiv.). The mixture was stirred for 20 minutes at 23 °C, then diluted with dry THF (10.2 mL). A

solution of alkenyl ketone **3.42** in THF (5.1 mL) was added and the mixture was stirred for 12 hours. The reaction mixture was poured into ice (40 g), then diluted with saturated aqueous NH_4Cl : H_2O (1:1, 100 mL) and Et_2O (80 mL). The biphasic mixture was shaken vigorously and allowed to stand for 10 minutes. The layers were separated and the aqueous layer was further extracted with Et_2O (3 x 30 mL), washed with H_2O : brine (1:1, 3 x 40 mL), dried over $MgSO_4$ and concentrated under reduced pressure (*Note: **3.43** is volatile; solvent removed at P = 120 mmHg*). The crude residue was purified by flash column chromatography (SiO_2, 2 g, 0–4% Et_2O in hexanes) to provide **3.43** (8 mg, ~75% purity, 55%) as an inseparable mixture of diastereomers. An analytical sample of this mixture was obtained by distillation of the crude material under reduced pressure (b.p. = 59 °C at 24 mmHg).

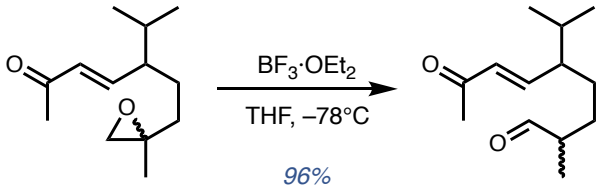
Please note that the NMR spectra reported is for the mixture of diastereomers.

^{1}H NMR (500 MHz, $CDCl_3$) δ 5.57 – 5.47 (m, 1H), 5.02 (app dt, J = 10.2, 2.1 Hz, 1H), 4.92 (app dd, J = 17.1, 2.2 Hz, 1H), 2.62 – 2.55 (m, 2H), 1.77 – 1.69 (m, 1H), 1.67 – 1.47 (m, 3H), 1.44 – 1.31 (m, 2H), 1.30 (s, 3H), 0.88 (d, J = 6.7 Hz, 3H), 0.85 – 0.82 (m, 3H).

^{13}C NMR (125 MHz, $CDCl_3$) δ 140.44, (140.04), 115.85, (115.84), 54.03, (53.97), 50.8, (50.6), 34.9, (34.7), 31.7, 27.33, (27.32), 21.15, (21.07), 20.7, (20.6), 18.9.

HRMS (ES+) *m/z* calc'd for $C_{11}H_{20}O$ $[M+H]^+$: 169.1591, found 169.1615.

TLC: R_f = 0.61 (20% EtOAc in hexanes, visualized by PMA)

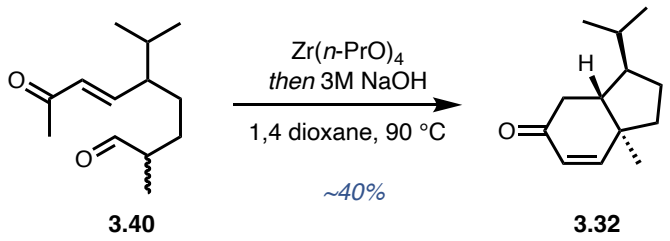


3.41 **3.40**

Based on a previously reported procedure.[6] Epoxide **3.41**[6] (1.76 g, 8.37 mmol, 1 equiv.) was dissolved in dry THF (42 mL) and cooled to –78 °C with a dry ice/acetone bath. $BF_3{\cdot}OEt_2$ (2.10 mL, 16.7 mmol, 2 equiv.) was slowly added, then the reaction mixture was removed from the cooling bath and allowed to stir for 30 minutes while warming to 23 °C. The reaction was quenched with the addition of saturated aqueous $NaHCO_3$ (40 mL). The layers of the newly formed biphasic mixture were separated, and the aqueous phase was further extracted with Et_2O (2 x 40 mL). The combined organic extracts were washed with brine (60 mL), dried over anhydrous $MgSO_4$, and concentrated under reduced pressure. The crude residue was dissolved once more in Et_2O (40 mL), washed with brine (3 x 20 mL), dried over $MgSO_4$, filtered through Celite (10 g, eluting with Et_2O), and concentrated under reduced pressure to form aldehyde **3.40** (1.7 g, 96%) as a clear oil. The spectral data matched those previously reported.[6]

^{1}H NMR (500 MHz, $CDCl_3$) δ 9.59 (dd, J = 4.1, 2.0 Hz, 1H), 6.58 (ddd, J = 15.9, 9.7, 3.2 Hz, 1H), 6.05 (d, J = 15.9 Hz, 1H), 2.35 – 2.28 (m, 1H), 2.26 (d, J = 2.4 Hz, 3H), 2.00 – 1.91 (m, 1H), 1.74 – 1.67 (m, 1H), 1.59 – 1.51 (m, 2H), 1.39 – 1.19 (m, 2H), 1.10 (dd, J = 7.1, 2.6 Hz, 3H), 0.90 (dd, J = 6.9, 1.3 Hz, 3H), 0.86 (dd, J = 6.9, 2.4 Hz, 3H).

TLC: R_f = 0.43 (30% EtOAc in hexanes, visualized by CAM)

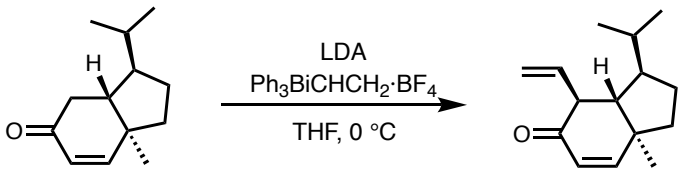


3.40 **3.32**

Based on a previously reported procedure.[6] Aldehyde **3.40** (1.6 g, 7.61 mmol, 1 equiv.) was dissolved in dry 1,4-dioxane (76 mL). A solution of zirconium(IV) propoxide (70 wt% in *i*-PrOH, 3.38 mL, 7.61 mmol, 1 equiv.) was added, and the mixture was stirred at 23 °C for 2 hours. An aqueous solution of NaOH (3 M, 12.7 mL, 38.0 mmol, 5 equiv.) was added to form a slurry, which was heated to 90 °C and stirred for 12 hours. The reaction was quenched with aqueous HCl (1 M, 100 mL) and the layers were separated. The aqueous phase was further extracted with Et_2O (3 x 50 mL), washed with brine (80 mL), dried over $MgSO_4$, and concentrated under reduced pressure. The crude residue was purified by flash column chromatography (SiO_2, 100 g, 0–5% EtOAc in hexanes) to afford hydrindenone **3.32** (800 mg, ~75% purity, ~40%) as an inseparable mixture of stereoisomers (major depicted). The spectral data matched those previously reported.[6]

^{1}H NMR (500 MHz, $CDCl_3$) δ 7.13 (d, *J* = 9.8 Hz, 1H), 5.83 (d, *J* = 9.8 Hz, 1H), 2.58 (dd, *J* = 17.4, 4.2 Hz, 1H), 2.29 (dd, *J* = 17.5, 14.1 Hz, 1H), 1.90 – 1.80 (m, 2H), 1.78 – 1.65 (m, 2H), 1.62 – 1.56 (m, 1H), 1.52 – 1.43 (m, 2H), 0.99 (s, 3H), 0.92 (d, *J* = 6.7 Hz, 3H), 0.85 (d, *J* = 6.6 Hz, 3H).

TLC: R_f = 0.20 (5% EtOAc in hexanes, visualized by CAM)



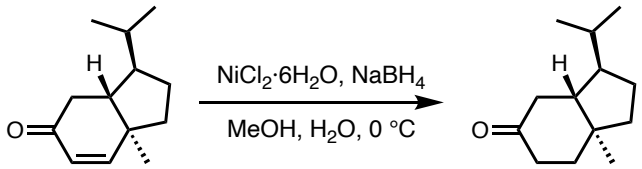
3.32 **3.9**

A solution of *n*-butyllithium (1.66 M in hexanes, 38 µL, 1.2 equiv.) was added to a solution of diisopropylamine (8.8 µL, 0.062 mmol, 1.2 equiv.) in dry THF (200 µL) at 0 °C. The mixture was stirred for 5 minutes, then cooled to –78 °C with a dry ice/acetone bath. A solution of hydrindenone **3.32** (10 mg, 0.052 mmol, 1 equiv.) in dry THF (200 µL) was added dropwise, and the mixture was stirred for 30 minutes. The enolate solution was then transferred by syringe to a separate vial containing a solution of triphenyl(vinyl)bismuth(V) tetrafluoroborate (43 mg, 0.078 mmol, 1.5 equiv.) in dry THF (200 µL) at –78 °C. The reaction mixture was stirred for 2 hours, then diluted with hexanes (3 mL) and quenched with H_2O (2 mL). The layers were then separated and the aqueous phase was further extracted with hexanes (2 x 3 mL). The combined organic layers were washed with brine (6 mL), dried over anhydrous Na_2SO_4, and concentrated under reduced pressure. The crude residue was purified by flash column chromatography (SiO_2, 2 g, 0–10% PhMe in hexanes *then* 0–2% EtOAc in hexanes) to afford ketone **3.9** (2.0 mg, ~20%).

^{1}H NMR (600 MHz, $CDCl_3$) δ 7.13 (d, J = 9.7 Hz, 1H), 5.88 (d, J = 9.7 Hz, 1H), 5.67 (ddd, J = 16.9, 10.0, 9.2 Hz, 1H), 5.26 (dd, J = 10.1, 1.7 Hz, 1H), 5.19 (dd, J = 17.0, 1.8 Hz, 1H), 2.99 (dd, J = 13.0, 9.2 Hz, 1H), 2.11 – 2.05 (m, 1H), 2.01 – 1.95 (m, 1H), 1.88 (dd, J = 13.0, 11.7 Hz, 1H), 1.74 – 1.66 (m, 1H), 1.61 – 1.52 (m, corrected 2H – *please see HMQC*), 1.43 – 1.37 (m, 1H), 1.07 (d, J = 0.9 Hz, 3H), 0.85 (d, J = 6.9 Hz, 3H), 0.74 (d, J = 6.8 Hz, 3H).

^{13}C NMR (151 MHz, $CDCl_3$) δ 201.3, 159.0, 135.5, 127.6, 119.3, 55.9, 50.4, 45.4, 44.5, 35.4, 27.1, 22.6, 21.0, 20.0, 14.7.

TLC: R_f = 0.22 (10% EtOAc in hexanes, visualized by CAM)

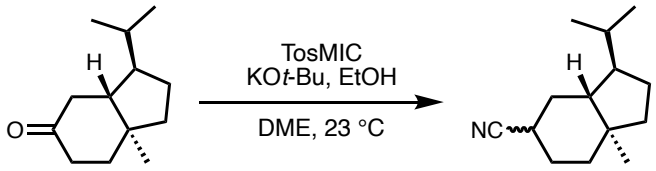


3.32 **3.49**

Hydrindenone **3.32** (10 mg, 0.052 mmol, 1 equiv.) and $NiCl_2{\cdot}6H_2O$ (124 mg, .52 mmol, 10 equiv.) were dissolved in MeOH : H_2O (6:1, 743 µL). The mixture was stirred vigorously to form a clear green solution, then $NaBH_4$ (7.9 mg, 0.21 mmol, 4 equiv.) was added in one portion, and the mixture was stirred for 1 hour. The reaction was quenched with MeOH (500 µL) and the mixture was filtered through Celite (1 g, eluted with MeOH). The methanol filtrate was diluted with H_2O (6 mL) and extracted with Et_2O (2 x 3 mL). The combined organic extracts were dried over $MgSO_4$ and concentrated under reduced pressure to afford crude **3.49** (8 mg, ~90% purity, 72%). The spectral data matched those previously reported.[7]

^{1}H NMR (600 MHz, $CDCl_3$) δ 2.47 – 2.39 (m, 2H), 2.35 – 2.30 (m, 1H), 2.17 (app t, J = 14.7 Hz, 1H), 1.91 – 1.82 (m, 2H), 1.71 – 1.58 (m, 3H), 1.55 – 1.46 (m, 3H), 1.19 (app q, J = 10.8 Hz, 1H), 1.01 (s, 3H), 0.89 (d, J = 6.1 Hz, 3H), 0.80 (d, J = 6.3 Hz, 3H).

TLC: R_f = 0.25 (10% EtOAc in hexanes, visualized by *p*-anisaldehyde)



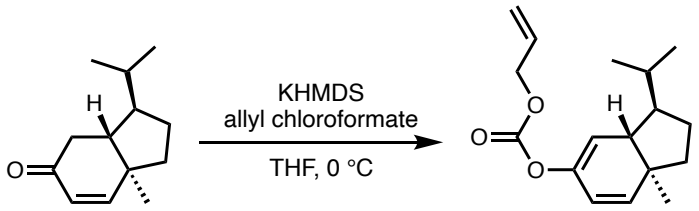
3.49 **3.50**

EtOH (6.0 µL, 0.10 mmol, 2 equiv.) was added to a solution of ketone**3.49** (10 mg, 0.051 mmol, 1 equiv.) and tosylmethyl isocyanide (12 mg, 0.062 mmol, 1.2 equiv.) in dry DME (510 µL). The reaction mixture was cooled to 0 °C, then anhydrous potassium *tert*-butoxide (17 mg, 0.15 mmol, 3 equiv.) was added in one portion. The reaction mixture was stirred for 30 minutes at 0 °C, removed from the cooling bath and stirred at 23 °C for 12 hours. The reaction mixture was diluted with Et_2O (2 mL) and the reaction was quenched with saturated aqueous $NaHCO_3$ (2 mL). The layers were separated and the aqueous layer was further extracted with Et_2O (2 x 2 mL). The combined organic extracts were washed with brine, dried over anhydrous $MgSO_4$, and concentrated under reduced pressure. The crude residue was purified by flash column chromatography (SiO_2, 2 g, 0–10% EtOAc in hexanes) to afford **3.50** (5.5 mg, ~55%) as an equal mixture of diastereomers.

Please note that the NMR spectra reported is for the mixture of diastereomers.

^{13}C NMR (151 MHz, $CDCl_3$) δ 123.2, 122.9, 49.6, 46.2, 45.9, 45.7, 41.4, 40.9, 39.2, 39.1, 38.3, 36.0, 29.2, 29.1, 29.0, 28.7, 27.6, 27.6, 25.9, 24.7, 23.0, 22.8, 22.1, 22.1, 17.8, 17.8, 17.6, 17.3.

TLC: R_f = 0.59 (20% EtOAc in hexanes, visualized by $KMnO_4$)



3.32 **3.51**

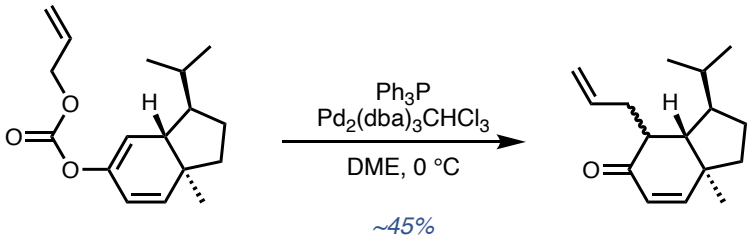
KHMDS (0.5 M in PhMe, 620 µL, 0.31 mmol, 3 equiv.) was added to a solution of hydrindenone **3.32** (20 mg, 0.10 mmol, 1 equiv.) in dry THF (1 mL) at –78 °C and the resulting mixture was stirred for 30 minutes. Allyl chloroformate (99 µL, 0.94 mmol, 9 equiv.) was added in one portion, the reaction mixture was removed from the cooling bath and stirred for 2 hours while warming to 23 °C. The reaction was quenched with brine (2 mL) and diluted with Et_2O. The layers were separated and the organic phase was dried over $MgSO_4$ and concentrated under reduced pressure. The crude residue was purified by flash column chromatography (SiO_2, 4 g, 0–2% EtOAc in hexanes to afford **3.51** (25 mg, 86%).

^{1}H NMR (600 MHz, $CDCl_3$) δ 6.17 (d, J = 10.1 Hz, 1H), 5.99 – 5.91 (m, 1H), 5.72 – 5.67 (m, 2H), 5.38 (d, J = 17.2 Hz, 1H), 5.29 (d, J = 10.5 Hz, 1H), 4.66 (d, J = 5.8 Hz, 2H), 2.37 (dd, J = 12.2, 2.8 Hz, 1H), 1.97 – 1.89 (m, 1H), 1.78 – 1.70 (m, 1H), 1.66 – 1.60 (m, 1H), 1.55 – 1.48 (m, 2H), 1.45 (t, J = 9.4 Hz, 1H), 0.94 (d, J = 6.7 Hz, 3H), 0.91 (s, 3H), 0.88 (d, J = 6.6 Hz, 3H).

^{13}C NMR (151 MHz, $CDCl_3$) δ 153.6, 147.0, 142.0, 131.4, 121.8, 119.3, 115.7, 68.9, 49.5, 43.8, 42.9, 33.4, 32.2, 27.0, 21.7, 19.9, 16.0.

TLC: R_f = 0.41 (10% EtOAc in hexanes, visualized by $KMnO_4$)

HRMS (ES+) *m/z* calc'd for $C_{17}H_{24}O_3$ $[M+Na]^+$: 299.1623, found 299.1635.



3.51 **3.52**

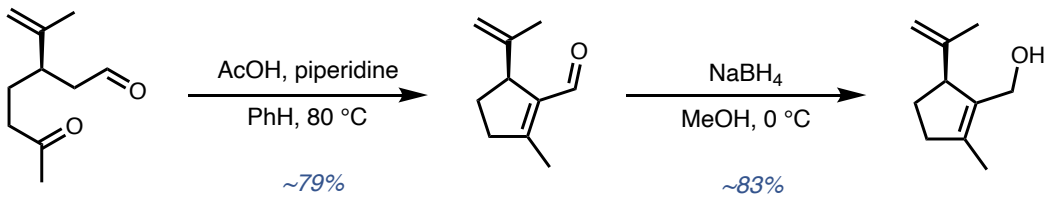
A solution of allyl carbonate **3.51** (12 mg, 0.043 mmol, 1 equiv.) in dry DME (220 µL) was added dropwise added to a solution of $Pd_2(dba)_3CHCl_3$ (4.5 mg, 0.0043 mmol, 0.1 equiv.) and Ph_3P (4.6 mg, 0.017 mmol, 0.4 equiv.) in dry DME (220 µL). The reaction mixture was stirred for 2 hours, then diluted with EtOAc (2 mL) and filtered through SiO_2 (1 g, elute w/ EtOAc). The filtrate was then concentrated under reduced pressure and the crude residue purified by flash column chromatography (SiO_2, 2 g, 0–4% EtOAc in hexanes) to afford **3.52** (4.5 mg, ~45%) as a single isomer. The configuration of the major stereoisomer was unable to be determined.

^{1}H NMR (600 MHz, $CDCl_3$) δ 7.10 (d, J = 9.6 Hz, 1H), 5.83 (d, J = 9.6 Hz, 1H), 5.80 – 5.71 (m, 1H), 5.05 (dd, J = 17.2, 1.6 Hz, 1H), 5.02 (d, J = 10.8 Hz, 1H), 2.73 – 2.67 (m, 1H), 2.54 – 2.49 (m, 2H), 2.02 (td, J = 9.2, 3.0 Hz, 2H), 1.86 (dd, J = 14.1, 9.8 Hz, 1H), 1.75 – 1.68 (m, 1H), 1.61 – 1.55 (m, 2H), 1.38 (app q, J = 11.1 Hz, 1H), 1.04 (s, 3H), 0.91 (d, J = 6.8 Hz, 3H), 0.80 (d, J = 6.4 Hz, 3H).

*Please note that only the signals that could be conclusively attributed to **3.52** are reported (n =15/16).*

^{13}C NMR (151 MHz, $CDCl_3$) δ 203.0, 158.4, 136.0, 128.1, 116.7, 49.5, 49.0, 45.3, 35.7, 31.9, 28.3, 22.9, 21.5, 20.2, 15.2.

TLC: R_f = 0.21 (10% EtOAc in hexanes, visualized by CAM)



3.54 **3.55** **3.56**

Based on a previously reported procedure.[8] Ketoaldehyde **3.54**[8] (1.8 g, 11 mmol, 1 equiv.) was dissolved in dry PhH (110 mL). Piperidine (0.53 mL, 5.3 mmol, 0.5 equiv.) and AcOH (0.31 mL, 5.3 mmol, 0.5 equiv.) were added sequentially. The reaction mixture was placed in a pre-heated oil bath at 85 °C and stirred for 1 hour. The flask was removed from the oil bath and cooled to 23 °C, then the reaction was quenched with aqueous HCl (1 M, 50 mL). The biphasic mixture was stirred vigorously for 10 minutes, then the layers were separated, and the aqueous phase was further extracted with EtOAc (2 x 20 mL). The combined organic extracts were washed with saturated aqueous $NaHCO_3$ (50 mL), brine (100 mL), dried over anhydrous Na_2SO_4, and concentrated under reduced pressure to afford enal **3.55** (1.3 g, ~79%) could be used without purification in the following step. The spectral data matched those previously reported.[8]

^{1}H NMR (600 MHz, $CDCl_3$) δ 9.88 (s, 1H), 4.61 (s, 1H), 4.52 (s, 1H), 3.52 (d, J = 9.6 Hz, 1H), 2.58 – 2.48 (m, 1H), 2.41 – 2.32 (m, 1H), 2.09 (s, 3H), 2.04 – 1.97 (m, 1H), 1.59 (app s, 4H).

^{13}C NMR (151 MHz, $CDCl_3$) δ 203.0, 158.4, 136.0, 128.1, 116.7, 49.5, 49.0, 45.3, 35.7, 31.9, 28.3, 22.9, 21.5, 20.2, 15.2.

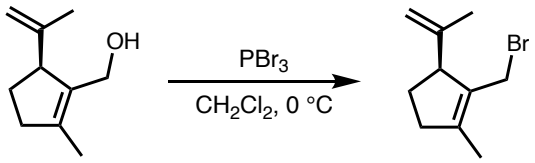
TLC: R_f = 0.53 (30% EtOAc in hexanes, visualized by *p*-anisaldehyde)

Based on a previously reported procedure.[8] $NaBH_4$ (208 mg, 5.50 mmol, 0.65 equiv.) was added to a solution of enal **3.55** (1.27 g, 8.45 mmol, 1 equiv.) in MeOH (17 mL) at 0 °C. After 1 hour, the reaction was quenched with saturated aqueous NH_4Cl : H_2O (1:1, 40 mL) and the heterogenous reaction mixture was extracted with EtOAc (4 x 20 mL). The combined organic extracts were washed with brine, dried over anhydrous Na_2SO_4, and concentrated under reduced pressure to afford **3.56** (1.3 g, ~80% purity, 83%). The spectral data matched those previously reported.[8]

^{1}H NMR (500 MHz, $CDCl_3$) δ 4.77 (d, J = 2.3 Hz, 1H), 4.74 – 4.72 (m, 1H), 4.21 (d, J = 12.1 Hz, 1H), 4.01 (d, J = 12.1 Hz, 1H), 3.49 (d, J = 9.1 Hz, 1H), 2.43 – 2.35 (m, 1H), 2.33 – 2.23 (m, 1H), 2.08 – 1.99 (overlapping m, 1H), 1.74 (d, J = 1.9 Hz, 3H), 1.71 – 1.65 (app m, 1H), 1.64 (s, 3H).

^{13}C NMR (125 MHz, $CDCl_3$) δ 149.1, 138.5, 135.5, 110.8, 58.3, 54.9, 38.0, 27.9, 19.0, 14.2.

TLC: R_f = 0.45 (30% EtOAc in hexanes, visualized by CAM)



3.56 **3.12**

Based on a previously reported procedure.[9] Allyl alcohol **3.56** (10 mg, 0.066 mmol, 1 equiv.) was suspended in Et_2O (880 µL) and cooled to 0 °C, then PBr_3 (6 µL, 0.066 mmol, 1 equiv.) was added dropwise by syringe. After 30 minutes, the reaction was quenched with MeOH (150 µL). The mixture was stirred vigorously for 30 minutes and diluted with H_2O. The layers were separated, and the aqueous layer was further extracted with Et_2O (3 x 2 mL). The combined organic extracts

were washed with brine (4 mL), dried over $MgSO_4$, and concentrated under reduced pressure to a clear oil that darkened over time. The yield of **3.12** (~60%) was determined by quantitative NMR using 5,6-dibromo-1,3-benzodioxole as an internal standard. The spectral data matched those previously reported.[9]

^{1}H NMR (500 MHz, $CDCl_3$) δ 4.79 – 4.73 (m, 2H), 4.15 (d, *J* = 9.7 Hz, 1H), 3.78 (d, *J* = 9.7 Hz, 1H), 3.58 – 3.52 (m, 1H), 2.41 – 2.24 (m, 2H), 2.09 – 2.01 (m, 1H), 1.74 (s, 3H), 1.72 – 1.64 (m, 1H), 1.58 (s, 3H).

3.11.3 Supplemental References

(1) Deng, J.; Ning, Y.; Tian, H.; Gui, J. *J. Am. Chem. Soc.* **2020**, *142*, 4690–4695.

(2) Zhang, M.; Fan, H.; Wang, Y.; Gui, J. *Org. Lett.* **2022**, *24*, 7383–7387.

(3) Sun, D.; Chen, R.; Tang, D.; Xia, Q.; Zhao, Y.; Liu, C.-H.; Ding, H. *J. Am. Chem. Soc.* **2023**.

(4) Bera, K.; Namboothiri, I. N. N. *Org. Lett.* **2012**, *14*, 980–983.

(5) Chen, K.; Ishihara, Y.; Galán, M. M.; Baran, P. S. *Tetrahedron* **2010**, *66*, 4738–4744.

(6) Attah-Poku, S. K.; Chau, F.; Yadav, V. K.; Fallis, A. G. *J. Org. Chem.* **1985**, *50*, 3418–3419.

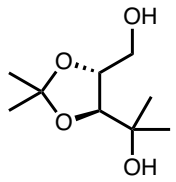
(7) Hog, D. T.; Huber, F. M. E.; Jiménez-Osés, G.; Mayer, P.; Houk, K. N.; Trauner, D. *Chem. Eur. J.* **2015**, *21*, 13646–13665.

(8) Wang, Y.-Q.; Xu, K.; Min, L.; Li, C.-C. *J. Am. Chem. Soc.* **2022**, *144*, 10162–10167.

(9) Yim, H.-K.; Liao, Y.; Wong, H. N. C. *Tetrahedron* **2003**, *59*, 1877–1884.

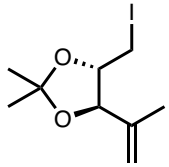
Appendix A

A1: NMR Data



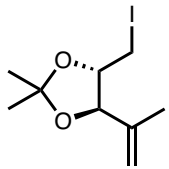
1.17

^{1}H NMR
500 MHz, $CDCl_3$



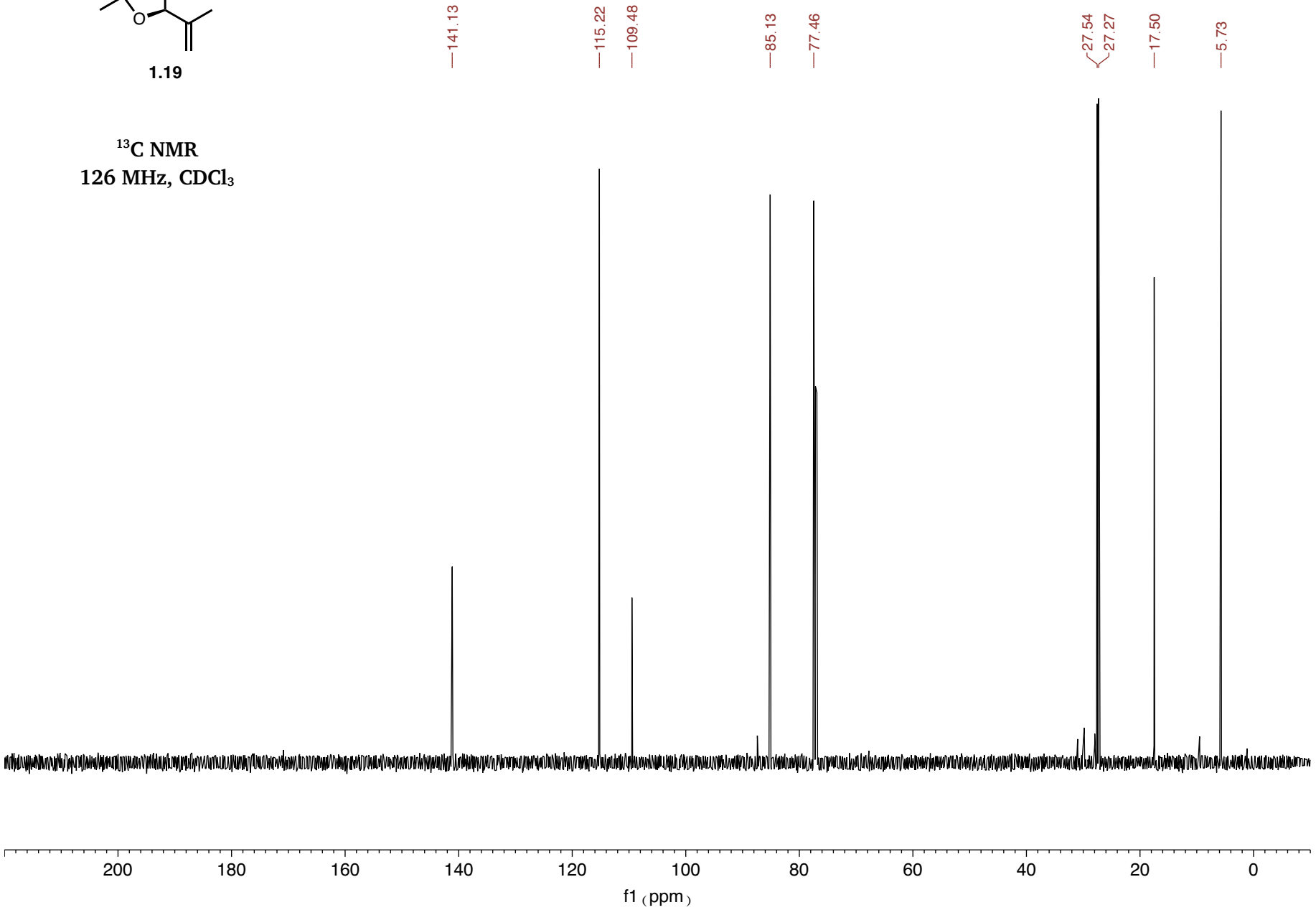
1.19

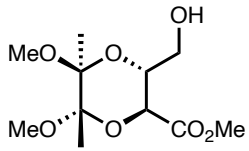
^{1}H NMR
500 MHz, $CDCl_3$



1.19

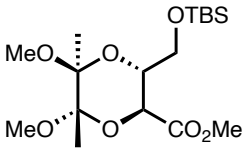
^{13}C NMR
126 MHz, $CDCl_3$





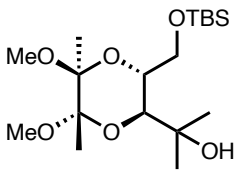
1.24

^{1}H NMR
500 MHz, $CDCl_3$



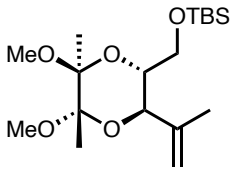
1.25

^{1}H NMR
500 MHz, $CDCl_3$



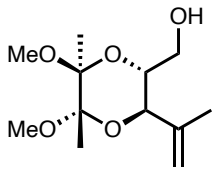
1.26

^{1}H NMR
500 MHz, $CDCl_3$



1.27

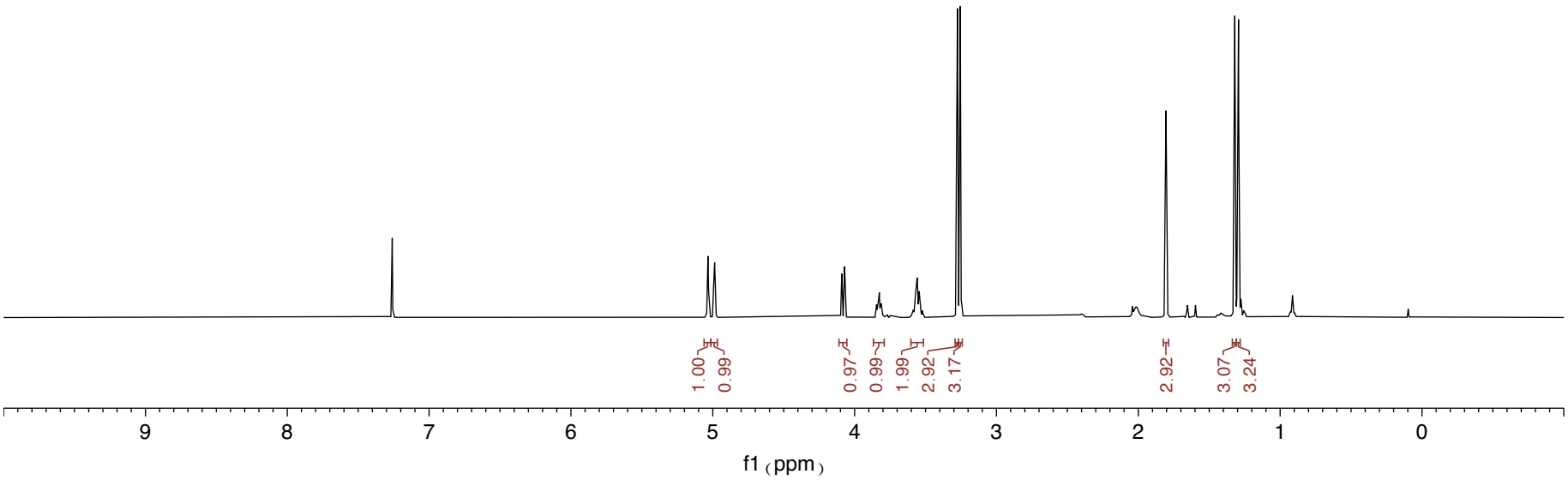
^{1}H NMR
500 MHz, $CDCl_3$

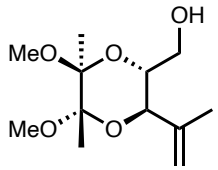


1.28

^{1}H NMR
500 MHz, $CDCl_3$

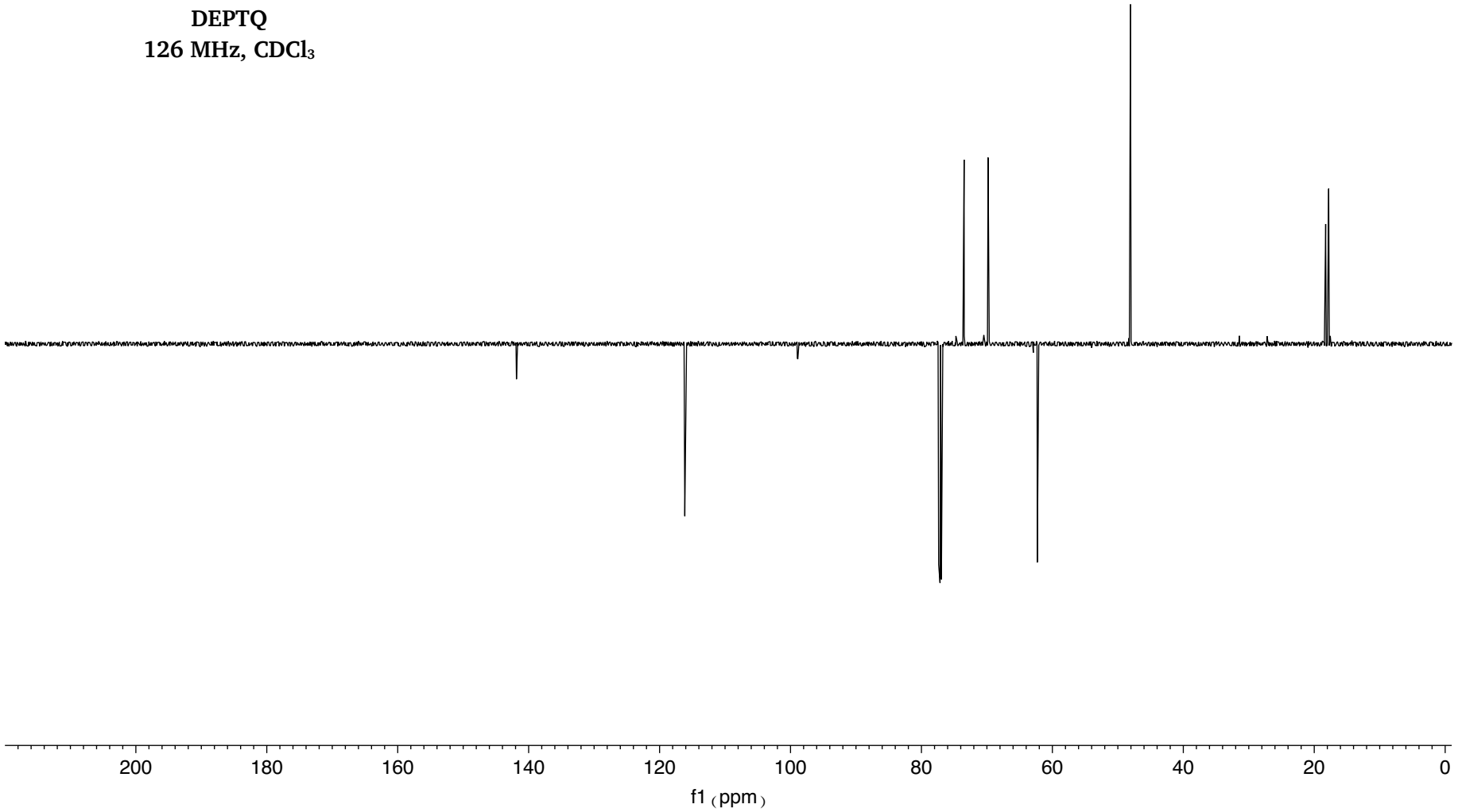


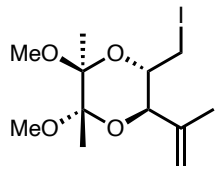




1.28

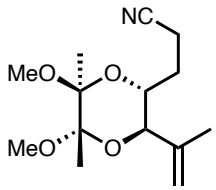
DEPTQ
126 MHz, $CDCl_3$





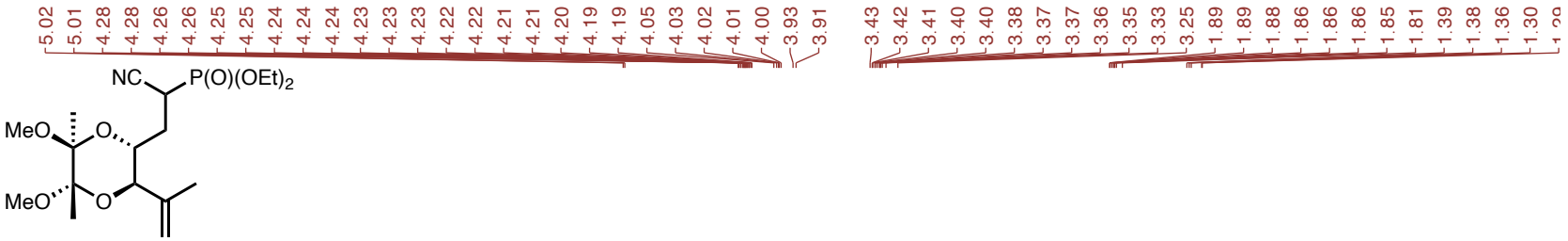
1.29

^{1}H NMR
500 MHz, $CDCl_3$



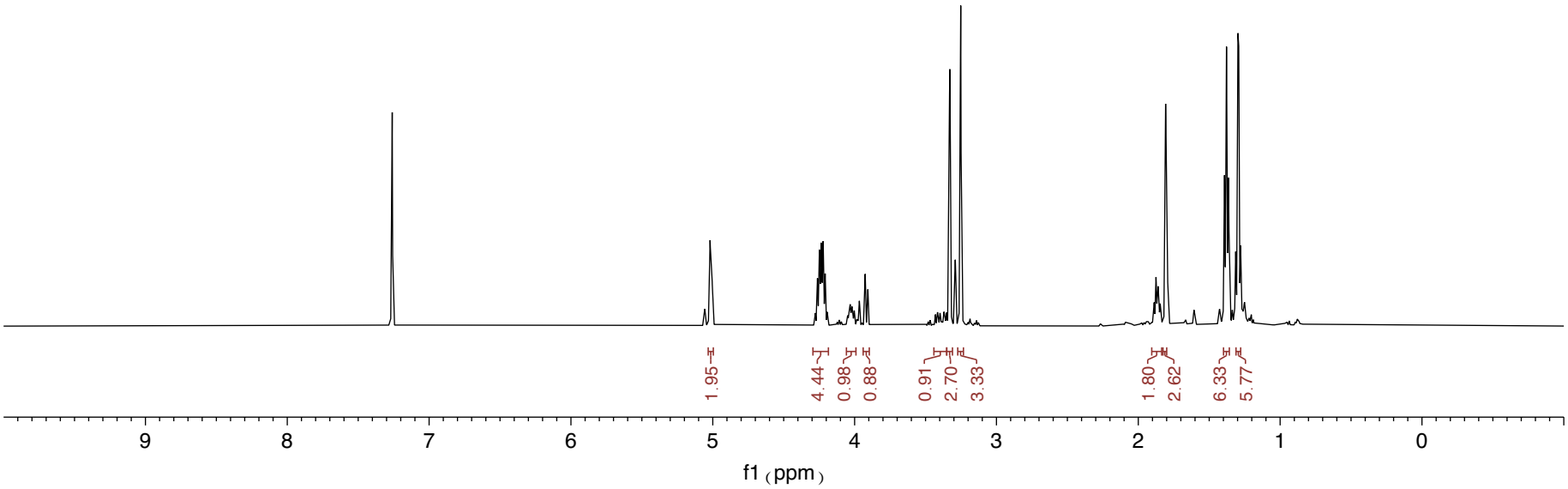
1.30

^{1}H NMR
500 MHz, $CDCl_3$

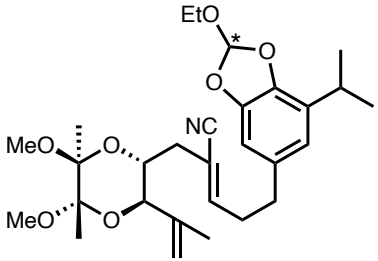


1.31

^{1}H NMR
500 MHz, $CDCl_3$

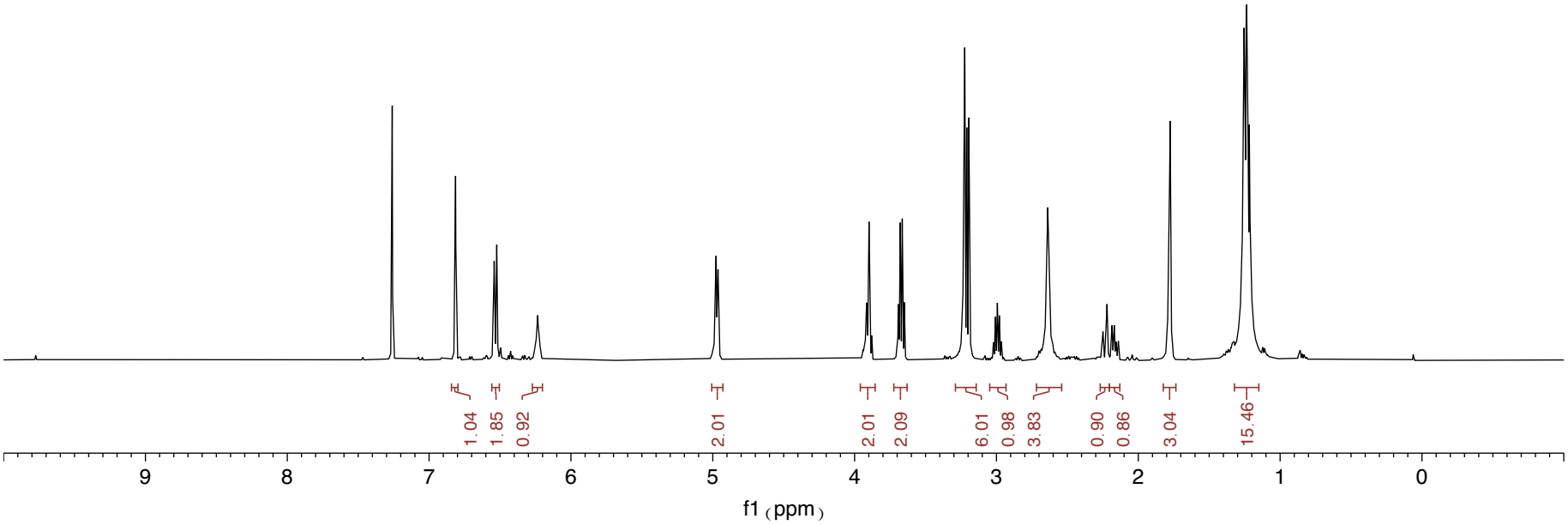


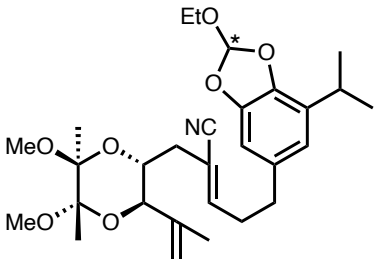




1.32

^{1}H NMR
500 MHz, $CDCl_3$





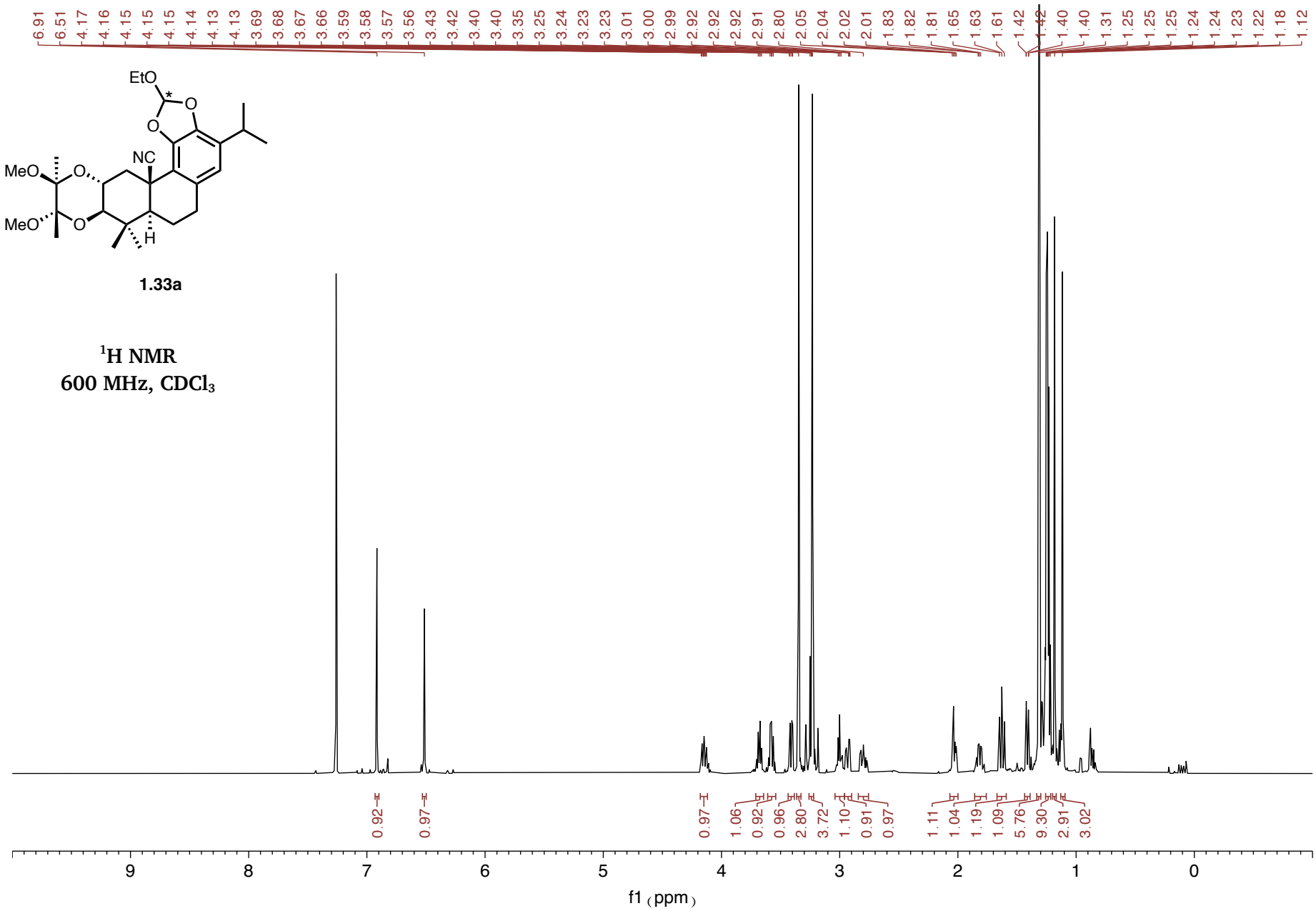
1.32

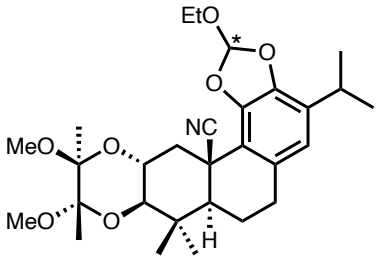
^{13}C NMR
151 MHz, $CDCl_3$

149.32
149.29
145.83
145.82
141.76
141.64
133.73
133.72
129.39
119.27
118.62
117.26
116.61
111.34
105.88
105.83
98.91
98.85
77.37
76.34
67.03
58.91
48.00
47.98
47.86
35.77
34.67
34.65
33.37
33.30
29.15
22.17
22.07
17.87
17.62
17.60
14.89

200 180 160 140 120 100 80 60 40 20 0

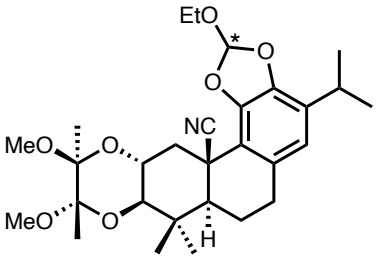
f1 (ppm)


EtO
O
O
NC
MeO
O
MeO
O
H
1.33a
^{1}H NMR
600 MHz, $CDCl_3$
f1 (ppm)



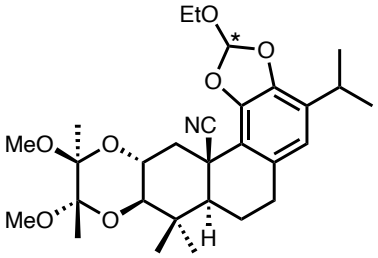
1.33b

^{1}H NMR
600 MHz, $CDCl_3$



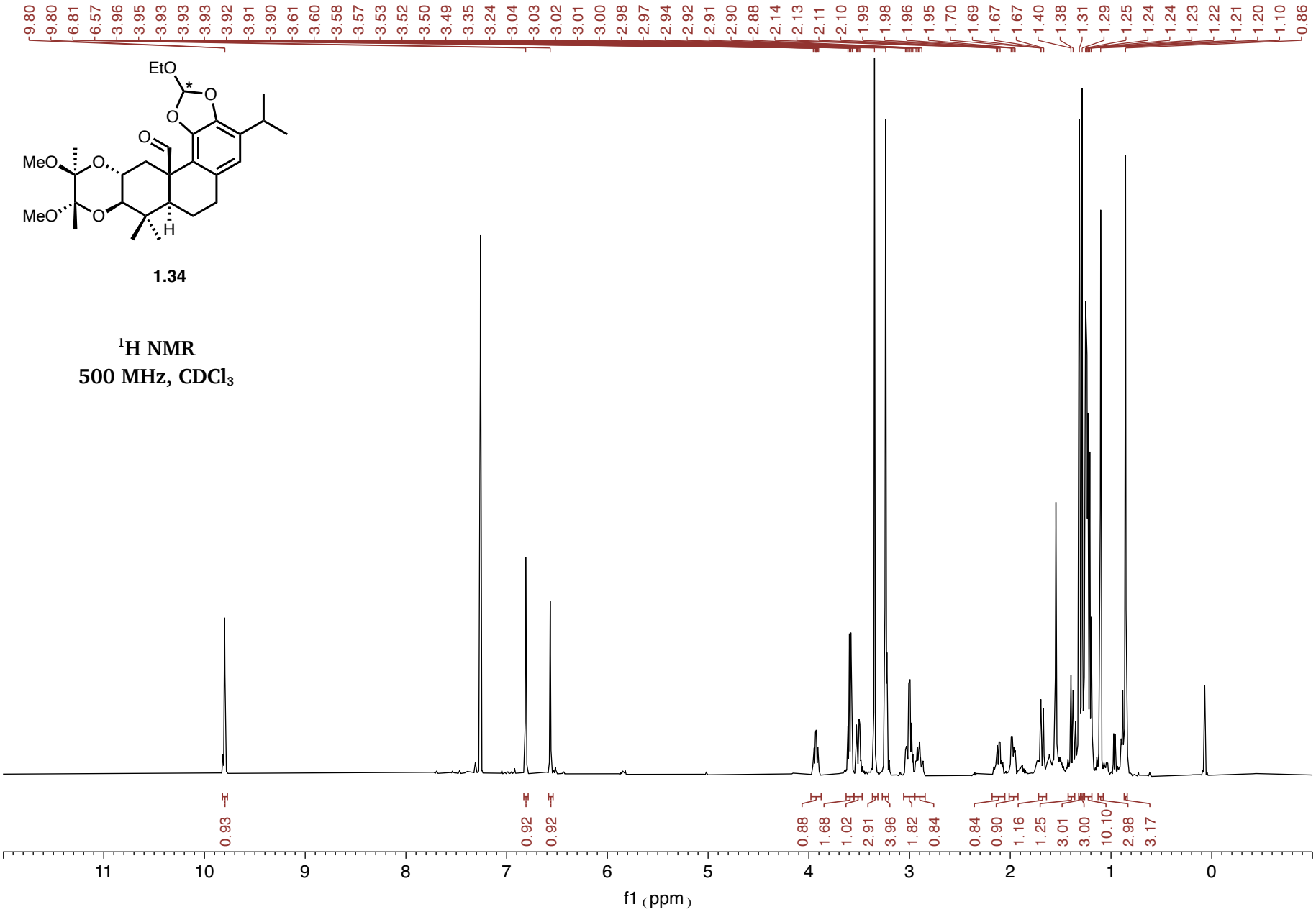
1.33a

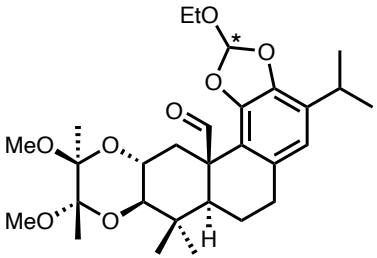
DEPTQ
151 MHz, $CDCl_3$



1.33b

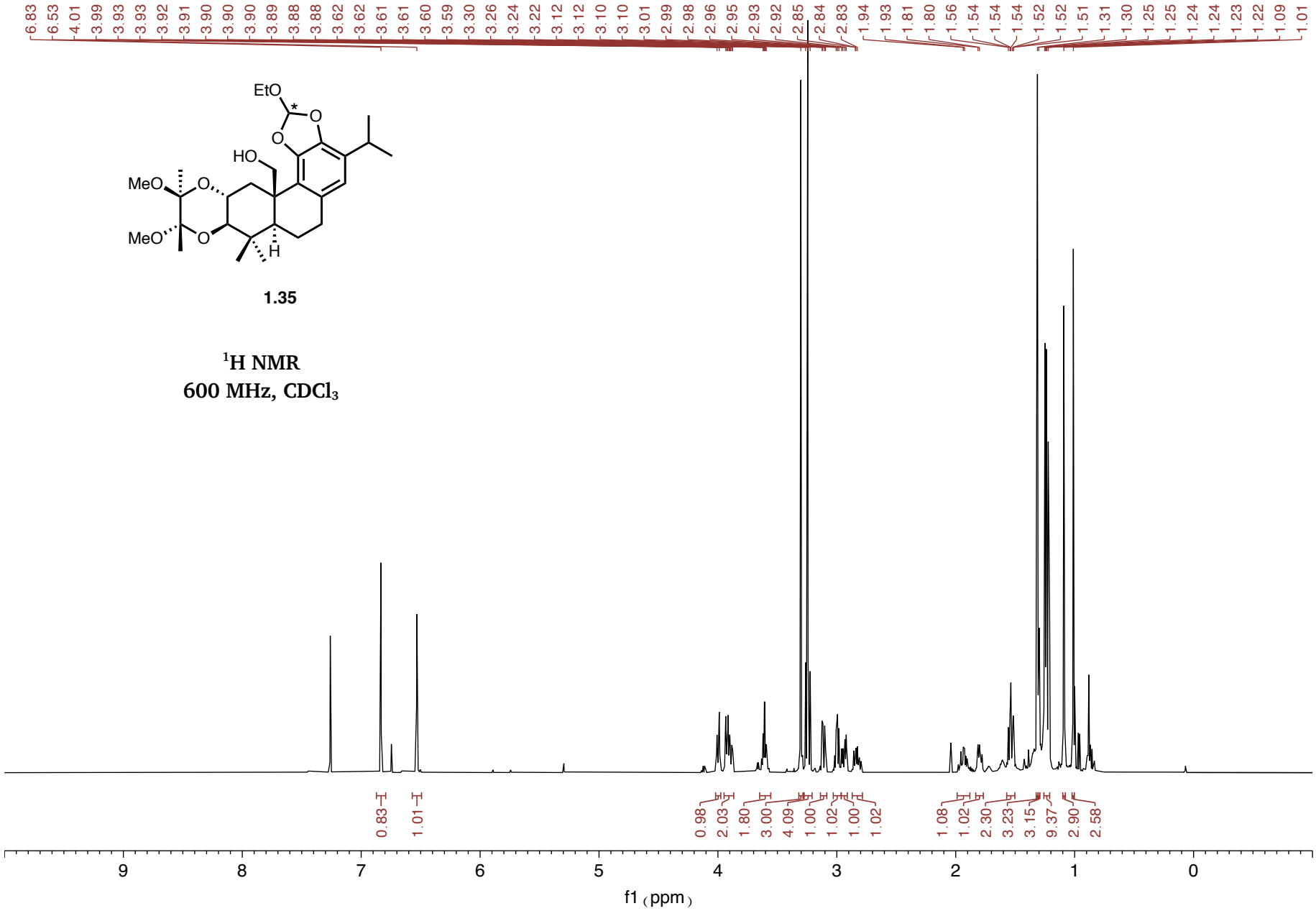
DEPTQ
151 MHz, $CDCl_3$


EtO
O
O
O
MeO
O
MeO
O
H
1.34
^{1}H NMR
500 MHz, $CDCl_3$
f1 (ppm)



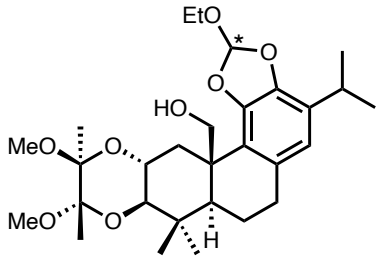
1.34

^{13}C NMR
151 MHz, $CDCl_3$



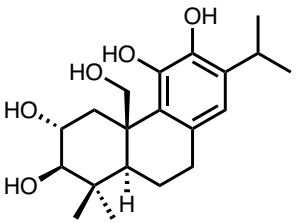
1.35

^{1}H NMR
600 MHz, $CDCl_3$



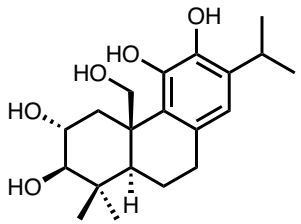
1.35

DEPTQ
151 MHz, $CDCl_3$



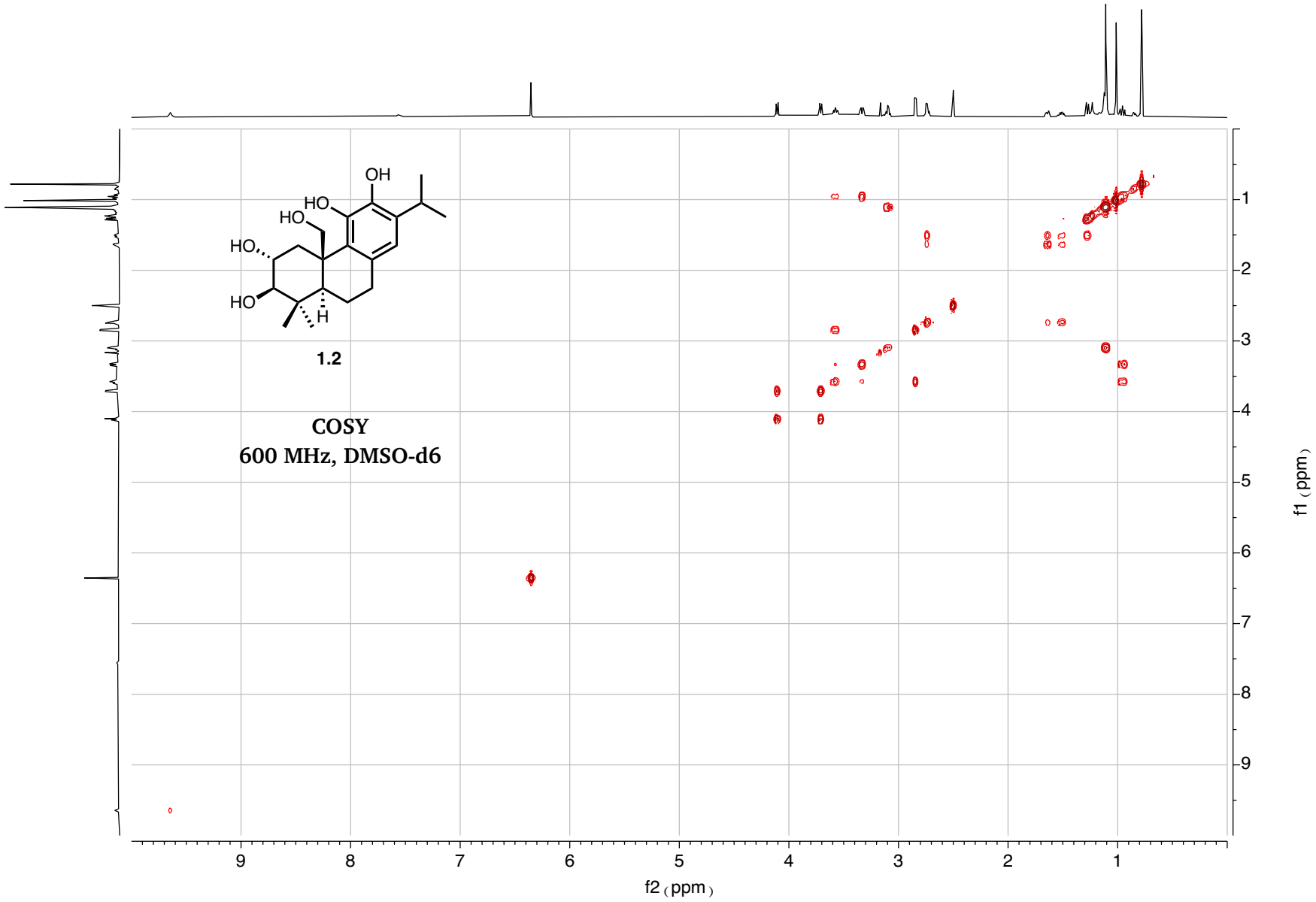
1.2

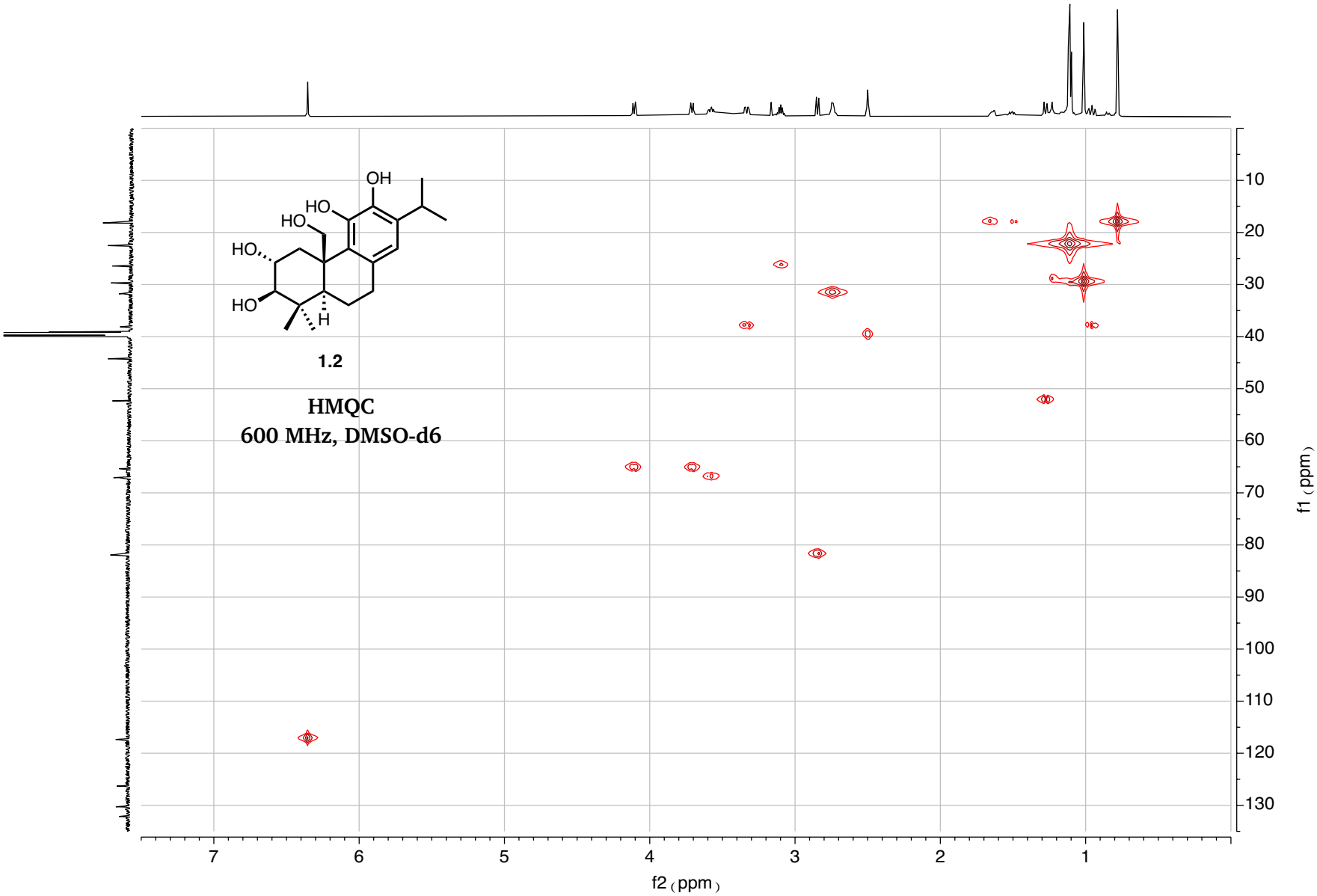
^{1}H NMR
500 MHz, DMSO-d_6

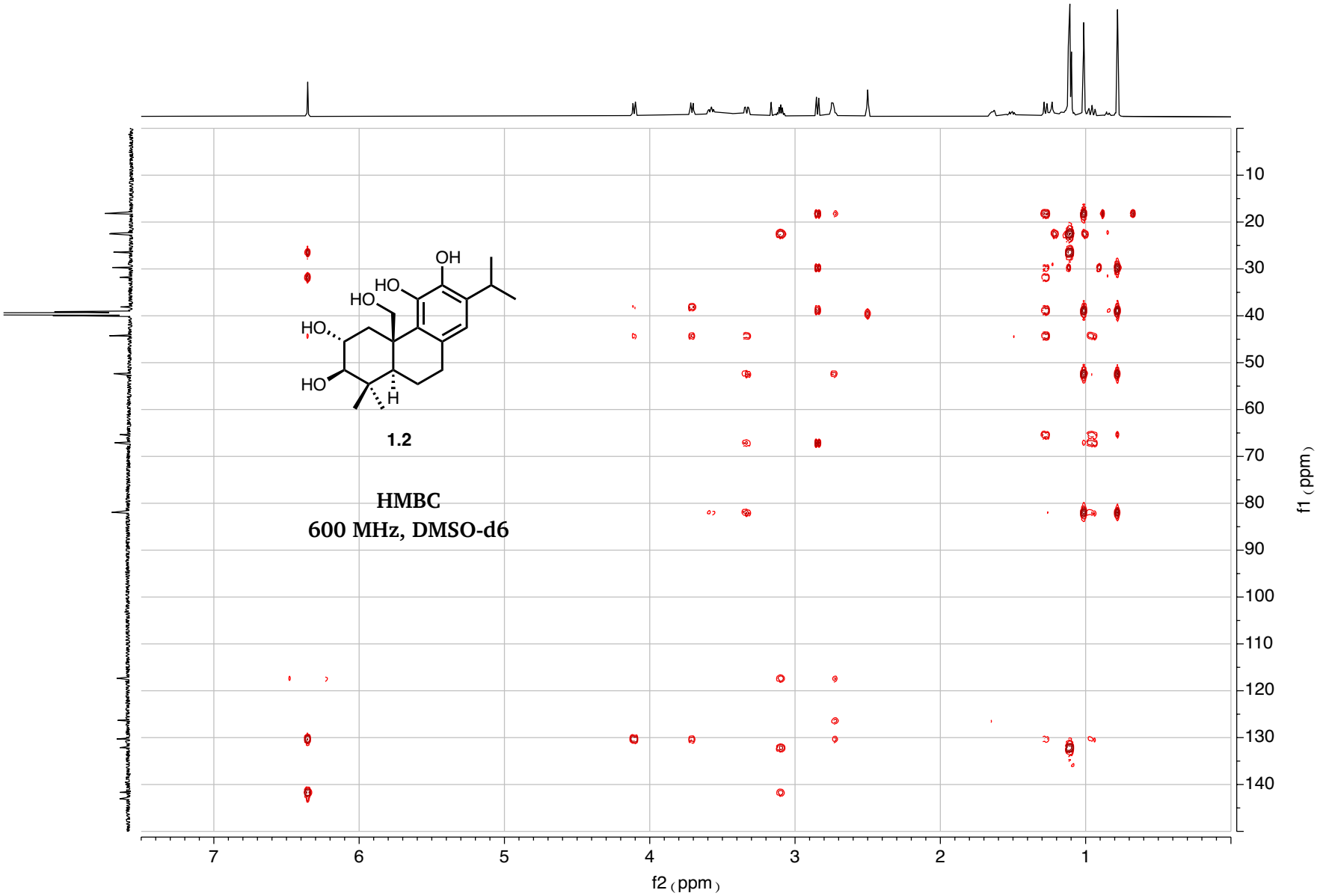


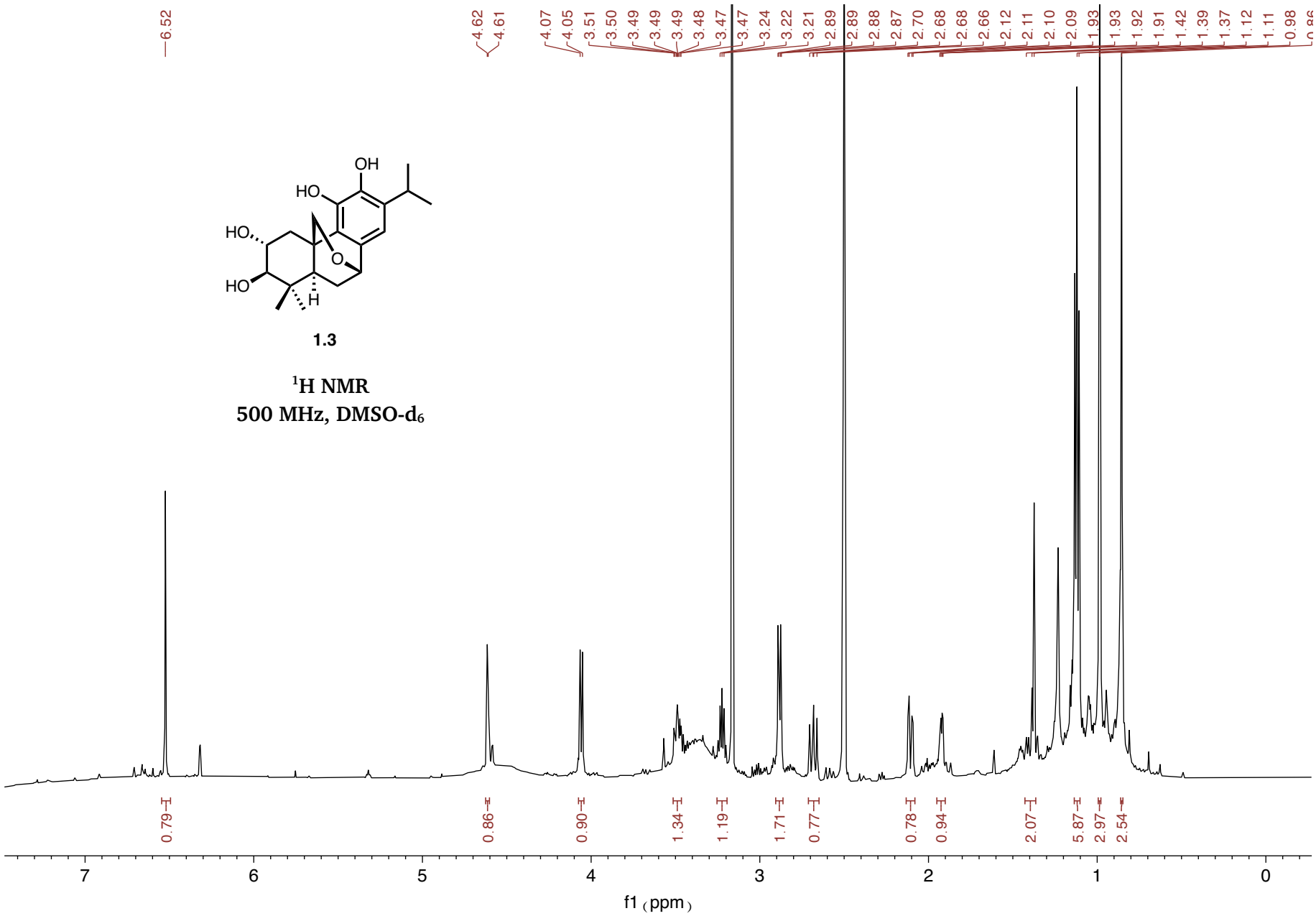
1.2

^{13}C NMR
151 MHz, DMSO-d_6


OH
HO
HO
HO
HO
H
1.2
COSY
600 MHz, DMSO-d6
f2 (ppm)
f1 (ppm)

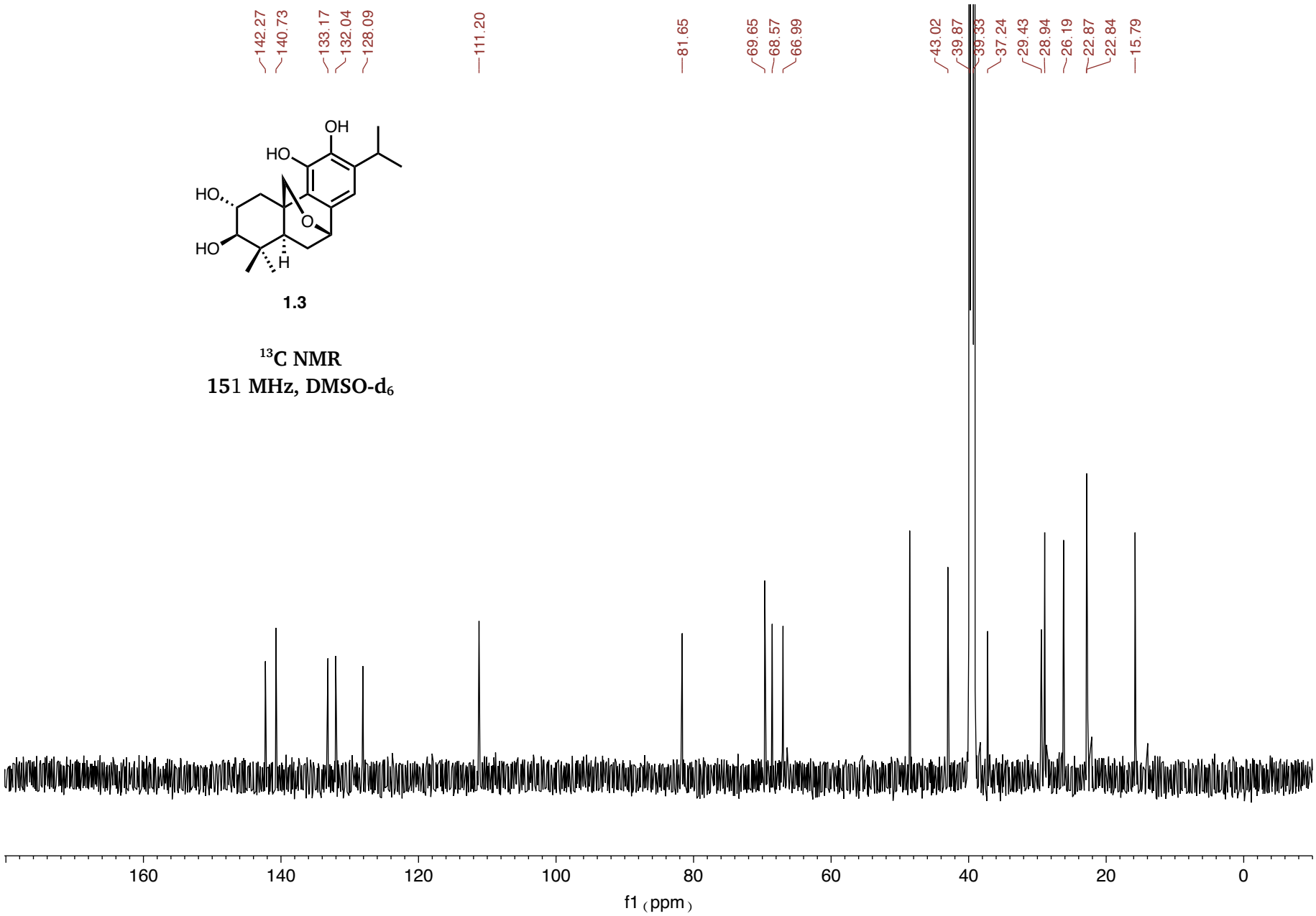

OH
HO
HO
HO
HO
H
1.2
HMQC
600 MHz, DMSO-d6
f2 (ppm)
f1 (ppm)


OH
HO
HO
HO
HO
H
1.2
HMBC
600 MHz, DMSO-d6
7
6
5
4
3
2
1
f2 (ppm)
10
20
30
40
50
60
70
80
90
100
110
120
130
140
f1 (ppm)



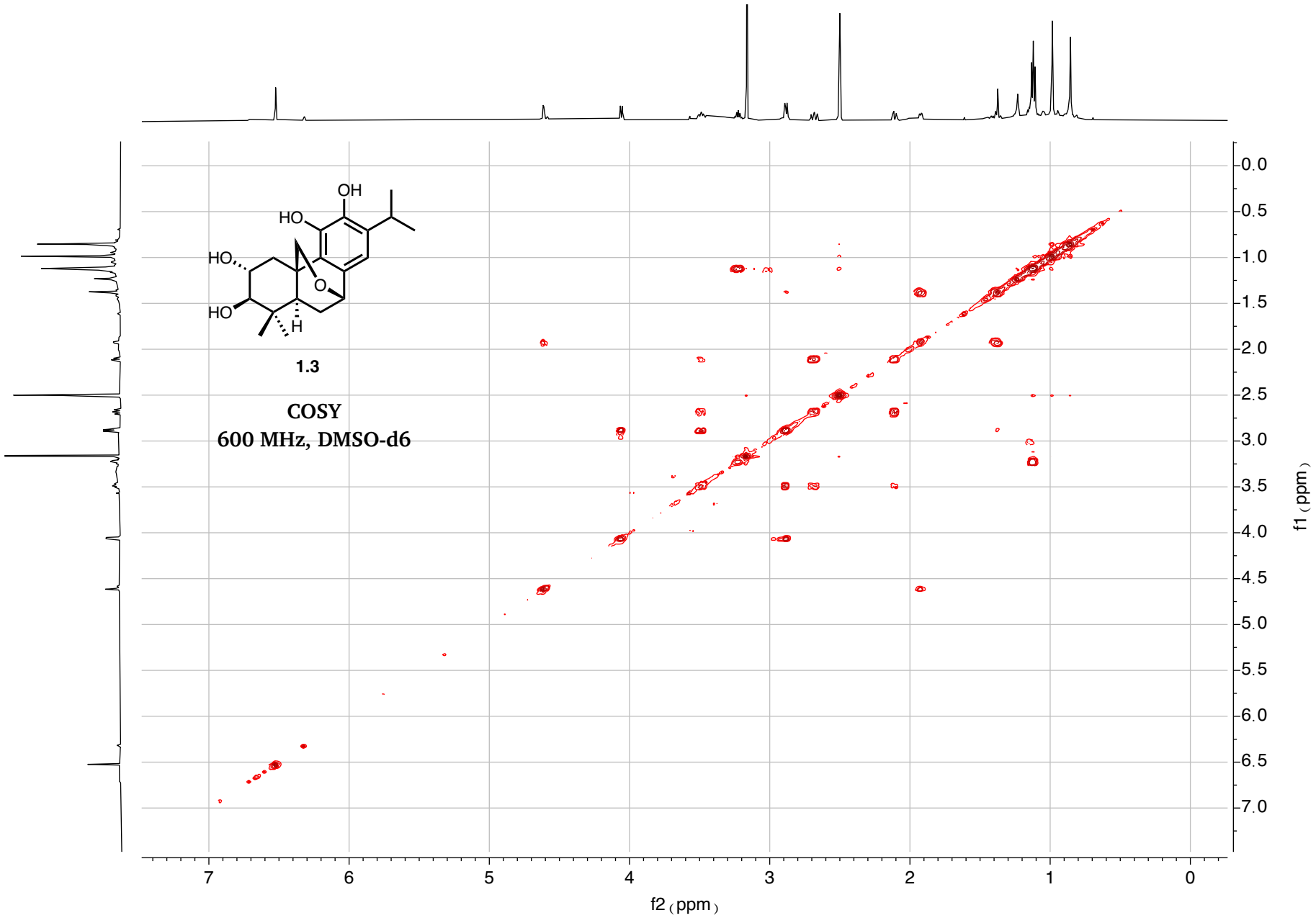
1.3

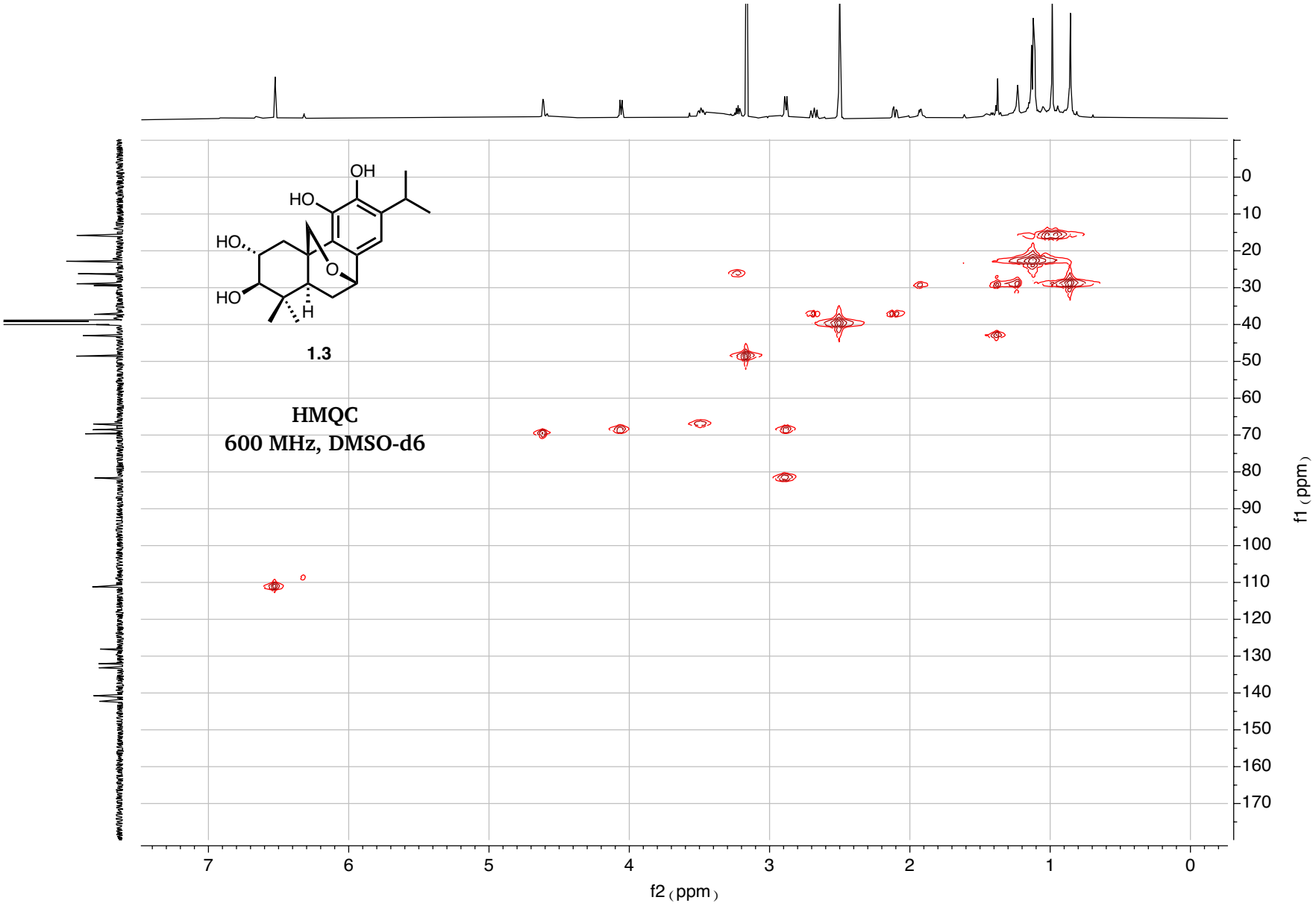
^{1}H NMR
500 MHz, DMSO-d_6



1.3

^{13}C NMR
151 MHz, DMSO-d_6


OH
HO
HO
O
HO
H
1.3
COSY
600 MHz, DMSO-d6
f2 (ppm)
f1 (ppm)


OH
HO
HO
O
HO
H
1.3
HMQC
600 MHz, DMSO-d6
f2 (ppm)
f1 (ppm)

Appendix A

A2: Predicted ^{13}C Shifts and Comparison of Spectral Data

Cartesian coordinates for lowest energy conformer of **1.1** optimized at HF/3-21G

C	-2.278836	-0.353964	0.170491
C	-0.076068	0.530044	-0.581053
C	-2.107643	0.805708	-2.026427
C	-0.730078	1.401433	-1.711113
C	-2.964381	0.596664	-0.797522
C	-0.940023	0.235104	0.688743
C	-0.182198	-0.785829	1.572755
C	1.20174	-0.979429	1.452584
C	2.103433	-0.132166	0.542059
C	1.326775	0.994337	-0.171507
O	-4.182752	0.019046	-1.337277
O	-2.783352	1.672695	-2.950523
C	1.846081	-1.925332	2.23755
C	1.148729	-2.699465	3.136481
C	-0.198123	-2.486106	3.306147
C	-0.850591	-1.523669	2.562911
C	2.971641	-1.021198	-0.406154
C	4.050137	-0.191289	-1.134457
C	2.178736	-1.866574	-1.418404
H	0.037987	-0.445679	-1.034125
C	-1.181361	1.501882	1.536502
O	-2.224395	1.209494	2.517369
C	0.106141	1.255831	-3.008186
C	-0.849748	2.917574	-1.439652
O	-2.17307	-1.337699	2.883537
O	1.855555	-3.630378	3.859102
H	-2.059087	-1.275329	-0.357228
H	-2.937354	-0.607063	0.978607
H	-1.971156	-0.175795	-2.470612
H	-3.193615	1.544115	-0.328737
H	2.816982	0.343963	1.209774
H	1.883738	1.315965	-1.036873
H	1.25657	1.853422	0.485106
H	-4.822194	-0.167651	-0.637923
H	-3.6915	1.349907	-3.042427
H	2.902294	-2.071488	2.173656

H	-0.773462	-3.024726	4.030137
H	3.499529	-1.713993	0.236151
H	4.609471	0.424008	-0.436848
H	3.616952	0.452838	-1.890116
H	4.749395	-0.855457	-1.631135
H	1.398843	-2.435051	-0.927034
H	1.73571	-1.247378	-2.186751
H	2.848588	-2.566781	-1.907059
H	-1.509382	2.329665	0.938997
H	-0.272827	1.772987	2.052944
H	-2.34677	1.93503	3.141375
H	0.317013	0.214311	-3.221565
H	-0.468984	1.6635	-3.828842
H	1.043621	1.794383	-2.945954
H	-1.629925	3.167771	-0.737151
H	-1.102216	3.410887	-2.366593
H	0.089532	3.318745	-1.077008
H	-2.392165	-0.379096	2.868701
H	1.29806	-4.132724	4.464575

ωB97X-D/6-311+G(2DF,2P) [6-311G*] = –1156.3493933 hartrees

Cartesian coordinates for lowest energy conformer of **1.2** optimized at HF/3-21G

C	-0.961456	2.044844	0.086975
C	0.307444	0.576445	1.639934
C	-0.782555	2.667062	2.511475
C	0.355387	1.661668	2.764886
C	-0.817089	3.185733	1.083373
C	0.229236	1.058818	0.154096
C	-0.008583	-0.171469	-0.753745
C	0.246803	-1.481085	-0.298914
C	0.821193	-1.773748	1.073359
C	1.350401	-0.533494	1.781573
C	-0.032403	-2.570997	-1.119804
C	-0.542353	-2.44536	-2.408798
C	-0.732498	-1.151921	-2.88337
C	-0.449524	-0.039831	-2.079238
C	1.543178	1.736468	-0.294961
O	1.314975	2.481142	-1.498455
H	-0.667395	0.088164	1.794542
C	0.050638	0.975915	4.113278
C	1.702807	2.390855	2.929598
O	-0.676267	3.738965	3.423458
O	-1.934971	4.06783	1.040209
O	-0.654127	1.156115	-2.727829
O	-1.172234	-0.939767	-4.15202
C	-0.836601	-3.64945	-3.28242
C	0.449159	-4.415358	-3.622221
C	-1.874703	-4.574292	-2.634256
H	-1.098302	2.456074	-0.912919
H	-1.879858	1.491396	0.317676
H	-1.739864	2.136748	2.666258
H	0.101377	3.7573	0.881559
H	1.609098	-2.530552	0.978693
H	0.039695	-2.224215	1.701983
H	2.31365	-0.227804	1.355505
H	1.540973	-0.768169	2.832303
H	0.164022	-3.56812	-0.729603
H	1.925212	2.419234	0.464913

H	2.301084	0.966648	-0.477092
H	2.167067	2.686578	-1.898184
H	-0.184829	1.738809	4.860444
H	-0.807407	0.297857	4.034481
H	0.906046	0.402133	4.483027
H	1.846583	3.206062	2.216701
H	2.540684	1.691963	2.834057
H	1.754223	2.845033	3.921748
H	-1.321918	4.393047	3.121502
H	-1.939275	4.50665	0.181672
H	0.061456	1.766456	-2.455266
H	-1.180269	0.02428	-4.26631
H	-1.259601	-3.275128	-4.219507
H	0.917387	-4.821966	-2.717734
H	1.176726	-3.76095	-4.112843
H	0.233143	-5.254082	-4.293826
H	-1.49742	-5.002121	-1.697827
H	-2.120664	-5.405415	-3.30483
H	-2.797479	-4.031	-2.40731

ωB97X-D/6-311+G(2DF,2P) [6-311G*] = –1156.3619383 hartrees

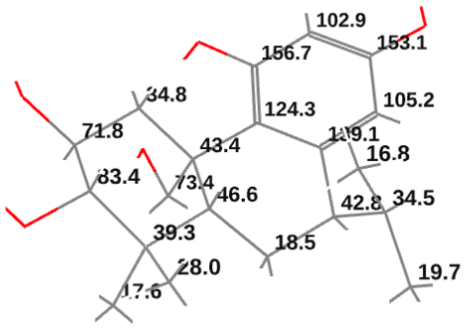
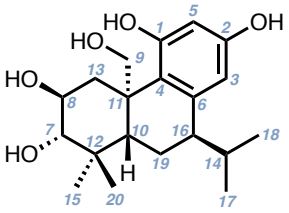


Figure A1.1. Plebeianiol A structure **1.1** optimized at HF/3-21G

Table A1.1. Isolated experimental and calculated ^{13}C chemical shifts for **1.1**
[these resonances are tabulated in order of decreasing chemical shift]

Carbon #	Isolated Exp.	ωB97X-D/6-31G*	Δ	| Δ |
1	**143.0**	**156.7**	**-13.7**	**13.7**
2	**141.6**	**153.1**	**-11.5**	**11.5**
3	131.9	139.1	-7.2	7.2
4	130.2	124.3	5.9	5.9
5	**126.3**	**105.2**	**21.1**	**21.1**
6	**117.5**	**102.9**	**14.6**	**14.6**
7	81.8	83.4	-1.6	1.6
8	66.8	73.4	-6.6	6.6
9	65.3	71.8	-6.5	6.5
10	52.1	46.6	5.5	5.5
11	43.8	43.4	0.4	0.4
12	38.6	42.8	-4.2	4.2
13	38.0	39.3	-1.3	1.3
14	31.7	34.8	-3.1	3.1
15	29.6	34.5	-4.9	4.9
16	26.4	28.0	-1.6	1.6
17	22.4	19.7	2.7	2.7
18	22.3	18.5	3.8	3.8
19	18.1	17.6	0.5	0.5
20	18.1	16.8	1.3	1.3

Average | Δ |: 5.9
Max | Δ |: 21.1



1.1 [reported structure]

Table A1.2. Isolated experimental and calculated ^{13}C chemical shifts for **1.1**
[these resonances are tabulated according to the assignments made by Liang, Wu, and co-workers, in order of decreasing chemical shift for the reported resonances]

Carbon #	Isolated Exp.	ωB97X-D/6-31G*	Δ	| Δ |
1	**143.0**	**156.7**	**-13.7**	**13.7**
2	**141.6**	**153.1**	**-11.5**	**11.5**
3	**131.9**	**105.2**	**26.7**	**26.7**
4	130.2	124.3	5.9	5.9
5	**126.3**	**102.9**	**23.4**	**23.4**
6	**117.5**	**139.1**	**-21.6**	**21.6**
7	81.8	83.4	-1.6	1.6
8	66.8	71.8	-5	5
9	65.3	73.4	-8.1	8.1
10	52.1	46.6	5.5	5.5
11	43.8	43.4	0.4	0.4
12	38.6	39.3	-0.7	0.7
13	38.0	34.8	3.2	3.2
14	31.7	34.5	-2.8	2.8
15	29.6	28.0	1.6	1.6
16	**26.4**	**42.8**	**-16.4**	**16.4**
17	22.4	19.7	2.7	2.7
18	22.3	16.8	5.5	5.5
19	18.1	18.5	-0.4	0.4
20	18.1	16.8	1.3	1.3

Average | Δ |: 7.9
Max | Δ |: 26.7

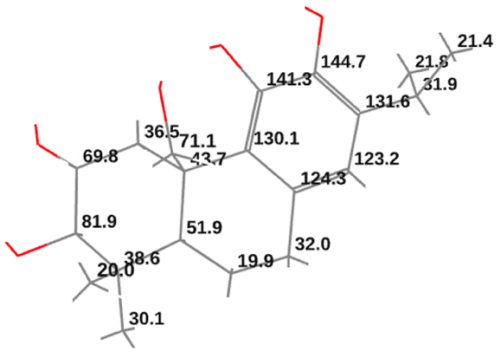


Figure A1.2. Plebeianiol A structure **1.2** optimized at HF/3-21

Table A1.3. Synthetic experimental and calculated ^{13}C chemical shifts for **1.2**
[these resonances are tabulated in order of decreasing chemical shift]

Carbon #	Synthetic Exp.	ωB97X-D/6-31G*	Δ	| Δ |
1	143.0	144.7	-1.7	1.7
2	141.6	141.3	0.3	0.3
3	132.2	131.6	0.6	0.6
4	130.2	130.1	0.1	0.1
5	126.3	124.3	2.0	2.0
6	117.4	123.2	-5.8	5.8
7	81.9	81.9	0.0	0.0
8	67.1	71.1	-4.0	4.0
9	65.4	69.8	-4.4	4.4
10	52.3	51.9	0.4	0.4
11	44.3	43.7	0.6	0.6
12	38.9	38.6	0.3	0.3
13	38.1	36.5	1.6	1.6
14	31.8	32.0	-0.2	0.2
15	29.7	31.9	-2.2	2.2
16	26.4	30.1	-3.7	3.7
17	22.5	21.8	0.7	0.7
18	22.4	21.4	1.0	1.0
19	18.2	20.0	-1.8	1.8
20	18.2	19.9	-1.7	1.7

Average | Δ |: 1.7
Max | Δ |: 5.8

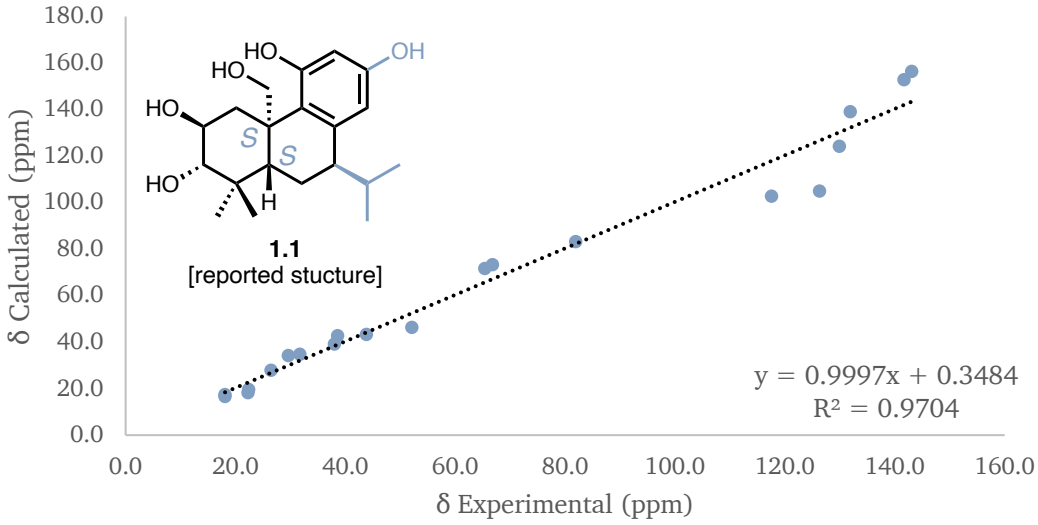


Figure A1.3. Linear correlation plot for **1.1** [based on data from **Table A1.1**]

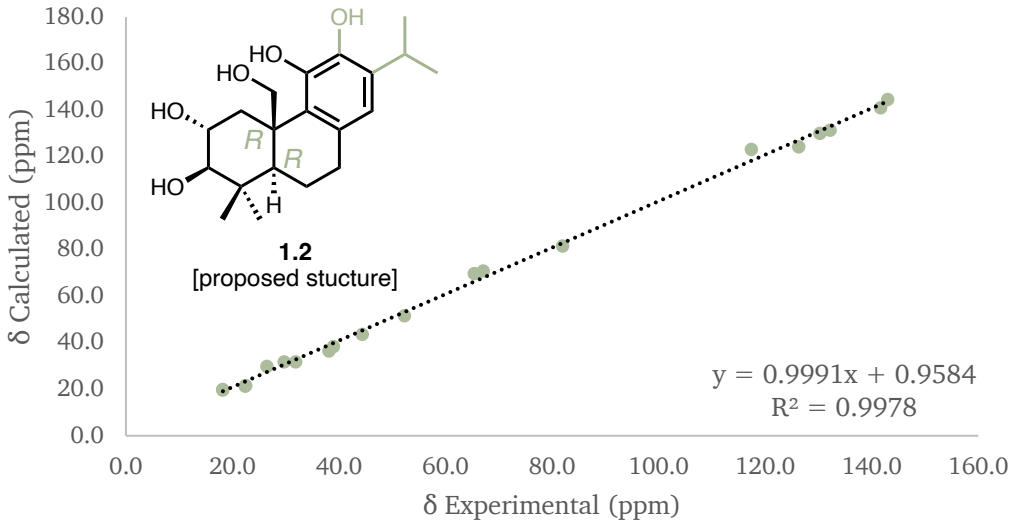


Figure A1.4. Linear correlation plot for **1.2** [based on data from **Table A1.3**]

Table A1.4. Comparison of isolated experimental and synthetic experimental ^{13}C chemical shifts for plebeianiol A in DMSO-d_6

Carbon #	Isolated	Synthetic	Δ	| Δ |
1	143.0	143.0	0.0	0.0
2	141.6	141.6	0.0	0.0
3	131.9	132.2	-0.3	0.3
4	130.2	130.2	0.0	0.0
5	126.3	126.3	0.0	0.0
6	117.5	117.4	0.1	0.1
7	81.8	81.9	-0.1	0.1
8	66.8	67.1	-0.3	0.3
9	65.3	65.4	-0.1	0.1
10	52.1	52.3	-0.2	0.2
11	**43.8**	**44.3**	**-0.5**	**0.5**
12	38.6	38.9	-0.3	0.3
13	38.0	38.1	-0.1	0.1
14	31.7	31.8	-0.1	0.1
15	29.6	29.7	-0.1	0.1
16	26.4	26.4	0.0	0.0
17	22.4	22.5	-0.1	0.1
18	22.3	22.4	-0.1	0.1
19	18.1	18.2	-0.1	0.1
20	18.1	18.2	-0.1	0.1

Average | Δ |: 0.1
Max | Δ |: 0.5

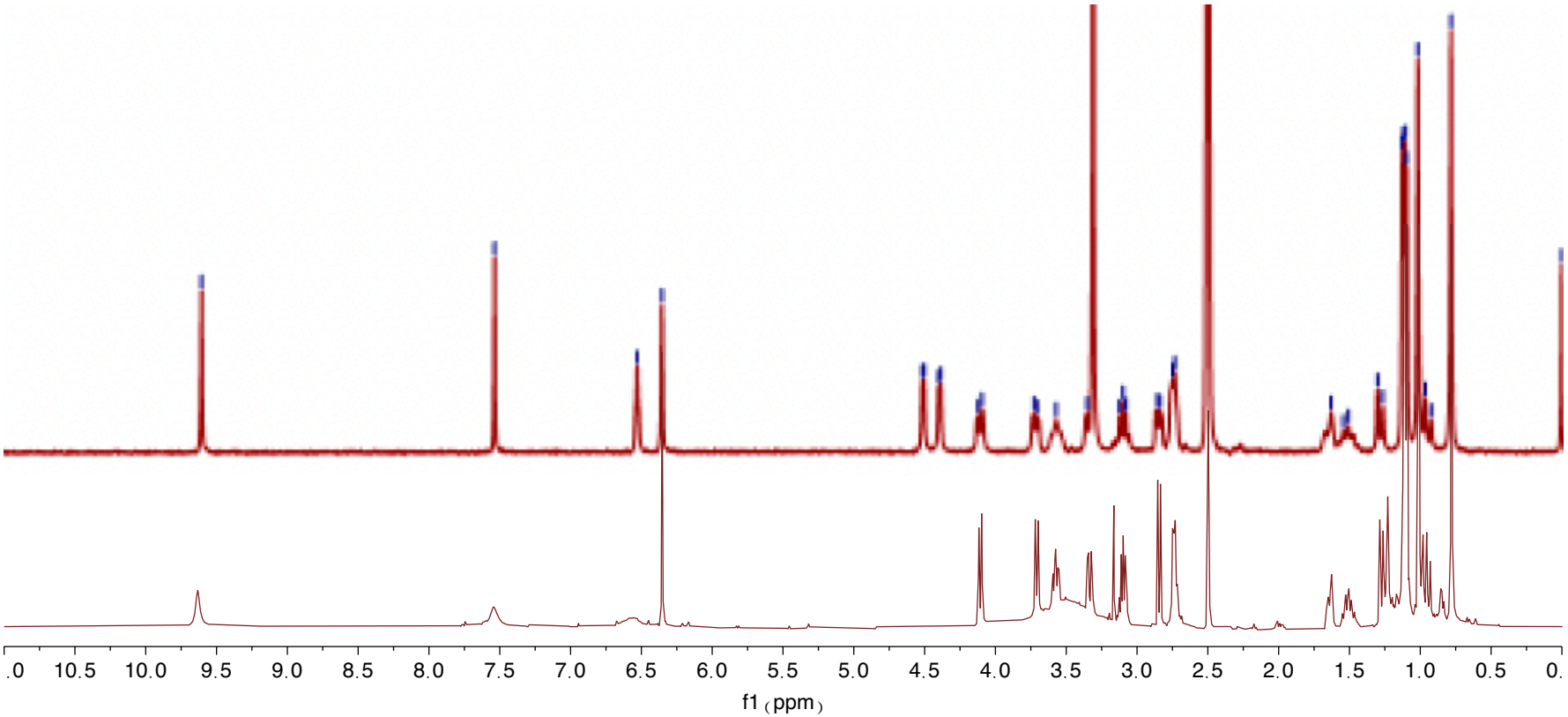


Figure A1.5. Comparison of ^{1}H NMR spectrum of isolated (top) plebeianiol A versus synthetic (bottom) plebeianiol A. Please note that the ^{1}H NMR spectrum for synthetic plebeianiol A displays broadening of the catechol O–H's and primary alcohol O–H at 9.63 ppm, 7.54 ppm, and 6.36 ppm. Also note that the exchangeable O–H protons of the secondary alcohols reported at 4.51 ppm and 4.39 ppm are absent.

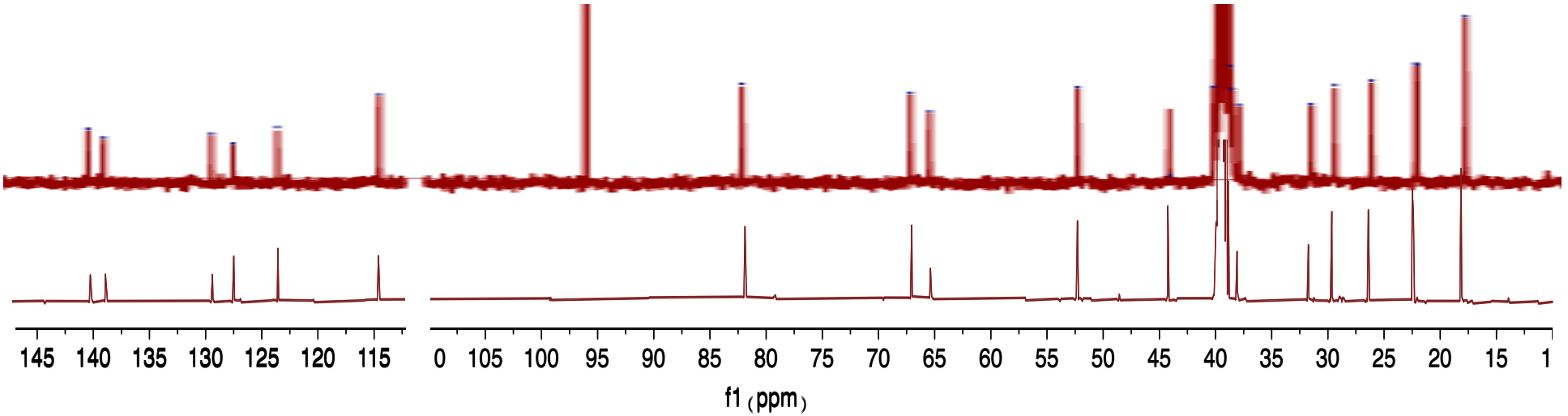
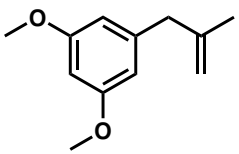


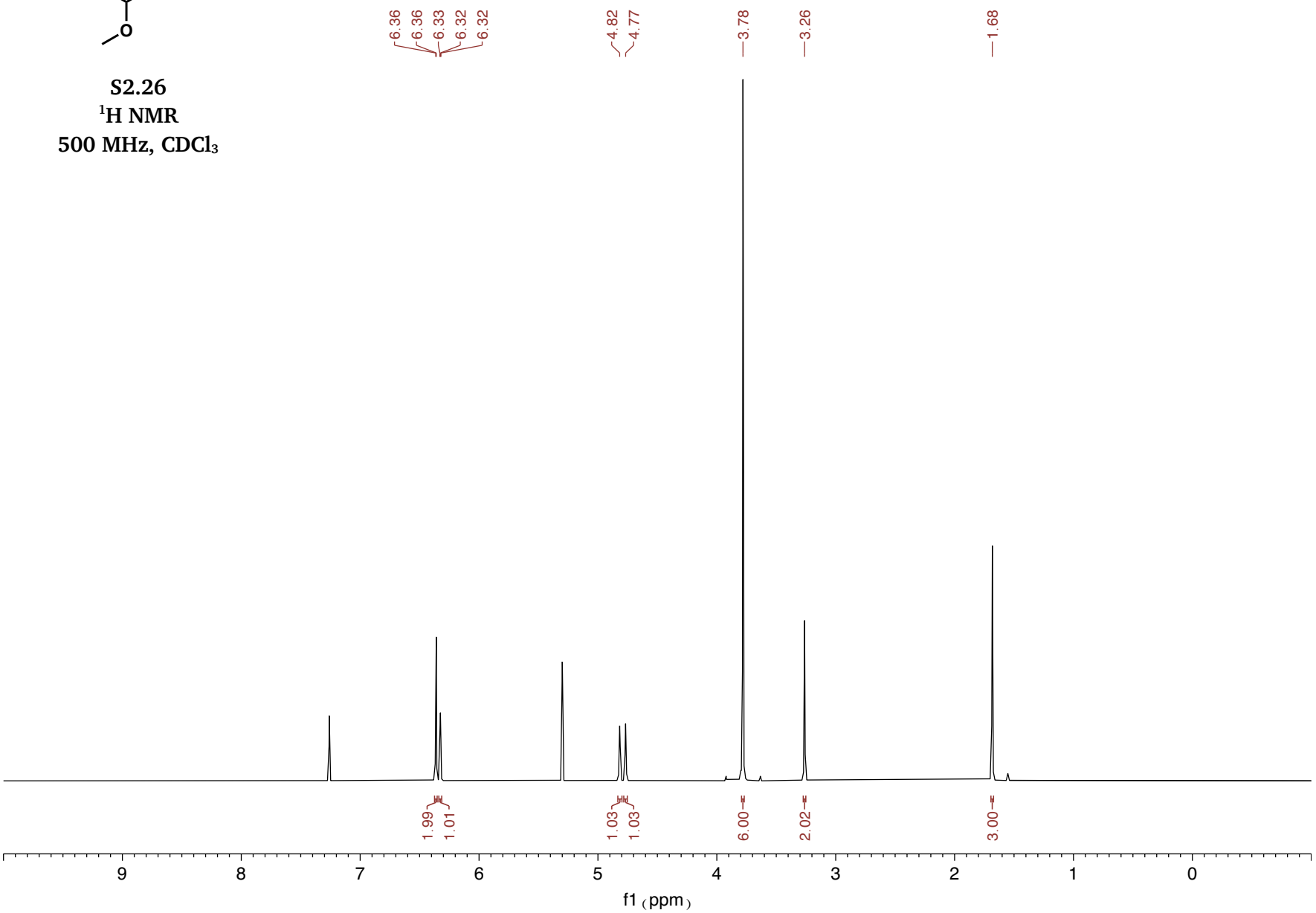
Figure A1.6. Comparison of ^{13}C NMR spectrum of isolated (top) plebeianiol A versus synthetic (bottom) plebeianiol A. Please note the presence of an unreported solvent/impurity observed at approximately 95 ppm in the ^{13}C NMR spectrum for isolated plebeianiol A

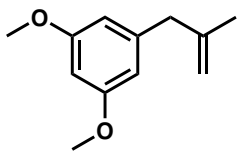
Appendix B

B1: NMR Data

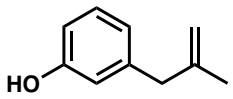


S2.26
^{1}H NMR
500 MHz, $CDCl_3$

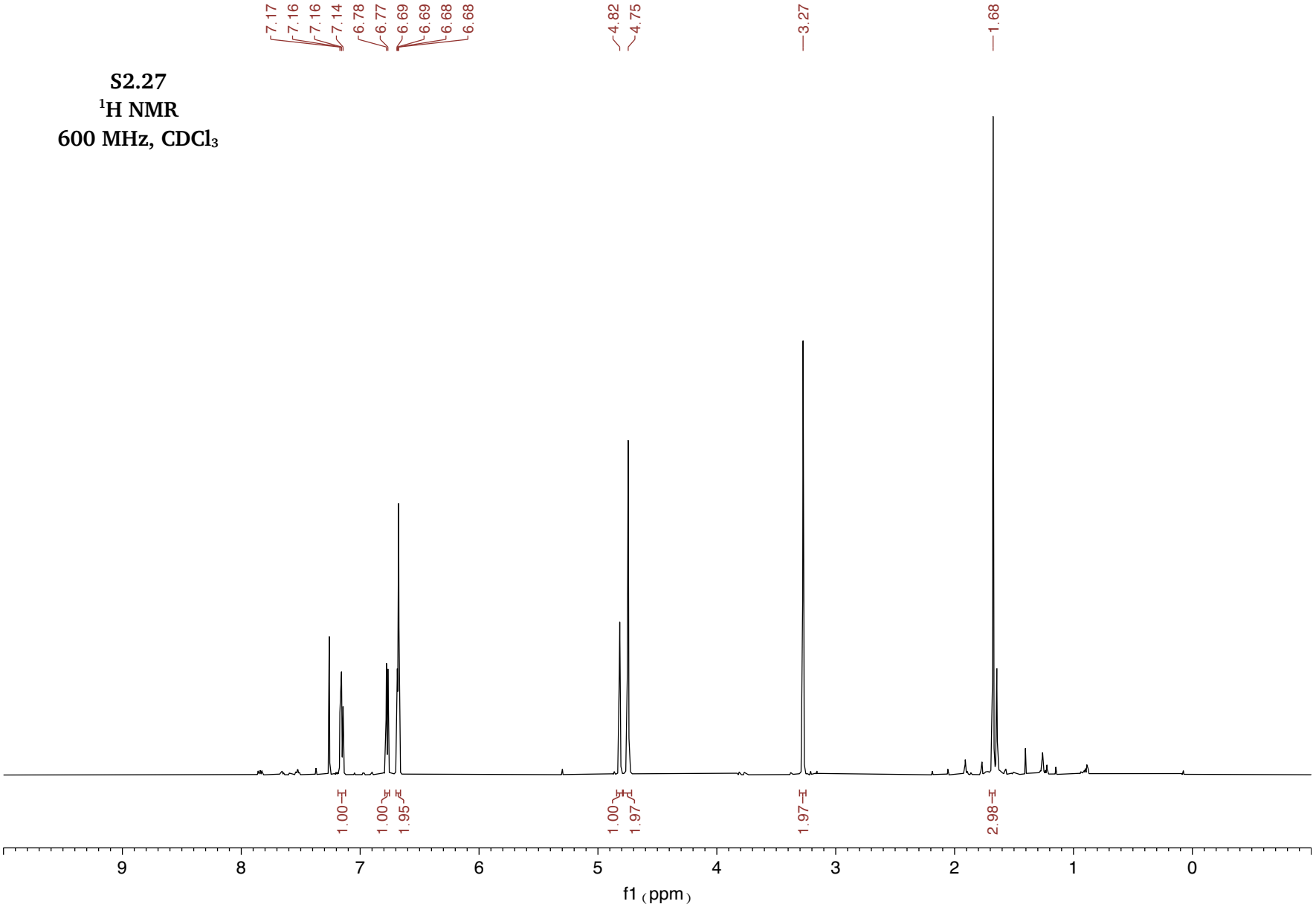


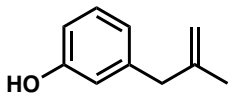


S2.26
^{13}C NMR
126 MHz, $CDCl_3$

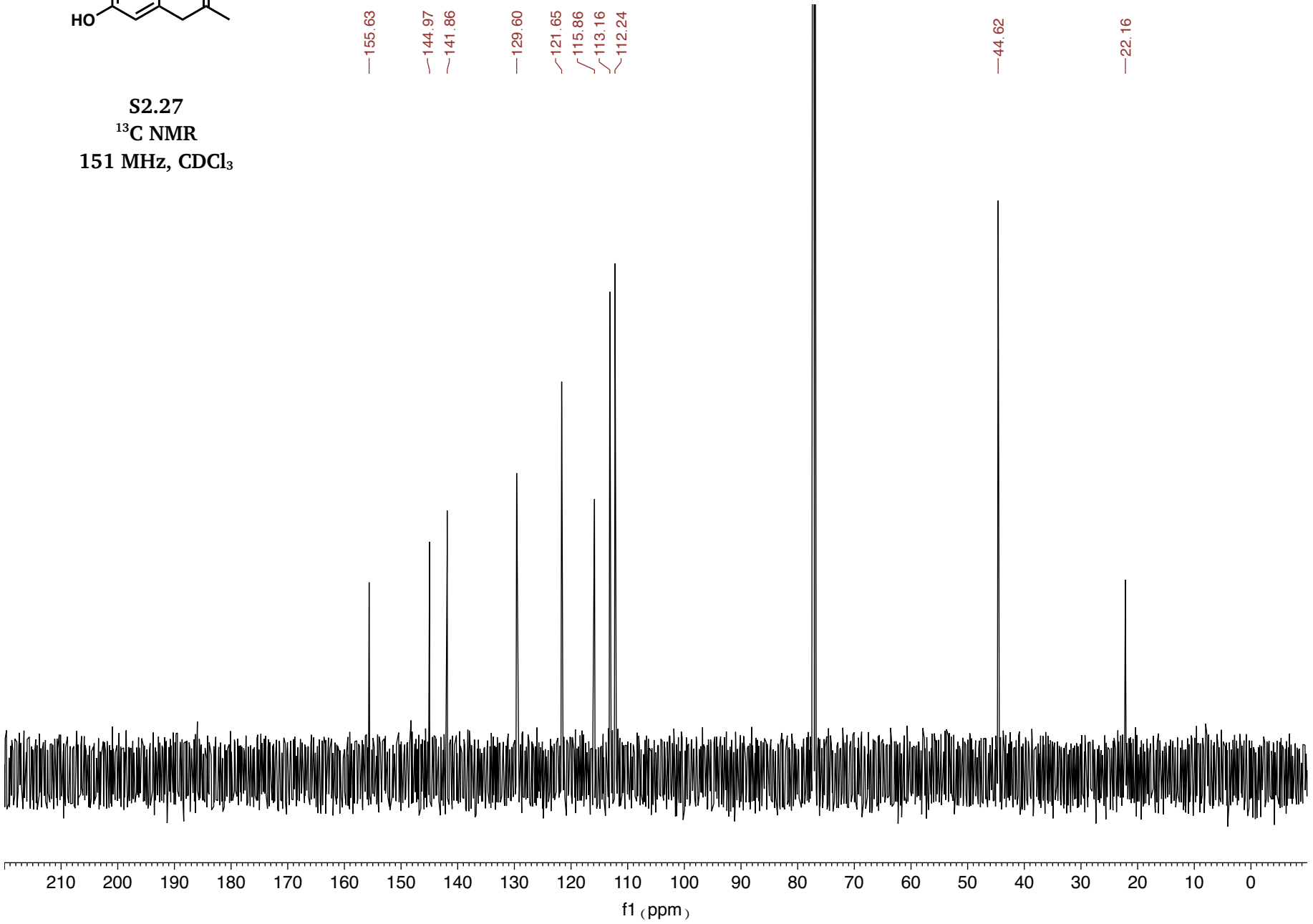


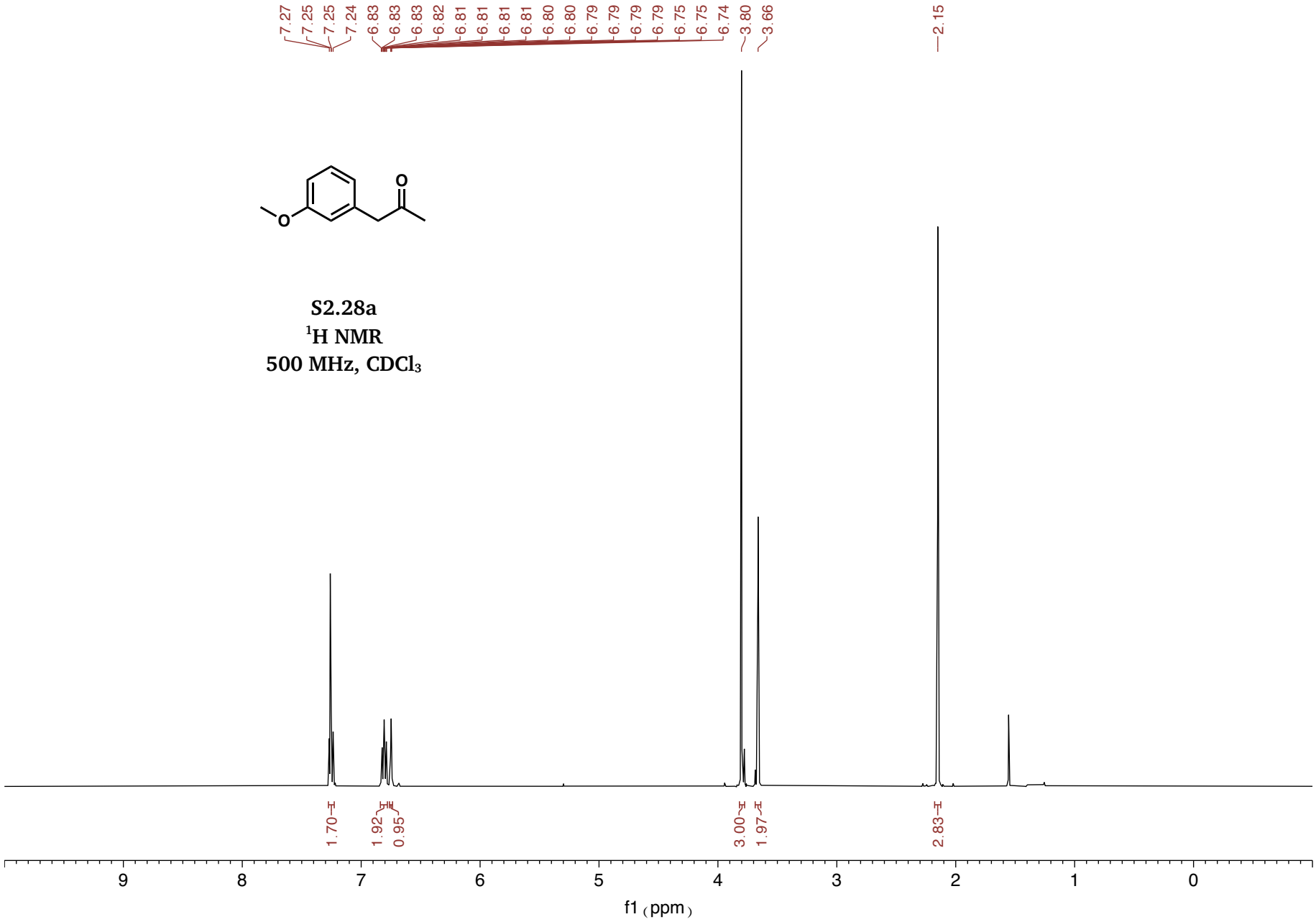
S2.27
^{1}H NMR
600 MHz, $CDCl_3$



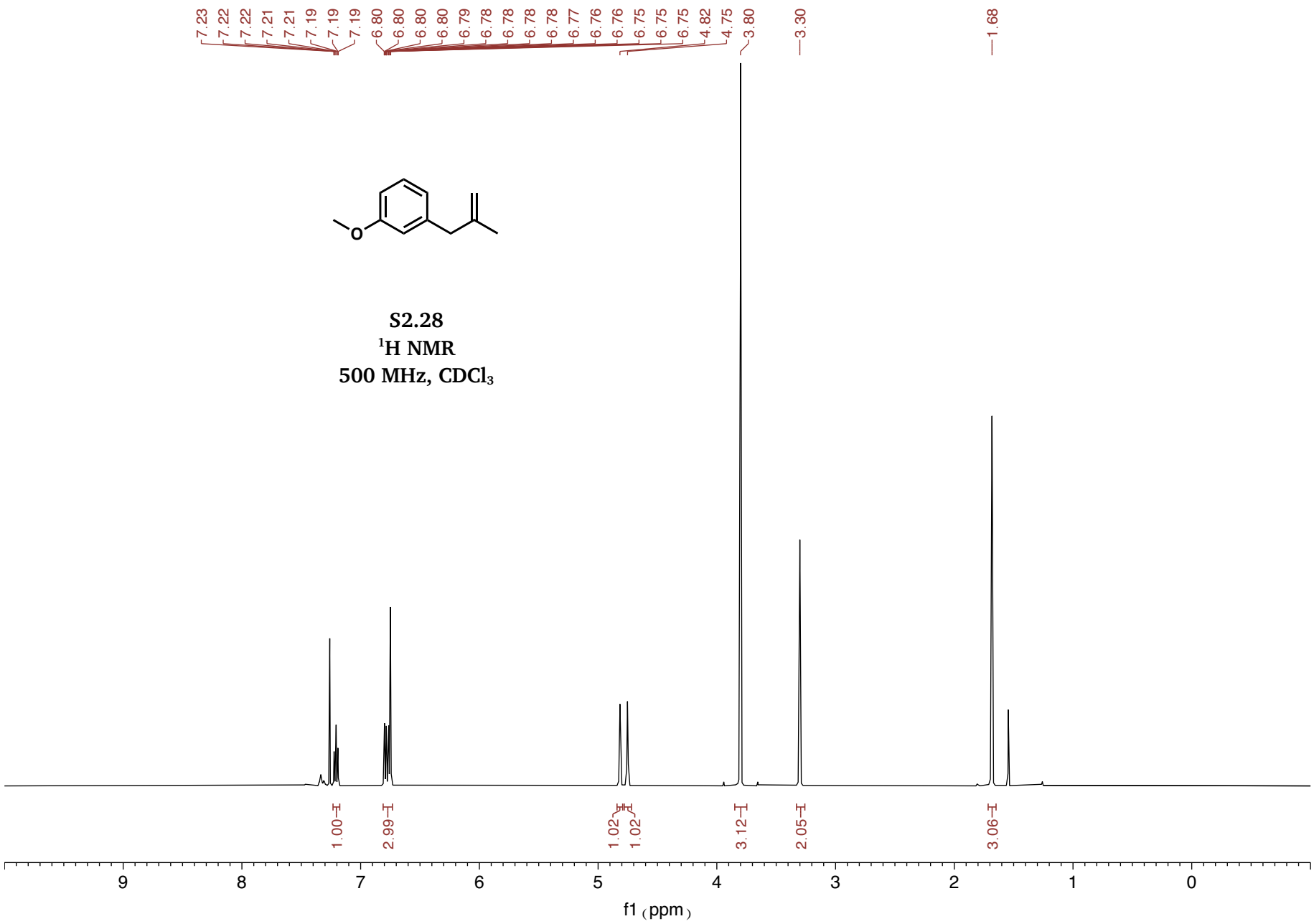


S2.27
^{13}C NMR
151 MHz, $CDCl_3$

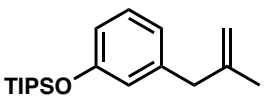




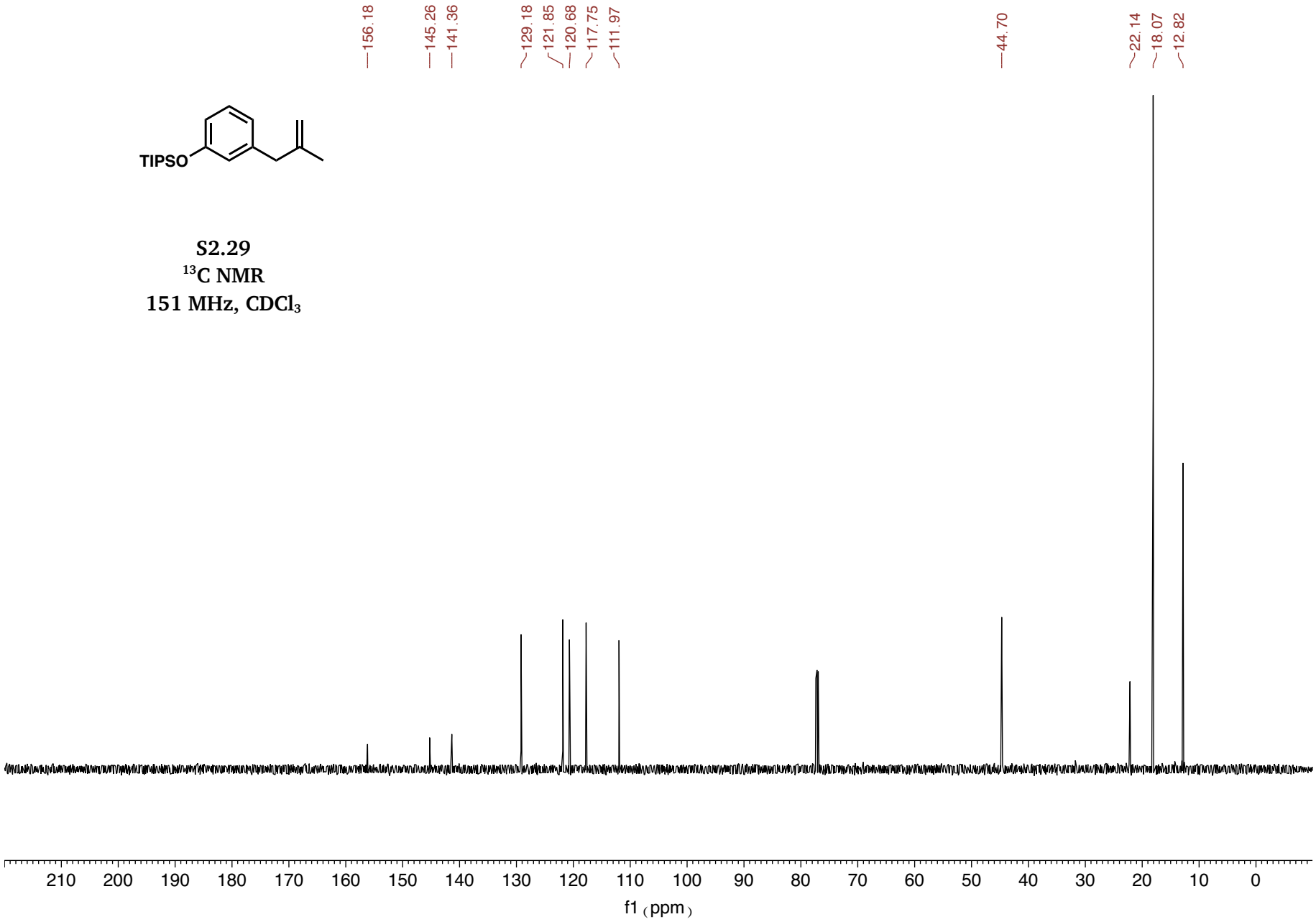
S2.28a
^{1}H NMR
500 MHz, $CDCl_3$



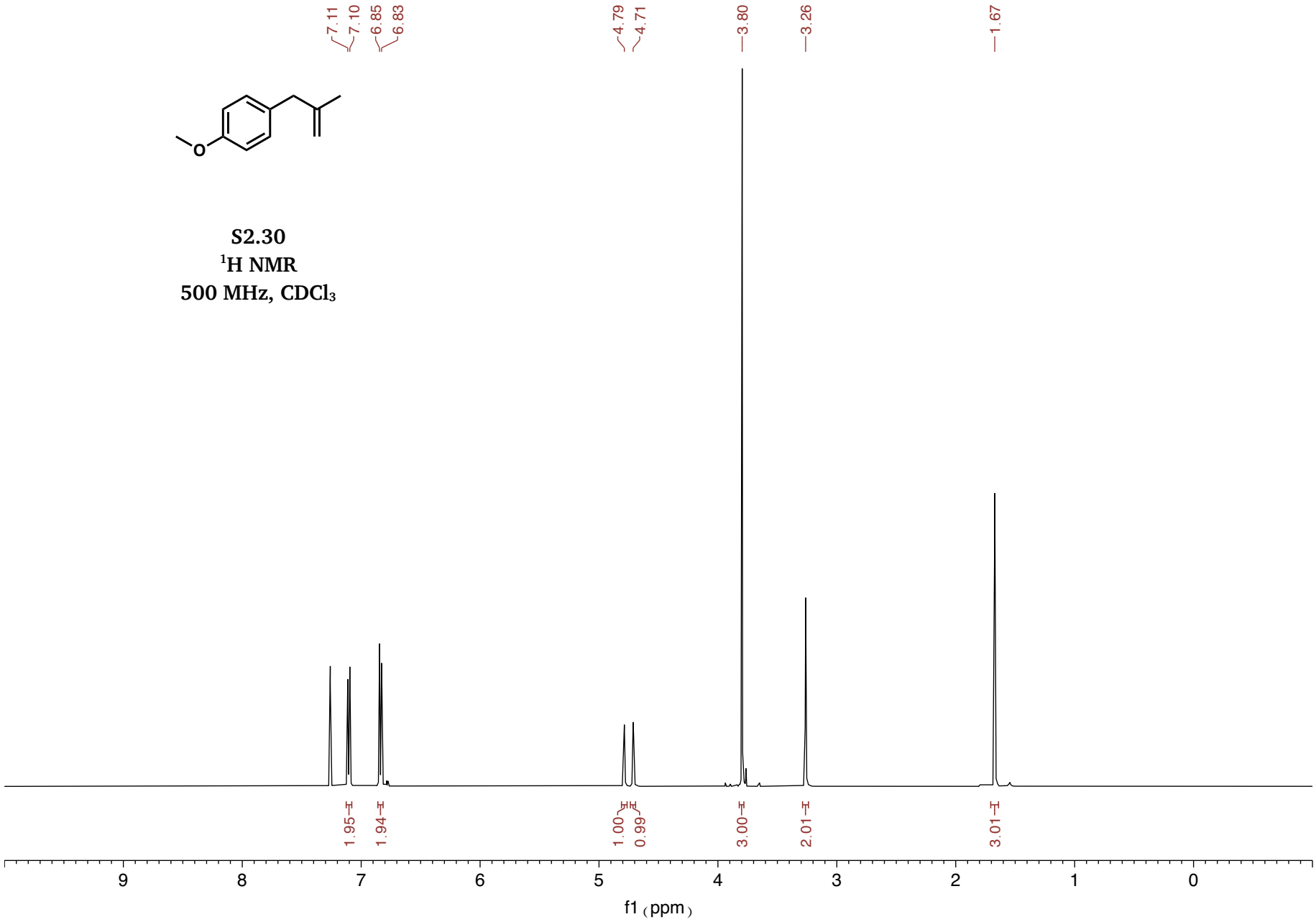
S2.28
^{1}H NMR
500 MHz, $CDCl_3$



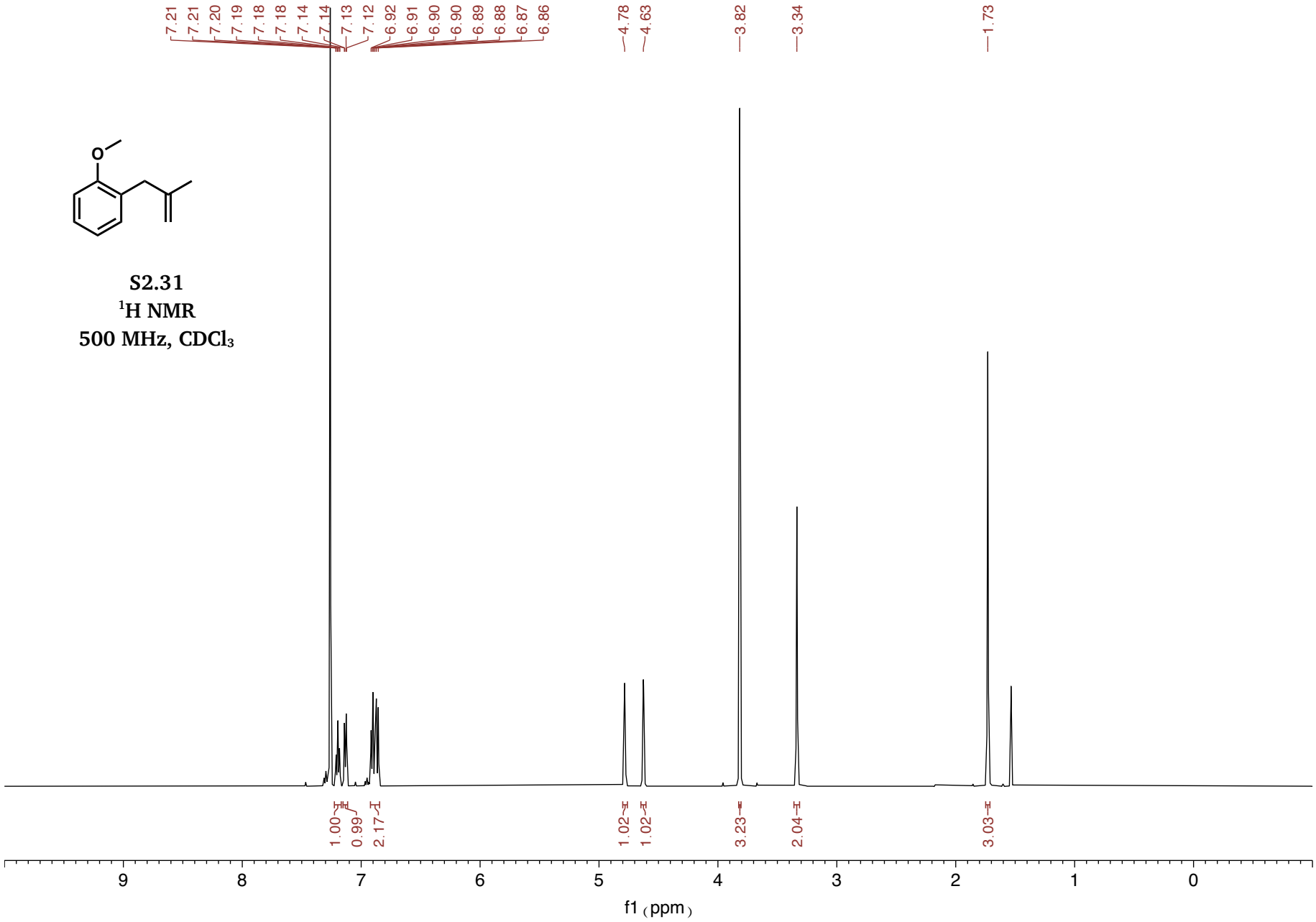
S2.29
^{1}H NMR
600 MHz, $CDCl_3$



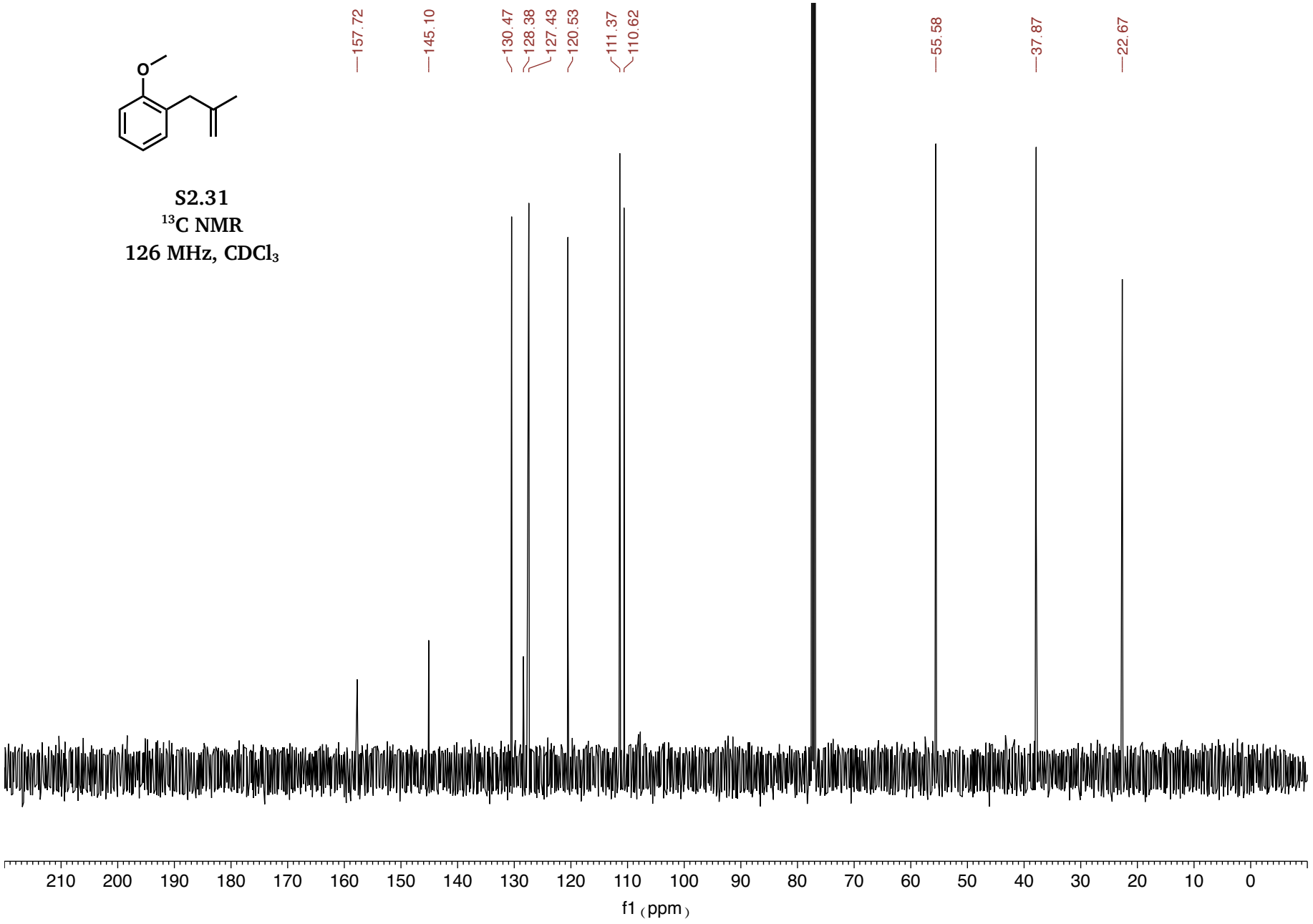
S2.29
^{13}C NMR
151 MHz, $CDCl_3$



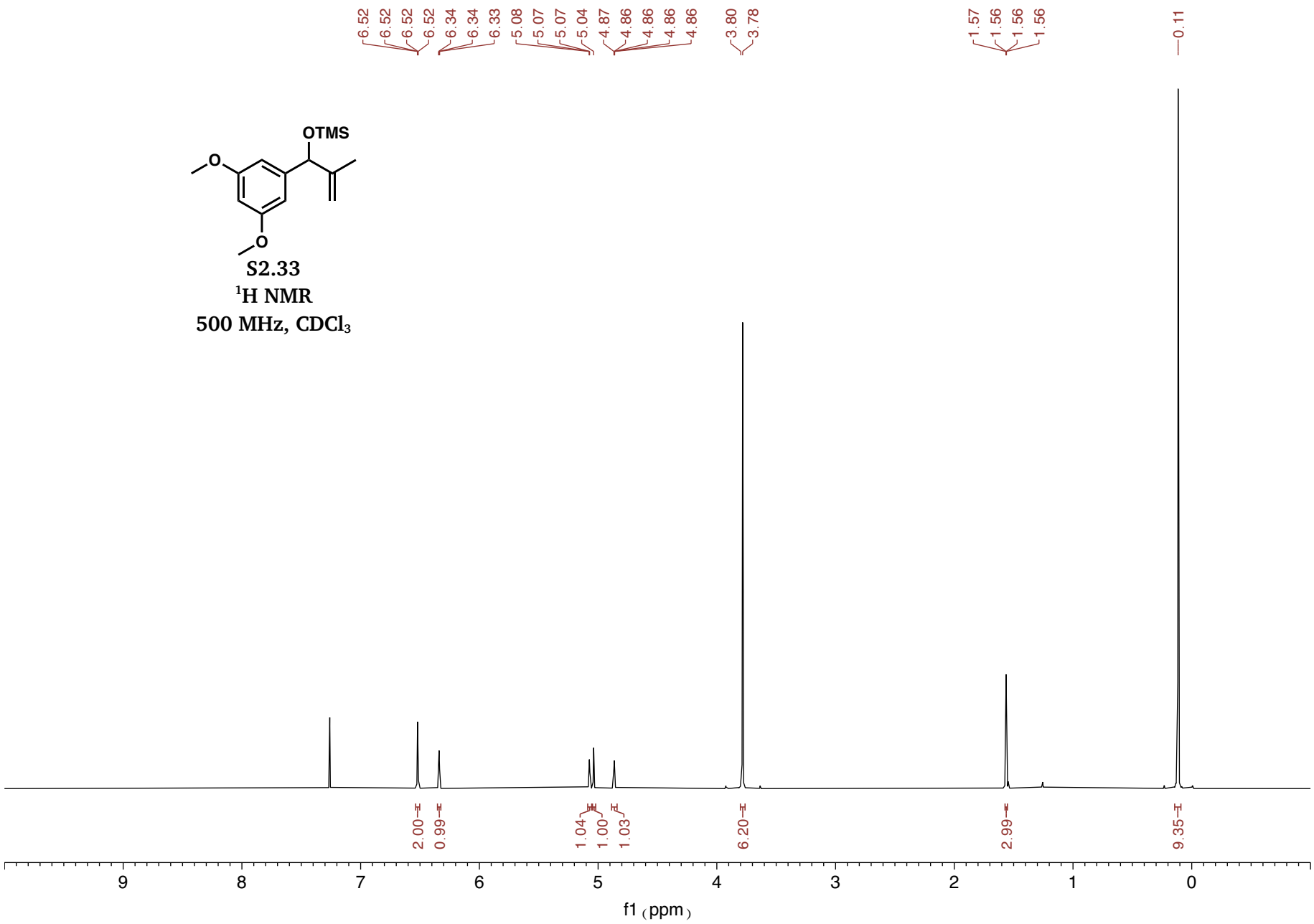
S2.30
^{1}H NMR
500 MHz, $CDCl_3$



S2.31
^{1}H NMR
500 MHz, $CDCl_3$



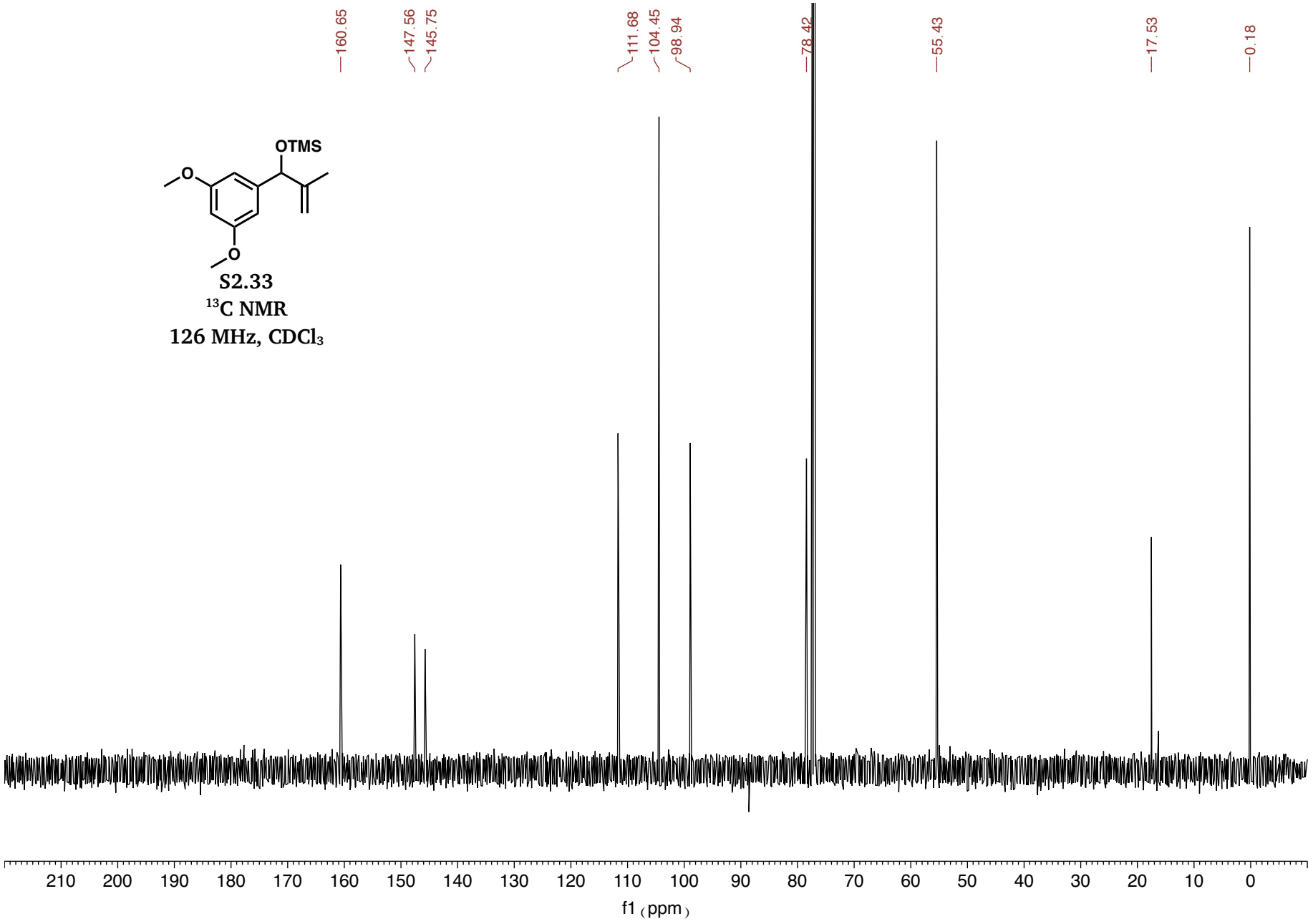
S2.31
^{13}C NMR
126 MHz, $CDCl_3$

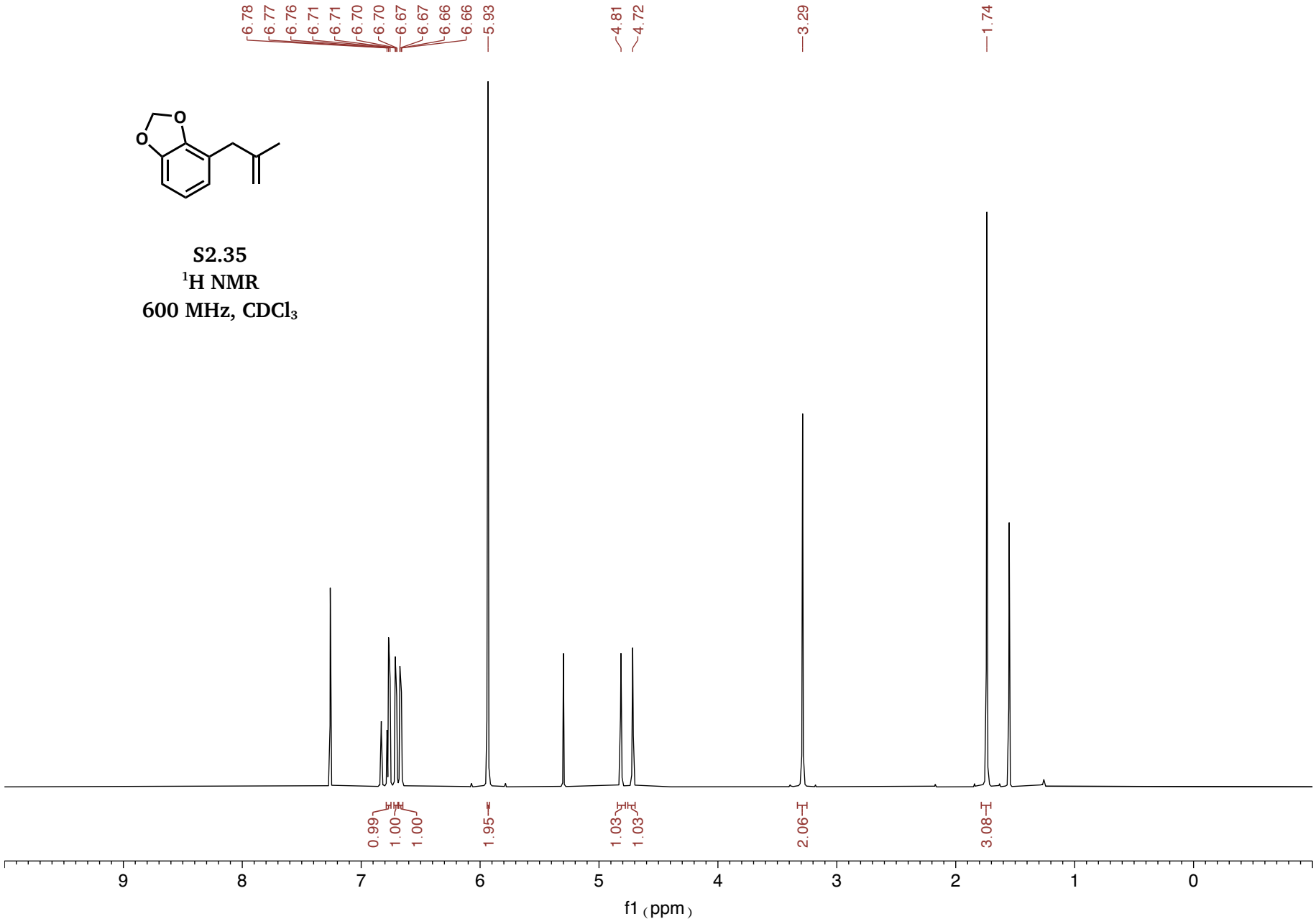


S2.33

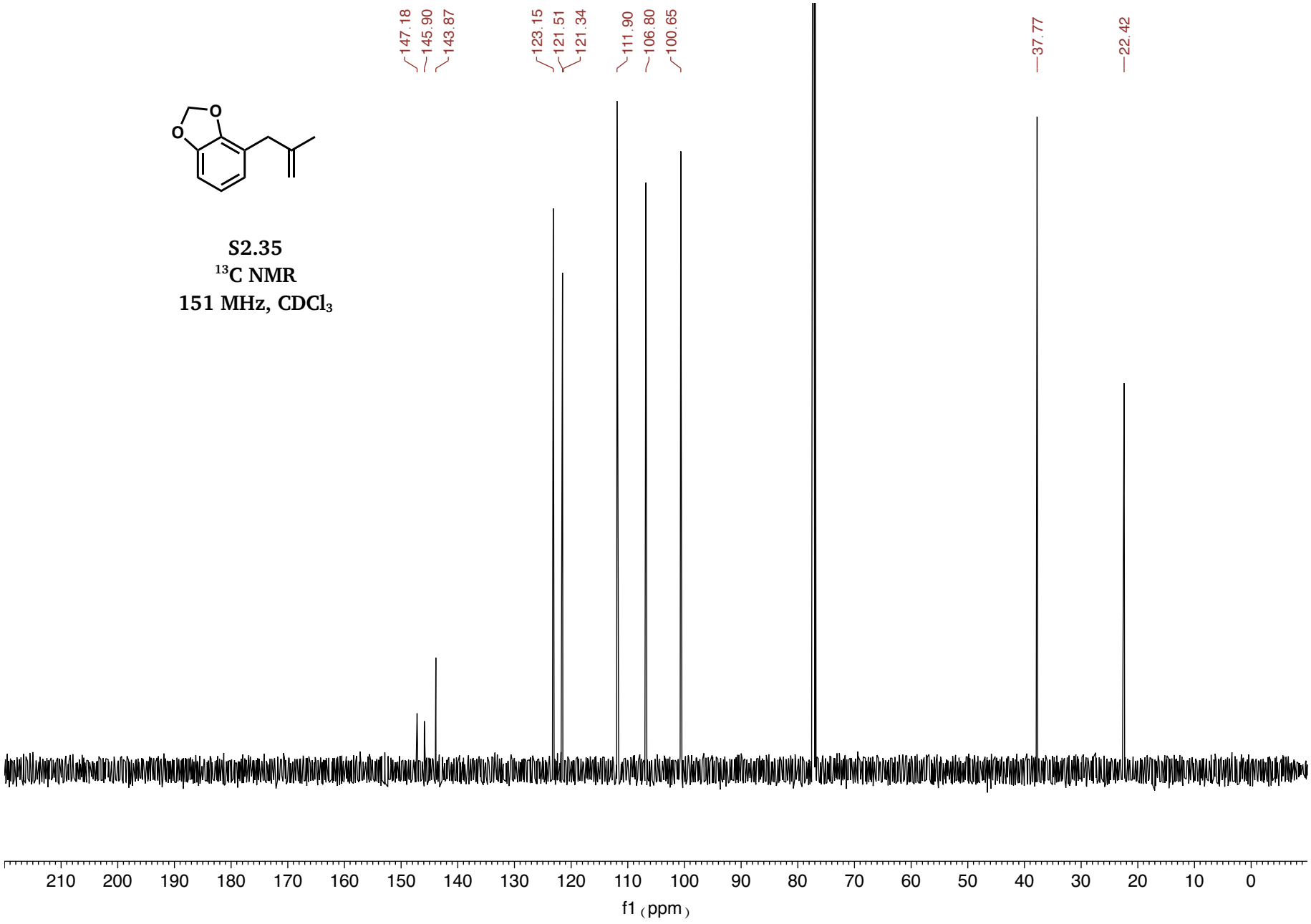
^{1}H NMR

500 MHz, $CDCl_3$

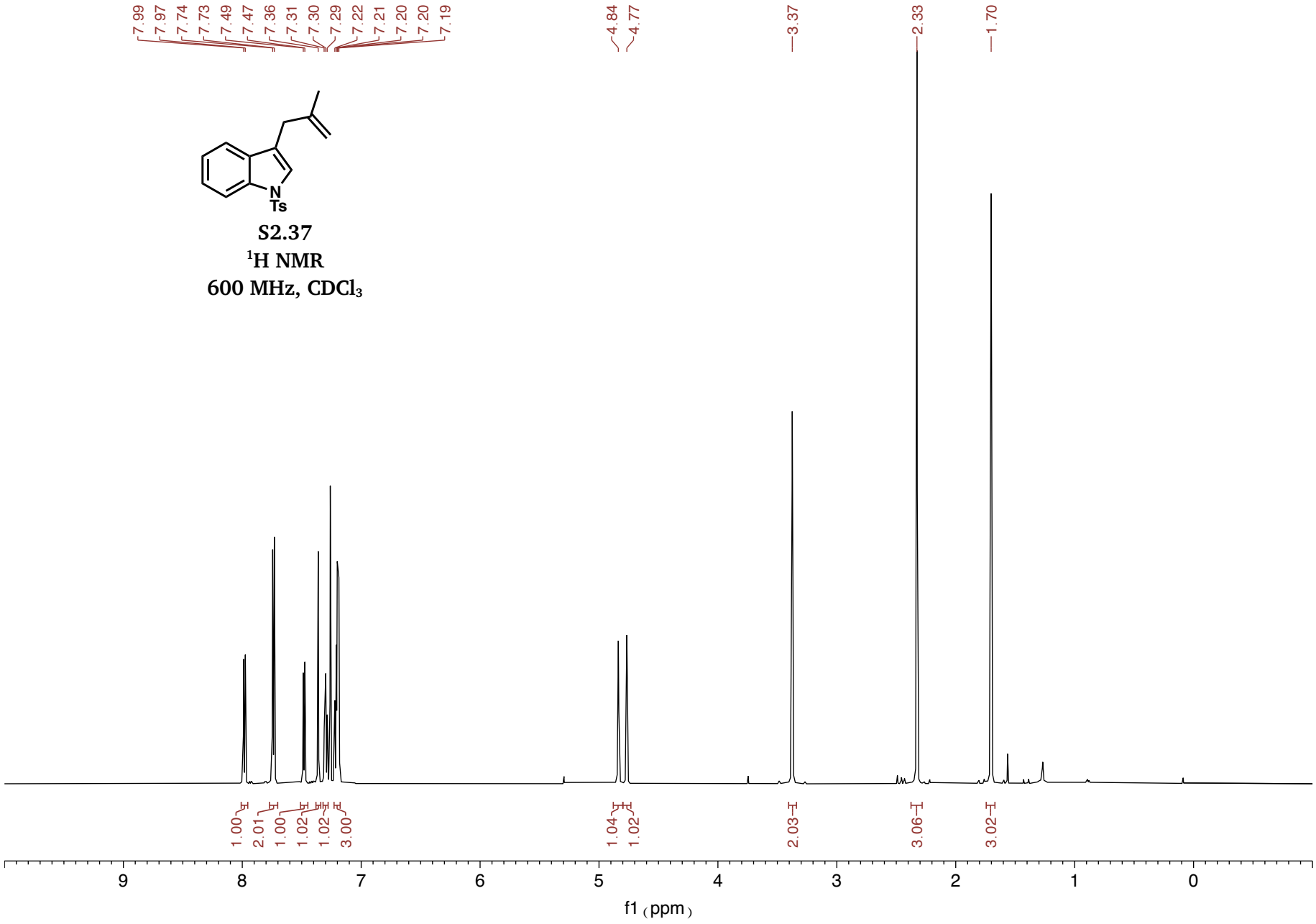

160.65
147.56
145.75
111.68
104.45
98.94
78.42
55.43
17.53
0.18
OTMS
O
O
S2.33
13C NMR
126 MHz, CDCl3
210 200 190 180 170 160 150 140 130 120 110 100 90 80 70 60 50 40 30 20 10 0
f1 (ppm)



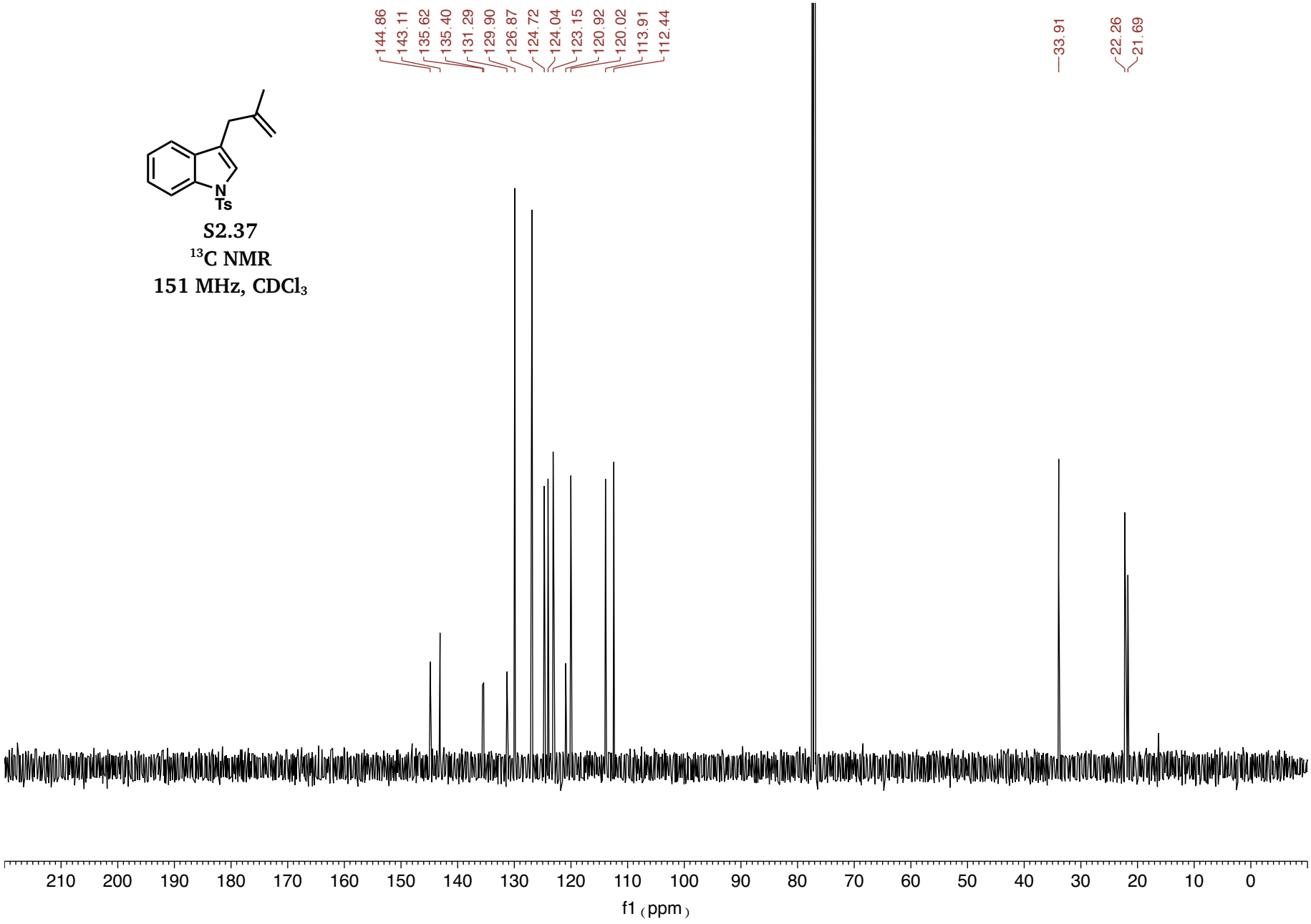
S2.35
^{1}H NMR
600 MHz, $CDCl_3$



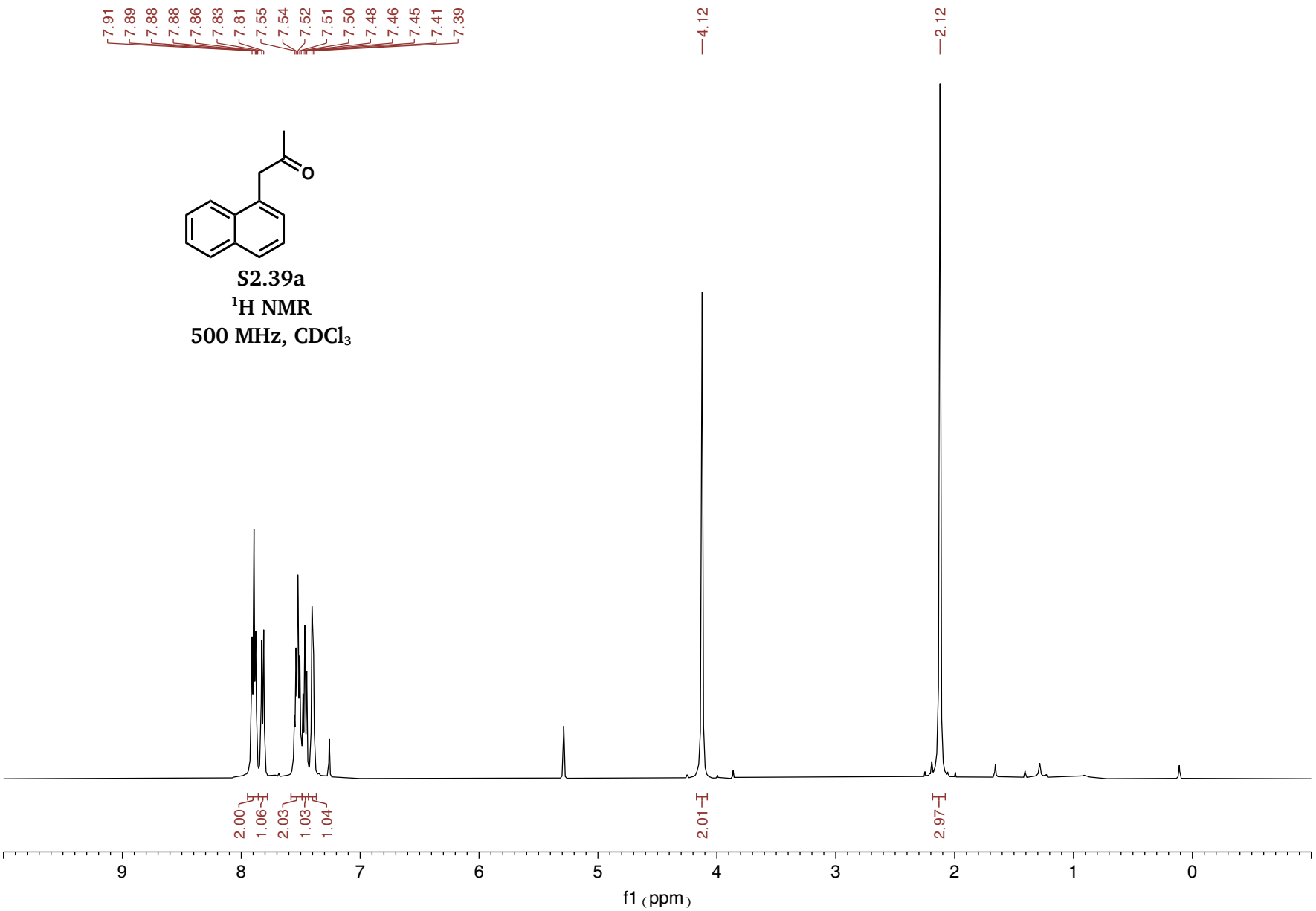
S2.35
^{13}C NMR
151 MHz, $CDCl_3$



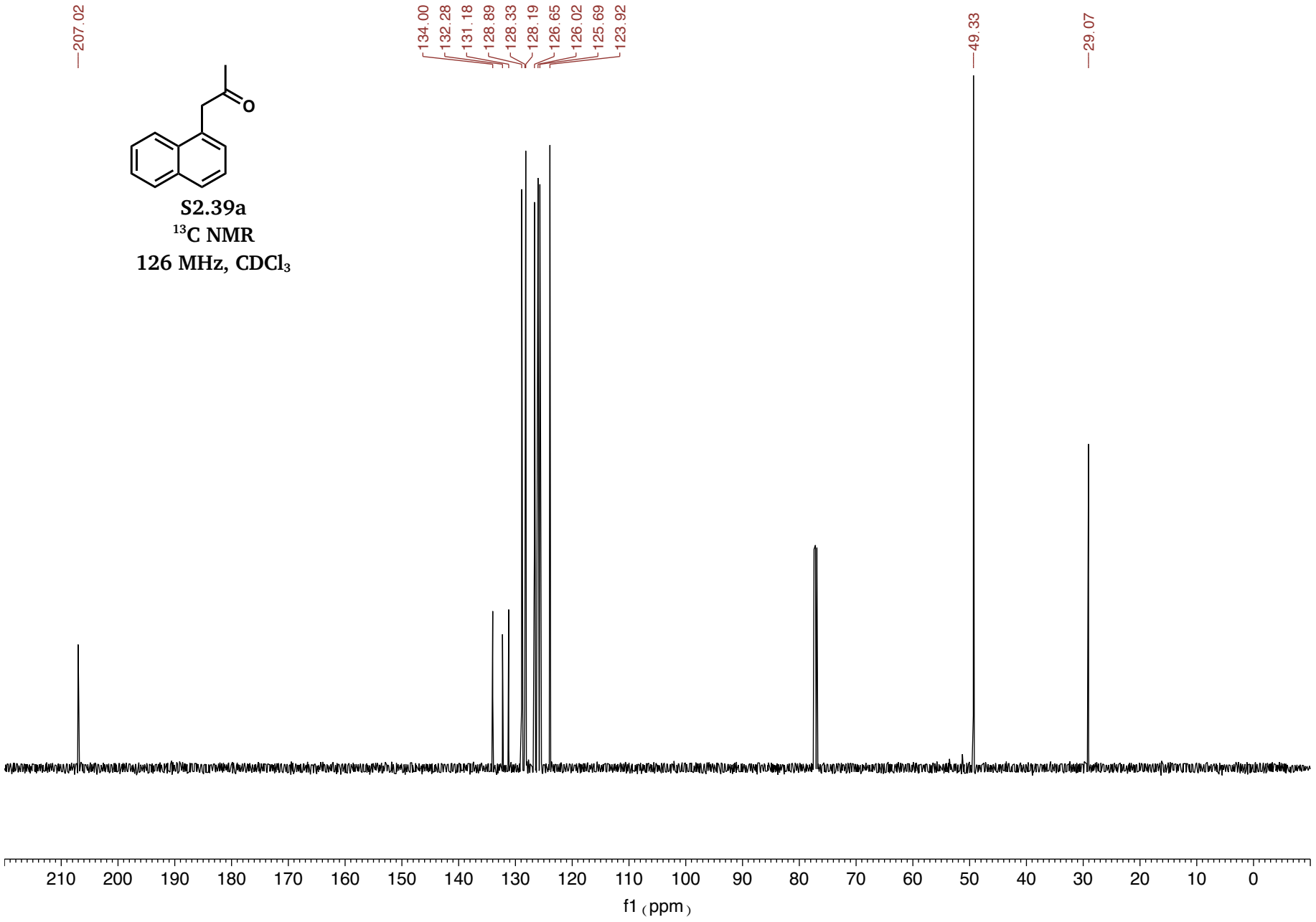
S2.37
^{1}H NMR
600 MHz, $CDCl_3$

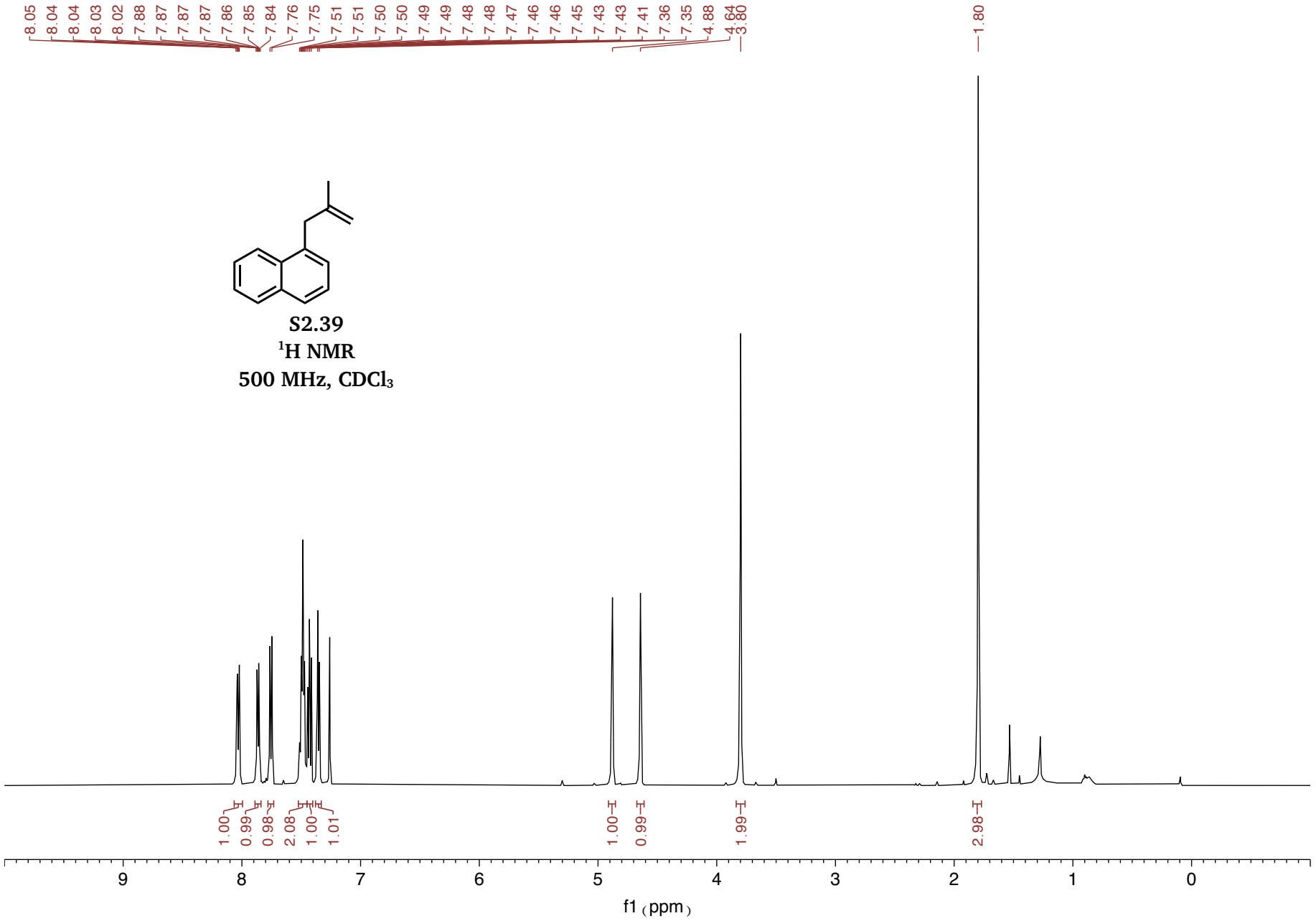


S2.37
^{13}C NMR
151 MHz, $CDCl_3$

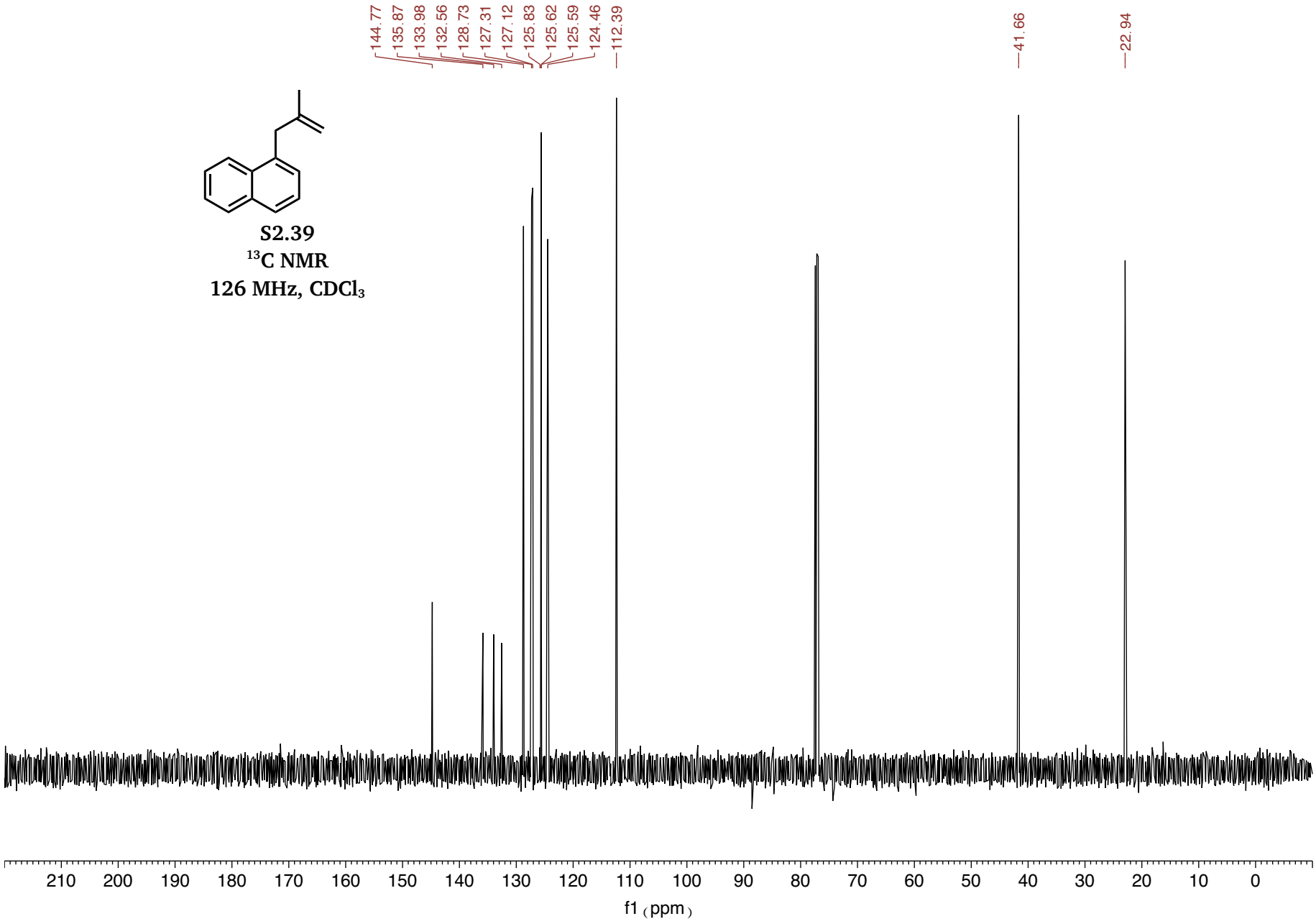


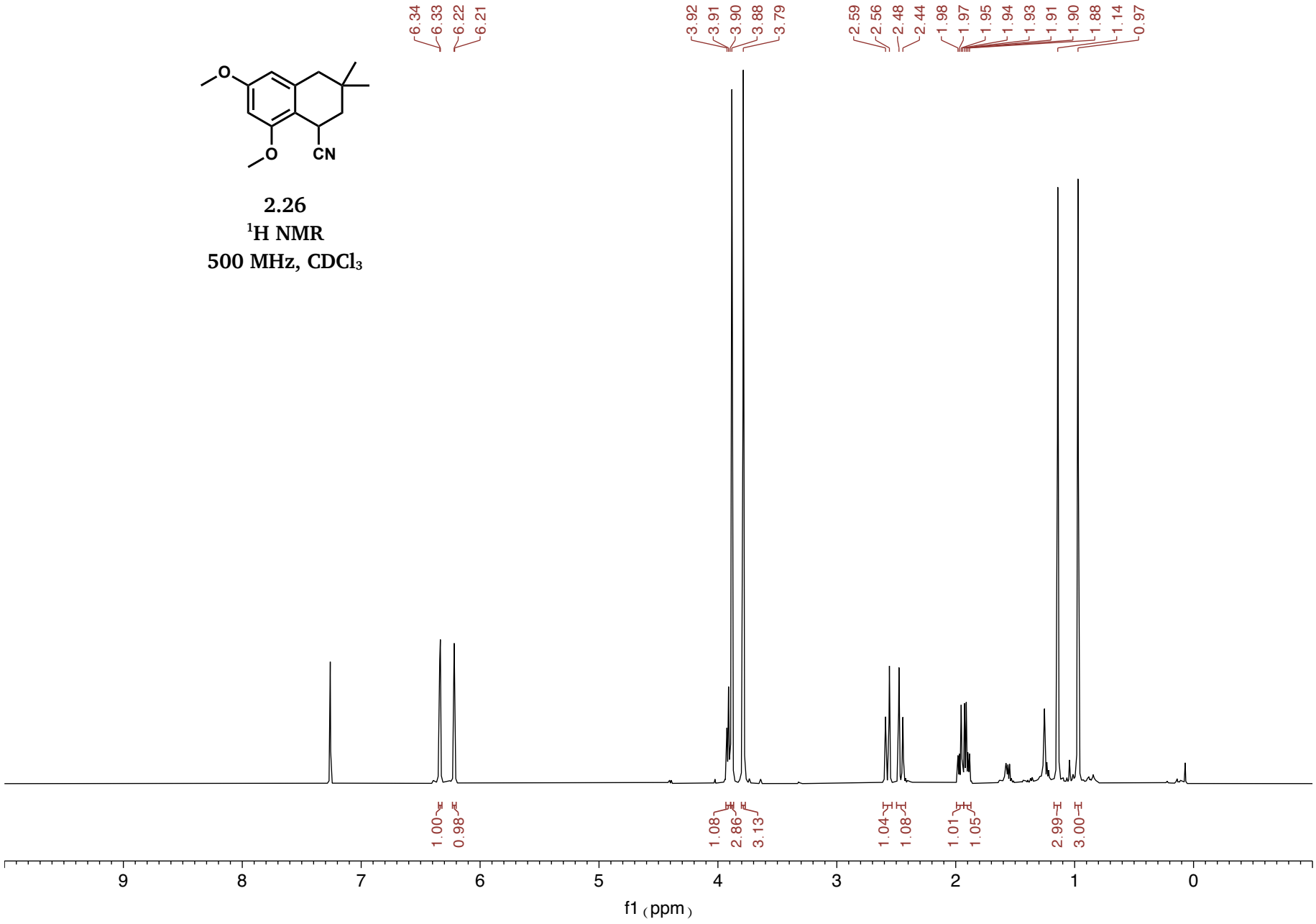
S2.39a
^{1}H NMR
500 MHz, $CDCl_3$


207.02
134.00
132.28
131.18
128.89
128.33
128.19
126.65
126.02
125.69
123.92
49.33
29.07
O
S2.39a
13C NMR
126 MHz, CDCl3
210 200 190 180 170 160 150 140 130 120 110 100 90 80 70 60 50 40 30 20 10 0
f1 (ppm)

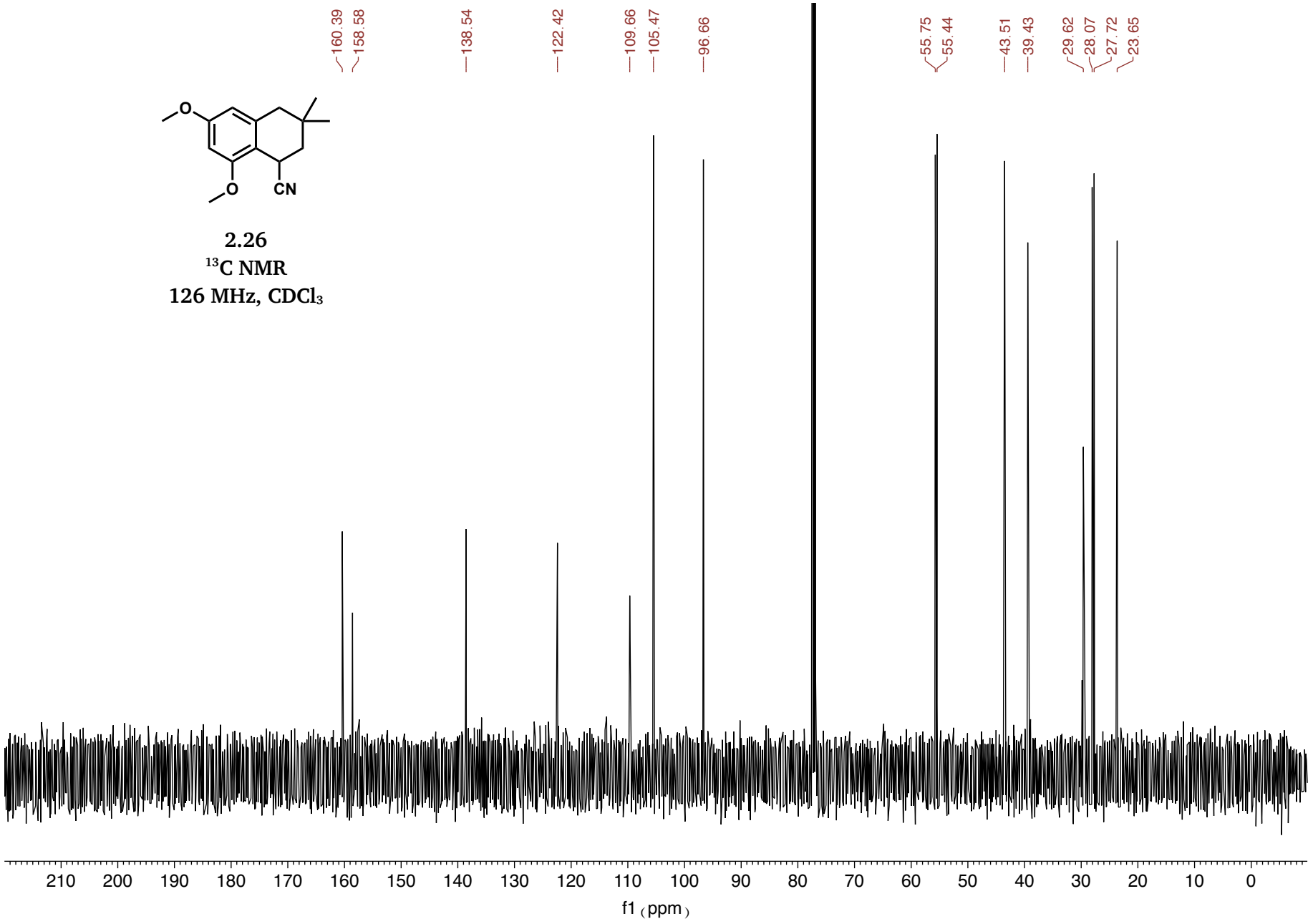


S2.39
^{1}H NMR
500 MHz, $CDCl_3$

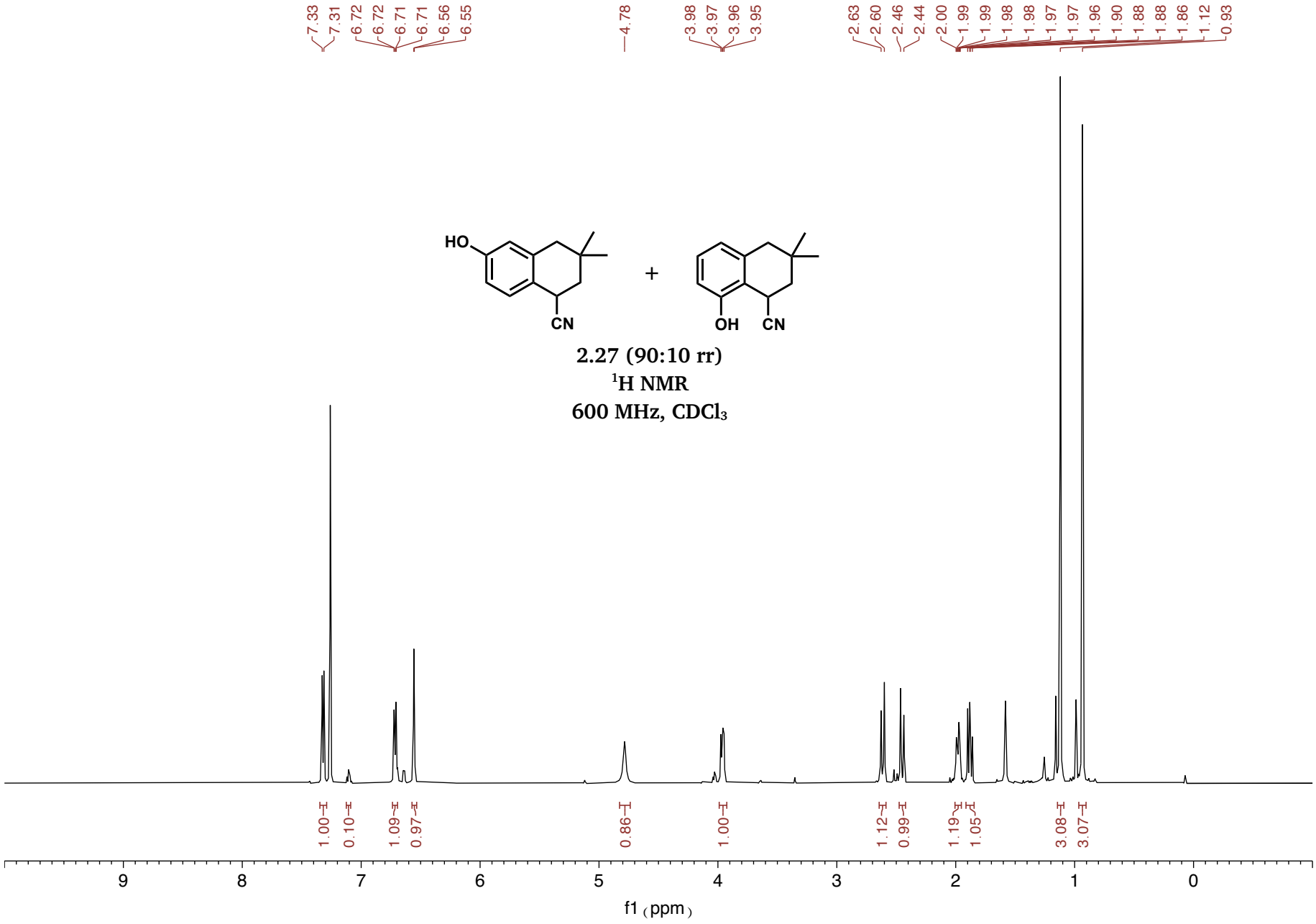

144.77
135.87
133.98
132.56
128.73
127.31
127.12
125.83
125.62
125.59
124.46
112.39
41.66
22.94
S2.39
13C NMR
126 MHz, CDCl3
210
200
190
180
170
160
150
140
130
120
110
100
90
80
70
60
50
40
30
20
10
0
f1 (ppm)



2.26
^{1}H NMR
500 MHz, $CDCl_3$



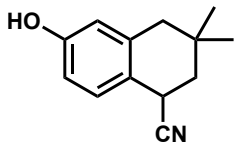
2.26
^{13}C NMR
126 MHz, $CDCl_3$



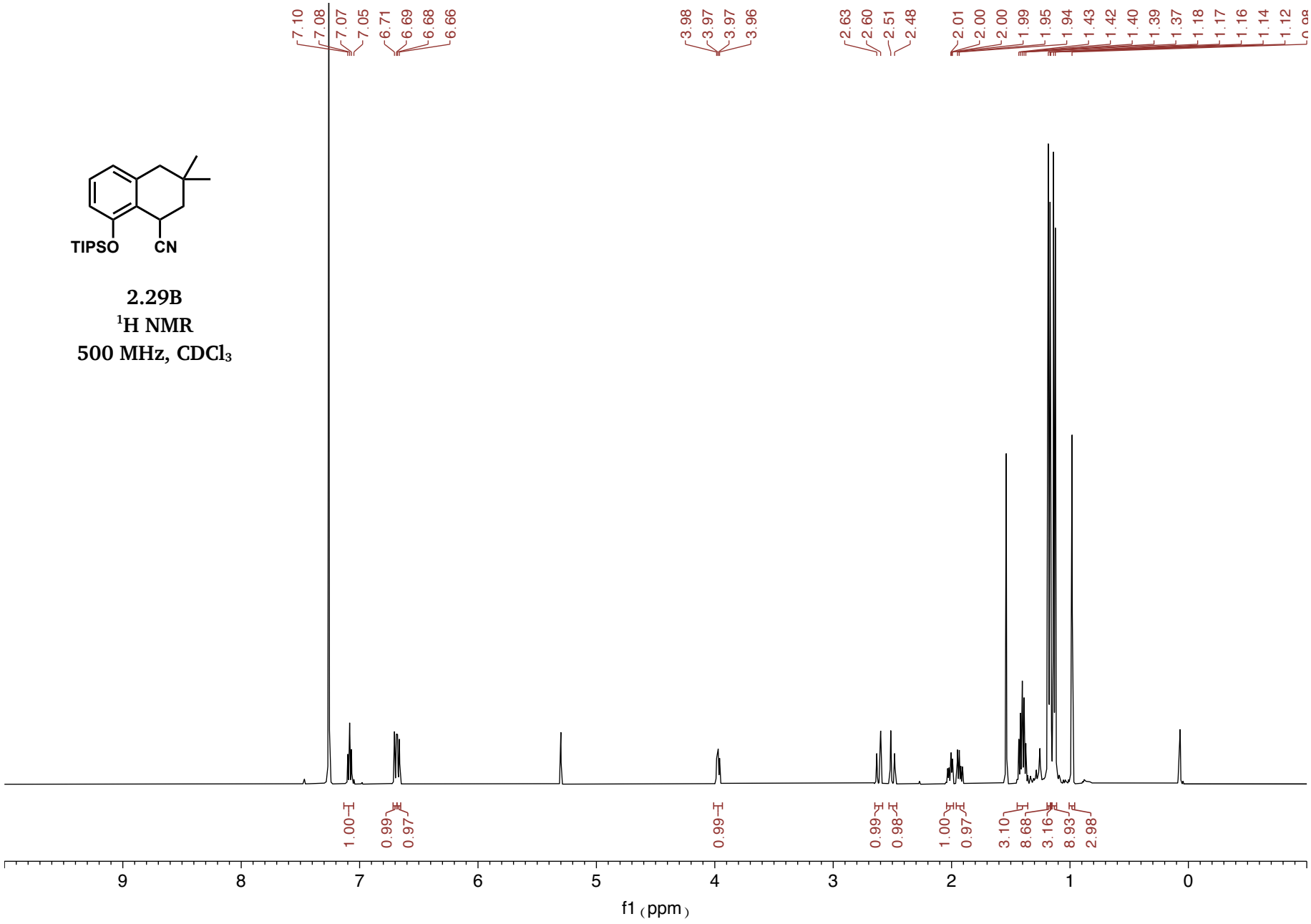
2.27 (90:10 rr)

^{1}H NMR

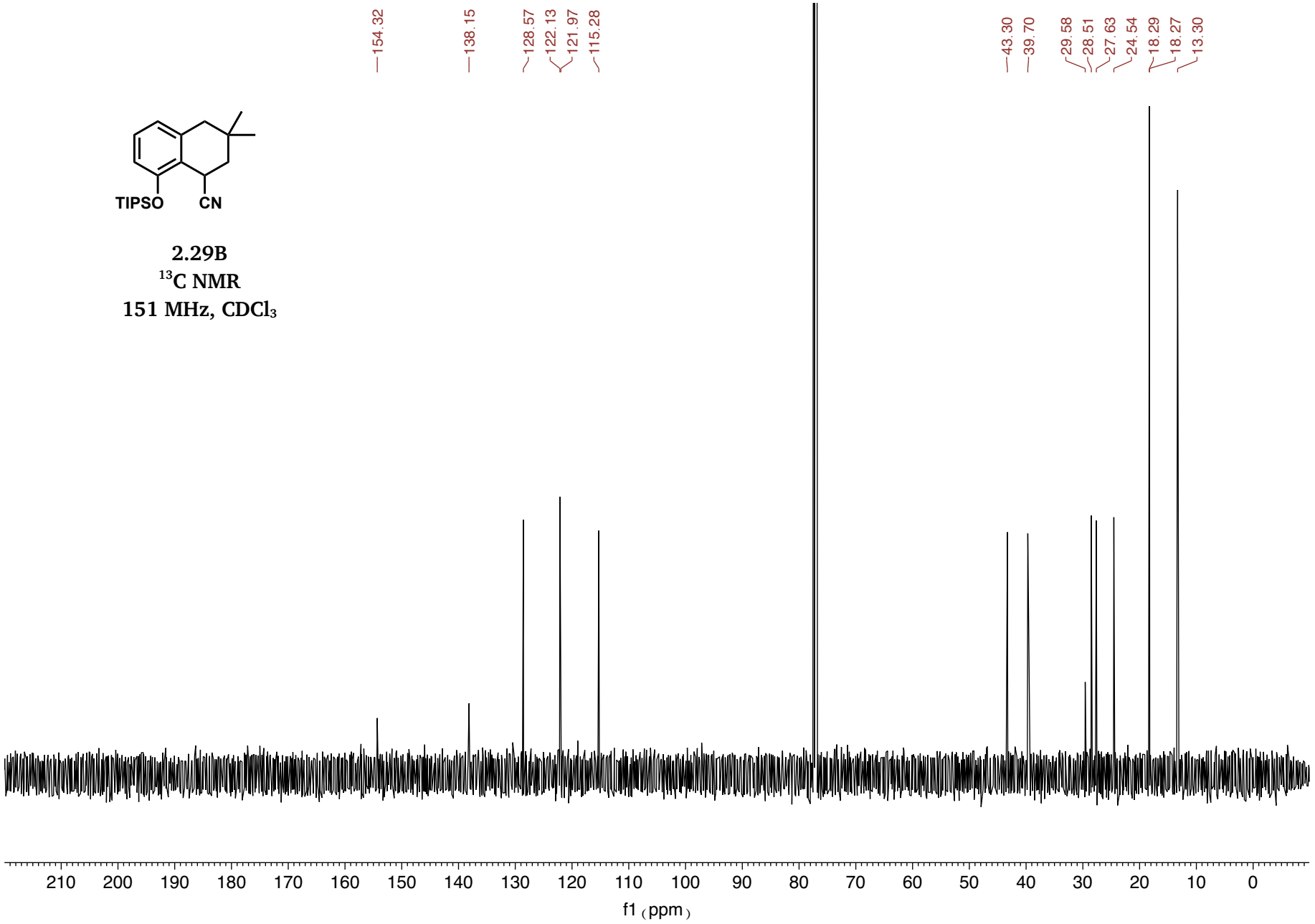
600 MHz, $CDCl_3$

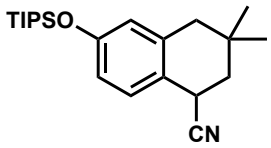


2.27
^{13}C NMR
151 MHz, $CDCl_3$

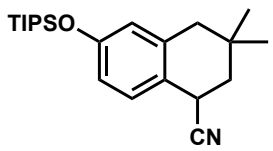


2.29B
^{1}H NMR
500 MHz, $CDCl_3$

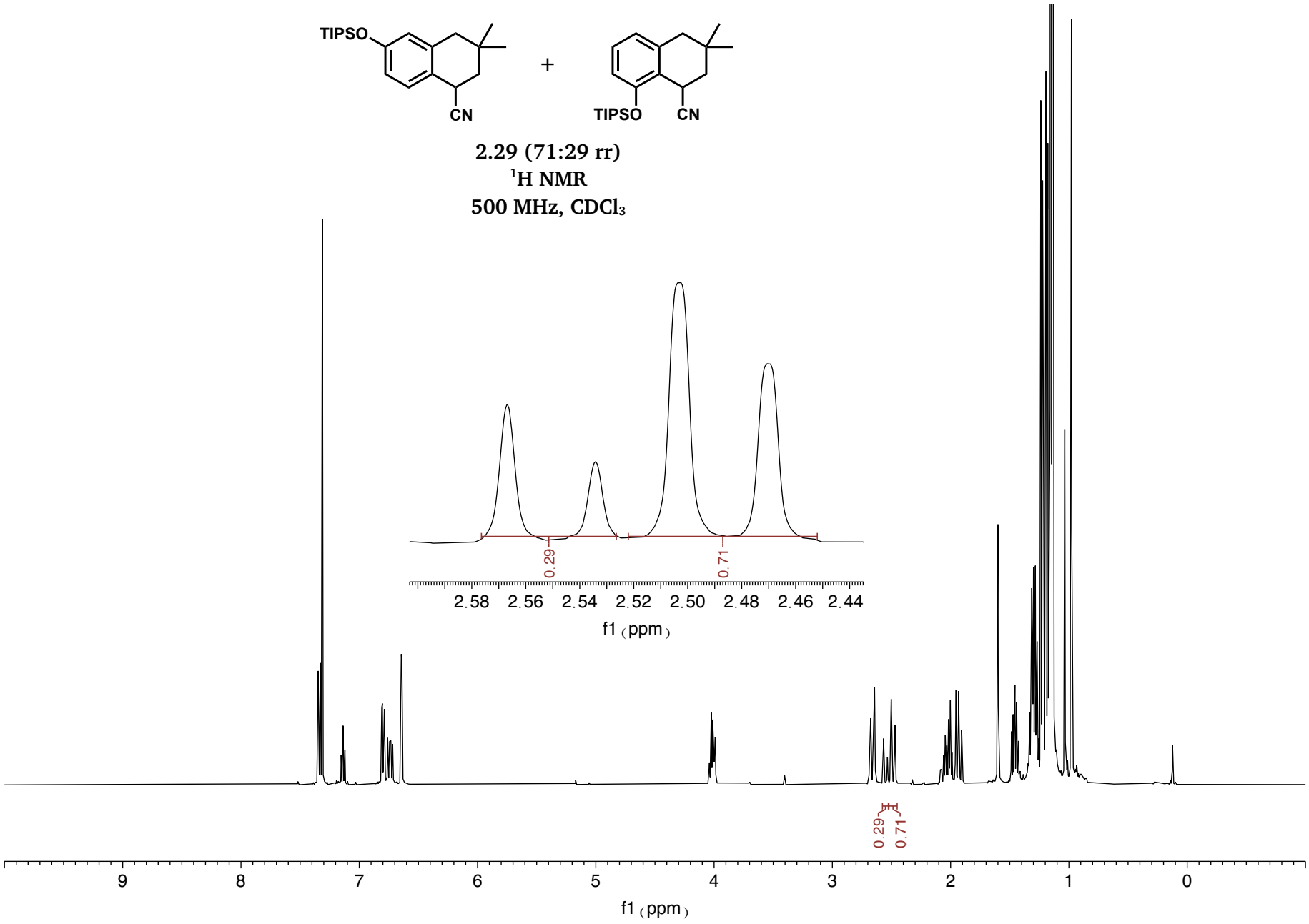

154.32
138.15
128.57
122.13
121.97
115.28
43.30
39.70
29.58
28.51
27.63
24.54
18.29
18.27
13.30
TIPSO
CN
2.29B
13C NMR
151 MHz, CDCl3
210 200 190 180 170 160 150 140 130 120 110 100 90 80 70 60 50 40 30 20 10 0
f1 (ppm)

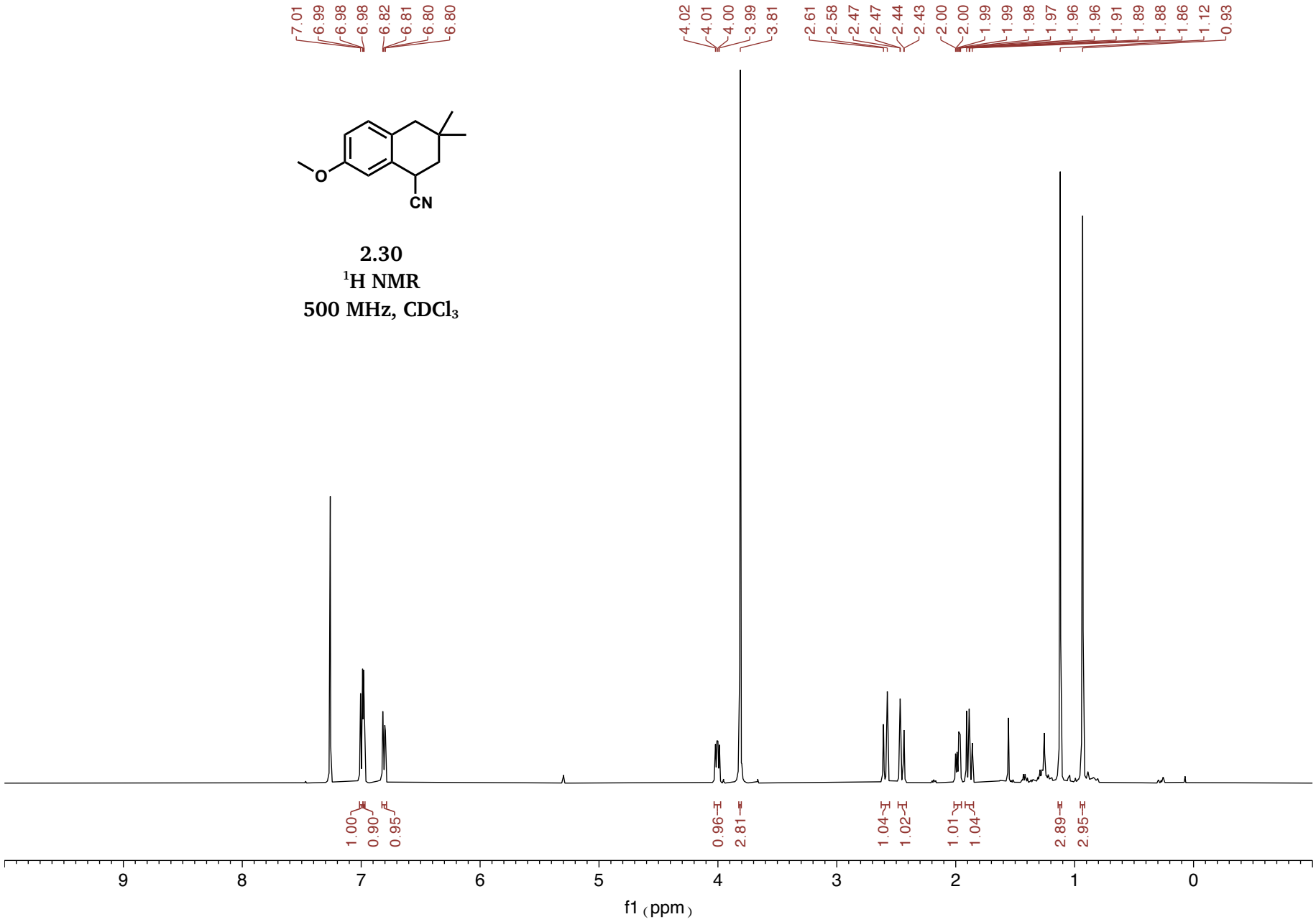


2.29A
^{1}H NMR
500 MHz, $CDCl_3$

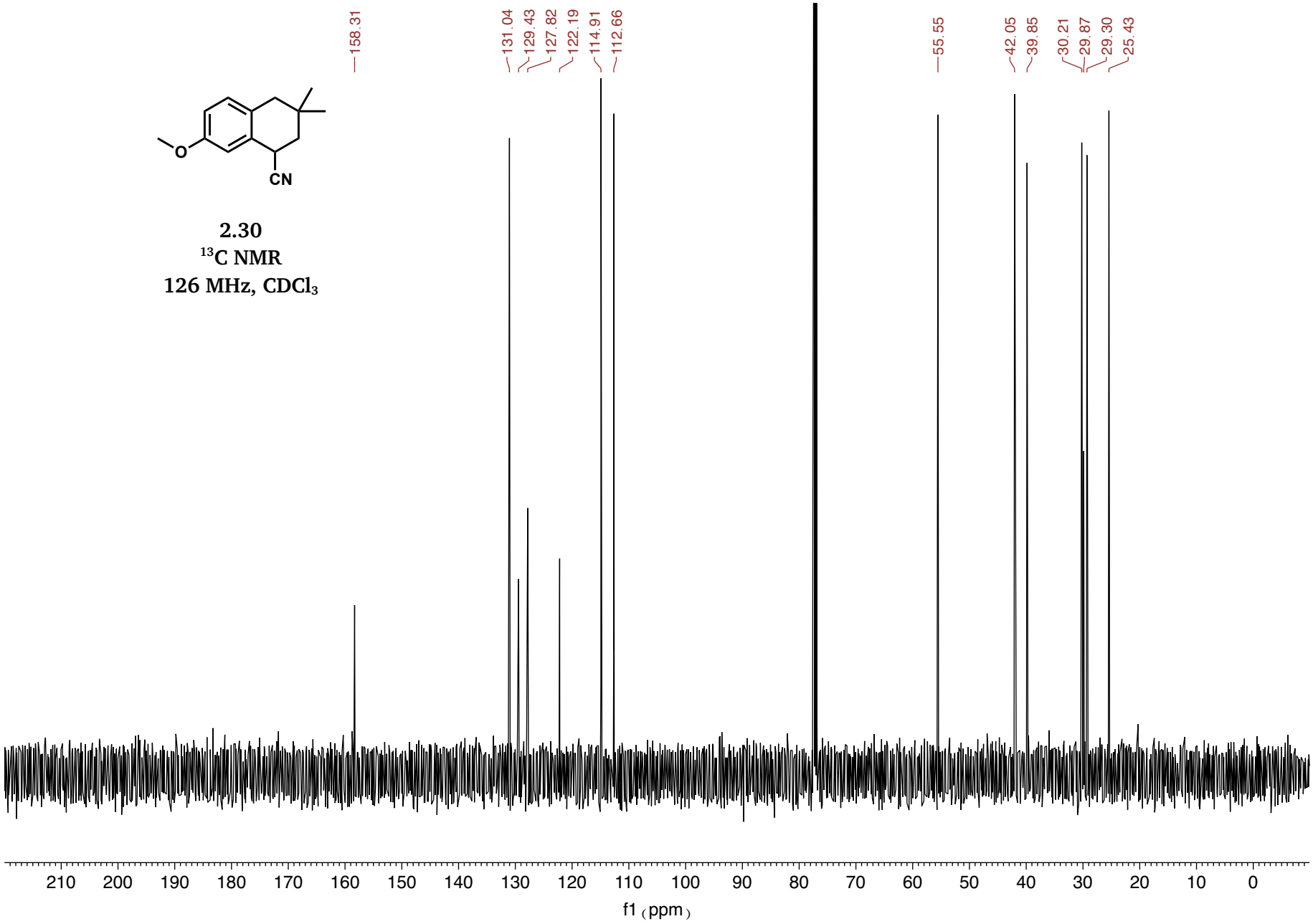


2.29A
^{13}C NMR
151 MHz, $CDCl_3$

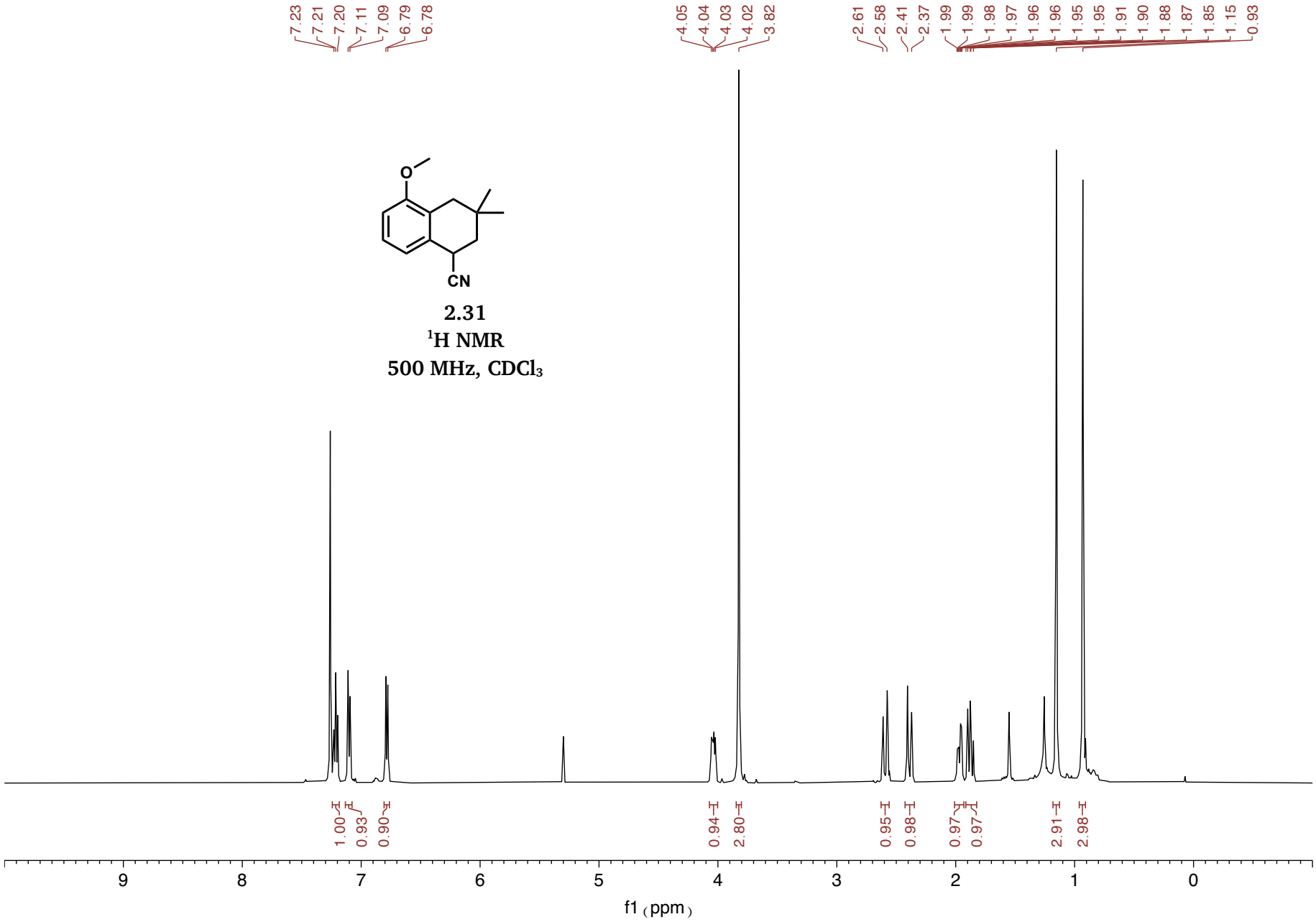

TIPSO
CN
+
TIPSO
CN
2.29 (71:29 rr)
1H NMR
500 MHz, CDCl3
0.29
0.71
2.58 2.56 2.54 2.52 2.50 2.48 2.46 2.44
f1 (ppm)
0.29
0.71
9 8 7 6 5 4 3 2 1 0
f1 (ppm)



2.30
^{1}H NMR
500 MHz, $CDCl_3$



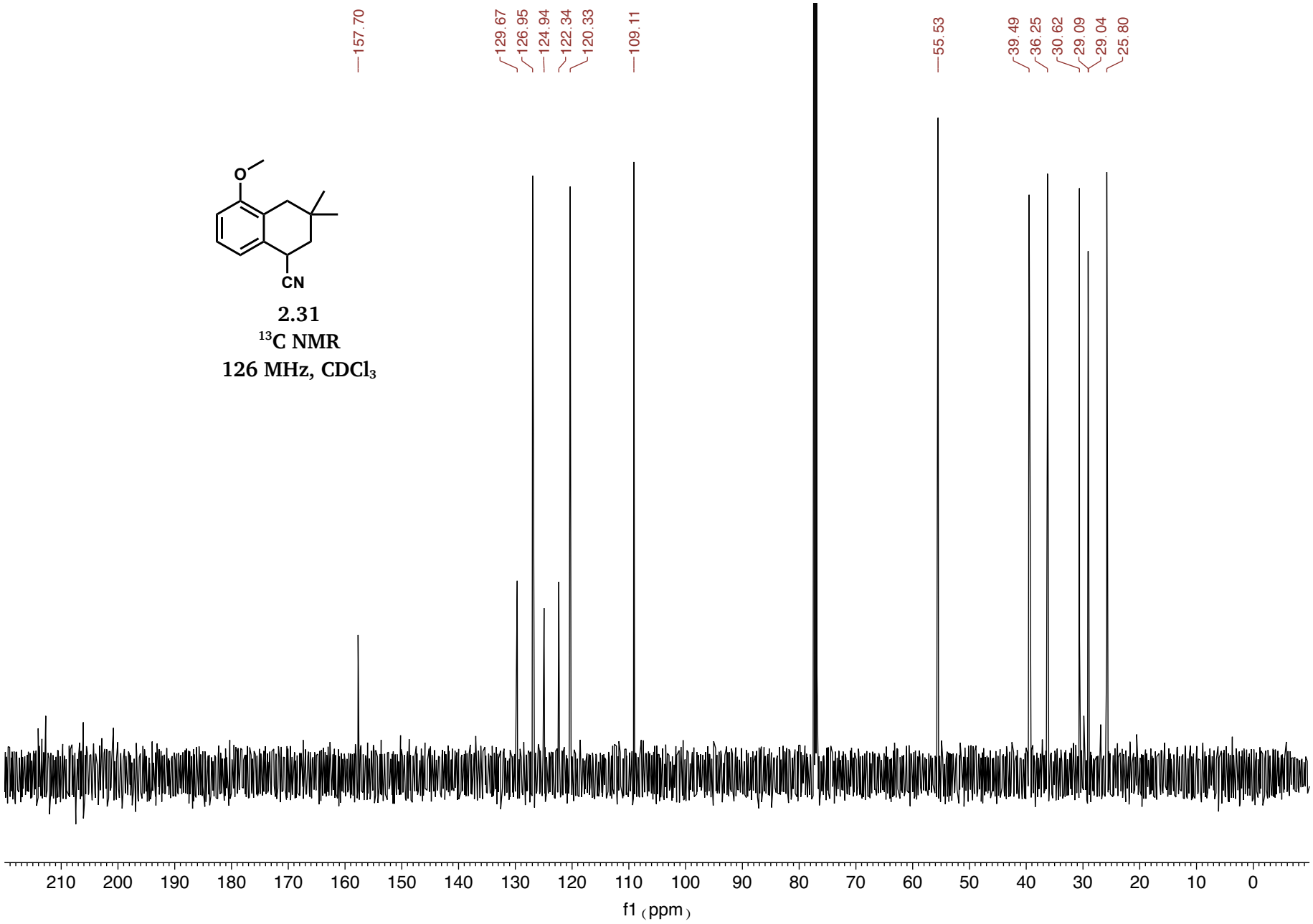
2.30
^{13}C NMR
126 MHz, $CDCl_3$



2.31

^{1}H NMR

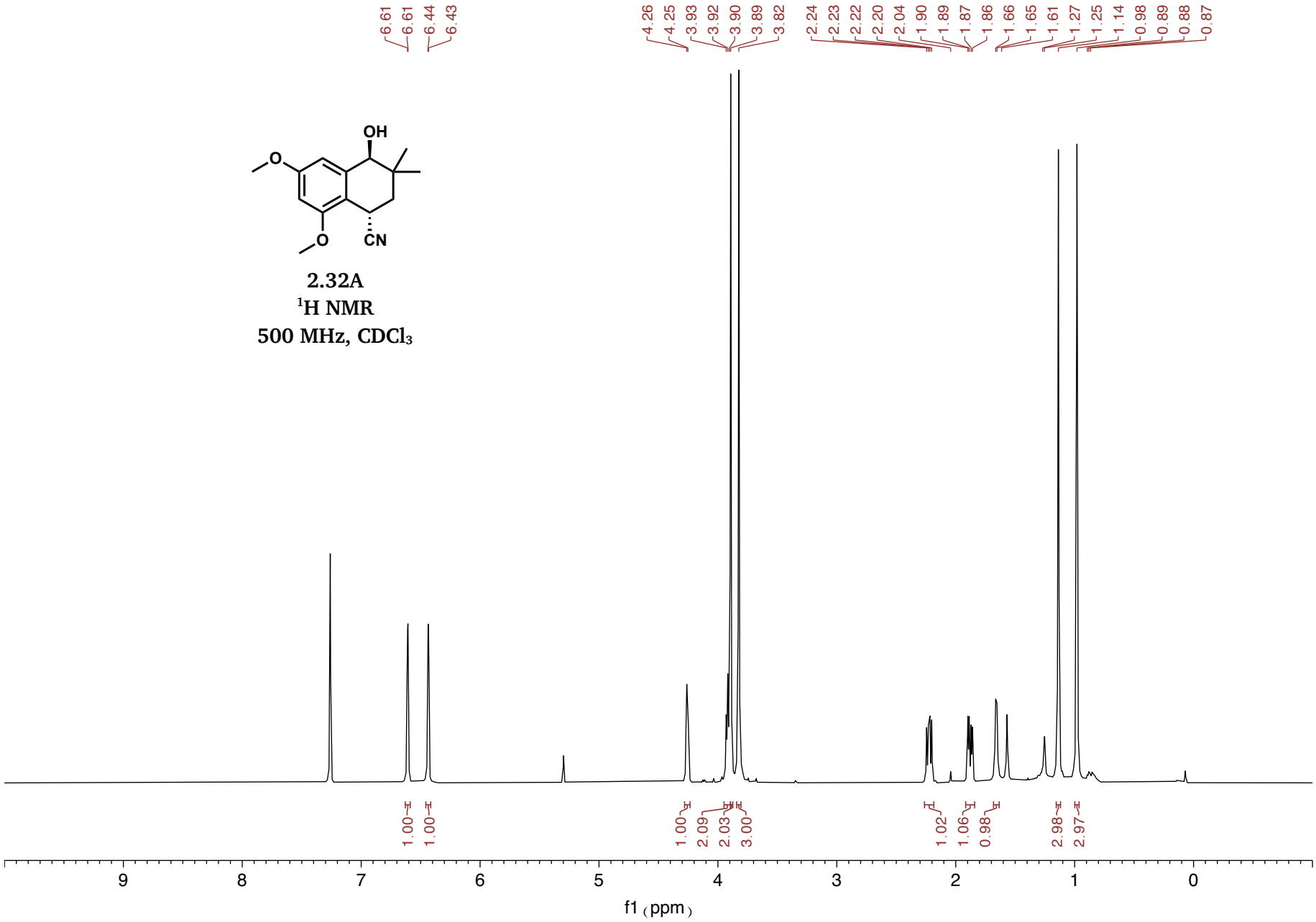
500 MHz, $CDCl_3$



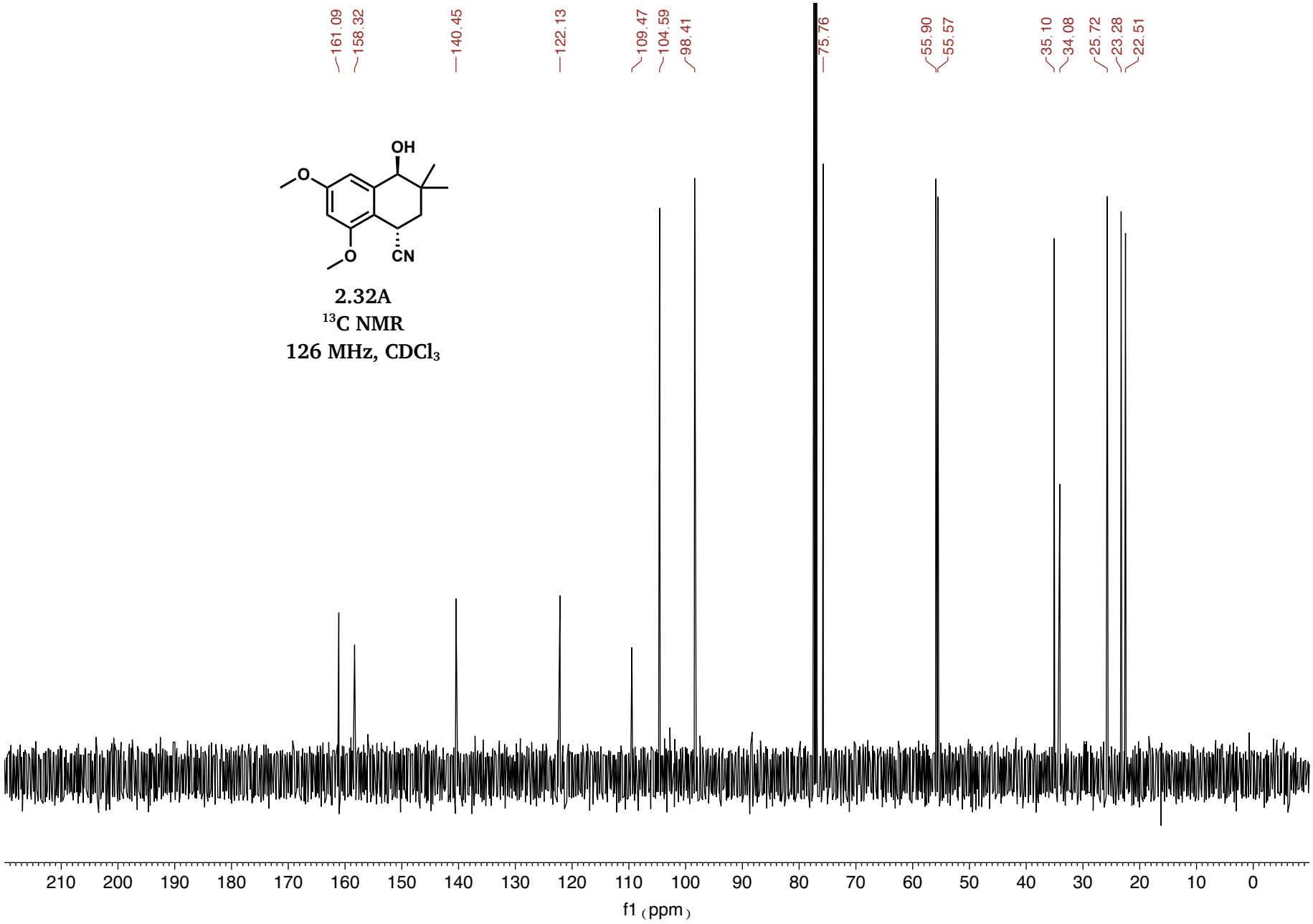
2.31

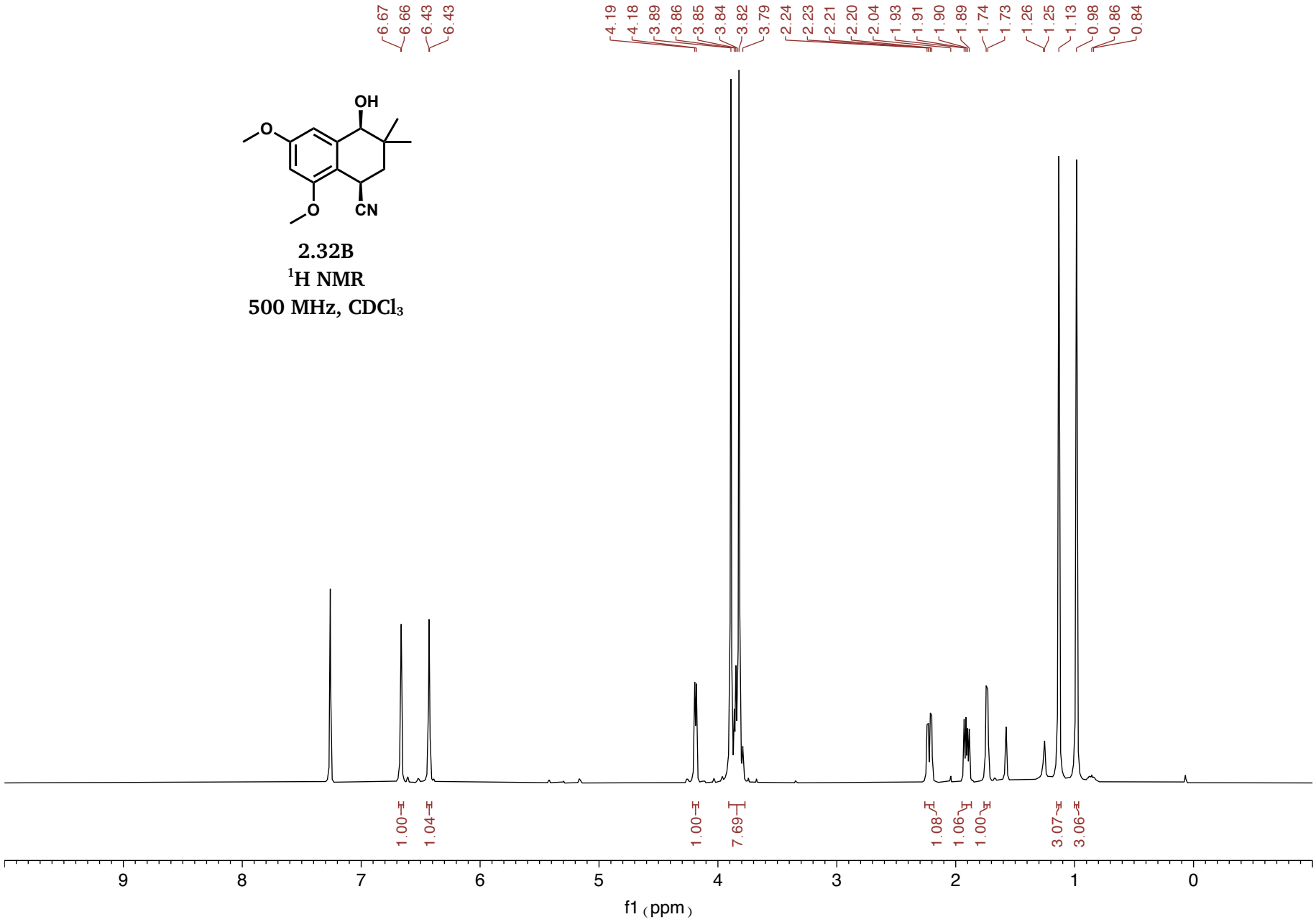
^{13}C NMR

126 MHz, $CDCl_3$

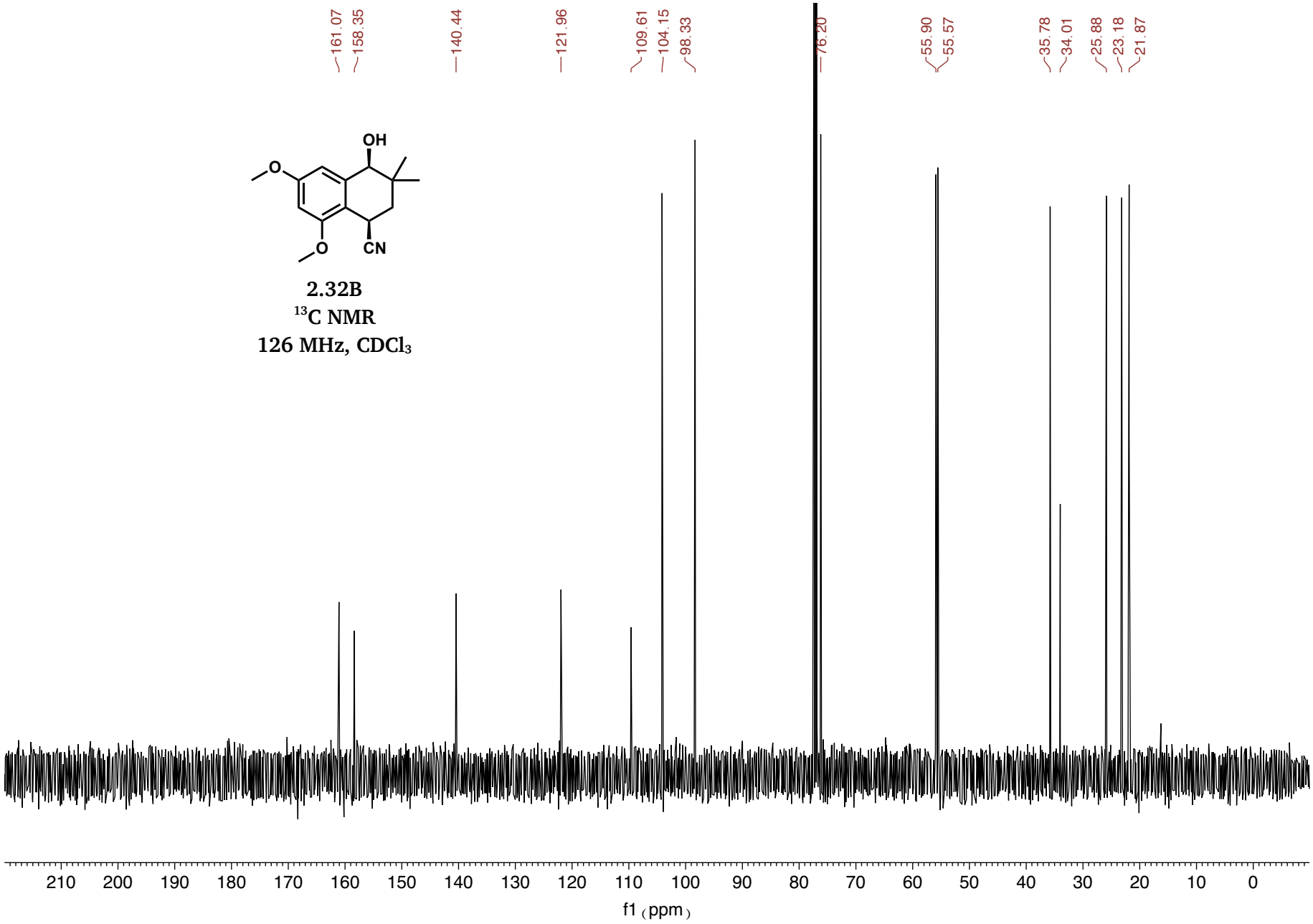


2.32A
^{1}H NMR
500 MHz, $CDCl_3$

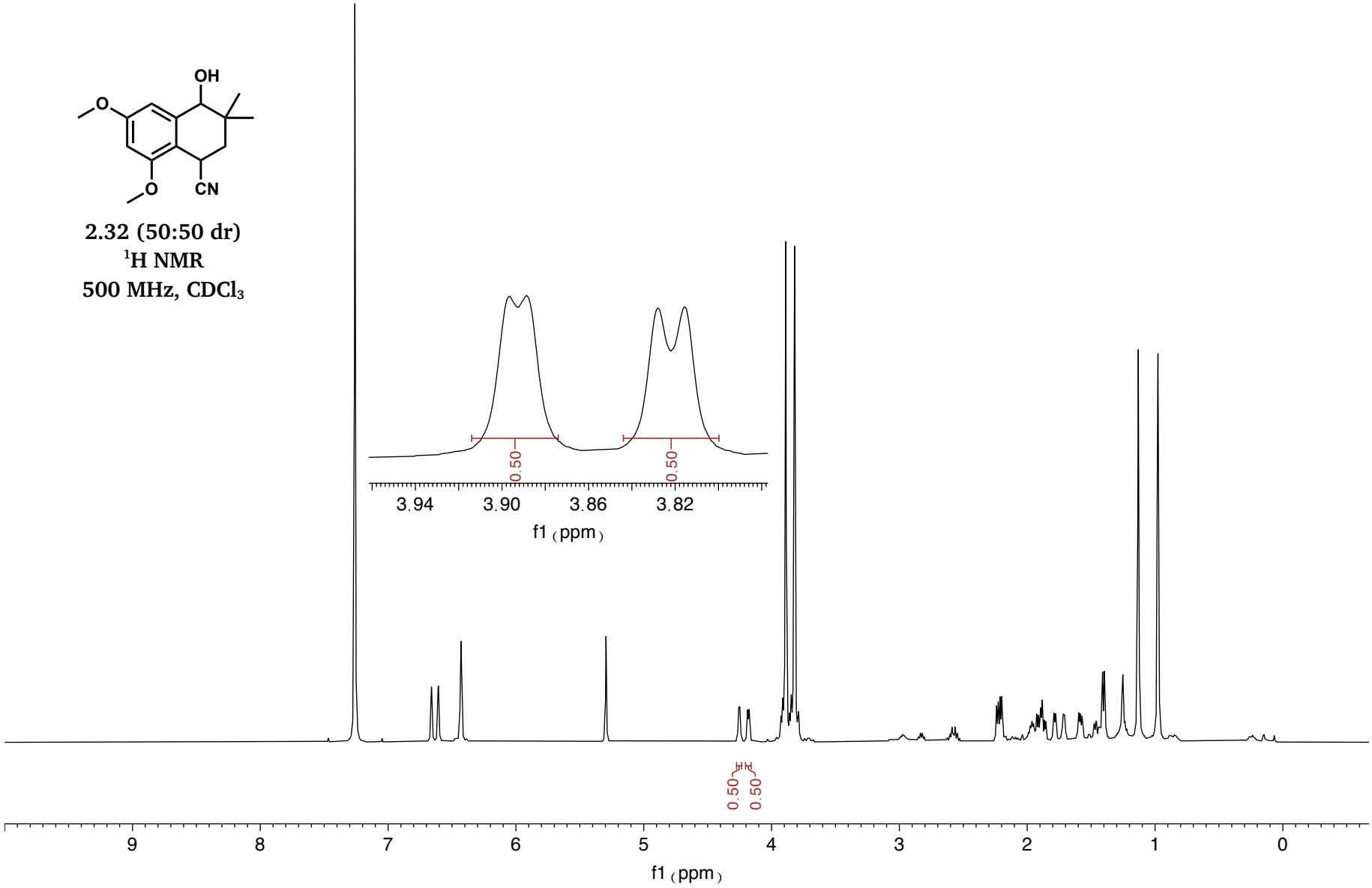

161.09
158.32
140.45
122.13
109.47
104.59
98.41
75.76
55.90
55.57
35.10
34.08
25.72
23.28
22.51
OH
O
O
CN
2.32A
13C NMR
126 MHz, CDCl3
210
200
190
180
170
160
150
140
130
120
110
100
90
80
70
60
50
40
30
20
10
0
f1 (ppm)



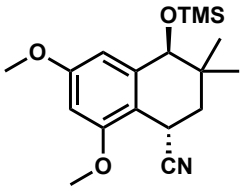
2.32B
^{1}H NMR
500 MHz, $CDCl_3$



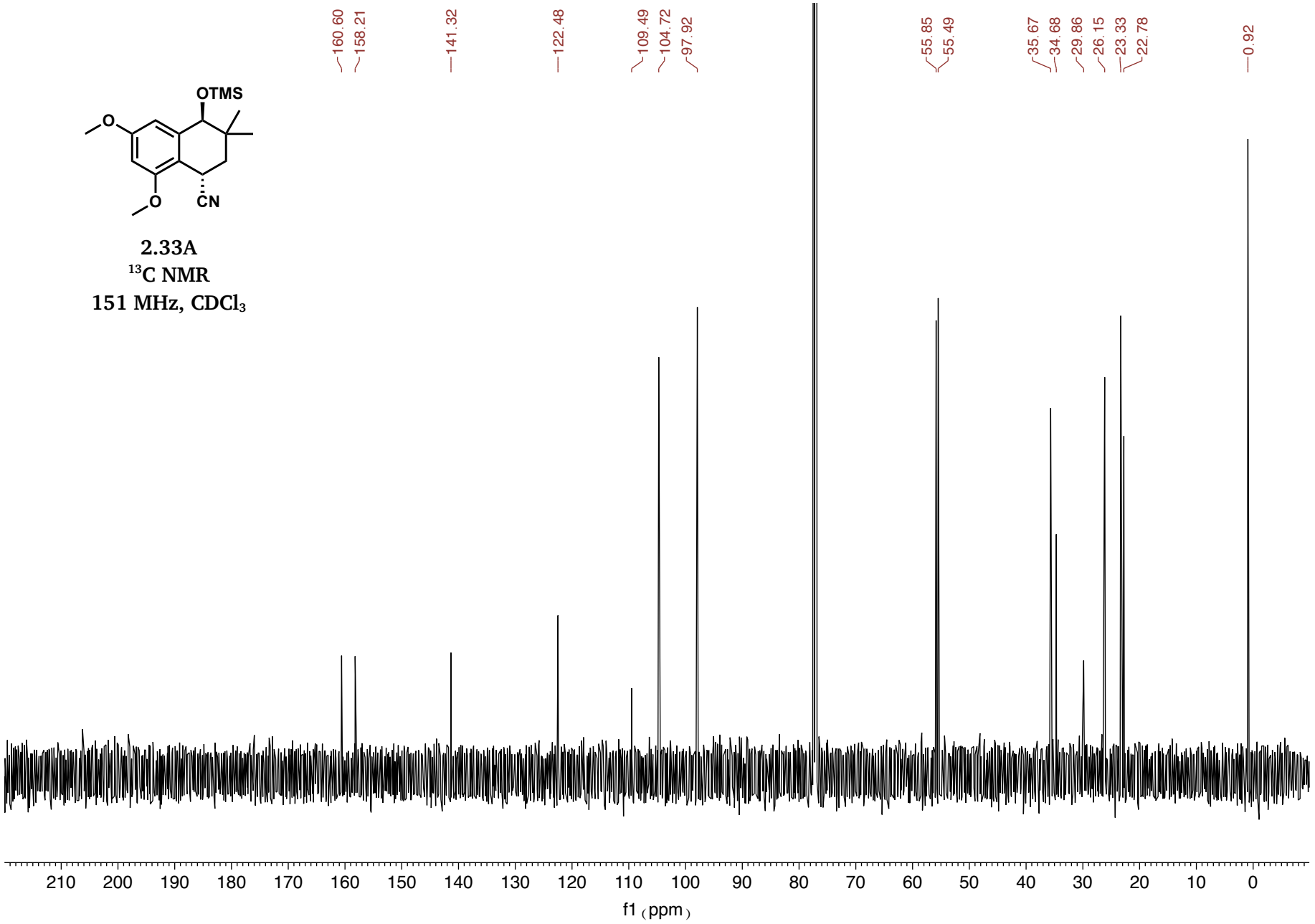
2.32B
^{13}C NMR
126 MHz, $CDCl_3$



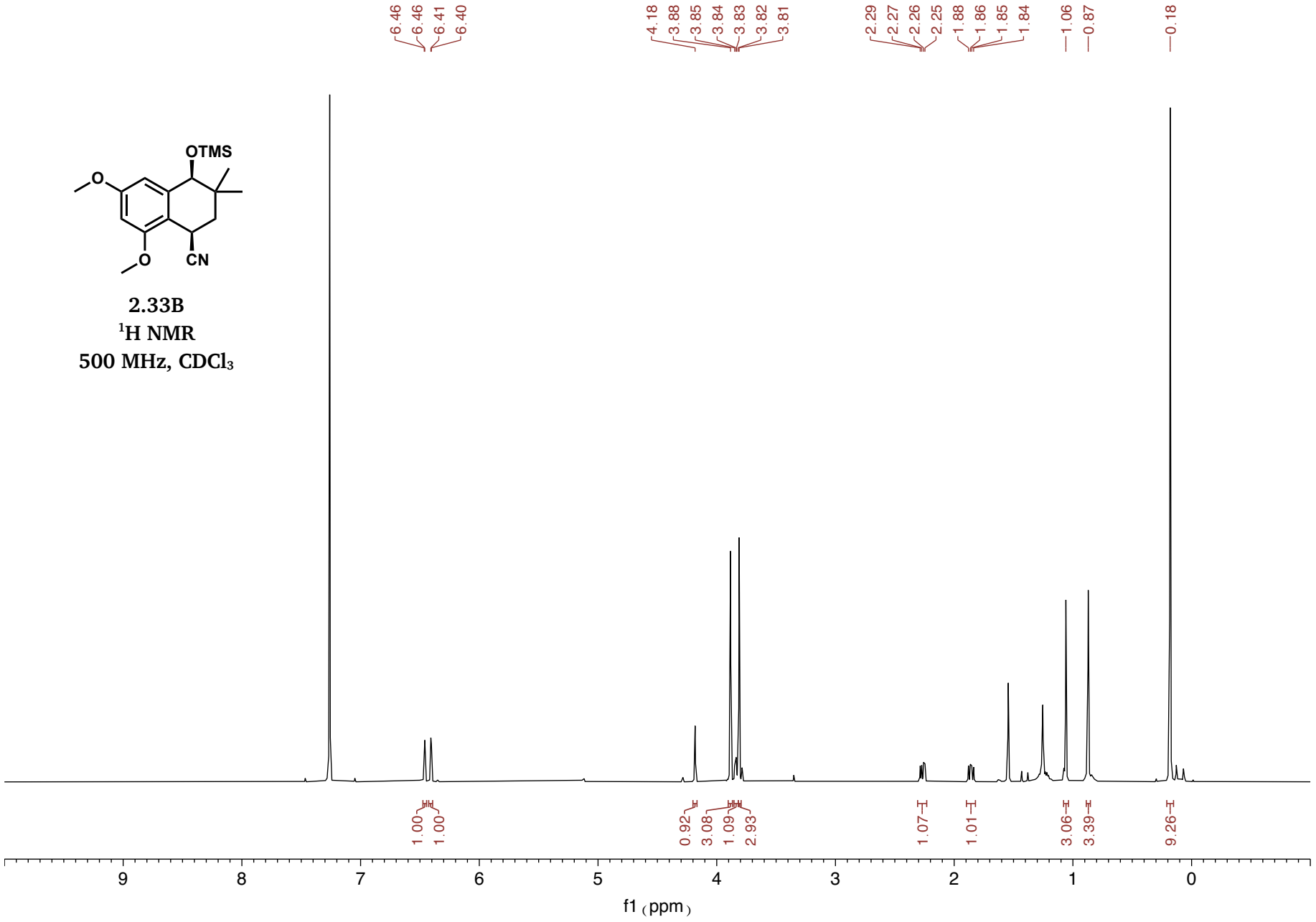
2.32 (50:50 dr)
^{1}H NMR
500 MHz, $CDCl_3$



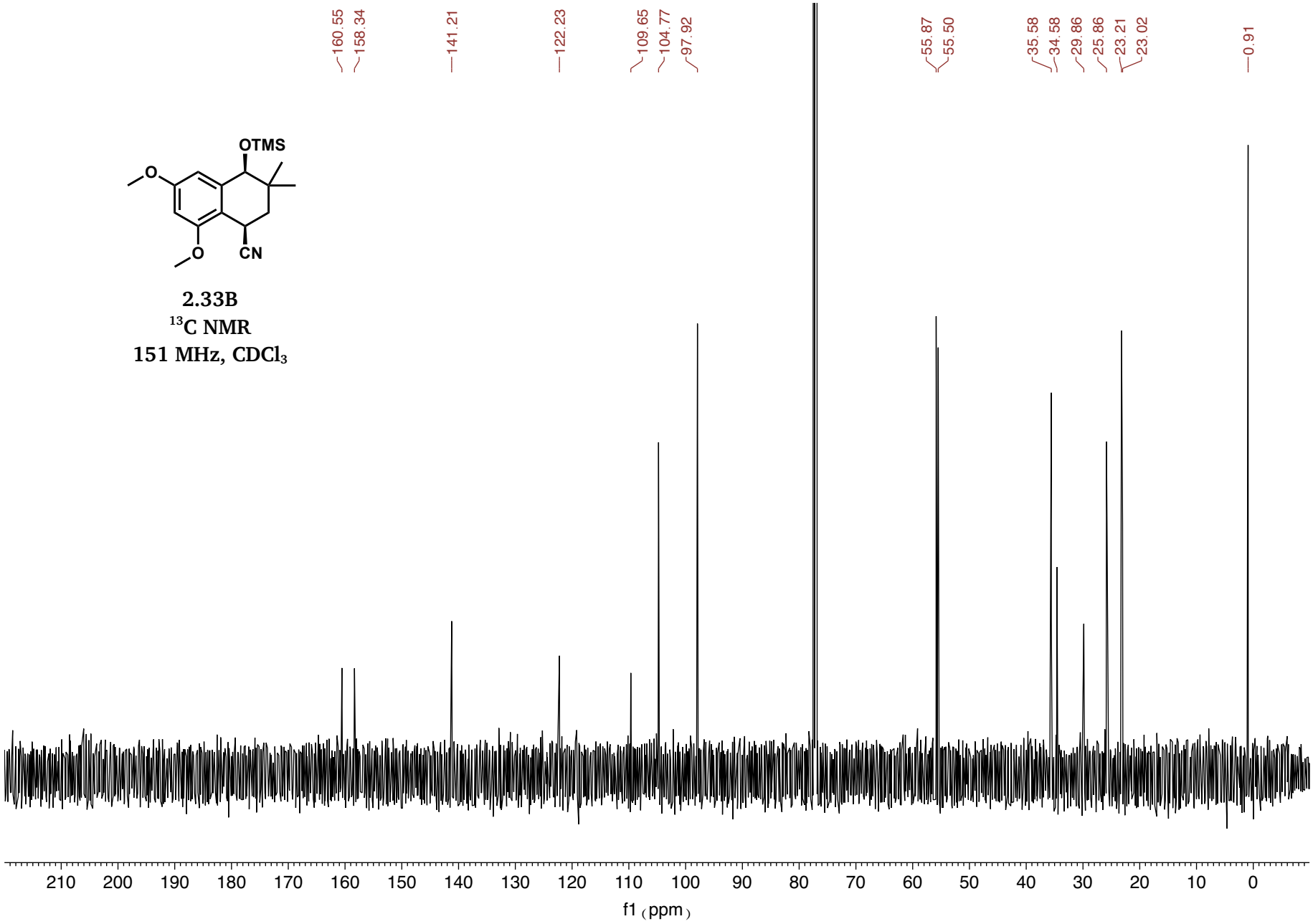
2.33A
^{1}H NMR
500 MHz, $CDCl_3$



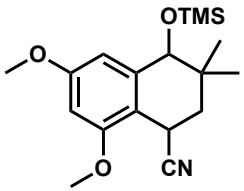
2.33A
^{13}C NMR
151 MHz, $CDCl_3$



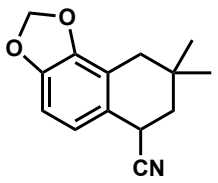
2.33B
^{1}H NMR
500 MHz, $CDCl_3$



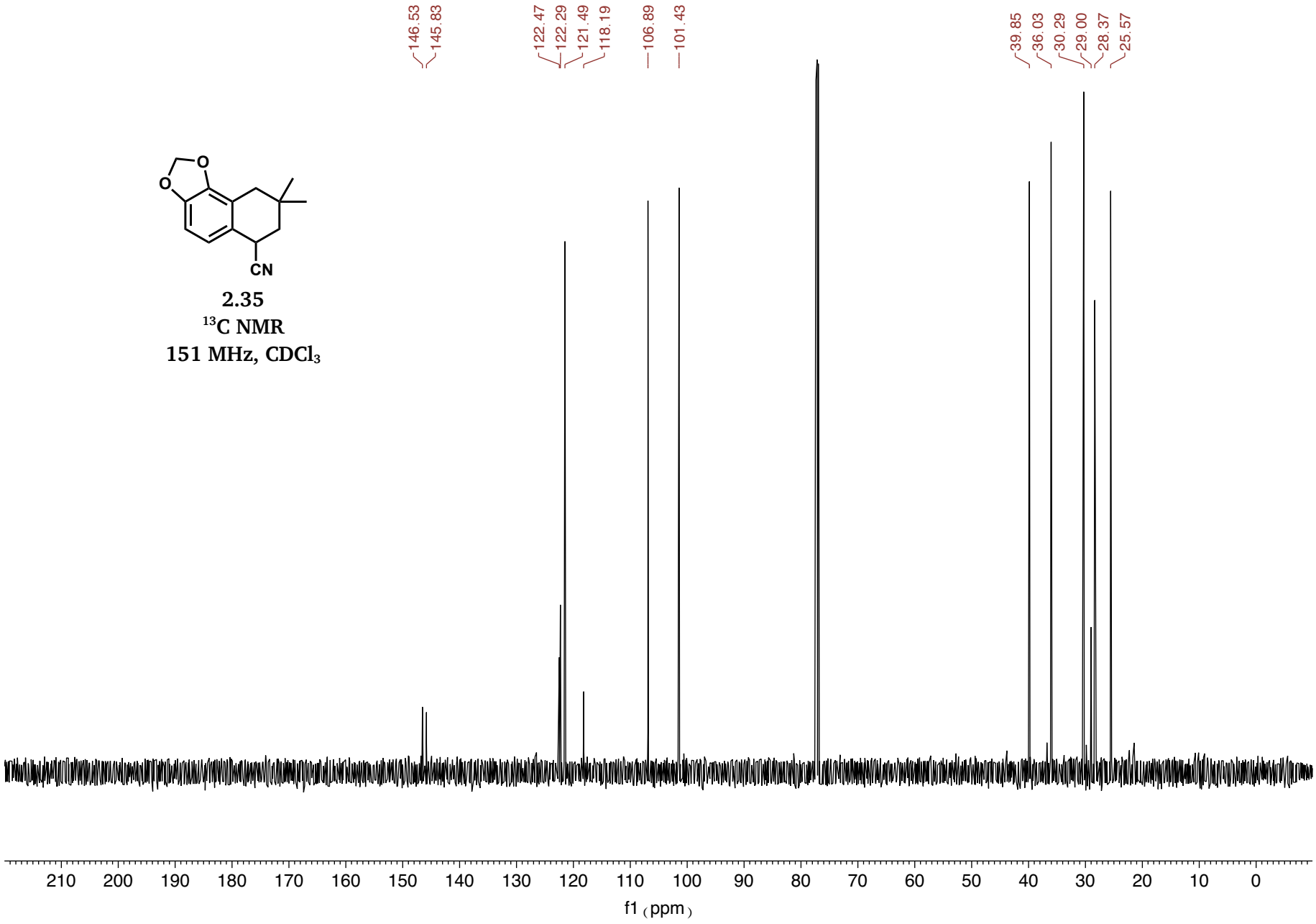
2.33B
^{13}C NMR
151 MHz, $CDCl_3$



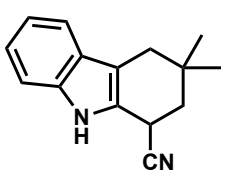
2.33 (50:50 dr)
^{1}H NMR
500 MHz, $CDCl_3$



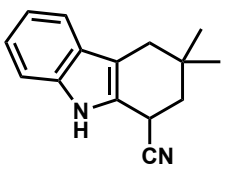
2.35
^{1}H NMR
600 MHz, $CDCl_3$



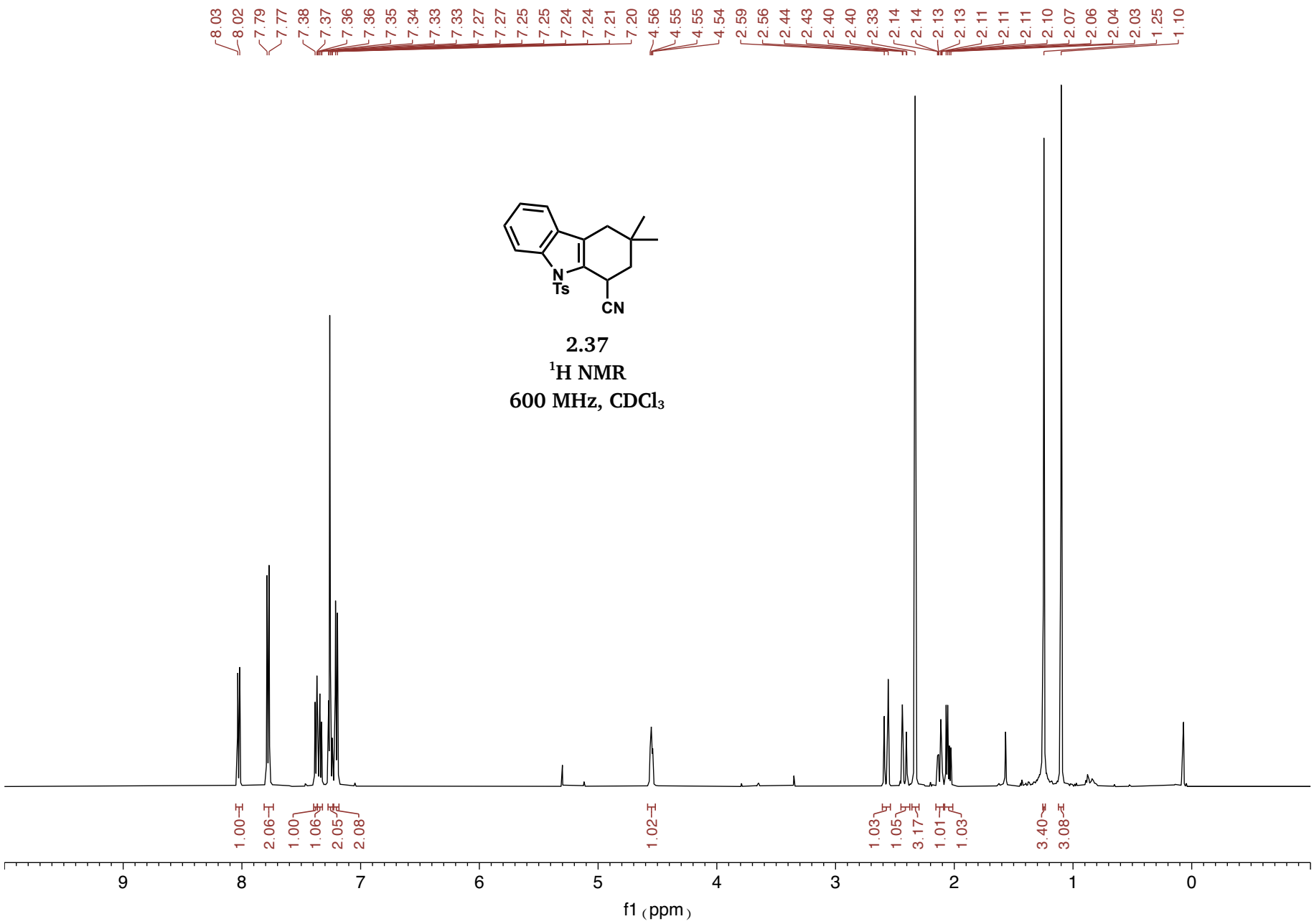
2.35
^{13}C NMR
151 MHz, $CDCl_3$



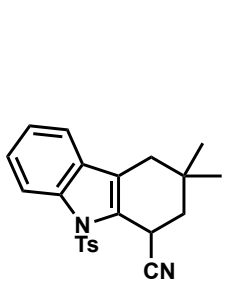
2.36
^{1}H NMR
500 MHz, $CDCl_3$



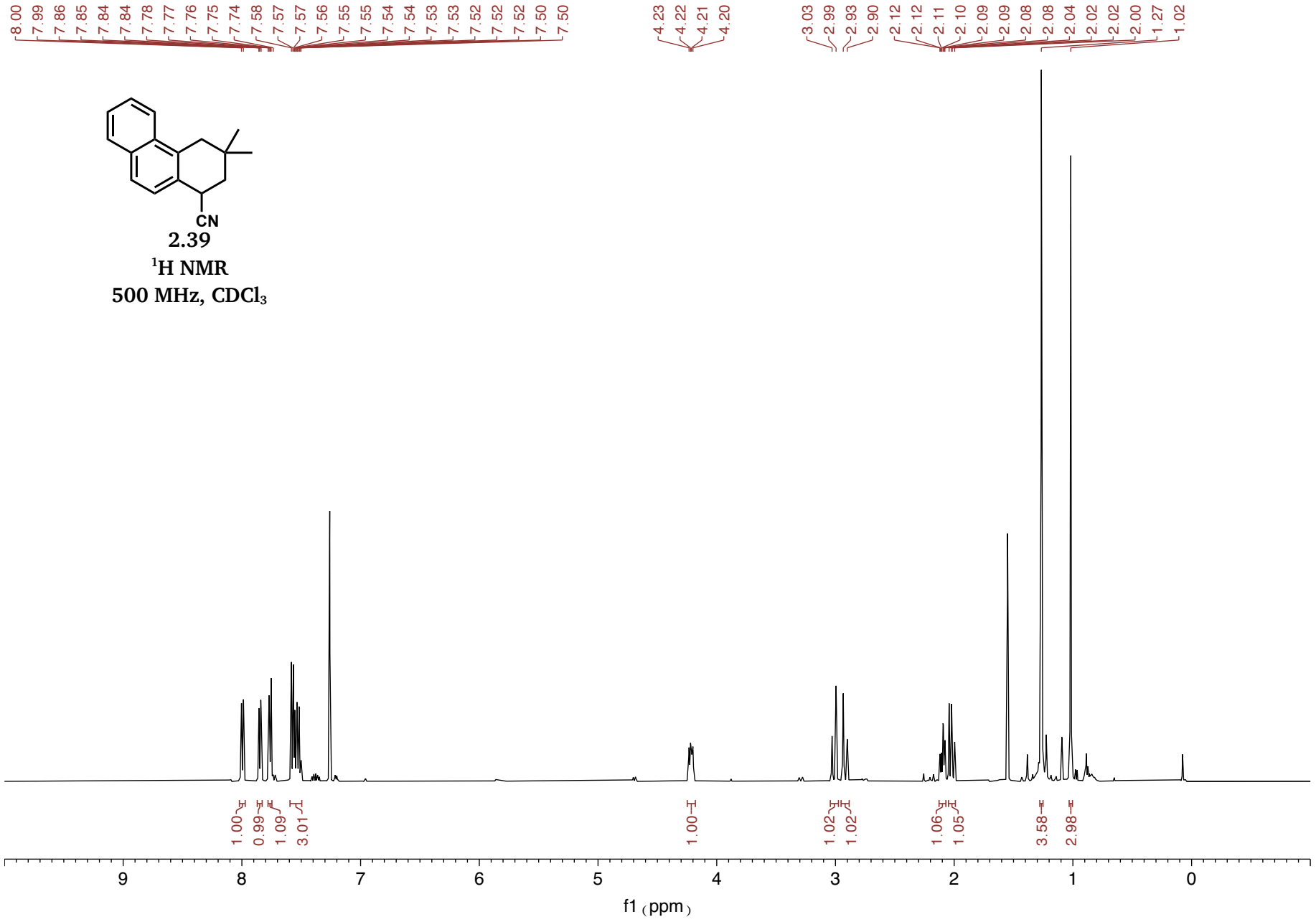
2.36
^{13}C NMR
151 MHz, $CDCl_3$



2.37
^{1}H NMR
600 MHz, $CDCl_3$



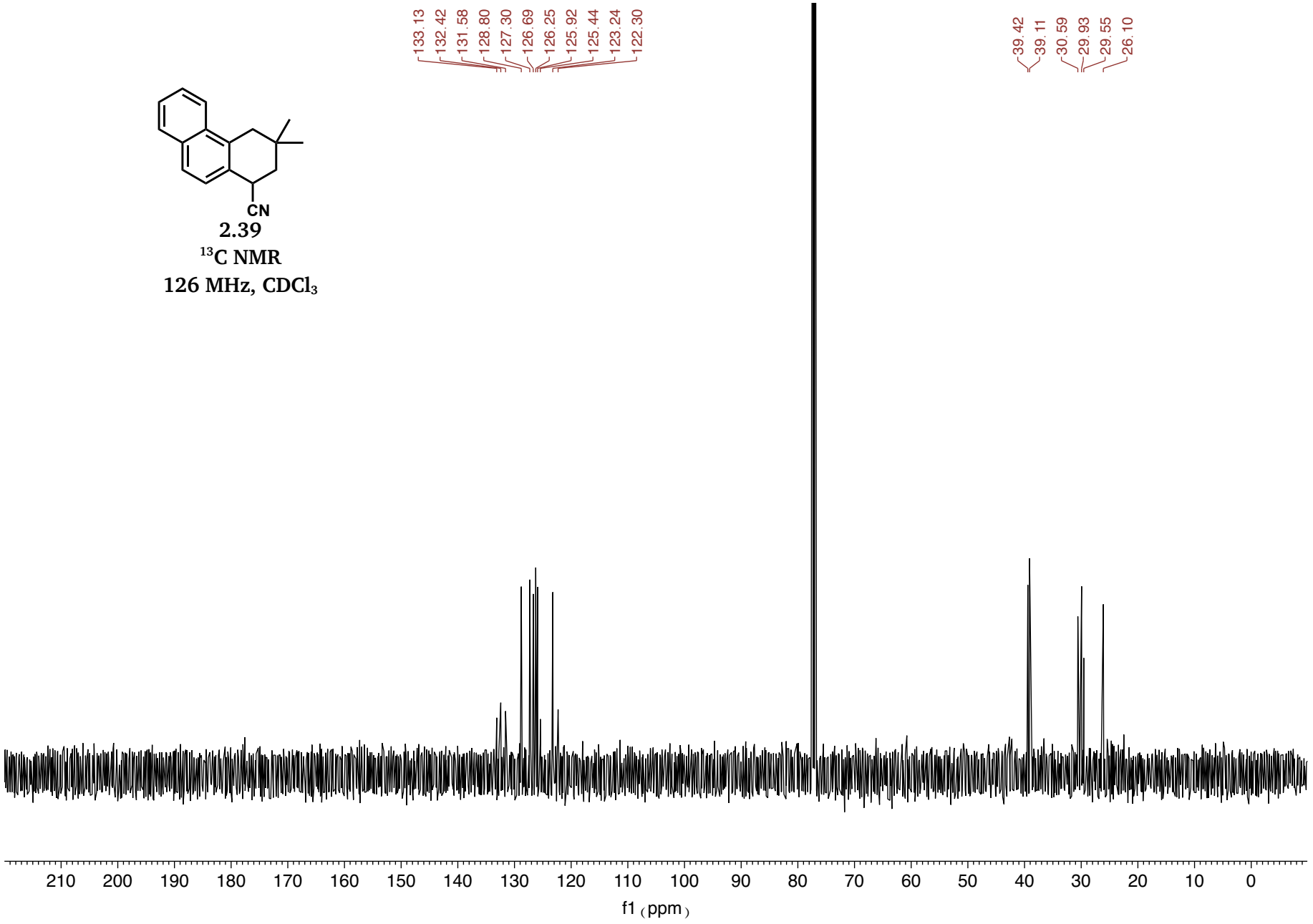
2.37
^{13}C NMR
126 MHz, $CDCl_3$

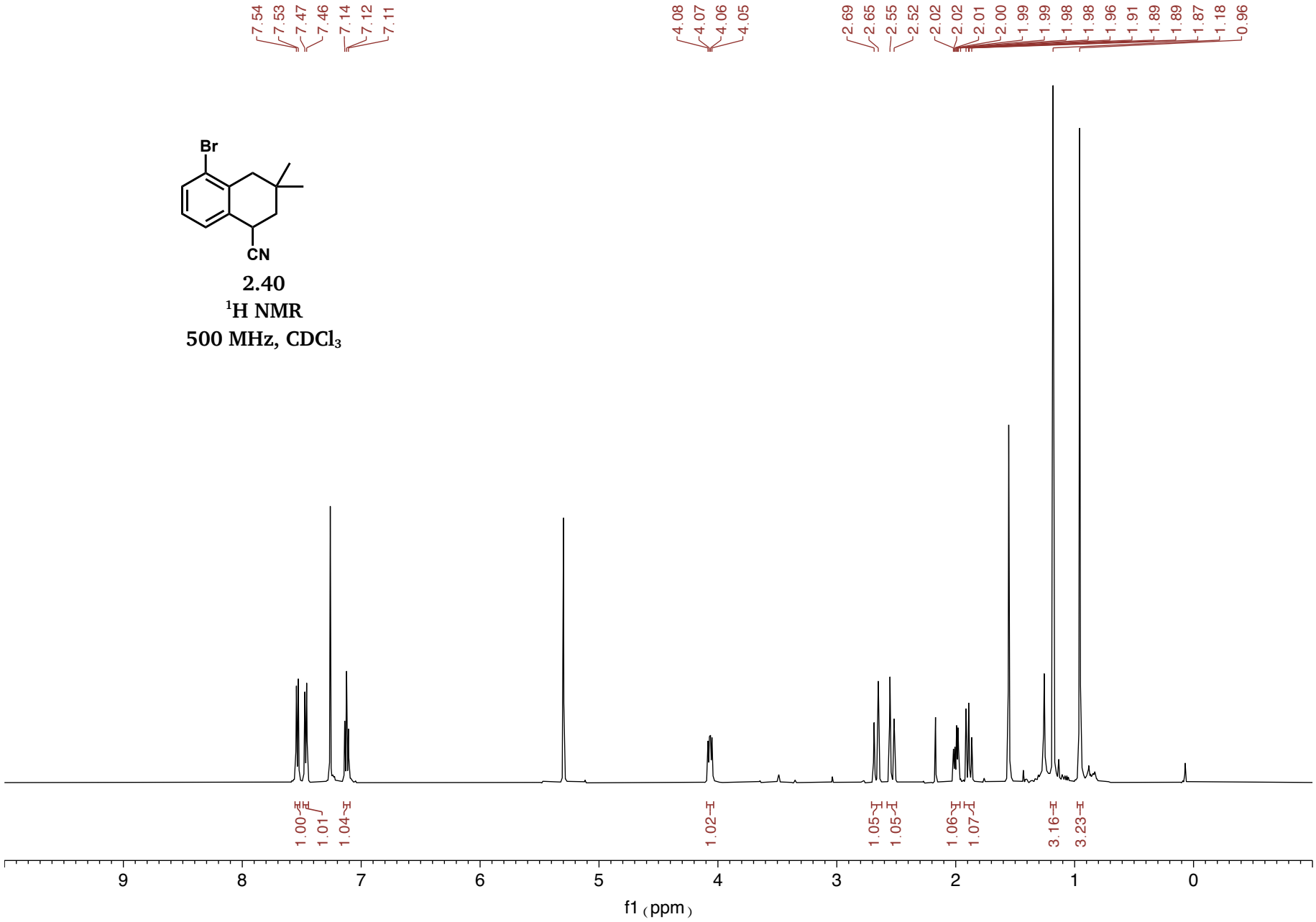


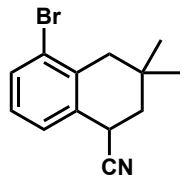
2.39

^{1}H NMR

500 MHz, $CDCl_3$


133.13
132.42
131.58
128.80
127.30
126.69
126.25
125.92
125.44
123.24
122.30
39.42
39.11
30.59
29.93
29.55
26.10
CN
2.39
^{13}C NMR
126 MHz, $CDCl_3$
210 200 190 180 170 160 150 140 130 120 110 100 90 80 70 60 50 40 30 20 10 0
f1 (ppm)

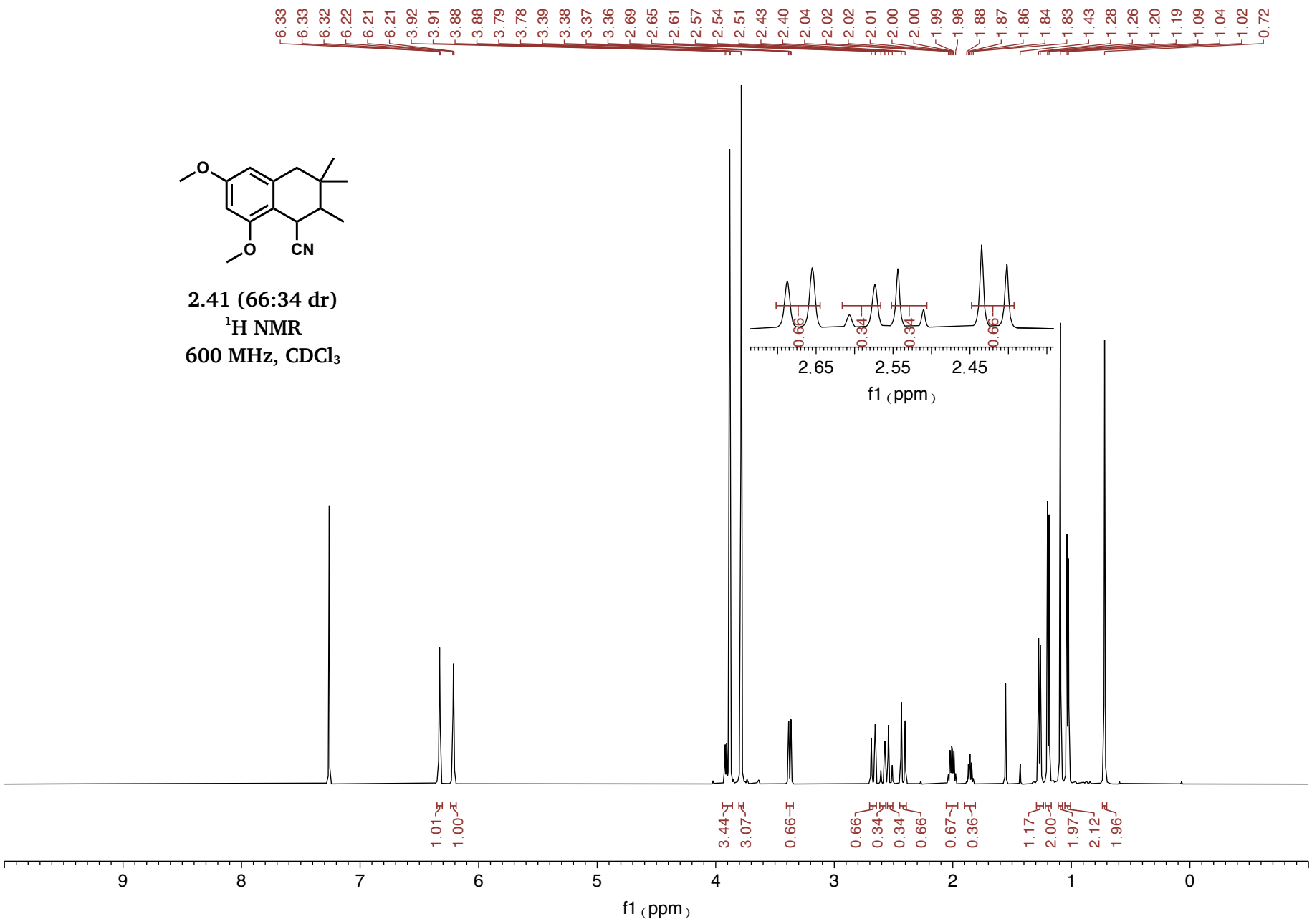

7.54
7.53
7.47
7.46
7.14
7.12
7.11
4.08
4.07
4.06
4.05
2.69
2.65
2.55
2.52
2.02
2.02
2.01
2.00
1.99
1.99
1.98
1.98
1.96
1.91
1.89
1.89
1.87
1.18
0.96
Br
CN
2.40
1H NMR
500 MHz, CDCl3
1.00
1.01
1.04
1.02
1.05
1.05
1.06
1.07
3.16
3.23
9
8
7
6
5
4
3
2
1
0
f1 (ppm)

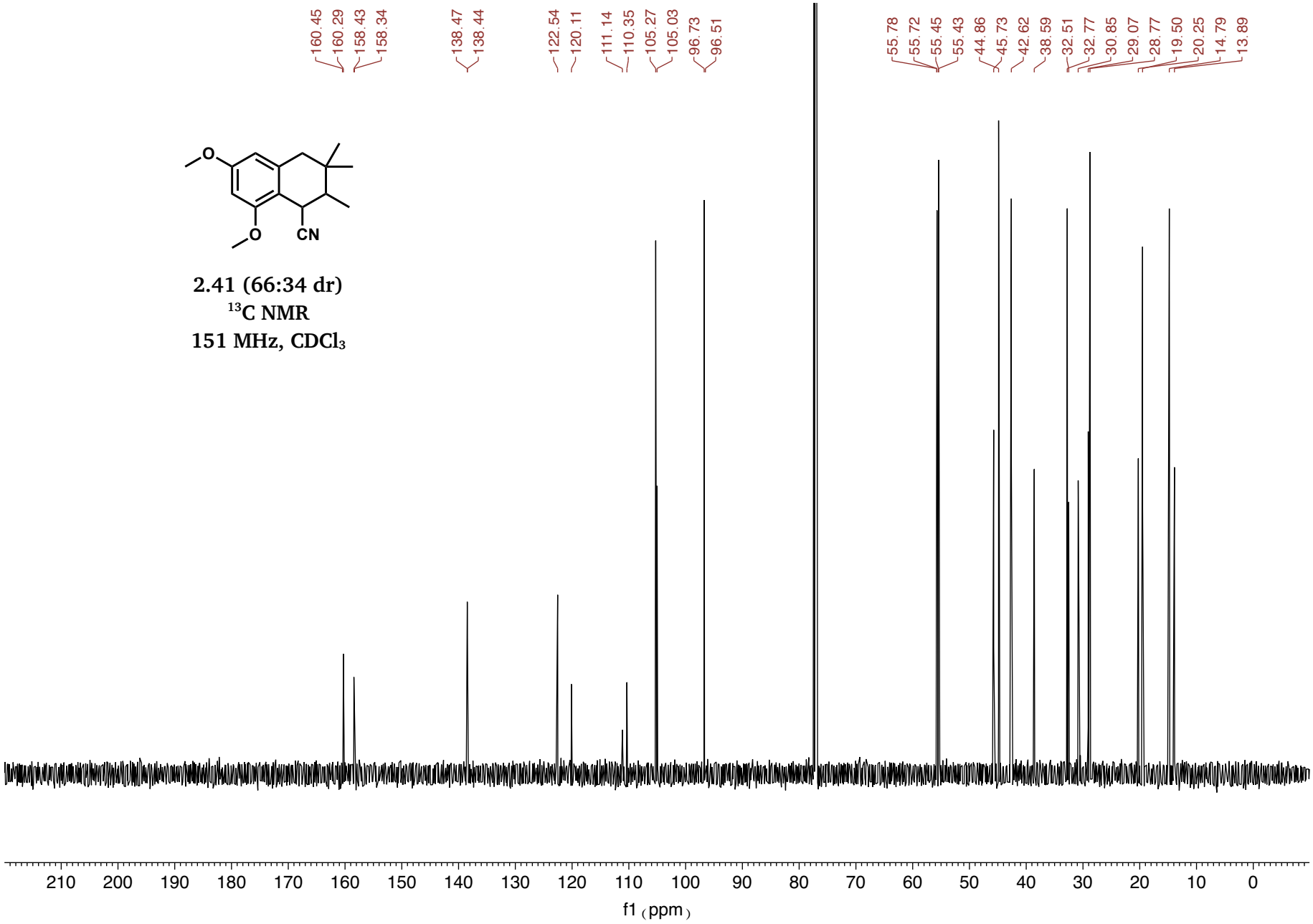


2.40

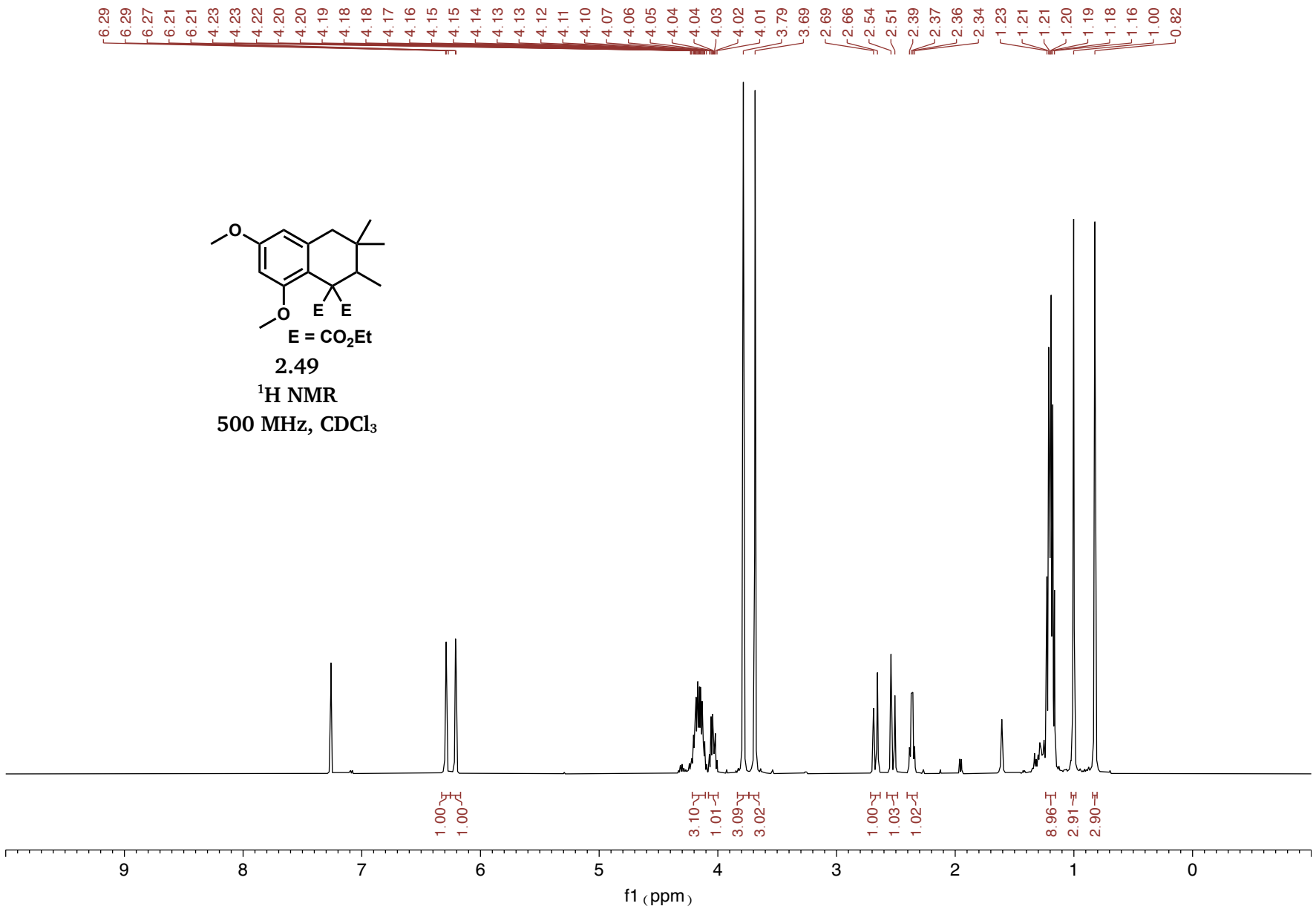
^{13}C NMR

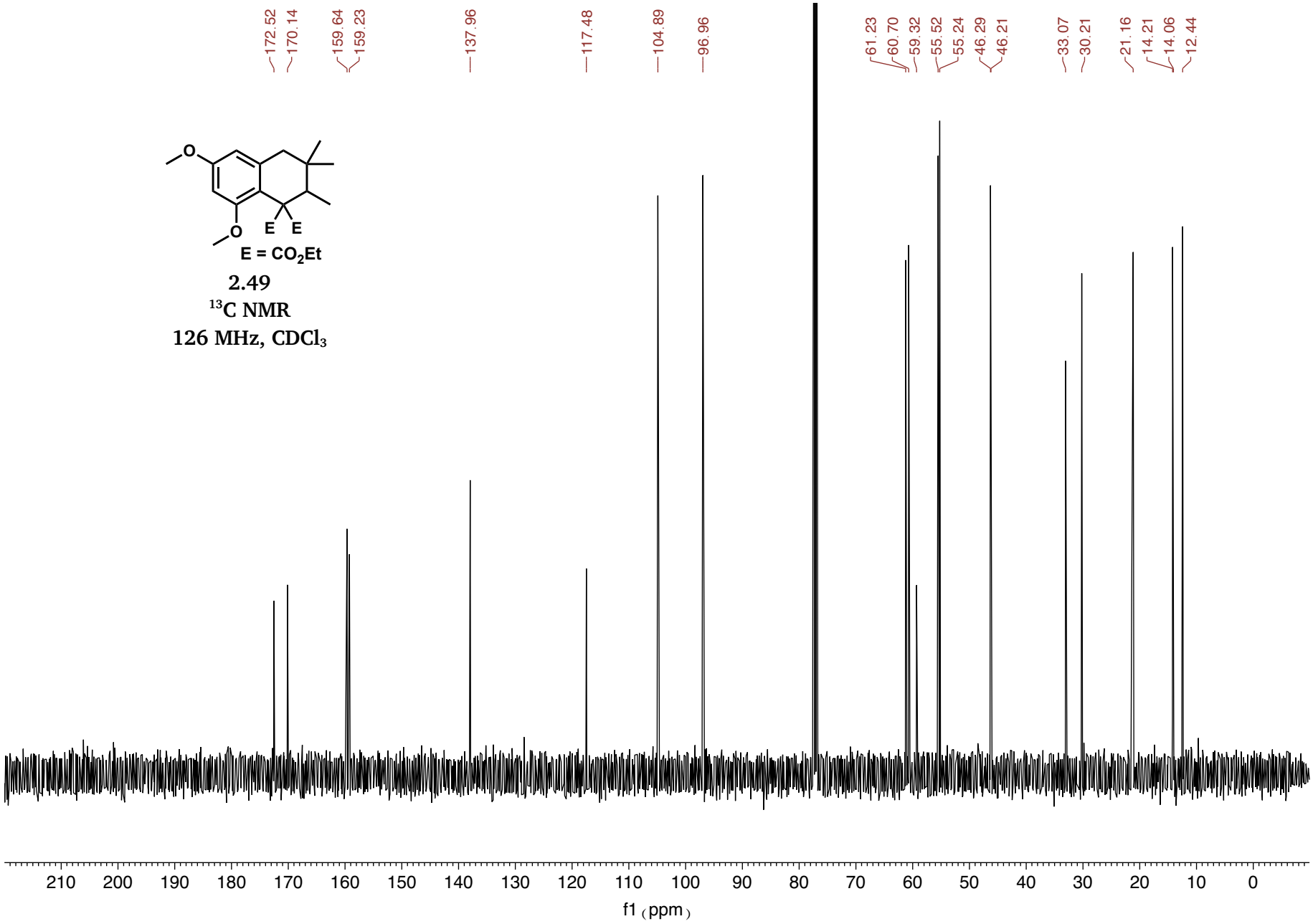
126 MHz, $CDCl_3$

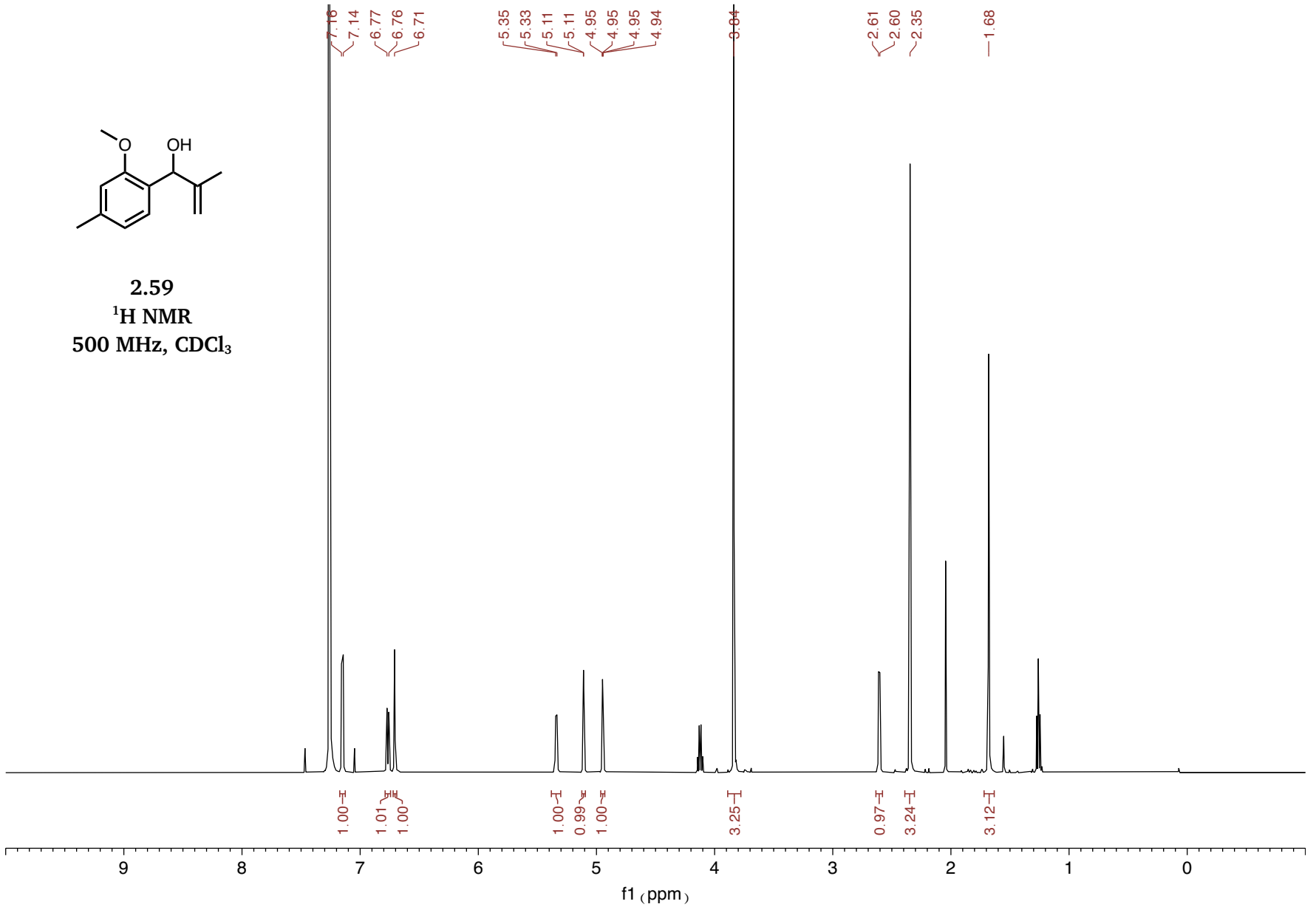

6.33 6.33 6.32 6.22 6.21 6.21 3.92 3.91 3.88 3.88 3.79 3.78 3.39 3.38 3.37 3.36 2.69 2.65 2.61 2.57 2.54 2.51 2.43 2.40 2.04 2.02 2.02 2.01 2.00 2.00 1.99 1.98 1.88 1.87 1.86 1.84 1.83 1.43 1.28 1.26 1.20 1.19 1.09 1.04 1.02 0.72
O
O
CN
2.41 (66:34 dr)
1H NMR
600 MHz, CDCl3
0.66 0.34 0.34 0.66
2.65 2.55 2.45
f1 (ppm)
1.01 1.00 3.44 3.07 0.66 0.66 0.34 0.34 0.66 0.67 0.36 1.17 2.00 1.97 2.12 1.96
9 8 7 6 5 4 3 2 1 0
f1 (ppm)



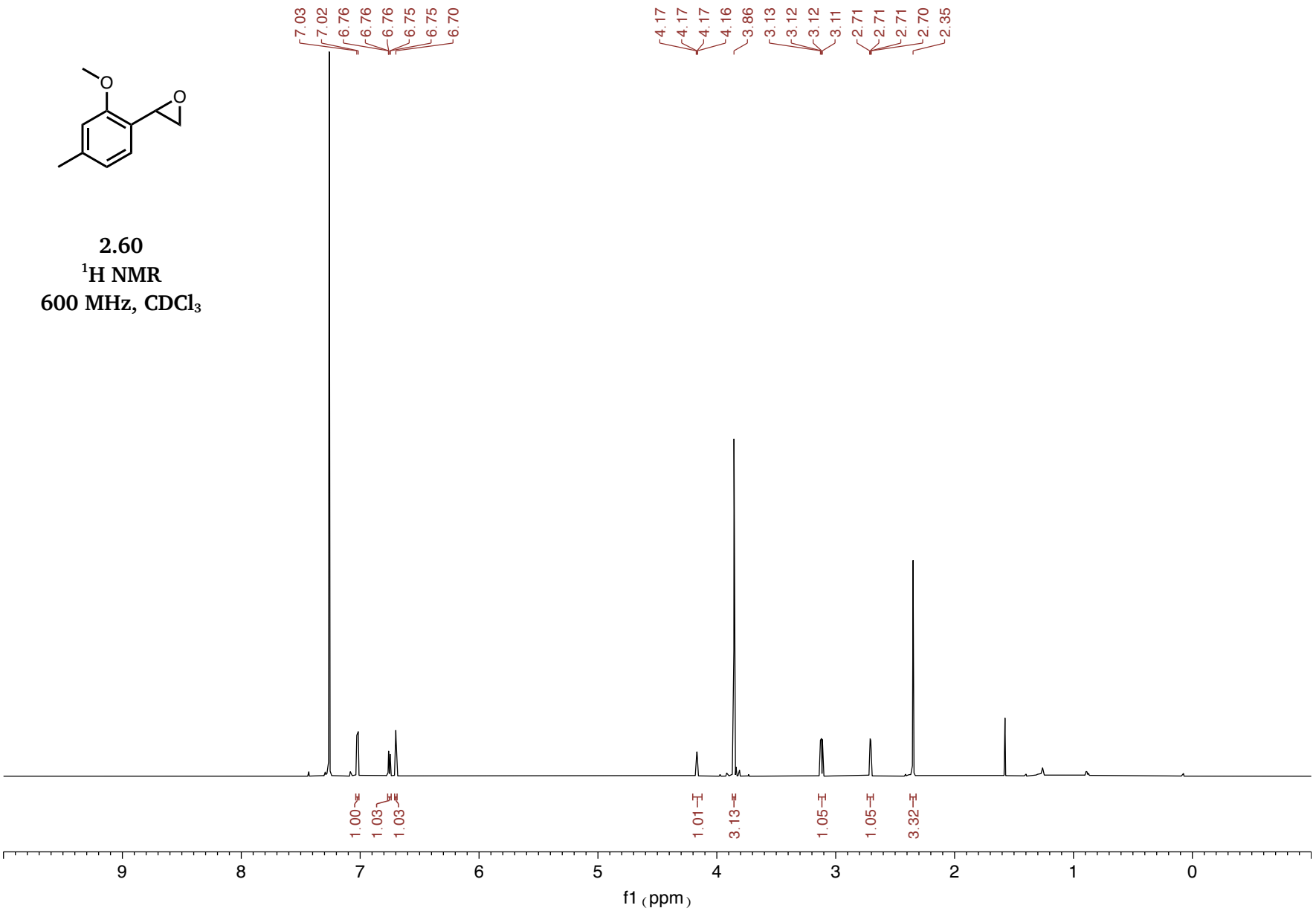
2.41 (66:34 dr)
^{13}C NMR
151 MHz, $CDCl_3$


6.29 6.29 6.27 6.21 6.21 6.23 4.23 4.22 4.20 4.20 4.19 4.18 4.18 4.17 4.16 4.15 4.15 4.14 4.13 4.13 4.12 4.11 4.10 4.07 4.06 4.05 4.04 4.04 4.03 4.02 4.01 3.79 3.69 2.69 2.66 2.54 2.51 2.39 2.37 2.36 2.34 1.23 1.21 1.21 1.20 1.19 1.18 1.16 1.00 0.82
O
O
E E
E = CO2Et
2.49
1H NMR
500 MHz, CDCl3
1.00 1.00 3.10 1.01 3.09 3.02 1.00 1.03 1.02 8.96 2.91 2.90
9 8 7 6 5 4 3 2 1 0
f1 (ppm)

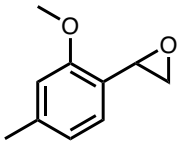

172.52
170.14
159.64
159.23
137.96
117.48
104.89
96.96
61.23
60.70
59.32
55.52
55.24
46.29
46.21
33.07
30.21
21.16
14.21
14.06
12.44
O
O
E E
E = CO2Et
2.49
13C NMR
126 MHz, CDCl3
210 200 190 180 170 160 150 140 130 120 110 100 90 80 70 60 50 40 30 20 10 0
f1 (ppm)



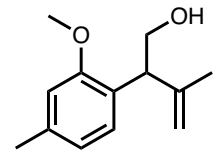
2.59
^{1}H NMR
500 MHz, $CDCl_3$



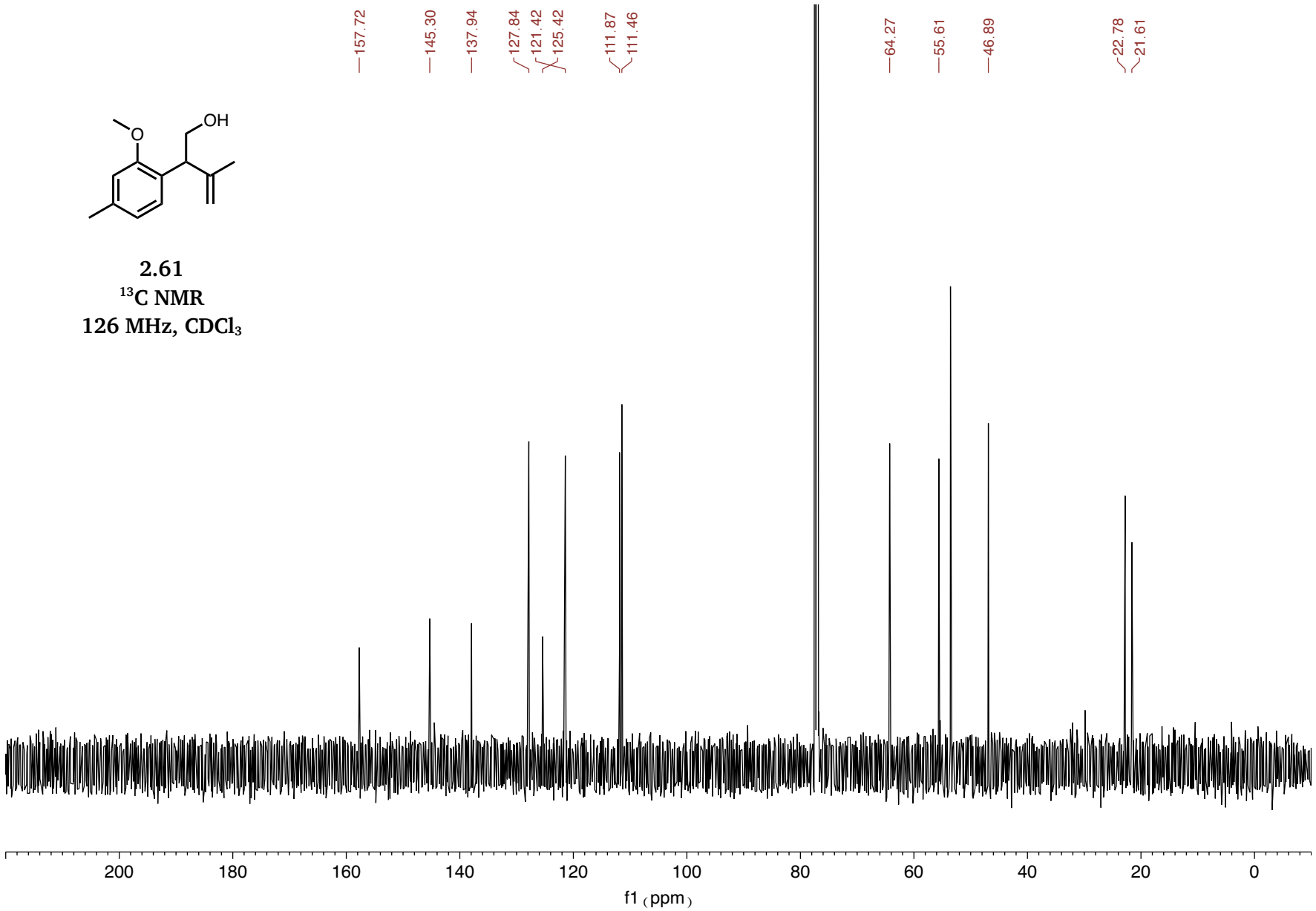
2.60
^{1}H NMR
600 MHz, $CDCl_3$



2.60
^{13}C NMR
151 MHz, $CDCl_3$



2.61
^{1}H NMR
500 MHz, $CDCl_3$



2.61
^{13}C NMR
126 MHz, $CDCl_3$

Appendix B

B2: X-Ray Crystallographic Data

X-ray Data Collection, Structure Solution and Refinement for cdv98

A colorless crystal of approximate dimensions 0.149 x 0.162 x 0.180 mm was mounted in a cryoloop and transferred to a Bruker X8 Prospector diffractometer system. The APEX3[1] program package was used to determine the unit-cell parameters and for data collection (10-15 sec/frame scan time). The raw frame data was processed using SAINT[2] and SADABS[3] to yield the reflection data file. Subsequent calculations were carried out using the SHELXTL[4] program package. The diffraction symmetry was 2/*m* and the systematic absences were consistent with the monoclinic space group $P2_1/n$ that was later determined to be correct.

The structure was solved by direct methods and refined on F^2 by full-matrix least-squares techniques. The analytical scattering factors[5] for neutral atoms were used throughout the analysis. Hydrogen atoms were included using a riding model.

Least-squares analysis yielded wR2 = 0.0863 and Goof = 1.061 for 180 variables refined against 2475 data (0.83 Å), R1 = 0.0340 for those 2307 data with $I > 2.0\sigma(I)$.

References.

1. APEX3 Version 2018.1-0, Bruker AXS, Inc.; Madison, WI 2018.

2. SAINT Version 8.38a, Bruker AXS, Inc.; Madison, WI 2013.

3. Sheldrick, G. M. SADABS, Version 2014/5, Bruker AXS, Inc.; Madison, WI 2014.

4. Sheldrick, G. M. SHELXTL, Version 2014/7, Bruker AXS, Inc.; Madison, WI 2014.

5. International Tables for Crystallography 1992, Vol. C., Dordrecht: Kluwer Academic Publishers.

Definitions:

$wR2 = [\Sigma[w(F_o^2-F_c^2)^2] / \Sigma[w(F_o^2)^2]]^{1/2}$

$R1 = \Sigma||F_o|-|F_c|| / \Sigma|F_o|$

Goof = $S = [\Sigma[w(F_o^2-F_c^2)^2] / (n-p)]^{1/2}$ where n is the number of reflections and p is the total number of parameters refined.

The thermal ellipsoid plot is shown at the 50% probability level.

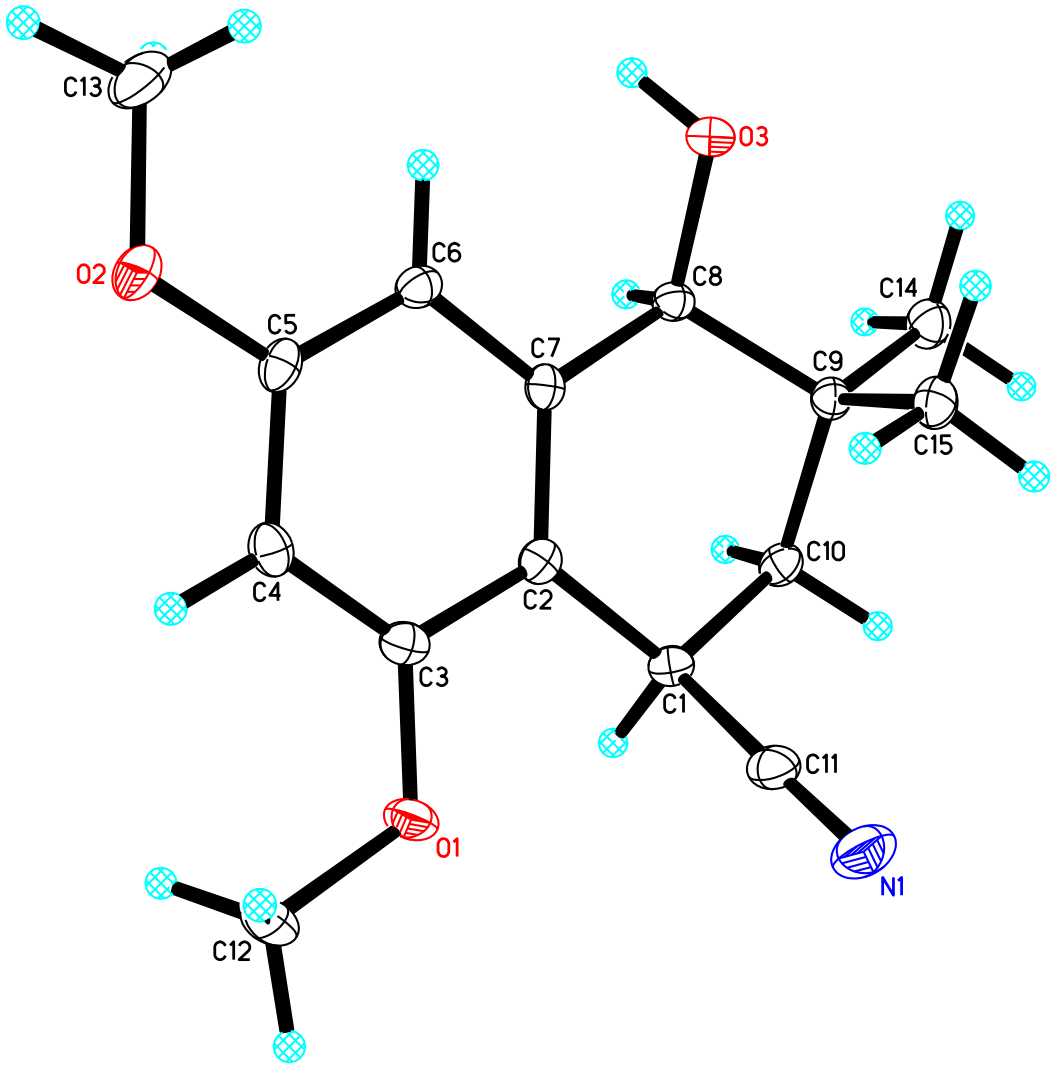

C13
O3
O2
C6
C8
C14
C5
C7
C9
C15
C10
C4
C2
C3
C1
C11
O1
N1
C12

Table 1. Crystal data and structure refinement for cdv98.

Identification code	cdv98 (Lucas Johnson)	
Empirical formula	C15 H19 N O3	
Formula weight	261.31	
Temperature	93(2) K	
Wavelength	1.54178 Å	
Crystal system	Monoclinic	
Space group	$P2_1/n$	
Unit cell dimensions	a = 8.3399(3) Å	α = 90°.
	b = 12.0490(5) Å	β = 101.8534(17)°.
	c = 13.8599(6) Å	γ = 90°.
Volume	1363.05(10) $Å^3$	
Z	4	
Density (calculated)	1.273 Mg/m^3	
Absorption coefficient	0.718 mm^{-1}	
F(000)	560	
Crystal color	colorless	
Crystal size	0.180 x 0.162 x 0.149 mm^3	
Theta range for data collection	4.909 to 68.667°	
Index ranges	$-10 \le h \le 9$, $-14 \le k \le 14$, $-16 \le l \le 16$	
Reflections collected	21040	
Independent reflections	2475 [R(int) = 0.0316]	
Completeness to theta = 67.679°	98.9 %	
Absorption correction	Semi-empirical from equivalents	

Max. and min. transmission	0.8643 and 0.8072
Refinement method	Full-matrix least-squares on F^2
Data / restraints / parameters	2475 / 0 / 180
Goodness-of-fit on F^2	1.061
Final R indices [I>2sigma(I) = 2307 data]	R1 = 0.0340, wR2 = 0.0847
R indices (all data, 0.83 Å)	R1 = 0.0360, wR2 = 0.0863
Largest diff. peak and hole	0.227 and -0.226 e.$Å^{-3}$

Table 2. Atomic coordinates (x 10^4) and equivalent isotropic displacement parameters ($Å^2$ x 10^3) for cdv98. U(eq) is defined as one third of the trace of the orthogonalized U^{ij} tensor.

	x	y	z	U(eq)
N(1)	10896(1)	4277(1)	6649(1)	24(1)
O(1)	8199(1)	3132(1)	4614(1)	18(1)
O(2)	3659(1)	1154(1)	5363(1)	18(1)
O(3)	4315(1)	4520(1)	7605(1)	16(1)
C(1)	7910(1)	4877(1)	5801(1)	13(1)
C(2)	6710(1)	3912(1)	5698(1)	12(1)
C(3)	6915(1)	3014(1)	5083(1)	13(1)
C(4)	5885(1)	2102(1)	4979(1)	14(1)
C(5)	4623(1)	2082(1)	5504(1)	13(1)
C(6)	4393(1)	2955(1)	6112(1)	13(1)
C(7)	5434(1)	3878(1)	6204(1)	11(1)
C(8)	5075(1)	4861(1)	6823(1)	12(1)
C(9)	6616(1)	5538(1)	7247(1)	12(1)
C(10)	7381(1)	5865(1)	6372(1)	14(1)
C(11)	9584(1)	4512(1)	6274(1)	17(1)
C(12)	8471(2)	2260(1)	3966(1)	22(1)
C(13)	2332(2)	1112(1)	5869(1)	26(1)
C(14)	6130(1)	6610(1)	7708(1)	17(1)
C(15)	7790(1)	4863(1)	8028(1)	16(1)

Table 3. Bond lengths [Å] and angles [°] for cdv98.

N(1)-C(11)	1.1461(16)
O(1)-C(3)	1.3689(14)
O(1)-C(12)	1.4309(14)
O(2)-C(5)	1.3675(14)
O(2)-C(13)	1.4273(15)
O(3)-C(8)	1.4238(13)
C(1)-C(11)	1.4820(16)
C(1)-C(2)	1.5214(15)
C(1)-C(10)	1.5434(15)
C(2)-C(7)	1.3906(16)
C(2)-C(3)	1.4097(16)
C(3)-C(4)	1.3835(16)
C(4)-C(5)	1.3974(16)
C(5)-C(6)	1.3858(16)
C(6)-C(7)	1.4007(16)
C(7)-C(8)	1.5274(15)
C(8)-C(9)	1.5337(15)
C(9)-C(14)	1.5313(15)
C(9)-C(10)	1.5336(15)
C(9)-C(15)	1.5352(15)
C(3)-O(1)-C(12)	117.50(9)

C(5)-O(2)-C(13)	116.80(9)
C(11)-C(1)-C(2)	110.90(9)
C(11)-C(1)-C(10)	110.20(9)
C(2)-C(1)-C(10)	112.71(9)
C(7)-C(2)-C(3)	118.91(10)
C(7)-C(2)-C(1)	122.12(10)
C(3)-C(2)-C(1)	118.96(10)
O(1)-C(3)-C(4)	124.24(10)
O(1)-C(3)-C(2)	114.26(10)
C(4)-C(3)-C(2)	121.50(10)
C(3)-C(4)-C(5)	118.55(10)
O(2)-C(5)-C(6)	123.85(10)
O(2)-C(5)-C(4)	115.07(10)
C(6)-C(5)-C(4)	121.08(10)
C(5)-C(6)-C(7)	119.89(10)
C(2)-C(7)-C(6)	120.07(10)
C(2)-C(7)-C(8)	121.27(10)
C(6)-C(7)-C(8)	118.58(10)
O(3)-C(8)-C(7)	111.88(9)
O(3)-C(8)-C(9)	109.31(9)
C(7)-C(8)-C(9)	112.49(9)
C(14)-C(9)-C(10)	107.60(9)
C(14)-C(9)-C(8)	109.60(9)
C(10)-C(9)-C(8)	106.56(9)

C(14)-C(9)-C(15)	109.73(9)
C(10)-C(9)-C(15)	112.70(9)
C(8)-C(9)-C(15)	110.55(9)
C(9)-C(10)-C(1)	114.59(9)
N(1)-C(11)-C(1)	177.06(13)

Table 4. Anisotropic displacement parameters ($Å^2$ x 10^3) for cdv98. The anisotropic displacement factor exponent takes the form: $-2\pi^2[h^2 a^{*2}U^{11} + ... + 2 h k a^* b^* U^{12}]$

	U^{11}	U^{22}	U^{33}	U^{23}	U^{13}	U^{12}
N(1)	14(1)	28(1)	32(1)	-2(1)	6(1)	0(1)
O(1)	19(1)	17(1)	21(1)	-5(1)	12(1)	-2(1)
O(2)	18(1)	14(1)	21(1)	-3(1)	5(1)	-6(1)
O(3)	14(1)	20(1)	15(1)	-1(1)	6(1)	-3(1)
C(1)	13(1)	14(1)	14(1)	1(1)	4(1)	-1(1)
C(2)	12(1)	12(1)	12(1)	2(1)	1(1)	1(1)
C(3)	12(1)	16(1)	12(1)	2(1)	3(1)	2(1)
C(4)	16(1)	12(1)	13(1)	-1(1)	1(1)	2(1)
C(5)	13(1)	12(1)	13(1)	2(1)	-1(1)	-2(1)
C(6)	10(1)	15(1)	13(1)	2(1)	2(1)	0(1)
C(7)	11(1)	12(1)	9(1)	2(1)	-1(1)	1(1)
C(8)	11(1)	14(1)	12(1)	1(1)	3(1)	1(1)
C(9)	12(1)	12(1)	12(1)	-1(1)	2(1)	0(1)
C(10)	13(1)	11(1)	16(1)	0(1)	3(1)	-2(1)
C(11)	16(1)	15(1)	21(1)	-2(1)	8(1)	-3(1)
C(12)	23(1)	22(1)	25(1)	-9(1)	13(1)	-1(1)
C(13)	24(1)	22(1)	34(1)	-4(1)	12(1)	-11(1)
C(14)	17(1)	16(1)	19(1)	-4(1)	3(1)	-1(1)
C(15)	15(1)	18(1)	14(1)	0(1)	0(1)	0(1)

Table 5. Hydrogen coordinates (x 10^4) and isotropic displacement parameters ($Å^2$ x 10^3) for cdv98.

	x	y	z	U(eq)
H(3)	3240(20)	4449(15)	7356(14)	44(5)
H(1A)	7947	5142	5123	16
H(4A)	6033	1503	4560	17
H(6A)	3531	2927	6466	15
H(8A)	4293	5363	6382	14
H(10A)	8351	6337	6617	16
H(10B)	6578	6318	5909	16
H(12A)	9405	2451	3670	34
H(12B)	7491	2163	3446	34
H(12C)	8704	1568	4340	34
H(13A)	1698	432	5685	39
H(13B)	1623	1759	5687	39
H(13C)	2765	1116	6582	39
H(14A)	7111	7058	7950	26
H(14B)	5606	6426	8260	26
H(14C)	5363	7030	7211	26
H(15A)	8033	4153	7744	24
H(15B)	7277	4725	8593	24

H(15C)	8809	5279	8247	24

Table 6. Torsion angles [°] for cdv98.

C(11)-C(1)-C(2)-C(7)	114.52(12)
C(10)-C(1)-C(2)-C(7)	-9.57(15)
C(11)-C(1)-C(2)-C(3)	-64.38(13)
C(10)-C(1)-C(2)-C(3)	171.53(9)
C(12)-O(1)-C(3)-C(4)	0.82(16)
C(12)-O(1)-C(3)-C(2)	-179.22(10)
C(7)-C(2)-C(3)-O(1)	179.56(10)
C(1)-C(2)-C(3)-O(1)	-1.50(14)
C(7)-C(2)-C(3)-C(4)	-0.48(16)
C(1)-C(2)-C(3)-C(4)	178.46(10)
O(1)-C(3)-C(4)-C(5)	179.67(10)
C(2)-C(3)-C(4)-C(5)	-0.28(17)
C(13)-O(2)-C(5)-C(6)	1.01(16)
C(13)-O(2)-C(5)-C(4)	-178.57(10)
C(3)-C(4)-C(5)-O(2)	-179.97(9)
C(3)-C(4)-C(5)-C(6)	0.44(17)
O(2)-C(5)-C(6)-C(7)	-179.39(10)
C(4)-C(5)-C(6)-C(7)	0.17(16)
C(3)-C(2)-C(7)-C(6)	1.09(16)
C(1)-C(2)-C(7)-C(6)	-177.81(10)
C(3)-C(2)-C(7)-C(8)	-175.59(10)
C(1)-C(2)-C(7)-C(8)	5.51(16)

C(5)-C(6)-C(7)-C(2)	-0.94(16)
C(5)-C(6)-C(7)-C(8)	175.82(10)
C(2)-C(7)-C(8)-O(3)	-152.81(10)
C(6)-C(7)-C(8)-O(3)	30.47(13)
C(2)-C(7)-C(8)-C(9)	-29.30(14)
C(6)-C(7)-C(8)-C(9)	153.98(10)
O(3)-C(8)-C(9)-C(14)	-64.50(11)
C(7)-C(8)-C(9)-C(14)	170.58(9)
O(3)-C(8)-C(9)-C(10)	179.35(8)
C(7)-C(8)-C(9)-C(10)	54.43(11)
O(3)-C(8)-C(9)-C(15)	56.58(12)
C(7)-C(8)-C(9)-C(15)	-68.34(12)
C(14)-C(9)-C(10)-C(1)	-178.68(9)
C(8)-C(9)-C(10)-C(1)	-61.20(12)
C(15)-C(9)-C(10)-C(1)	60.22(12)
C(11)-C(1)-C(10)-C(9)	-85.80(12)
C(2)-C(1)-C(10)-C(9)	38.68(13)

Table 7. Hydrogen bonds for cdv98 [Å and °].

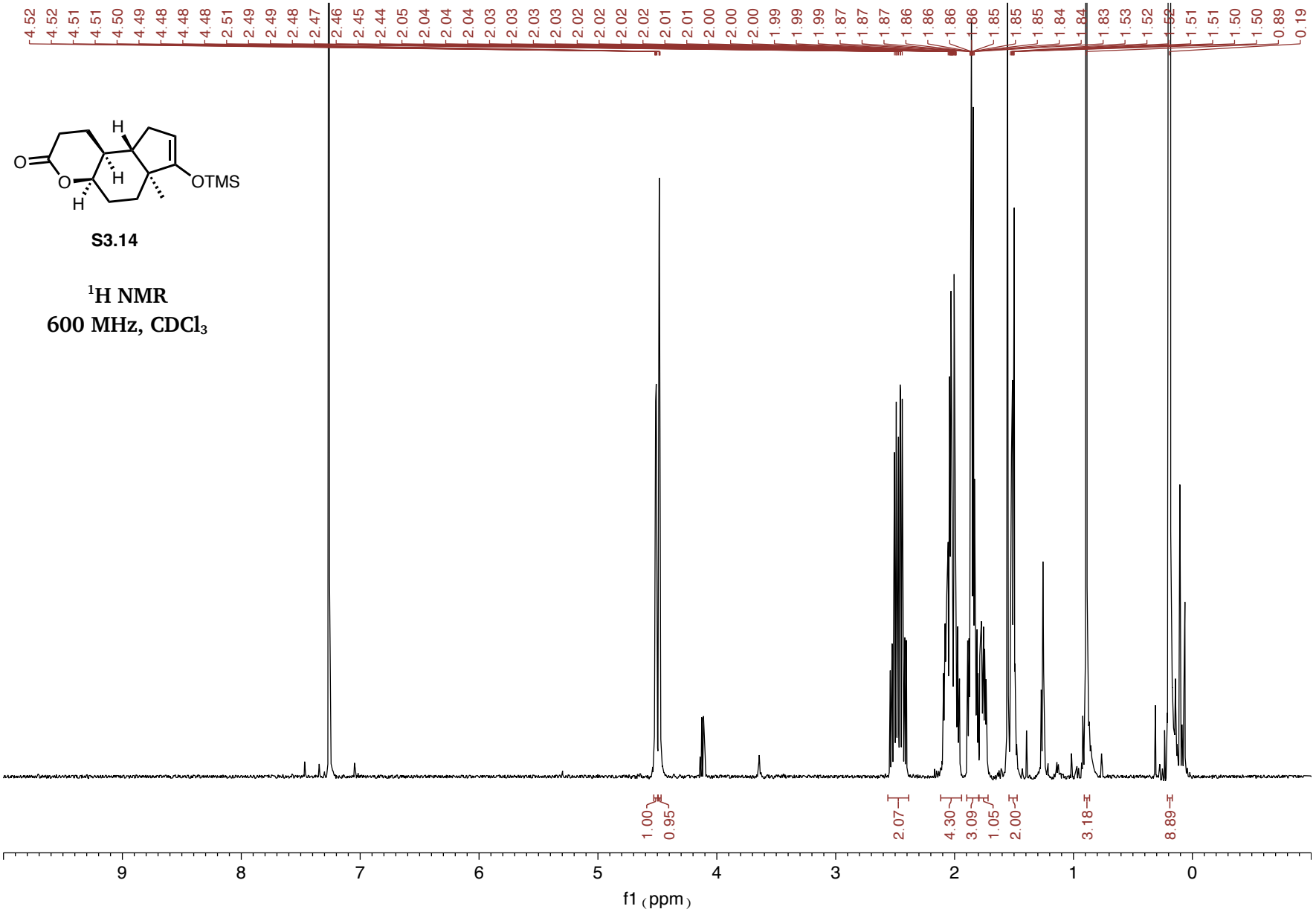
D-H...A	d(D-H)	d(H...A)	d(D...A)	<(DHA)
O(3)-H(3)...N(1)#1	0.89(2)	2.01(2)	2.9020(14)	173.7(17)

Symmetry transformations used to generate equivalent atoms:

#1 x-1,y,z

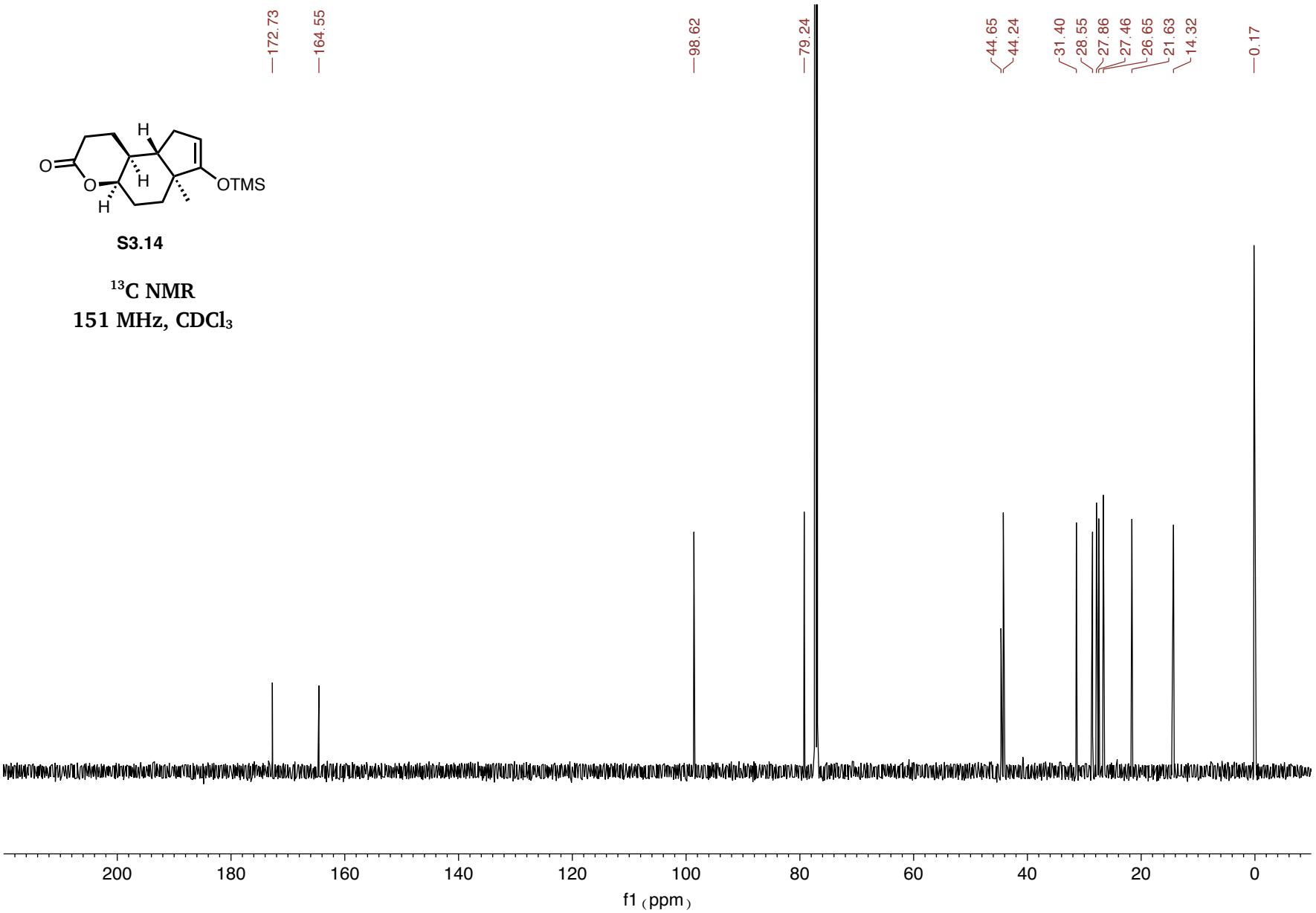
Appendix C

C1: NMR Data



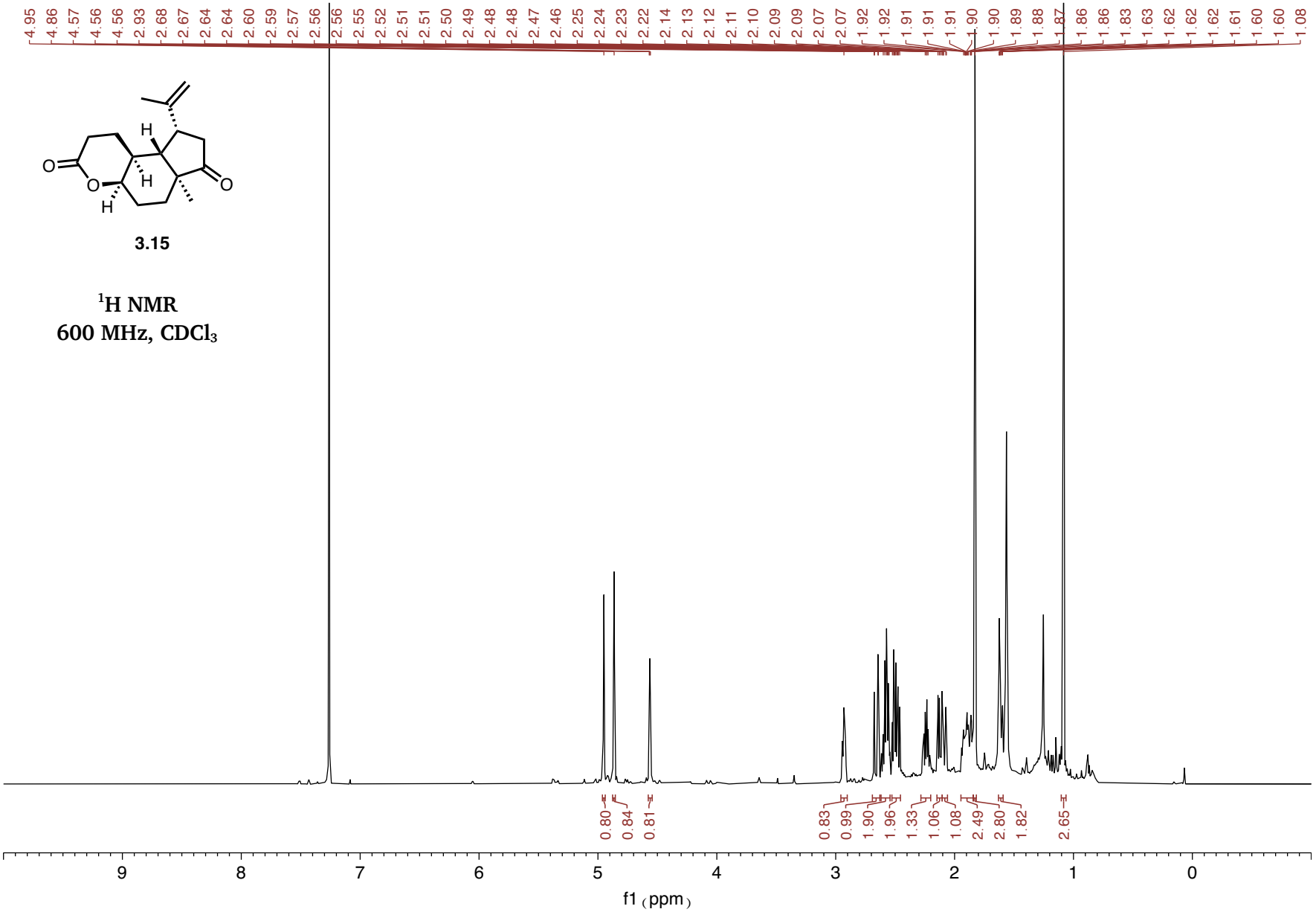
S3.14

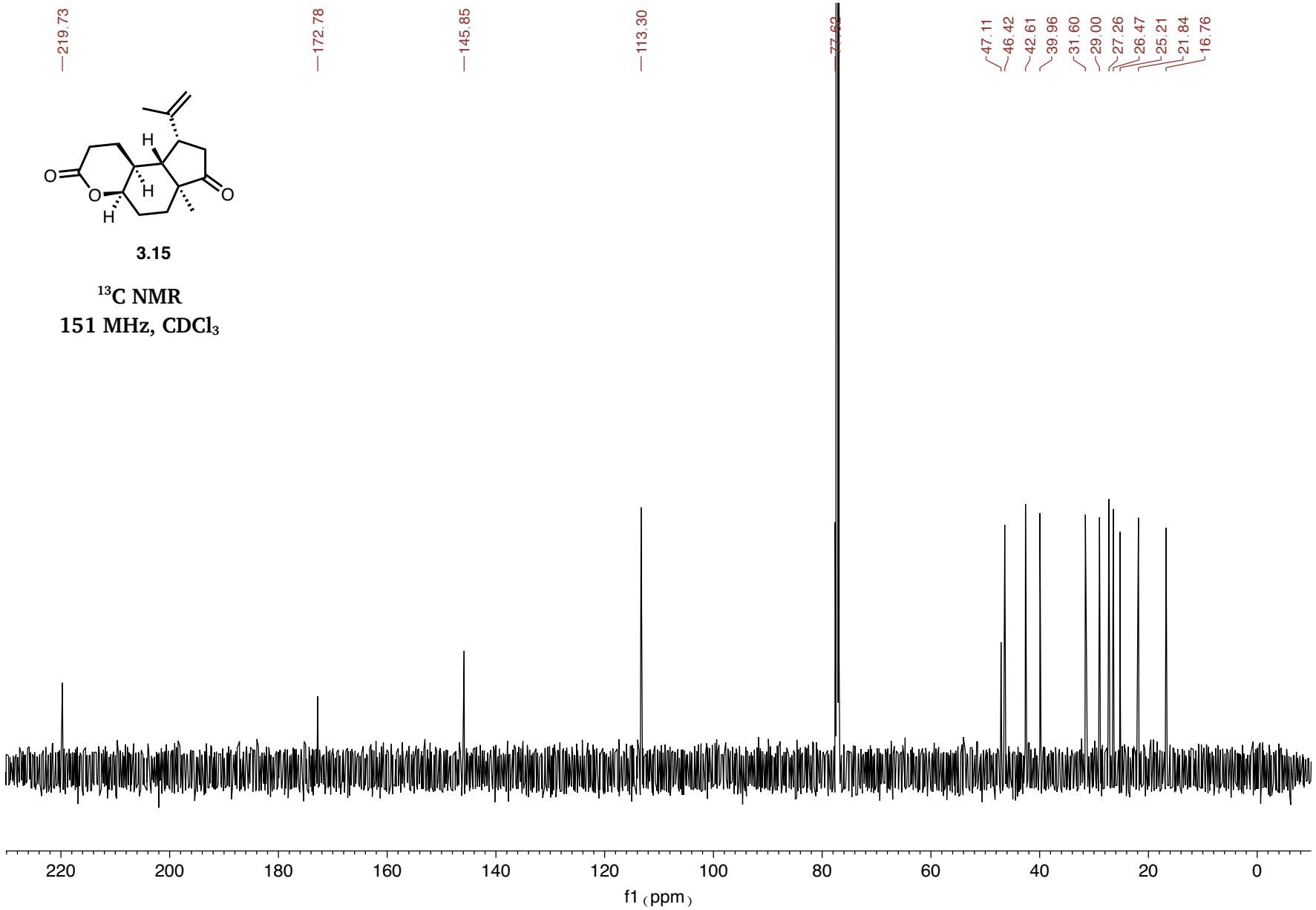
^{1}H NMR
600 MHz, $CDCl_3$



S3.14

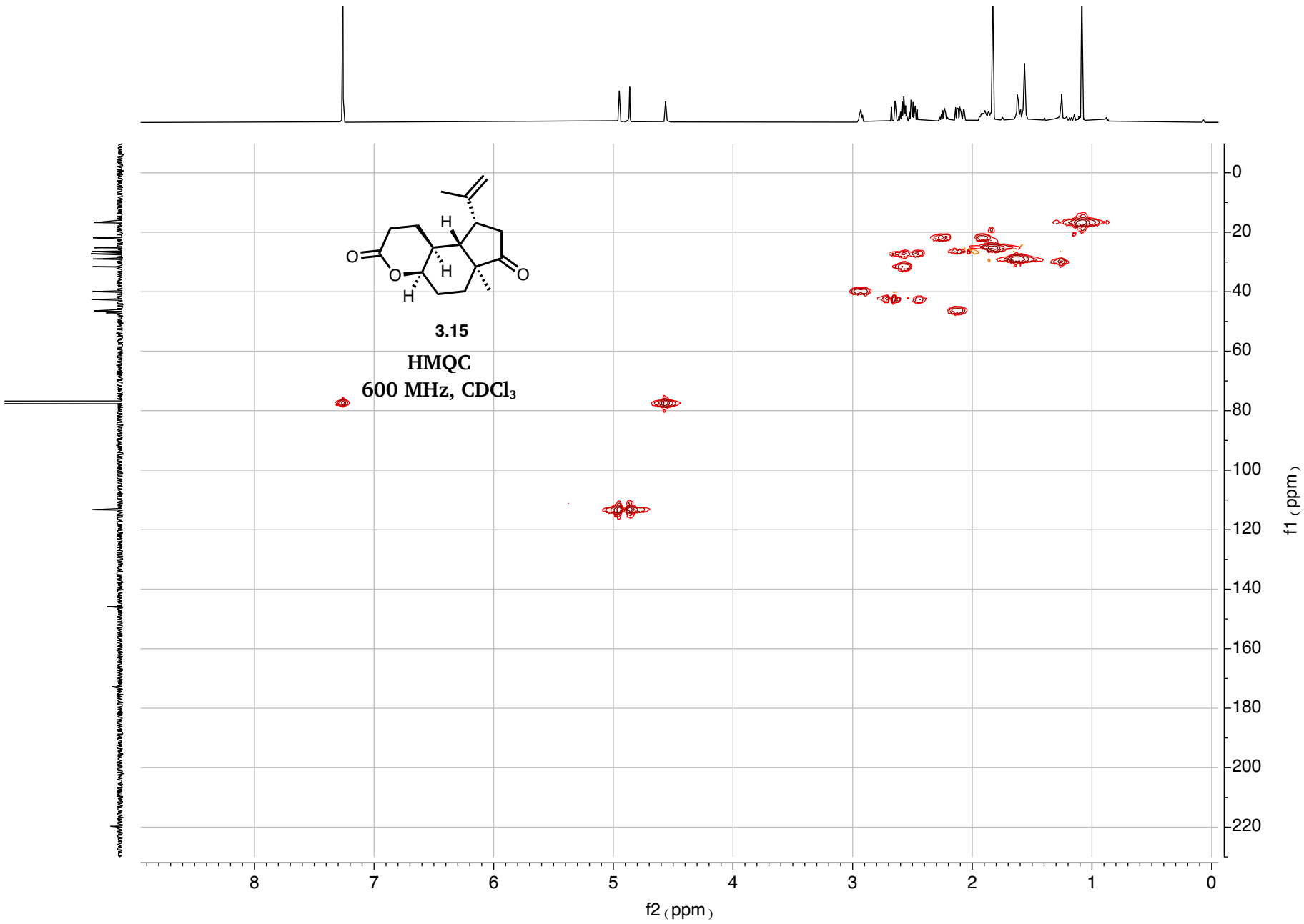
^{13}C NMR
151 MHz, $CDCl_3$

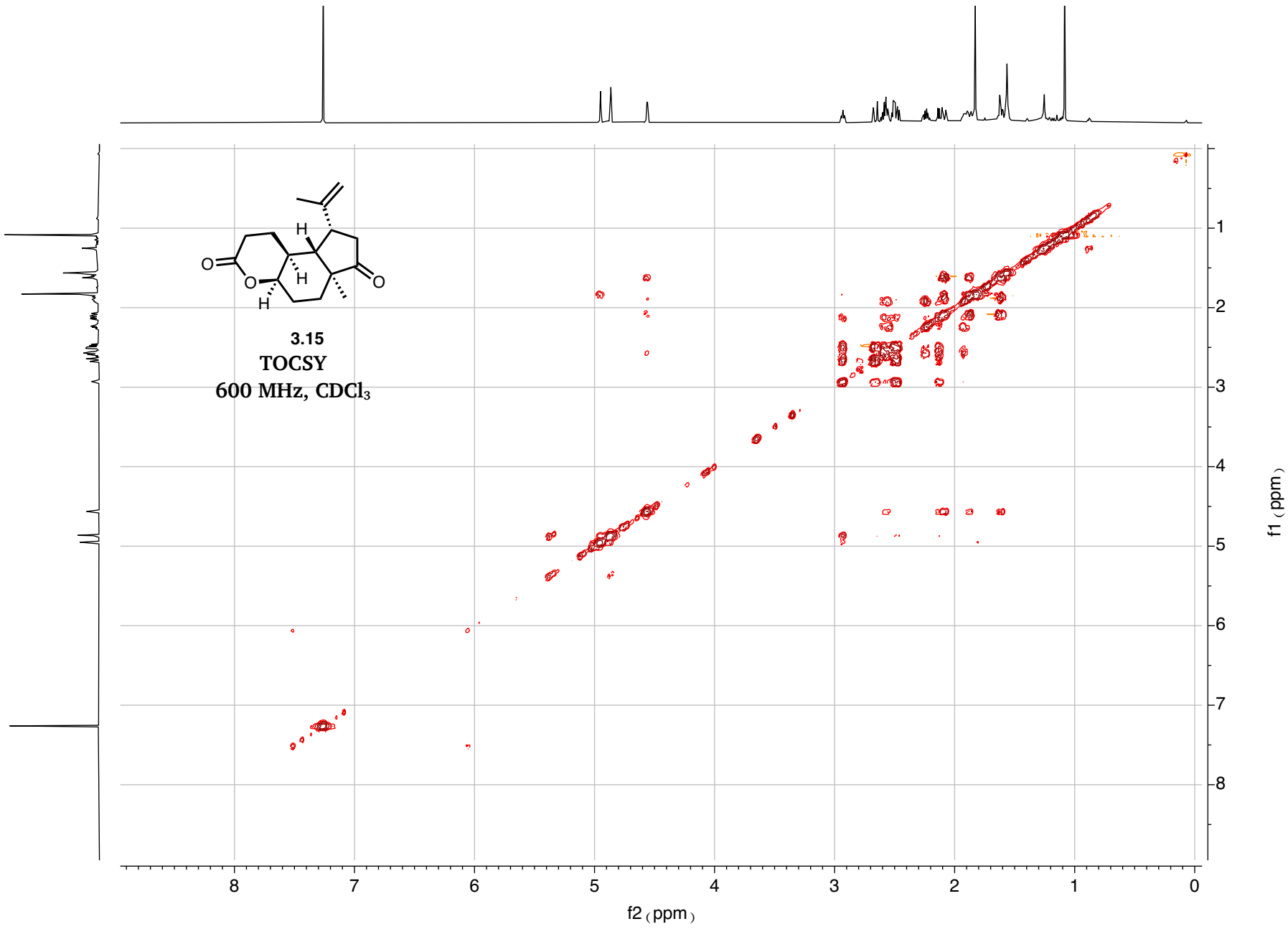

4.95 4.86 4.57 4.56 4.56 2.93 2.68 2.67 2.64 2.64 2.60 2.59 2.57 2.56 2.56 2.55 2.52 2.51 2.51 2.50 2.49 2.48 2.48 2.47 2.46 2.25 2.24 2.23 2.22 2.14 2.13 2.12 2.11 2.10 2.09 2.09 2.07 2.07 1.92 1.92 1.91 1.91 1.91 1.90 1.90 1.89 1.88 1.87 1.86 1.86 1.83 1.63 1.62 1.62 1.62 1.61 1.60 1.60 1.08
O
O
O
H
H
H
3.15
1H NMR
600 MHz, CDCl3
0.80 0.84 0.81 0.83 0.99 1.90 1.96 1.33 1.06 1.08 2.49 2.80 1.82 2.65
9 8 7 6 5 4 3 2 1 0
f1 (ppm)

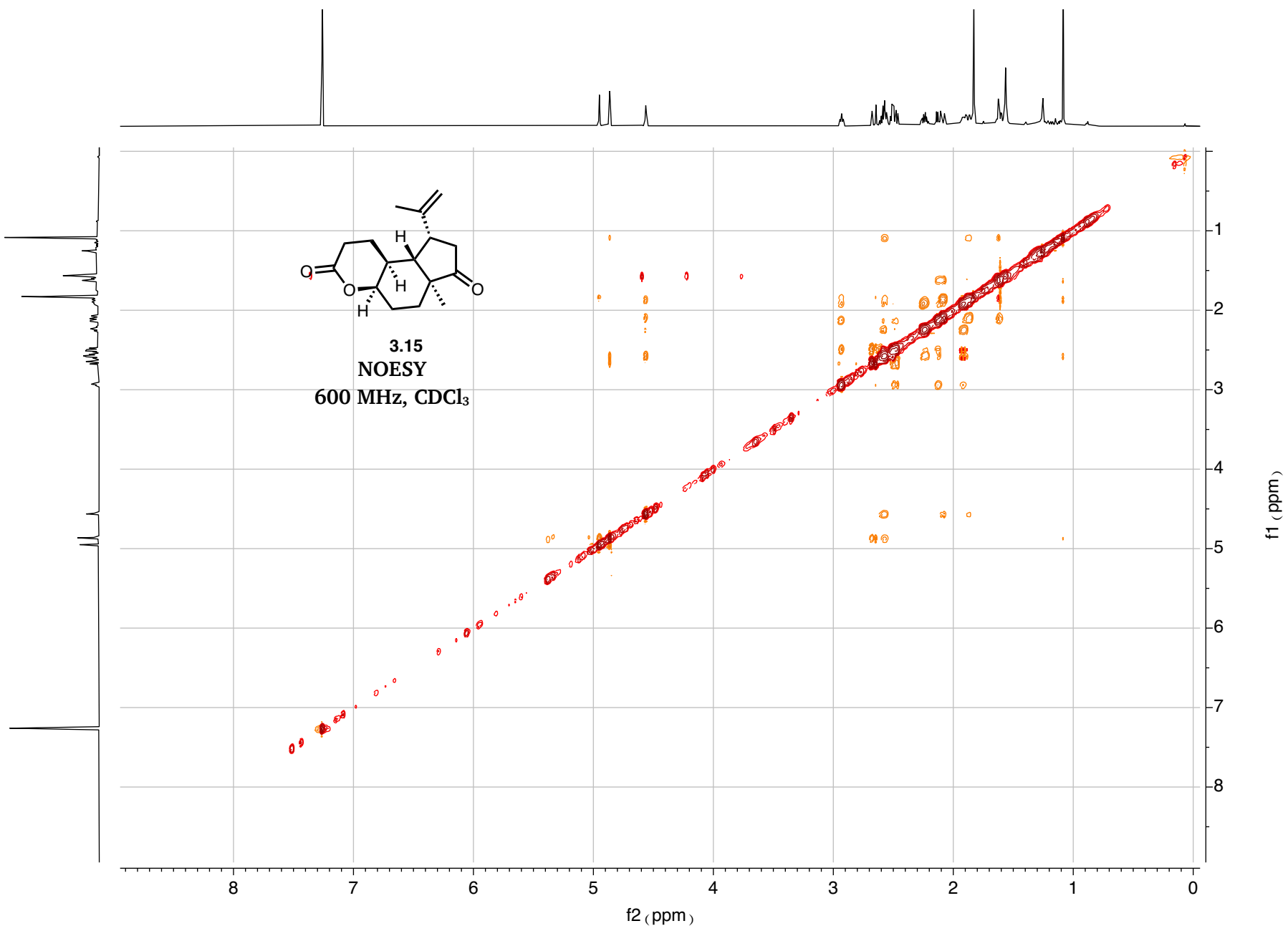


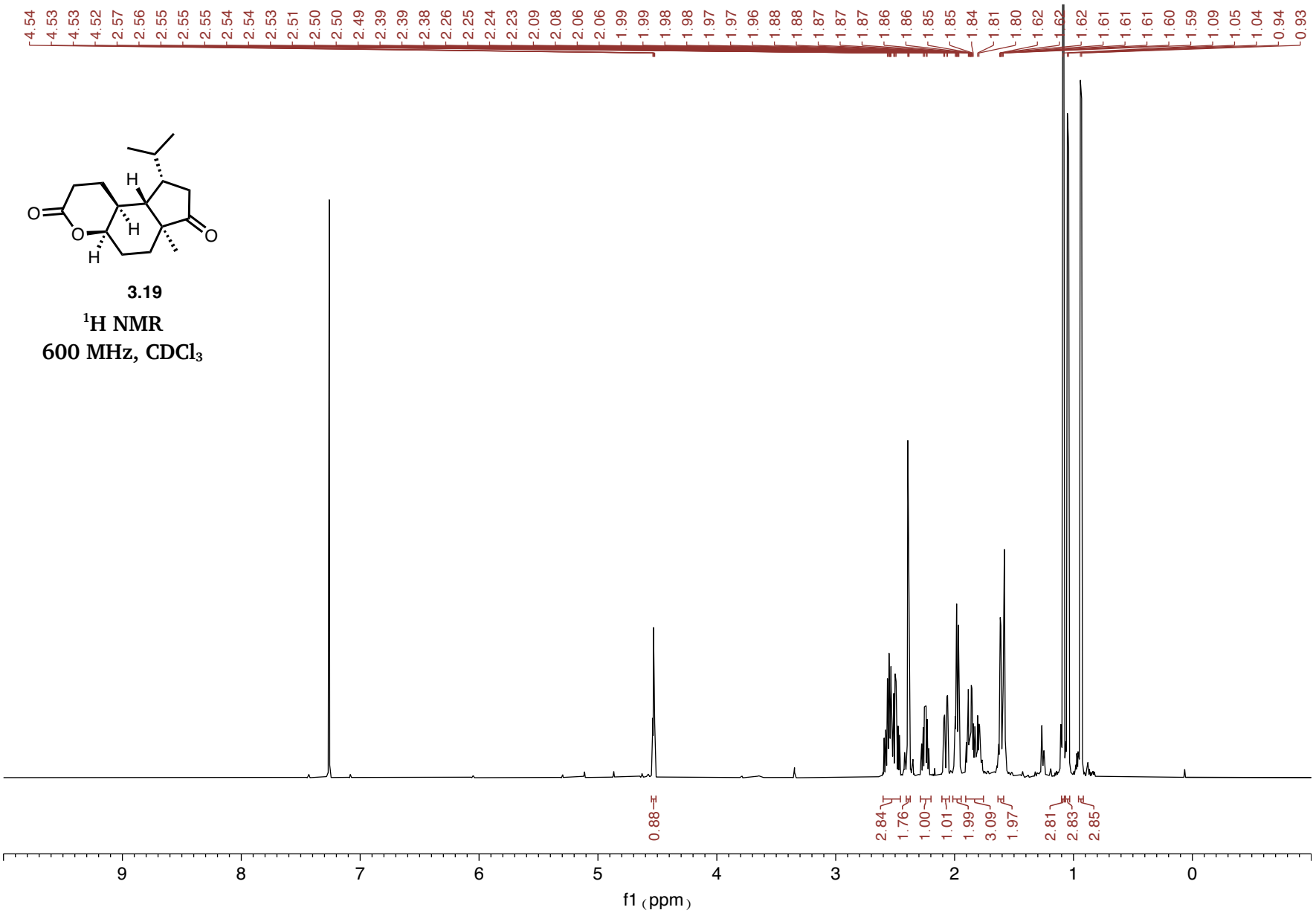
3.15

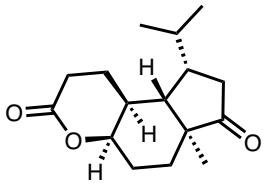
^{13}C NMR
151 MHz, $CDCl_3$


3.15
HMQC
600 MHz, CDCl3
f2 (ppm)
f1 (ppm)


3.15
TOCSY
600 MHz, CDCl3
f2 (ppm)
f1 (ppm)

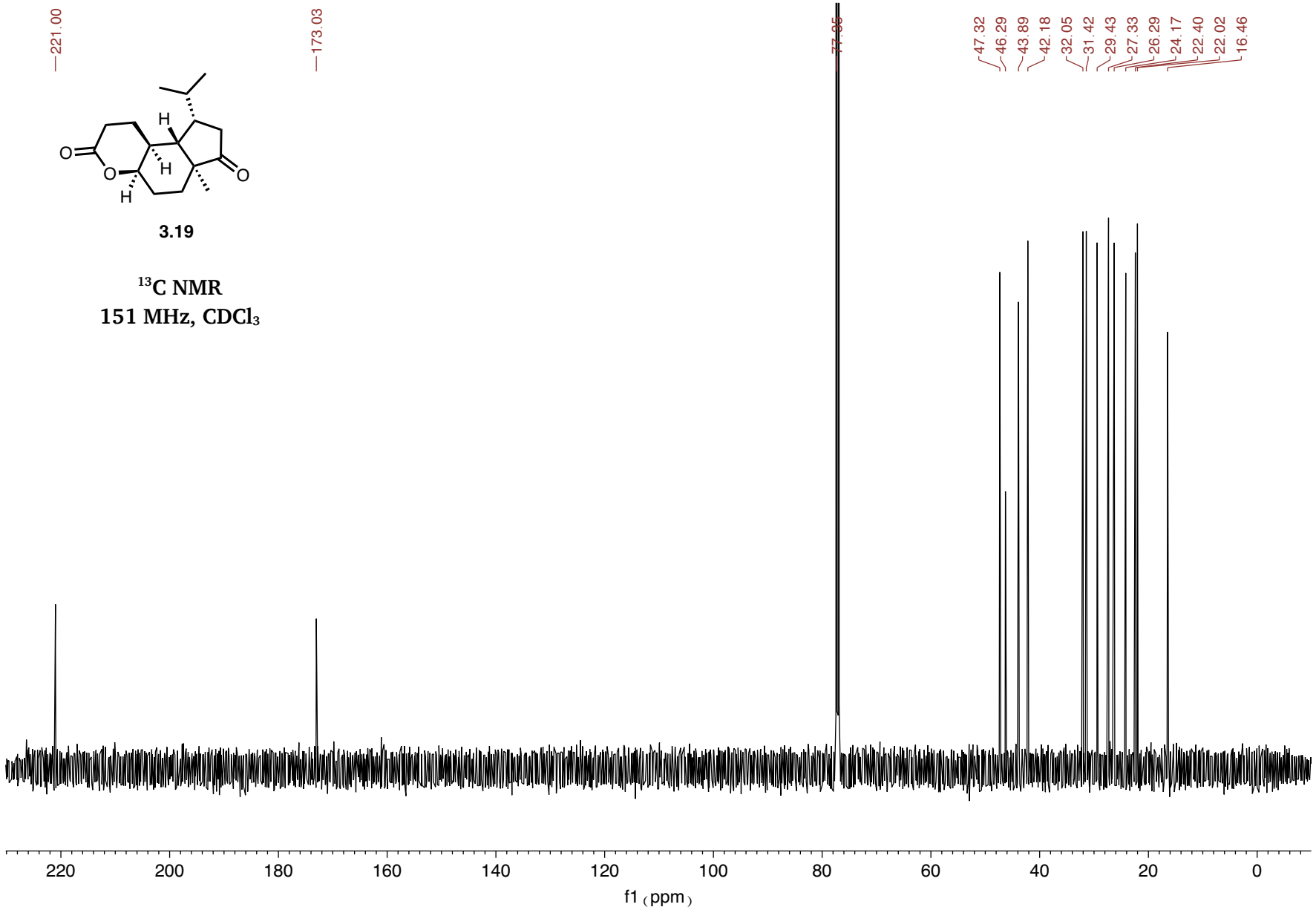

3.15
NOESY
600 MHz, CDCl3
f2 (ppm)
f1 (ppm)


4.54 4.53 4.53 4.52 2.57 2.56 2.55 2.55 2.55 2.54 2.54 2.53 2.51 2.50 2.50 2.49 2.39 2.39 2.38 2.26 2.25 2.24 2.23 2.09 2.08 2.06 2.06 1.99 1.99 1.98 1.98 1.97 1.97 1.96 1.88 1.88 1.87 1.87 1.87 1.86 1.86 1.85 1.85 1.84 1.81 1.80 1.62 1.62 1.62 1.61 1.61 1.61 1.60 1.59 1.09 1.05 1.04 0.94 0.93
O
O
O
H
H
H
3.19
^{1}H NMR
600 MHz, $CDCl_3$
0.88
2.84 1.76 1.00 1.01 1.99 3.09 1.97 2.81 2.83 2.85
9 8 7 6 5 4 3 2 1 0
f1 (ppm)



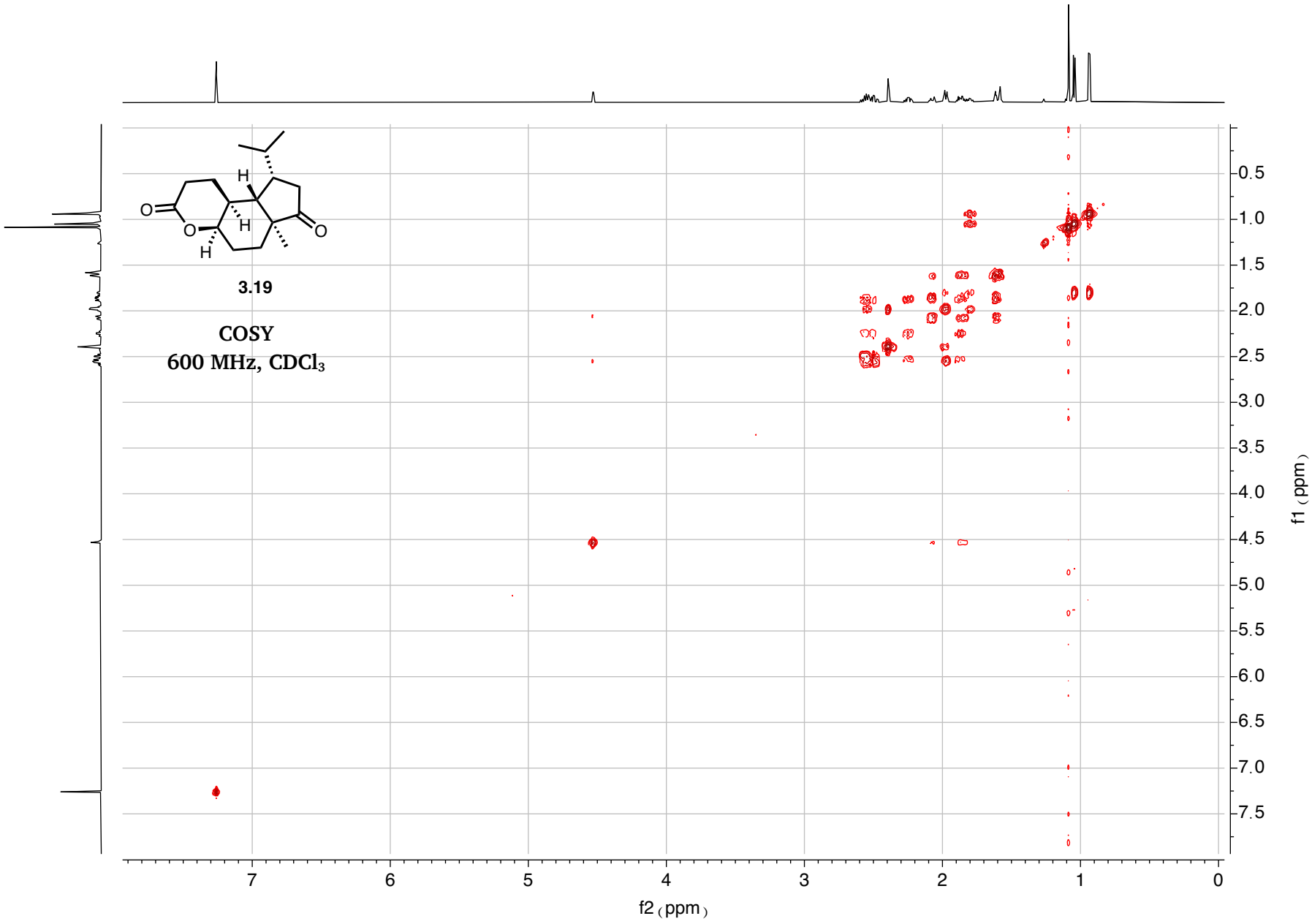
3.19

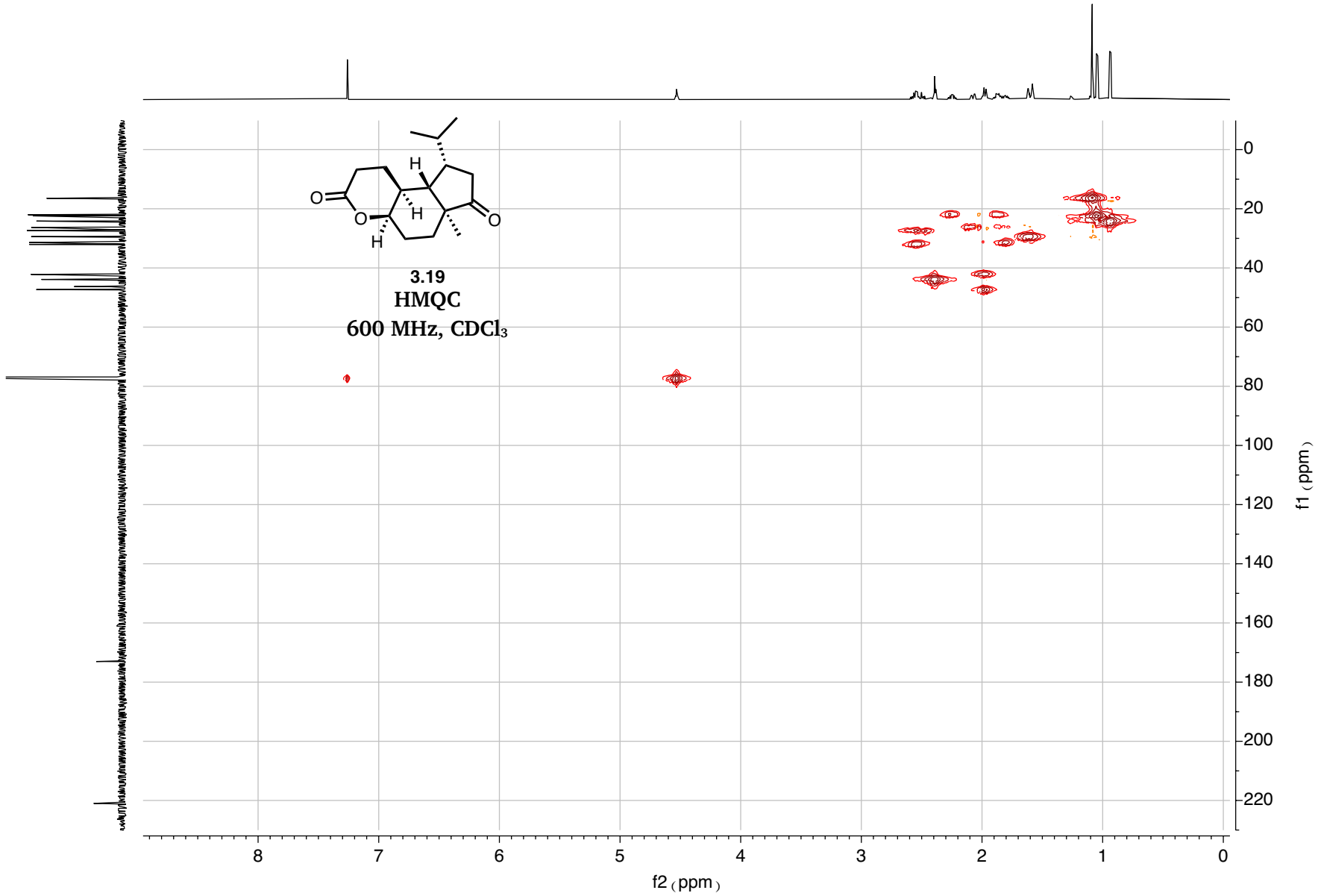
^{1}H NMR
500 MHz, $CDCl_3$

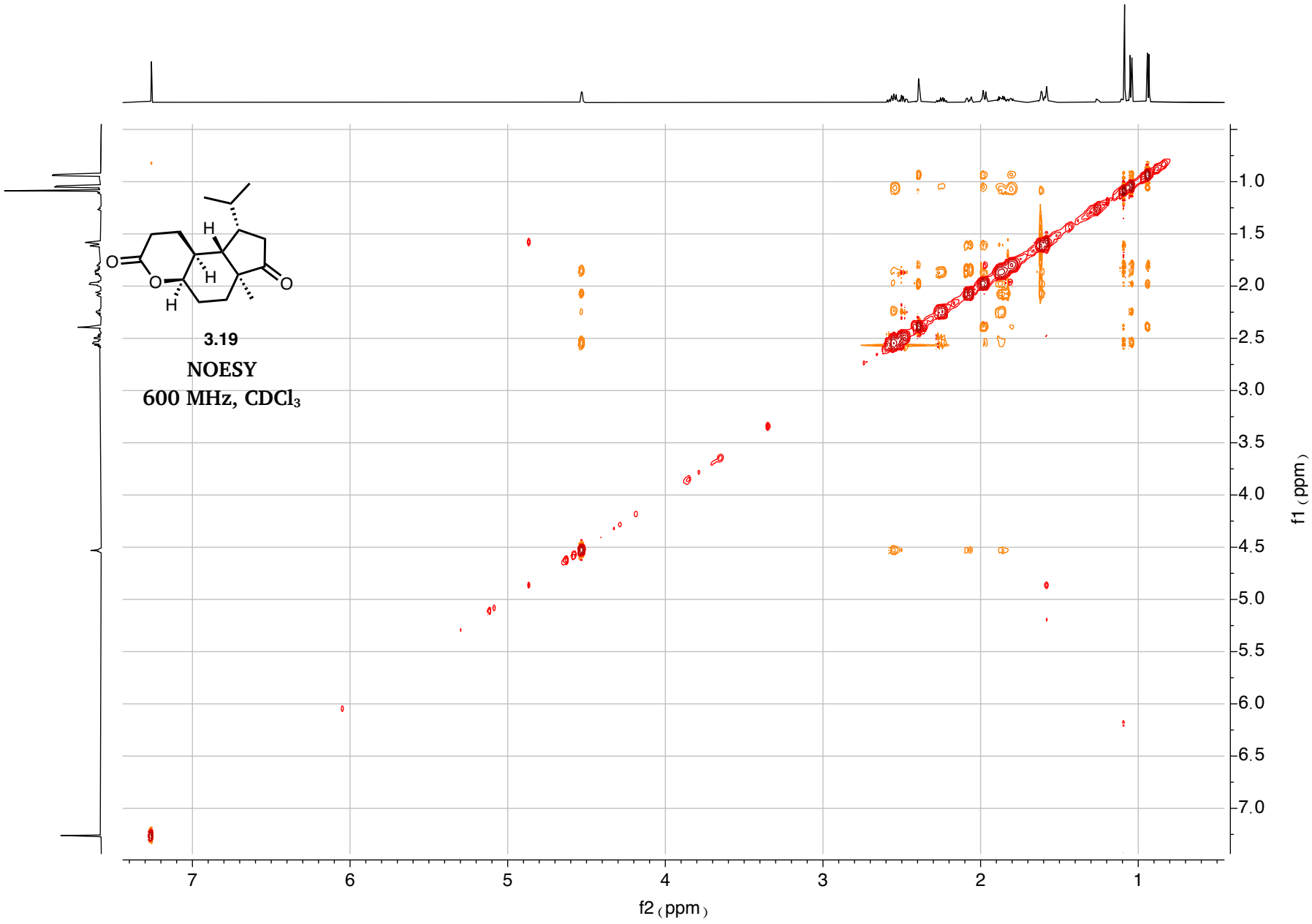


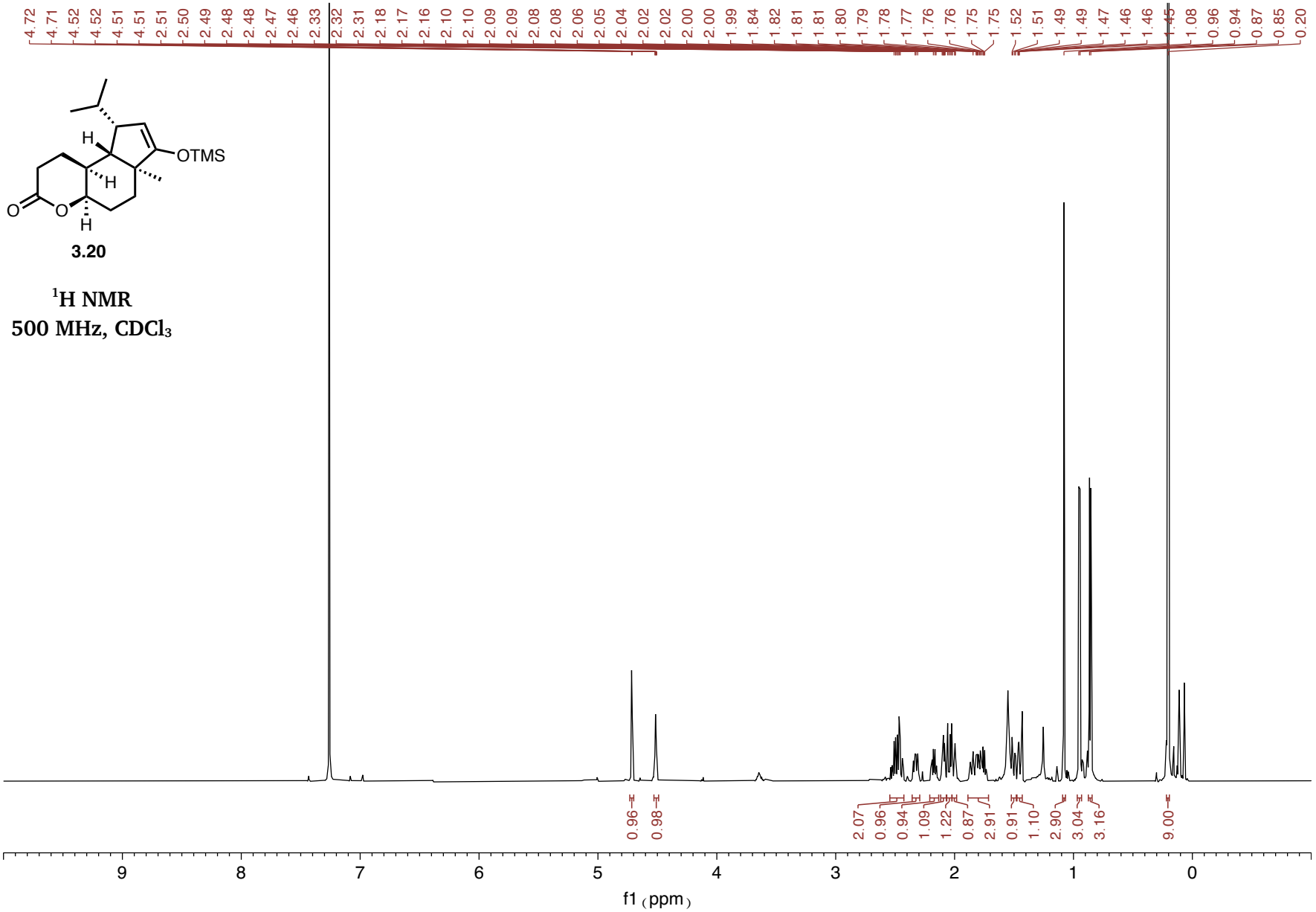
3.19

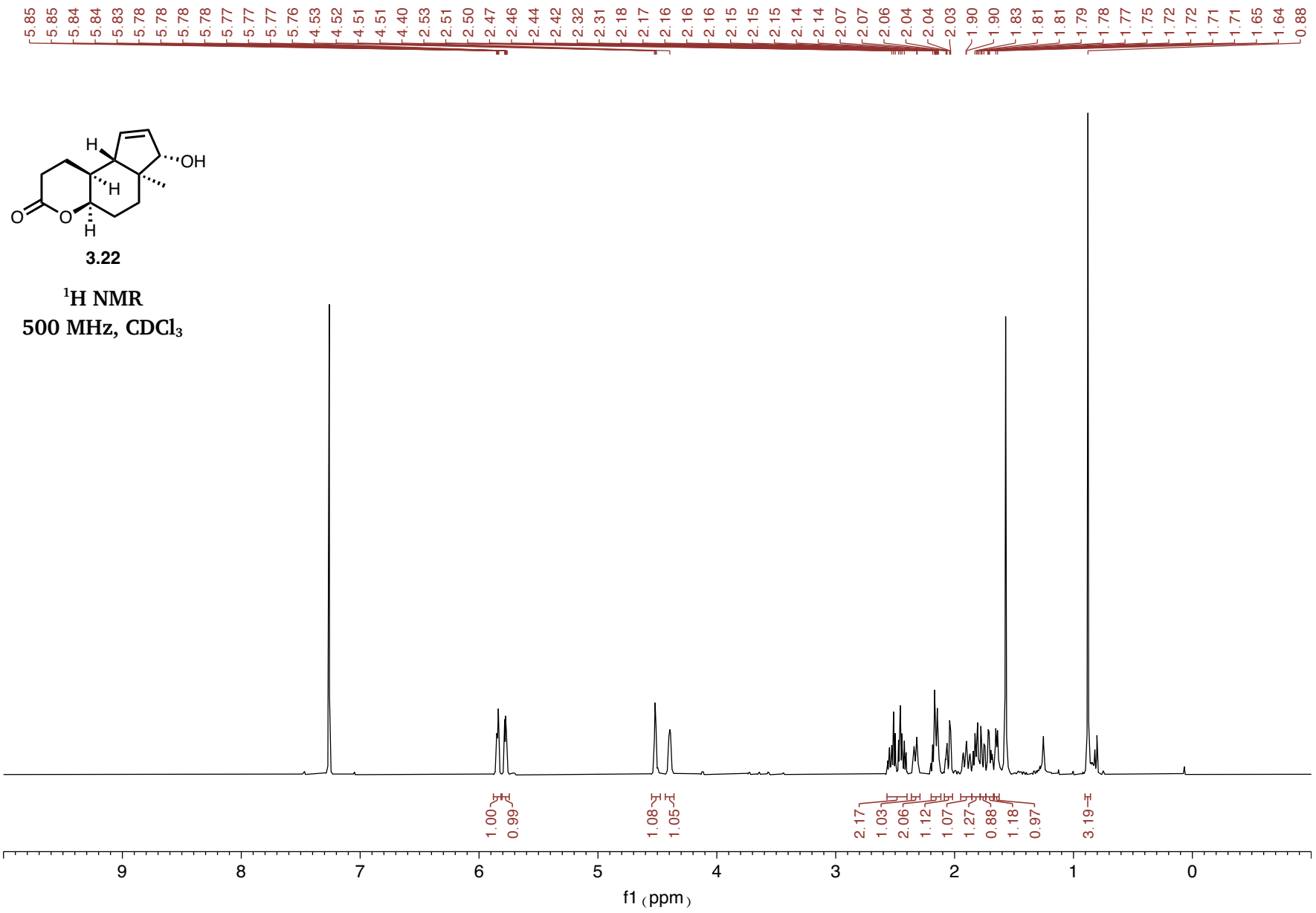
^{13}C NMR
151 MHz, $CDCl_3$

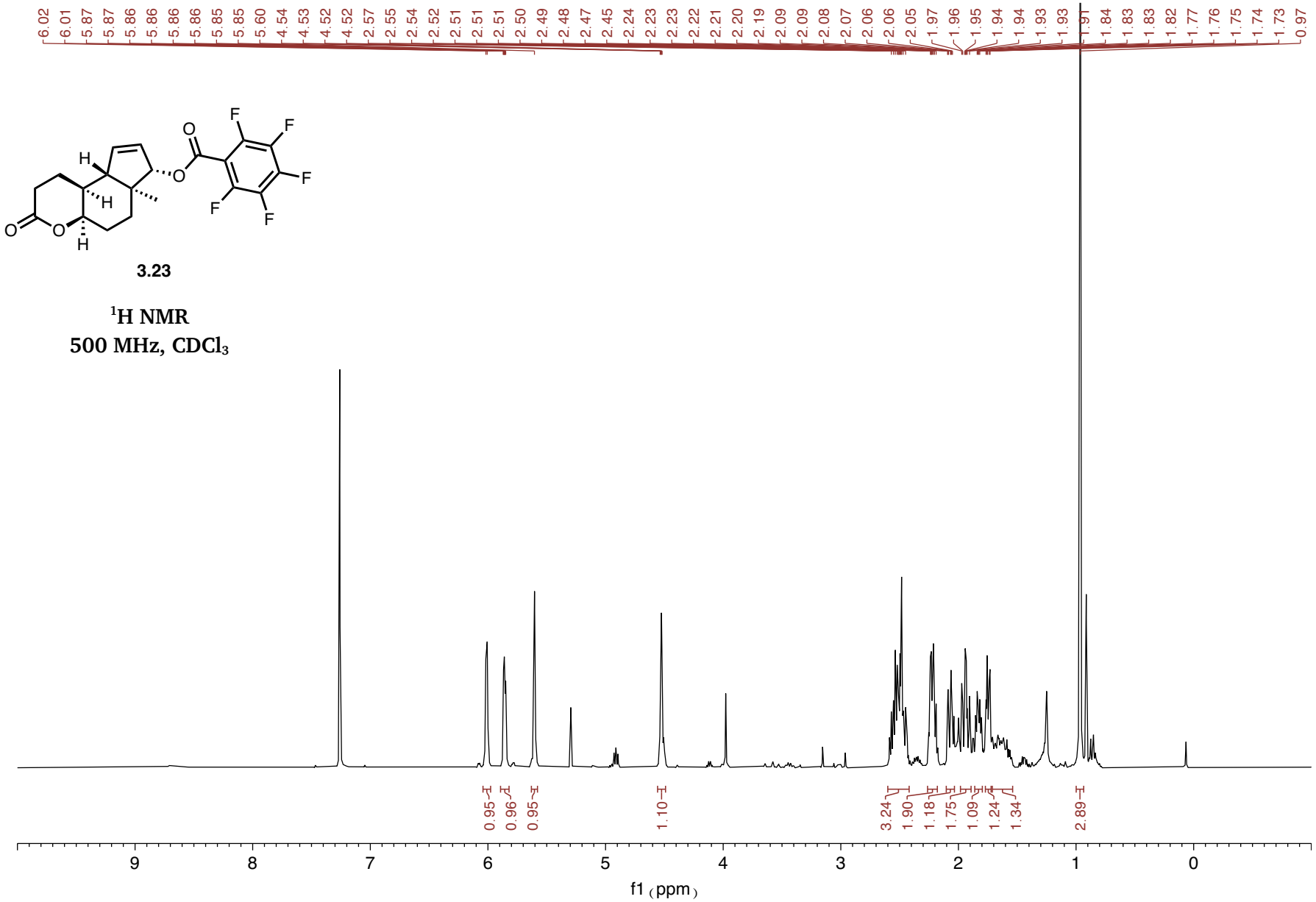

3.19
COSY
600 MHz, CDCl3
f2 (ppm)
f1 (ppm)


3.19
HMQC
600 MHz, CDCl3
f2 (ppm)
f1 (ppm)


3.19
NOESY
600 MHz, CDCl3
f2 (ppm)
f1 (ppm)

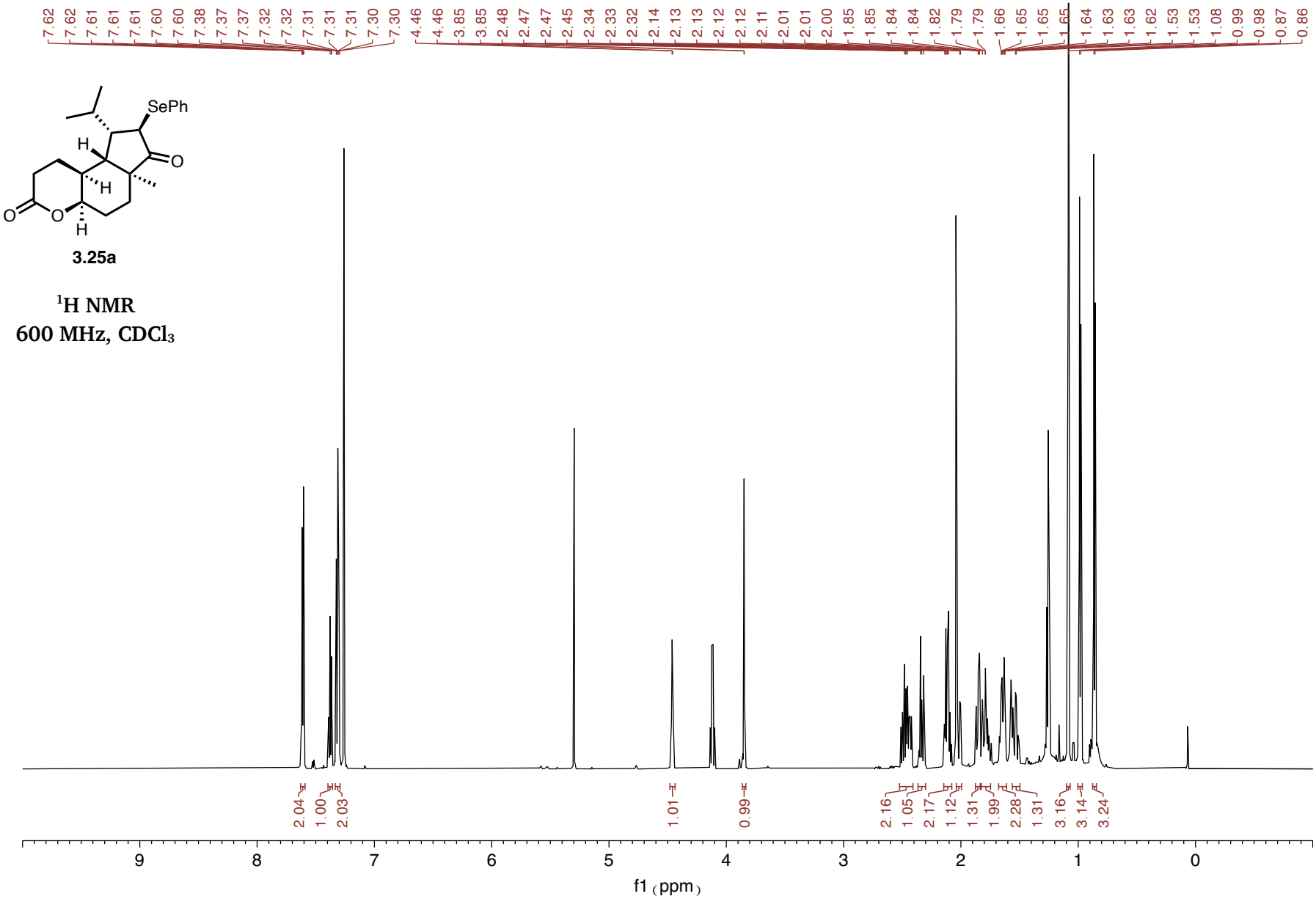

4.72 4.71 4.52 4.52 4.51 4.51 2.51 2.50 2.49 2.48 2.48 2.47 2.46 2.33 2.32 2.31 2.18 2.17 2.16 2.10 2.10 2.09 2.09 2.08 2.08 2.06 2.05 2.04 2.02 2.02 2.00 2.00 1.99 1.84 1.82 1.81 1.81 1.80 1.79 1.78 1.77 1.76 1.76 1.75 1.75 1.52 1.51 1.49 1.49 1.47 1.46 1.46 1.45 1.08 0.96 0.94 0.87 0.85 0.20
H
OTMS
H
O
O
H
3.20
1H NMR
500 MHz, CDCl3
0.96 0.98 2.07 0.96 0.94 1.09 1.22 0.87 2.91 0.91 1.10 2.90 3.04 3.16 9.00
9 8 7 6 5 4 3 2 1 0
f1 (ppm)

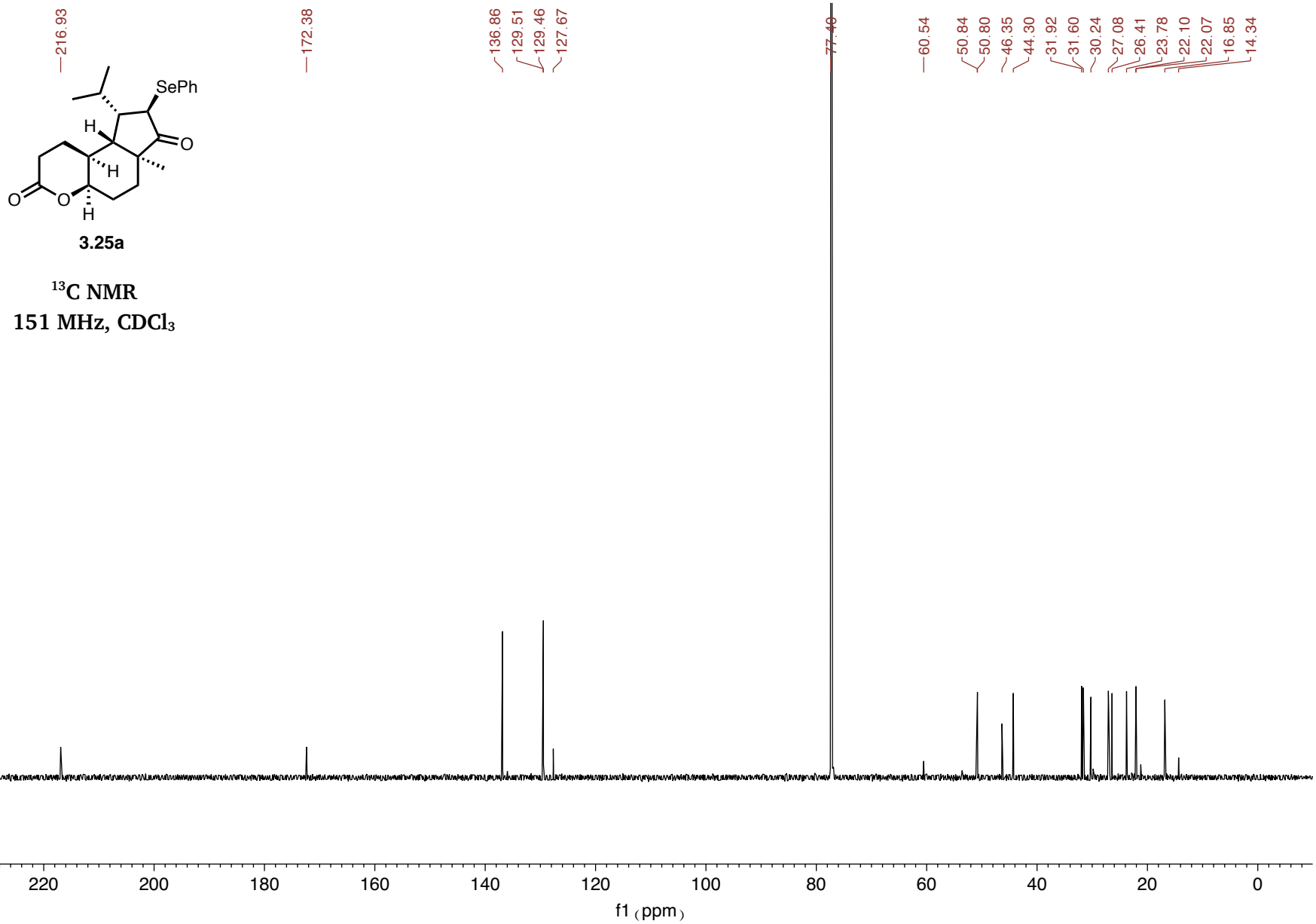

5.85 5.85 5.84 5.84 5.83 5.78 5.78 5.78 5.78 5.77 5.77 5.77 5.76 4.53 4.52 4.51 4.51 4.40 2.53 2.51 2.50 2.47 2.46 2.44 2.42 2.32 2.31 2.18 2.17 2.16 2.16 2.16 2.15 2.15 2.15 2.14 2.14 2.07 2.07 2.06 2.04 2.04 2.03 1.90 1.90 1.83 1.81 1.81 1.79 1.78 1.77 1.75 1.72 1.72 1.71 1.71 1.65 1.64 0.88
H
OH
H
O
O
H
3.22
1H NMR
500 MHz, CDCl3
1.00 0.99 1.08 1.05 2.17 1.03 2.06 1.12 1.07 1.27 0.88 1.18 0.97 3.19
9 8 7 6 5 4 3 2 1 0
f1 (ppm)



3.23

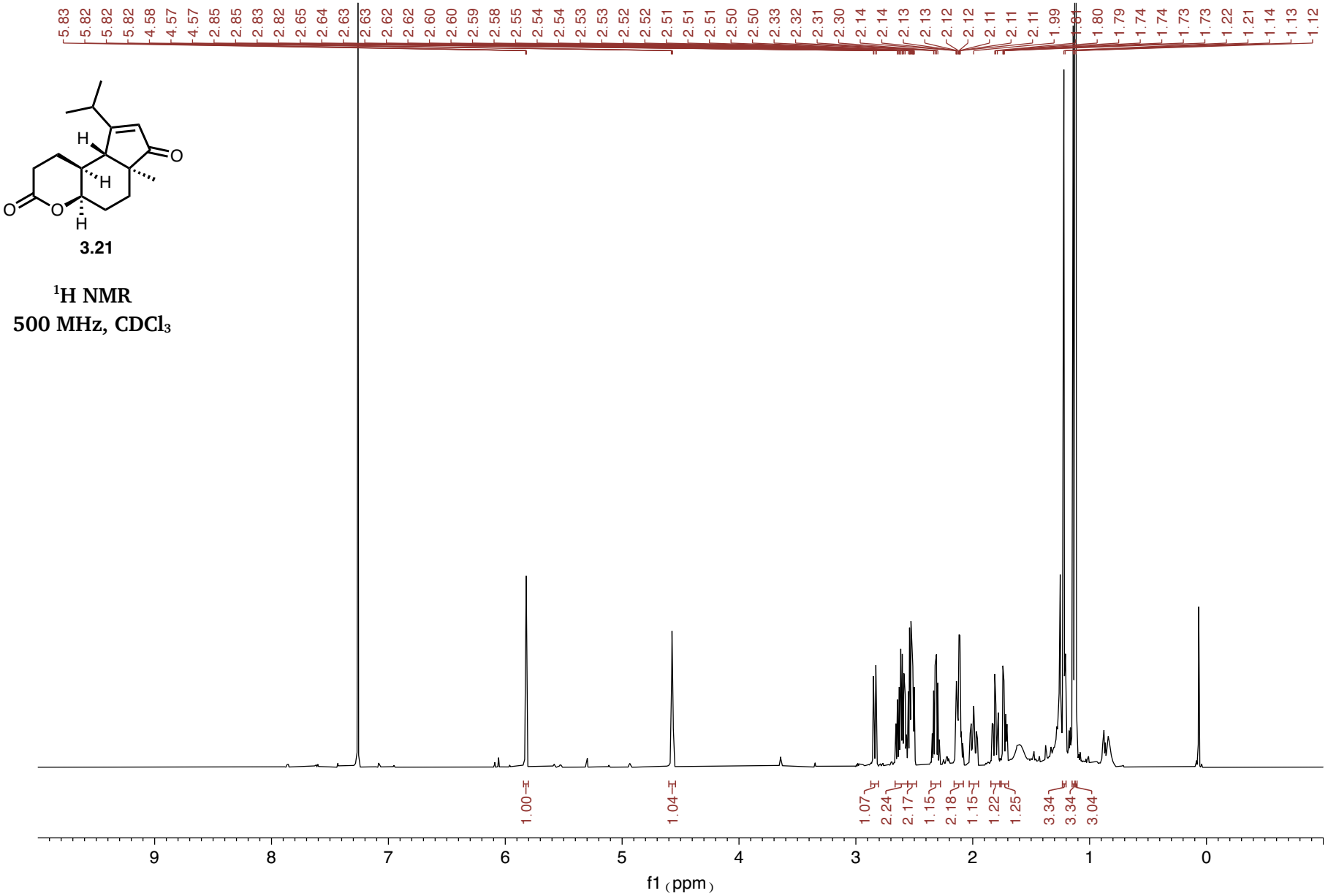
^{1}H NMR
500 MHz, $CDCl_3$


SePh
H
O
H
O
O
H
3.25a
1H NMR
600 MHz, CDCl3
f1 (ppm)



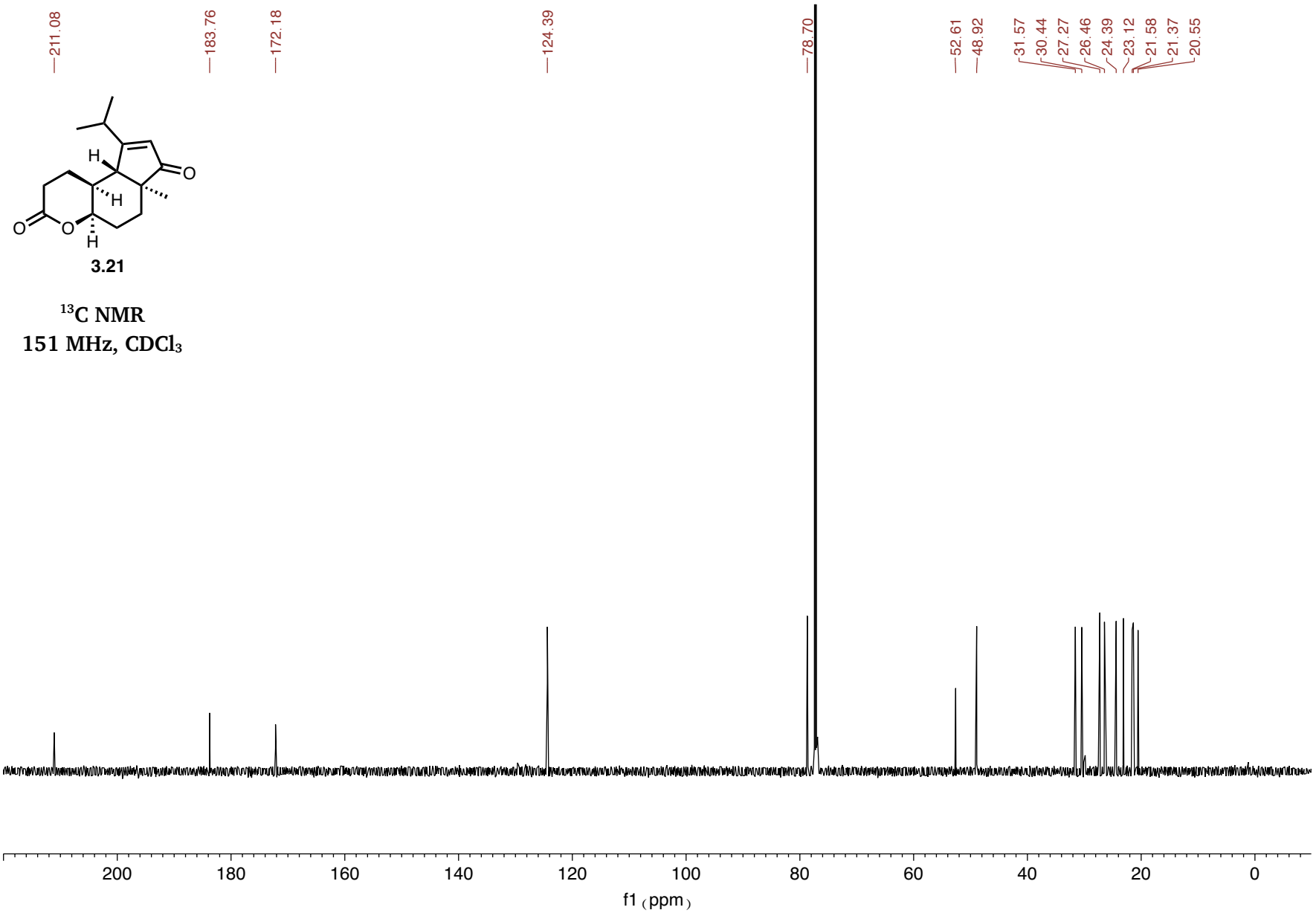
3.25a

^{13}C NMR
151 MHz, $CDCl_3$



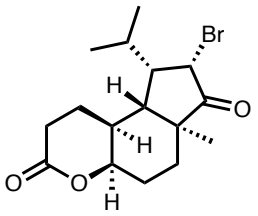
3.21

^{1}H NMR
500 MHz, $CDCl_3$



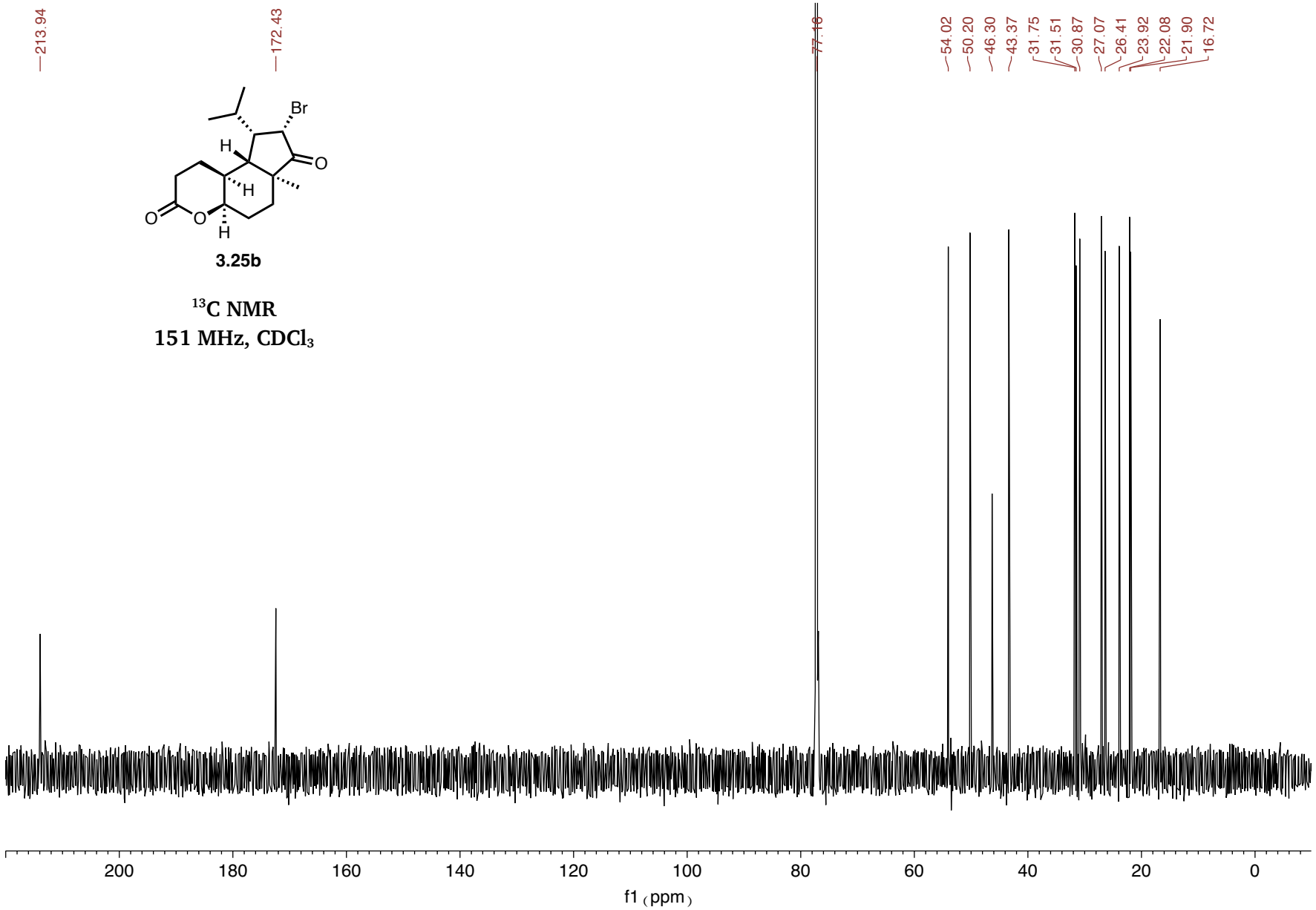
3.21

^{13}C NMR
151 MHz, $CDCl_3$



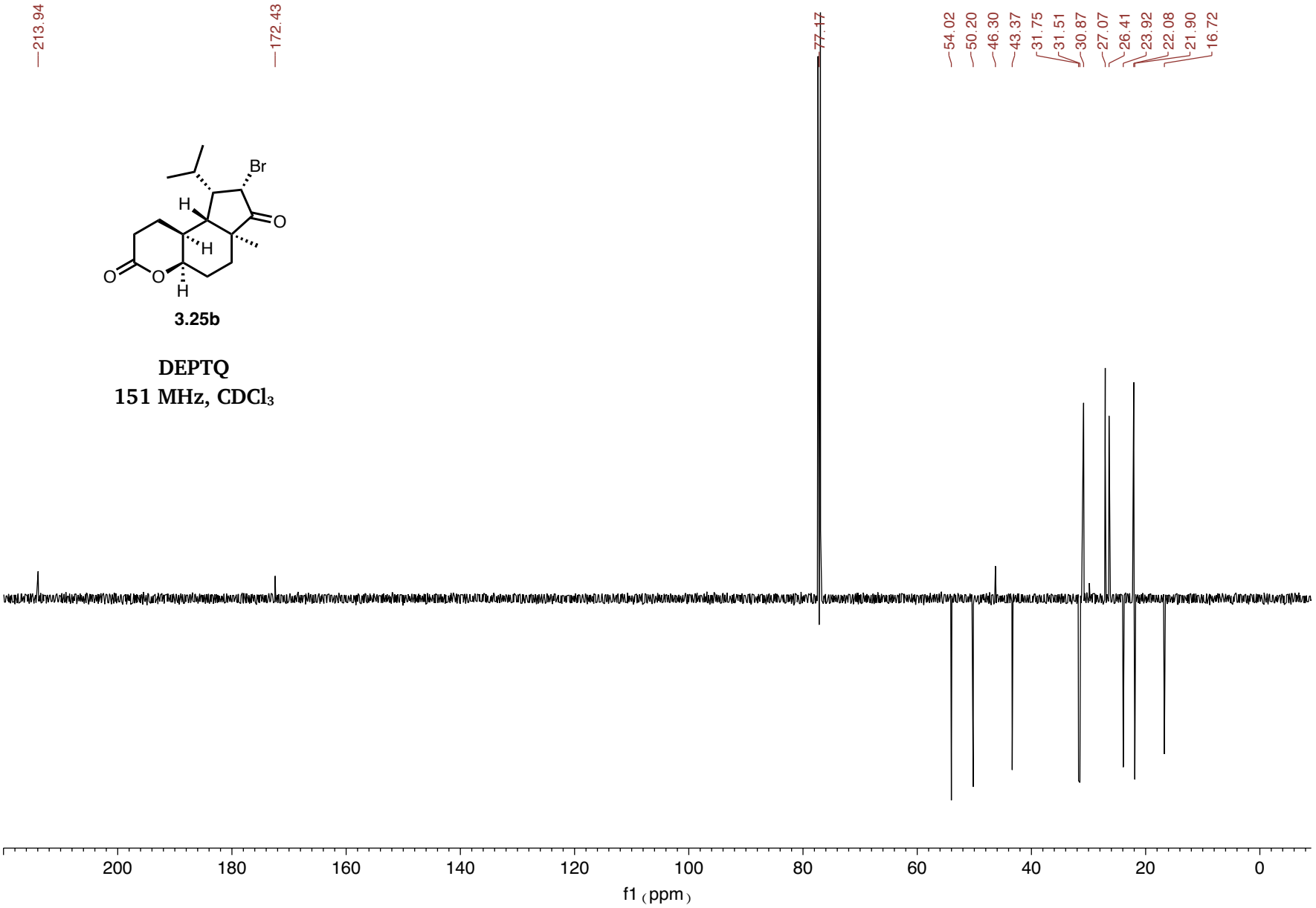
3.25b

^{1}H NMR
600 MHz, $CDCl_3$



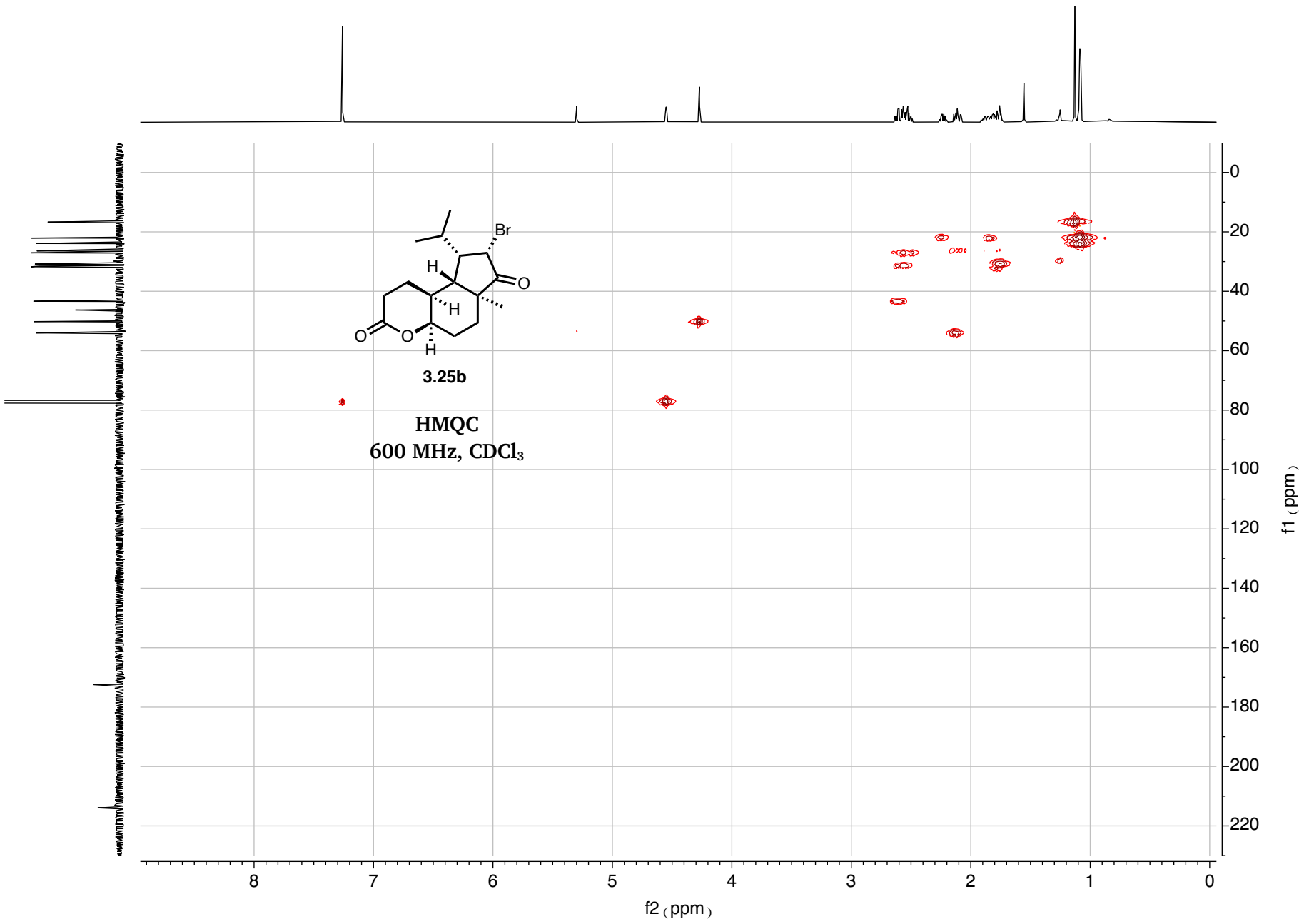
3.25b

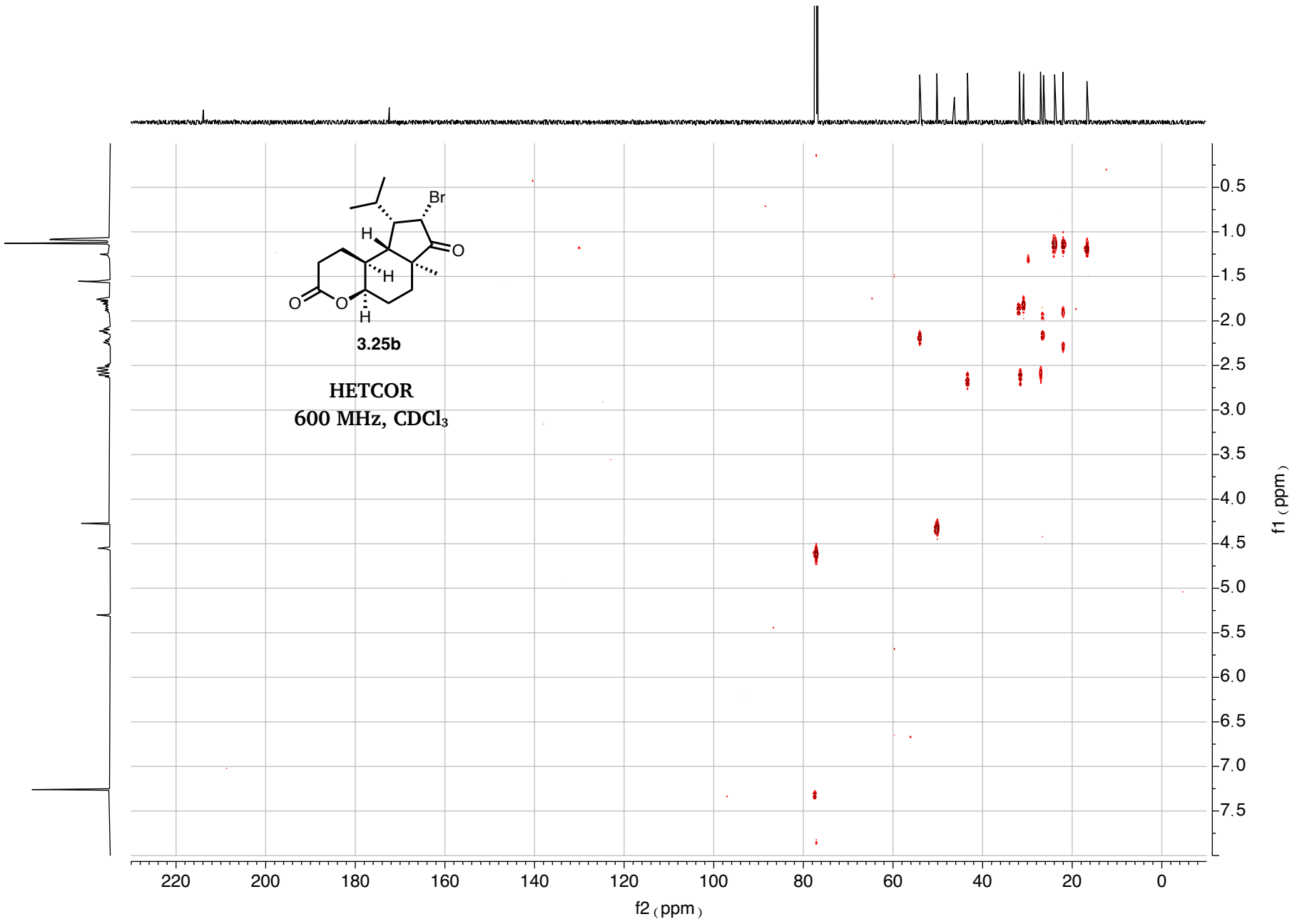
^{13}C NMR
151 MHz, $CDCl_3$

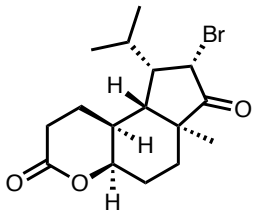


3.25b

DEPTQ
151 MHz, $CDCl_3$

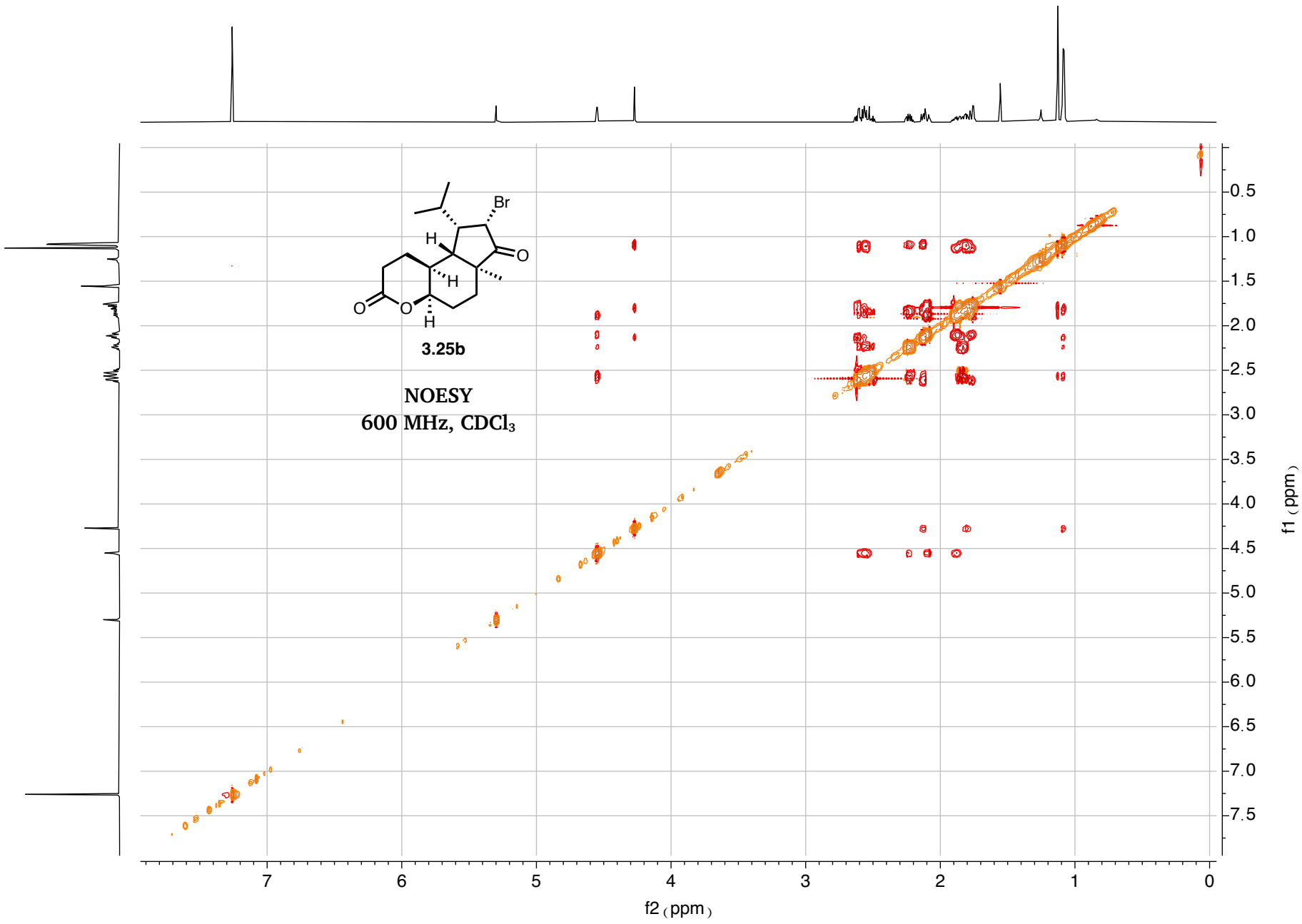

Br
H
O
H
O
O
H
3.25b
HMQC
600 MHz, CDCl3
f2 (ppm)
f1 (ppm)
8
7
6
5
4
3
2
1
0
0
20
40
60
80
100
120
140
160
180
200
220

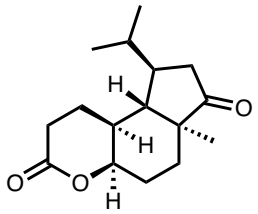

Br
H
H
H
O
O
O
3.25b
HETCOR
600 MHz, CDCl3
220
200
180
160
140
120
100
80
60
40
20
0
f2 (ppm)
0.5
1.0
1.5
2.0
2.5
3.0
3.5
4.0
4.5
5.0
5.5
6.0
6.5
7.0
7.5
f1 (ppm)



3.25b

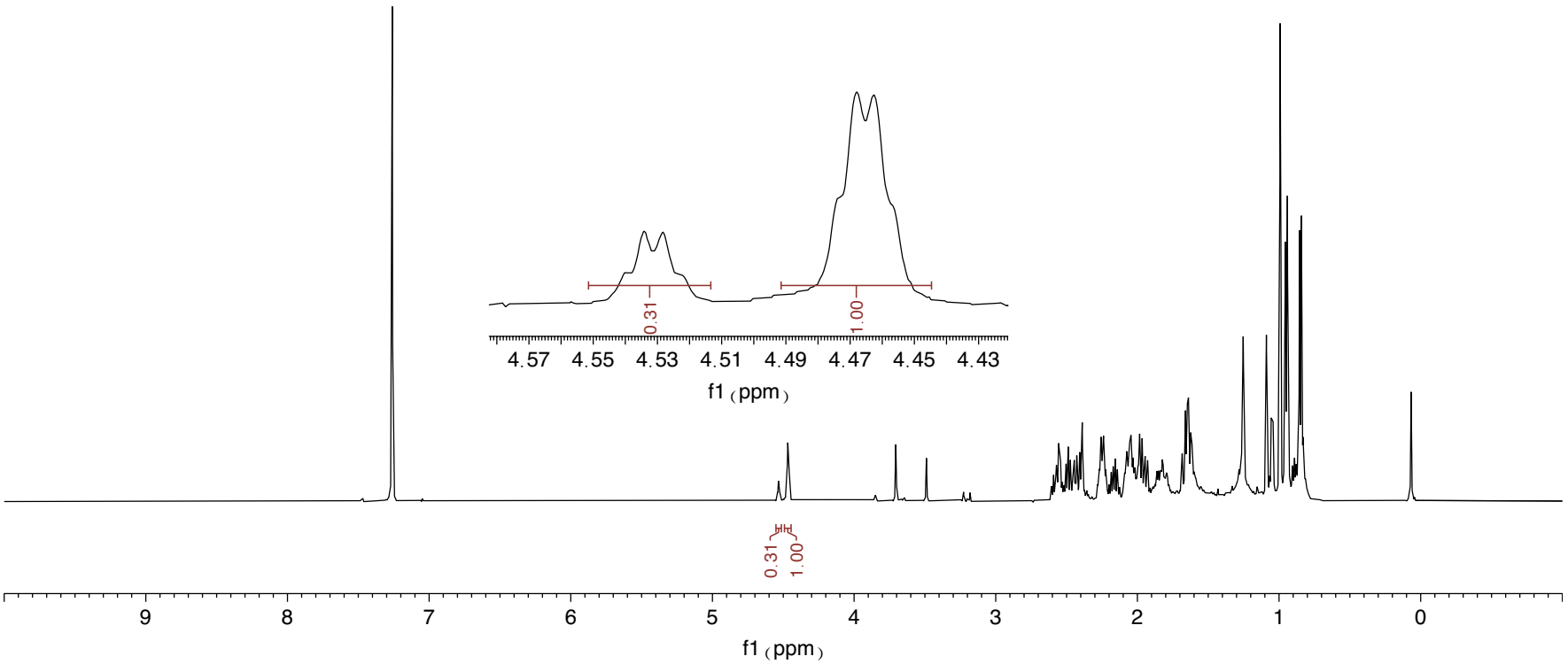
NOE
600 MHz, $CDCl_3$

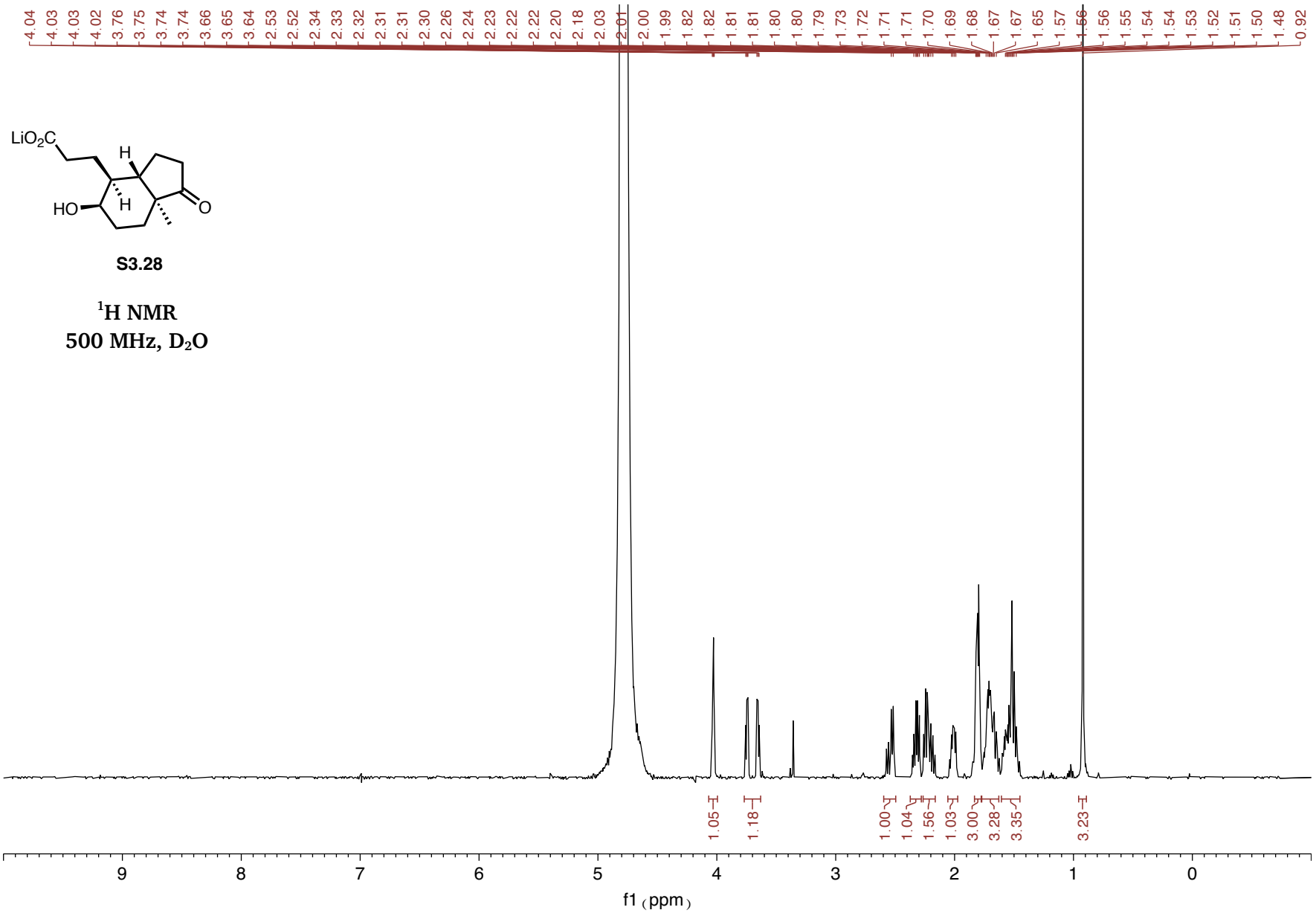

Br
H
H
H
O
O
O
3.25b
NOESY
600 MHz, CDCl3
f2 (ppm)
f1 (ppm)



3.27

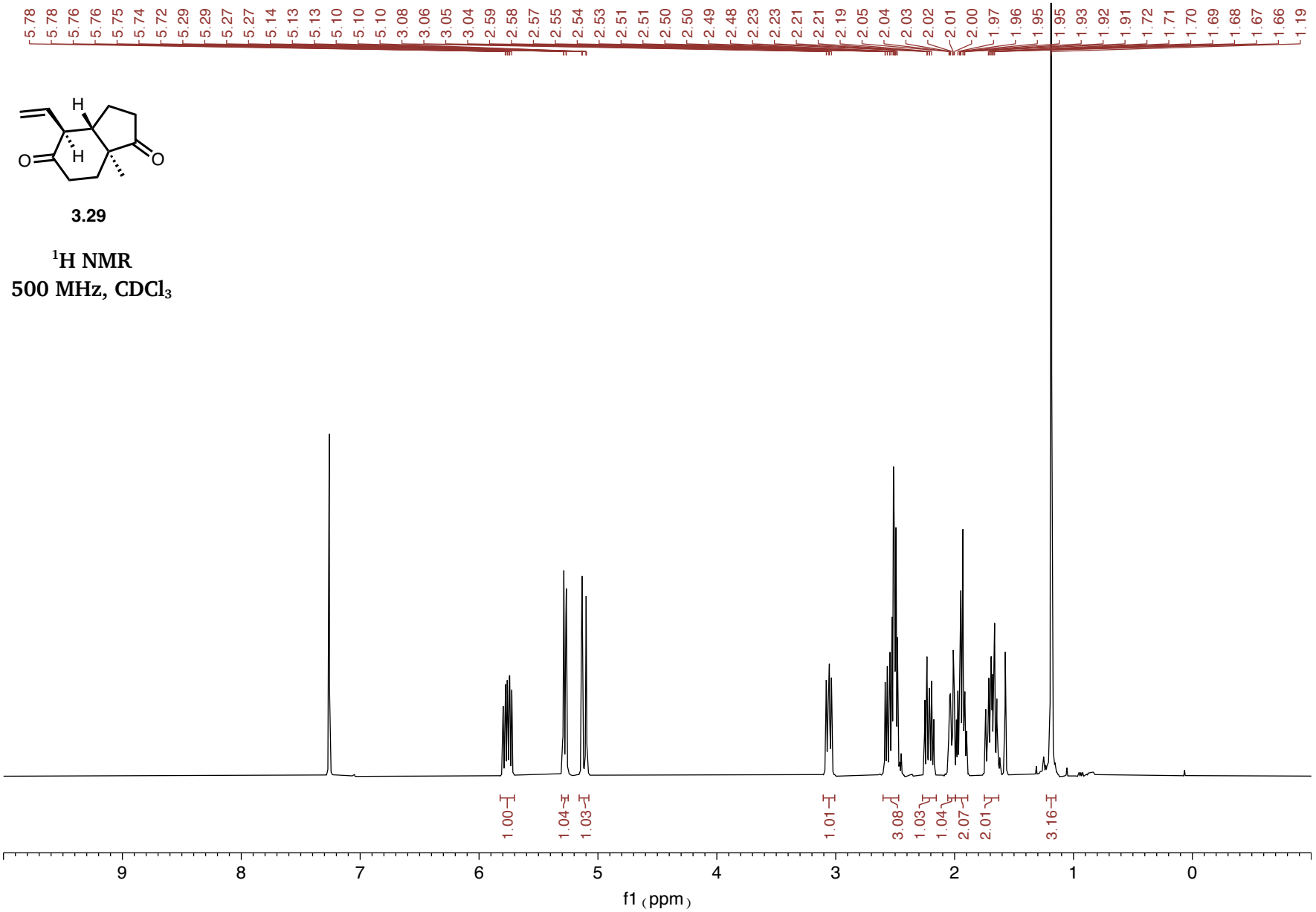
^{1}H NMR
600 MHz, $CDCl_3$





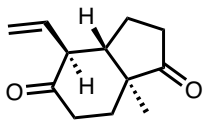
S3.28

^{1}H NMR
500 MHz, D_2O



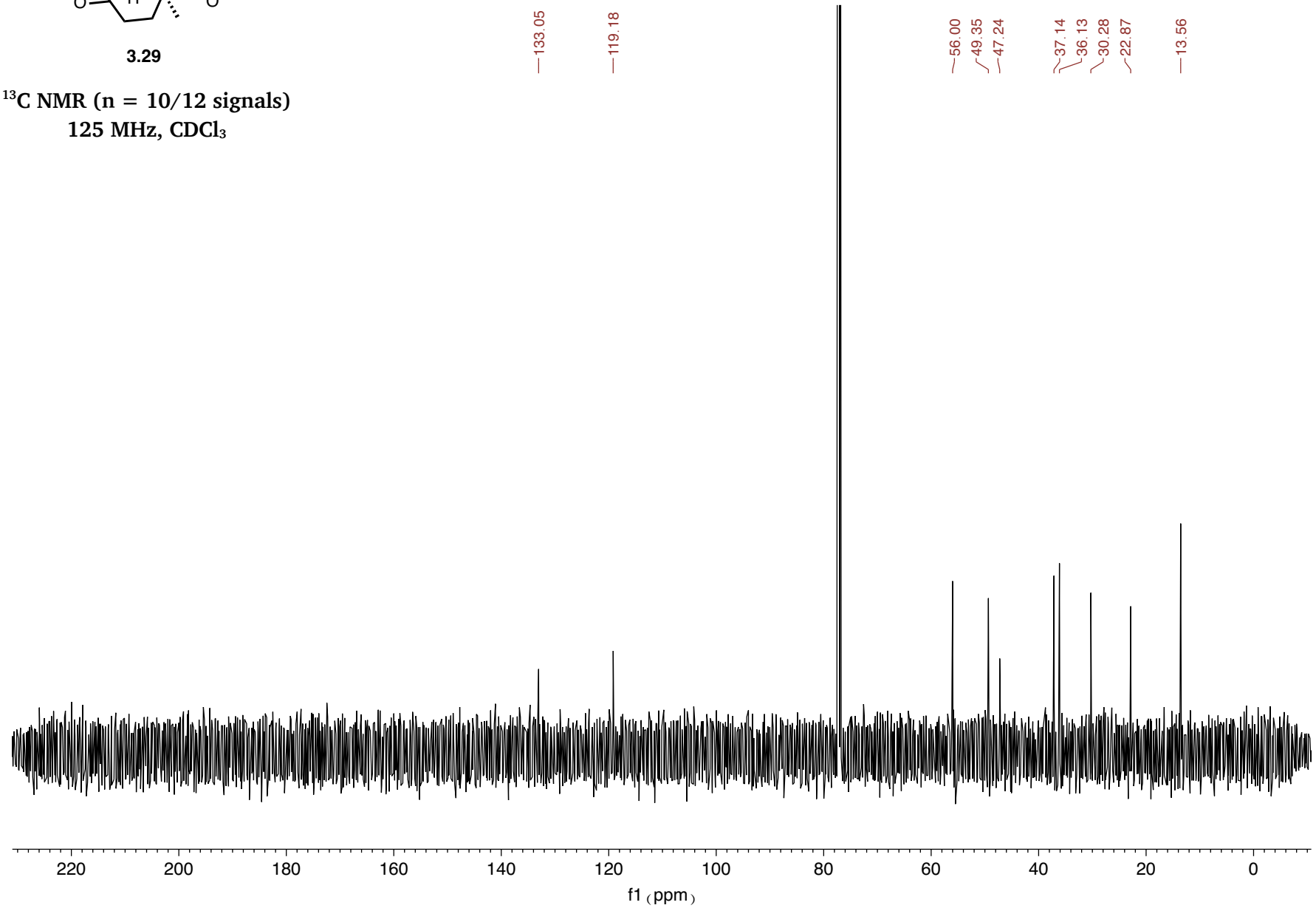
3.29

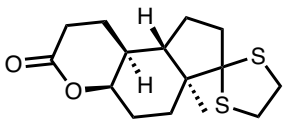
^{1}H NMR
500 MHz, $CDCl_3$



3.29

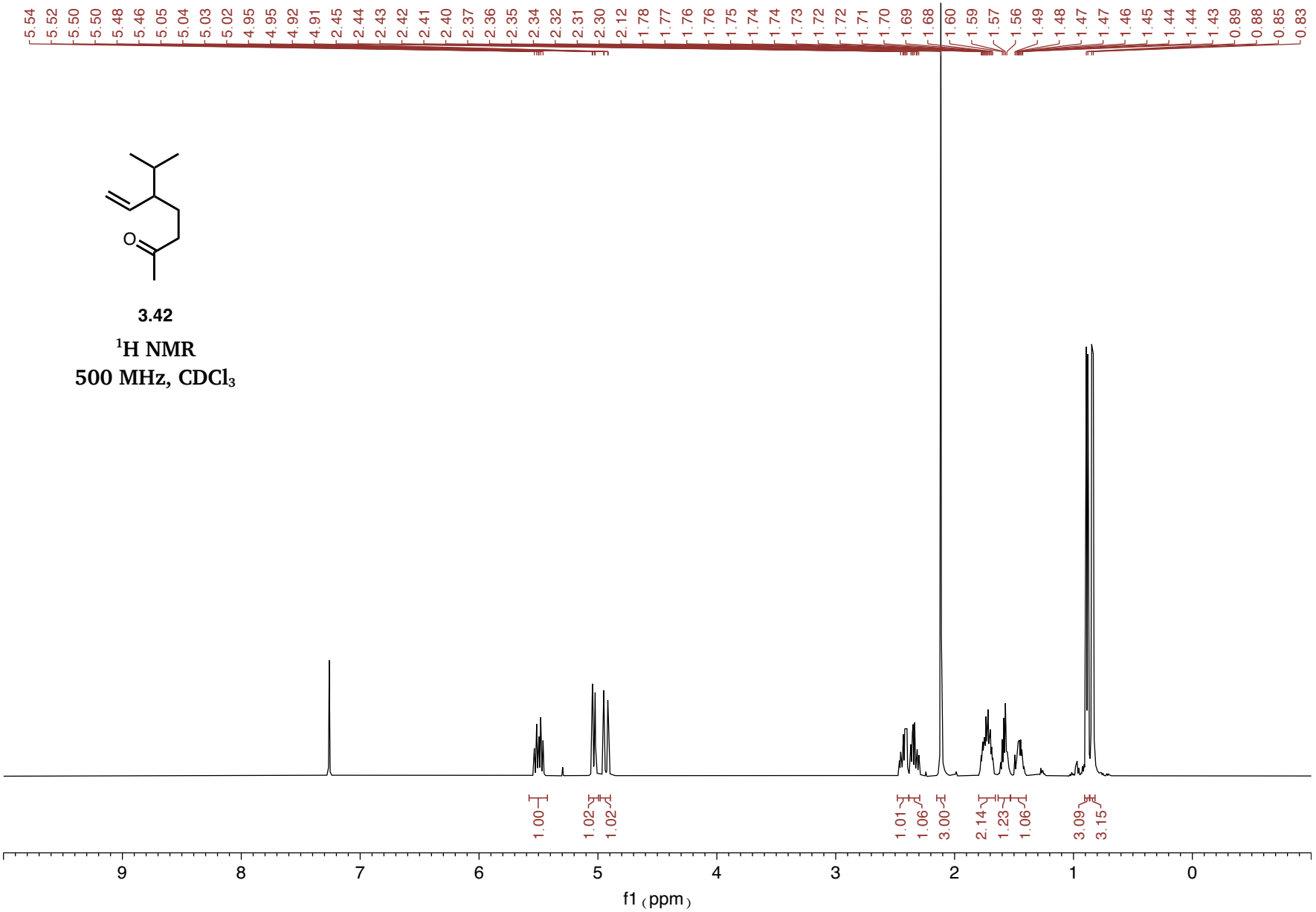
^{13}C NMR (n = 10/12 signals)
125 MHz, $CDCl_3$

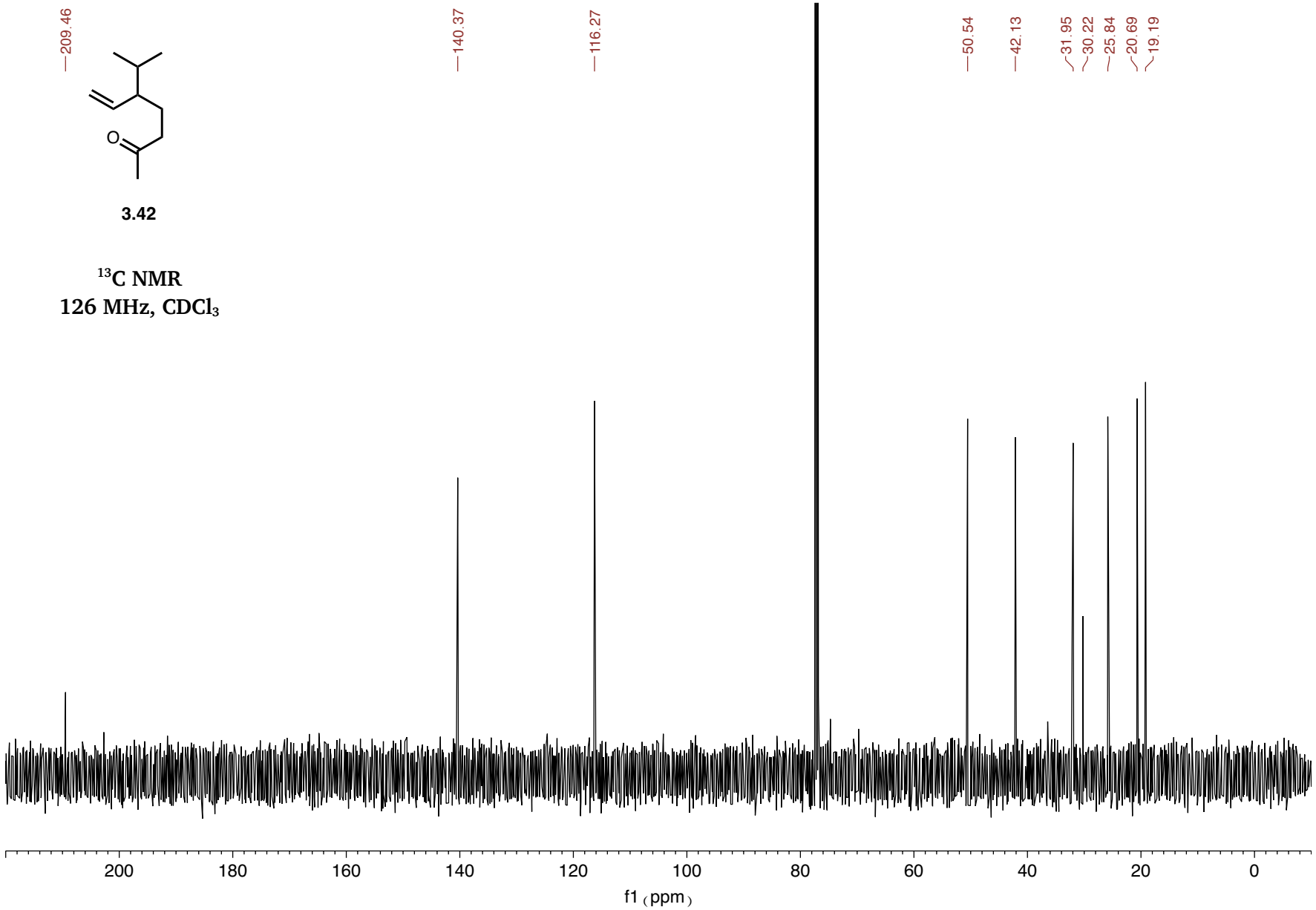




3.30

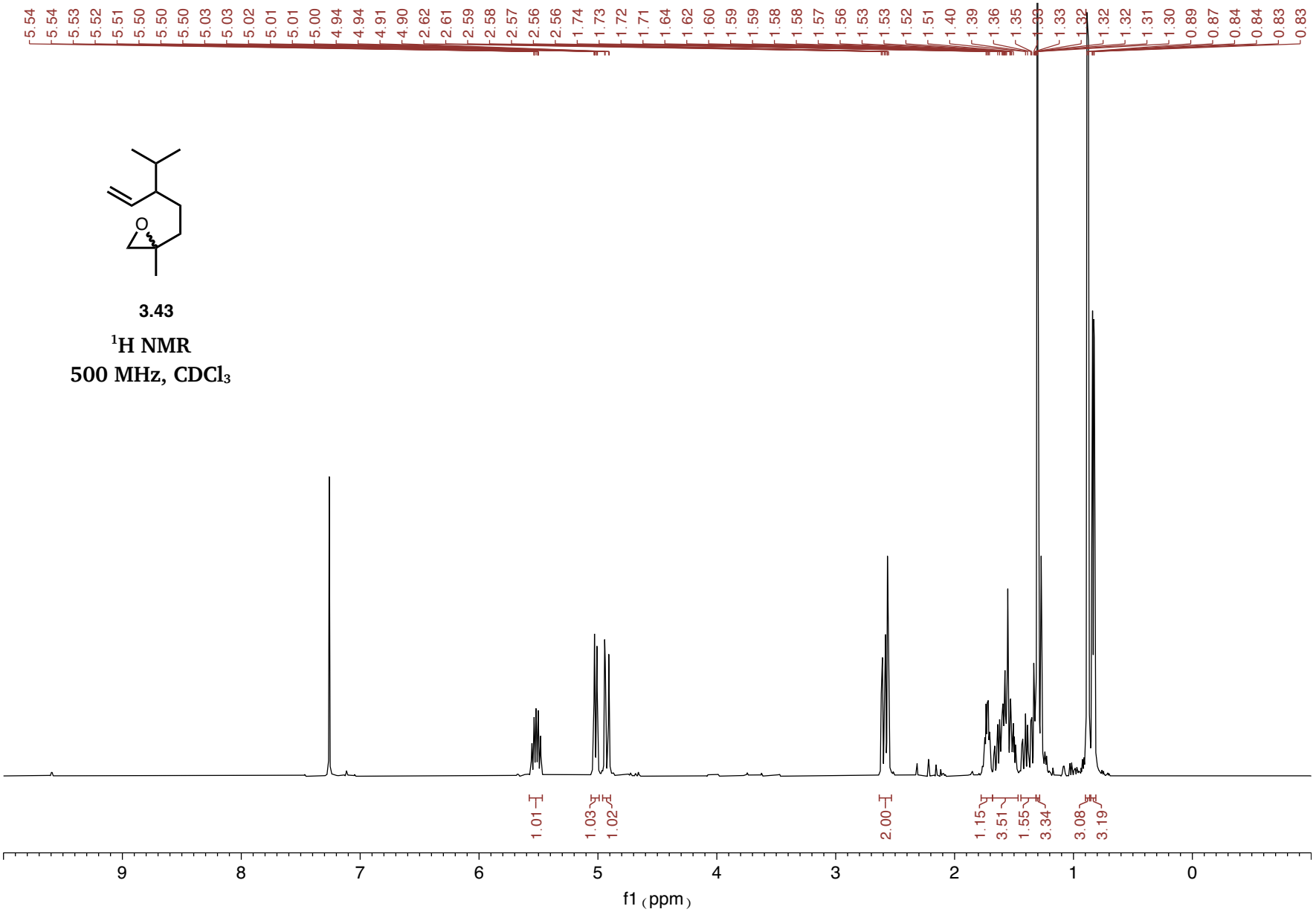
^{1}H NMR
600 MHz, $CDCl_3$

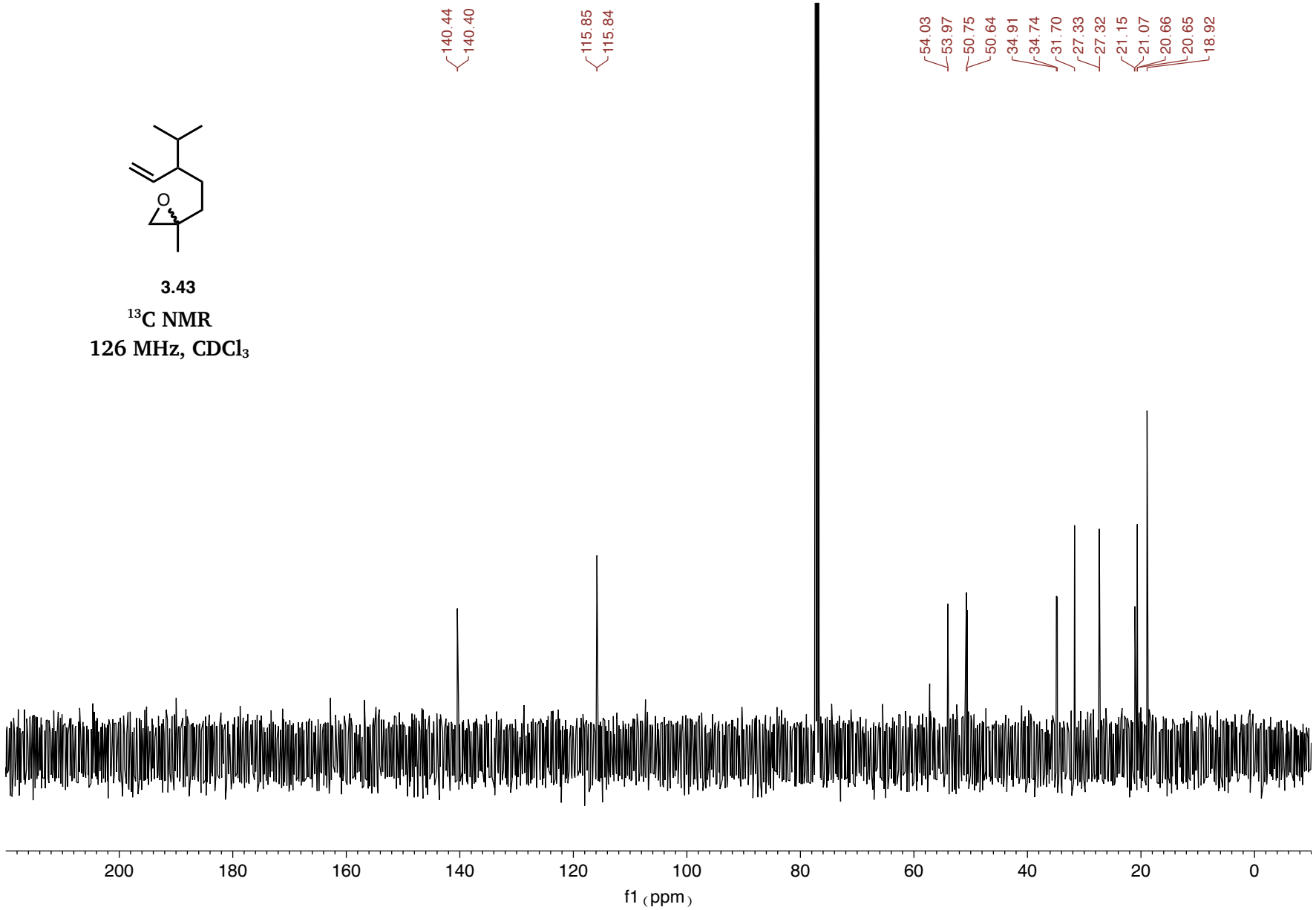

5.54 5.52 5.50 5.50 5.48 5.46 5.05 5.04 5.03 5.02 4.95 4.95 4.92 4.91 2.45 2.44 2.43 2.42 2.41 2.40 2.37 2.36 2.35 2.34 2.32 2.31 2.30 2.12 1.78 1.77 1.76 1.76 1.75 1.74 1.74 1.73 1.72 1.72 1.71 1.70 1.69 1.68 1.60 1.59 1.57 1.56 1.49 1.48 1.47 1.47 1.46 1.45 1.44 1.44 1.43 0.89 0.88 0.85 0.83
O
3.42
1H NMR
500 MHz, CDCl3
1.00 1.02 1.02 1.01 1.06 3.00 2.14 1.23 1.06 3.09 3.15
9 8 7 6 5 4 3 2 1 0
f1 (ppm)



3.42

^{13}C NMR
126 MHz, $CDCl_3$

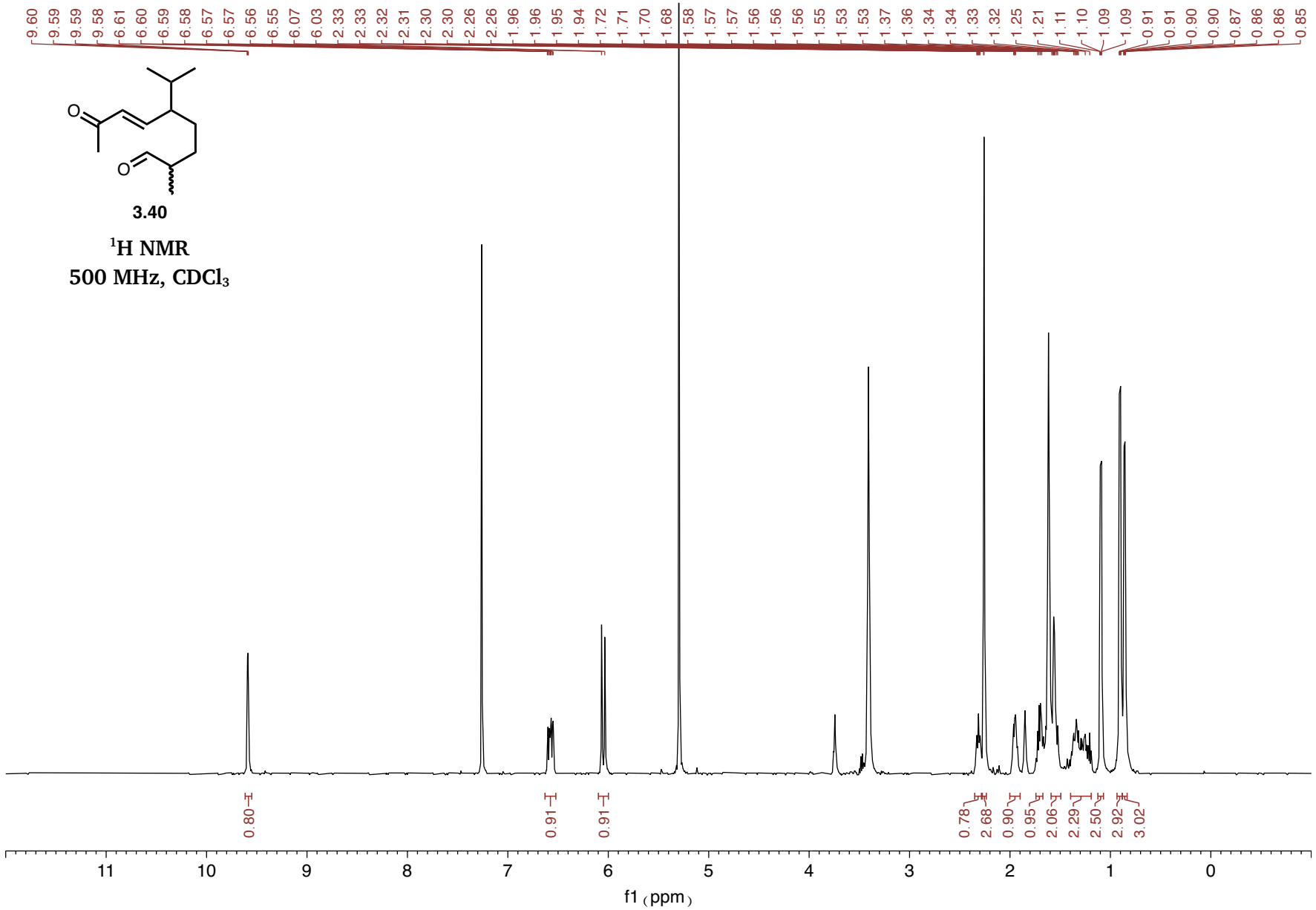

5.54 5.54 5.53 5.52 5.51 5.50 5.50 5.50 5.03 5.03 5.02 5.01 5.01 5.00 4.94 4.94 4.91 4.90 2.62 2.61 2.59 2.58 2.57 2.56 2.56 1.74 1.73 1.72 1.71 1.64 1.62 1.60 1.59 1.59 1.58 1.58 1.57 1.56 1.53 1.53 1.52 1.51 1.40 1.39 1.36 1.35 1.33 1.33 1.32 1.32 1.32 1.31 1.30 0.89 0.87 0.84 0.84 0.83 0.83
O
3.43
1H NMR
500 MHz, CDCl3
1.01 1.03 1.02 2.00 1.15 3.51 1.55 3.34 3.08 3.19
9 8 7 6 5 4 3 2 1 0
f1 (ppm)

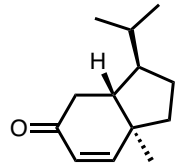


3.43

^{13}C NMR

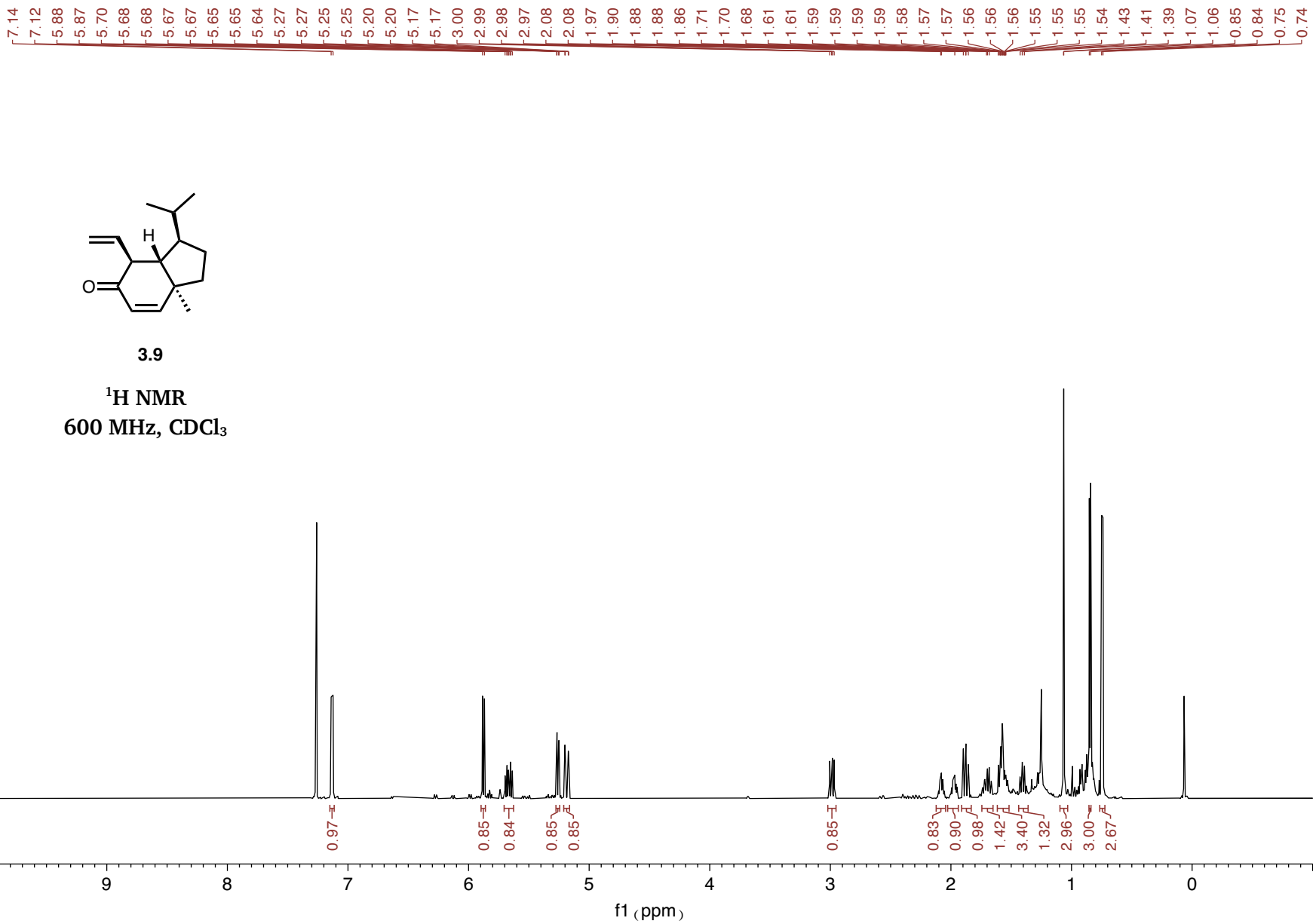
126 MHz, $CDCl_3$


9.60 9.59 9.59 9.58 6.61 6.60 6.59 6.58 6.57 6.57 6.56 6.55 6.07 6.03 2.33 2.33 2.32 2.31 2.30 2.30 2.26 2.26 1.96 1.96 1.95 1.94 1.72 1.71 1.70 1.68 1.58 1.57 1.57 1.56 1.56 1.56 1.55 1.53 1.53 1.37 1.36 1.34 1.34 1.33 1.32 1.25 1.21 1.11 1.10 1.09 1.09 0.91 0.91 0.90 0.90 0.87 0.86 0.86 0.85
O
O
3.40
1H NMR
500 MHz, CDCl3
0.80 0.91 0.91 0.78 2.68 0.90 0.95 2.06 2.29 2.50 2.92 3.02
11 10 9 8 7 6 5 4 3 2 1 0
f1 (ppm)



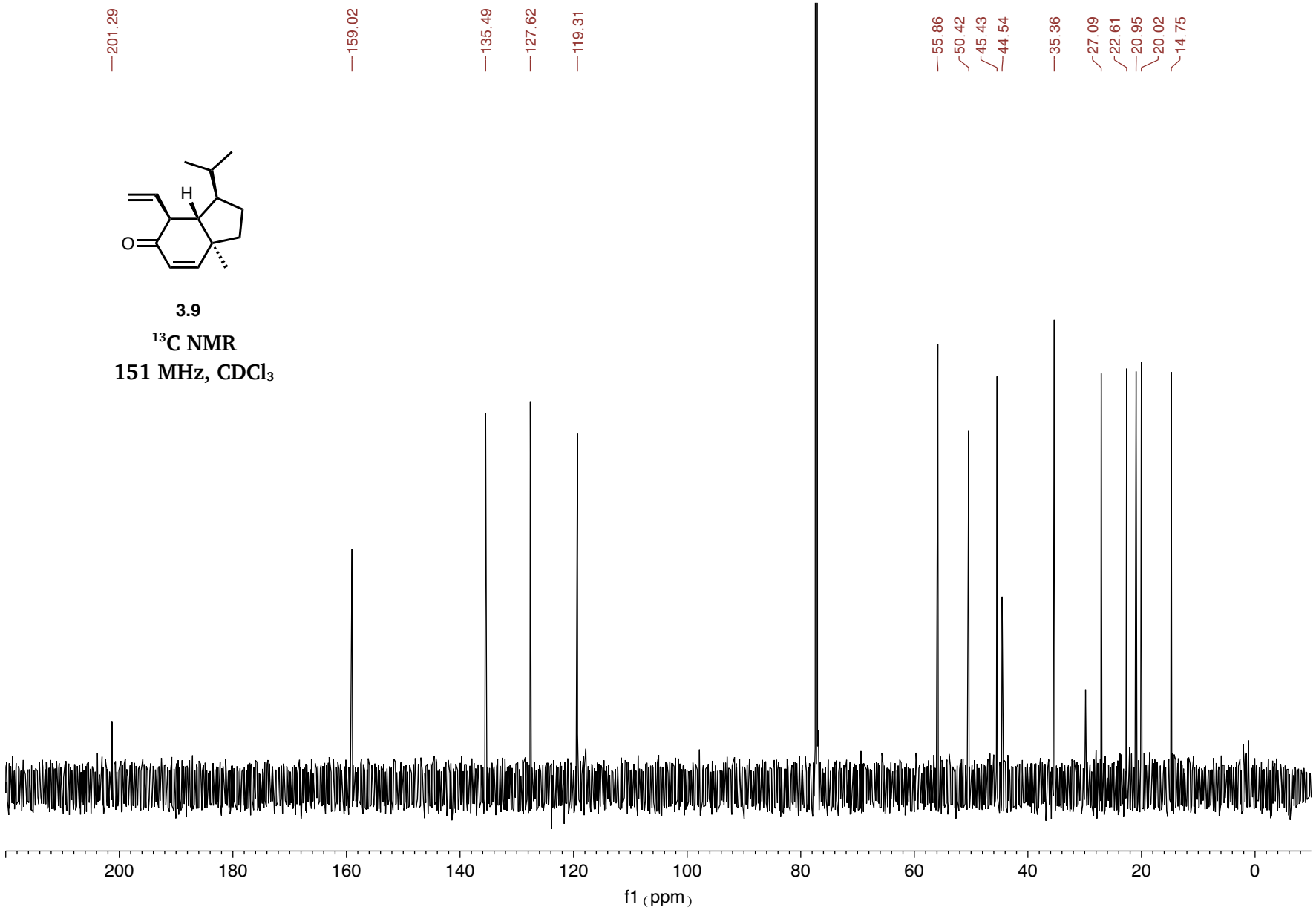
3.32

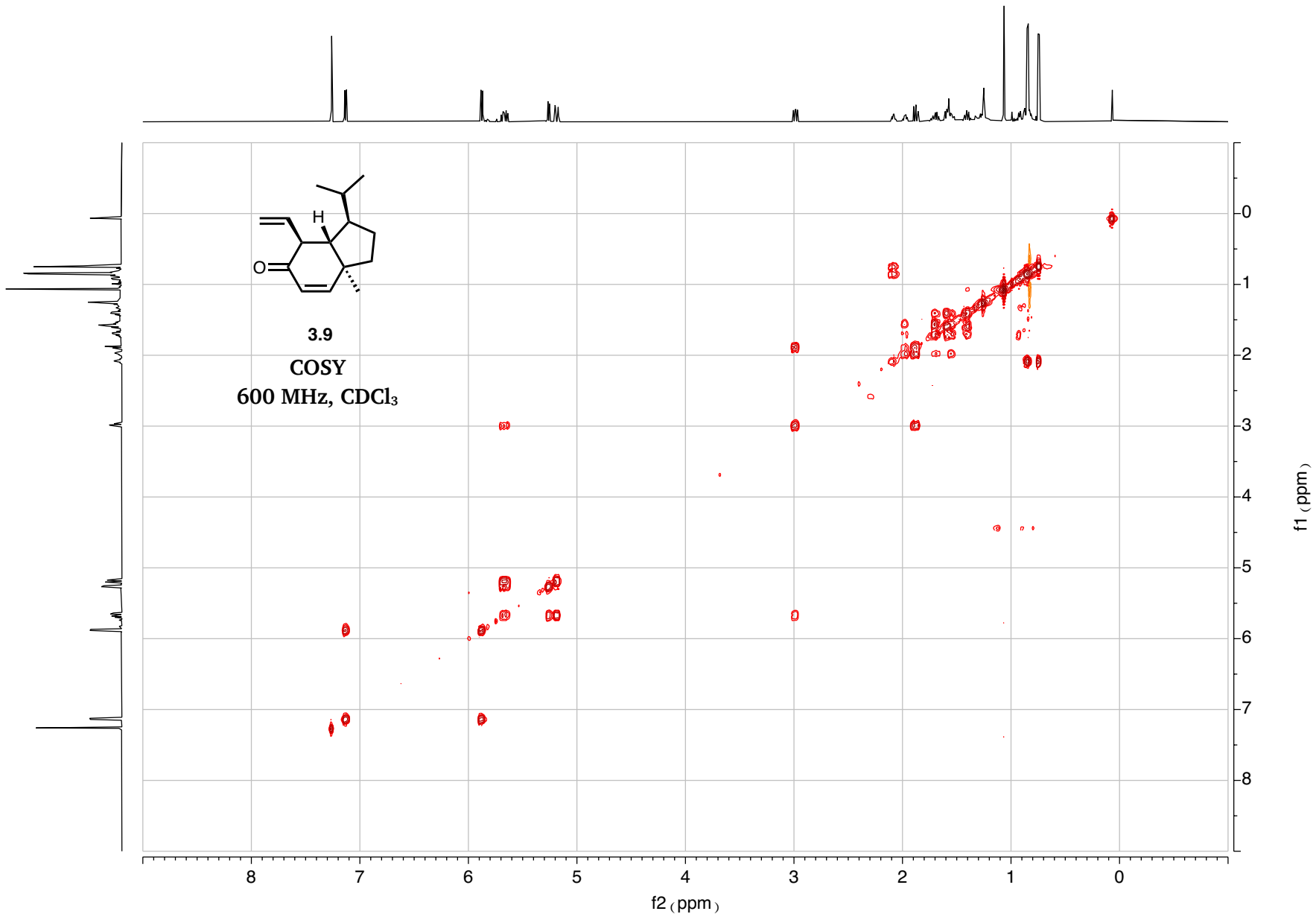
^{1}H NMR
500 MHz, $CDCl_3$

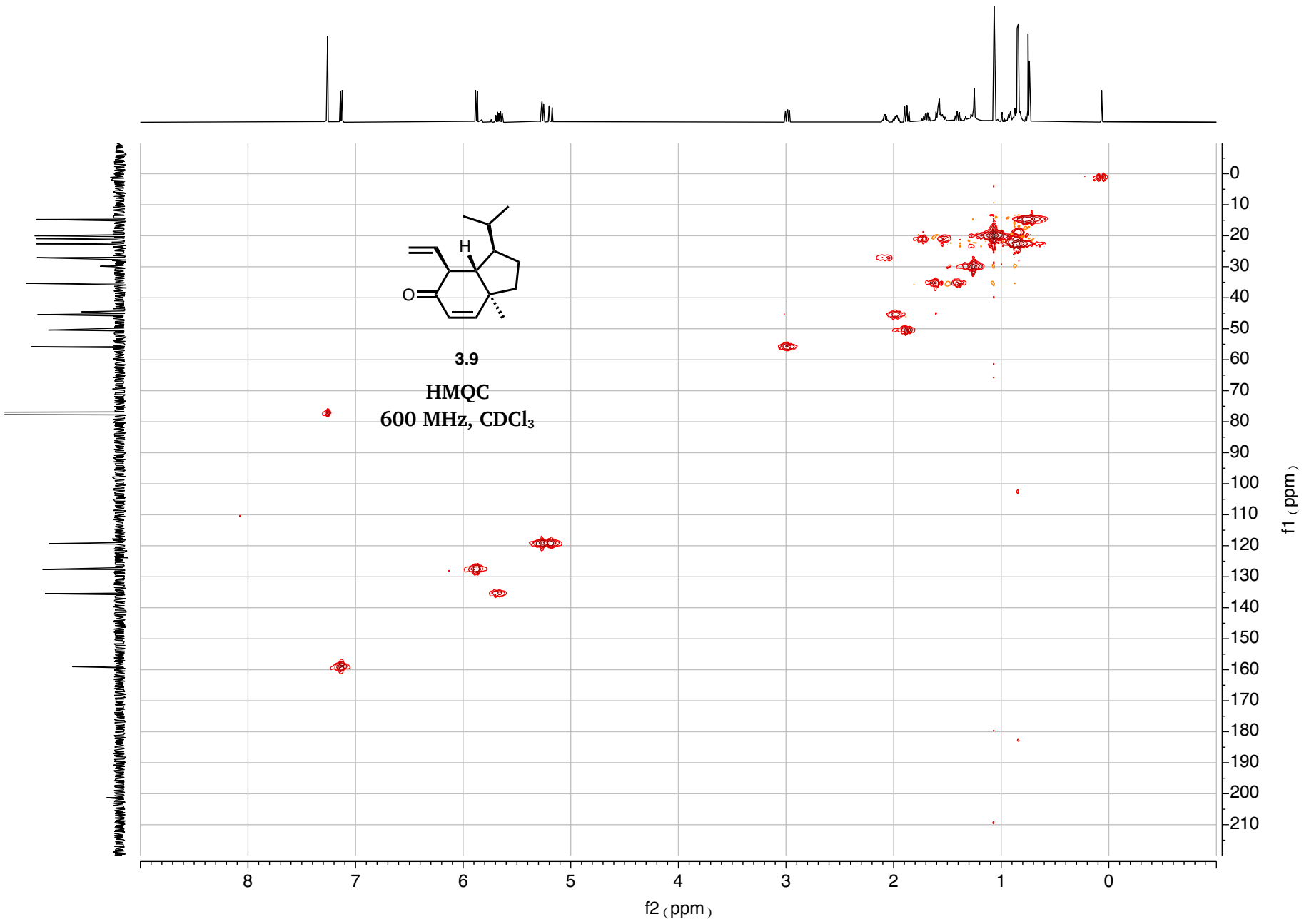


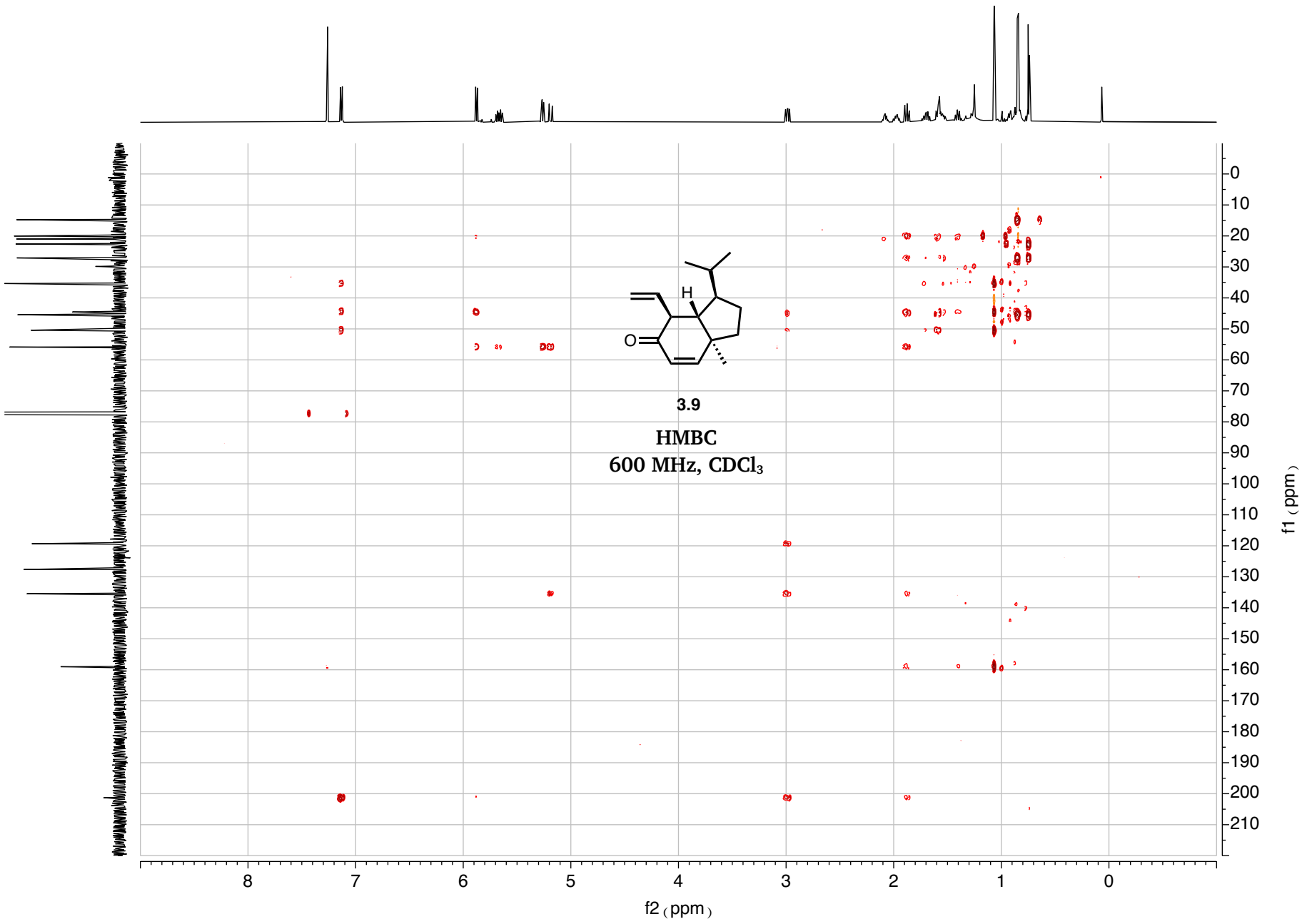
3.9

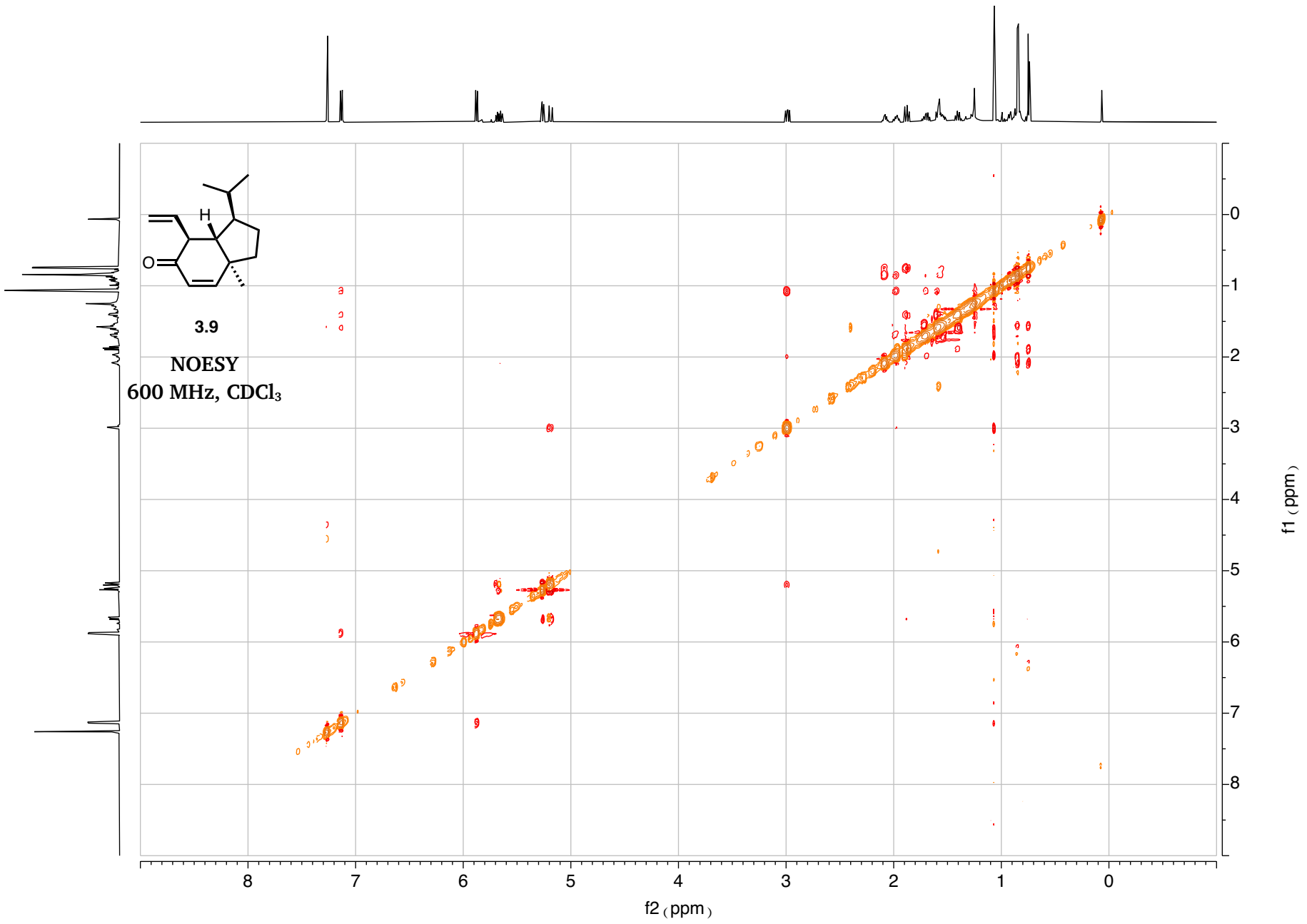
^{1}H NMR
600 MHz, $CDCl_3$

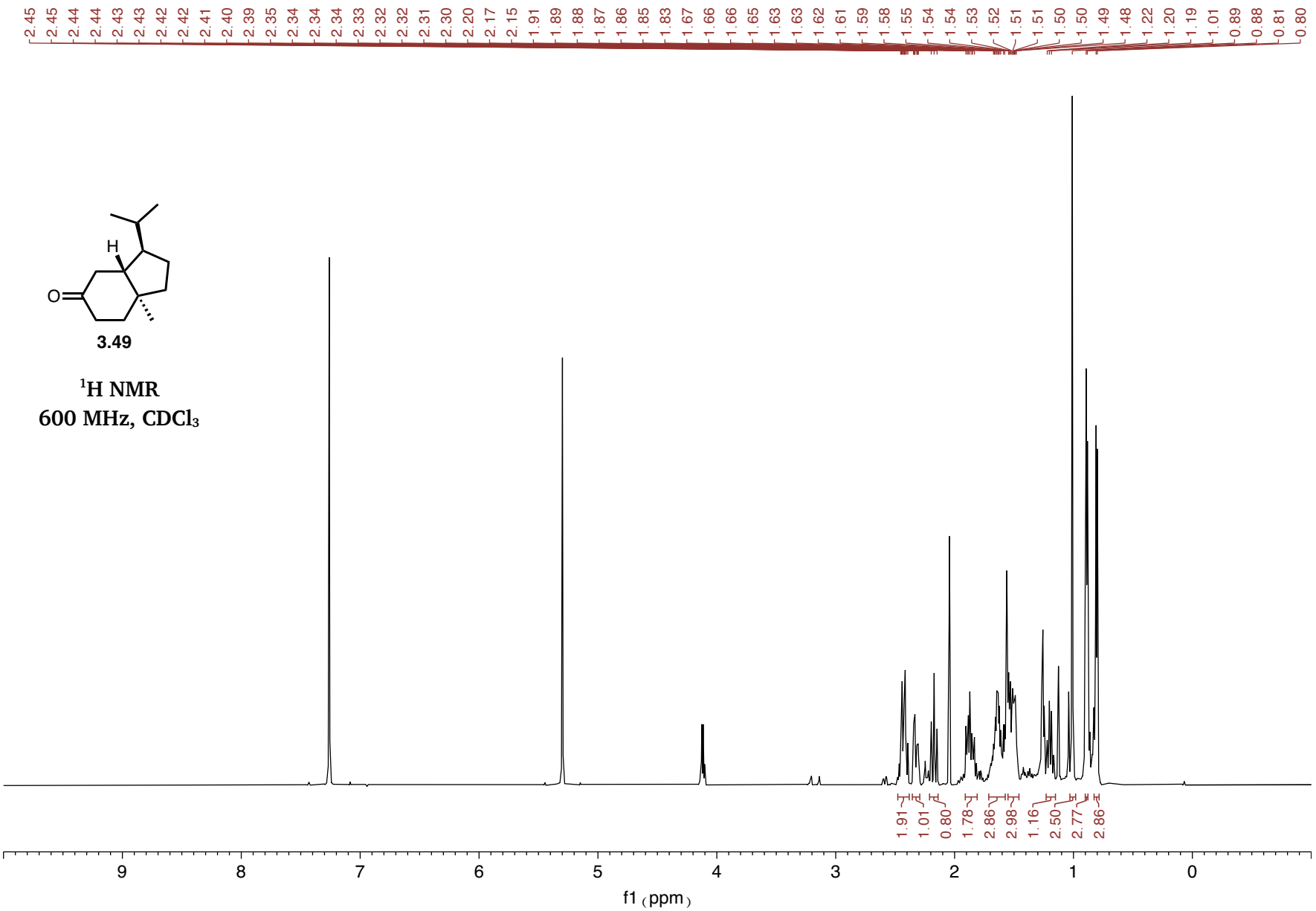

201.29
159.02
135.49
127.62
119.31
55.86
50.42
45.43
44.54
35.36
27.09
22.61
20.95
20.02
14.75
H
O
3.9
13C NMR
151 MHz, CDCl3
200
180
160
140
120
100
80
60
40
20
0
f1 (ppm)

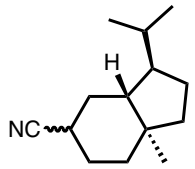

H
O
3.9
COSY
600 MHz, CDCl3
f2 (ppm)
f1 (ppm)


H
O
3.9
HMQC
600 MHz, CDCl3
f2 (ppm)
f1 (ppm)


H
O
3.9
HMBC
600 MHz, CDCl3
f2 (ppm)
f1 (ppm)

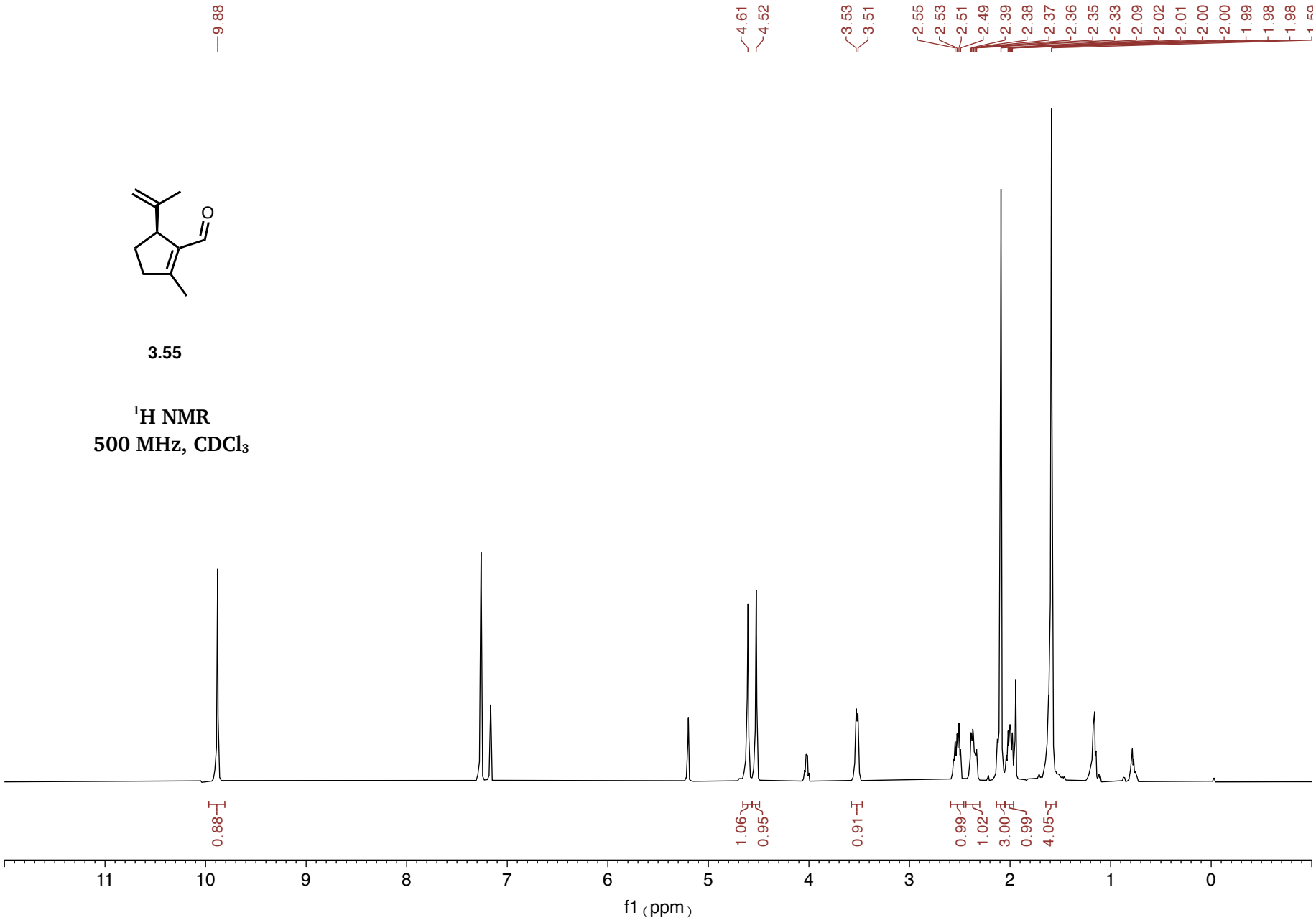

H
O
3.9
NOESY
600 MHz, CDCl3
f2 (ppm)
f1 (ppm)


2.45 2.45 2.44 2.44 2.43 2.43 2.42 2.42 2.41 2.40 2.39 2.35 2.34 2.34 2.34 2.33 2.32 2.32 2.31 2.30 2.20 2.17 2.15 1.91 1.89 1.88 1.87 1.86 1.85 1.83 1.67 1.66 1.66 1.65 1.63 1.63 1.62 1.61 1.59 1.58 1.55 1.54 1.54 1.53 1.52 1.51 1.51 1.50 1.50 1.49 1.48 1.22 1.20 1.19 1.01 0.89 0.88 0.81 0.80
H
O
3.49
1H NMR
600 MHz, CDCl3
1.91 1.01 0.80 1.78 2.86 2.98 1.16 2.50 2.77 2.86
9 8 7 6 5 4 3 2 1 0
f1 (ppm)



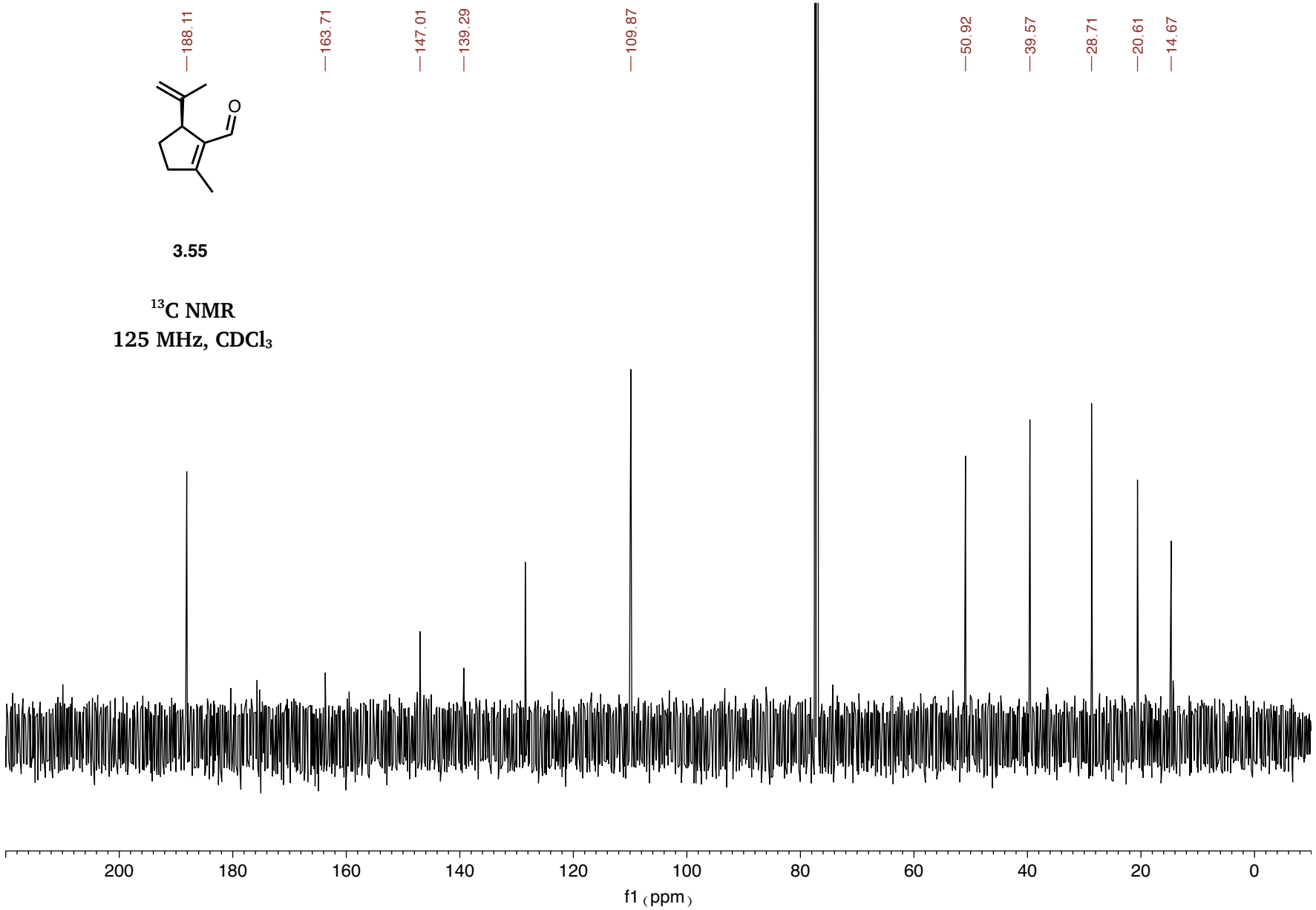
3.50

^{13}C NMR
151 MHz, $CDCl_3$



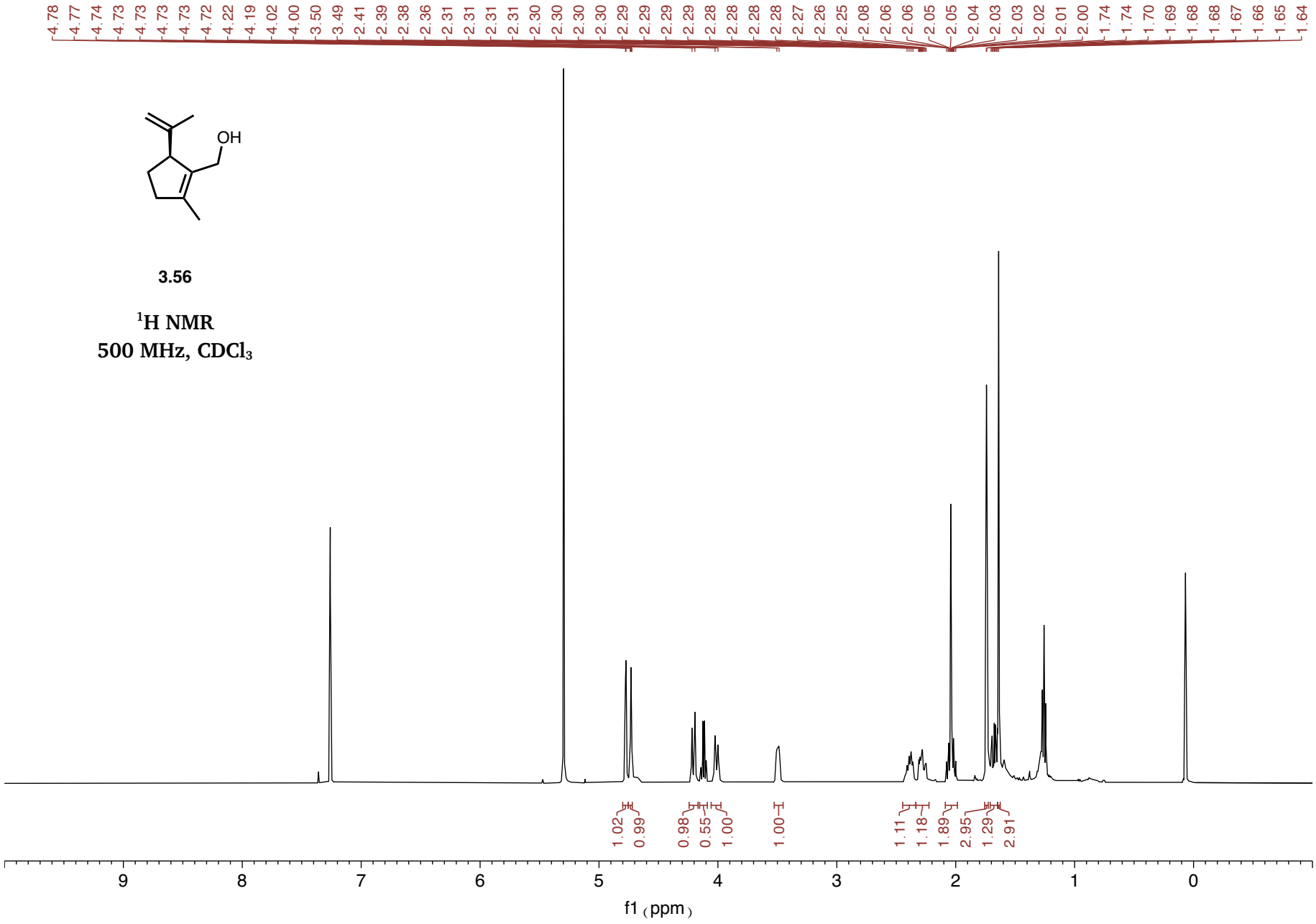
3.55

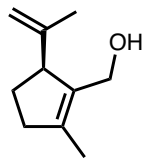
^{1}H NMR
500 MHz, $CDCl_3$



3.55

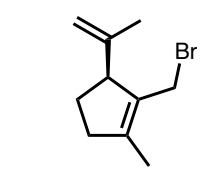
^{13}C NMR
125 MHz, $CDCl_3$


4.78 4.77 4.74 4.73 4.73 4.73 4.73 4.72 4.22 4.19 4.02 4.00 3.50 3.49 2.41 2.39 2.38 2.36 2.31 2.31 2.31 2.31 2.30 2.30 2.30 2.30 2.29 2.29 2.29 2.29 2.28 2.28 2.28 2.28 2.27 2.26 2.25 2.08 2.06 2.06 2.05 2.05 2.04 2.03 2.03 2.02 2.01 2.00 1.74 1.74 1.70 1.69 1.68 1.68 1.67 1.66 1.65 1.64
OH
3.56
1H NMR
500 MHz, CDCl3
1.02 0.99 0.98 0.55 1.00 1.00 1.11 1.18 1.89 2.95 1.29 2.91
9 8 7 6 5 4 3 2 1 0
f1 (ppm)



3.56

^{13}C NMR
125 MHz, $CDCl_3$



3.12

^{1}H NMR
500 MHz, $CDCl_3$

Appendix C

C2: X-Ray Crystallographic Data

X-ray Data Collection, Structure Solution and Refinement for cdv114.

A colorless crystal of approximate dimensions 0.095 x 0.115 x 0.276 mm was mounted on a glass fiber and transferred to a Bruker X8 Prospector diffractometer system. The APEX3[1] program package was used to determine the unit-cell parameters and for data collection (15 sec/frame scan time). The raw frame data was processed using SAINT[2] and SADABS[3] to yield the reflection data file. Subsequent calculations were carried out using the SHELXTL[4] program package. The diffraction symmetry was *mmm* and the systematic absences were consistent with the orthorhombic space group $P2_12_12_1$ that was later determined to be correct.

The structure was solved by direct methods and refined on F^2 by full-matrix least-squares techniques. The analytical scattering factors[5] for neutral atoms were used throughout the analysis. Hydrogen atoms were located from a difference-Fourier map and refined (x,y,z and U_{iso}). There are two molecules of the formula-unit present in the asymmetric unit.

Least squares analysis yielded wR2 = 0.1106 and Goof = 1.150 for 520 variables refined against 4971 data (0.83 Å), R1 = 0.0476 for those 4864 data with $I > 2.0\sigma(I)$. The absolute structure was assigned by refinement of the Flack parameter[6].

References.

1. APEX3 Version 2018.1-0, Bruker AXS, Inc.; Madison, WI 2018.

1. SAINT Version 8.38a, Bruker AXS, Inc.; Madison, WI 2013.

2. Sheldrick, G. M. SADABS, Version 2014/5, Bruker AXS, Inc.; Madison, WI 2014.

3. Sheldrick, G. M. SHELXTL, Version 2014/7, Bruker AXS, Inc.; Madison, WI 2014.

4. International Tables for Crystallography 1992, Vol. C., Dordrecht: Kluwer Academic Publishers.

5. Parsons, S., Flack, H. D., Wagner, T. Acta Cryst. B69, 249-259, 2013.

Definitions:

$wR2 = [\Sigma[w(F_o^2-F_c^2)^2] / \Sigma[w(F_o^2)^2]]^{1/2}$

$R1 = \Sigma||F_o|-|F_c|| / \Sigma|F_o|$

Goof = $S = [\Sigma[w(F_o^2-F_c^2)^2] / (n-p)]^{1/2}$ where n is the number of reflections and p is the total number of parameters refined.

The thermal ellipsoid plot is shown at the 50% probability level.

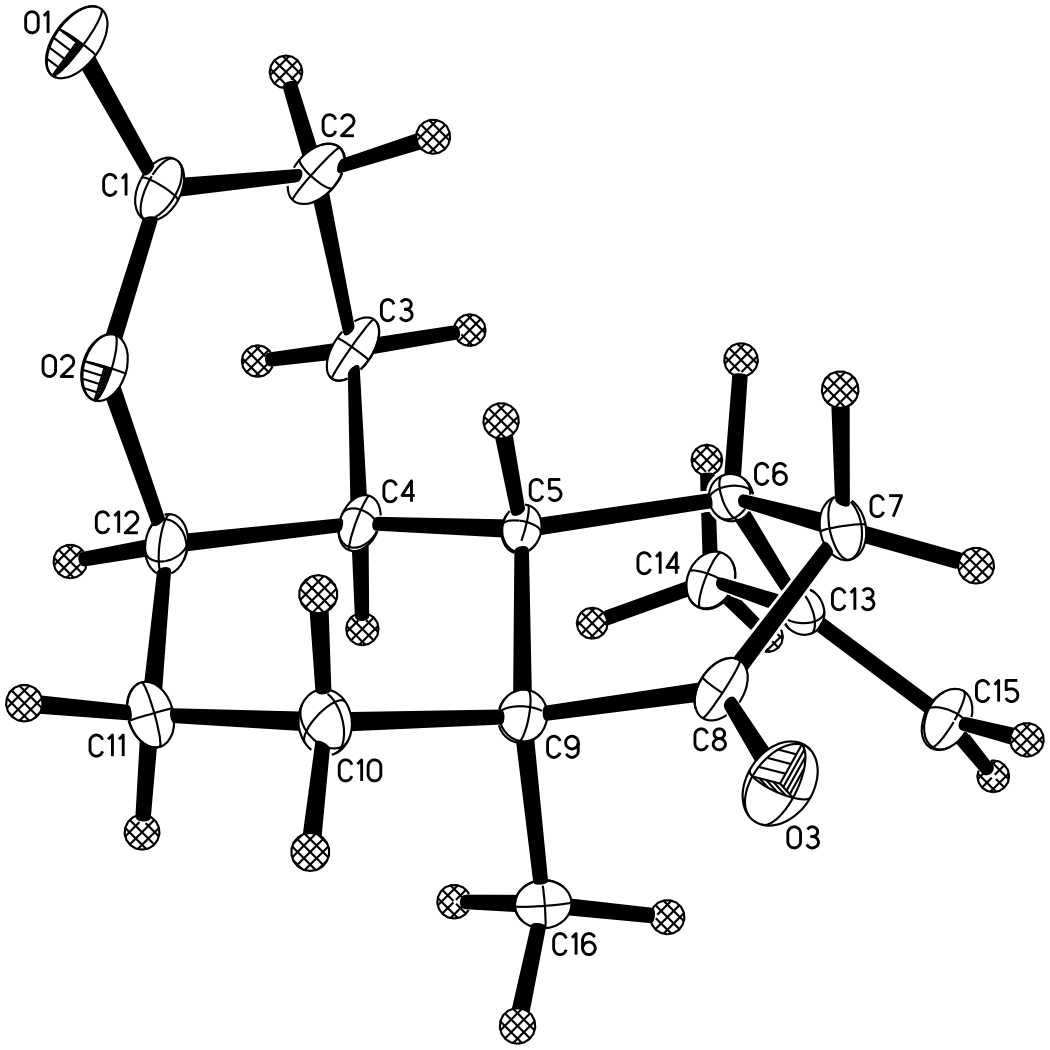

O1
C2
C1
C3
O2
C4
C5
C6
C7
C12
C14
C13
C15
C11
C10
C9
C8
O3
C16

Table 1. Crystal data and structure refinement for cdv114.

Identification code	cdv114 (Lucas Johnson)	
Empirical formula	C_{16} H_{22} O_3	
Formula weight	262.33	
Temperature	93(2) K	
Wavelength	1.54178 Å	
Crystal system	Orthorhombic	
Space group	$P2_12_12_1$	
Unit cell dimensions	a = 7.22090(10) Å	α = 90°.
	b = 13.3211(2) Å	β = 90°.
	c = 28.2631(5) Å	γ = 90°.
Volume	2718.64(7) $Å^3$	
Z	8	
Density (calculated)	1.282 Mg/m^3	
Absorption coefficient	0.696 mm^{-1}	
F(000)	1136	
Crystal color	colorless	
Crystal size	0.276 x 0.115 x 0.095 mm^3	
Theta range for data collection	3.127 to 68.322°	
Index ranges	$-8 \leq h \leq <8$, $-15 \leq k \leq 16$, $-33 \leq l \leq 33$	
Reflections collected	34713	
Independent reflections	4971 [R(int) = 0.0609]	
Completeness to theta = 67.679°	100.0 %	
Absorption correction	Semi-empirical from equivalents	

Max. and min. transmission	0.7531 and 0.6194
Refinement method	Full-matrix least-squares on F^2
Data / restraints / parameters	4971 / 0 / 520
Goodness-of-fit on F^2	1.150
Final R indices [I>2sigma(I) = 4864 data]	R1 = 0.0476, wR2 = 0.1096
R indices (all data, 0.83 Å)	R1 = 0.0483, wR2 = 0.1106
Absolute structure parameter	-0.01(8)
Extinction coefficient	0.0066(8)
Largest diff. peak and hole	0.415 and -0.388 e.$Å^{-3}$

Table 2. Atomic coordinates (x 10^4) and equivalent isotropic displacement parameters ($Å^2$ x 10^3) for cdv114. U(eq) is defined as one third of the trace of the orthogonalized U^{ij} tensor.

	x	y	z	U(eq)
O(1)	3549(2)	6534(1)	6540(1)	20(1)
O(2)	3090(2)	5170(1)	6123(1)	18(1)
O(3)	8478(2)	3939(1)	4823(1)	23(1)
C(1)	3088(3)	6172(2)	6164(1)	15(1)
C(2)	2604(3)	6819(2)	5743(1)	17(1)
C(3)	1545(3)	6273(2)	5351(1)	17(1)
C(4)	2361(3)	5234(2)	5255(1)	14(1)
C(5)	4355(3)	5255(2)	5080(1)	11(1)
C(6)	4994(3)	5861(2)	4638(1)	11(1)
C(7)	7061(3)	5550(2)	4638(1)	15(1)
C(8)	7119(3)	4473(2)	4827(1)	14(1)
C(9)	5216(3)	4204(2)	5025(1)	14(1)
C(10)	5259(3)	3699(2)	5514(1)	20(1)
C(11)	3280(4)	3626(2)	5706(1)	23(1)
C(12)	2268(3)	4631(2)	5718(1)	18(1)
C(13)	3992(3)	5720(2)	4167(1)	13(1)
C(14)	1989(3)	6036(2)	4149(1)	16(1)
C(15)	4826(3)	5408(2)	3776(1)	19(1)
C(16)	4247(4)	3523(2)	4659(1)	19(1)

O(4)	7357(2)	6403(1)	5869(1)	19(1)
O(5)	8324(2)	5249(1)	6361(1)	18(1)
O(6)	2702(3)	3952(2)	7578(1)	26(1)
C(17)	7921(3)	6211(2)	6265(1)	14(1)
C(18)	8153(3)	7003(2)	6641(1)	14(1)
C(19)	9204(3)	6664(2)	7083(1)	14(1)
C(20)	8629(3)	5600(2)	7227(1)	11(1)
C(21)	6563(3)	5506(2)	7340(1)	10(1)
C(22)	5528(3)	6185(2)	7703(1)	11(1)
C(23)	3591(3)	5703(2)	7664(1)	15(1)
C(24)	3896(3)	4591(2)	7563(1)	15(1)
C(25)	5934(3)	4420(2)	7441(1)	12(1)
C(26)	6287(3)	3796(2)	6994(1)	17(1)
C(27)	8347(3)	3832(2)	6867(1)	19(1)
C(28)	9087(3)	4896(2)	6815(1)	15(1)
C(29)	6254(3)	6303(2)	8208(1)	14(1)
C(30)	8096(3)	6812(2)	8262(1)	18(1)
C(31)	5269(4)	6076(2)	8593(1)	21(1)
C(32)	6829(3)	3923(2)	7880(1)	17(1)

Table 3. Bond lengths [Å] and angles [°] for cdv114.

O(1)-C(1)	1.214(3)
O(2)-C(1)	1.340(3)
O(2)-C(12)	1.475(3)
O(3)-C(8)	1.212(3)
C(1)-C(2)	1.509(3)
C(2)-C(3)	1.530(3)
C(2)-H(2A)	1.01(3)
C(2)-H(2B)	0.98(4)
C(3)-C(4)	1.528(3)
C(3)-H(3A)	0.98(4)
C(3)-H(3B)	1.02(3)
C(4)-C(5)	1.522(3)
C(4)-C(12)	1.537(3)
C(4)-H(4)	1.03(3)
C(5)-C(9)	1.539(3)
C(5)-C(6)	1.559(3)
C(5)-H(5)	0.96(3)
C(6)-C(13)	1.526(3)
C(6)-C(7)	1.550(3)
C(6)-H(6)	1.04(3)
C(7)-C(8)	1.531(3)
C(7)-H(7A)	1.05(4)

C(7)-H(7B)	0.93(4)
C(8)-C(9)	1.526(3)
C(9)-C(10)	1.536(3)
C(9)-C(16)	1.545(3)
C(10)-C(11)	1.532(3)
C(10)-H(10A)	1.02(3)
C(10)-H(10B)	0.99(4)
C(11)-C(12)	1.526(3)
C(11)-H(11A)	1.01(4)
C(11)-H(11B)	0.95(4)
C(12)-H(12)	0.98(3)
C(13)-C(15)	1.327(3)
C(13)-C(14)	1.507(3)
C(14)-H(14A)	0.98(3)
C(14)-H(14B)	0.96(4)
C(14)-H(14C)	0.94(3)
C(15)-H(15A)	0.94(4)
C(15)-H(15B)	1.04(4)
C(16)-H(16A)	1.02(4)
C(16)-H(16B)	0.96(3)
C(16)-H(16C)	1.01(5)
O(4)-C(17)	1.216(3)
O(5)-C(17)	1.342(3)
O(5)-C(28)	1.474(3)

O(6)-C(24)	1.212(3)
C(17)-C(18)	1.508(3)
C(18)-C(19)	1.528(3)
C(18)-H(18A)	0.99(4)
C(18)-H(18B)	0.98(4)
C(19)-C(20)	1.533(3)
C(19)-H(19A)	0.97(3)
C(19)-H(19B)	0.99(3)
C(20)-C(21)	1.530(3)
C(20)-C(28)	1.532(3)
C(20)-H(20)	0.98(3)
C(21)-C(25)	1.543(3)
C(21)-C(22)	1.559(3)
C(21)-H(21)	1.00(3)
C(22)-C(29)	1.528(3)
C(22)-C(23)	1.542(3)
C(22)-H(22)	1.01(3)
C(23)-C(24)	1.525(3)
C(23)-H(23A)	0.99(4)
C(23)-H(23B)	1.04(3)
C(24)-C(25)	1.529(3)
C(25)-C(26)	1.533(3)
C(25)-C(32)	1.549(3)
C(26)-C(27)	1.531(3)

C(26)-H(26A)	1.04(3)
C(26)-H(26B)	1.00(4)
C(27)-C(28)	1.522(3)
C(27)-H(27A)	0.92(3)
C(27)-H(27B)	1.02(4)
C(28)-H(28)	0.95(3)
C(29)-C(31)	1.335(3)
C(29)-C(30)	1.501(3)
C(30)-H(30A)	1.01(4)
C(30)-H(30B)	0.94(4)
C(30)-H(30C)	0.99(4)
C(31)-H(31A)	0.95(4)
C(31)-H(31B)	0.99(4)
C(32)-H(32A)	0.95(4)
C(32)-H(32B)	0.99(3)
C(32)-H(32C)	0.93(4)

C(1)-O(2)-C(12)	123.43(17)
O(1)-C(1)-O(2)	118.1(2)
O(1)-C(1)-C(2)	121.8(2)
O(2)-C(1)-C(2)	120.07(19)
C(1)-C(2)-C(3)	114.5(2)
C(1)-C(2)-H(2A)	103.6(18)
C(3)-C(2)-H(2A)	109.9(18)

C(1)-C(2)-H(2B)	108.8(18)
C(3)-C(2)-H(2B)	111.8(19)
H(2A)-C(2)-H(2B)	108(3)
C(4)-C(3)-C(2)	111.49(18)
C(4)-C(3)-H(3A)	109(2)
C(2)-C(3)-H(3A)	108.5(19)
C(4)-C(3)-H(3B)	111.3(19)
C(2)-C(3)-H(3B)	107.0(19)
H(3A)-C(3)-H(3B)	109(3)
C(5)-C(4)-C(3)	113.94(18)
C(5)-C(4)-C(12)	109.09(17)
C(3)-C(4)-C(12)	107.74(18)
C(5)-C(4)-H(4)	113.9(17)
C(3)-C(4)-H(4)	107.1(17)
C(12)-C(4)-H(4)	104.5(17)
C(4)-C(5)-C(9)	113.48(17)
C(4)-C(5)-C(6)	123.36(17)
C(9)-C(5)-C(6)	105.69(16)
C(4)-C(5)-H(5)	105.7(16)
C(9)-C(5)-H(5)	105.0(15)
C(6)-C(5)-H(5)	101.6(15)
C(13)-C(6)-C(7)	115.05(17)
C(13)-C(6)-C(5)	119.68(17)
C(7)-C(6)-C(5)	98.43(16)

C(13)-C(6)-H(6)	105.0(18)
C(7)-C(6)-H(6)	111.2(19)
C(5)-C(6)-H(6)	107.4(18)
C(8)-C(7)-C(6)	106.06(17)
C(8)-C(7)-H(7A)	108(2)
C(6)-C(7)-H(7A)	108(2)
C(8)-C(7)-H(7B)	111(2)
C(6)-C(7)-H(7B)	117(2)
H(7A)-C(7)-H(7B)	107(3)
O(3)-C(8)-C(9)	126.5(2)
O(3)-C(8)-C(7)	124.6(2)
C(9)-C(8)-C(7)	108.87(17)
C(8)-C(9)-C(10)	114.47(18)
C(8)-C(9)-C(5)	100.82(17)
C(10)-C(9)-C(5)	108.41(16)
C(8)-C(9)-C(16)	107.40(17)
C(10)-C(9)-C(16)	110.75(18)
C(5)-C(9)-C(16)	114.78(18)
C(11)-C(10)-C(9)	109.09(19)
C(11)-C(10)-H(10A)	109.6(18)
C(9)-C(10)-H(10A)	109.4(18)
C(11)-C(10)-H(10B)	108(2)
C(9)-C(10)-H(10B)	113(2)
H(10A)-C(10)-H(10B)	108(3)

C(12)-C(11)-C(10)	113.54(19)
C(12)-C(11)-H(11A)	104(2)
C(10)-C(11)-H(11A)	115(2)
C(12)-C(11)-H(11B)	107(2)
C(10)-C(11)-H(11B)	108(2)
H(11A)-C(11)-H(11B)	108(3)
O(2)-C(12)-C(11)	104.63(19)
O(2)-C(12)-C(4)	112.88(18)
C(11)-C(12)-C(4)	114.69(19)
O(2)-C(12)-H(12)	105.1(18)
C(11)-C(12)-H(12)	109.0(18)
C(4)-C(12)-H(12)	109.9(18)
C(15)-C(13)-C(14)	119.7(2)
C(15)-C(13)-C(6)	123.5(2)
C(14)-C(13)-C(6)	116.70(18)
C(13)-C(14)-H(14A)	113.3(18)
C(13)-C(14)-H(14B)	111(2)
H(14A)-C(14)-H(14B)	107(3)
C(13)-C(14)-H(14C)	111.7(19)
H(14A)-C(14)-H(14C)	105(3)
H(14B)-C(14)-H(14C)	108(3)
C(13)-C(15)-H(15A)	124(2)
C(13)-C(15)-H(15B)	122(2)
H(15A)-C(15)-H(15B)	114(3)

C(9)-C(16)-H(16A)	113(2)
C(9)-C(16)-H(16B)	113.4(19)
H(16A)-C(16)-H(16B)	104(3)
C(9)-C(16)-H(16C)	108(3)
H(16A)-C(16)-H(16C)	111(3)
H(16B)-C(16)-H(16C)	108(3)
C(17)-O(5)-C(28)	124.23(17)
O(4)-C(17)-O(5)	117.3(2)
O(4)-C(17)-C(18)	122.6(2)
O(5)-C(17)-C(18)	120.04(18)
C(17)-C(18)-C(19)	115.17(19)
C(17)-C(18)-H(18A)	106.7(19)
C(19)-C(18)-H(18A)	110.6(19)
C(17)-C(18)-H(18B)	107.0(19)
C(19)-C(18)-H(18B)	110(2)
H(18A)-C(18)-H(18B)	107(3)
C(18)-C(19)-C(20)	110.85(18)
C(18)-C(19)-H(19A)	109.3(19)
C(20)-C(19)-H(19A)	110.7(18)
C(18)-C(19)-H(19B)	110.2(16)
C(20)-C(19)-H(19B)	111.5(16)
H(19A)-C(19)-H(19B)	104(2)
C(21)-C(20)-C(28)	108.61(17)
C(21)-C(20)-C(19)	113.25(17)

C(28)-C(20)-C(19)	107.77(17)
C(21)-C(20)-H(20)	111.8(18)
C(28)-C(20)-H(20)	106.2(18)
C(19)-C(20)-H(20)	108.8(18)
C(20)-C(21)-C(25)	113.69(17)
C(20)-C(21)-C(22)	123.91(17)
C(25)-C(21)-C(22)	106.31(16)
C(20)-C(21)-H(21)	105.9(17)
C(25)-C(21)-H(21)	103.8(17)
C(22)-C(21)-H(21)	100.7(17)
C(29)-C(22)-C(23)	114.92(17)
C(29)-C(22)-C(21)	120.67(16)
C(23)-C(22)-C(21)	98.41(16)
C(29)-C(22)-H(22)	107.0(19)
C(23)-C(22)-H(22)	109.9(19)
C(21)-C(22)-H(22)	105.2(19)
C(24)-C(23)-C(22)	106.70(17)
C(24)-C(23)-H(23A)	108(2)
C(22)-C(23)-H(23A)	107(2)
C(24)-C(23)-H(23B)	113.8(18)
C(22)-C(23)-H(23B)	120.6(17)
H(23A)-C(23)-H(23B)	99(3)
O(6)-C(24)-C(23)	125.0(2)
O(6)-C(24)-C(25)	126.1(2)

C(23)-C(24)-C(25)	108.97(18)
C(24)-C(25)-C(26)	115.22(18)
C(24)-C(25)-C(21)	100.73(17)
C(26)-C(25)-C(21)	107.92(17)
C(24)-C(25)-C(32)	106.51(17)
C(26)-C(25)-C(32)	111.02(18)
C(21)-C(25)-C(32)	115.25(17)
C(27)-C(26)-C(25)	109.74(18)
C(27)-C(26)-H(26A)	109.2(18)
C(25)-C(26)-H(26A)	106.3(17)
C(27)-C(26)-H(26B)	111.1(19)
C(25)-C(26)-H(26B)	110.3(18)
H(26A)-C(26)-H(26B)	110(3)
C(28)-C(27)-C(26)	113.12(18)
C(28)-C(27)-H(27A)	108(2)
C(26)-C(27)-H(27A)	109.1(19)
C(28)-C(27)-H(27B)	110(2)
C(26)-C(27)-H(27B)	109(2)
H(27A)-C(27)-H(27B)	108(3)
O(5)-C(28)-C(27)	104.56(18)
O(5)-C(28)-C(20)	112.72(17)
C(27)-C(28)-C(20)	114.84(17)
O(5)-C(28)-H(28)	105.3(19)
C(27)-C(28)-H(28)	108.3(19)

C(20)-C(28)-H(28)	111(2)
C(31)-C(29)-C(30)	119.5(2)
C(31)-C(29)-C(22)	123.7(2)
C(30)-C(29)-C(22)	116.48(18)
C(29)-C(30)-H(30A)	113(2)
C(29)-C(30)-H(30B)	109(3)
H(30A)-C(30)-H(30B)	107(3)
C(29)-C(30)-H(30C)	112(2)
H(30A)-C(30)-H(30C)	107(3)
H(30B)-C(30)-H(30C)	110(3)
C(29)-C(31)-H(31A)	124(2)
C(29)-C(31)-H(31B)	117(2)
H(31A)-C(31)-H(31B)	119(3)
C(25)-C(32)-H(32A)	109(2)
C(25)-C(32)-H(32B)	112.4(17)
H(32A)-C(32)-H(32B)	111(3)
C(25)-C(32)-H(32C)	108(2)
H(32A)-C(32)-H(32C)	109(3)
H(32B)-C(32)-H(32C)	107(3)

Table 4. Anisotropic displacement parameters ($Å^2$ x 10^3) for cdv114. The anisotropic displacement factor exponent takes the form: $-2\pi^2[h^2 a^{*2}U^{11} + ... + 2 h k a^* b^* U^{12}]$

	U^{11}	U^{22}	U^{33}	U^{23}	U^{13}	U^{12}
O(1)	19(1)	30(1)	10(1)	-3(1)	-1(1)	5(1)
O(2)	22(1)	23(1)	10(1)	2(1)	2(1)	0(1)
O(3)	20(1)	28(1)	22(1)	1(1)	2(1)	10(1)
C(1)	11(1)	22(1)	11(1)	-1(1)	3(1)	3(1)
C(2)	19(1)	22(1)	11(1)	-2(1)	0(1)	7(1)
C(3)	14(1)	28(1)	10(1)	-3(1)	1(1)	7(1)
C(4)	12(1)	20(1)	10(1)	-1(1)	3(1)	-1(1)
C(5)	11(1)	13(1)	8(1)	1(1)	1(1)	0(1)
C(6)	11(1)	12(1)	11(1)	0(1)	0(1)	-1(1)
C(7)	10(1)	18(1)	16(1)	2(1)	2(1)	-2(1)
C(8)	14(1)	19(1)	10(1)	-1(1)	1(1)	4(1)
C(9)	17(1)	13(1)	12(1)	1(1)	2(1)	0(1)
C(10)	29(1)	14(1)	16(1)	6(1)	6(1)	4(1)
C(11)	33(1)	18(1)	17(1)	4(1)	8(1)	-5(1)
C(12)	18(1)	22(1)	13(1)	-1(1)	6(1)	-5(1)
C(13)	15(1)	12(1)	12(1)	2(1)	0(1)	-1(1)
C(14)	13(1)	23(1)	13(1)	0(1)	-1(1)	1(1)
C(15)	19(1)	25(1)	12(1)	-2(1)	3(1)	1(1)
C(16)	26(1)	14(1)	18(1)	-3(1)	5(1)	-3(1)

O(4)	19(1)	27(1)	11(1)	2(1)	0(1)	0(1)
O(5)	23(1)	20(1)	11(1)	-2(1)	2(1)	2(1)
O(6)	21(1)	29(1)	29(1)	2(1)	2(1)	-12(1)
C(17)	11(1)	20(1)	11(1)	2(1)	4(1)	0(1)
C(18)	14(1)	16(1)	12(1)	2(1)	1(1)	-1(1)
C(19)	10(1)	18(1)	12(1)	2(1)	0(1)	-2(1)
C(20)	10(1)	14(1)	10(1)	0(1)	0(1)	1(1)
C(21)	9(1)	11(1)	8(1)	2(1)	0(1)	0(1)
C(22)	10(1)	11(1)	12(1)	1(1)	1(1)	2(1)
C(23)	10(1)	22(1)	13(1)	2(1)	0(1)	1(1)
C(24)	14(1)	21(1)	9(1)	2(1)	-1(1)	-5(1)
C(25)	14(1)	12(1)	12(1)	1(1)	1(1)	-2(1)
C(26)	23(1)	12(1)	16(1)	-2(1)	1(1)	-3(1)
C(27)	26(1)	14(1)	16(1)	-2(1)	3(1)	6(1)
C(28)	14(1)	18(1)	13(1)	0(1)	1(1)	3(1)
C(29)	16(1)	12(1)	12(1)	0(1)	-1(1)	2(1)
C(30)	20(1)	22(1)	13(1)	-3(1)	-3(1)	-1(1)
C(31)	28(1)	22(1)	12(1)	2(1)	0(1)	-1(1)
C(32)	21(1)	14(1)	15(1)	4(1)	-2(1)	1(1)

Table 5. Hydrogen coordinates (x 10^4) and isotropic displacement parameters ($Å^2$ x 10^3) for cdv114.

	x	y	z	U(eq)
H(2A)	3850(50)	7050(30)	5621(11)	21(7)
H(2B)	1940(50)	7410(30)	5855(11)	20(7)
H(3A)	240(50)	6200(20)	5450(12)	22(7)
H(3B)	1610(50)	6720(20)	5058(12)	23(8)
H(4)	1460(40)	4870(20)	5030(11)	16(7)
H(5)	5060(40)	5570(19)	5327(9)	5(6)
H(6)	4840(50)	6620(20)	4717(11)	20(7)
H(7A)	7760(50)	6020(30)	4880(13)	32(9)
H(7B)	7690(50)	5600(30)	4353(12)	21(7)
H(10A)	6050(40)	4120(20)	5740(11)	19(7)
H(10B)	5790(50)	3020(30)	5503(13)	28(8)
H(11A)	2420(50)	3170(30)	5519(13)	30(8)
H(11B)	3340(50)	3380(30)	6020(13)	27(8)
H(12)	970(40)	4520(20)	5808(11)	16(7)
H(14A)	1170(40)	5610(20)	4340(11)	15(7)
H(14B)	1850(50)	6710(30)	4264(13)	31(9)
H(14C)	1510(40)	6000(20)	3839(11)	17(7)
H(15A)	6100(50)	5260(30)	3756(11)	23(7)

H(15B)	4140(50)	5390(30)	3450(13)	27(8)
H(16A)	2840(50)	3520(30)	4696(13)	32(9)
H(16B)	4430(40)	3740(20)	4336(11)	17(7)
H(16C)	4760(60)	2820(30)	4694(16)	47(11)
H(18A)	6890(50)	7230(30)	6726(12)	23(8)
H(18B)	8780(50)	7580(30)	6493(12)	23(8)
H(19A)	10520(50)	6700(20)	7022(11)	18(7)
H(19B)	9010(40)	7150(20)	7345(10)	9(6)
H(20)	9400(40)	5380(20)	7493(12)	18(7)
H(21)	5900(40)	5690(20)	7042(10)	12(6)
H(22)	5510(50)	6870(30)	7557(12)	22(7)
H(23A)	2970(50)	6000(30)	7387(12)	27(8)
H(23B)	2580(50)	5840(20)	7920(11)	18(7)
H(26A)	5520(50)	4130(20)	6724(11)	21(7)
H(26B)	5860(50)	3090(30)	7043(11)	21(7)
H(27A)	9020(40)	3520(20)	7102(11)	16(7)
H(27B)	8560(50)	3450(30)	6561(13)	28(8)
H(28)	10390(50)	4860(20)	6768(11)	19(7)
H(30A)	9140(50)	6430(30)	8107(12)	26(8)
H(30B)	8040(60)	7440(30)	8113(14)	36(9)
H(30C)	8440(50)	6900(30)	8599(13)	31(9)
H(31A)	4090(50)	5770(30)	8583(12)	26(8)
H(31B)	5860(50)	6200(30)	8905(12)	25(8)
H(32A)	8130(50)	3910(30)	7842(11)	23(7)

H(32B)	6490(40)	4270(20)	8178(11)	15(6)
H(32C)	6390(60)	3270(30)	7902(13)	34(9)

Table 6. Torsion angles [°] for cdv114.

C(12)-O(2)-C(1)-O(1)	169.27(19)
C(12)-O(2)-C(1)-C(2)	-13.4(3)
O(1)-C(1)-C(2)-C(3)	-163.5(2)
O(2)-C(1)-C(2)-C(3)	19.3(3)
C(1)-C(2)-C(3)-C(4)	-43.1(3)
C(2)-C(3)-C(4)-C(5)	-62.3(2)
C(2)-C(3)-C(4)-C(12)	58.9(2)
C(3)-C(4)-C(5)-C(9)	175.08(17)
C(12)-C(4)-C(5)-C(9)	54.6(2)
C(3)-C(4)-C(5)-C(6)	-55.2(3)
C(12)-C(4)-C(5)-C(6)	-175.64(18)
C(4)-C(5)-C(6)-C(13)	-52.7(3)
C(9)-C(5)-C(6)-C(13)	80.2(2)
C(4)-C(5)-C(6)-C(7)	-177.97(19)
C(9)-C(5)-C(6)-C(7)	-45.09(19)
C(13)-C(6)-C(7)-C(8)	-95.6(2)
C(5)-C(6)-C(7)-C(8)	32.9(2)
C(6)-C(7)-C(8)-O(3)	170.5(2)
C(6)-C(7)-C(8)-C(9)	-10.5(2)
O(3)-C(8)-C(9)-C(10)	45.7(3)
C(7)-C(8)-C(9)-C(10)	-133.33(19)
O(3)-C(8)-C(9)-C(5)	161.8(2)

C(7)-C(8)-C(9)-C(5)	-17.2(2)
O(3)-C(8)-C(9)-C(16)	-77.7(3)
C(7)-C(8)-C(9)-C(16)	103.3(2)
C(4)-C(5)-C(9)-C(8)	177.29(16)
C(6)-C(5)-C(9)-C(8)	39.15(19)
C(4)-C(5)-C(9)-C(10)	-62.2(2)
C(6)-C(5)-C(9)-C(10)	159.69(17)
C(4)-C(5)-C(9)-C(16)	62.2(2)
C(6)-C(5)-C(9)-C(16)	-75.9(2)
C(8)-C(9)-C(10)-C(11)	170.89(19)
C(5)-C(9)-C(10)-C(11)	59.2(2)
C(16)-C(9)-C(10)-C(11)	-67.5(2)
C(9)-C(10)-C(11)-C(12)	-54.4(3)
C(1)-O(2)-C(12)-C(11)	156.02(19)
C(1)-O(2)-C(12)-C(4)	30.7(3)
C(10)-C(11)-C(12)-O(2)	-74.8(2)
C(10)-C(11)-C(12)-C(4)	49.4(3)
C(5)-C(4)-C(12)-O(2)	72.3(2)
C(3)-C(4)-C(12)-O(2)	-51.9(2)
C(5)-C(4)-C(12)-C(11)	-47.4(3)
C(3)-C(4)-C(12)-C(11)	-171.59(19)
C(7)-C(6)-C(13)-C(15)	-3.6(3)
C(5)-C(6)-C(13)-C(15)	-120.5(2)
C(7)-C(6)-C(13)-C(14)	-178.65(18)

C(5)-C(6)-C(13)-C(14)	64.4(3)
C(28)-O(5)-C(17)-O(4)	177.62(18)
C(28)-O(5)-C(17)-C(18)	-3.1(3)
O(4)-C(17)-C(18)-C(19)	-169.2(2)
O(5)-C(17)-C(18)-C(19)	11.5(3)
C(17)-C(18)-C(19)-C(20)	-40.8(2)
C(18)-C(19)-C(20)-C(21)	-59.9(2)
C(18)-C(19)-C(20)-C(28)	60.2(2)
C(28)-C(20)-C(21)-C(25)	55.0(2)
C(19)-C(20)-C(21)-C(25)	174.64(16)
C(28)-C(20)-C(21)-C(22)	-173.41(18)
C(19)-C(20)-C(21)-C(22)	-53.7(3)
C(20)-C(21)-C(22)-C(29)	-52.7(3)
C(25)-C(21)-C(22)-C(29)	81.8(2)
C(20)-C(21)-C(22)-C(23)	-178.33(19)
C(25)-C(21)-C(22)-C(23)	-43.82(18)
C(29)-C(22)-C(23)-C(24)	-96.9(2)
C(21)-C(22)-C(23)-C(24)	32.64(19)
C(22)-C(23)-C(24)-O(6)	168.7(2)
C(22)-C(23)-C(24)-C(25)	-11.3(2)
O(6)-C(24)-C(25)-C(26)	48.5(3)
C(23)-C(24)-C(25)-C(26)	-131.50(18)
O(6)-C(24)-C(25)-C(21)	164.3(2)
C(23)-C(24)-C(25)-C(21)	-15.7(2)

O(6)-C(24)-C(25)-C(32)	-75.1(2)
C(23)-C(24)-C(25)-C(32)	104.92(19)
C(20)-C(21)-C(25)-C(24)	177.16(16)
C(22)-C(21)-C(25)-C(24)	37.43(19)
C(20)-C(21)-C(25)-C(26)	-61.7(2)
C(22)-C(21)-C(25)-C(26)	158.57(17)
C(20)-C(21)-C(25)-C(32)	63.0(2)
C(22)-C(21)-C(25)-C(32)	-76.7(2)
C(24)-C(25)-C(26)-C(27)	170.56(18)
C(21)-C(25)-C(26)-C(27)	58.9(2)
C(32)-C(25)-C(26)-C(27)	-68.3(2)
C(25)-C(26)-C(27)-C(28)	-54.8(2)
C(17)-O(5)-C(28)-C(27)	149.78(19)
C(17)-O(5)-C(28)-C(20)	24.4(3)
C(26)-C(27)-C(28)-O(5)	-73.8(2)
C(26)-C(27)-C(28)-C(20)	50.2(3)
C(21)-C(20)-C(28)-O(5)	71.3(2)
C(19)-C(20)-C(28)-O(5)	-51.7(2)
C(21)-C(20)-C(28)-C(27)	-48.3(2)
C(19)-C(20)-C(28)-C(27)	-171.32(18)
C(23)-C(22)-C(29)-C(31)	-4.3(3)
C(21)-C(22)-C(29)-C(31)	-121.9(2)
C(23)-C(22)-C(29)-C(30)	-177.33(18)
C(21)-C(22)-C(29)-C(30)	65.1(3)